Published by Empress Catherine II
Saint Petersburg Mining University

SINCE 1907

ISSN 2411-3336
E-ISSN 2541-9404

JOURNAL OF MINING INSTITUTE

ZAPISKI GORNOGO INSTITUTA

SCIENTIFIC JOURNAL

Volume 275

N 5 • 2025

SCOPUS (Q1, CITESCORE – 8.8)
WEB OF SCIENCE (Q1, JIF – 2.9)
SJR 2024 – 1.351

WWW.PMI.SPMI.RU

Journal of Mining Institute
Scientific journal

Empress Catherine II Saint Petersburg Mining University

The International Competence Center for Mining Engineering Education under the auspices of **UNESCO**

The peer-reviewed scientific periodical “Journal of Mining Institute” is published since 1907 by Empress Catherine II Saint Petersburg Mining University – the first higher technical educational institution in Russia, founded in 1773 by the decree of Catherine II as the embodiment of the ideas of Peter I and M.V.Lomonosov on the training of engineers for the development of mining business.

The International Competence Center for Mining Engineering Education under the auspices of UNESCO operates on the basis of Empress Catherine II Saint Petersburg Mining University and contributes to active interaction of the Journal with the international scientific community.

The purpose of the Journal is to create an information space in which Russian and foreign scientists can present results of their theoretical and empirical research on the problems of the mining sector. The journal invites the leading specialists to publish scientific articles and promotes them in the international scientific community.

Published articles cover the issues of geology, geotechnical engineering and engineering geology, mining and petroleum engineering, mineral processing, energy, geoecology and life safety, economics of raw materials industries.

The Journal is indexed by Scopus (Q1, CiteScore – 8.8), Web of Science (JCR – Q1, JIF – 2.9), SJR 2024 – 1.351, DOAJ, RSCI, GeoRef, Islamic World Science Citation Database (ISC), Google Scholar. It is included in the White list of the Ministry of Education and Science of the Russian Federation.

The Journal is published six times a year. The average first decision time is one month.

Articles are published free of charge. Translation is provided by the author.

The cover shows an exhibit of the Mining Museum – a sawn off piece of the Carlton iron meteorite with regmaglypts on the natural surface. Etching revealed the structure of fine-structured octahedrite with kamacite beams about 0.2 mm wide. There are elongated, hieroglyph-shaped inclusions of schreibersite, bordered by kamacite. In 1994, the Carlton meteorite attracted special attention because a new mineral, chladniite, was first discovered in it. Chladniite was subsequently found on Earth as well – in metamorphic rocks and in phosphate-rich granite pegmatites.

The Mining Museum is the world’s third largest natural-science exposition, it contains more than 230 thousand exhibits, including precious metals and stones, unique collections of minerals, ores, rocks, paleontological remains, meteorites, a collection of models and prototypes of mining equipment, pieces of stone-cutting and jewelry art.

JOURNAL OF MINING INSTITUTE

ZAPISKI GORNOGO INSTITUTA

PEER-REVIEWED SCIENTIFIC JOURNAL

Published since 1907

ISSN 2411-3336
e-ISSN 2541-9404

Volume 275
№ 5 • 2025

ST. PETERSBURG

Journal founder: Empress Catherine II Saint Petersburg Mining University

Guest science editors of the volume: Doctor of Engineering Sciences **Yuriy L. Zhukovskiy,** Candidate of Engineering Sciences **Ilya I. Beloglazov,** Candidate of Engineering Sciences **Dmitrii A. Klebanov,** Doctor of Engineering Sciences **Igor O. Temkin**

Sections

• Geology • Geotechnical Engineering and Engineering Geology • Economic Geology • Energy

The journal invites the leading specialists to publish scientific articles and promotes them in the international scientific community
Registration Certificate PI N FS 77-70453 dated 20 July 2017

PH License N 06517 dated 09.01.02

Editorial staff: Head of the Editorial Center V.L.Lebedev, Editors E.S.Dribinskaya, M.G.Khachirova, L.V.Nabieva, A.I.Yakovleva, E.D.Bokareva
Bibliographer A.A.Belova. Computer Design N.N.Sedykh, V.I.Kashirina, E.A.Golovinskaya

Publishing date 31.10.2025. Format 60 × 84/8. Academic Publishing Division 46.
Circulation: 100 copies. Order 634. Printed by RIC of Empress Catherine II Saint Petersburg Mining University. Free sale price.

Editorial and publisher address 2, 21st Line, St. Petersburg, 199106, Russia
Phone: +7 (812) 328-8416; +7 (812) 328-8216
E-mail: pmi@spmi.ru Journal website: pmi.spmi.ru

CONTENTS

Energy and Energy Efficiency

Oil and Gas Industry

Mining and Metallurgy Industry

Journal of Mining Institute. 2025. Vol. 275. P. 3-4

Editorial

Editorial: Digital transformation in process and equipment management at Fuel and Energy Complex and Mineral Resources companies

In the context of the rapid development of digital technologies and increasing demands on energy efficiency, sustainability and competitiveness of industrial enterprises, the fuel and energy (FEC) and mineral resources (MR) complexes are undergoing major changes. Digital transformation is becoming a key factor in improving the efficiency, reliability, and sustainability of production processes, as well as an important element of the strategy for technological sovereignty and the modernization of production systems. Modern approaches to managing equipment and process chains are based on the use of machine learning methods, big data analysis, digital modeling, and the creation of digital twins, which, in turn, allows not only the optimization of technological and business processes, but also the formation of new control architectures from local systems to industrial metauniverses.

This thematic volume presents research studies united by the common theme of digital transformation at fuel and energy complex and mineral resources companies. It covers three key areas: energy, oil and gas, and mining and metallurgy, demonstrating a wide range of applications of end-to-end digital technologies, from load identification to reservoir property prediction and the creation of ontological enterprise models.

Incorporation of three key industries in one volume suggests that digital transformation today extends beyond individual automated systems, creating a holistic ecosystem of intelligent industrial process control with the potential for sustainable lifecycle management of energy and mineral resources.

The articles presented reflect both fundamental scientific research and practical solutions in demand in the context of import substitution and the growth of domestic technological potential. Particular attention is paid to the interpretability of models, economic efficiency, and practical applicability of solutions. The materials in this volume will be useful to a wide range of specialists – scientists, engineers, business managers, and software developers – working in the field of industrial digitalization and will serve as a stimulus for further research and implementation.

The “Energy and Energy Efficiency” section presents research aimed at improving the energy efficiency of electrical complexes of industrial enterprises.

The article by *Yuriy L. Zhukovskiy* and *Pavel K. Suslikov* is devoted to the identification and classification of the electrical load of mining enterprises based on signal decomposition, which makes it possible to create conditions for the classification of loads for the purpose of implementing electricity demand management.

Aleksandr V. Nikolaev and *Aleksei V. Kychkin* propose a service for managing electricity demand for ventilation in underground workings, opening up opportunities for adaptive regulation of energy consumption.

Natalia I. Koteleva, *Vladislav V. Valnev*, *Aleksandr S. Simakov* and *Maysam M. Shirazi* examine the process of creating a cyber-physical service engineer avatar as the basis for constructing an industrial metauniverse where physical and digital processes interact in a single information space.

Roman R. Khalikov, *Mikhail Yu. Chernetskiy*, *Ilia E. Revin* and *Vadim A. Potemkin* propose an automated machine learning technology using a model composition framework for fault detection in pumping systems based on motor current signature analysis.

Irina Yu. Semykina, *Valery M. Zavyalov*, *Yaroslava A. Nechiporenko* and *Elena N. Taran* develop a model of wireless charging infrastructure for battery-powered dump trucks at open-pit mining enterprises, which is relevant for improving environmental efficiency and reducing the use of diesel fuel.

The "Oil and Gas Industry" section examines the use of digital technologies to improve drilling efficiency, production, and environmental safety.

Vasiliy I. Nikitin, *Mikhail V. Dvoynikov*, *Kirill S. Kupavykh* and *Tatiana A. Panteleeva* model the influence of rheological parameters of nonlinear viscous drilling mud on the quality of cuttings removal using machine learning methods.

Andrei V. Soromotin and *Dmitrii A. Martyushev* apply machine learning approaches to modeling synthetic hydrodynamic well tests and predicting the permeability of oil formations.

Ildar M. Ishkulov and *Irik G. Fattakhov* use interpretable machine learning to detect well leaks, providing not only high prediction accuracy but also an understanding of the causes of defects.

Pavel S. Tsvetkov proposes a cluster approach to capture and transport of industrial CO_2 demonstrating economic advantages due to the effects of scale when combining stationary emission sources into a single network with a shared infrastructure.

The "Mining and Metallurgical Industry" section presents solutions for digitalization of ore flow management, geoinformation support, and equipment localization.

Sergei A. Deryabin and *Igor O. Temkin* develop an ontological model for the digital transformation of mining enterprise architecture, which allows for the formalization of knowledge and ensures consistency between IT systems.

Egor A. Knyazkin, *Dmitrii A. Klebanov* and *Roman O. Yuvakaev* propose new methods for assessing the variability of the quality of minerals based on big data analysis to improve the efficiency of the produced quality of minerals.

Sergei V. Lukichev and *Oleg V. Nagovitsyn* highlight the development of MGIS, demonstrating the practical results of the implementation of modern geographic information systems in large mining companies.

Mikhail S. Nikitenko, *Danila Yu. Khudonogov* and *Sergei A. Kizilov* examine alternative approaches to determining the position of equipment in quarries to solve dispatching and navigation problems within technological areas for the operation of highly automated vehicles without the use of navigation equipment.

Onalethata Saubi, *Rodrigo S. Jamisola Jr.*, *Raymond S. Suglo* and *Oduetse Matsebe* predict and optimize particle size distribution in blasting waste using hybrid artificial intelligence methods at a diamond mine contributing to improved overburden mining efficiency.

Sergei V. Khokhlov presents alternative approaches to digital modeling of blasted rock muckpile, which allows for the prediction of particle size distribution and optimization of subsequent processing.

***Guest science editors of the volume*: Yuriy L. Zhukovskiy,** *Doctor of Engineering Sciences, Head of Department* (*Empress Catherine II Saint Petersburg Mining University, Saint Petersburg, Russia*), *Zhukovskiy_Yul@ pers.spmi.ru*, https://orcid.org/0000-0003-0312-0019, **Ilya I. Beloglazov,** *Candidate of Engineering Sciences, Associate Professor* (*Empress Catherine II Saint Petersburg Mining University, Saint Petersburg, Russia*), https://orcid.org/0000-0002-1224-2117, **Dmitrii A. Klebanov,** *Candidate of Engineering Sciences, Head of the Laboratory* (*Institute of Comprehensive Exploitation of Mineral Resources RAS, Moscow, Russia*), https://orcid.org/0000-0002-3289-9212, **Igor O. Temkin,** *Doctor of Engineering Sciences, Head of Department* (*National University of Science and Technology MISiS, Moscow, Russia*), https://orcid.org/0000-0001-8150-6529.

ISSN 2411-3336; e-ISSN 2541-9404

JOURNAL OF MINING INSTITUTE
Zapiski Gornogo instituta
Journal homepage: pmi.spmi.ru

Research article
Geotechnical Engineering and Engineering Geology

Identification and classification of electrical loads in mining enterprises based on signal decomposition methods

Yuriy L. Zhukovskiy✉, **Pavel K. Suslikov**
Empress Catherine II Saint Petersburg Mining University, Saint Petersburg, Russia

***How to cite this article*:** Zhukovskiy Yu.L., Suslikov P.K. Identification and classification of electrical loads in mining enterprises based on signal decomposition methods. Journal of Mining Institute. 2025. Vol. 275, p. 5-17.

Abstract
This study investigates the use of Singular value decomposition to decompose time series of electricity consumption from substation feeders. The goal is to identify and classify the electrical load patterns of mining enterprises. The need for continuous improvement in process efficiency is dictated by current trends and tendencies towards increased consumption of fossil fuels and energy resources. The proposed algorithm uses the decomposition results to identify similarities in consumption patterns, enabling the categorization of loads into broader groups. Based on the results of the analysis of electricity consumption data for two independent feeders, the formation of similar recurring characteristic load changes (temporal patterns) with a period of three days was identified. The results facilitate the automated typification and classification of load profiles. This is vital for integrating economic incentives into demand management and for assessing the feasibility and potential of consumer participation in load schedule regulation via demand side management technologies. The proposed algorithms enable the use of these typical consumption profiles to calculate quasi-dynamic electrical modes, supporting tasks related to the long-term development of energy supply systems and energy efficiency improvements for mining enterprises.

Keywords
demand side management; classification of electrical loads; management in power grids; power grids; data analysis; machine learning; energy efficiency

Funding
The work was carried out as part of a State assignment from the Ministry of Science and Higher Education of the Russian Federation N FSRW-2023-0002 “Fundamental interdisciplinary research into the Earth's interior and processes of integrated development of georesources”.

Received: 13.02.2025 ***Accepted: 02.09.2025*** ***Online: 02.10.2025*** ***Published: 31.10.2025***

Introduction

The need to improve the efficiency of mining operations is dictated by current trends and tendencies, in particular the increase in the consumption of minerals [1-3]. Digital transformation, based on the use of digital technologies and mathematical methods that enable the processing and analysis of large volumes of data generated by mining equipment, improves the efficiency of technological processes throughout the entire mineral extraction chain from geological exploration to resource consumption [4-6]. Similar to the tasks of improving electricity quality [7, 8], methods, based on models of the object under study, must be used to ensure a sufficient level of energy efficiency [9, 10].

The article discusses an approach to improving the efficiency of power supply system to a mining enterprise based on the identification and classification of electrical loads through signal decomposition. Signal decomposition is the breakdown of the original signal (time series) into components represented as modes, components, etc. Signal decomposition methods are determined based on the characteristics of the analysed time series [11, 12] (Table 1).

Table 1

Characteristics of decomposition methods used in power grids

Method	Scope of application	Disadvantages	Literary source
Fourier transform	Harmonic analysis in electrical networks (THD, harmonic distortion). Identification of seasonal components in the load. Detection of equipment faults based on the current or voltage spectrum	Assumes signal stationarity, which is rarely the case in real loads. Not suitable for analyzing nonlinear and non-stationary processes, which are common in the mining industry	[13-16]
Singular value decomposition, SVD	Decomposition of load time series into trend and cyclical components. Signal noise removal. Analysis of non-stationary processes in power grids	No shortcomings found	[17-20]
Empirical mode decomposition, EMD	Analysis of non-stationary electrical loads in mines and quarries. Equipment diagnostics based on vibrations and currents. Improved real-time load forecasting	The method is prone to modal mixing (different frequencies in one IMF). High noise sensitivity	[13, 21-23]
Variational mode decomposition, VMD	Analysis and forecasting of electrical load under variable production conditions. Identification of abnormal equipment operating modes. Joint use with AI models (e.g., LSTM) for forecasting	Dependence on initial parameters. High computational complexity, problems with processing signals with sharp jumps or pulses. Does not guarantee complete separation of overlapping frequency components	[24, 25]
Hilbert – Huang transformation (HHT)	Analysis of transient processes in mining enterprise networks. Diagnosis of faults in electric motors and pumps. Monitoring of electricity quality	The problem of modal mixing. Edge effects. High sensitivity to noise. Complexity of automation and standardisation	[26-28]

Various decomposition methods are used in different technological processes related to energy supply for mining enterprises [29, 30]. The choice of a specific method depends on the volume of data, its statistical characteristics, and other factors that are currently not the subject of this study.

Research involving Fourier transform as a research method is most often devoted to analysing power quality parameters in power supply networks. In the papers of Russian and foreign scientists, the use of singular value decomposition has recently become very popular and is associated with solving a large number of problems. For example, in the study [24], the singular value decomposition method is applied as part of a singular spectrum analysis complex when solving problems of electricity consumption forecasting in an isolated hybrid electrical engineering complex.

Despite the fact that in the mining industry, a significant part of research on the analysis of the condition of electromechanical equipment is based on the use of spectral analysis methods, such as Fourier transform and singular value decomposition, in most cases they are used to diagnose the condition of individual components, such as bearings, or generally to analyze the vibration characteristics of the equipment. At the same time, the influence of the structure and parameters of the electric drive, including the type of motor, control system, operating modes and interaction with the technological process, on the nature of electricity consumption from the grid remains insufficiently studied. This limits the possibilities for comprehensive analysis of electrical modes and reduces the accuracy of load forecasting, especially when using adaptive signal analysis methods. Thus, in further research, it is advisable to take into account not only the external manifestations of signals (vibration, current, voltage), but also the internal parameters of the electric drive that affect the formation of load in the power grid of mining enterprise.

Methods

Signal decomposition methods are essential analytical techniques used in various disciplines, including complex signal processing, data analysis, and engineering, to extract meaningful components. Well-known methods include Fourier transform, SVD, EMD, and multi-scale singular value decomposition (MSVD) [31, 32], VMD, HHT. These methods provide valuable information about signal characteristics when dealing with problems such as nonlinearity, non-stationarity, noise, and multimodal data, making them indispensable tools in modern analysis. The areas of application of these methods vary and have their own characteristics when applied to different types of problems.

SVD is a fundamental method of linear algebra that allows a matrix to be decomposed into three components, revealing the internal properties of the original matrix. This method is widely used for dimensionality reduction, noise suppression, and data compression in various fields, such as image processing and machine learning. SVD is particularly effective for revealing hidden structures in data, allowing us to understand underlying patterns and relationships. However, this method is sensitive to data outliers, and the decomposition of large matrices must be carried out with considerable computational resources in mind.

EMD is a data-driven method that breaks down a signal into intrinsic modes (IMF) that reflect different frequency components of the signal without relying on predefined basis functions. This method is particularly effective for analyzing non-linear and non-stationary signals, making it suitable for use in condition monitoring and other areas. The EMD process includes a screening algorithm that iteratively extracts IMF from the original signal until the remainder has no apparent variations. In recent studies, the EMD method has been extended to bi-dimensional empirical mode decomposition (BEMD), allowing it to be applied to two-dimensional signals and images.

VMD is a relatively new method aimed at decomposing a signal into a set of frequency-band-limited eigenmode functions. It eliminates some of the limitations of EMD and SVD by applying a variational approach that optimally separates modes based on their own passband frequencies. This method is particularly useful for signals with closely spaced frequency components and provides improved performance in carrier frequency estimation and signal analysis.

HHT combines EMD and Hilbert transform to provide time-frequency analysis of signals. By applying the Hilbert transform to the IMF obtained using EMD, HHT allows the generation of a Hilbert spectrum that shows the instantaneous distribution of signal frequency and energy over time. This approach is particularly effective for analyzing complex signals with time-varying characteristics.

General limitations and selection criteria for any method:

• Non-stationarity and non-linearity. Many real signals have non-stationary and non-linear characteristics. The presence of these characteristics can complicate the analysis and interpretation of signals. Traditional signal processing methods often assume that signals are stationary, which leads to inaccurate conclusions when applied to non-stationary data.

• Noise and data outliers are another serious problem in signal processing. They can distort the true signal and lead to unreliable results. Decomposition methods help solve this problem by isolating meaningful signal components from noise.

• Resolution and feature extraction. Signal decomposition methods also aim to improve their resolution, allowing more information to be extracted. Methods such as discrete wavelet transform (DWT) increase frequency resolution while reducing time resolution, providing a comprehensive representation of the signal at different scales.

• Multimodal data processing. In modern signal processing applications, there is an increasing need to analyse multimodal data that combines different types of signals. Signal decomposition methods facilitate the effective combination of these modalities, improving classification efficiency and allowing for a more complete understanding of the underlying processes.

To obtain the components of the original time series of electricity consumption, it was decided to use the SVD method due to its stability with regard to noisy data. The method also allows processing non-stationary signals (such as the time series under study) by extracting the trend component.

In accordance with the singular analysis method, it is necessary to obtain a trajectory matrix from the initial time series. To do this, the initial time series, which has N values $\{p_1, \ldots, p_N\}$, is embedded in a space with dimension L. In Russian literature, this method of obtaining a trajectory matrix from a time series is called "Gusenica" (eng. Caterpillar), while in foreign literature it is called Embedding. The value L determines the dimension of the trajectory matrix and is called the window length. The procedure for determining the window length is a separate scientific task, but when considering time series with known periodicity, the window length is selected based on the duration of the known period. For example, when analyzing the dependence of solar radiation on time over a weekly cycle, it is advisable to set the window length to be equal to, or a multiple of, one day (the period of the observed cycle). In other cases, additional calculations are required to determine the optimal window size.

The result of embedding a time series into an L-dimensional space is an Ln-dimensional (trajectory) matrix (the Hankel matrix):

$$A = \begin{pmatrix} p_1 & p_2 & p_3 & & p_n \\ p_2 & p_3 & p_4 & \cdots & p_{n+1} \\ p_3 & p_4 & p_5 & & p_{n+2} \\ & \vdots & & \ddots & \vdots \\ p_L & p_{L+1} & p_{L+2} & \cdots & p_N \end{pmatrix},$$

where $p_1, p_2, \ldots, p_n$ – values of the time series at times $t = 1, 2, 3, \ldots, N$; $n = N - L + 1$ – number of columns in the matrix (the number of lagged vectors); the number of rows is the window length and must satisfy the condition $L \le \left[(N+1)/2\right]$.

According to [33] any matrix can be represented as:

$$A = U\Sigma V^T;$$

$$\begin{pmatrix} \\ A \\ \\ \end{pmatrix}_{Ln} = \begin{pmatrix} \\ U \\ \\ \end{pmatrix}_{LL} \begin{pmatrix} \sigma_1 & 0 & 0 \\ 0 & \cdots & 0 \\ 0 & 0 & \sigma_N \end{pmatrix}_{Ln} \begin{pmatrix} \\ V \\ \\ \end{pmatrix}^T_{nn},$$

where matrix U consists of the left singular vectors, i.e. columns of the matrix U consist of the eigenvectors of the matrix AA^T; matrix V consists of the right singular vectors, i.e. the columns of the matrix V consist of the eigenvectors of the matrix A^TA; σ_N – singular values of the matrix AA^T ($\sigma = \sqrt{\lambda}$, λ – eigenvalue of the matrix AA^T), singular values are located on the main diagonal in descending order.

Let us assume that $\lambda_1 \ldots \lambda_L$ – eigenvalues of a matrix AA^T, at the same time $\lambda_1 \ge \lambda_2 \ldots \ge \lambda_L$. We will also assume $U_1 \ldots U_L$ as columns of a matrix U, taken in accordance with singular values λ.

If we write $V_i = X^T U_i / \sqrt{\lambda_i}$, at the same time $i = 1, \ldots, rank(A)$, then the singular value decomposition of matrix A can be written as follows:

$$A = A_1 + A_2 + \ldots + A_{rank(A)},$$

where $A_i = \sqrt{\lambda_i} U_i V_i^T$.

Each of the matrices A_i has rank 1, so they can be called elementary matrices. Each of $\sqrt{\lambda_i}, U_i, V_i$ is called the i-th singular triplets.

At the final stage of the algorithm, each of the matrices A_i obtained from the decomposition is converted back to the form of the original object. This operation is performed by means of matrix Hankelisation (diagonal averaging),

$$\tilde{A} = \begin{cases} \dfrac{1}{j}\sum_{i=1}^{j} \tilde{a}_{i,\, j-i+1}, 1 \le j \le L; \\ \dfrac{1}{L}\sum_{i=1}^{L} \tilde{a}_{i,\, j-i+1}, L \le j \le n; \\ \dfrac{1}{N-j+1}\sum_{i=1}^{N-j+1} \tilde{a}_{i+j-n,\, n-i+1}, n \le j \le N. \end{cases}$$

Using diagonal averaging of the components from the obtained matrix, we reconstruct the time series. Thus, the original series is decomposed into the sum of the reconstructed components.

The research [34] presents an original study of time series of electrical energy consumption. This study used graphs of electrical loads of eight substation feeders over a year of observation. The data was obtained directly from the electrical energy and power meter Mercury (a commercial meter with an accuracy class of 0.5). The time series has a sampling interval of 30 min, i.e. the power consumption values are averaged over a 30-minute period.

The original time series consists of 17,520 points. The entire data set includes 140,160 values, which corresponds to the number of feeder connections at the substation. A segment of the original time series for the first feeder, shown on a monthly time scale, is plotted as the purple curve in Fig.1. The results of the SVD decomposition are also shown as the first 12 components reconstructed from the original time series.

Before applying any mathematical transformations, the data was normalized using the min-max method. The original time series was intentionally not pre-processed to remove noise or outliers, to test the algorithm's robustness to input data quality.

Algorithm implementation

The entire algorithm was implemented in the Jupyter Notebook development environment using Python. Aside from auxiliary steps such as importing libraries and defining functions, the main stages of the algorithm are as follows:

• Data import and pre-processing for further analysis. Creating a Pandas DataFrame containing timestamps and power consumption values for each feeder.

• Feature engineering based on datetime data: creating new columns for the day of the month, day of the week, month, quarter, etc. This step is necessary for subsequent data aggregation and dependency analysis across different time periods.

• Performing preliminary correlation analysis by calculating Pearson correlation coefficients (Fig.2). This is used to determine the linear relationship between feeders through pairwise comparison.

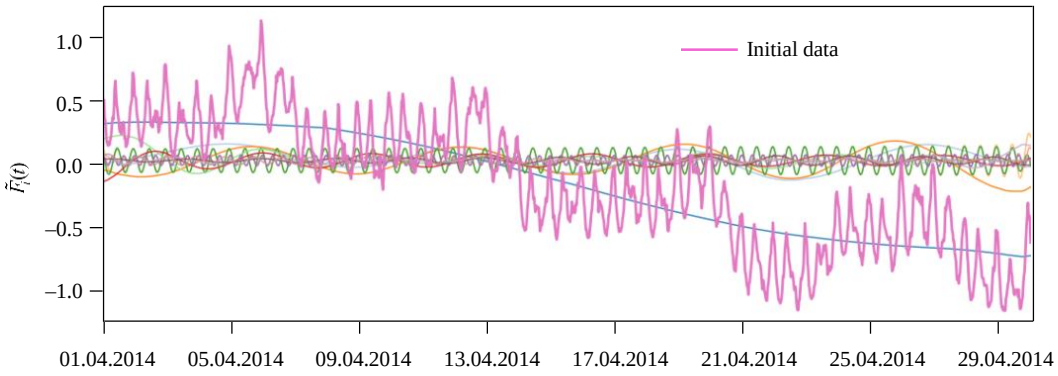

Fig.1. Electricity consumption graph for April 2014 and 12 components of the time series [34]

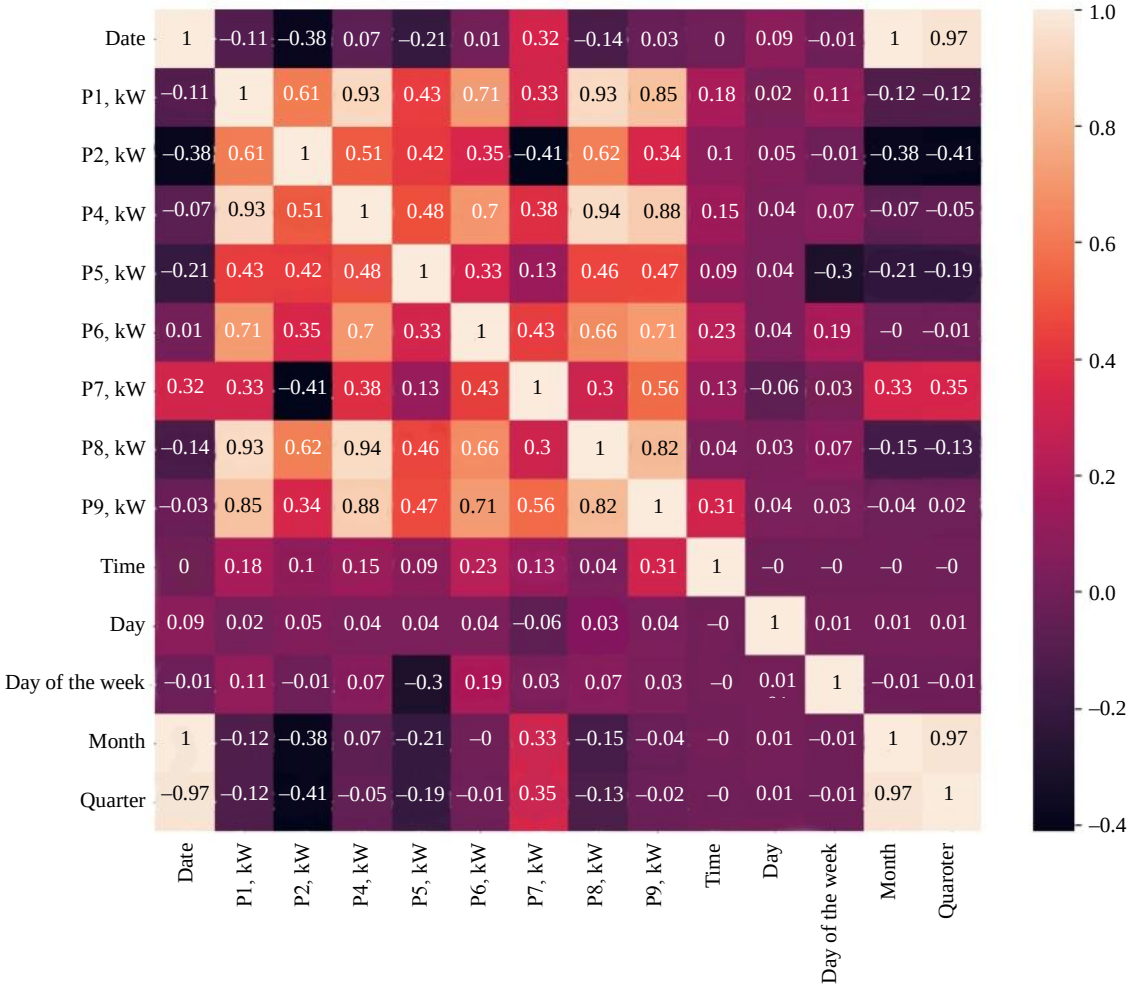

Fig.2. Correlation matrix of initial data using Pearson's method

• Setting the window width L. When analysing the entire year, the window width is set to L_{year} = 1460 data units. based on the average number of points per month. When considering the scale of a month, the window length was defined as the amount of data per week, i.e. L_{month} = 336. Similarly, when considering a single week, the window size was set to L_{week} = 48 in accordance with the amount of data per day.

• Creating a trajectory matrix for a single feeder (Fig.3).

• Singular decomposition of the previously created trajectory matrix, verification of the correctness of the decomposition by summing all elementary matrices and then comparing the result with the original matrix.

• Calculation of the relative and cumulative contribution of components to the initial time series for subsequent determination of the required volume of components when grouping them (Fig.4).

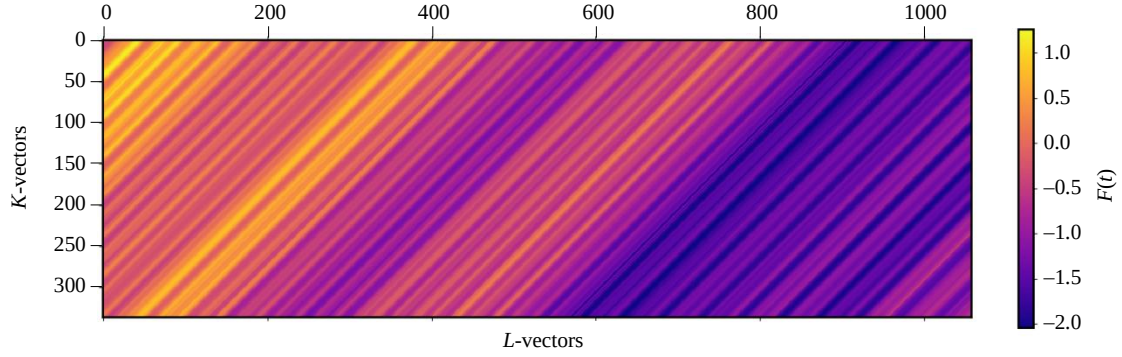

Fig.3. Trajectory matrix of normalized initial data. The time series of feeder 1 is represented as a matrix

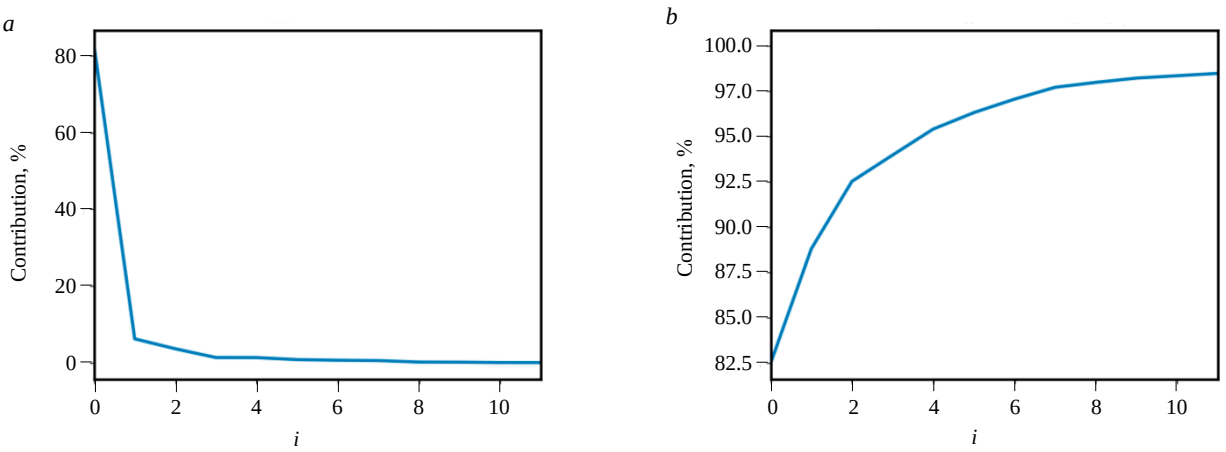

Fig.4. Relative (*a*) and cumulative (*b*) contribution of components using the example of a feeder 1

• Time series reconstruction. Each elementary matrix is transformed back into a one-dimensional time series component through diagonal averaging (a process also known as Hankelization). The resulting reconstructed components are saved to separate files for subsequent analysis.

• A *W*-correlation matrix is constructed to quantify the dependence between the reconstructed components. The components are reordered along the matrix's main diagonal according to their contribution (measured by their singular values) to the total variance of the original time series.

• Components are grouped into interpretable modes based on the analysis of the *W*-correlation matrix. This grouping reveals consumption patterns for each feeder (Fig.5).

The *W*-correlation matrix reveals a high degree of correlation between specific pairs of components. These components are grouped together based on their strong correlation. For example, a distinct group is formed by components (2, 3, 5, 6), while another group comprises components (3, 4, 7, 8, 11, 12).

Results

The study [34] contains the results of manual component grouping using the *W*-correlation matrix (Fig.6). In this paper the principle of grouping based on the *W*-correlation matrix was extended using amplitude-frequency clustering and taking into account multiple feeders (Fig.7). For feeder 1, within the time interval under consideration, the components were grouped as follows:

• trend group: 0;
• periodical group 1: 1, 2, 5, 6, 9, 10;
• periodical group 2: 3, 4, 7, 8, 11, 12;
• periodical group 3: 19, 20, 21, 27, 28, 29.

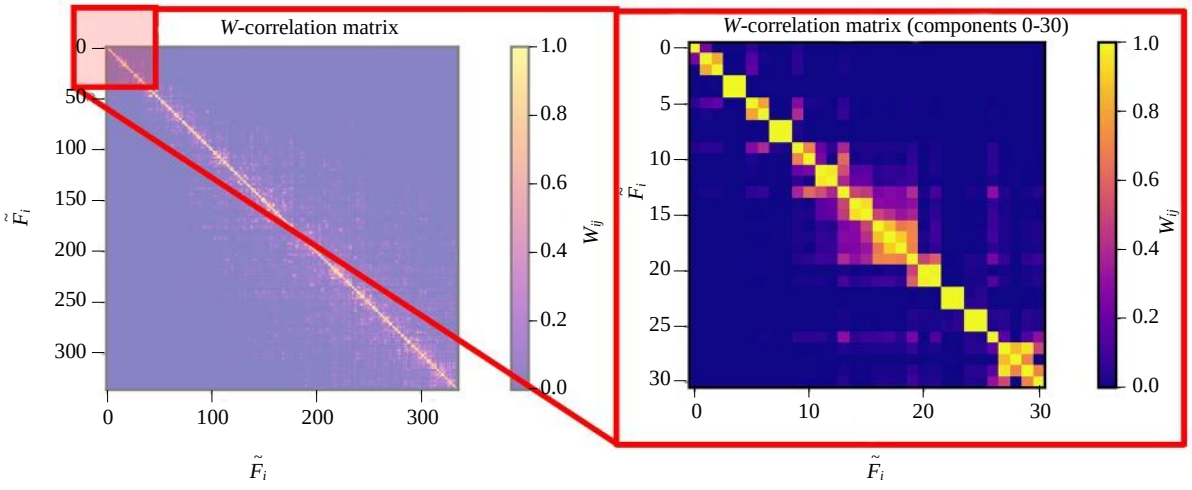

Fig.5. *W*-correlation matrix for feeder 1 [34]

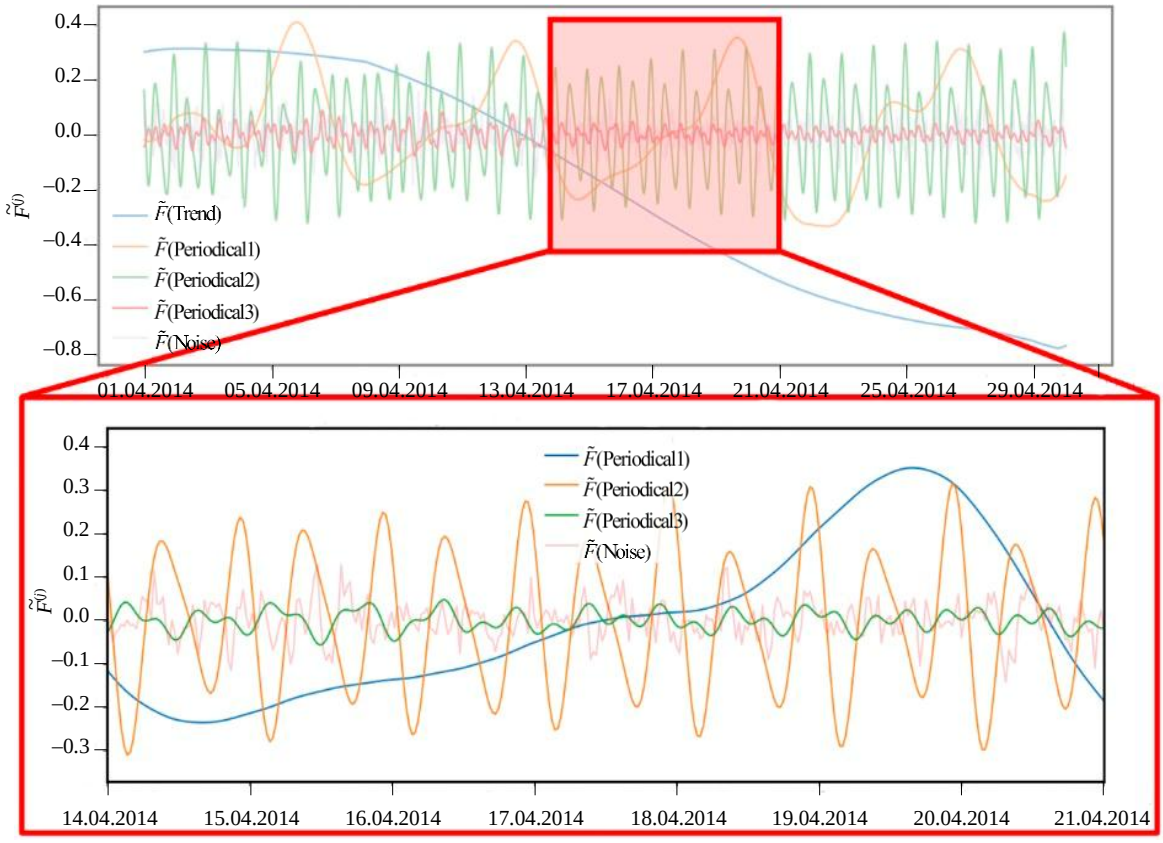

Fig.6. Grouped components of a time series: one trend component and three groups of periodic components [34]

The trend group is characterised by a weekly pattern in the consumption power graph. At the same time, when looking at the original time series, this pattern is difficult to discern.

Periodical group 1 is characterised by a daily consumption pattern with strong morning and evening peaks. However, the shape of the curve remains unchanged even with significant changes in the nature of the power consumed and an increase in noise levels.

For periodical group 2, a pattern is formed with a period of occurrence twice a day. The pattern visually resembles a daily one, but the amplitude of its maxima is several times smaller.

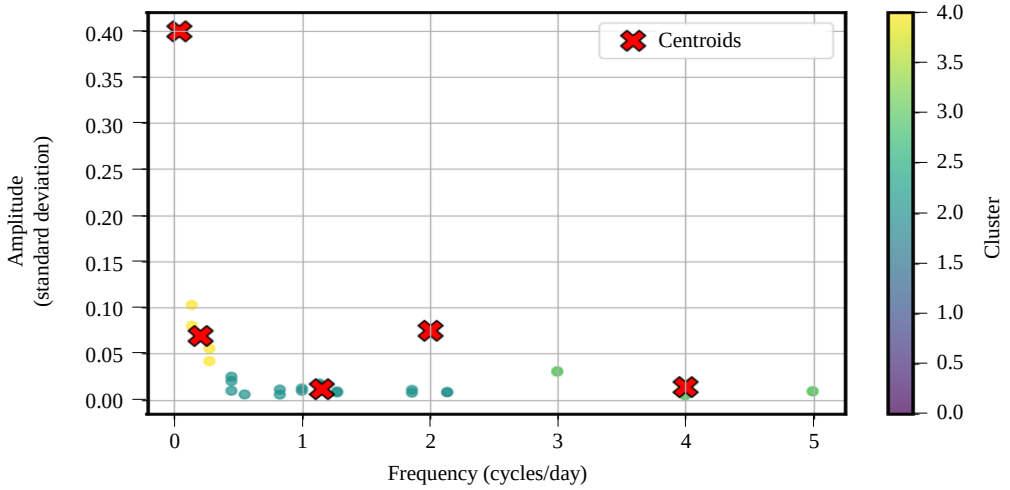

Fig.7. Clustering by frequency and amplitude of the first 10 components of eight feeders

The given example is valid for feeder 1 when considering a monthly volume of data. However, the formation of distinct patterns with a certain periodicity holds true for each of the datasets considered in the study. Furthermore, the patterns are unique for each feeder and vary depending on the type of connected load. Table 2 presents the analysis results for the entire dataset.

Based on the assumption of constant frequency and amplitude of a component over the entire segment under consideration, an amplitude-frequency plane was constructed. In this plane, the vertical axis represents the RMS value of the component, and the horizontal axis represents the frequencies calculated using the Fourier transform. As a result of analyzing the feeder components using this method, a family of points was obtained on the plane, where each point represents an individual feeder component (Fig.7).

Table 2

Results of applying the SVD method and grouping components via the *W*-correlation matrix

Feeder	Component	Characteristic	Group	Description	Note
9	0	Trend	0	–	Formation of a daily pattern. Deviant values are determined by a drop in consumption over a period of 1.5 h on Thursday, 17 April 2014, in the middle of the day. The power graph does not depend on the day of the week
	1	Period – half a day, the maximum matches the morning peak	1	Formation of daily consumption pattern	
	2		1		
	3	Period – one day for both components. Strong mutual *W*-correlation	1		
	4		1		
	5	–	2	The formation of a harmonic component with a frequency of 3.5 times per day is characteristic	
	6	–	2		
8	0	Trend	0	–	Minimum consumption in the evening period, reaching its first peak at midnight. A decrease in consumption is observed at midday
	1	Period – one day, the maximum matches with the morning period	1	Formation of daily consumption pattern	
	2		1		
	3	Period – half a day, the maximum matches at noon and midnight	1		
	4		1		
	5	–	2	Formation of a harmonic component with a frequency of three times per day	
	6	–	2		
7	0	Trend	0	–	Formation of a pronounced daily pattern with recurring sections during the daytime on weekdays, which were separated into a separate pair of components 7 and 8
	1	Period – half a day, the maximums match the consumption peaks	1	Formation of daily consumption pattern	
	2		1		
	3	Period – one day, the maximum matches the daily peak load	1		
	4		1		
	5	Period – 1/3 of the day, the maximum matches midnight	1		
	6		1		
	7	Period – 1/5 of the day, the maximum matches with 11 p.m.	2	The amplitude varies depending on the day. On weekends, the amplitude decreases to 0	
	8		2		
	9	Period – 1/4 of the day, the minimum matches midnight	3	The amplitude and frequency vary slightly within narrow limits depending on the day of the week	
	10		3		

Table 2 continued

Feeder	Component	Characteristic	Group	Description	Note
6	0	Trend	0	–	Formation of an electricity consumption curve that remains virtually unchanged over time. There is no visible daily pattern. On weekdays, consumption ranges from 800 to 1000 kW. On weekends, the values exceed these limits
	1		0	–	
	2	Period – half a day, the maximum occurs at noon and midnight	1	Contrary to expectations, the group does not form a daily pattern. The frequency and amplitude of the group varies widely	
	3		1		
	4	The component correlates weakly with the trend	0	–	
	5	Period – 1/4 of the day, the maximum matches midday	2	The component group generates oscillations with an amplitude of less than 3 % of the base signal with a stable frequency and an amplitude that varies within wide limits	
	6		2		
	7		2		
	8		2		
	9	Period – more than 1/7 of the day, the minimum matches midnight	3	The component group forms the high-frequency harmonic component of the signal	
	10		3		
5	0	Trend	0	–	Formation of a daily pattern. Consumption depends on the day of the week: on weekends, the daily pattern disappears. The increase in energy consumption is concentrated in the daytime and evening hours. There is a characteristic drop in energy consumption between 1 and 2 p.m. The amplitude of all components and component groups considered falls to zero on weekends
	1	Period – one day, the maximum matches the daily peak consumption	1	The component group forms a daily energy consumption pattern. It can be used to classify the type of load as a component group, purified from noise	
	2		1		
	3	Period – half a day, the maximum matches at noon and midnight	1		
	4		1		
	5	Period – 1/4 of the day, the minimum matches midnight	2	The component group changes its amplitude insignificantly. The minimums coincide with consumption dips between 1 and 2 p.m.	
	6		2		
	7		2		
	8	Period – 1/10 of the day, high-frequency component	3	The component group forms the high-frequency harmonic component of the signal	
	9		3		
4	0	Trend	0	–	The time series is characterised by pronounced periodicity throughout the day with a slight deviation from the average daily energy consumption. A decrease in energy consumption is observed on Sundays
	1	Period – half a day, the maximum matches the morning and evening peaks	1	The component group forms the daily energy consumption pattern	
	2		1		
	4	Period – 1/3 of the day, the minimum matches midnight	1		
	5		1		
	7	Period – 1/5 of the day, the minimum matches midnight	2	The component group generates oscillations with low amplitude and medium frequency	
	8		2		
2	0	Trend	0	–	The time series is characterised by an implicit periodicity throughout the day with a slight deviation from the average daily energy consumption. There is a deviation from the average over a seven-hour period in the middle of the week
	1	Period – half a day, the maximum matches at noon and midnight	1	The component group forms the daily energy consumption pattern	
	2		1		
	3		1		
	4		1		
	5	Period – 1/3 of the day, the maximum matches midnight	2	The components have a stable frequency regardless of data differences. The amplitude increases when significant deviations occur	
	6		2		

End of Table 2

Feeder	Component	Characteristic	Group	Description	Note
1	0	Trend	0	–	The time series is characterised by pronounced periodicity with a slight deviation from average daily energy consumption. A decrease in energy consumption is observed at the end of the week over the course of one day
	1	Period – half a day, the maximum occurs two hours before noon and midnight	1	The component group forms the daily energy consumption pattern	
	2		1		
	4	Period – 1/3 of the day, the maximum matches midnight	1		
	5		1		
	7	Period – 1/5 of the day, the peak occurs two hours before midnight	2	The group of components has a variable amplitude. The frequency remains constant throughout the interval under consideration. The amplitude is minimal on the second day	
	8		2		

The research yielded the following findings:

• When using the SVD method for analyzing the time series of power consumption for a substation feeder, the resulting components of the original signal exhibit, to a first approximation, stable frequency and amplitude.

• The zeroth decomposition component always represents the trend and typically accounts for more than 70 % of the original signal, according to the metric of the components' relative contribution to the original signal.

• Grouping components using the *W*-correlation matrix, based on the intensity of correlation, leads to the formation of weekly, daily, daytime, and higher-frequency patterns, which are unique for each feeder.

• The formation of a pattern requires only the first three to four pairs of components; the inverse matrix transformation and reconstruction of the component into a time series should be performed only for the first 30 components.

• To enhance the informativeness of the graphs when examining components plotted on the amplitude-frequency plane, an exponential scale for the *OY* axis should be used.

• Analysis of Fig.7 and similar figures with different time intervals revealed that the components cluster in regions of characteristic frequencies. This indirectly indicates a similarity at the component level among consumer groups of the considered feeders. This information can be utilized in various scenarios: from consumption forecasting to generating control actions for electricity demand management algorithms.

Conclusion

The application of the research results is relevant for the automated typification of load profiles, wherein the specific application can vary depending on the conditions and initial data. The results can be applied to tasks related to integrating economic incentives into the retail market, assessing a consumer's suitability and potential from the perspective of electricity demand management, and automating the process of locating unauthorized electricity access. The method will demonstrate changes in the component composition of the time series and the emergence of changes in the load profile. In this context, for more effective application of this method, it is advisable to develop a system incorporating a classifier based on an artificial neural network [35] for use in various applications.

The creation of a “consumption fingerprint” or “typical consumption profile” is also necessary for solving tasks associated with integrating economic incentives into demand management. Information about the consumption profile should be used to formulate individual requests for managing a group of loads with interdependent and/or common consumption patterns, thereby forming a management strategy based on motivation [36] for active participation in the electricity demand management process.

Using the results of component grouping for a single feeder allows for assessing a consumer's suitability and potential from the perspective of electricity demand management. Furthermore, implementing the results of component clustering on the amplitude-frequency plane is possible in applications addressing feeder similarity in dynamics. i.e., not an overall similarity of graph shapes, but their similarity at the component level, for instance, an almost complete match of consumption graphs on specific days of the week.

Additionally, the SVD method can be applied to the task of analyzing generation trends from stochastic energy sources. such as wind or solar power plants. No adaptation of the method is required; as described in [37], for forecasting renewable energy generation, it is necessary to extract periodic components from the overall set of components using the *W*-correlation matrix as an indicator for selecting periodic components.

The proposed algorithms will enable the use of the obtained typical electricity consumption profiles for calculating quasi-dynamic electrical regimes when solving tasks related to the prospective development of electrotechnical complexes and selecting rational methods of energy supply and improving the energy efficiency of mining enterprises [38].

REFERENCES

1. Nikolaev A.V., Vöth S., Kychkin A.V. Application of the cybernetic approach to price-dependent demand response for underground mining enterprise electricity consumption. *Journal of Mining Institute.* 2023. Vol. 261, p. 403-414. DOI: 10.31897/PMI.2022.33

2. Rylnikova M.V., Klebanov D.A., Makeev M.A., Kadochnikov M.V. Application of artificial intelligence and the future of big data analytics in the mining industry. *Russian Mining Industry.* 2022. N 3, p. 89-92 (in Russian). DOI: 10.30686/1609-9192-2022-3-89-92

3. Skamyin A.N., Dobush V.S., Jopri M.H. Determination of the grid impedance in power consumption modes with harmonics. *Journal of Mining Institute.* 2023. Vol. 261, p. 443-454. DOI: 10.31897/PMI.2023.25

4. Shklyarskiy Ya., Skvortsov I., Sutikno T., Manap M. The optimization technique for a hybrid renewable energy system based on solar-hydrogen generation. *International Journal of Power Electronics and Drive Systems*. 2024. Vol. 15. N 1, p. 639-650. DOI: 10.11591/ijpeds.v15.i1.pp639-650

5. Shklyarskiy Ya., Andreeva Iu., Sutikno T., Jopri M.H. Energy management in hybrid complexes based on wind generation and hydrogen storage. *Bulletin of Electrical Engineering and Informatics*. 2024. Vol. 13. N 3, p. 1483-1494. DOI: 10.11591/eei.v13i3.6757

6. Beloglazov I., Plaschinsky V. Development MPC for the Grinding Process in SAG Mills Using DEM Investigations on Liner Wear. *Materials.* 2024. Vol. 17. Iss. 4. N 795. DOI: 10.3390/ma17040795

7. Sychev Yu.A., Aladin M.E., Aleksandrovich S.V. Developing a hybrid filter structure and a control algorithm for hybrid power supply. *International Journal of Power Electronics and Drive Systems*. 2022. Vol. 13. N 3, p. 1625-1634. DOI: 10.11591/ijpeds.v13.i3.pp1625-1634

8. Serikov V.A., Kostin V.N., Sychev Yu.A., Haidar S. Evaluation method of power quality in mine supply systems with high-powered high-voltage variable frequency drives. *Mining Informational and Analytical Bulletin.* 2024. N 12, p. 162-177 (in Russian). DOI: 10.25018/0236_1493_2024_12_0_162

9. Zhukovskiy Yu.L., Suslikov P.K. Assessment of the potential effect of applying demand management technology at mining enterprises. *Sustainable Development of Mountain Territories.* 2024. Vol. 16. N 3 (61), p. 895-908 (in Russian). DOI: 10.21177/1998-4502-2024-16-3-895-908

10. Xiang Jing, Wenping Qin, Hongmin Yao et al. Resilience-oriented planning strategy for the cyber-physical ADN under malicious attacks. *Applied Energy*. 2024. Vol. 353. Part 4. N 122052. DOI: 10.1016/j.apenergy.2023.122052

11. Zarate-Perez E., Rosales-Asensio E., González-Martínez A. et al. Battery energy storage performance in microgrids: A scientific mapping perspective. *Energy Reports*. 2022. Vol. 8. Suppl. 9, p. 259-268. DOI: 10.1016/j.egyr.2022.06.116

12. Fedorova E., Morgunov V., Lobko K., Pupysheva E. Review: Axial Motion of Material in Rotary Kilns. *Eng.* 2025. Vol. 6. Iss. 6. N 106. DOI: 10.3390/eng6060106

13. Beloglazov I. Review of Advanced Digital Technologies. Modeling and Control Applied in Various Processes. *Symmetry*. 2024. Vol. 16. Iss. 5. N 536. DOI: 10.3390/sym16050536

14. Koteleva N.I., Valnev V.V., Korolev N.A. Augmented reality as a means of metallurgical equipment servicing. *Tsvetnye metally*. 2023. N 4, p. 14-23 (in Russian). DOI: 10.17580/tsm.2023.04.02

15. Skamyin A., Shklyarskiy Ya., Lobko K. et al. Impedance analysis of squirrel-cage induction motor at high harmonics condition. *Indonesian Journal of Electrical Engineering and Computer Science*. 2024. Vol. 33. N 1, p. 31-41. DOI: 10.11591/ijeecs.v33.i1.pp31-41

16. Kvasnikov V.P., Stakhova A.P. Spectral analysis of vibration signal using Fourier transform. *Collection of scientific works of the Odesa State Academy of Technical Regulation and Quality.* 2022. N 2 (21), p. 28-33 (in Ukrainian). DOI: 10.32684/2412-5288-2022-2-21-28-33

17. Yingguan Lu. Applications of Fourier transforms in engineering. *Theoretical and Natural Science*. 2024. Vol. 43, p. 26-32. DOI: 10.54254/2753-8818/43/20241142

18. Zihui Yin, Rongwen Guo, Hang Chen. Multi-station Magnetotelluric Data Processing Based on Singular Value Decomposition. *Journal of Physics: Conference Series*. 2023. Vol. 2651. N 012067. DOI: 10.1088/1742-6596/2651/1/012067

19. Zhukovskiy Y., Buldysko A., Revin I. Induction Motor Bearing Fault Diagnosis Based on Singular Value Decomposition of the Stator Current. *Energies.* 2023. Vol. 16. Iss. 8. N 3303. DOI: 10.3390/en16083303

20. Javadnejad F., Sharifi M.R., Basiri M.H., Ostadi B. Optimization Model for Maintenance Planning of Loading Equipment in Open Pit Mines. *European Journal of Engineering and Technology Research*. 2022. Vol. 7. Iss. 5, p. 94-101. DOI: 10.24018/ejeng.2022.7.5.2907

21. Zeyang Zhou, Mingzhu Zhang, Jie Tian, Jingwen Huang. Experimental study on classification and identification method for fault signals of mining steel wire ropes. *Journal of Physics: Conference Series*. 2024. Vol. 2798. N 012043. DOI: 10.1088/1742-6596/2798/1/012043

22. MingAng Guo, Xiaotong Tu, Abbas S. et al. Time-frequency analysis-based impulse feature extraction method for quantitative evaluation of milling tool wear. *Structural Health Monitoring*. 2024. Vol. 23. Iss. 3, p. 1766-1778. DOI: 10.1177/14759217231192003

23. Ninawe S., Deshmukh R. Efficient vibration analysis system using empirical mode decomposition residual signal and multi-axis data. *Journal of Vibration and Control*. 2025. Vol. 31. Iss. 15-16, p. 2993-3006. DOI: 10.1177/10775463241262117

24. Guolong Fu, Jintian Yin, Shengyi Wu et al. Composite Fault Signal Detection Method of Electromechanical Equipment Based on Empirical Mode Decomposition. Advanced Hybrid Information Processing: 6th EAI International Conference. 29-30 September 2022. Changsha. China. Springer. 2023. Part 2, p. 1-13. DOI: 10.1007/978-3-031-28867-8_1

25. Kharchenko K.V., Zubets A.Zh., Moskvitina E.I. et al. Analyzing the efficiency of implementing predictive maintenance of mining equipment based on Industry 4.0 technologies. *Russian Mining Industry*. 2024. N 4, p. 130-138 (in Russian). DOI: 10.30686/1609-9192-2024-4-130-138

26. Zexian Sun, Mingyu Zhao, Guohong Zhao. Hybrid model based on VMD decomposition. clustering analysis. long short memory network, ensemble learning and error complementation for short-term wind speed forecasting assisted by Flink platform. *Energy*. 2022. Vol. 261. Part B. N 125248. DOI: 10.1016/j.energy.2022.125248

27. Khalkhali Shandiz S., Khezrzadeh H. Application of moving vehicle response and variational mode decomposition (VMD) for indirect damage detection in bridges. *Modares Civil Engineering journal*. 2021. Vol. 21. Iss. 1, p. 31-46.

28. Ahmad Zaki Maulana, Subekti Subekti, Nur Indah. Detecting damage on engine mounts using hilbert-huang transform vibration analysis. *JTTM: Jurnal Terapan Teknik Mesin*. 2024. Vol. 5. N 2, p. 235-240. DOI: 10.37373/jttm.v5i2.1108

29. Prasshanth C.V., Venkatesh S.N., Mahanta T.K. et al. Deep learning for fault diagnosis of monoblock centrifugal pumps: a Hilbert–Huang transform approach. *International Journal of System Assurance Engineering and Management*. 2024. DOI: 10.1007/s13198-024-02447-z

30. Ziyu Guo. Robot terrain classification based on improved Hilbert-Huang transform and long short-term memory network. *Applied and Computational Engineering*. 2024. Vol. 95, p. 49-56. DOI: 10.54254/2755-2721/95/2024BJ0060

31. Hong Lu, Wei Zhang, Zhimin Chen et al. Rotating machinery early fault detection integrating variational mode decomposition and multiscale singular value decomposition. *Measurement Science and Technology*. 2024. Vol. 35. N 12. N 126128. DOI: 10.1088/1361-6501/ad7a1f

32. Khan M.U., Hasan M.A.H. Hybrid EEG-fNIRS BCI Fusion Using Multi-Resolution Singular Value Decomposition (MSVD). *Frontiers in Human Neuroscience*. 2020. Vol. 14. N 599802. DOI: 10.3389/fnhum.2020.599802

33. Golyandina N. Particularities and commonalities of singular spectrum analysis as a method of time series analysis and signal processing. *WIREs Computational Statistics*. 2020. Vol. 12. Iss. 4. N e1487. DOI: 10.1002/wics.1487

34. Suslikov P., Zhukovskiy Yu. Determination of hidden dependencies of multiple time series of electricity consumption for the purpose of classification and management of load profiles. Elektroenergetika glazami molodezhi – 2024: Materialy XIV Mezhdunarodnoi nauchno-tekhnicheskoi konferentsii, 1-4 oktyabrya 2024, Stavropol, Rossiya. V 2 tomakh. T. 2. Stavropol: Severo-Kavkazskii federalnyi universitet, 2024, p. 127-130 (in Russian).

35. Ustinov D.A., Aysar Abou Rashid. Using Artificial Neural Network Methods to Increase the Sensitivity of Distance Protection. *International Journal of Engineering – Transactions B: Applications*. 2024. Vol. 37. Iss. 11, p. 2192-2199. DOI: 10.5829/IJE.2024.37.11B.06

36. Shushpanov I., Suslov K., Ilyushin P., Sidorov D.N. Towards the Flexible Distribution Networks Design Using the Reliability Performance Metric. *Energies*. 2021. Vol. 14. Iss. 19. N 6193. DOI: 10.3390/en14196193

37. Kavakci G., Cicekdag B., Ertekin S. Time Series Prediction of Solar Power Generation Using Trend Decomposition. *Energy Technology*. 2024. Vol. 12. Iss. 2. N 2300914. DOI: 10.1002/ente.202300914

38. Ilyushin P., Papkov B., Kulikov A., Suslov K. Algorithm and Methods for Analyzing Power Consumption Behavior of Industrial Enterprises Considering Process Characteristics. *Algorithms*. 2025. Vol. 18. Iss. 1. N 49. DOI: 10.3390/a18010049

***Authors*: Yuriy L. Zhukovskiy,** *Doctor of Engineering Sciences, Head of Department* (*Empress Catherine II Saint Petersburg Mining University, Saint Petersburg, Russia*), *Zhukovskiy_Yul@pers.spmi.ru, https://orcid.org/0000-0003-0312-0019*, **Pavel K. Suslikov,** *Postgraduate Student* (*Empress Catherine II Saint Petersburg Mining University, Saint Petersburg, Russia*), *https://orcid.org/0000-0002-0607-660X*.

The authors declare no conflict of interests.

ISSN 2411-3336; e-ISSN 2541-9404

JOURNAL OF MINING INSTITUTE

Zapiski Gornogo instituta

Journal homepage: pmi.spmi.ru

Research article

Geotechnical Engineering and Engineering Geology

Development and integration of an underground mining enterprise ventilation process simulations into the demand response

Aleksandr V. Nikolaev[1]✉, **Aleksei V. Kychkin**[2]

[1] *Perm National Research Polytechnic University, Perm, Russia*

[2] *National Research University Higher School of Economics – Perm, Perm, Russia*

***How to cite this article*:** Nikolaev A.V., Kychkin A.V. Development and integration of an underground mining enterprise ventilation process simulations into the demand response. Journal of Mining Institute. 2025. Vol. 275, p. 18-29.

Abstract

Controlling the ventilation in underground mining enterprises (UME), characterized by high inertia and numerous influencing external factors, based on real-time sensor data located in mine workings and on the surface, with a high level of accuracy in regulating air supply by the main ventilation unit (MVU), is feasible only under conditions of a pre-defined sequence of control actions. This task can be classified as an approximate dynamic programming (ADP) problem, which involves synthesizing a suboptimal control function for MVU operation in a predictive modeling mode of air distribution, given a known space of possible states and the selection of the optimal control strategy that meets a specified criterion. A simulation model of a digital twin subsystem for ventilation process control is presented, using the example of two types of UME (potash mines and oil shafts), which can be used to solve ADP tasks. For predictive modeling of air distribution and determining the energy efficiency criterion of the MVU, which consumes up to half of the total electricity of the UME, the digital twin is integrated with external data, based on which energy consumption is evaluated while maintaining the required volume of supplied air. This control approach enables not only safe and energy-efficient management of the ventilation process but also participation in the planning and implementation of measures for price-dependent electricity demand management.

Keywords

electricity demand management; cybernetic approach; Internet of Things platform; underground mining enterprise; short-term load forecasting; digital twin

Funding

The research was funded by the Ministry of Science and Higher Education of the Russian Federation (Project N FSNM-2024-0005).

Received: 09.08.2024 ***Accepted: 02.07.2025*** ***Online: 24.09.2025*** ***Published: 31.10.2025***

Introduction

The mining industry is among the most energy-intensive sectors in Russia [1, 2] and abroad [3, 4], with the energy component accounting for 37-40 % of the production cost of finished products [5], which has a detrimental impact on the economy given the persistent trend of rising energy prices.

However, the methods and devices developed to reduce electricity consumption often do not allow for simultaneous efficient and safe management of underground mining enterprises (UME) [6, 7], necessitating the development of the company's energy policy. In addition to the complexity of implementing energy-saving programs at hazardous production facilities, there is the challenge of aligning generation and consumption patterns [8, 9]. This is because most power plants in industrial areas produce electricity continuously throughout the day, while energy consumption exhibits a pronounced cyclic pattern tied to a 24-hour time interval, i.e., there are

periods of high and low electricity demand within a day [10, 11]. One solution to this second issue is price-dependent electricity demand management (Demand Response – DR) – a change in electricity consumption by end users relative to their normal profile in response to time-varying electricity prices or incentive payments provided for reducing energy consumption during peak demand hours.

The actual state of power grids in industrial regions, combined with the operating modes of energy consumers, weather conditions, and other factors, largely determines the imbalanced values of electricity generation and consumption indicators. The simultaneous activation of various equipment units throughout the day creates instantaneous energy demand, leading to a sharp increase in grid load and, consequently, a reduction in reliability. The practice of deploying and maintaining reserve grid capacities can address issues of high demand, including in energy-deficient regions, but it results in significant increases in capital expenditures and the cost of electricity transmission services.

The complexity of load balancing, including for overloaded substations, unpredictable consumption volumes, the inability to store electricity locally on an industrial scale, the need for more accurate forecasting (predictive analytics) and dynamic electricity distribution during peak load hours (preventive analytics), as well as the economically viable interpretation of modern energy market conditions, drive the demand for electricity demand management worldwide [12, 13] and in Russia [14-16]. To reduce financial costs in underground mining, it is necessary to develop mechanisms that not only reduce electricity consumption without compromising production safety but also do so at specific times to enable the enterprise to participate in DR.

Considering that the primary electricity consumption in UME is associated with ventilation (up to half [17-19], and according to some sources, up to 70 % [20]), the search for solutions in the areas of DR and energy conservation was focused on this domain. An essential condition was ensuring safety, as the critical ventilation process directly impacts it.

Despite the differences among enterprises based on the type of extracted raw material and mining methods, depending on the depth of the deposit, ventilation methods, the number of mine shafts, etc., a general action plan for process management can be developed, taking into account the most significant factors. This study examines two types of UME: potash mines (using the example of the Verkhnekamskoye deposit of potassium-magnesium salts – VKMKS) and oil shafts (Yaregskoye deposit).

Construction of the digital twin simulation subsystem for the ventilation control

In recent years, digital technologies have been increasingly applied across all spheres of human activity, including the mining industry. In the mining sector, an example is the creation of digital twins (DT), i.e., virtual replicas of physical systems that enable monitoring, modeling, and managing the behavior of the simulated system in real time. This solution allows mining companies to optimize equipment performance and reduce downtime [21-23]. It is expected that the use of digital twins in Industry 4.0 and the Internet of Things (IoT) will grow in the coming years as more companies adopt this technology [24].

Implementing a digital twin requires a high level of integration of data and information from various sources and systems. A digital twin is typically created by integrating multiple technologies, including sensors, data analysis tools, and modeling tools. In the context of cyber-physical systems (CPS), a digital twin comprises several subsystems, with the simulation subsystem being one of the key components, used to model the behavior of the physical system and its interaction with the environment [25]. Developing the simulation subsystem of a digital twin requires a structure that accounts for the physical and cyber components of the system, as well as the interaction between these components. This structure may include co-simulation, where the digital twin and the physical system are

modeled together, as well as hardware-in-the-loop testing, where the digital twin is integrated with physical equipment to simulate real-world scenarios.

The ventilation process, which is the most energy-intensive, in potash mines and oil shafts is carried out using the main ventilation unit (MVU). Unjustified changes to energy consumption, and thus the operating mode of the MVU, are prohibited, as it supplies the underground mining enterprise with the air necessary for the survival of miners and the safety of mining operations. Changes to the MVU's operating modes must be carried out based on a written order from the technical manager of the UME*. Therefore, to utilize this resource for reducing energy consumption and participating in DR, it is necessary to provide justified recommendations for such actions.

The study [6] established that the most significant factor affecting the operation of the main ventilation unit (MVU) is the mine-wide natural draft – a phenomenon resulting from the difference in air densities in interconnected mine shafts [26, 27]. The primary parameter influencing the magnitude of the natural draft is the temperature of the outside air, as well as the air supplied to and exiting from the mine shafts [28]. The mine-wide natural draft can be negative, i.e., hindering ventilation, or positive, facilitating air supply and, consequently, the operation of the MVU [29, 30]. Based on this, it follows that when a positive natural draft is present, it becomes possible to reduce the MVU's output while still ensuring the supply of the required volume of air to the mine shafts [6, 31].

Previously derived mathematical relationships allow for determining the magnitude and direction of the mine-wide natural draft with a specified confidence probability, based on the parameters of the outside air, as well as the air supplied to and exiting from the mine shafts [32]. By knowing the technical characteristics of the underground mining enterprise, the parameters of the main ventilation unit, and the parameters of the outside air during the regulation of the ventilation process, it is possible to predetermine the magnitude and direction of the mine-wide natural draft and forecast the required operating mode of the MVU. In this case, changes to the MVU's operating mode are made based on changes in the outside air parameters, rather than relying on air flow sensor readings. The ventilation process is inertial, and after adjusting the MVU's output, air distribution between the mine shafts occurs only after a certain time interval, which for the considered potash mines and oil shafts is up to 6-7 min. Therefore, managing ventilation solely based on sensor readings, without accounting for the process's inertia, is not feasible.

To predict air distribution between mine shafts and select the required operating mode of the main ventilation unit in real time based on the provided simplified ventilation scheme (Fig.1), a simulation subsystem of a digital twin (simplified model) for ventilation control was developed in OpenModelica using the example of the BKPRU-4 mine (Uralkali PJSC) (Fig.2).

The presented graphical scheme of the ventilation control process for the digital twin simulation subsystem in OpenModelica includes components described in the Table. Each element is a software object from the Fluid library, which contains components for modeling air, liquid, and steam flows. Each software object implements specific physical behavior and has interfaces for interacting with other objects to receive and transmit computed values. The objects are described by corresponding differential equations, interconnected to form a system of 8170 equations, solved by the OpenModelica environment during the simulation of the ventilation process.

The Table provides information about the Pipe element of the Modelica.Fluid.Pipes.DynamicPipe software class, interpreted as a mine working. The parameters of this component correlate with the example of the BKPRU-4 mine scheme as follows: if the elevation parameters of the initial and final points are specified, the working is interpreted as horizontal if the values are the same, vertical if the values differ by the length of the section, and inclined in other cases. The cross-section of the mine working is assumed as circular, but an equivalent diameter is used, calculated according to the methodology [33].

* Order of Rostekhnadzor N 505 dated 8 December 2020 “On the Approval of Federal Standards and Rules in the Field of Industrial Safety “Safety Rules for Mining Operations and Processing of Solid Minerals”.

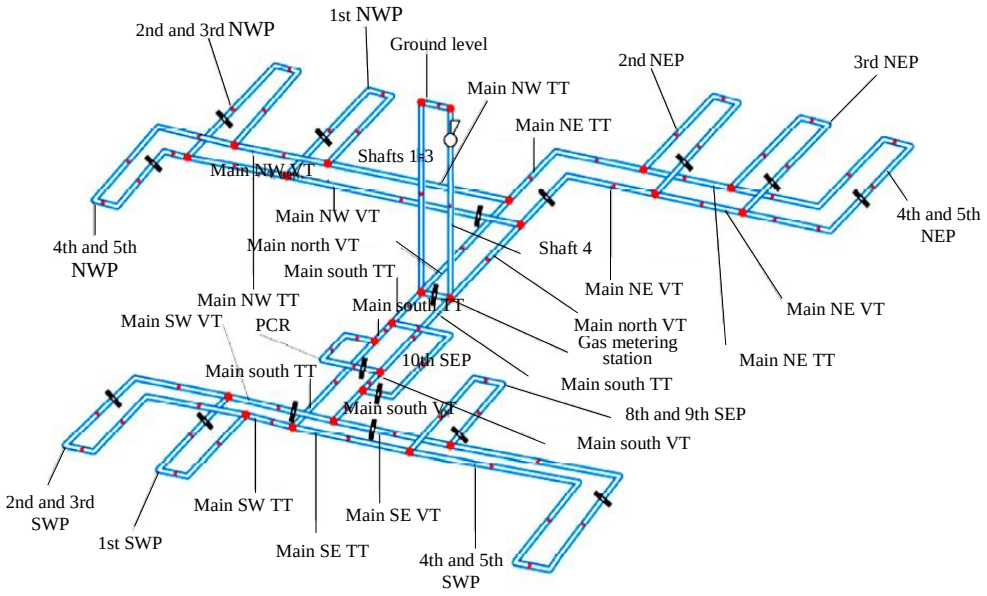

Fig.1. Simplified ventilation scheme of the BKPRU-4 mine

TT – transport tunnel; VT – ventilation tunnel; NWP – north-west panel; NEP – north-east panel; SEP – south-east panel; SWP – south-west panel

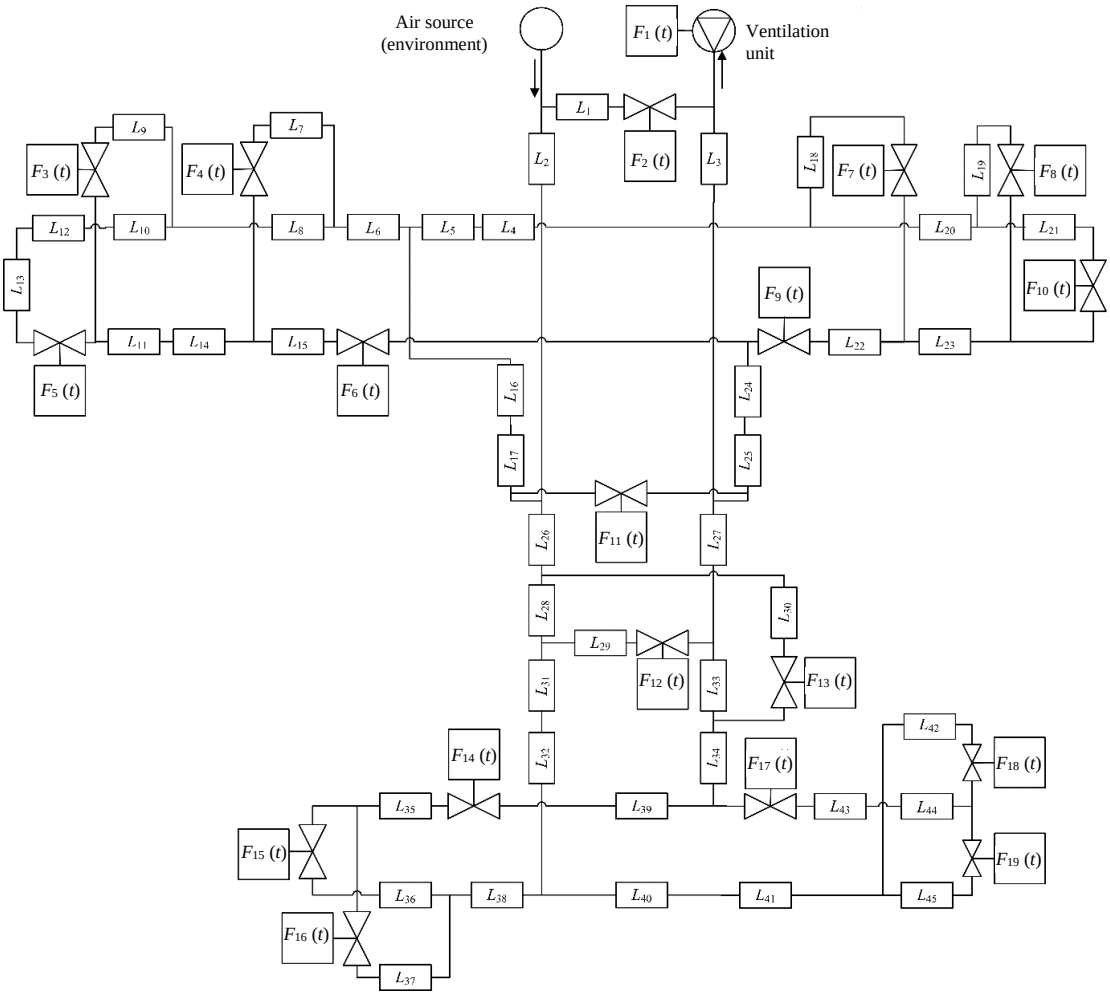

Fig.2. Ventilation control model of a digital twin simulation subsystem

Technical description of the components of the digital twin simulation subsystem

Block type	Notation		Description
	Fig.2	OpenModelica	
FixedBoundary	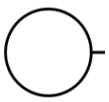	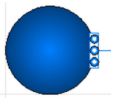	An air source with a specified temperature, pressure, density, specific enthalpy, and composition of gases in the form of impurities described by mass fractions
Pipe	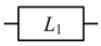	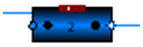	A straight section of a mine workings with a specified length, cross-sectional area, wall unevenness, and the heights of the starting and ending points relative to the uniform horizontal level established for the entire mine
MassFlowSource_T	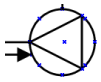	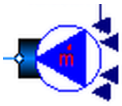	MVU fan simulating air supply with a specified mass flow rate per unit time, specified temperature, and impurity composition
ValveLinear (valve with linear control)	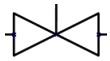	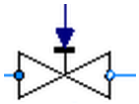	Valves that simulate various types of isolating devices, such as jumpers and ventilation doors, with a specified nominal mass air flow rate when fully open and a pressure drop when fully open
Step (step control function)	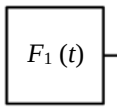	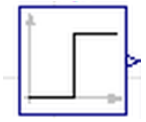	Control element for valves with a set signal level and its time offset *t* relative to the start of ventilation simulation

During the research, the results of the digital twin simulation subsystem were confirmed to be consistent with previously obtained experimental calculations [31].

To automatically "load" data on outdoor air parameters, a software was developed to connect to the digital twin simulation subsystem via its digital interface [34]. Examples of connections to the weather service, the block for reading and transferring data from .csv files, and the block for reading and writing data to the time series database have been developed. The software is launched by the user via the console and reads data on the outside air temperature from the weather service, data on the temperature at several points in the mine workings from files, fills in the gaps in the data, converts formats and exports the result to a measurement table in the database. In this case, it becomes possible to predict the value of the overall natural draft depending on the hydrometeorological forecast.

The simulation subsystem of the digital twin of the ventilation control process allows, based on the forecast values of outdoor air parameters using mathematical dependencies, to determine with high accuracy the value of the overall natural draft, which in this case will act between the mine shafts. This will allow the selection of the required mode of operation of the ventilation system, taking into account the inertia of the ventilation process, in which the required volume of air will be supplied to the mine air supply shafts. Also, when negative natural draft acts on the entire mine, there will be no unjustified increase in the air supply system's performance, but only compensation for its effect on the ventilation process. When positive natural draft acts on the entire mine, a decrease in performance is possible, and therefore, a decrease in the air supply system's energy consumption.

The second type considered in the UME study is oil mines, in which air is supplied by suction ventilation (similar to the ventilation scheme used in potash mines) – through two air supply shafts due to the vacuum created by the MVU located on the ventilation shaft. However, a sectional ventilation scheme is currently recommended [35, 36], in which, in addition to supplying air to the oil mine through mine shafts, air is supplied separately to each inclined block (production area) through air supply and ventilation wells. Through the air supply well, outside air enters the slope (air supply working), washes the drilling gallery where oil is produced, and is removed through the ventilation well drilled in the passage (air exhaust well) to the surface. With this ventilation scheme, natural

draft will act not only between the mine shafts, but also between the inclined block wells. This makes it even more difficult to control the ventilation process, as it is necessary to take into account the effect of natural draft between each pair of inclined block wells on the operation of the ventilation system.

Using the air distribution between underground mine workings in a digital twin

The simulation subsystem allows determining the air distribution between mine shafts and selecting the MVU operating mode at which the required volume of air will be supplied to the UME. However, it should be noted that due to the constant growth in the volume of minerals extracted, the increase in the number of depleted mining areas and the distance between them and the air supply shafts, the process of supplying all working areas with fresh air is becoming more complicated and, consequently, there is no guarantee that the air will not be distributed throughout the mine workings, resulting in a shortage of air in the mining areas. In this case, the digital twin should consider the processes of air distribution between underground mine workings.

Since potash mines have low aerodynamic resistance [37], even slight temperature differences caused by heated sections of the conveyor belt or other heat sources will affect ventilation stability [33]. In addition, study [38] found that when light gases (mainly methane) are released in mined and mined chambers, additional natural draft occurs between mine workings due to the different specific weights of gas-air mixtures. In this regard, additional adjustments must be made to the digital twin to account for this effect.

In oil mines, air distribution between mining workings is an even more complex process, as there are heat sources in the production areas. Their presence is due to the unique method of extracting high-viscosity oil – thermal mining [39, 40]. When using this method, steam is injected into the oil reservoir, which reduces the viscosity of the oil and increases its fluidity. At the same time, the air temperature in the inclined block to high values – in the drilling gallery (the place where steam is injected into the reservoir) and in the outgoing mine workings. Solutions aimed at reducing the air temperature in the inclined block and outgoing mine workings have no significant effect.

A method for reducing the air temperature in mountain oil mine workings while ensuring resource and energy conservation is described in [41]. A heat-insulating partition is installed in the inclined block in front of the heated oil layer (Fig.3), as a result of which the air supplied through the incline is divided into two streams – one stream passes between the heat-insulating partition and the oil layer (the non-working part of the drilling gallery), and the second enters the drilling gallery on the other side of the partition (the working part of the drilling gallery). In the non-working part of the drilling gallery, the air is heated and then removed to the surface through the ventilation well. The non-working part of the drilling gallery is limited by the heat-insulating partition to the base of the ventilation well. Air that meets the required sanitary standards enters the working part of the drilling gallery, i.e. it is possible to ensure comfortable working conditions in the inclined blocks and the oil shaft as a whole.

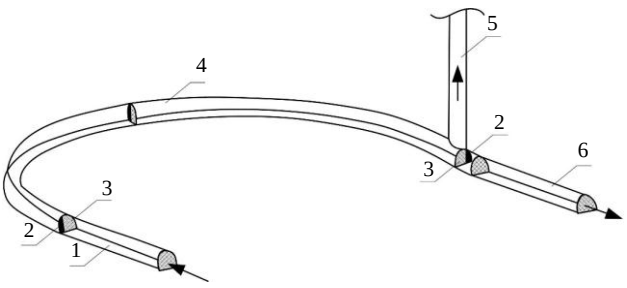

Fig.3. Ventilation of the inclined block of an oil mine using a heat-insulating partition

1 – slope; 2 – non-working part of the drill gallery; 3 – working part of the drill gallery; 4 – drill gallery; 5 – ventilation shaft; 6 – walkway

However, the presence of ventilation holes originating from inclined blocks, through which air of varying volumes and temperatures escapes, makes the ventilation process less stable and significantly complicates control.

When modelling the ventilation process in potash mines and oil wells, it is necessary to consider the release of harmful and hazardous gases in mine workings. For example, to account for methane, an additional FixedBoundary source with a

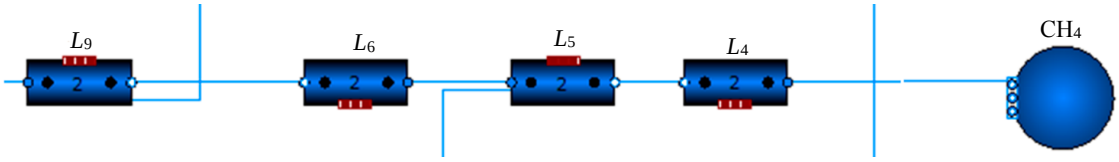

Fig.4. Example of adding a new source of gas-air mixture with excess methane content in OpenModelica

specified air mixture composition describing a high methane content is installed in the simulation subsystem of the digital twin at one of the levels of the mine workings, which is connected to one of the transport workings (Fig.4).

General natural draft can be incorporated into the simulation subsystem at the level of the valve control algorithm in the ventilation shaft (for oil wells – additionally in ventilation wells), as well as in adjacent branches. To simulate the action of general mine natural draft in a positive direction, i.e. when it promotes ventilation, the corresponding time delays and the level of air flow increase on the Step control device for the MVU must be set (see Table). To simulate the effect of natural draft in the mine in a negative direction, i.e. hindering ventilation, the corresponding air flow rate on the Step control device for the ventilation system must be reduced. To simulate a change in the direction of air between mine shafts, time delays for the damper must be set (Fig.5).

The following parameters are specified with the model:

• temperature and atmospheric pressure of the outside air entering the mine shafts;

• location and/or inclination of mine workings, their cross-sectional area and length;

• condition of insulating devices, including those used to simulate the operation of mining machinery;

• MVU capacity, including for simulating unloading during demand management events.

Energy demand management system for underground mining operations

Energy flows and accompanying data between automation objects can be effectively used to regulate equipment operation and reduce load during periods of increased demand [13], but demand management strategies can vary significantly [42]. There are numerous publications by Russian scientists [43-46] describing the theoretical foundations of the functioning of such services and systems, including those based on the regulations of the Decree of the Government of the Russian Federation N 287 of 20 March 2019. It is known that the loads of a wide variety of electricity consumers can participate in demand management, including industrial equipment of mining enterprises,

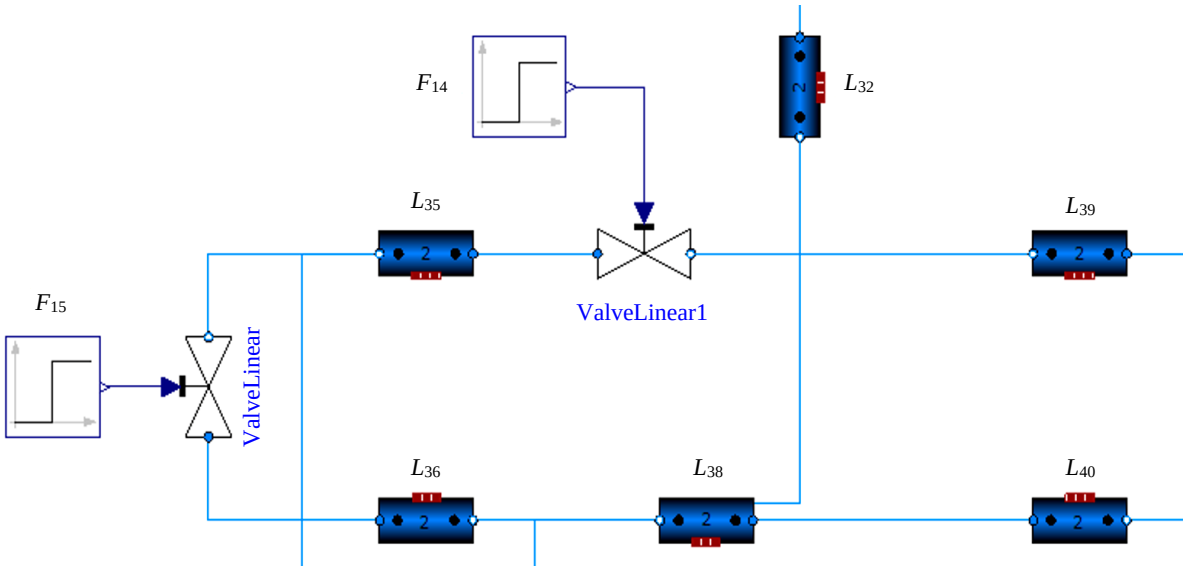

Fig.5. Example of damper control on a ventilation shaft (and ventilation well) to simulate the action of general natural draught in OpenModelica

which can be combined into larger units with dispatch control. Due to the wide variety of current and potentially connectable industrial equipment units and the multitude of factors affecting their operation, avoiding energy consumption during peak demand hours in aggregated groups requires support from control room operators in terms of higher quality planning, which can be achieved through the development and implementation of digital twins.

Managing electricity demand during ventilation involves the following tasks:

• Planning energy consumption for the next day, i.e. planning tasks for the MVU control system. It is necessary to calculate the required amount of electricity per hour for the next day. Deviations from the plan lead to financial penalties. Determining energy consumption mainly depends on the performance of the MVU system, i.e. it is directly related to the volume of air supplied to the UME. Solving this problem using energy consumption forecasting methods allows you to take into account observation statistics, identify patterns and factors affecting the system, determine a planned energy consumption profile for the MVU system that is close to reality, and plan unloading operations taking into account the electricity tariff grid and possible time intervals, considering the effect of natural draft between the UME workings.

• Implementation of the declared energy consumption plan during the day. In real time, it is necessary to monitor the compliance of energy consumption with the declared plan and compensate for any deviations that arise. Deviations from the energy consumption plan may arise in the event of a mismatch between the predicted values of disturbances to the system during planning. For example, a significant error in the weather forecast and, as a result, a change in the value of the overall natural draft or interference caused by the movement of people, transport, and equipment within the UME, which leads to a change in air distribution between mine workings. Solving this problem using a digital twin simulation subsystem allows you to search for the optimal MVU control trajectory in simulation mode to minimize deviations from the declared energy consumption plan.

The optimal control problem is represented as a functional of the form:

$$J\left(x, u^*\right) = \min J\left(x, u\right),\ \ x \in X,\ \ u \in D;$$

$$g_k(x) \geq 0,\ \ k = 1...N;$$

$$J(x, u) = \int_0^T f(t, x, u)dt;$$

$$x'(t) = f\left[t, x(t), u(t)\right];$$

$$x(0) = x_0,$$

where D – control actions set; X – stateset; $g(x)$ – constraints; $J(x, u)$ – control criterion; $x(t)$ – state vector; $u(t)$ – control actions vector.

The constraints $g_k(x) \geq 0$, $k = 1...N$ include requirements for ensuring the necessary air volume flow for each section of the mine and requirements for the concentration level of harmful gases. This problem can be solved using linear programming, which determines the time intervals for unloading and its magnitude.

The results of calculations, daily energy consumption forecasting, and a simulation subsystem of a digital twin ventilation system in the OpenModelica environment were jointly integrated with the InfluxData Internet of Things platform based on the TICK technology stack. Instead of the built-in visualization unit, the external Grafana service was used to clearly display energy consumption values in the form of time series. As part of the integration, standard screen forms were

implemented for UME demand response specialists, including an example of an operator panel for planning unloading and monitoring plan implementation, including the display of graphs, histograms, and average values (Fig.6).

The operator panel displays a widget with a base load graph (GBN), i.e. a calculated daily electricity consumption plan for the next day according to the System Operator's GBN calculation method (Fig.6, *a*). According to the action plan and weather conditions, OpenModelica estimates air distribution considering the effect of general natural draft and determines the permissible reduction value for a given unloading time. Based on the implemented models, the software calculates the cost of electricity for the month ahead for two profile states, namely the profile without power changes ("as is" according to the GBN) and after the change ("as will be" according to the GBN – the permissible power calculated in the digital twin), including a histogram and average values.

During testing, demand management event dates were selected at random in accordance with the accepted rules. After that, the necessary calculations were performed and unloading plans were obtained in accordance with the permissible values for each specific case. Figure 6, *b* also shows the

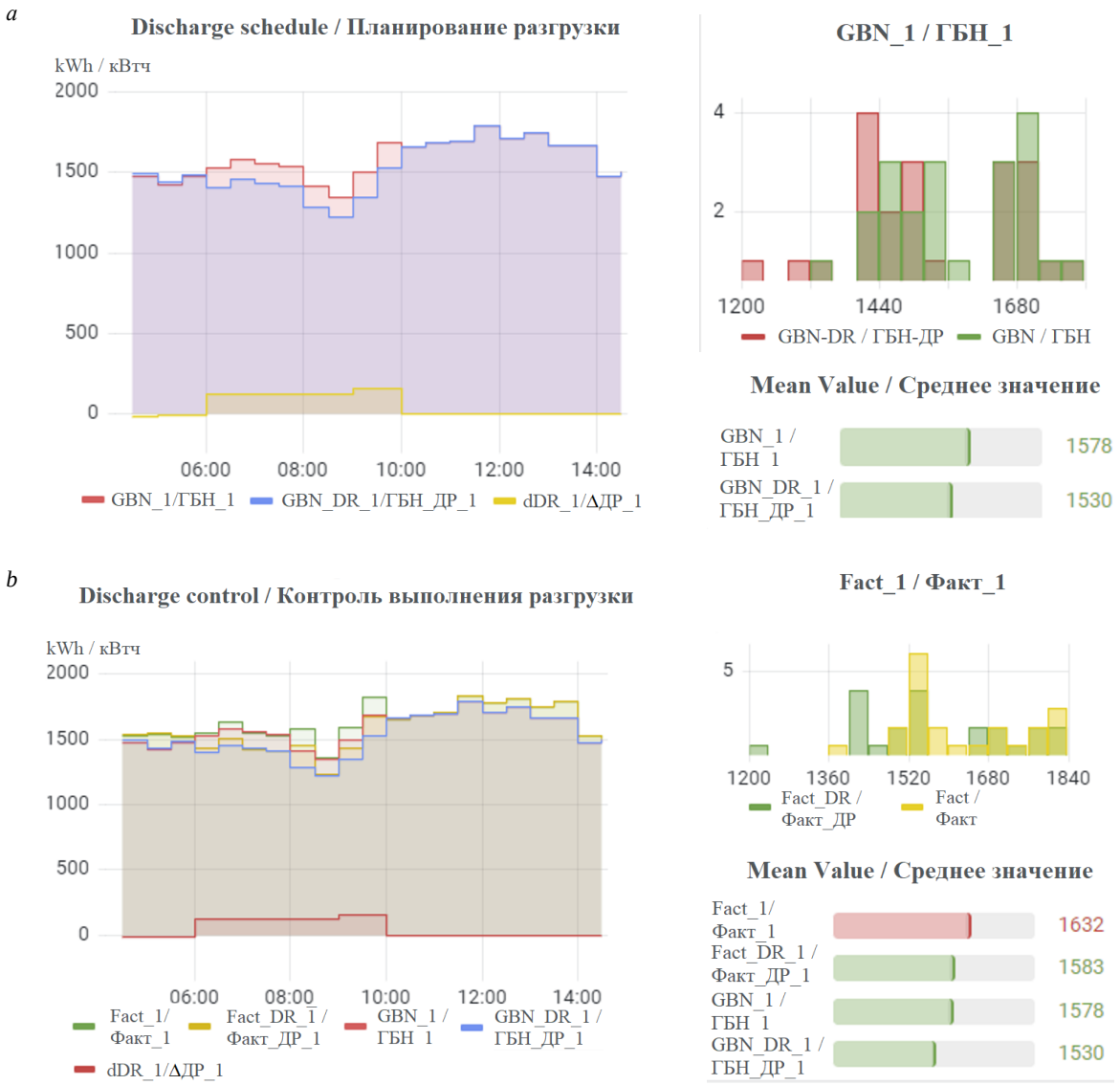

Fig.6. Operator panel to support the process of managing electricity demand during ventilation of the UME based on a digital twin simulation subsystem: *a* – GBN; *b* – difference between GBN and actual values

GBN / ГБН (orange); GBN_DR / ГБН _ДР (blue) – with a marked reduction plan;
Fact / Факт (green) – electricity consumption without demand response events;
Fact_DR / Факт_ДР (yellow) – electricity consumption, taking into account demand response events

difference between the GBN or actual values, as well as the GBN or actual values with unloading, respectively, including a histogram and average values. For example, unloading was simulated for 19 January 2022 from 06:00 to 10:00, including calculations of the base load of the GBN and power reduction in a given interval based on the parameters of the model in OpenModelica, assuming natural draft.The results presented show that during the specified four-hour period, the amount of power reduction that can be declared in advance and then guaranteed to be implemented is 171 kW, while in some hours the reduction potential may be significantly higher, for example 222 kW.

The results of integrating and testing a simulation model as part of the InfluxData energy management platform using external meteorological data are demonstrated, allowing the possibility of reducing the load on the MVU system through natural ventilation to be assessed. Aligning the moments when draft is active with demand management events and controlled reduction of the load on the ventilation system allows maintaining the required level of air distribution, both in the case of a shaft and for a mine under conditions of perfectly accurate weather forecasting. The results of modelling permissible unloading showed a wide range of possibilities for reducing power from 51 to 224 kW at a nominal fan power of 2 MW (~ 11 % of the MVU power).

Conclusion

The solutions described allow natural processes to be used to reduce electricity consumption for the most energy-intensive process – ventilation of the UME. At the same time, air distribution, the operating mode of the MVU system and, consequently, energy consumption can be determined in advance based on hydrometeorological forecast data.

Currently, according to [47], the success rate (accuracy) of hydrometeorological forecasts and warnings about atmospheric phenomena reaches 85-90 %. Consequently, once meteorological data has been obtained, it is possible to calculate the value of the overall natural draft in advance and select the operating mode of the MVU system that will ensure the required ventilation mode.

In this case, it becomes possible not only to reduce the consumption of electricity for the operation of the ventilation system, but also to participate in the planning and implementation of DR. If energy consumption is reduced at a specified time, the mining company will receive financial compensation, thereby reducing the cost of mineral extraction.

Given that seasonal and daily changes in outdoor air parameters are stochastic in nature, when developing an electricity DR system, it is necessary to consider the conditions under which a reduction in electricity consumption will be possible if climatic changes do not allow the ventilation process to be controlled.

Other data can also be exported to the digital twin:

• daily electricity rates – potentially higher electricity consumption at a lower price;

• scheduled equipment shutdowns, inspections and repairs – these activities may be carried out during peak load hours.

The proposed model of electricity demand management using a digital twin simulation subsystem is an important technological solution that can be adapted to solve alternative problems in other industries. In particular, the technology can be used to implement energy consumption management algorithms with Model Predictive Control (MPC) predictive models, one of the modern methods of control theory used mainly in the management of production processes, for example in the chemical industry and oil refining [48]. In this case, the use of the service allows for more effective energy management strategies for technological processes and production facilities, implementing the concept of an intelligent power complex with a smart network (MicroGrid), which is particularly relevant for geographically distributed industrial sites and production facilities based on cyber-physical architectures [49, 50].

A key feature of the implementation of simulation modelling of the ventilation process is an object-oriented approach that allows the formation of model scenarios for related areas of knowledge,

for example, to develop sequences of control commands to minimize environmental impact, to develop a management strategy considering personnel safety requirements, etc. A promising area of research is the introduction of elements of specialized intelligence (NarrowAI) into the energy consumption control loop, which, together with the proposed model, will allow the construction of hybrid forms of artificial intelligence (HybridAI) that use the strengths of machine learning together with the results of calculations based on accurate mathematical models [51].

The solutions developed in the study can be used to generate various energy consumption scenarios to obtain datasets that can be used to train more complex deep learning models for virtual energy managers, as well as, for example, to verify the results of generative artificial intelligence (GenAI), which together can be used to support decision-making on improving energy efficiency [52].

REFERENCES

1. Nevskaya M.A., Raikhlin S.M., Chanysheva A.F. Assessment of Energy Efficiency Projects at Russian Mining Enterprises within the Framework of Sustainable Development. *Sustainability*. 2024. Vol. 16. Iss. 17. N 7478. DOI: 10.3390/su16177478
2. Dmitrieva D., Solovyova V. Russian Arctic Mineral Resources Sustainable Development in the Context of Energy Transition, ESG Agenda and Geopolitical Tensions. *Energies*. 2023. Vol. 16. Iss. 13. N 5145. DOI: 10.3390/en16135145
3. Aramendia E., Brockway P.E., Taylor P.G., Norman J. Global energy consumption of the mineral mining industry: Exploring the historical perspective and future pathways to 2060. *Global Environmental Change*. 2023. Vol. 83. N 102745. DOI: 10.1016/j.gloenvcha.2023.102745
4. Liu Xiaomeng, Meng Xiangrui. Evaluation and empirical research on the energy efficiency of 20 mining cities in Eastern and Central China. *International Journal of Mining Science and Technology*. 2018. Vol. 28. Iss. 3, p. 525-531. DOI: 10.1016/j.ijmst.2018.01.002
5. Knyazkin E.A. Justification of parameters for energy-efficient drainage schemes for underground mines using hydropower: Avtoref. dis. … kand. tekhn. nauk. Moscow: Institut problem kompleksnogo osvoeniya nedr im. akademika N.V.Melnikova, 2021, p. 18.
6. Nikolaev A.V., Lyalkina G.B., Kychkin A.V., Vöth S. Season-oriented mine ventilation modes analysis. *Eurasian Mining*. 2021. Vol. 36. N 2, p. 81-85. DOI: 10.17580/em.2021.02.17
7. Zharikov I.F. Energy efficiency and energy-saving technologies in open-pit coal mining. *Tendentsii razvitiya nauki i obrazovaniya*. 2018. N 42-5, p. 38-41.
8. Göransson L. Balancing Electricity Supply and Demand in a Carbon-Neutral Northern Europe. *Energies*. 2023. Vol. 16. Iss. 8. N 3548. DOI: 10.3390/en16083548
9. Kiviluoma J., Rinne E., Helistö N. Comparison of flexibility options to improve the value of variable power generation. *International Journal of Sustainable Energy*. 2018. Vol. 37. Iss. 8, p. 761-781. DOI: 10.1080/14786451.2017.1357554
10. Torriti J. Household electricity demand, the intrinsic flexibility index and UK wholesale electricity market prices. *Environmental Economics and Policy Studies*. 2022. Vol. 24. Iss. 1, p. 7-27. DOI: 10.1007/s10018-020-00296-1
11. Sperber E., Frey U., Bertsch V. Reduced-order models for assessing demand response with heat pumps – Insights from the German energy system. *Energy and Buildings*. 2020. Vol. 223. N 110144. DOI: 10.1016/j.enbuild.2020.110144
12. Eid C., Codani P., Perez Y. et al. Managing electric flexibility from Distributed Energy Resources: A review of incentives for market design. *Renewable and Sustainable Energy Reviews*. 2016. Vol. 64, p. 237-247. DOI: 10.1016/j.rser.2016.06.008
13. Ugurlu U., Tas O., Kaya A., Oksuz I. The Financial Effect of the Electricity Price Forecasts' Inaccuracy on a Hydro-Based Generation Company. *Energies*. 2018. Vol. 11. Iss. 8. N 2093. DOI: 10.3390/en11082093
14. Dzyuba A.P., Solovyeva I.A. Prospects for Energy Demand Management in Russian Regions. *Economy of Region.* 2021. Vol. 17. Iss. 2, p. 502-519 (in Russian). DOI: 10.17059/ekon.reg.2021-2-11
15. Afanasyev D.O., Fedorova E.A. On the impact of outlier filtering on the electricity price forecasting accuracy. *Applied Energy*. 2019. Vol. 236, p. 196-210. DOI: 10.1016/j.apenergy.2018.11.076
16. Zhukovskiy Yu.L., Suslikov P.K. Assessment of the potential effect of applying demand management technology at mining enterprises. *Sustainable Development of Mountain Territories.* 2024. Vol. 16. N 3, p. 895-908 (in Russian). DOI: 10.21177/1998-4502-2024-16-3-895-908
17. Sibo Nan, Ming Zhou, Gengyin Li. Optimal residential community demand response scheduling in smart grid. *Applied Energy*. 2018. Vol. 210, p. 1280-1289. DOI: 10.1016/j.apenergy.2017.06.066
18. De Souza E. Improving the energy efficiency of mine fan assemblages. *Applied Thermal Engineering*. 2015. Vol. 90, p. 1092-1097. DOI: 10.1016/j.applthermaleng.2015.04.048
19. Wallace K., Prosser B., Stinnette J.D. The practice of mine ventilation engineering. *International Journal of Mining Science and Technology*. 2015. Vol. 25. Iss. 2, p. 165-169. DOI: 10.1016/j.ijmst.2015.02.001
20. de Vilhena Costa L., Margarida da Silva J. Cost-saving electrical energy consumption in underground ventilation by the use of ventilation on demand. *Mining Technology*. 2020. Vol. 129. Iss. 1, p. 1-8. DOI: 10.1080/25726668.2019.1651581
21. Ting Yu Lin, Zhengxuan Jia, Chen Yang et al. Evolutionary digital twin: A new approach for intelligent industrial product development. *Advanced Engineering Informatics*. 2021. Vol. 47. N 101209. DOI: 10.1016/j.aei.2020.101209
22. Aheleroff S., Xu X., Zhong R.Y., Lu Y. Digital Twin as a Service (DTaaS) in Industry 4.0: An Architecture Reference Model. *Advanced Engineering Informatics*. 2021. Vol. 47. N 101225. DOI: 10.1016/j.aei.2020.101225
23. Steindl G., Stagl M., Kasper L. et al. Generic Digital Twin Architecture for Industrial Energy Systems. *Applied Sciences*. 2020. Vol. 10. Iss. 24. N 8903. DOI: 10.3390/app10248903
24. Lo C.K., Chen C.H., Zhong R.Y. A review of digital twin in product design and development. *Advanced Engineering Informatics*. 2021. Vol. 48. N 101297. DOI: 10.1016/j.aei.2021.101297
25. Saad A., Faddel S., Mohammed O. IoT-Based Digital Twin for Energy Cyber-Physical Systems: Design and Implementation. *Energies*. 2020. Vol. 13. Iss. 18. N 4762. DOI: 10.3390/en13184762

26. Jianwei Cheng, Yan Wu, Xu H. et al. Comprehensive and Integrated Mine Ventilation Consultation Model – CIMVCM. *Tunnelling and Underground Space Technology*. 2015. Vol. 45, p. 166-180. DOI: 10.1016/j.tust.2014.09.004

27. Fomin A.I., Grunskoy T.V. Improvement of the Working Conditions of Oil Miners During the Transition from the Thermoshaft Method of High-Viscosity Oil Production to the Modular Mine Method of the Yaregskoye Field Development. *Occupational Safety in Industry*. 2020. N 12, p. 58-65 (in Russian). DOI: 10.24000/0409-2961-2020-12-58-65

28. Nie B.S., Peng B., Guo J.H. et al. Research on Characteristics of Air Flow Disorder in Inlet Shafts. *Journal of Mining Science*. 2018. Vol. 54. N 3, p. 444-457. DOI: 10.1134/S1062739118033846

29. Hao Shao, Qingzi Lu, Shuguang Jiang. Effect of Frequency Conversion Ventilation on Coal Spontaneous Combustion. *Combustion Science and Technology*. 2021. Vol. 193. Iss. 10, p. 1766-1781. DOI: 10.1080/00102202.2020.1713769

30. Fetri M., Shahabi R.S., Namin F.S. et al. Analyzing the effects of natural ventilation caused by excavating the waste pass on the ventilation network of Anguran mine. *International Journal of Mining and Geo-Engineering*. 2023. Vol. 57. Iss. 3, p. 231-240. DOI: 10.22059/IJMGE.2022.342133.594970

31. Kychkin A.V., Nikolaev A.V. Architecture of a Cyber-Physical System for the Mining Enterprise Ventilation Control Based on the Internet of Things Platform. *Mekhatronika, avtomatizatsiya, upravlenie*. 2021. Vol. 22. N 3, p. 115-123 (in Russian). DOI: 10.17587/mau.22.115-123

32. Lyalkina G.B., Nikolaev A.V. Natural Draft and Its Direction in a Mine at the Preset Confidence Coefficient. *Journal of Mining Science*. 2015. Vol. 51. N 2, p. 342-346. DOI: 10.1134/S1062739115020180

33. Mokhirev N.N., Radko V.V. Engineering calculations for mine ventilation. Construction. Reconstruction. Operation. Moscow: Nedra, 2007, p. 324.

34. Nikolaev A.V., Zhebelev D.D., Presnyakov A.A. Certificate of state registration of computer program N 2023685311 MineVent DT-Connector. Program for integrating a simulation subsystem of a digital twin of an underground mining enterprise. Publ. 24.11.2023. Bul. N 12 (in Russian).

35. Gendler S.G., Fazylov I.R. Application efficiency of closed gathering system toward microclimate normalization in operating galleries in oil mines. *Mining Informational and Analytical Bulletin*. 2021. N 9, p. 65-78 (in Russian). DOI: 10.25018/0236_1493_2021_9_0_65

36. Rudakov M.L., Korobitsyna M.A. On the possibility of normalizing air temperature in the mine workings of the oil mines. *Occupational Safety in Industry*. 2019. N 8, p. 66-71 (in Russian). DOI: 10.24000/0409-2961-2019-8-66-71

37. Alymenko N.I. Research and development of methods and means to improve the efficiency and reliability of ventilation in underground mines with large equivalent openings (using potash mines as an example): Avtoref. dis. ... d-ra tekhn. nauk. St. Petersburg: Sankt-Peterburgskii gosudarstvennyi gornyi institut im. G.V.Plekhanova, 1998, p. 44.

38. Nikolaev A.V., Maksimov P.V., Fajnburg G.Z., Konotop D.A. Efficiency of a new ventilation method for a tilted block in an oil mine. *Mining Informational and Analytical Bulletin*. 2023. N 5, p. 83-98 (in Russian). DOI: 10.25018/0236_1493_2023_5_0_83

39. Konoplev Yu.P., Buslaev V.F., Yagubov Z.Kh., Tskhadaya N.D. Thermomine development of oil fields. Moscow: Nedra, 2006, p. 288 (in Russian).

40. Chertenkov M.V., Mulyak V.V., Konoplev Y.P. The Yarega Heavy Oil Field – History, Experience, and Future. *Journal of Petroleum Technology*. 2012. Vol. 64. Iss. 4, p. 153-160. DOI: 10.2118/0412-0153-JPT

41. Nikolaev A.V., Maksimov P.V., Lialkina G.B., Konotop D.A. The effect of methane emission on air distribution in potash mine production units. *News of the Higher Institutions. Mining Journal*. 2021. N 6, p. 87-97 (in Russian). DOI: 10.21440/0536-1028-2021-6-87-97

42. dos Santos S.A.B., Soares J.M., Barroso G.C., Prata B. de A. Demand response application in industrial scenarios: A systematic mapping of practical implementation. *Expert Systems with Applications*. 2023. Vol. 215. N 119393. DOI: 10.1016/j.eswa.2022.119393

43. Savard C., Iakovleva E., Ivanchenko D., Rassõlkin A. Accessible Battery Model with Aging Dependency. *Energies*. 2021. Vol. 14. Iss. 12. N 3493. DOI: 10.3390/en14123493

44. Senchilo N.D., Ustinov D.A. Method for Determining the Optimal Capacity of Energy Storage Systems with a Long-Term Forecast of Power Consumption. *Energies*. 2021. Vol. 14. Iss. 21. N 7098. DOI: 10.3390/en14217098

45. Shabalov M.Yu., Zhukovskiy Yu.L., Buldysko A.D. et al. The influence of technological changes in energy efficiency on the infrastructure deterioration in the energy sector. *Energy Reports*. 2021. Vol. 7, p. 2664-2680. DOI: 10.1016/j.egyr.2021.05.001

46. Zhukovskiy Y.L., Kovalchuk M.S., Batueva D.E., Senchilo N.D. Development of an Algorithm for Regulating the Load Schedule of Educational Institutions Based on the Forecast of Electric Consumption within the Framework of Application of the Demand Response. *Sustainability*. 2021. Vol. 13. Iss. 24. N 13801. DOI: 10.3390/su132413801

47. Mukashev D., Abitova G., Uskenbayeva G., Shaikhanova A. Weather prediction with artificial intelligence in meteorology. *The Bulletin of KazATC*. 2024. N 1 (130), p. 414-425. DOI: 10.52167/1609-1817-2024-130-1-414-425

48. Raimondi Cominesi S., Farina M., Giulioni L. et al. A Two-Layer Stochastic Model Predictive Control Scheme for Microgrids. *IEEE Transactions on Control Systems Technology*. 2018. Vol. 26. Iss. 1, p. 1-13. DOI: 10.1109/TCST.2017.2657606

49. Razmi D., Lu T. A Literature Review of the Control Challenges of Distributed Energy Resources Based on Microgrids (MGs): Past, Present and Future. *Energies*. 2022. Vol.15. Iss. 13. N 4676. DOI: 10.3390/en15134676

50. Blesslin S.T., Wessley G.J.J., Kanagaraj V. et al. Microgrid Optimization and Integration of Renewable Energy Resources: Innovation, Challenges and Prospects. Integration of Renewable Energy Sources with Smart Grid. Wiley, 2021, p. 239-262. DOI: 10.1002/9781119751908.ch11

51. Corrigan C.C., Ikonnikova S.A. A review of the use of AI in the mining industry: Insights and ethical considerations for multi-objective optimization. *The Extractive Industries and Society*. 2024. Vol. 17. N 101440. DOI: 10.1016/j.exis.2024.101440

52. Kaur S., Kumar R., Singh K., Yinglai Huang. Leveraging Artificial Intelligence for Enhanced Sustainable Energy Management. *Journal of Sustainability for Energy*. 2024. Vol. 3. Iss. 1, p. 1-20. DOI: 10.56578/jse030101

***Authors*: Aleksandr V. Nikolaev,** *Doctor of Engineering Sciences, Professor* (*Perm National Research Polytechnic University, Perm, Russia*), *nikolaev0811@mail.ru, https://orcid.org/0000-0002-4601-5780*, **Aleksei V. Kychkin,** *Candidate of Engineering Sciences, Associate Professor, Head of Center* (*National Research University Higher School of Economics – Perm, Perm, Russia*), *https://orcid.org/0000-0003-0626-5803*.

The authors declare no conflict of interests.

ISSN 2411-3336; e-ISSN 2541-9404

JOURNAL OF MINING INSTITUTE

Zapiski Gornogo instituta

Journal homepage: pmi.spmi.ru

Research article

Geotechnical Engineering and Engineering Geology

Digital transformation of industrial machinery repair and maintenance to build an industrial metaverse

Natalia I. Koteleva[1]✉, **Vladislav V. Valnev**[1], **Aleksandr S. Simakov**[1], **Maysam Mohammadzadeh Shirazi**[2]

[1] *Empress Catherine II Saint Petersburg Mining University, Saint Petersburg, Russia*

[2] *Shiraz University, Shiraz, Iran*

***How to cite this article*:** Koteleva N.I., Valnev V.V., Simakov A.S., Shirazi M.M. Digital transformation of industrial machinery repair and maintenance to build an industrial metaverse. Journal of Mining Institute. 2025. Vol. 275, p. 30-41.

Abstract

Industrial metaverse is a new direction for development of industrial enterprises. Nowadays the process of full understanding term "industrial metaverse", its conception, its effectiveness for enterprises is not actualy completed. The methodology, tools, and methods for building an industrial metaverse have not been clearly defined. Therefore, it is advisable to experimentally implement a part of the metaverse on one or several processes with future scaling to other processes. The process of industrial machinery repair and maintenance is proposed as an experimental zone for implementing the industrial metaverse. This process is well suited as an experimental zone. Launching the industrial metaverse concept on it will solve a number of problems, such as the diversity of equipment with unique diagnostic and repair methods, human errors made during repair work, etc. This article presents the concept of building and the architecture of industrial metaverse. A general description of the physical, cyber-physical, and social spaces and the interaction layer between them is provided, without any details of qualitative and quantitative indicators. The avatar of a service engineer is highlighted as one of the elements of the cyber-physical space. The process of creating an avatar of a cyber-physical service engineer is considered: a description of the main functionality is provided, it is shown that a combined system of wearable devices – a glove and a video camera integrated into glasses, a vest, a helmet, or represented by an independent device – is sufficient for its creation. Laboratory experiments were conducted, where the created avatar was tested to determine the task of servicing a centrifugal pump. The results of processing 518 experimental datasets of 10 points, each of which belongs to one of six classes corresponding to a specific technological operation during servicing of a centrifugal pump are shown. Three types of models were obtained (accuracy on training data 0.99; 1.0; 1.0, accuracy on test data 0.625; 0.7; 1.0). It has been shown that achieving 1.0 accuracy on training and test data requires first identifying features representing frequency and temporal characteristics obtained through time series processing. The obtained results allow to make conclusions about the readiness of these technologies for industrial implementation.

Keywords

industrial machinery repair and maintenance; industrial metaverse; digital transformation; Industry 5.0; service engineer avatar; wearable devices; artificial intelligence

Received: 21.02.2025 ***Accepted: 02.09.2025*** ***Online: 07.10.2025*** ***Published: 31.10.2025***

Introduction

Modern industrial machinery repair and maintenance is a guarantee of operational safety of any industrial enterprise [1, 2]. Modern maintenance is understood as equipment maintenance performed on time in the required volume, during which the decrease in the enterprise's operational efficiency is either absent or minimal [3, 4]. During maintenance, enterprises can flow to four strategies [5, 6]: 1) reactive maintenance or maintenance that must be performed upon an incident (repair, accident, etc.); 2) preventive maintenance or scheduled maintenance (according to the manufacturer's recommendations or regulations); 3) predictive maintenance or maintenance based on defect development forecasts; 4) maintenance based on actual condition (i.e., only when really necessary).

Modern enterprises try to move to maintenance based on actual condition and reduce the need for reactive maintenance [7, 8]. During maintenance, enterprises face a number of problems [9, 10], for example:

- lack of labor;
- a huge variety of equipment with unique diagnostic and repair methods;
- a lack of personnel skills and competencies in equipment maintenance;
- a lack of tools for monitoring the actual condition, assessing the service life, and predicting the development of various equipment defects;
- personnel errors occurred during installation or maintenance of equipment, timely logging of these errors and diagnosis;
- a lack of an automated system for monitoring maintenance and personnel actions;
- limited access to real-time information about the life condition of equipment at the facility during repairs.

To solve these and other problems arising during an industrial machinery repair and maintenance, it is necessary to develop new approaches. It made possible by the digital transformation, which is making the transition through Industry 4.0 to Industry 5.0 [11, 12]. Digital transformation today spreads almost all types of human activity [13, 14]. Of course, industry is not immune to it [15, 16]. One of the areas of digital transformation of enterprises and the concept of Industry 5.0 is the creation of an industrial metaverse [17, 18]. The metaverse is a new concept describing a completely immersive digital environment in which people can interact both with digital objects and with each other in virtual space [19]. However, the concept of the "industrial metaverse" is quite new, the principles, methodology and tools of the industrial metaverse have not been clearly defined [20, 21]. There are several problems that hinder its creation in enterprises [22, 23]. For example, the adaptation of existing technological solutions to a specific process and enterprise, the lack of a regulatory framework and standards, insufficient information security, and the absence of a data management system and resource distribution between the real, virtual, and mixed reality. Considering these problems, researchers agree that implementation, i.e., the creation of an industrial metaverse, is necessary today [24, 25].

According to the authors, the implementation of the industrial metaverse should be realized conservatively: a part of the industrial metaverse should be experimentally deployed on one or more processes and then scaled up. However, it is important to remember that even the experimental implementation of a part of the metaverse should not harm the activities of the enterprise or reduce its operational efficiency. The correct selection of an object or process is an important task for the initial deployment of the industrial metaverse. A study [26], the purpose of which was to find out how companies perceive the potential for using the industrial metaverse, showed that maintenance and repair processes have the greatest potential for the implementation of the industrial metaverse: 44 % of votes (first place) versus 15 % for design and planning (second place). This gap proves the advisability of choosing maintenance and repair processes as an experimental zone for the implementation of the industrial metaverse concept. Other studies [27, 28] directly or indirectly choose the equipment maintenance and repair process as the most suitable for the initial implementation of the industrial metaverse concept at an industrial enterprise.

The aim of this work is to develop technical solutions for creating a part of the industrial metauniverse for the equipment maintenance and repair process.

Methods

To build an industrial metaverse of the industrial machinery repair and maintenance process, four mandatory levels or layers are assumed: the physical level (real-world objects), the level of interaction between the physical and virtual worlds (IoT devices, wearable devices, special interaction

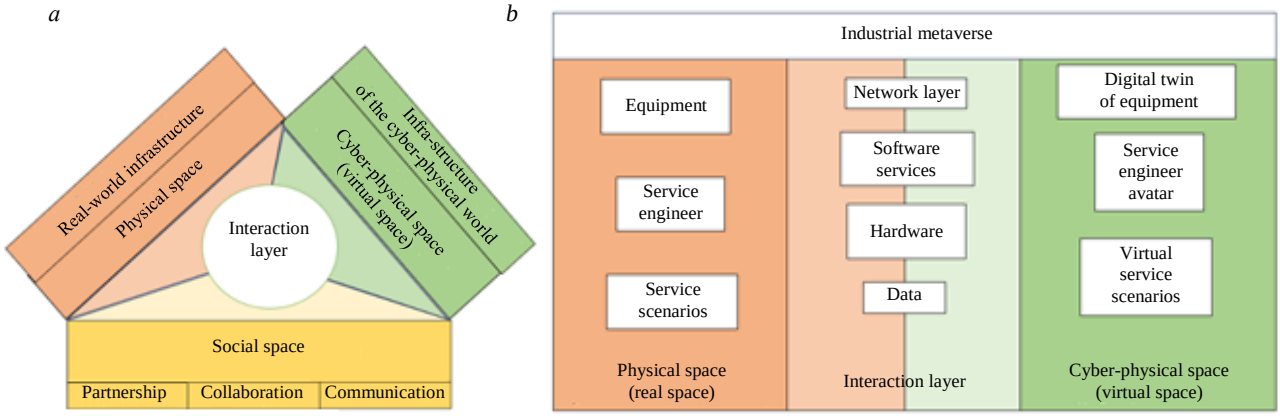

Fig.1. The architecture of the industrial metaverse of industrial machinery repair and maintenance:
a – the whole model; *b* – model in the plane of physical and cyber-physical space

protocols, communication systems, robots and drones), the mixed reality level (virtual world objects, digital twins, virtual and augmented reality), the decision-making level (objects and algorithms that synchronize the operation of the real and virtual parts of the metaverse). For example, in [29] the industrial metaverse includes physical, cyber-physical, and social spaces. According to this terminology and expanding the industrial metaverse concept, a model of the industrial metaverse was developed, the architecture of which is presented in Fig.1, *a*.

The difference between this model and the one presented in [29], is that the common layer is called the interaction layer (in [29] the common layer is called the fusion layer, the interaction layer is the layer between the social and cyber-physical space, and additionally introduced are the configuration layer – the layer between the social and physical space, the network layer – the layer between the physical and cyber-physical space, and the perception layer – the layer between the physical and cyber-physical space). The developed architecture allows for a more detailed presentation of the interactions of the three spatial components from different planes. For example, Fig.1, *b* presents an examination of the industrial metaverse in the plane of interaction between the physical and cyber-physical space.

The real and virtual parts of the industrial metaverse overlap. At the intersection of each part there are data (information models), software services, hardware, and a network layer. At the same time, there is data generated only by the real part of the metaverse, and there is only that which relates to the virtual part, also with software services and hardware. However, the infrastructure should be built in such a way that the parts are independent and can interact with each other.

For the presented industrial metaverse architecture, the decision-making system [30] will be located in layers of social space, as shown in Fig.2. The light colors used in Fig.2 for each of the three spaces indicate the boundaries of interaction between the spaces.

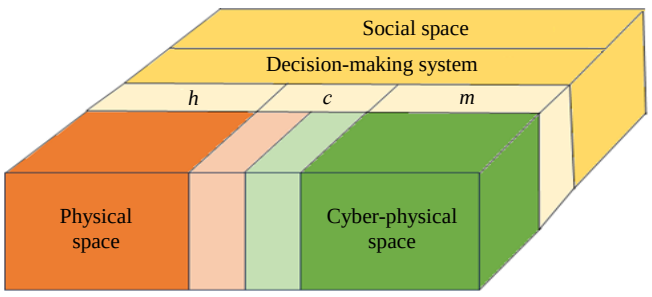

Fig.2. Decision-making system in industrial metaverse for industrial machinery repair and maintenance:
h – only human, *m* – only machine, *c* – collaboration mode

The decision-making system can operate in three modes: human-only, system-only, and interaction mode (expert assistant, where the system generates possible solutions to the problem, and the human makes the final decision). Companies are more willing to delegate decision-making to humans. The system is involved in fewer cases. As trust increases, the degree of system participation in decision-making should certainly increase.

The creation of an industrial metaverse does not occur from scratch. Conceptually, this is certainly a new question, but it is based on existing developments and solutions. For example, for the equipment maintenance and repair process, the physical space exists completely, while the cyber-physical space exists partially. This means that to build an industrial metaverse and understand it in terms of the plane of interaction between the physical and cyber-physical space, it is necessary to improve or supplement the cyber-physical space, as well as the interaction layer. Today, almost all parts of the model in Fig.2 are presented in one form or another as specific technological solutions [31, 32]. The authors see only one element that has not been sufficiently developed in the form of specific software and hardware solutions. This is the avatar of a service engineer or a digital model of a service engineer in cyber-physical space. The experimental part of this study allows to obtaining an avatar of a service engineer. It allows for recording the actions of a service engineer and comparing them with the actual actions performed during repairs. Data suppliers for the development of a service engineer can be special sensors [33, 34] or a machine vision system [35, 36], but the main devices are wearable devices, the range of which on the market is quite wide – helmets [37], glasses [38], vests [39] and even insoles [40].

The hypothesis of experimental part of this research is that to create a digital avatar of a service engineer and implement a system for comparing real maintenance scenes, it is necessary and sufficient to use a combination of devices: a smart glove and a wearable video camera (either a standalone device or integrated into glasses or a hard hat). We emphasize that, despite a certain degree of readiness, even existing solutions require certain upgrades. For example, at the physical level, when interacting with social space, it is necessary to assess personnel's readiness to use various technologies (cognitive-psychological state when using wearable devices, adaptation to interaction with virtual experts, advisory agents, increasing the degree of trust in these technologies), readiness to partner with robots and drones, the availability of regulatory documentation, and ensuring industrial safety of facilities when building a metaverse.

Experiments

Building an industrial metaverse is a resource-intensive process that defies a comprehensive solution. The experiments demonstrate the implementability of only part of the proposed concept. Specifically, they demonstrate the implementation of an avatar of the service engineer in the cyber-physical space of the metaverse. A service engineer in cyber-physical space is defined as an information model with different types of data: the service engineer's position in time and space during repairs; the service engineer's actions and their sequence; and the types and methods of interaction between the service engineer and the equipment.

The functionality of the industrial metaverse that can be realized with the implementation of the cyber-physical avatar of the service engineer: generation and creation of maintenance and repair instructions (using digital twins) and their issuance to the service engineer (AR, XR); verification of instruction execution (sequence and correctness of actions); maintenance and repair logging (recording, manual input, voice command, photo recording, video recording, neural interface); assessment of the service engineer competence level; optimization of maintenance and repair process; assessment of the psychophysical and emotional state of the service engineer during maintenance and repair (Fig.3).

Figure 3 shows a workflow for obtaining a service engineer avatar in the cyber-physical space of the metaverse.

To obtain an avatar of a service engineer in the industrial metaverse, three subsystems were developed: a subsystem for determining the position of the service engineer in space, a subsystem for obtaining information about maintenance and repair by processing a video sequence received through a wearable video camera [41], and a subsystem for processing data coming from a smart glove [42].

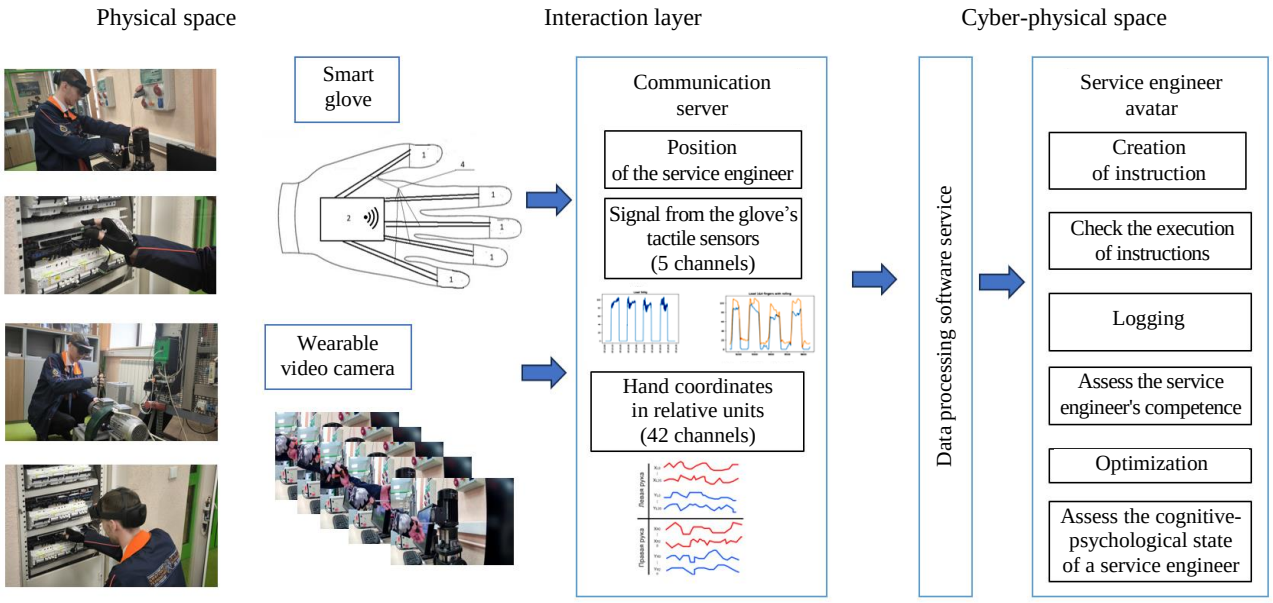

Fig.3. A workflow for obtaining a service engineer avatar in the cyber-physical space of the metaverse

The subsystem for determining the position of a service engineer in space can be implemented in several ways, at least three. The first method is the simplest, using a locator beacon. The system scans the position of a service engineer relative to the locator beacon. When a service engineer approaches the beacon, the service engineer is within the equipment's service area [43]. The second method is the use of spatial computing (via augmented reality glasses) [44]. The third method is via ZigBee modems [45], for example, using ToF and RSSI methods [46].

Below is the pseudocode for the system's operating algorithm:

Algorithm 1. Get a service engineer avatar in the cyber-physical space of the metaverse.
Output data. Object coordinates (x_{ob}, y_{ob}, z_{ob}), instruction list ($a_1 \dots a_n$), mode (collaboration, glove, video).
Step 1. Determine the service engineer's position in space (x, y, z).
Step 2. Check whether the object coordinates match the service engineer's coordinates → **Step 1**.
Step 3. Accuse hand coordinates and signals from tactile sensors.
Step 4. Check if the mode is collaboration mode → **Step 8**.
Step 5. Calculate the probability for each class using the video processing system **(**$\rho Sa_1 \dots \rho Sa_n$) and the glove signal processing system **(**$\rho Ga_1 \dots \rho Ga_n$).
Step 6. Determine action $\exists a_n \in N$, max($\rho Sa_1 \dots \rho Sa_n, \rho Ga_1 \dots \rho Ga_n$).
Step 7. Output data a_n, t, where a_n – action from input instruction list, t – current time (timestamp).
Step 8. Check if the mode is glove mode → **Step 11**.
Step 9. Calculate the probability for each class using the glove signal processing system **(**$\rho Ga_1 \dots \rho Ga_n$).
Step 10. Determine action $\exists a_n \in N$, max($\rho Ga_1 \dots \rho Ga_n$) → **Step 7**.
Step 11. Check if the mode is video mode → **Step 4**.
Step 12. Calculate the probability for each class using the video processing system **(**$\rho Sa_1 \dots \rho Sa_n$).
Step 13. Determine action $\exists a_n \in N$, max($\rho Sa_1 \dots \rho Sa_n$) → **Step 7**.

While solving the same problem, subsystems can be used to label data during model training. For example, a trained video processing subsystem divides the data into specific stages, labeling them, and this information is then used to train a glove signal processing subsystem, and vice versa.

To create a classification model for two processing subsystems, several feature extraction methods were selected and subsequently used for training. Feature extraction significantly improves the quality of time series classification, allowing the model to focus on the most important parts of the data [47]. The wavelet transform method, whose values are characterized by the entropy and energy of the wavelet transform coefficients, was used as a feature extraction method, as well as the calculation of statistical parameters of the time series.

For the video processing subsystem, a dimensionality reduction unit was additionally added. The 42 time series at the input of the dimensionality reduction unit were transformed into 12 time series, 10 of which are the Euler distance between the fingertips and key points of hand N 2, 3, 5, 9, and 17. Two time series are the area of the figure formed by each hand of the service engineer.

Results

The replacement of the lip seals during maintenance and repair of a centrifugal pump is carried out in the following sequence: removing the protective covers of the coupling; removing the half coupling; removing four nuts from the screws; disconnecting the engine. The following technological operations were used to check the operability of the glove signal processing subsystem: removing and installing the nuts securing the main parts of the pump; loosening and tightening the screws securing the protective cover of the pump electronics unit; recording values in the repair log – recording

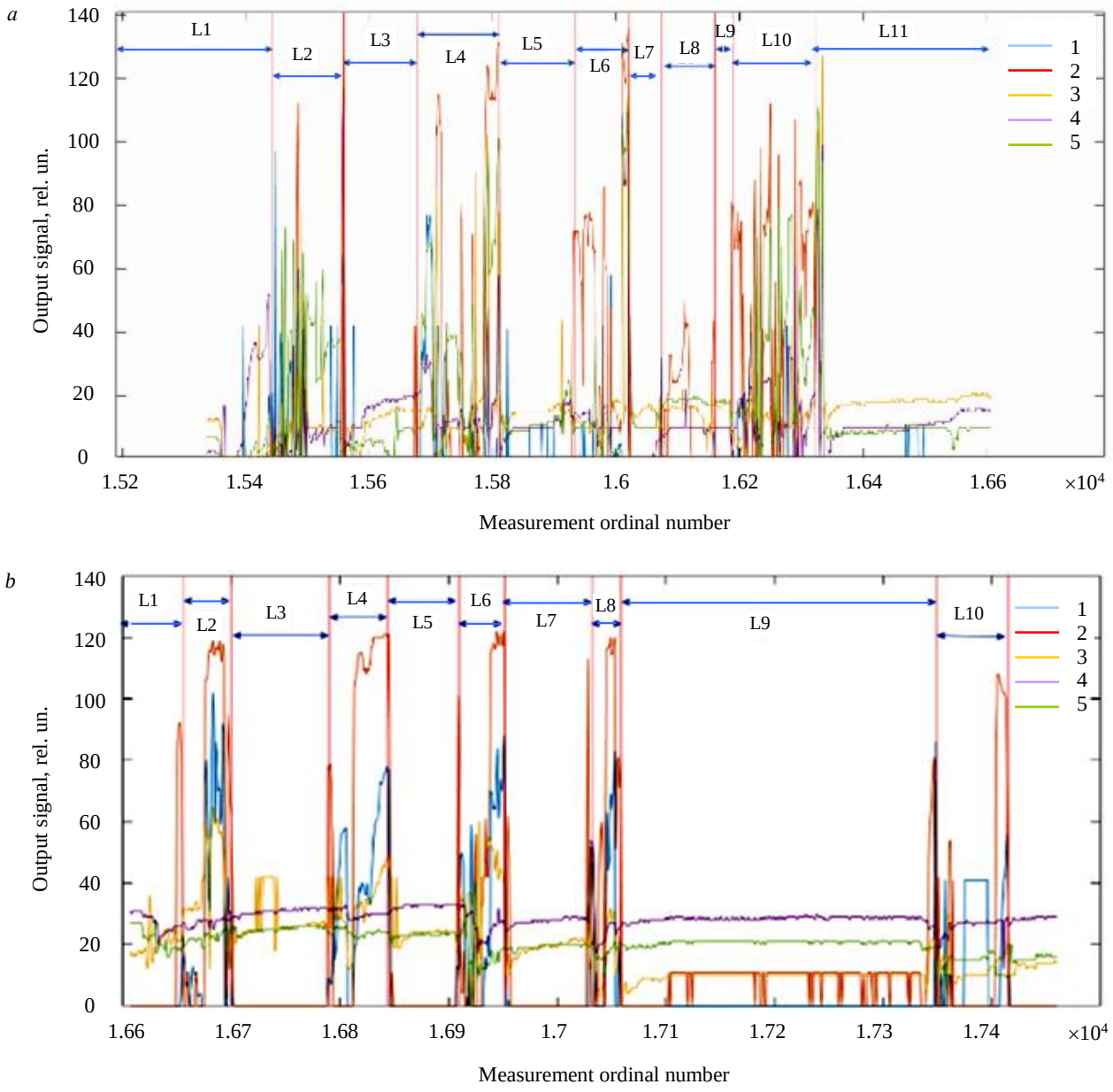

Fig.4. Sensors data from smart glove, getting during different service operation:
a – removing a nut; *b* – writing a short word

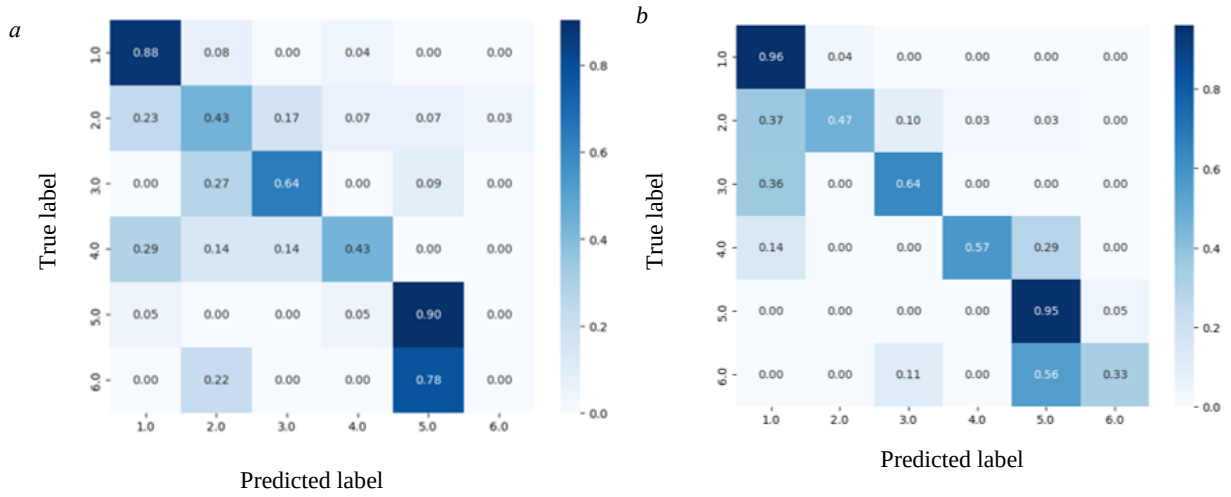

Fig.5. Confusion matrix: *a* – for method Elastic Ensemble (accuracy train = 0.99, accuracy test = 0.625); *b* – for method Rocket (accuracy train = 1, accuracy test = 0.7)

a short word (parameter value) and recording a long word – recording the features of the repair being performed. The video processing subsystem was not tested, because its description was given earlier [41]. For the experiments, the following classes were determined: class 1 – removing nuts, class 2 – installing nuts, class 3 – loosening a screw, class 4 – tightening a screw, class 5 – recording a short word, class 6 – recording a long word. Figure 4 shows the signal received from five glove sensors.

As Fig.4, *a* shows, the data was divided into 11 areas. The initial labeling areas L2, L4, L6, L8, and L10 were revealed as significant. During the servicing, it was additionally recorded that the service engineer removed the nut four times instead of five. Accordingly, one of the regions was identified incorrectly. The video processing system was also launched. Using this system's data, it was determined that region L8 had been labeled incorrectly and that data from regions L2, L4, L6, and L10 should be used for training.

In Fig.4, *b*, the initial labeling revealed significant regions L2, L4, L6, L8, and L10. The video processing system was also launched. Further verification revealed that all five regions were identified and labeled correctly. Thus, data from five regions was added for training.

Figure 5 shows the results of training the AutoML model using algorithms without preprocessing. The Aeon package and two of its methods suitable for processing multivariable time series data – Rocket [48] and Elastic Ensemble [49] – were used for training. The accuracy values for the Elastic Ensemble training set were 0.99, for Rocket – 1.00, and for the test set – Elastic Ensemble – 0.625, for Rocket – 0.7.

The results obtained during training demonstrate, on the one hand, easy trainability, distinguishability, and satisfactory performance on the task. As can be seen in Fig.5, on the test set, the model most often confused classes are 5 and 6 – “recording a short word” and “recording a long word”. On the other hand, we see signs of overfitting, specifically high performance on the training set and lower performance on the test set. To improve results, it is necessary to perform preprocessing transformations of the time series data and additionally apply feature extraction methods to the algorithms.

Figure 6 shows a plot of class distinguishability after applying feature extraction methods. Figure 6, *a* shows class 1 for datasets 0 and 1, and Fig.6, *b* shows class 2 for datasets 70 and 71. Despite the classes being very similar in the nature of the actions performed, they are visually distinguishable from each other and similar internally.

The model using feature extraction methods trained perfectly on both the training and test sets, with an accuracy of 1.00.

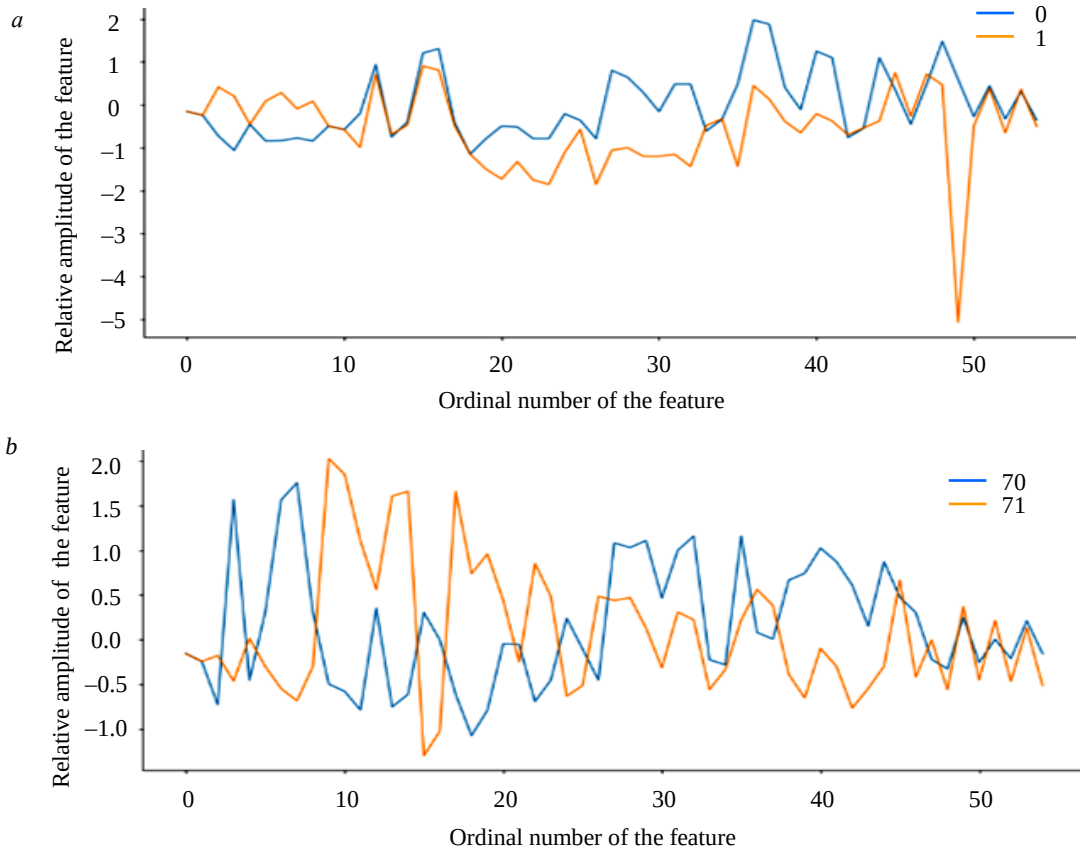

Fig.6. Class distinguishability graph: *a* – class 1, data set numbers 0 and 1*; b* – class 2, data set numbers 70 and 71

Figure 7 shows the contribution of each feature (the top 20), based on the values of which the model obtained the results. It should be noted that the fingers in the study were coded as follows: 1 – thumb, 2 – index, 3 – middle, 4 – ring, 5 – little finger. It is noteworthy that the index and little fingers made it into the top 10.

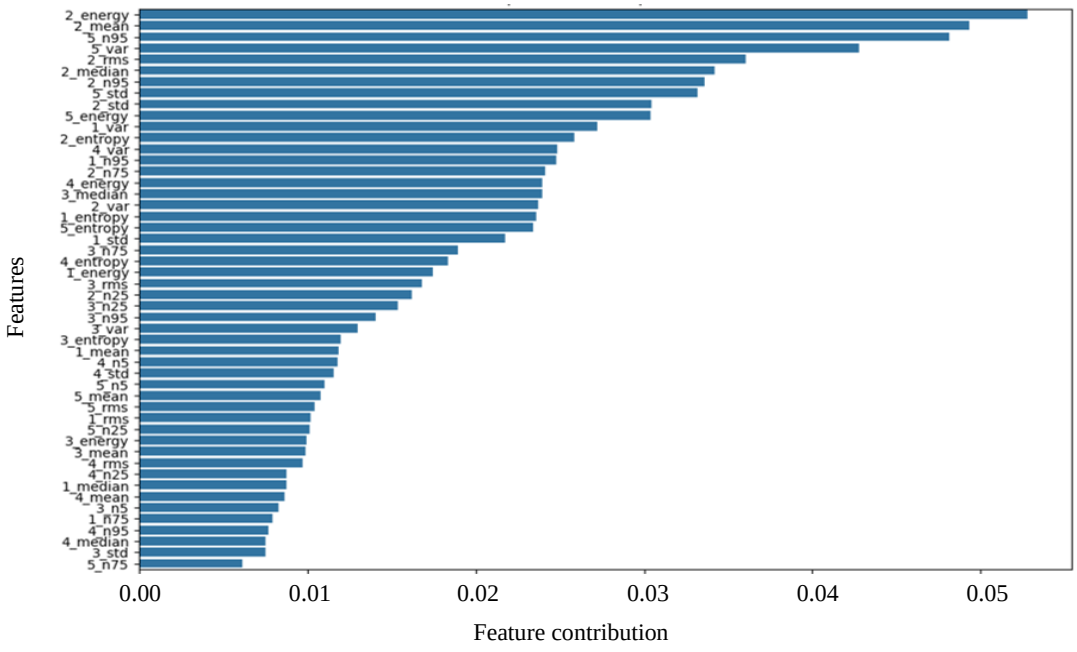

Fig.7. Feature contribution

Further analysis of such information can help determine the qualifications, work characteristics of the service engineer and other useful information.

Discussion

Building an industrial metaverse is an important task and provides a foundation for the future development of an industrial enterprise. However, it is important to remember that many solutions have been developed that can be integrated and adapted into the industrial metaverse concept. The collaboration of new and existing solutions and their use within a single conceptual framework should bring profit to the enterprise and open new horizons for production operations.

An example of the new solutions discussed in this article is the creation of a service engineer avatar for use in cyberspace. Integrating the service engineer avatar and its interaction with digital twins of equipment will take an industrial machinery repair and maintenance to a new level.

The experimental part of the study demonstrates the development of only a part of the industrial metaverse for an industrial machinery repair and maintenance. Further work can be focused on various directions, but the most interesting is the following workflow for creating an industrial metaverse: development of a subsystem for monitoring the position of a service engineer in space (especially simplified methods, for example, based on ZigBee network data), development of automatic maintenance and repair scenarios and work plans for the maintenance and repair system, development of a system for evaluating the maintenance and repair system's actions, development of methods for machine-human interaction during maintenance and repair processes, development of methods for optimizing maintenance and repair processes, adaptation of digital twins for use in the industrial metaverse, and verification of the full concept of implementing an industrial metaverse for an industrial machinery repair and maintenance. The extensive plan for further work clearly demonstrates that this work is the initial stage in the construction of an industrial metaverse for the maintenance and repair process.

We emphasize that the smart glove and wearable video camera represent the minimum set of wearable devices that can be used to determine the actions of the service engineer during maintenance and repair. The list of devices and the data obtained from them can be expanded, provided that their data expands the existing functionality. The specified devices and the data obtained from them are sufficient for the presented functions.

When implementing an industrial metaverse, it is necessary to consider potential scaling issues with these solutions. Such issues may include network limitations when using a large number of devices, an exponentially increasing load on the system computing nodes (however, the modularity inherent in the conceptual model will allow for parallelization of computations), and low reliability characteristics of wearable devices, especially when operating in the field.

At all stages of building an industrial metaverse, information security issues must be additionally considered [50]. The interactions of physical space and its operation in unified layers with cyber-physical and social space raise the major issue of information security. The use of new approaches, network protocols, and modern cybersecurity principles (e.g., zero trust security [51, 52], etc.) is key to building an industrial metauniverse. However, it is important to remember that these technologies introduce adjustments to established principles and may require significant changes to the network, software, and hardware implementation of the proposed solutions.

Conclusion

A concept for building an industrial metaverse presents in this article. The applicability of this concept to an industrial machinery repair and maintenance is demonstrated. The analytical section reveals that this process offers the most promising initial approach to building an industrial metaverse. Three types of spaces – physical, cyber-physical, and social – are considered for the industrial metaverse, as well as the interaction layer between them. When considering

the industrial metaverse in terms of physical and cyber-physical space, it is necessary to develop missing technological solutions, such as solutions for creating a service engineer's avatar in the cyber-physical space. The experimental section of the study demonstrates that two types of wearable devices – a wearable video camera and a smart glove – are necessary and sufficient for creating an avatar. The process of creating models for comparing data obtained from wearable devices and the work performed by a service engineer is considered. Current developments and future research will reduce costs and maximize profits not only during the operation of the finished "industrial metaverse" product, but also during its development. The company's transition to Industry 5.0 through Industry 4.0 will enable a new level of production. A key step in implementing new technologies is assessing their readiness and adaptability to existing production realities. Informed decisions, avoiding blind adherence to new trends, ensuring information security, and understanding the global nature of processes during the transition to a new industrial era are essential components of digital transformation.

REFERENCES

1. Bouabid D.A., Hadef H., Innal F. Maintenance as a sustainability tool in high-risk process industries: A review and future directions. *Journal of Loss Prevention in the Process Industries*. 2024. Vol. 89. N 105318. DOI: 10.1016/j.jlp.2024.105318

2. Tokarev I.S., Nazarychev A.N., Shklyarsky Ya.E., Skvortsov I.V. Ensuring the sustainable operation of autonomous power systems in the gas industry. *Energetik.* 2024. N 7, p. 15-19 (in Russian).

3. Mallioris P., Aivazidou E., Bechtsis D. Predictive maintenance in Industry 4.0: A systematic multi-sector mapping. *CIRP Journal of Manufacturing Science and Technology*. 2024. Vol. 50, p. 80-103. DOI: 10.1016/j.cirpj.2024.02.003

4. Nedashkovskaya E.S., Sheshukova E.I., Korogodin A.S. et al. Structure of the system of maintenance and repair of mining machines. *Transport, mining and construction engineering: science and production.* 2024. N 25, p. 155-162 (in Russian). DOI: 10.26160/2658-3305-2024-25-155-162

5. Dayo-Olupona O., Genc B., Celik T., Bada S. Adoptable approaches to predictive maintenance in mining industry: An overview. *Resources Policy*. 2023. Vol. 86. Part A. N 104291. DOI: 10.1016/j.resourpol.2023.104291

6. Wari E., Weihang Zhu, Gino Lim. Maintenance in the downstream petroleum industry: A review on methodology and implementation. *Computers & Chemical Engineering*. 2023. Vol. 172. N 108177. DOI: 10.1016/j.compchemeng.2023.108177

7. Zhukovsky Yu.L., Suslikov P.K. Assessment of the potential effect of applying demand management technology at mining enterprises. *Sustainable Development of Mountain Territories.* 2024. Vol. 16. N 3 (61), p. 895-908 (in Russian). DOI: 10.21177/1998-4502-2024-16-3-895-908

8. Psarommatis F., May G., Azamfirei V. Envisioning maintenance 5.0: Insights from a systematic literature review of Industry 4.0 and a proposed framework. *Journal of Manufacturing Systems*. 2023. Vol. 68, p. 376-399. DOI: 10.1016/j.jmsy.2023.04.009

9. Alves F.F., Ravetti M.G. Hybrid proactive approach for solving maintenance and planning problems in the scenario of Industry 4.0. *IFAC-PapersOnLine*. 2020. Vol. 53. Iss. 3, p. 216-221. DOI: 10.1016/j.ifacol.2020.11.035

10. Palmitessa E., Premoli A., Roda I., Macchi M. Integrating maintenance and energy problems through a Digital Twin-based decision support framework under the guidance of Asset Management. *IFAC-PapersOnLine*. 2024. Vol. 58. Iss. 8, p. 7-12. DOI: 10.1016/j.ifacol.2024.08.042

11. Kans M., Campos J. Digital capabilities driving industry 4.0 and 5.0 transformation: Insights from an interview study in the maintenance domain. *Journal of Open Innovation: Technology, Market, and Complexity*. 2024. Vol. 10. Iss. 4. N 100384. DOI: 10.1016/j.joitmc.2024.100384

12. Ahmed Murtaza A., Saher A., Hamza Zafar M et al. Paradigm shift for predictive maintenance and condition monitoring from Industry 4.0 to Industry 5.0: A systematic review, challenges and case study. *Results in Engineering*. 2024. Vol. 24. N 102935. DOI: 10.1016/j.rineng.2024.102935

13. Litvinenko V.S. Digital Economy as a Factor in the Technological Development of the Mineral Sector. *Natural Resources Research*. 2020. Vol. 29. Iss. 3, p. 1521-1541. DOI: 10.1007/s11053-020-09716-1

14. Korolev N., Kozyaruk A., Morenov V. Efficiency Increase of Energy Systems in Oil and Gas Industry by Evaluation of Electric Drive Lifecycle. *Energies*. 2021. Vol. 14. Iss. 19, p. 6074. DOI: 10.3390/en14196074

15. Cherepovitsyn A., Solovyova V., Dmitrieva D. New challenges for the sustainable development of the rare-earth metals sector in Russia: Transforming industrial policies. *Resources Policy*. 2023. Vol. 81. N 103347. DOI: 10.1016/j.resourpol.2023.103347

16. Makhovikov A.B., Filyasova Yu.A. Information technologies for solid mineral extraction in the Arctic. *Sustainable Development of Mountain Territories.* 2024. Vol. 16. N 3 (61), p. 1110-1117 (in Russian). DOI: 10.21177/1998-4502-2024-16-3-1110-1117

17. Xiao Wang, Yutong Wang, Jing Yang et al. The survey on multi-source data fusion in cyber-physical-social systems: Foundational infrastructure for industrial metaverses and industries 5.0. *Information Fusion*. 2024. Vol. 107. N 102321. DOI: 10.1016/j.inffus.2024.102321

18. Martínez-Gutiérrez A., Díez-González J., Perez H., Araújo M. Towards industry 5.0 through metaverse. *Robotics and Computer-Integrated Manufacturing*. 2024. Vol. 89. N 102764. DOI: 10.1016/j.rcim.2024.102764

19. Alkaeed M., Qayyum A., Qadir J. Privacy preservation in Artificial Intelligence and Extended Reality (AI-XR) metaverses: A survey. *Journal of Network and Computer Applications*. 2024. Vol. 231. N 103989. DOI: 10.1016/j.jnca.2024.103989
20. Hosseini S., Abbasi A., Magalhaes L.G. et al. Immersive Interaction in Digital Factory: Metaverse in Manufacturing. *Procedia Computer Science*. 2024. Vol. 232, p. 2310-2320. DOI: 10.1016/j.procs.2024.02.050
21. Starly B., Koprov P., Bharadwaj A. et al. "Unreal" factories: Next generation of digital twins of machines and factories in the Industrial Metaverse. *Manufacturing Letters*. 2023. Vol. 37, p. 50-52. DOI: 10.1016/j.mfglet.2023.07.021
22. Hosseini S., Abbasi A., Magalhaes L.G. Immersive Interaction in Digital Factory: Metaverse in Manufacturing. *Procedia Computer Science*. 2024. Vol. 232, p. 2310-2320. DOI: 10.1016/j.procs.2024.02.050
23. Shankar A., Gupta R., Kumar A. et al. Exploring the adoption of Enterprise Metaverse in Business-to-Business (B2B) organisations. *Industrial Marketing Management*. 2025. Vol. 124, p. 224-238. DOI: 10.1016/j.indmarman.2024.11.017
24. Kumar A., Shankar A., Behl A. et al. Implementing enterprise metaverse as a means of enhancing growth hacking performance: Will adopting the metaverse be a success in organizations? *Journal of Business Research*. 2025. Vol. 188. N 115079. DOI: 10.1016/j.jbusres.2024.115079
25. Shahzad K., Ashfaq M., Zafar A.U., Basahel S. Is the future of the metaverse bleak or bright? Role of realism, facilitators, and inhibitors in metaverse adoption. *Technological Forecasting and Social Change*. 2024. Vol. 209. N 123768. DOI: 10.1016/j.techfore.2024.123768
26. Salminen K., Aromaa S. Industrial metaverse – company perspectives. *Procedia Computer Science*. 2024. Vol. 232, p. 2108-2116. DOI: 10.1016/j.procs.2024.02.031
27. Shufei Li, Hai-Long Xie, Pai Zheng, Lihui Wang. Industrial Metaverse: A proactive human-robot collaboration perspective. *Journal of Manufacturing Systems*. 2024. Vol. 76, p. 314-319. DOI: 10.1016/j.jmsy.2024.08.003
28. Menezes C., Cunha H., Siqueira G. et al. Metaverse framework for power systems: Proposal and case study. *Electric Power Systems Research*. 2024. Vol. 237. N 111039. DOI: 10.1016/j.epsr.2024.111039
29. Junlang Guo, Jiewu Leng, J. Leon Zhao et al. Industrial metaverse towards Industry 5.0: Connotation, architecture, enablers, and challenges. *Journal of Manufacturing Systems*. 2024. Vol. 76, p. 25-42. DOI: 10.1016/j.jmsy.2024.07.007
30. Oliveri L.M., Lo Iacono N., Chiacchio F. et al. A Decision Support System tailored to the Maintenance Activities of Industry 5.0 Operators. *IFAC-PapersOnLine*. 2024. Vol. 58. Iss. 8, p. 186-191. DOI: 10.1016/j.ifacol.2024.08.118
31. Fede G., Sgarbossa F., Paltrinieri N. Integrating production and maintenance planning in process industries using Digital Twin: A literature review. *IFAC-PapersOnLine*. 2024. Vol. 58. Iss. 19, p. 151-156. DOI: 10.1016/j.ifacol.2024.09.124
32. Sai S., Sharma P., Gaur A., Chamola V. Pivotal role of digital twins in the metaverse: A review. *Digital Communications and Networks*. 2024. DOI: 10.1016/j.dcan.2024.12.003
33. Brahma M., Rejula M.A., Srinivasan B. et al. Learning impact of recent ICT advances based on virtual reality IoT sensors in a metaverse environment. *Measurement: Sensors*. 2023. Vol. 27. N 100754. DOI: 10.1016/j.measen.2023.100754
34. Khokhlov S., Abiev Z., Makkoev V. The Choice of Optical Flame Detectors for Automatic Explosion Containment Systems Based on the Results of Explosion Radiation Analysis of Methane- and Dust-Air Mixtures. *Applied Sciences*. 2022. Vol. 12. Iss. 3. N 1515. DOI: 10.3390/app12031515
35. Romashev A.O., Nikolaeva N.V., Gatiatullin B.L. Adaptive approach formation using machine vision technology to determine the parameters of enrichment products deposition. *Journal of Mining Institute*. 2022. Vol. 256, p. 677-685. DOI: 10.31897/PMI.2022.77
36. Boykov A.V., Payor V.A. Machine vision system for monitoring the process of levitation melting of non-ferrous metals. *Tsvetnye Metally*. 2023. N 4, p. 85-89 (in Russian). DOI: 10.17580/tsm.2023.04.11
37. Lee P., Heepyung Kim, Zitouni M.S. et al. Trends in Smart Helmets With Multimodal Sensing for Health and Safety: Scoping Review. *JMIR mHealth and uHealth*. 2022. Vol. 10. N 11. N e40797. DOI: 10.2196/40797
38. Wagner M., Leubner C., Strunk J. Mixed Reality or Simply Mobile? A Case Study on Enabling Less Skilled Workers to Perform Routine Maintenance Tasks. *Procedia Computer Science*. 2023. Vol. 217, p. 728-736. DOI: 10.1016/j.procs.2022.12.269
39. Rajendran S.D., Wahab S.N., Yeap S.P. Design of a Smart Safety Vest Incorporated With Metal Detector Kits for Enhanced Personal Protection. *Safety and Health at Work*. 2020. Vol. 11. Iss. 4, p. 537-542. DOI: 10.1016/j.shaw.2020.06.007
40. Abdollahi M., Quan Zhou, Wei Yuan. Smart wearable insoles in industrial environments: A systematic review. *Applied Ergonomics*. 2024. Vol. 118. N 104250. DOI: 10.1016/j.apergo.2024.104250
41. Koteleva N., Valnev V. Automatic Detection of Maintenance Scenarios for Equipment and Control Systems in Industry. *Applied Science*. 2023. Vol. 13. Iss. 24. N 12997. DOI: 10.3390/app132412997
42. Koteleva N., Simakov A., Korolev N. Smart Glove for Maintenance of Industrial Equipment. *Sensors*. 2025. Vol. 25. Iss. 3. N 722. DOI: 10.3390/s25030722
43. Surian D., Kim V., Menon R. et al. Tracking a moving user in indoor environments using Bluetooth low energy beacons. *Journal of Biomedical Informatics*. 2019. Vol. 98. N 103288. DOI: 10.1016/j.jbi.2019.103288
44. Yuhao Guo, Yicheng Li, Shaohua Wang et al. Pedestrian multi-object tracking combining appearance and spatial characteristics. *Expert Systems with Applications*. 2025. Vol. 272. N 126772. DOI: 10.1016/j.eswa.2025.126772
45. Padma B., Erukala S.B. End-to-end communication protocol in IoT-enabled ZigBee network: Investigation and performance analysis. *Internet of Things*. 2023. Vol. 22. N 100796. DOI: 10.1016/j.iot.2023.100796
46. Pease S.G., Conway P.P., West A.A. Hybrid ToF and RSSI real-time semantic tracking with an adaptive industrial internet of things architecture. *Journal of Network and Computer Applications*. 2017. Vol. 99, p. 98-109. DOI: 10.1016/j.jnca.2017.10.010
47. Mingsen Du, Yanxuan Wei, Yupeng Hu et al. Multivariate time series classification based on fusion features. *Expert Systems with Applications*. 2024. Vol. 248. N 123452. DOI: 10.1016/j.eswa.2024.123452
48. Dempster A., Petitjean F., Webb G.I. ROCKET: exceptionally fast and accurate time series classification using random convolutional kernels. *Data Mining and Knowledge Discovery*. 2020. Vol. 34. Iss. 5, p. 1454-1495. DOI: 10.1007/s10618-020-00701-z
49. Lines J., Bagnall A. Time series classification with ensembles of elastic distance measures. *Data Mining and Knowledge Discovery*. 2015. Vol. 29. Iss. 3, p. 565-592. DOI: 10.1007/s10618-014-0361-2

50. Chaudhuri A., Behera R.K., Bala P.K. Factors impacting cybersecurity transformation: An Industry 5.0 perspective. *Computers & Security*. 2025. Vol. 150. N 104267. DOI: 10.1016/j.cose.2024.104267

51. Azad M.A., Abdullah S., Arshad J. et al. Verify and trust: A multidimensional survey of zero-trust security in the age of IoT. *Internet of Things*. 2024. Vol. 27. N 101227. DOI: 10.1016/j.iot.2024.101227

52. Itodo C., Ozer M. Multivocal literature review on zero-trust security implementation. *Computers & Security*. 2024. Vol. 141. N 103827. DOI: 10.1016/j.cose.2024.103827

***Authors*: Natalia I. Koteleva,** *Candidate of Engineering Sciences, Associate Professor* (*Empress Catherine II Saint Petersburg Mining University, Saint Petersburg,* Russia), *koteleva_ni@pers.spmi.ru, https://orcid.org/0000-0002-5970-4534*, **Vladislav V. Valnev,** *Postgraduate Student* (*Empress Catherine II Saint Petersburg Mining University, Saint Petersburg, Russia*), *https://orcid.org/0000-0001-6642-8585*, **Aleksandr S. Simakov,** *Candidate of Engineering Sciences, Associate Professor* (*Empress Catherine II Saint Petersburg Mining University, Saint Petersburg, Russia*), *https://orcid.org/0000-0002-9237-4469*, **Maysam Mohammadzadeh Shirazi,** *PhD, Head of Department* (*Shiraz University, Shiraz, Iran*), *https://orcid.org/0000-0001-8382-9460*.

The authors declare no conflict of interests.

ISSN 2411-3336; e-ISSN 2541-9404

JOURNAL OF MINING INSTITUTE

Zapiski Gornogo instituta

Journal homepage: pmi.spmi.ru

Research article

Geotechnical Engineering and Engineering Geology

Centrifugal pump and electrical motor fault detection with motor current signature analysis and automated machine learning

Roman R. Khalikov[1], **Mikhail Yu. Chernetskiy**[1], **Ilia E. Revin**[2], **Vadim A. Potemkin**[2]✉

[1] *ROTEC Digital Solutions JSC, Moscow, Russia*

[2] *ITMO University, Saint Petersburg, Russia*

***How to cite this article*:** Khalikov R.R., Chernetskiy M.Yu., Revin I.E., Potemkin V.A. Centrifugal pump and electrical motor fault detection with motor current signature analysis and automated machine learning. Journal of Mining Institute. 2025. Vol. 275, p. 42-55.

Abstract

Centrifugal pumps, as key components of hydraulic systems, play a fundamental role in ensuring the reliable operation of numerous industrial processes in sectors such as energy, chemical production, and oil refining, where uninterrupted equipment performance is of critical importance. Failures of centrifugal pumps can result in substantial financial losses due to costly repairs and unplanned production downtime. This paper presents an innovative approach to diagnosing and detecting faults in centrifugal pumps. The method is based on the application of Motor Current Signature Analysis (MCSA) in combination with automated machine learning (AutoML) technologies. Such an approach enables efficient and highly accurate identification of early signs of equipment malfunction. The experimental study was conducted using an open dataset collected under conditions close to real-world operation. The proposed method achieved a fault detection accuracy of 89 %, which significantly exceeds the performance of the traditional gradient boosting method. This confirms the advantage of a comprehensive model developed through AutoML. Further improvement in diagnostic accuracy was made possible by applying an enhanced Park's vector transformation to the raw current and voltage data. This approach makes it possible to detect even subtle anomalies in pump operation, thereby strengthening the capability for early fault prediction. The study not only highlights the potential of MCSA as a non-invasive and scalable tool for equipment condition monitoring but also demonstrates the promise of AutoML for technical diagnostics of industrial pumps.

Keywords

machine learning; electric motor; gradient boosting; composite model; AutoML; fault detection; time series

Received: 09.04.2025 ***Accepted: 25.08.2025*** ***Online: 13.10.2025*** ***Published: 31.10.2025***

Introduction

The global pump market reached a volume of USD 59.2 billion in 2023*, with centrifugal pumps representing its largest segment. These pumps are critically important for combined-cycle power plants, coal-fired thermal power stations, nuclear reactors, chemical facilities, and other industries [1, 2]. According to data from the European Association of Pump Manufacturers, an oil refinery with a capacity of 300,000 barrels per day may operate up to 650 pumps, each of which requires thorough monitoring to prevent failures. Without intelligent systems capable of automatically analyzing sensor data and detecting anomalies [3], timely monitoring of such a fleet of equipment becomes impossible.

* Global Pump Market Outlook. Spring 2024. Sample Material. URL: https://www.oxfordeconomics.com/resource/global-pump-market-outlook-2024/ (accessed 10.04.2025).

One of the promising methods for pump condition monitoring is Motor Current Signature Analysis (MCSA). This approach enables the assessment of equipment condition based on the analysis of consumed current using low-cost sensors and well-established signal processing techniques. MCSA is particularly effective for centrifugal pumps, as it allows the detection of problems at an early stage without direct access to the pump, in contrast to vibration, acoustic or pressure analysis methods.

Despite the potential of MCSA, its manual or semi-automated application requires significant effort from experts and developers, which hinders scalability across a large number of units. A possible solution lies in diagnostic systems based on machine learning (ML), which have been investigated for more than 15 years. Most MCSA-related studies focus on motor diagnostics – such as rotor bar breakage [4, 5], stator winding faults [6], and bearing defects [7-9]. Typical approaches include feature extraction in the time, frequency, and time-frequency domains [10-12], demodulation transformations [13, 14] and their combinations with various ML models. However, research dedicated specifically to pumps is very limited due to the lack of high-quality data. The majority of studies rely on synthetic datasets [8] or laboratory test rigs [15, 16], which constrains the applicability of their findings under real operating conditions. An exception is the study by C.E.Sunal et al. [9], which employed industrial data from centrifugal pumps. Nevertheless, its technical implementation details are insufficiently disclosed.

Classical machine learning methods and deep learning (DL) approaches are promising [17], yet they are constrained by the limited availability of labeled data. In practice, traditional ML is capable of solving tasks under conditions of data scarcity. However, in such cases the creation of an informative feature space becomes critically important. An effective method for generating additional informative signals for equipment analysis and feature construction remains the use of the Extended Park's Vector Approach, which mitigates the influence of supply frequency and highlights fault-related features [18]. The development of automated machine learning (AutoML) further opens new opportunities. AutoML simplifies data preprocessing, model construction, and hyperparameter tuning, enabling efficient utilization of data even in the presence of class imbalance [19-21].

The objective of this study is to develop a methodology for fault detection in pump units with electric motors based on current signature analysis under conditions of limited data availability. To this end, the research addressed the task of identifying an optimal combined approach that integrates MCSA techniques, the generation of an informative feature space, and AutoML for early-stage fault classification of centrifugal pumps and electric motors using an open dataset simulating real operating conditions. The study considers a scenario in which a fault with similar signal manifestations may occur either in the motor or in the pump. A series of experiments evaluated the impact of the Extended Park's Vector Approach on diagnostic accuracy. The results demonstrated that AutoML is capable of automatically generating models with accuracy exceeding 89 %, outperforming optimized gradient boosting. This confirms the potential of AutoML for industrial diagnostic applications.

Related works

Motor current signature analysis of pumps and electric motors. Several approaches have been proposed for anomaly detection and fault classification of pumps and motors using MCSA [22]. One of the more recent methods, presented by Y.Han et al. [15], focuses on unsupervised anomaly detection through a comprehensive framework combining MCSA, the Extended Park's Vector Approach, a CNN-LSTM attention model, and spectral analysis. The model attempts to reconstruct the instantaneous current amplitude by leveraging the original phase signals along with additional voltage features. The authors conducted an in-depth analysis and manually identified three levels of cavitation as well as the number of damaged impeller blades. Decision-making was based on a statistically computed threshold in the frequency domain and on the residual difference between measured and predicted values. All tasks were performed under variable flow conditions.

C.E.Sunal et al. [9] applied a classical approach by visualizing the components of the Park's vector. They achieved an accuracy ranging from 85.5 to 100 % (depending on the signal sampling frequency) in the image classification task using a fine-tuned ResNet-34 model. The visual representation addressed the data imbalance problem by effectively augmenting the existing dataset. The model was trained and validated at frequencies of 1500 and 3000 Hz, while the test data included 1500, 3000, and 4500 Hz. The data were collected from pumps operating under different working conditions. This approach enabled the supervised detection of anomalies by identifying defective pumps. A detailed review by the same authors [8] demonstrates that deep learning models are capable of solving motor and pump fault detection tasks with high accuracy. Only a small fraction of classical machine learning models achieve accuracy above 90 %.

However, these studies lack information regarding the severity of faults. Signals of advanced defects can be identified visually through frequency analysis, yet experts may encounter difficulties in detecting weak anomalies. Faults may be masked within the sidebands of the carrier frequency or bearing frequencies, remaining unnoticed after demodulation due to the low spectral power of defect harmonics and high noise levels. Machine learning methods allow for the prediction of emerging faults, but the limited volume of available data can critically affect deep learning models, leading to overfitting. An additional challenge arises when the operating conditions of the pump or motor change, necessitating the collection of new data.

Application of AutoML in fault detection. Initially, AutoML was focused on automating typical tasks of ML engineers, thereby making machine learning more accessible to domain experts. However, the evolution of the field has demonstrated that AutoML can outperform humans in designing model architectures for both classical ML [23, 24], and deep learning [25]. A variety of AutoML frameworks exist, but to the best of the authors' knowledge, only two of them – FEDOT and TPOT [26]) – are capable not only of automating model search and hyperparameter optimization, but also of generating composite models using genetic algorithms to improve performance. A composite model is a special type of ensemble, resembling stacking. It can be represented as a graph, where each node corresponds to a model or a data processing method. By combining nodes and connections, it is possible to obtain an optimal structure tailored to the specific dataset.

Previous studies on fault diagnosis using AutoML demonstrate that such approaches enable the development of complex models with higher accuracy than individual algorithms. J.Zhang et al. [12] showed that TPOT outperformed SVM and XGBoost, achieving accuracy between 95.8 and 99.3 % under different signal-to-noise ratios in vibration signals. Using wavelet decomposition, A.S.Maliuk et al. [27] successfully classified three types of bearing faults (inner race, outer race, and ball) as well as the normal condition. Similarly, R.H.Hadi et al. [28] reported that the AutoML framework PyCaret achieved 95.6 % accuracy on new data without employing composite models. M.Cerrada et al. [29] compared the results of TPOT and H2O [30] in the task of classifying the severity of three types of gear faults. Both frameworks demonstrated comparable accuracy (exceeding 96 %) across all scenarios, on par with other ML and DL methods. The authors noted that the key features used by the models were consistent, despite differences in their architectures.

The main advantage of FEDOT over TPOT and other frameworks is its ability to generate models with high variability. High variability of composite models refers to the capability of constructing a directed acyclic graph, where the nodes represent data preprocessing operations or trained models, and the edges define the flow of results between nodes. FEDOT allows the connection of preceding nodes to any subsequent nodes. In this way, FEDOT generalizes the approach to composite model construction implemented in TPOT. Moreover, FEDOT supports diverse data types and tasks, offering a flexible interface for interaction. Studies employing FEDOT for motor diagnostics are very

limited. In the work of I.Revin et al. [31] FEDOT was tested on time series classification tasks using public datasets. In 90 % of cases, the performance of FEDOT's composite models exceeded or approached that of state-of-the-art algorithms, confirming their applicability to tasks analogous to fault detection.

Methods

Experimental data. Publicly available datasets for analyzing motor current and voltage, particularly for motors coupled with pumps, are limited. Most existing datasets cover only a narrow range of fault types, motor power ratings, and operating modes. However, S.Bruinsma et al. [7] introduced a dataset that partially addresses these issues. The dataset includes three-phase currents and voltages recorded after a frequency converter for induction motors rated at 11 and 22 kW, as well as vibration signals measured at five points on the motor and pump. The data were collected at a sampling frequency of 20 kHz. Electrical signals were recorded for 15 s with a 2 min interval between measurements. The signals were not processed in any way; the raw 24-bit data were stored directly in CSV files. In total, 20 fault types were recorded, each with three severity levels. Data for healthy states were measured 94 times, while the number of records for other faults varied from 3 to 10. Based on this, the dataset is unbalanced, with the proportion of healthy states exceeding faulty ones by approximately 5:1. Data labeling was performed automatically at the time of acquisition, with each fault recorded separately. The dataset was not validated by independent experts, but it was collected at different motor speeds, which increases its applicability to real industrial conditions. Despite the authors' efforts, this dataset has rarely been used in studies on current-based diagnostics of pumps.

For the experiments, the minimum severity level of faults was selected, as the primary objective was early detection. Measurements were carried out at 100 % motor speed. The task was formulated as a multiclass classification problem with seven classes: healthy state, motor bearing faults (inner race, outer race, ball), pump bearing fault (simultaneous inner and outer race), and looseness of motor and pump mountings. The data were pre-analyzed to examine signal properties before and after pre-processing, as well as to identify outliers. The seven selected classes represent the most challenging cases for defect analysis. The faults in the dataset were artificially induced. Bearing race damages were introduced from the rolling element side using a milling cutter, resulting in grooves spanning the entire width of the race with a length of 1 mm and a depth of 350 μm. The degree of damage varied depending on the number of such scratches. The rolling elements themselves were damaged with a rotary engraver across the entire ball surface, producing scratch-like defects over the ball surfaces [7]. Looseness of the mountings was simulated by reducing the tightness of already fastened bolts.

Data preprocessing and feature extraction. The original dataset contains files for each phase and signal type, where the columns correspond to 15-second measurements. The files were transformed into an array of size $N_{\text{samp}} \times N_{\text{chan}}$, where $N_{\text{chan}} = 6$ (three current phases and three voltage phases). The array includes all available data for both healthy and faulty states, with corresponding class labels. Thirty percent of the measurements for each state were reserved for the test set.

In part of the experiments, additional data channels were introduced using the Extended Park's Vector Approach (up to six channels). This transformation enhances the diagnostics of three-phase electrical machines by minimizing the influence of the fundamental supply frequency (50 Hz) and highlighting fault-related features. For example, the extended Park's transformation for current is defined as a linear combination of the three phases, which simplifies the analysis of asymmetry and harmonics:

$$\begin{cases} i_a = \left(2i_u - i_v - i_w\right)/3; \\ i_b = \left(i_u - i_w\right)/\sqrt{3}, \end{cases}$$

where i_u, i_v, i_w correspond to the three current phases, and i_a, i_b represent the real and imaginary components of the Park's vector.

The linear transformation makes it possible to obtain up to four data channels (two for current and two for voltage). These vectors can also be used to generate up to four additional channels by computing the squared modulus of the Park's vector:

$$i_{\text{inst}} = \left| i_a + j i_b \right|,$$

where i_{inst} denotes the instantaneous amplitude.

This transformation removes the fundamental 50 Hz component from the signal. After generating the additional channels, the sample array was divided into time windows of 1 s (20,000 samples per window) and converted into a three-dimensional tensor. The tensor dimensions corresponded to the number of windows, window size, and number of data channels. For each window, feature extraction was performed according to standard MCSA practices [32]. Features in the time and frequency domains were calculated, including mean value, variance, root mean square (RMS), crest factor, kurtosis, and skewness.

The energy of the approximation coefficients from the first, second, and third levels of the wavelet packet decomposition was added in the time-frequency domain. In total, 28 features were calculated for each data channel, resulting in up to 224 features. The complete list of features is presented in Table 1. At the final stage, min-max scaling was applied to both the training and test datasets.

Table 1

Generated functions

Time domain		Frequency domain	
Mean value	$\bar{x} = \frac{1}{n}\sum_{i=1}^{n} x_i$	Mean value	$\overline{F(x)} = \frac{1}{n}\sum_{i=1}^{n} F_i(x)$
Variance	$\sigma^2_{\text{time}} = \frac{1}{n}\sum_{i=1}^{n}(x_i - \bar{x})^2$	Variance	$\sigma^2_{\text{freq}} = \frac{1}{n}\sum_{i=1}^{n}(F_i(x) - \overline{F(x)})^2$
RMS	$RMS_{\text{time}} = \sqrt{\frac{1}{n}\sum_{i=1}^{n} x_i^2}$	RMS	$RMS_{\text{freq}} = \sqrt{\frac{1}{n}\sum_{i=1}^{n} F_i(x)^2}$
Peak value	$PV_{\text{time}} = \max(\lvert x \rvert)$	Peak value	$PV_{\text{freq}} = \max\left(\left\lvert F(x) \right\rvert\right)$
Crest-factor	$CF_{\text{time}} = \frac{PV_{\text{time}}}{RMS_{\text{time}}}$	Crest-factor	$CF_{\text{freq}} = \frac{P\upsilon T_{\text{freq}}}{RMS_{\text{freq}}}$
Kurtosis	$Kurt_{\text{time}} = \frac{\sum_{i=1}^{n}(x_i - \bar{x})^4}{n(\sigma^2_{\text{time}})^2} - 3$	Kurtosis	$Kurt_{\text{freq}} = \frac{\sum_{i=1}^{n}(F_i - \overline{F(x)})^4}{n(\sigma^2_{\text{freq}})^2} - 3$
Skewness	$Sk_{\text{time}} = \frac{\sum_{i=1}^{n}(x_i - \bar{x})^3}{n\left(\frac{1}{n}\sum_{i=1}^{n}(x_i - \bar{x})^2\right)^{\frac{3}{2}}}$	Skewness	$Sk_{\text{freq}} = \frac{\sum_{i=1}^{n}(F_i(x) - \overline{F(x)})^3}{n\left(\frac{1}{n}\sum_{i=1}^{n}(F_i(x) - \overline{F(x)})^2\right)^{\frac{3}{2}}}$
Clearance factor	$Clf = \frac{PV_{\text{time}}}{\left(\frac{1}{n}\sum_{i=1}^{n}\sqrt{\lvert x_i \rvert}\right)^2}$	FFT peak value frequency	$PF = \arg\max\left(\left\lvert F(x) \right\rvert\right)$
Line integral	$LI = \sum_{i=1}^{n}\lvert x_{i+1} - x_i \rvert$	Spectrum energy	$E = \sum_{i=1}^{n} F_i(x)^2$
Impulse factor	$IF = \frac{PV_{\text{time}}}{\frac{1}{n}\sum_{i=1}^{n}\lvert x_i \rvert}$	Time and frequency domain	
Shape factor	$SF = \frac{RMS_{\text{time}}}{\frac{1}{n}\sum_{i=1}^{n}\lvert x_i \rvert}$	Wavelet packet decomposition detail coefficient energy	$cD_i = \sum_{j=1}^{n_i} D_{i,j},\ i = 1, 2, 3$
Peak-to-peak value	$PtP = \max x_i - \min x_i$	Wavelet packet decomposition approximate coefficient energy	$cA_i = \sum_{j=1}^{n_i} A_{i,j},\ i = 1, 2, 3$

Shannon's entropy	$H = -\sum_{i1}^{n} x_i^2 \log\left(x_i^2\right)$

As part of the study, four datasets were constructed to investigate the impact of additional channels on the effectiveness of fault diagnostics using MCSA. The first dataset (NoPark) contained only the preprocessed raw current and voltage data and served as the baseline for evaluating classification accuracy improvements obtained by adding Park's vector components. The second dataset consisted solely of instantaneous current and voltage vectors. This dataset was used to assess the demodulation effect of the Extended Park's Vector Approach and to compare the expressiveness of the data against unprocessed current and voltage signals. The third dataset combined the previous two and served as the primary dataset for evaluating the effectiveness of the proposed algorithms, as it contained the largest amount of signal information. The fourth dataset included Park's vector components as well as the instantaneous amplitude. This dataset was used to evaluate the amount of fault-related information contained in the Park's vector components (each component representing a linear combination of three phases) and to reduce the dimensionality of the feature space. Table 2 summarizes the characteristics of each dataset used in the experiments.

Table 2

Datasets

Experiment	Data	Training dataset size (number of samples × number of features)
NoPark	Three current and voltage phases	1680 × 168
OnlyInstAmp	Instantaneous current and voltage amplitude	1680 × 56
WithInstAmp	Three phases and instantaneous current and voltage amplitude	1680 × 224
FullPark	Park's vectors and instantaneous amplitude	1680 × 168

Classification algorithms. Two approaches were used for fault classification. During preliminary training, the gradient boosting algorithm demonstrated superior performance compared to other classical machine learning methods. This result is consistent with the general consensus that gradient boosting is among the most effective techniques for such tasks. Thus, the first approach involved the use of gradient boosting on decision trees implemented through the CatBoost library [33]. The CatBoost classifier was trained using hyperparameters optimized with the Optuna tuning framework [23].

For hyperparameter sampling in Optuna, the Tree-structured Parzen Estimator algorithm [24, 34] was applied with 10 initial trials. As the adaptive pruning algorithm (pruner), Hyperband [34] was used with a minimum resource allocation of 50, a maximum of 400, a reduction factor of 2, and 10 bootstrap samples. Thanks to Optuna's multithreading capabilities, hyperparameter optimization was significantly accelerated, with approximately 3000 configurations tested in each experimental scenario. The maximum number of training iterations for CatBoost was set to 400.

During the optimization process, Optuna tuned the following hyperparameters: loss function – MultiClass (multiclass) or MultiClassOneVsAll (multiclass OneVsAll); learning rate – from 0.01 to 1 with a step of 0.001; L2 regularization on leaves – from 1 to 200 with a step of 1; boosting type – Ordered or Plain; class weight calculation formula – Balanced or SqrtBalanced; tree depth – from 1 to 10 with a step of 1; and feature fraction (percentage of random subspace) – from 0.01 to 1 with a step of 0.01.

In the second approach, the open-source AutoML platform FEDOT [20] was applied to solve the same classification task. The FEDOT platform is capable of automatically generating, optimizing, and tuning composite models using a directed acyclic graph representation and genetic algorithms. In this study, the best quality preset was used, which allows the inclusion of any available machine learning models in the construction of the composite model.

The early stopping criterion was set to 10 generations without improvement, and the maximum number of generations was limited to 100. During hyperparameter tuning with Optuna, the objective was to maximize the macro-averaged F1-score on the test dataset. In the case of composite model construction, the FEDOT framework autonomously attempted to maximize the macro-averaged F1-score using five-fold cross-validation. To minimize the effect of class imbalance, macro-averaging was applied. Since the FEDOT framework does not support macro-averaging natively, a custom metric was implemented.

Results

Exploratory data analysis. The original recorded signal is shown in Fig.1. The waveform deviates substantially from an ideal sinusoid due to the use of a frequency converter, with the largest distortions observed in the voltage. Analysis of the signal distributions revealed no significant differences between the raw data for healthy and faulty states. However, in the healthy state data (healthy 1 at 100 % speed, 15th measurement), a motor shutdown process was detected, which was excluded as an outlier.

The Extended Park's Vector Approach enabled an alternative representation of the data. The effect of the transformation on the signal spectrum is shown in Fig.2. As severity level 3, a motor signal with a damaged bearing outer race was used. Demodulation redistributes the spectral amplitude to other frequencies, thereby facilitating fault detection. Park's transformation suppresses the supply carrier frequency while amplifying other significant harmonics. This alters the distribution of the signal when comparing healthy and faulty states, which in turn affects the distribution of the extracted features.

A visual analysis of the Park's vector components was conducted. Figure 3 illustrates the difference between a bearing outer race fault (BPFO) at severity levels 1 and 3 at 100 % motor speed. The main distinction between the healthy state and both faulty states is driven by the larger volume of healthy state data. However, it is evident that the pattern at severity level 3 is more distorted and asymmetric compared to severity level 1, which remains closer to the healthy state. This indirectly indicates the difficulty of detecting faults at early stages, even when applying machine learning methods.

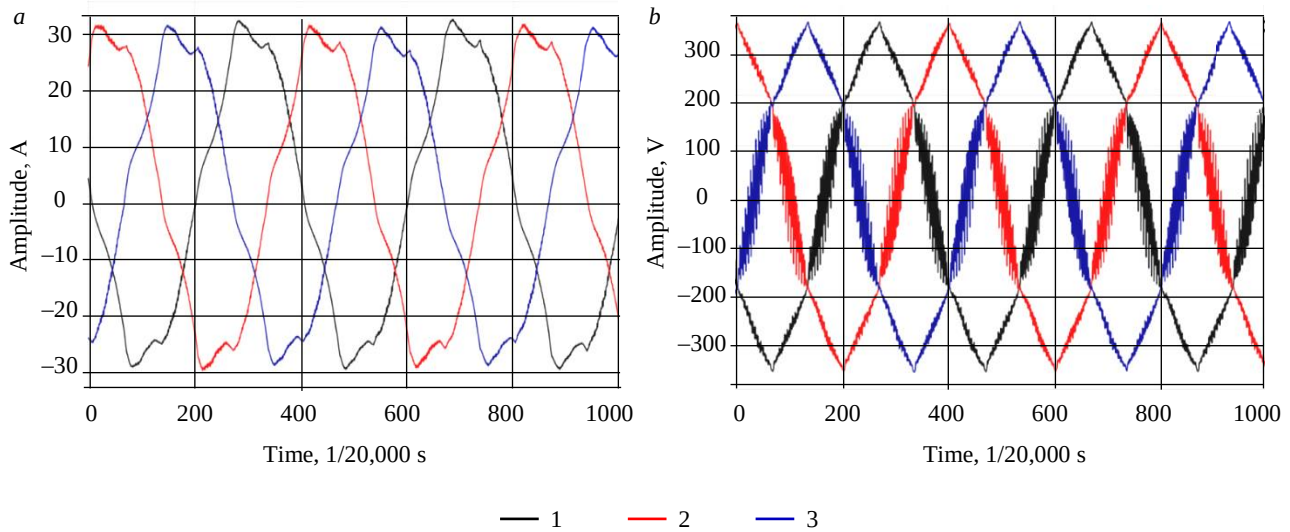

Fig.1. Original current signal (*a*) and voltage signal (*b*)
1, 2, 3 – phases

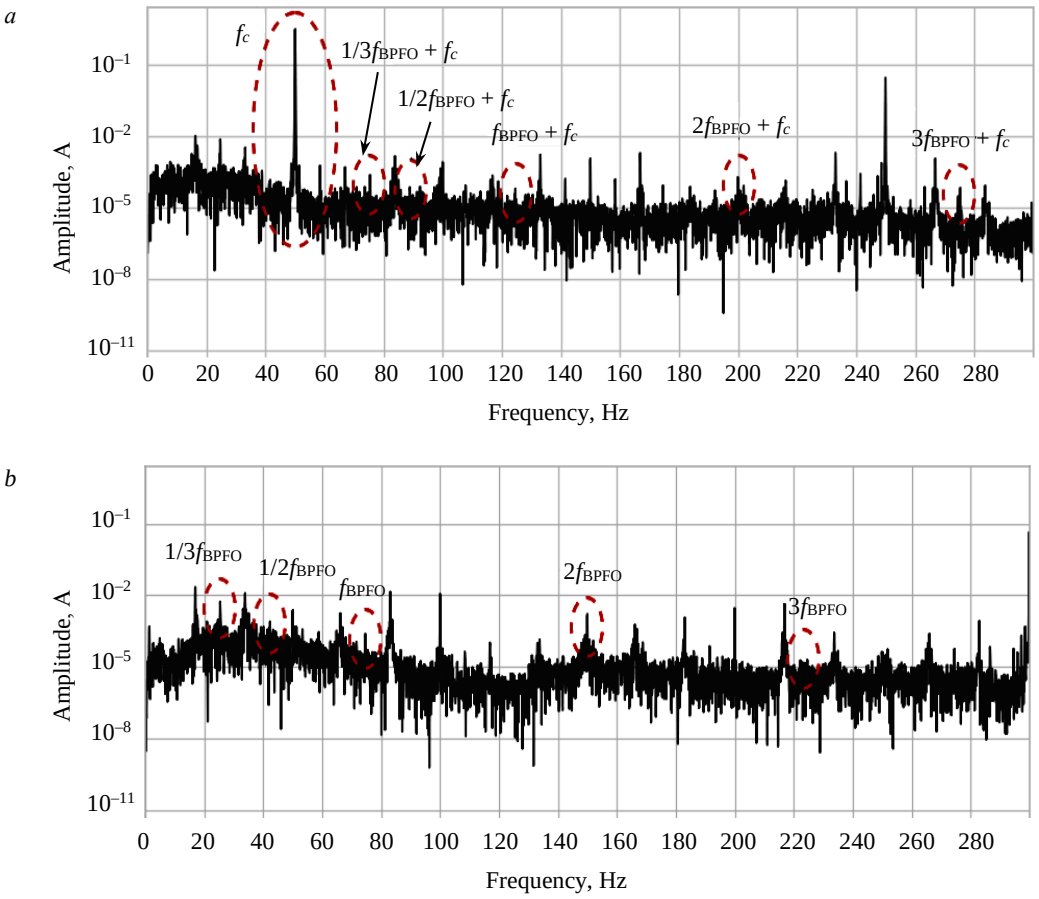

Fig.2. Comparison of the spectra of the original current signal and the instantaneous amplitude: *a* – spectrum of the instantaneous current phase; *b* – spectrum of the generalized current after Park's transformation

f_c – carrier frequency 50 Hz; $f_{BPFO} \approx 74{,}7$ Hz depending on the bearing and motor rotational frequency

Analysis of feature distributions using boxplots confirmed that the proposed features capture class differences and can improve classification performance. Figure 4 presents three informative features: one generated from the raw voltage data; one obtained from the spectrum of the α-component of Park's transformation; and one computed through wavelet packet decomposition of the instantaneous current. Each of these features can be effectively used for training ML models.

Analysis of AutoML results. A time budget of 30 min was allocated for generating composite machine learning models, and 5 min for hyperparameter tuning. The experiments were carried out in three stages:

• Baseline: a combination of a quantile feature generator and a random forest model.

• Comparison with SOTA: the best result of the proposed approach was compared with the performance of other time series classification models using the F1-score metric.

• Ensembling: features from the top-performing models were combined into a single matrix, after which the model selection process was repeated.

Figure 5 visualizes the process of model composition. An improvement in model quality is observed with each generation, followed by metric stabilization, which confirms FEDOT's ability to converge to an optimal solution within a reasonable time. Analysis of the diversity within the model population showed that, at the beginning, the distribution of metrics was wide, reflecting variability

in

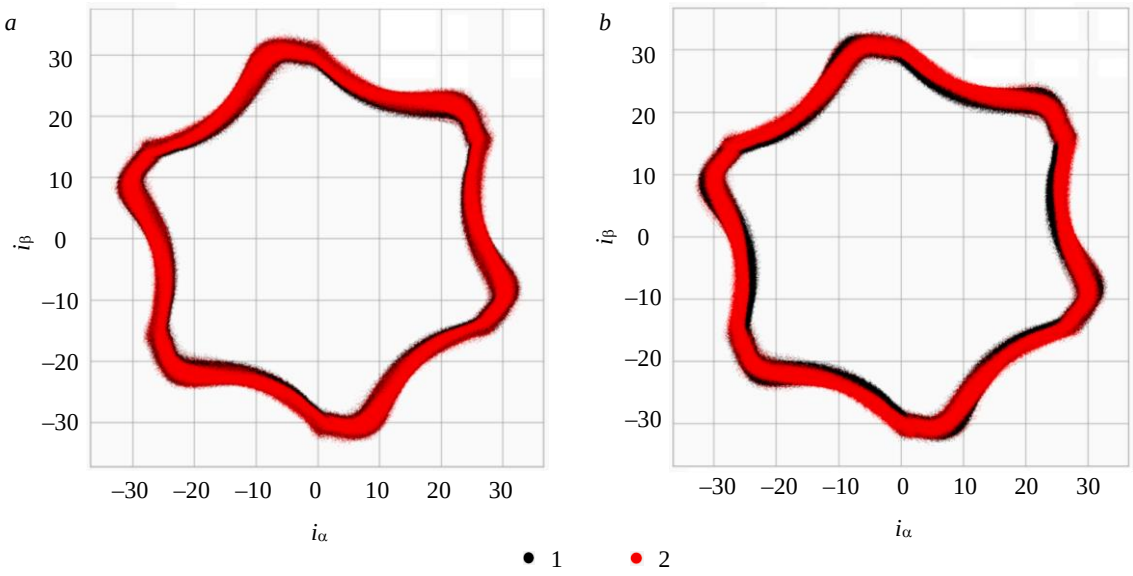

Fig.3. Comparison of the structure of Park's vector components for severity level 1 (*a*), severity level 3 (*b*), and the fault-free state

1 – components of Park's transformation unrelated to faults, identical in both plots;
2 – fault-related components that vary with the severity level in each case;
i_α and i_β are real and imaginary components of Park's vector

performance. At later stages, the distribution narrows as the target metric increases and the standard deviation decreases. Evolutionary optimization thus ensures both high model quality and the preservation of diversity, even in the final generations.

Advantages of the approach over traditional gradient boosting:

• Flexible model composition – examples of the generated pipelines (Fig.6) demonstrate the framework's ability to combine heterogeneous preprocessing methods and algorithms.

• Automation of labor-intensive stages – automatic feature selection, model choice, and hyperparameter tuning significantly reduce development time.

• Integration of AutoML and MCSA – the results confirm that combining AutoML with MCSA enables the development of effective diagnostic systems for industrial equipment.

Model evaluation. The macro F1-scores for both algorithms, measured on the test dataset, are presented in Table 3. The CatBoost algorithm achieved a maximum macro F1-score of 0.68 when trained on data without Park's transformation. Models trained on other datasets showed slightly lower performance with nearly comparable scores. The FEDOT framework demonstrated superior results, achieving a macro F1-score above 0.89. The best-performing model was trained on data combining raw and instantaneous amplitude signals. The composite model begins with a resampling node, which does not apply any transformations in the case of a multiclass task. The second node applies the FastICA algorithm with unit variance whitening, without dimensionality reduction, and passes the result to the next node. The third node is a logistic regression model with an inverse regularization strength of C = 5.88. The normalization node applies min-max scaling to the probabilities produced by the logistic regression. The final node performs quadratic discriminant analysis (QDA) on the normalized probabilities. The resulting pipeline is simple to understand and interpret; it confirms that the data are well-prepared and provides all the necessary information on the faults. Even in cases where pump and motor faults produce similar spectral characteristics, the algorithm clearly distinguishes them. A comparison of the confusion matrices for the best CatBoost and composite models is shown in Fig.7.

Table 3

F1-score for the CatBoost algorithm and the composite model

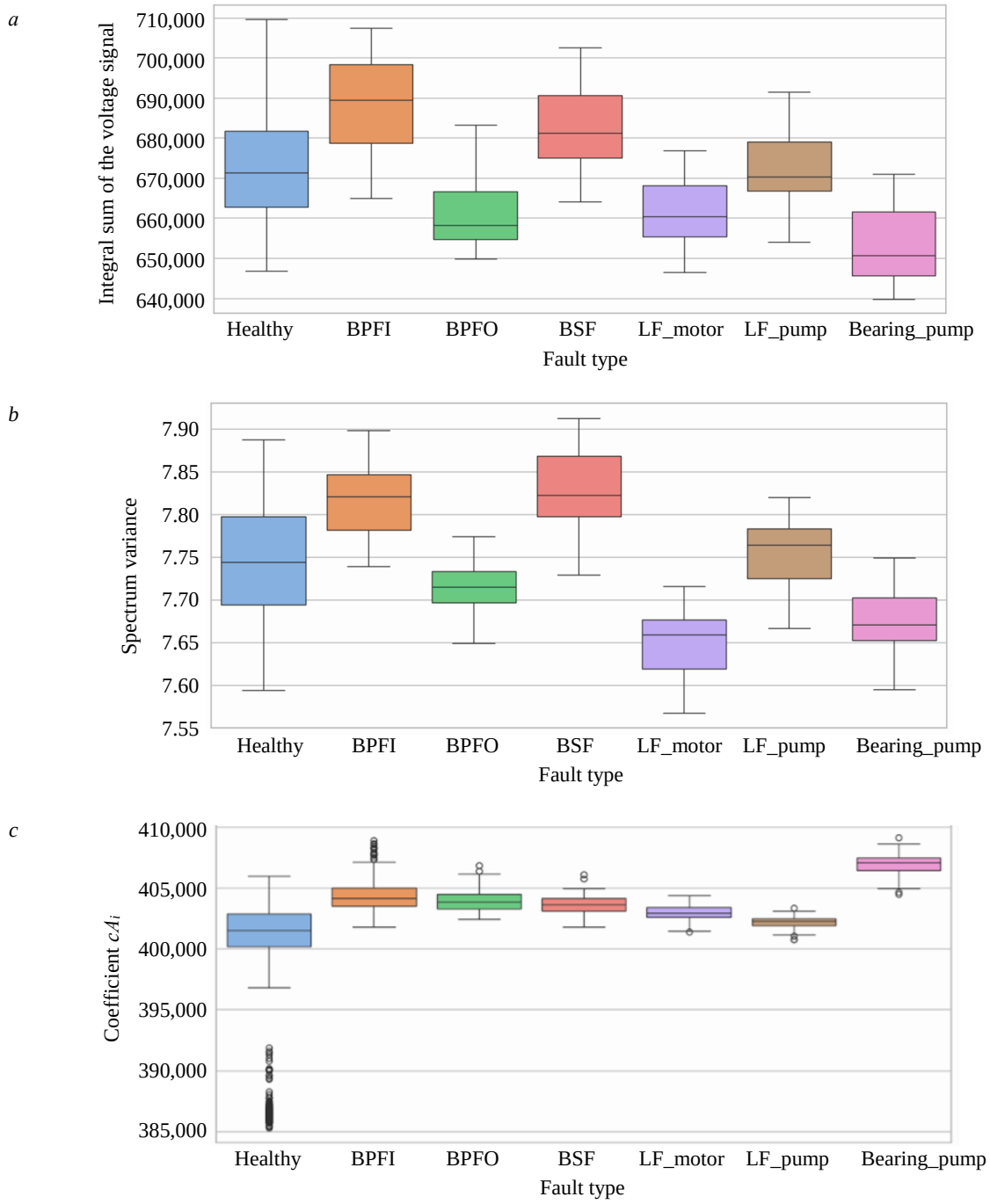

Fig.4. Example distributions of extracted features: *a* – first voltage phase, linear integral; *b* – computed spectrum variance; *c* – instantaneous current amplitude, coefficient *cAi* (energy of approximation coefficients from the wavelet packet decomposition)

Healthy – absence of any faults; BPFI, BPFO, and BSF – faults associated with inner race, outer race, and ball defects of the motor bearing; LF_motor and LF_pump – looseness in motor and pump mountings; Bearing_pump – pump bearing fault with damage to both races

Experiment	CatBoost	Composite model	Experiment	CatBoost	Composite model
NoPark	0.68	0.76	WithInstAmp	0.65	0.89
OnlyInstAmp	0.66	0.65	FullPark	0.64	0.86

The models experience the greatest difficulty in accurately classifying outer and inner race faults. Both models exhibit confusion between inner race defects and rolling element defects. This can be explained by the fact that the induced faults represent an early stage of defect development and are

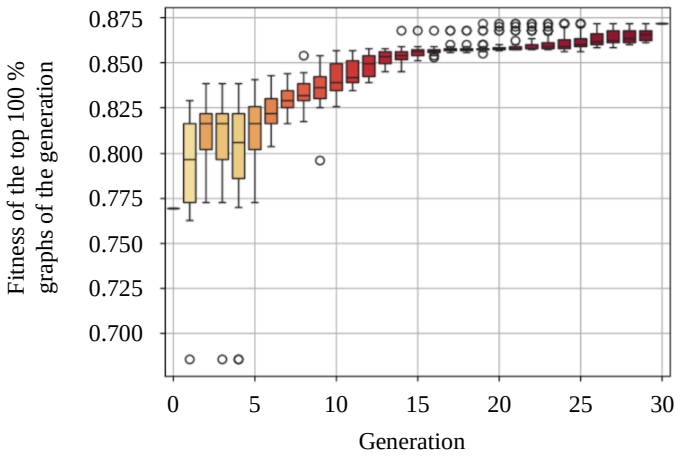

Fig.5. Evolution of model composition performance

weakly expressed in the signals, while the extracted features showed similar distributions for these confused fault types. For the composite model, inner race faults proved to be the most challenging to recognize. Similar behavior was observed during the preliminary selection of the best classical ML model, indicating the general difficulty of identifying this type of defect. The gradient boosting algorithm was able to clearly identify the inner race fault, but encountered problems with other fault types, which may suggest the existence of a trade-off between the decision boundaries separating the classes. It is worth noting that both classifiers did not confuse most of the identical faults of the motor and pump, which indicates a clear separation of these defects in terms of the generated features. The composite model also demonstrated the lowest false positive rate in detecting anomalies associated with healthy state labeling.

Discussions and limitations

The application of the CatBoost algorithm with various combinations of additional features did not achieve better results in detecting such pump unit faults as motor bearing defects (inner race, outer race, ball), pump bearing defect (simultaneous inner and outer race), and looseness of motor and pump mountings, compared to the approach proposed in this paper. The composite model demonstrated superior performance when using features generated from instantaneous current and voltage amplitudes. The results of the composite model confirm the preliminary analysis and clearly show that the Extended Park's Vector increases the amount of useful information. The study confirmed that this approach should be applied in combination with raw data to achieve the best results.

An important outcome of the study is the demonstration that the classifiers were able to distinguish between similar faults in the electric motor and the pump. The obtained results suggest that the proposed model can be trained to detect anomalies with a low false positive rate, even when using data corresponding to low fault severity levels.

It should be noted that several practical issues remain unresolved within the scope of this study and require further investigation. In this work, we used the maximum available motor speed, whereas in real applications the motor may operate under varying conditions. Variable frequency drives are often employed to regulate motor speed, and such drives were present during the recording of the dataset used. Variable frequency drives alter the amplitude and frequency of the motor supply, which fundamentally changes the recorded signals and the extracted features – resulting in data drift. The same effect would occur when replacing the motor or pump model. Due to data drift, the model's

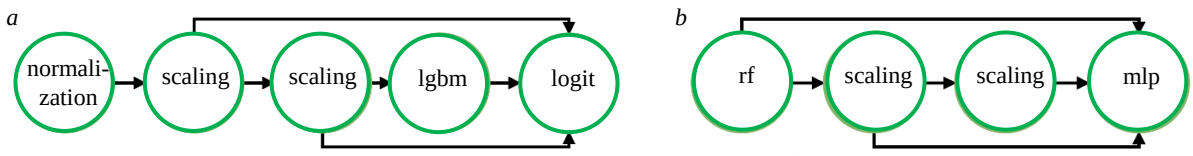

Fig.6. Examples of composite pipelines generated by AutoML: *a* – linear pipeline with boosting; *b* – linear pipeline with perceptron

Computational nodes: normalization; scaling; lgbm – light gradient boosting machine; logit – logistic regression; rf – random forest; mlp – multilayer perceptron

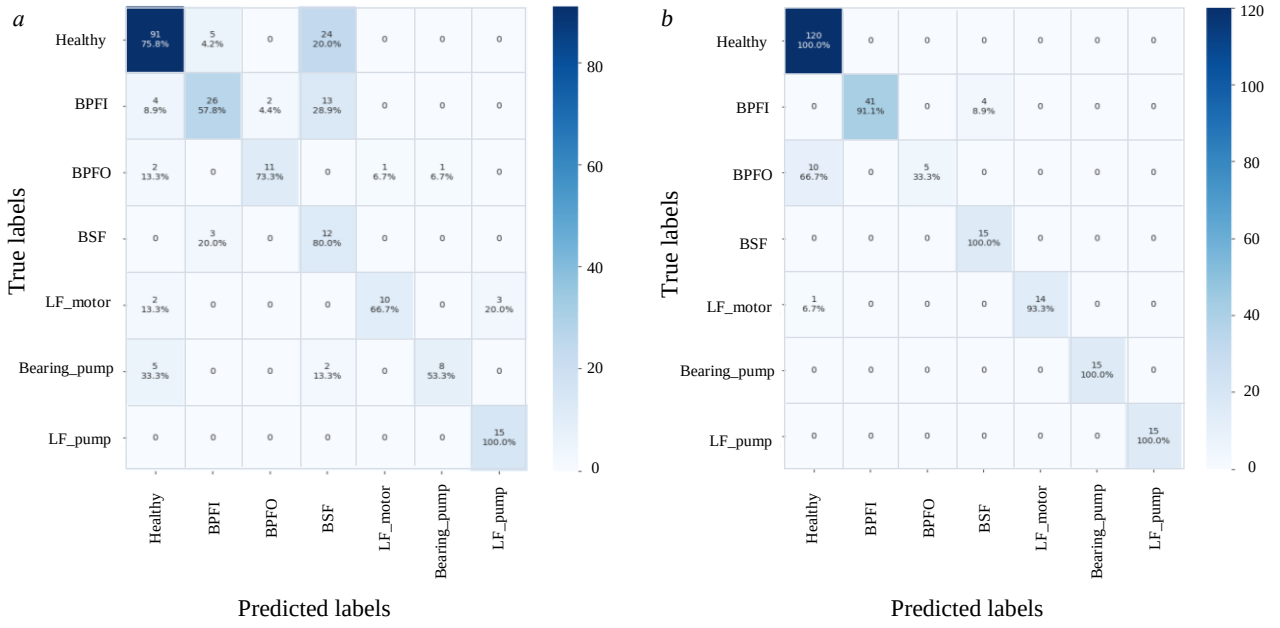

Fig.7. Comparison of confusion matrices between CatBoost (*a*) and the composite model (*b*).
The upper value indicates the total number of classified samples; the lower value shows the percentage of samples normalized with respect to the true set (100 % for each row)

Healthy – absence of any faults; BPFI, BPFO, and BSF – faults associated with inner race, outer race, and ball defects of the motor bearing; LF_motor, LF_pump – looseness in motor and pump mountings; Bearing_pump – pump bearing defects

performance may deteriorate, and therefore it must be retrained, and in some cases modified, to maintain its accuracy. The modification of pretrained models is possible within the FEDOT framework, and the fine-tuning of such models is simpler and faster compared to deep learning models. The authors believe that these limitations can be overcome either by normalizing the signal with respect to the speed and load of the diagnosed units, or by deriving features that are invariant to signal amplitude and frequency.

It is important to note the limitations of data collection, which represent a common challenge in industry. Recording large amounts of fault data is difficult, since damaged electric motors and pumps must be serviced immediately. The classical machine learning approach helps to mitigate this limitation compared to deep learning methods, even under conditions where only a small amount of fault data is available. Generative neural networks may improve this situation; however, they still face the same shortage of training data. Nevertheless, such methods are beginning to emerge.

Conclusions

An approach to classifying a range of industrial pump and electric motor faults using a model composition framework is presented, achieving a macro F1-score of 0.89. It has been shown that the use of the Extended Park's Vector in combination with raw data yields superior results under conditions of limited training data availability.

The study demonstrated that the proposed algorithm outperforms the gradient boosting algorithm when using the same additional features for the considered faults (motor bearing defects: inner race, outer race, ball; pump bearing defect: simultaneous inner and outer races; and looseness of motor and pump mountings).

It was established that, through current and voltage analysis using the proposed approach, it is possible to distinguish between bearing faults associated with both the electric motor and the pump.

This research highlights the potential of MCSA as a non-invasive and scalable tool for equipment condition monitoring, the importance of generating additional features, and the promise of AutoML for technical diagnostics of pump units.

With a view to practical implementation of the developed approach, further studies are planned, focusing on changes in pump rotational speed and the resulting data drift.

REFERENCES

1. Zhukovskiy Y., Buldysko A., Revin I. Induction Motor Bearing Fault Diagnosis Based on Singular Value Decomposition of the Stator Current. *Energies*. 2023. Vol. 16. Iss. 8. N 3303. DOI: 10.3390/en16083303

2. Korolev N.A., Zhukovskiy Y.L., Buldysko A.D. et al. Energy resource evaluation from technical diagnostics of electromechanical devices in minerals sector. *Mining Informational and Analytical Bulletin.* 2024. N 5, p. 158-181 (in Russian). DOI: 10.25018/0236_1493_2024_5_0_158

3. Bolón-Canedo V., Morán-Fernández L., Cancela B., Alonso-Betanzos A. A review of green artificial intelligence: Towards a more sustainable future. *Neurocomputing*. 2024. Vol. 599. N 128096. DOI: 10.1016/j.neucom.2024.128096

4. Garcia-Calva T., Morinigo-Sotelo D., Fernandez-Cavero V., Romero-Troncoso R. Early Detection of Faults in Induction Motors – A Review. *Energies*. 2022. Vol. 15. Iss. 21. N 7855. DOI: 10.3390/en15217855

5. Atta M.E.E.-D., Ibrahim D.K., Gilany M.I. Broken Bar Fault Detection and Diagnosis Techniques for Induction Motors and Drives: State of the Art. *IEEE Access*. 2022. Vol. 10, p. 88504-88526. DOI: 10.1109/ACCESS.2022.3200058

6. Ghanbari T., Mehraban A., Farjah E. Inter-turn fault detection of induction motors using a method based on spectrogram of motor currents. *Measurement*. 2022. Vol. 205. N 112180. DOI: 10.1016/j.measurement.2022.112180

7. Bruinsma S., Geertsma R.D., Loendersloot R., Tinga T. Motor current and vibration monitoring dataset for various faults in an E-motor-driven centrifugal pump. *Data in Brief*. 2024. Vol. 52. N 109987. DOI: 10.1016/j.dib.2023.109987

8. Sunal C.E., Dyo V., Velisavljevic V. Review of Machine Learning Based Fault Detection for Centrifugal Pump Induction Motors. *IEEE Access*. 2022. Vol. 10, p. 71344-71355. DOI: 10.1109/ACCESS.2022.3187718

9. Sunal C.E., Velisavljevic V., Dyo V. et al. Centrifugal Pump Fault Detection with Convolutional Neural Network Transfer Learning. *Sensors*. 2024. Vol. 24. Iss. 8. N 2442. DOI: 10.3390/s24082442

10. Chao Zhao, Zio E., Weiming Shen. Domain generalization for cross-domain fault diagnosis: An application-oriented perspective and a benchmark study. *Reliability Engineering & System Safety*. 2024. Vol. 245. N 109964. DOI: 10.1016/j.ress.2024.109964

11. Kim M.-C., Lee J.-H., Wang D.-H., Lee I.-S. Induction Motor Fault Diagnosis Using Support Vector Machine, Neural Networks, and Boosting Methods. *Sensors*. 2023. Vol. 23. Iss. 5. N 2585. DOI: 10.3390/s23052585

12. Jiusi Zhang, Ke Zhang, Yiyao An et al. An Integrated Multitasking Intelligent Bearing Fault Diagnosis Scheme Based on Representation Learning Under Imbalanced Sample Condition. *IEEE Transactions on Neural Networks and Learning Systems*. 2024. Vol. 35. Iss. 5, p. 6231-6242. DOI: 10.1109/TNNLS.2022.3232147

13. Kumar P., Hati A.S. Review on Machine Learning Algorithm Based Fault Detection in Induction Motors. *Archives of Computational Methods in Engineering*. 2021. Vol. 28. Iss. 3, p. 1929-1940. DOI: 10.1007/s11831-020-09446-w

14. Yakhni M.F., Cauet S., Sakout A. et al. Variable speed induction motors' fault detection based on transient motor current signatures analysis: A review. *Mechanical Systems and Signal Processing*. 2023. Vol. 184. N 109737. DOI: 10.1016/j.ymssp.2022.109737

15. Yuejiang Han, Jiamin Zou, Bo Gong et al. The use of model-based voltage and current analysis for torque oscillation detection and improved condition monitoring of centrifugal pumps. *Mechanical Systems and Signal Processing*. 2025. Vol. 222. N 111781. DOI: 10.1016/j.ymssp.2024.111781

16. Chen Liang, Yan Hao, Xie Tengzhou, Li Zhiguo. Identification of cavitation state of centrifugal pump based on current signal. *Frontiers in Energy Research*. 2023. Vol. 11. N 1204300. DOI: 10.3389/fenrg.2023.1204300

17. Gospodarikov A.P., Revin I.E., Morozov K.V. Composite model of seismic monitoring data analysis during mining operations on the example of the Kukisvumchorrskoye deposit of AO Apatit. *Journal of Mining Institute.* 2023. Vol. 262, p. 571-580. DOI: 10.31897/PMI.2023.9

18. Nath A.G., Udmale S.S., Singh S.K. Role of artificial intelligence in rotor fault diagnosis: a comprehensive review. *Artificial Intelligence Review*. 2021. Vol. 54. Iss. 4, p. 2609-2668. DOI: 10.1007/s10462-020-09910-w

19. Salehin I., Islam S., Saha P. et al. AutoML: A systematic review on automated machine learning with neural architecture search. *Journal of Information and Intelligence*. 2024. Vol. 2. Iss. 1, p. 52-81. DOI: 10.1016/j.jiixd.2023.10.002

20. Baratchi M., Can Wang, Limmer S. et al. Automated machine learning: past, present and future. *Artificial Intelligence Review*. 2024. Vol. 57. Iss. 5. N 122. DOI: 10.1007/s10462-024-10726-1

21. Alsharef A., Aggarwal K., Sonia et al. Review of ML and AutoML Solutions to Forecast Time-Series Data. *Archives of Computational Methods in Engineering*. 2022. Vol. 29. Iss. 7, p. 5297-5311. DOI: 10.1007/s11831-022-09765-0

22. Barandier P., Mendes M., Cardoso A.J.M. Comparative analysis of four classification algorithms for fault detection of heat pumps. *Energy and Buildings*. 2024. Vol. 316. N 114342. DOI: 10.1016/j.enbuild.2024.114342

23. Barbudo R., Ventura S., Romero J.R. Eight years of AutoML: categorisation, review and trends. *Knowledge and Information Systems*. 2023. Vol. 65. Iss. 12, p. 5097-5149. DOI: 10.1007/s10115-023-01935-1

24. Bischl B., Binder M., Lang M. et al. Hyperparameter optimization: Foundations, algorithms, best practices, and open challenges. *WIREs Data Mining and Knowledge Discovery*. 2023. Vol. 13. Iss. 2. N e1484. DOI: 10.1002/widm.1484

25. Morales-Hernández A., Van Nieuwenhuyse I., Rojas Gonzalez S. A survey on multi-objective hyperparameter optimization algorithms for machine learning. *Artificial Intelligence Review*. 2023. Vol. 56. Iss. 8, p. 8043-8093. DOI: 10.1007/s10462-022-10359-2

26. Dahiya S., Nanda H., Artwani J., Varshney J. Using Clustering techniques and Classification Mechanisms for Fault Diagnosis. *International Journal of Advanced Trends in Computer Science and Engineering*. 2020. Vol. 9. N 2, p. 2138-2146. DOI: 10.30534/ijatcse/2020/188922020

27. Maliuk A.S., Ahmad Z., Kim J.-M. A Technique for Bearing Fault Diagnosis Using Novel Wavelet Packet Transform-Based Signal Representation and Informative Factor LDA. *Machines*. 2023. Vol. 11. Iss. 12. N 1080. DOI: 10.3390/machines11121080

28. Hadi R.H., Hady H.N., Hasan A.M. et al. Improved Fault Classification for Predictive Maintenance in Industrial IoT Based on AutoML: A Case Study of Ball-Bearing Faults. *Processes*. 2023. Vol. 11. Iss. 5. N 1507. DOI: 10.3390/pr11051507

29. Cerrada M., Trujillo L., Hernández D.E. et al. AutoML for Feature Selection and Model Tuning Applied to Fault Severity Diagnosis in Spur Gearboxes. *Mathematical and Computational Applications*. 2022. Vol. 27. Iss. 1. N 6. DOI: 10.3390/mca27010006

30. Hutter F., Kotthoff L., Vanschoren J. Automated Machine Learning. Methods, Systems, Challenges. Springer, 2019, p. 219. DOI: 10.1007/978-3-030-05318-5

31. Revin I., Potemkin V.A., Balabanov N.R., Nikitin N.O. Automated machine learning approach for time series classification pipelines using evolutionary optimization. *Knowledge-Based Systems*. 2023. Vol. 268. N 110483. DOI: 10.1016/j.knosys.2023.110483

32. Javed K., Gouriveau R., Zerhouni N. State of the art and taxonomy of prognostics approaches, trends of prognostics applications and open issues towards maturity at different technology readiness levels. *Mechanical Systems and Signal Processing*. 2017. Vol. 94, p. 214-236. DOI: 10.1016/j.ymssp.2017.01.050

33. Khan A.A., Chaudhari O., Chandra R. A review of ensemble learning and data augmentation models for class imbalanced problems: Combination, implementation and evaluation. *Expert Systems with Applications*. 2024. Vol. 244. N 122778. DOI: 10.1016/j.eswa.2023.122778

34. Ozaki Y., Tanigaki Y., Watanabe S. et al. Multiobjective Tree-Structured Parzen Estimator. *Journal of Artificial Intelligence Research*. 2022. Vol. 73, p. 1209-1250. DOI: 10.1613/jair.1.13188

Authors: **Roman R. Khalikov**, *Specialist* (*ROTEC Digital Solutions JSC, Moscow, Russia*), *https://orcid.org/0009-0009-2369-4926*, **Mikhail Yu. Chernetskiy**, *Candidate of Engineering Sciences, Head of Department* (*ROTEC Digital Solutions JSC, Moscow, Russia*), *https://orcid.org/0000-0001-7444-6660*, **Ilia E. Revin**, *Candidate of Engineering Sciences, Researcher* (*ITMO University, Saint Petersburg, Russia*), *https://orcid.org/0000-0002-4459-8724*, **Vadim A. Potemkin**, *Candidate of Engineering Sciences, Researcher* (*ITMO University, Saint Petersburg, Russia*), *vadim_potemkin@itmo.ru, https://orcid.org/0000-0002-8019-7282*.

The authors declare no conflict of interests.

ISSN 2411-3336; e-ISSN 2541-9404

JOURNAL OF MINING INSTITUTE

Zapiski Gornogo instituta

Journal homepage: pmi.spmi.ru

Research article *Geotechnical Engineering and Engineering Geology*

The model of wireless charging infrastructure for electric transport of open-pit mining enterprises

Irina Yu. Semykina[1]✉, **Valery M. Zavyalov**[1], **Yaroslava A. Nechiporenko**[1], **Elena N. Taran**[2]

[1] *T.F.Gorbachev Kuzbass State Technical University, Kemerovo, Russia*

[2] *Sevastopol Station of Young Technicians, Sevastopol, Russia*

***How to cite this article*:** Semykina I.Yu., Zavyalov V.M., Nechiporenko Ya.A., Taran E.N. The model of wireless charging infrastructure for electric transport of open-pit mining enterprises. Journal of Mining Institute. 2025. Vol. 275, p. 56-69.

Abstract

The prospects for implementing battery-powered dump trucks at open-pit mining enterprises are considered. Main attention is on the problem of charging infrastructure for adopting the unmanned production concept. The suggestion is to use wireless charging stations to join charging with particular technological operations, thereby reducing battery capacity and increasing the utilization rate of electric vehicles. To determine effective charging infrastructure solutions, it is necessary to evaluate the interaction between the dump truck and charging stations. The research aims to develop a model reflecting the power flows between the charging infrastructure and the dump truck battery while an operational process is being executed. The model takes into account the work cycle parameters, dump truck parameters with powertrain options providing energy recovery at braking, and charging infrastructure parameters in three options: one stationary charging station located outside the operating routes designed for the simultaneous charging of several dump trucks (option A); stationary charging stations for one dump truck located at loading points (option B); and a dynamic charging station that charges in motion (option C). The method for determining the power of a single wireless charging station is proposed, along with a related method for determining battery capacity. When establishing capacity, the parameters of the charge-discharge cycle and the charging current ratio are considered. The described model is implemented in MATLAB Simulink using *m*-files for processing satellite data of route parameters from geographic information systems, as well as elements of the Stateflow and Simscape Electrical libraries. The capabilities of the model were demonstrated on the example of the Lebedinsky GOK, with the BelAZ-7558E selected as a battery-powered dump truck. In the example considered, the total capacity of the wireless charging infrastructure for options A, B, and C was 10.6; 6.3, and 13.5 MW, with option B providing the highest value of the battery average state of charge of 0.65 p.u., with the lowest specific power demand per dump truck of 2.4 MW·h. The simulation results allow us to determine various operating factors of the system, evaluate the power compliance of system elements, compare wireless charging infrastructure options, and make informed design decisions.

Keywords

dump truck; battery-powered electric vehicles; wireless charging station; charging infrastructure; work cycle; power flow; computer model

Funding

The research was supported by the State assignment of Ministry of Science and Higher Education of the Russian Federation (N 075-03-2024-082-2).

Received: 06.04.2025 ***Accepted: 02.09.2025*** ***Online: 13.10.2025*** ***Published: 31.10.2025***

Introduction

The widespread adoption of digital technologies in production machines and mechanisms is a basic prerequisite for designing unmanned production. This process is also typical for mining [1]. For example, unmanned down-the-hole drills, scrapers, mining trucks, and charging vehicles have been developed for underground metal mine [2]. For open-pit mining enterprises, intelligent systems for

unmanned shovels [3, 4], dump trucks [5-7], and dispatching in shovel-truck systems with unmanned transport [8, 9] are being actively developed.

It is worth noting the growing role of electric transport in this process. Battery-powered electric vehicles have been thoroughly developed as objects of automation [10, 11]. The use of electric motors and batteries enables a higher level of energy efficiency of the vehicle itself [12]. Their integration with the power supply optimizes the overall energy consumption at the enterprise level [13]. Active developments are ongoing for battery-powered electric vehicles for open-pit mining [14, 15], for instance, such battery-powered dump trucks as eDumper [16], BYD V60 [17, 18], BelAZ-7558E [19], as well as battery-powered and autonomous Volvo HX series [20].

The article discusses battery-powered dump trucks. For open-pit mining enterprises, extensive areas and complex relief are typical. Due to heavy loads, the dump truck must have a large battery reserve on board or recharge the battery during the operational process. The technologies currently used for charging batteries require a wired connection to the power supply [21] or removal of a discharged battery and replacement with a charged one at a special battery swapping station [22, 23]. Both technologies require human participation, which contradicts the unmanned production concept. This contradiction can be overcome by developing additional automation tools. For an unmanned wired connection, an automated system can be considered, which includes a specialized vision system for parking and robotic connectors [24]. For battery swapping stations, robotic systems that operate on similar principles as [25] can be considered. Currently, there are no ready-made solutions for such automation systems designed for powerful, large-sized electric vehicles operating in dusty and vibration-intensive conditions, and the need for their development is an additional obstacle to implementing unmanned electric transport.

An alternative solution to the problem of charging battery-powered dump trucks within the unmanned production concept could be the wireless charging systems [26, 27]. Their additional advantage is the ability to join battery charging with particular technological operations, which increases the utilization rate of electric vehicles and allows using batteries with a lower capacity. However, wireless charging technology is currently in the early stage of commercial application, with various circuit designs being developed for charging station infrastructure, and no general guidance for selecting a specific design solution that takes into account a wide range of technical and economic factors. Any open-pit mining project requires significant investment and energy costs. In this regard, making design decisions is associated with high risks and requires a comprehensive analysis of possible options for wireless charging infrastructure.

Examples of adopting this technology for systems with relatively high power relate to the freight and passenger transportation field. Like urban electric transport, the open-pit mining operational process has a cyclical nature. Existing methods cannot be directly applied to the problem under consideration but can serve as a basis. Requirements for batteries and charging infrastructure capacity can be established analogously with [28, 29], which are concerned with electric buses, while considering differences in their operating conditions. It should be taken into account that the type and capacity of the battery used are significantly influenced not only by the operating conditions, but also by the selected charging scenario. To determine effective charging infrastructure solutions for various charging scenarios, it is necessary to conduct a thorough assessment of the interaction between the dump truck and charging stations and develop a model reflecting the power flows between the charging infrastructure and the dump truck battery while an operational process is being executed. The development of such a model is the objective of this research.

Methods

General approaches to the model. The structure of the developed model is shown in Fig.1. The initial data used are the work cycle parameters and the dump truck parameters, which determine the power consumption of the battery.

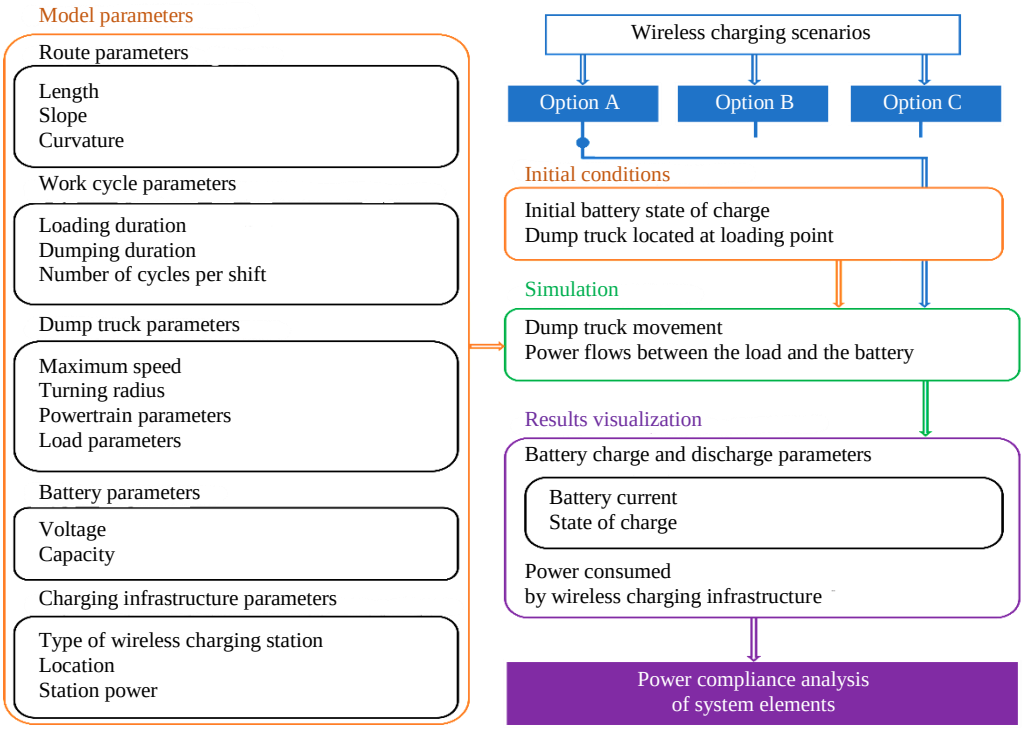

Fig.1. The model structure

The work cycle is considered in a simplified form, omitting the quality of face preparation and the shovel efficiency, which excludes from consideration the downtime at the face while waiting for loading. The basic technological operations are loading and dumping with durations T_l and T_d, as well as the trip on the route. The duration of trip on the route depends on the route length L and the route profile, including its slope α and curvature κ. The dump truck trip on straight sections of the route is assumed to be at a constant speed, and a slowdown occurs on sections with a curvature comparable to the turning radius of the dump truck R_t. Slowdowns due to traffic congestion or road surface deterioration are not taken into account.

The dump truck parameters for the model are divided into two groups: those describing the powertrain and those determining the load on the motor-wheels. The first group includes the gearbox gear ratio i, the radius of the dump truck wheels R_w, the efficiency of the gearbox η_g, and the motor-wheel η_m. The second group includes the dump truck empty weight M_d and its payload M_p, the coefficient of rolling friction f for the tire type used, the frontal area of the dump truck A, and the coefficient of frontal resistance C to air with density ρ. The simulation assumes that the dump truck trip to the unloading point is uphill (the average value of α is positive), the transported rock mass is constant and equal to the payload M_p, and the trip to the loading point is downhill with the empty dump truck. The coefficient f is assumed to be constant, regardless of seasons and possible precipitation.

During the simulation process, the shaft power consumed by the motor-wheel is determined, having the battery as the source. The power consumed by any other electrical receivers connected to the battery is negligible. The motor-wheel transients are not considered. The power electrical converters that control the motor-wheels and battery charging are assumed to be ideal. The powertrain is considered in two options: one that provides energy recovery to the battery at braking, and one that does not. The initial battery parameters for this model are the nominal voltage U and the capacity AH.

Battery is recharged using wireless charging stations, with the following options being considered: A. One stationary charging station located outside the operating routes and designed for the simultaneous charging of several dump trucks. B. Stationary charging stations for one dump truck located at loading points. C. A dynamic charging station that charges in motion. The input parameters of the wireless

charging infrastructure are the station power P_e, the efficiency η, and the location. In option A, it is assumed that the wireless charging station is located at a distance L_c from the unloading point, and the dump truck is sent there after a specified number N of loading and unloading cycles. In option B, the route section equipped with the proper infrastructure has a length of L_d and begins at a distance of L_s from the loading point. The battery charge duration for option A is limited by the specified time T_c, for option B by the duration T_l, and for option C by the duration of the dump truck trip on the equipped route section.

The battery charging occurs when the dump truck is at the location where the wireless charging infrastructure is located, provided that the current state of charge *SOC* has reached the lower threshold. The charging current value is determined by the battery type and is specified by the ratio K_c to the battery capacity in ampere-hours. If *SOC* reaches the upper threshold during charging, wireless power transfer ceases. While the battery is charging, the wireless charging station consumes power from the power supply. The idle power consumption of the station is set at 1 % of P_e.

Determining the battery load. Accurate assessment of energy consumption is crucial for electric vehicles due to the limited battery capacity. Various approaches to addressing this problem are outlined in [30-32]. This research primarily focuses on the route parameters that are associated with acceleration-deceleration patterns.

The power consumption from the battery is determined by the power consumed by the in-wheel motors:

$$P_m = M_m \omega_m \frac{1}{\eta_m}, \tag{1}$$

where ω_m is the motor angular speed; M_m is the torque on the motor shaft,

$$M_m = M_w \frac{1}{i\eta_g};$$

M_w is the torque on the wheel, calculated according to [33] from the ratio

$$\frac{M_w}{R_w} = mg\sin\alpha + \rho CA\frac{v^2}{2} + mgf\cos\alpha + v\frac{dv}{dt};$$

m is the dump truck weight, $m = M_d + M_p$ for the trip from the loading point to the unloading point, $m = M_d$ for the trip in any other direction; v is the dump truck velocity.

The angular speed is calculated according to equation

$$\omega_m = v\frac{i}{R_w}, \tag{2}$$

where the velocity v is changed to ensure a safe velocity of motion on the curved section. According to [34], this dependence is complex. In this research, assuming that the tire grip on the road is constant, it is approximated by an exponential function depending on the route curvature κ:

$$v = v_{\max}\left(1 - e^{\frac{-1}{2\kappa R_t}}\right), \tag{3}$$

where $v_{\max}$ is maximum velocity of the dump truck.

Parameters α and κ vary along the route length. Considering newly established open-pit mining enterprises, their design values should be used. For active enterprises, using geodetic information [35] is the best solution. If instrumental measurements are not possible, the satellite data from geographic information systems is used. It is proposed to use Google Maps API to obtain the latitude ϕ and

longitude λ coordinates of route points, and Elevation API to determine their above sea level height *h*. In this case, the slope in degrees is determined as

$$\alpha = \arctan\left(\frac{\Delta h}{\Delta d}\right), \tag{4}$$

where Δh is the difference in the two above sea level heights ($h_2 - h_1$) of two adjacent route points with latitude and longitude coordinates ϕ_1, λ_1, and ϕ_2, λ_2; Δd is the distance between these points, calculated using the haversine formula

$$\Delta d = 2r \arcsin\left(\sqrt{\sin^2\left(\frac{\phi_2 - \phi_1}{2}\right) + \cos(\phi_1)\cos(\phi_2)\sin^2\left(\frac{\lambda_2 - \lambda_1}{2}\right)}\right),$$

r is the radius of the Earth. The distance travelled by the dump truck along the route between these points will be equal to

$$\Delta l = \frac{\Delta d}{\cos\alpha}. \tag{5}$$

To determine κ, coordinates given by latitude and longitude are transformed into a Cartesian coordinate system with the *x*-axis pointing east and the *y*-axis pointing north:

$$\begin{aligned} x &= (r + h)\cos\phi\cos\lambda; \\ y &= (r + h)\cos\phi\sin\lambda, \end{aligned} \tag{6}$$

in which

$$\kappa = \frac{\left|\frac{\partial x}{\partial l}\frac{\partial^2 y}{\partial l^2} - \frac{\partial y}{\partial l}\frac{\partial^2 x}{\partial l^2}\right|}{\left(\left(\frac{\partial x}{\partial l}\right)^2 + \left(\frac{\partial y}{\partial l}\right)^2\right)^{3/2}}. \tag{7}$$

Since all parameters in equations (1)-(7), which describe both the powertrain and the load on the motor-wheels, are known with some error, when determining the power of the wireless charging stations and the battery capacity, the corresponding reserve factors should be set.

Determination of stations' power. The power of the single wireless charging station, as well as the entire infrastructure, is determined using the energy balance method similar to [36]. The basis is the power required to fully charge one dump truck after a single cycle. Depending on the scenario chosen, the maximum number of dump trucks *K* simultaneously charging from the station, the total number of technological routes of the enterprise *F*, and the number of sections *H* equipped with dynamic charging infrastructure are taken into account.

Table 1 presents the general calculation procedure, where T_o is the trip time from the loading point to the unloading point; T_m is the trip time from the unloading point to the wireless charging station location; T_{cd} is the trip time along the route section equipped with the dynamic charging infrastructure; P_l is the average power consumed from the battery by one cycle; P_e is the installed power of the wireless charging station.

The trip time on different sections:

$$T_o = \left\{t \middle| l(t) = \int v dt \to L^-\right\} - \left\{t \middle| l(t) \to 0^+\right\};$$

$$T_m = \left\{t \middle| l(t) = \int v dt \to L + L_c^-\right\} - \left\{t \middle| l(t) \to L^+\right\};$$

$$T_{cd} = \left\{t \middle| l(t) = \int v dt \to L_s + L_d^-\right\} - \left\{t \middle| l(t) \to L_s^+\right\}.$$

The average power is defined as

$$P_l = \frac{1}{T_{cd}} \int_0^{T_{cd}} P_m dt; \tag{8}$$

$$P_l = \frac{1}{T_{cd}} \int_0^{T_{cd}} \left\{ P_m \middle| P_m(t) > 0 \right\} dt, \tag{9}$$

formula (8) is used for the option when energy recovery to the battery at braking is provided, and formula (9) is used when it is not.

The installed power is defined as

$$P_e = P_s \frac{k_p}{\eta},$$

where k_p is the reserve factor.

Table 1

Calculation formulas depending on the wireless charging scenario chosen

Value	Option A	Option B	Option C
Discharge duration per cycle T_{cd}	$2\left(T_0 + \frac{T_m}{N}\right)$	$2T_0$	$2T_0$
Charge duration per cycle T_{ch}	$\frac{T_c}{N}$	T_l	$2T_{cd}$
Wireless charging station output power P_s	$P_l \frac{T_{cd}}{T_{ch}} K$	$P_l \frac{T_{cd}}{T_{ch}}$	$P_l \frac{T_{cd}}{T_{ch}} K;\ K = \left\lceil \frac{T_d}{L_d / \langle v \rangle} \right\rceil$
Total power of wireless charging infrastructure P_Σ	P_e	$\sum_{i=1}^{F} P_{e_i}$	$\sum_{i=1}^{H} P_{e_i}$

Relationship between station power and battery capacity. The battery capacity must be calculated based on the required run S, which depends on the wireless charging infrastructure option. For option A, the run S is determined as $2(LN+L_c)k_a$, and for options B and C is determined as $2Lk_a$, where k_a is the reserve factor. Under these conditions:

$$AH = \frac{P_l(T_{cd} + T_l + T_d)S}{3600UL}.$$

It should be noted that the battery charging current is limited. If the charging time is less than $3600/K_c$, the battery capacity must be increased proportionally. As the power of the wireless charging station is limited, the condition must be met

$$P_e \geq \frac{UAHK_c}{\eta},$$

otherwise, the installed power of the wireless charging station must be increased proportionally.

The consumed current of the battery (assumed positive) or its current output is determined from the ratio

$$IU = \begin{cases} UAHK_c - P_m \text{ while wireless charging;} \\ -P_m \text{ outside the charging station,} \end{cases}$$

besides, if the considered option is not providing energy recovery to the battery at braking, the value of P_m is only considered under the condition that $P_m > 0$.

The battery charge-discharge model can be implemented with different levels of detail [37-39]. In this research, the current state of charge of the battery is determined based on I using the coulometric method:

$$SOC = SOC_0 + \frac{1}{3600AH}\int Idt,$$

where SOC_0 is the initial state of charge, and the current battery voltage depends on SOC as follows:

$$V = U\left(\frac{SOC}{1-\beta(1-SOC)}\right),$$

β is the slope coefficient that is calculated so that the battery voltage is V_1 when the given current capacity is AH_1.

It should be also be taken into account that high K_c, ensuring rapid battery recharge, also contributes to accelerated fade. The main factors influencing battery fade are described in [40]. Based on them, rational parameters of the charge-discharge cycle should be formed (Fig.2).

The SOC_{on} and SOC_{off} values represent thresholds for activating and ceasing wireless power transfer when the dump truck is located at the wireless charging infrastructure location. When the dump truck is on the route, SOC may either increase above SOC_{off}, for example, due to energy recovery when downhill, or decrease below SOC_{on}. Reducing both $\langle SOC\rangle$ and $(SOC_{max} - SOC_{min})$ will help slow battery fade. Specific SOC_{on} and SOC_{off} values should be adjusted based on simulation results. However, to prevent battery overcharging, SOC_{off} should be set to less than one, proportionally increasing battery capacity.

Results and discussion

Computer model. The described mathematical model is implemented using MATLAB Simulink. Processing of the route parameters is implemented as separate *m*-files, whose results are exported to 1-D Lookup Table. The computer model uses two of these elements: the first contains the dependence $h(l)$, and the second contains $\kappa(l)$.

Scenarios for the choice of trip direction along the route and activating-and-ceasing of wireless power transfer are implemented using Stateflow.Chart (Fig.3). The initial state is assumed to be that the dump truck has arrived at the loading point, that is, at $t = 0$, the value $l = 0$, and its battery is charged to SOC_0.

The computer model of the battery is implemented using the Simscape Electrical library (Fig.4), while the remaining model elements are based on standard Simulink library blocks. The Battery block of the Simscape Electrical library provides additional tools to enhance the battery model parameters. For example, the Thermal port setting allows, if necessary, to include in calculations the dependence of battery voltage and discharge curve parameters on battery temperature, while the Battery fade setting allows for battery fade. By default, the settings Thermal port and Battery fade are disabled.

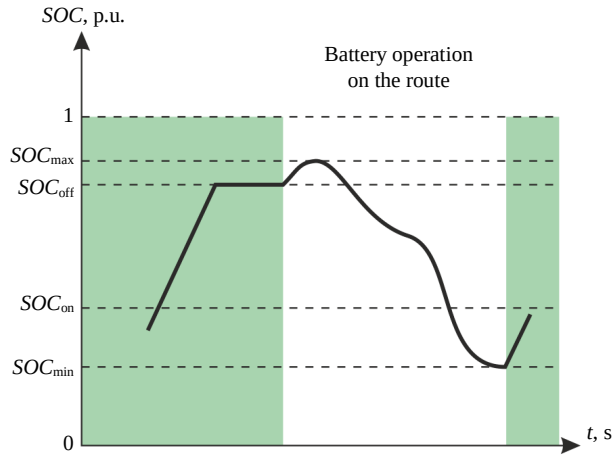

Fig.2. Charge-discharge cycle

Simulation results. The values of the computer model parameters are given in Table 2. The Lebedinsky GOK was taken as the model enterprise, for which the dump truck route location and the wireless charging infrastructure location were selected (Fig.5). The parameters of the wireless charging infrastructure were taken according to [36].

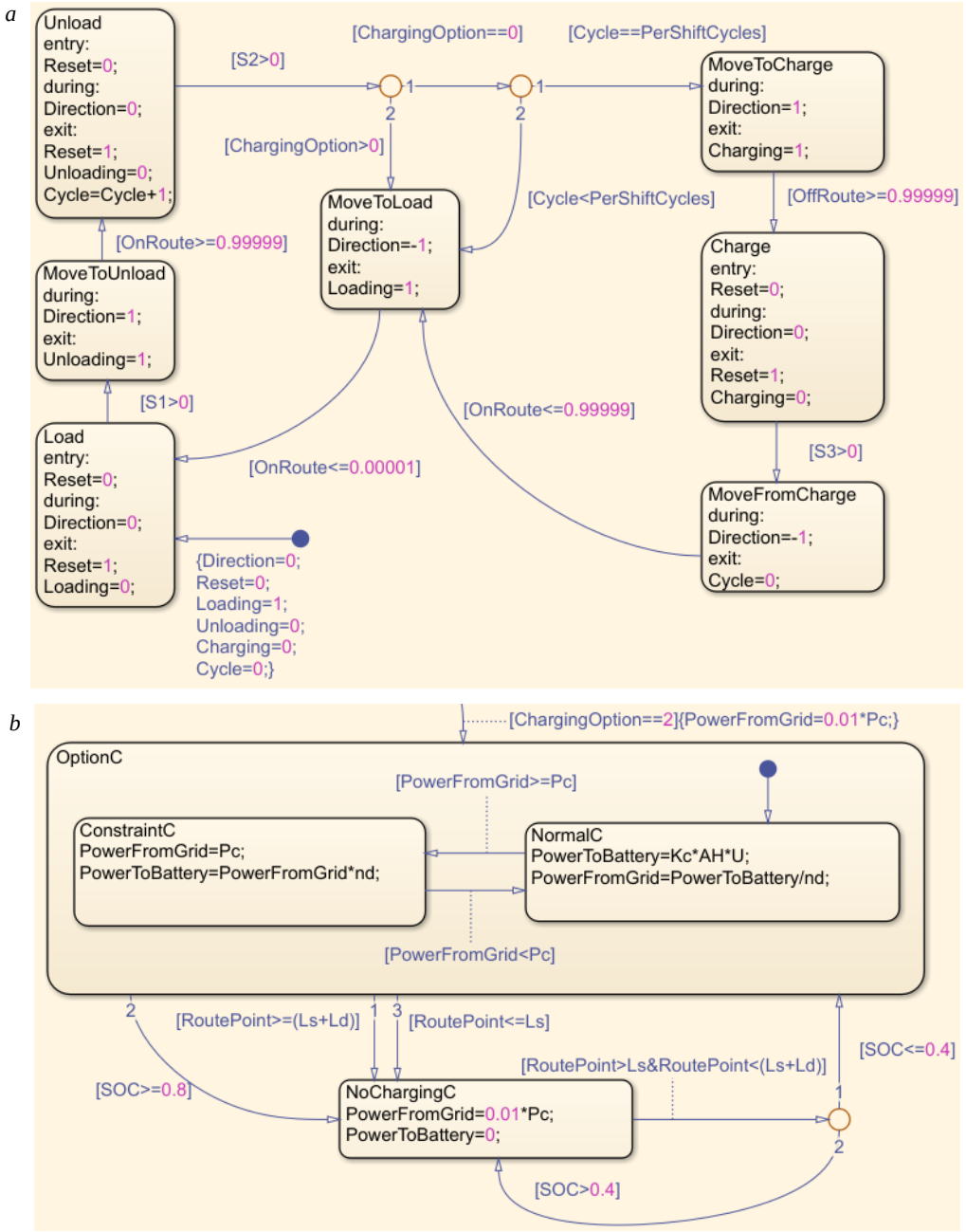

Fig.3. Fragments of the scenario interaction implementation:
a – choice of trip direction; *b* – wireless power transfer in option C

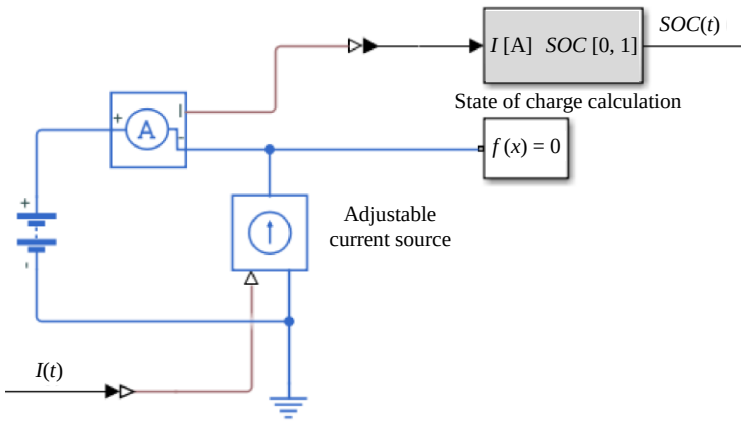

Fig.4. Implementation of the battery

Table 2

Computer model parameters

Parameter	Value	Parameter	Value		
			Option A	Option B	Option C
v_m, m/s	5.1667	P_e, MW	10.564	0.566	7.517
i, p.u.	30.36	η, p.u.	0.95	0.95	0.4
R_w, m	1.3395	AH, Ah	2472	412	412
R_t, m	11	AH_1, Ah	1236	206	206
M_d, t	74	SOC_{on}, p.u.	0.75	0.75	0.4
M_p, t	90	U, V	712.8		
η_g, p.u.	0.97	V_1, V	677.16		
η_m, p.u.	0.98	SOC_0, p.u.	0.8		
f, p.u.	0.008	SOC_{off}, p.u.	0.8		
C, p.u.	0.7	L, m	3860		
A, m^2	12.4	L_s, m	1620		
ρ, kg/m^3	1.2255	L_d, m	1300		
g, m/s^2	9.8	L_c, m	4200		
T_l, s	460	N	20		
T_d, s	100	T_c, s	1800		

The BelAZ-7558E was selected as the model for the dump truck, and its powertrain and load parameters were used. The battery parameters differ from those of the BelAZ-7558E and were selected with the above-described approach. The specific battery type and its parameters were chosen from the options outlined in [41-43]. The best match to the calculated battery parameters was found to be for a lithium-iron-phosphate battery with a nominal capacity of 412 Ah. This battery was used for options B and C, and 6 units connected in parallel were used for option A.

The work cycle parameters should ideally be determined in conjunction with the optimization tools of the shovel-truck systems, as mentioned in [8, 44]. If such tools are not available, operational indicators are used. The values of average durations described in [45] were used as parameters of the model work cycle.

The simulation results allow us to determine various operating factors of the system and evaluate the power compliance of system elements. As an example, Fig.6 provides the transient curves of motor torque and angular speed of the truck motor-wheel for the trip along the route. Analysis shows that the in-wheel motor spends most of the time of the dump truck trip in braking mode. If energy recovery to the battery at braking is not provided, then maintaining a rhythmic and continuous system operation is only possible by increasing the instantaneous power transferred to the battery from the wireless charging station. This increase can be achieved by increasing K_c.

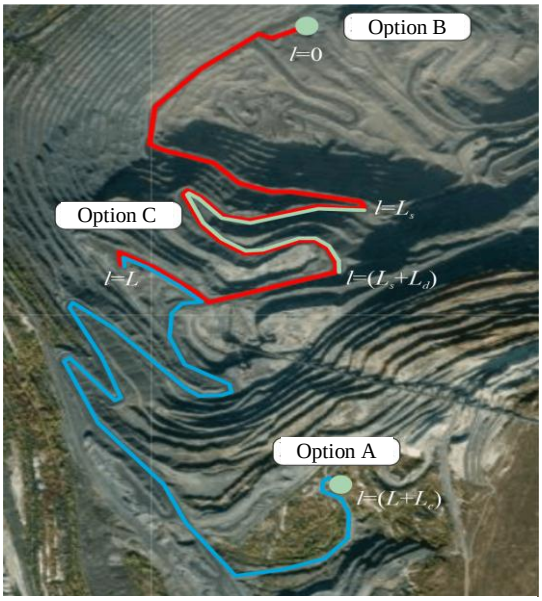

Fig.5. Location of the route
and the wireless charging infrastructure

As an illustration, Fig.7 shows transient curves of battery state of charge changes for different options of charging infrastructure. In the simulation, initially, $K_c = 3$ was used to bring the battery charging time closer to the corresponding for the BelAZ-7558E. As can be seen in Fig.7, *a*, *d*, if energy recovery is provided, the battery is fully charged by one charge per cycle for both static (option B) and dynamic charging (option C).

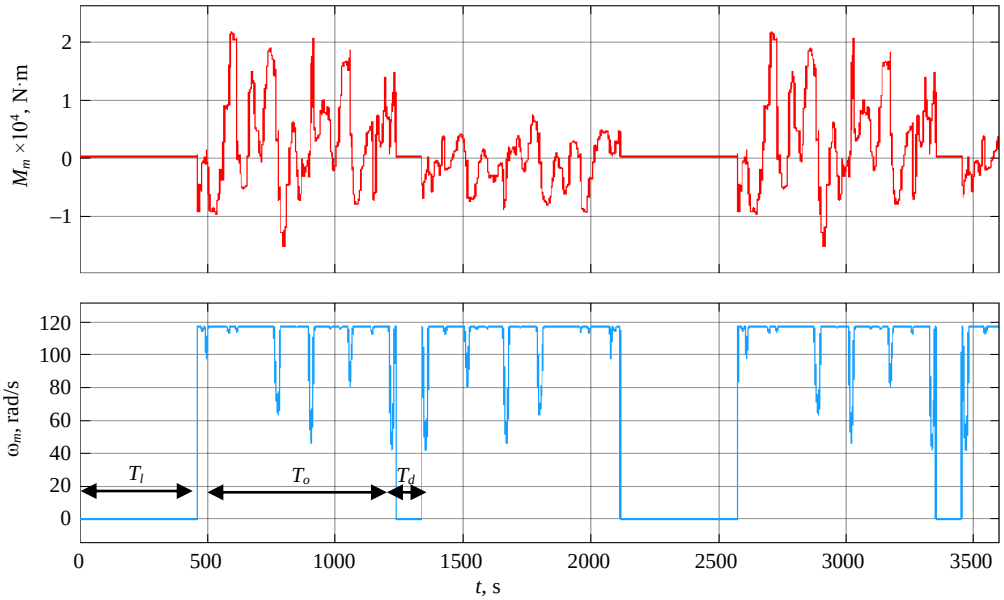

Fig.6. Transient curves of $\omega_m(t)$ and $M_m(t)$

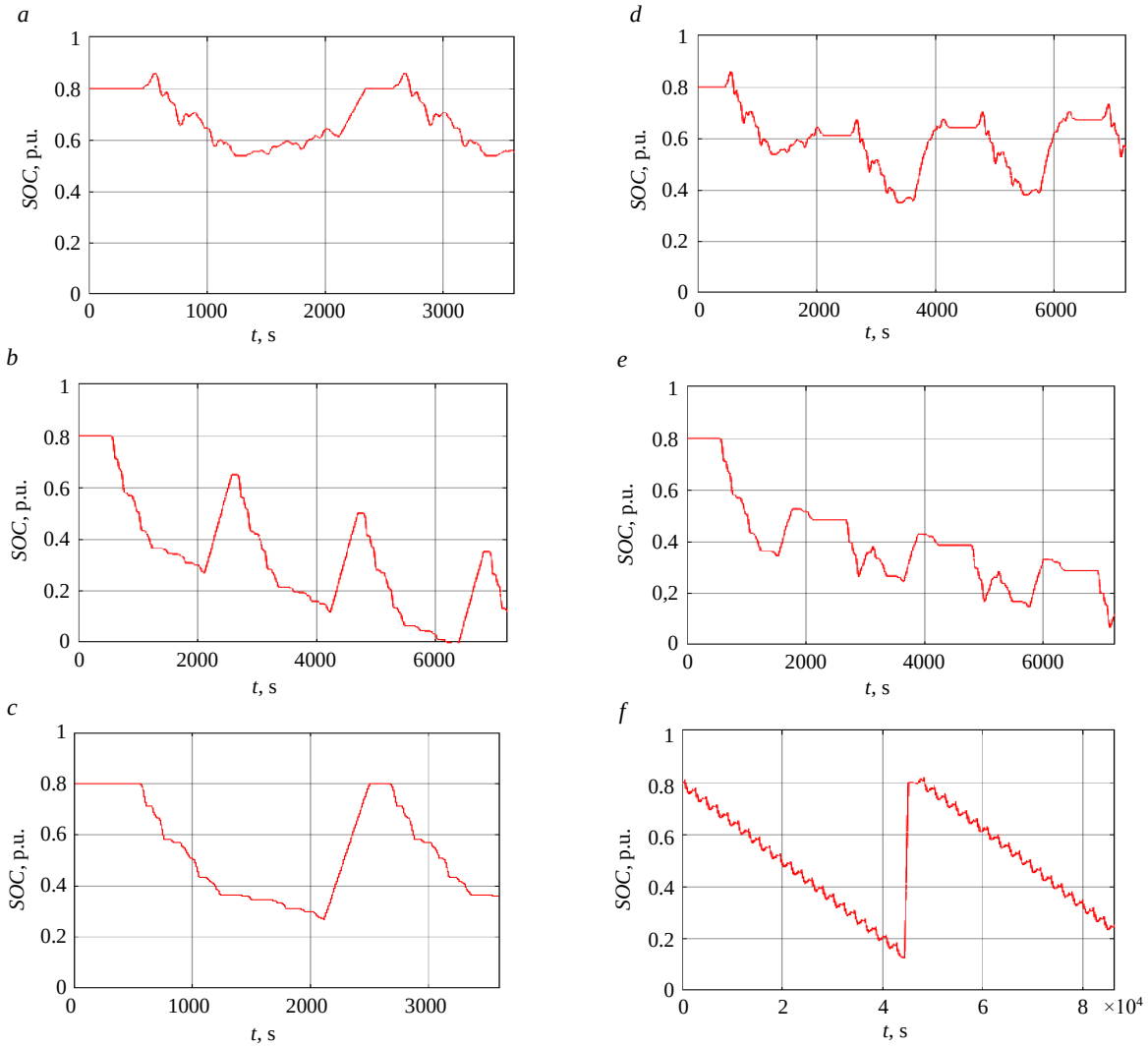

Fig.7. Transient curves of *SOC* (*t*): *a* – option B, with energy recovery, $K_c = 3$; *b* – option B, no energy recovery, $K_c = 3$; *c* – option B, no energy recovery, $K_c = 5$; *d* – option C, with energy recovery, $K_c = 3$; *e* – option C, no energy recovery, $K_c = 3$; *f* – option A, with energy recovery, $K_c = 3$

If energy recovery at braking is not provided, for option B and option C, the battery is fully discharged within three cycles (Fig.7, *b*, *e*). However, increasing the charging current to $K_c = 5$ maintains continuous operation of the dump truck (Fig.7, *c*).

In addition to operational continuity assessment, Fig.7 allows us to compare the rate of battery fade for different scenarios of interaction between the dump truck and the charging infrastructure. Figure 7, *c* demonstrates a higher difference ($SOC_{\max} - SOC_{\min}$) at a higher charging current, which indicates, in comparison with Fig.7, *a*, a known shortage of the battery life for the options where energy recovery is not provided. Similarly, comparing Fig.7, *a* and *d*, it can be noted that with the same charging current and a similar difference ($SOC_{\max} - SOC_{\min}$), the $\langle SOC \rangle$ value for option B is lower. Therefore, with dynamic wireless charging, the battery life will be longer than with static wireless charging once per cycle.

A similar comparison with option A (Fig.7, *f*) is not possible due to the different battery capacities and charge-discharge cycle durations. It should be noted that with $K_c = 3$ and one-charge operating range of more than 10 h, the $\langle SOC \rangle$ value is approximately 0.38 with ($SOC_{\max} - SOC_{\min}$) close to the 80-20 cycle recommended by battery manufacturers. This option is closest in battery parameters to the BelAZ-7558E, which operates with wired charging stations.

The comparison of power consumption by wireless charging infrastructure from the power supply is of interest. The results under consideration correspond to the single dump truck operation, while options A and B assume the possibility of simultaneous wireless cahrge for several vehicles. Thus, there is a good reason to consider the specific power consumption per dump truck and, taking into account the different charge-discharge cycle durations, to compare the daily power consumption W_e. If energy recovery at braking is provided and $K_c = 3$, the daily power consumption per dump truck for option A is 3.8 MW·h, for option B is 2.4 MW·h, and for option C is 7 MW·h. This is explained by the lower power of the wireless charging station for option B and a significantly higher efficiency for the stationary charging stations. As a result, although option A has a higher power of the charging station than option C, the power consumption for option A is lower. Moreover, options B and C have a higher specific utilization factor k_u.

A summary comparative analysis of the wireless charging infrastructure options when energy recovery at braking is provided, and $K_c = 3$ is presented in Table 3. The following conclusions can be drawn. An average battery state of charge is close to 0.5 for all options, which indicates similarly efficient aging of the battery. However, *AH* for option A is significantly higher, indicating higher investment and operating costs for battery replacement, as the battery life is significantly shorter than that of a dump truck. In terms of installed power, which reflects investment costs, and energy consumption, which reflects operating costs, option B is the best, while option C is the worst. Based on the entire set of operational characteristics, option B is the best.

Table 3

Summarizing model parameters

Parameter	Value		
	Option A	Option B	Option C
P_Σ, MW	10.6	6.3	13.5
P_e, MW	10.6	0.6	7.5
W_e, MW·h	3.8	2.4	7
k_u, p.u.	0.04	0.16	0.19
AH, Ah	2472	412	412
$SOC_{\min}$, p.u.	0.12	0.54	0.32
$SOC_{\max}$, p.u.	0.82	0.86	0.86
$\langle SOC \rangle$, p.u.	0.44	0.65	0.52

Conclusion

This paper proposes a mathematical model describing the interaction of the battery-powered dump truck with the wireless charging infrastructure under various charging scenarios. The model serves as a tool for comparing wireless charging infrastructure options and making design decisions. It describes the power flows between the charging infrastructure and the dump truck battery while an operational process is being executed. Under the assumptions of the constant duration of loading and dumping, the constant dump truck velocity on straight sections of the route, the constant coefficient of rolling friction, battery capacity and its discharge curve parameters, the

model allows us to calculate the parameters of the battery and wireless charging stations and to determine various operational characteristics of the system, in particular the power consumption of the charging stations.

The assumptions described restrict the application of the proposed mathematical model to the design stage. To improve its adequacy in actual practice, the model should be supplemented with components that more closely account for operational conditions, and the model parameters that affect energy consumption during route travel should be adjustable. For example, the coefficient of rolling friction f should be dynamic and dependent on the wear-out rate of the truck tire, temperature conditions, and precipitation. When determining the dump truck velocity v for the trip along the route, instead of the dependence on the curvature $\kappa(l)$, the dependence $v(l)$ generated by statistical processing of operational dump truck tachograms should be used. This will consider the road surface conditions and the likelihood of congestion for the specific route and the specific dispatching system used. The transported material weight should be dynamically adjusted depending on the quality of the face preparation, which determines the particle size distribution of the transported material. These modifications are the subject of further research.

To implement the proposed mathematical model, the computer model in MATLAB Simulink was developed. This model was used to carry out the research for a specific dump truck operating on a given route in conjunction with one stationary charging station located outside the route, several stationary charging stations at the loading points, or the dynamic charging station that charges in motion. Dump truck powertrain options are considered providing energy recovery at braking and not. It is shown that the option without energy recovery is less efficient in energy performance and causes more accelerated battery aging. Among the charging infrastructure options, the charging stations at the loading points demonstrated the best performance. In the considered example, this charging infrastructure option consumes 37 % less electricity than the infrastructure with a stationary charging station located outside the route, and 66 % less than with the dynamic charging station that charges in motion, while providing $\langle SOC \rangle$ higher by 48 and 25 %, respectively.

The research demonstrated that, given the parameters of the work cycle, the dump truck, and the route, it is possible to optimize the cooperative effort of electric vehicles at open-pit mining enterprises and the wireless charging infrastructure. The development of such optimization methods is the subject of further research. With the described model modification, periodic adjustments of the system power consumption parameters can be made while operating, taking into account the face advancing, the changes in condition of the operating routes, as well as seasonal changes, including temperature and precipitation. Based on these adjustments, regular adjustments to the optimization algorithms can be made.

The proposed model can also be used as a foundation for a more detailed analysis of the battery fade, evaluating the effects of temperature on it and identifying the technical and economic parameters of the system under consideration.

REFERENCES

1. Nobahar P., Chaoshui Xu, Dowd P., Shirani Faradonbeh R. Exploring digital twin systems in mining operations: A review. *Green and Smart Mining Engineering*. 2024. Vol. 1. Iss. 4, p. 474-492. DOI: 10.1016/j.gsme.2024.09.003

2. Jian-guo Li, Kai Zhan. Intelligent Mining Technology for an Underground Metal Mine Based on Unmanned Equipment. *Engineering*. 2018. Vol. 4. Iss. 3, p. 381-391. DOI: 10.1016/j.eng.2018.05.013

3. Zhengguo Hu, Shibin Lin, Xiuhua Long et al. Excavation trajectory planning for unmanned mining electric shovel using B-spline curves and point-by-point incremental strategy under uncertainty. *Automation in Construction*. 2025. Vol. 174. N 106135. DOI: 10.1016/j.autcon.2025.106135

4. Dongyang Huo, Jinshi Chen, Tongyang Wang. Chaos-based support vector regression for load power forecasting of excavators. *Expert Systems with Applications*. 2024. Vol. 246. N 123169. DOI: 10.1016/j.eswa.2024.123169

5. Yukun Yang, Wei Zhou, Jiskani I.M., Zhiming Wang. Extracting unstructured roads for smart Open-Pit mines based on computer vision: Implications for intelligent mining. *Expert Systems with Applications*. 2024. Vol. 249. Part C. N 123628. DOI: 10.1016/j.eswa.2024.123628

6. Lalezar M., Izadi I., Hoseinie S.H., Mohamadrezaie H. A Model Predictive Control Algorithm for Autonomous Mining Dump Trucks. *IFAC-PapersOnLine*. 2024. Vol. 58. Iss. 22, p. 60-65. DOI: 10.1016/j.ifacol.2024.09.291

7. Siyu Teng, Luxi Li, Yuchen Li et al. FusionPlanner: A multi-task motion planner for mining trucks via multi-sensor fusion. *Mechanical Systems and Signal Processing*. 2024. Vol. 208. N 111051. DOI: 10.1016/j.ymssp.2023.111051

8. Voronov Yu.E., Voronov A.Yu., Dubinkin D.M., Maksimova O.S. Dispatching in truck-shovel systems with unmanned transport at open-pit mines. *Ugol.* 2023. N 9 (1171), p. 75-83 (in Russian). DOI: 10.18796/0041-5790-2023-9-75-83

9. Li Zhang, Wenxuan Shan, Bin Zhou, Bin Yu. A dynamic dispatching problem for autonomous mine trucks in open-pit mines considering endogenous congestion. *Transportation Research Part C: Emerging Technologies*. 2023. Vol. 150. N 104080. DOI: 10.1016/j.trc.2023.104080

10. Yamini E., Zarnoush M., Jalilvand M. et al. Integration of emerging technologies in next-generation electric vehicles: Evolution, advancements, and regulatory prospects. *Results in Engineering*. 2025. Vol. 25. N 104082. DOI: 10.1016/j.rineng.2025.104082

11. Verma S., Sharma A., Tran B., Alahakoon D. A systematic review of digital twins for electric vehicles. *Journal of Traffic and Transportation Engineering*. 2024. Vol. 11. Iss. 5, p. 815-834. DOI: 10.1016/j.jtte.2024.04.004

12. Balboa-Espinoza V., Segura-Salazar J., Hunt C. et al. Comparative life cycle assessment of battery-electric and diesel underground mining trucks. *Journal of Cleaner Production*. 2023. Vol. 425. N 139056. DOI: 10.1016/j.jclepro.2023.139056

13. Qingsong Tang, Manjiang Hu, Yougang Bian et al. Optimal energy efficiency control framework for distributed drive mining truck power system with hybrid energy storage: A vehicle-cloud integration approach. *Applied Energy*. 2024. Vol. 374. N 123989. DOI: 10.1016/j.apenergy.2024.123989

14. Zamyatin I.D. Analysis of the development prospects of the design of the mining dump. *Voprosy ustoichivogo razvitiya obshchestva.* 2021. N 6, p. 641-651 (in Russian).

15. Cherepanov V.A., Zhuravlev A.G., Glebov I.A., Chendyrev M.A. Overview of transport with rower supply in focus of mining industry development. *Problems of Subsoil Use.* 2019. N 1 (20), p. 33-49 (in Russian). DOI: 10.25635/2313-1586.2019.01.033

16. Hunt J.D., Nascimento A., Wenxuan Tong et al. Perpetual motion electric truck, transporting cargo with zero fuel costs. *Journal of Energy Storage*. 2023. Vol. 72. Part D. N 108671. DOI: 10.1016/j.est.2023.108671

17. Khazin M.L. Electric trucks for underground and open pit mining. *News of the Ural State Mining University.* 2019. Iss. 1 (53), p. 128-135 (in Russian). DOI: 10.21440/2307-2091-2019-1-128-135

18. Dubinkin D.M., Kartashov A.B., Arutyunyan G.A. et al. Current state of the art and technologies in the field of quarry dump trucks with energy storage devices. *Mining Equipment and Electromechanics.* 2020. N 6 (152), p. 31-42 (in Russian). DOI: 10.26730/1816-4528-2020-6-31-42

19. Grachev A.I. Absolutely "green" BELAZ-7558E. *Gornaya promyshlennost*. 2022. N 2, p. 30-32 (in Russian).

20. Nguyen T.H., Vasiliev B.Yu. Analysis of autonomous robotic mining machines with autonomous electric propulsion systems. *Mining Equipment and Electromechanics.* 2022. N 5 (163), p. 59-69 (in Russian). DOI: 10.26730/1816-4528-2022-5-59-69

21. Sudev V., Sindhu M.R. State-of-the-art and future trends in electric vehicle charging infrastructure: A review. *Engineering Science and Technology, an International Journal*. 2025. Vol. 62. N 101946. DOI: 10.1016/j.jestch.2025.101946

22. Revankar S.R., Kalkhambkar V.N. Grid integration of battery swapping station: A review. *Journal of Energy Storage*. 2021. Vol. 41. N 102937. DOI: 10.1016/j.est.2021.102937

23. Weipeng Zhan, Zhenpo Wang, Lei Zhang et al. A review of siting, sizing, optimal scheduling, and cost-benefit analysis for battery swapping stations. *Energy*. 2022. Vol. 258. N 124723. DOI: 10.1016/j.energy.2022.124723

24. Mahaadevan V.C., Narayanamoorthi R., Logeshwer S.P.P. et al. Integrated design and YOLO based control framework for autonomous EV charging robot platforms. *Results in Engineering*. 2025. Vol. 26. № 105438. DOI: 10.1016/j.rineng.2025.105438

25. Santos G.R., Romeral P.A., Zancul E. et al. Exploring electric vehicle robot charging stations: A simulation-based approach for charging capacity improvement. *Research in Transportation Business & Management*. 2025. Vol. 60. N 101383. DOI: 10.1016/j.rtbm.2025.101383

26. Hao Chen, Zhongnan Qian, Ruoqi Zhang et al. Modular Four-Channel 50 kW WPT System With Decoupled Coil Design for Fast EV Charging. *IEEE Access*. 2021. Vol. 9, p. 136083-136093. DOI: 10.1109/ACCESS.2021.3116696

27. Zavyalov V.M., Semykina I.Yu., Dubkov E.A., Velilyaev A.S. The wireless charging system for mining electric locomotives. *Journal of Mining Institute.* 2023. Vol. 261, p. 428-442.

28. Rogge M., Wollny S., Sauer D.U. Fast Charging Battery Buses for the Electrification of Urban Public Transport – A Feasibility Study Focusing on Charging Infrastructure and Energy Storage Requirements. *Energies*. 2015. Vol. 8. Iss. 5, p. 4587-4606. DOI: 10.3390/en8054587

29. Rothgang S., Rogge M., Becker J., Sauer D.U. Battery Design for Successful Electrification in Public Transport. *Energies*. 2015. Vol. 8. Iss. 7, p. 6715-6737. DOI: 10.3390/en8076715

30. Basso R., Kulcsár B., Egardt B. et al. Energy consumption estimation integrated into the Electric Vehicle Routing Problem. *Transportation Research Part D: Transport and Environment*. 2019. Vol. 69, p. 141-167. DOI: 10.1016/j.trd.2019.01.006

31. Yang Xing, Chen Lv, Dongpu Cao, Chao Lu. Energy oriented driving behavior analysis and personalized prediction of vehicle states with joint time series modeling. *Applied Energy*. 2020. Vol. 261. N 114471. DOI: 10.1016/j.apenergy.2019.114471

32. Jia-Hao Syu, Lin J.C.-W., Yu P.S. Multi-head learning models for power consumption prediction of unmanned ground vehicles. *Information Fusion*. 2025. Vol. 118. N 102895. DOI: 10.1016/j.inffus.2024.102895

33. Xu Y., Ingelström P., Kersten A. et al. Improving powertrain efficiency through torque modulation techniques in single and dual motor electric vehicles. *Transportation Engineering*. 2024. Vol. 18. N 100289. DOI: 10.1016/j.treng.2024.100289

34. Burmistrova O.N., Plastinina E.V., Timokhova O.M. On the determination of dependence of the velocity of the car from the visibility distance on the curve plan. *Fundamental Research.* 2015. N 2-10, p. 2074-2078 (in Russian).

35. Bryn M.Ya., Mustafin M.G., Bashirova D.R., Vasilev B.Yu. Investigation of the accuracy of constructing digital elevation models of technogenic massifs based on satellite coordinate determinations. *Journal of Mining Institute.* 2025. Vol. 271, p. 95-107.

36. Semykina I.Yu., Zavyalov V.M., Dubkov E.A., Nechiporenko Ya.A. The evaluation of the power of technological connection to electrical systems for the wireless charging infrastructure of battery-powered dump trucks. Problemy i perspektivy razvitiya energetiki, elektrotekhniki i energoeffektivnosti: Materialy VIII Mezhdunarodnoi nauchno-tekhnicheskoi konferentsii, 22 noyabrya 2024. Cheboksary, Rossiya. V 2 chastyakh. Cheboksary: Chuvashskii gosudarstvennyi universitet im. I.N.Ulyanova, 2024. Part 1, p. 265-273 (in Russian).

37. Pechenko V.V. Single state dynamic battery cell model. *Radioengineering.* 2015. N 4, p. 58-60 (in Russian).

38. Hao Mu, Rui Xiong, Fengchun Sun. A Novel Multi-model Probability Based Battery State-of-charge Fusion Estimation Approach. *Energy Procedia*. 2016. Vol. 88, p. 840-846. DOI: 10.1016/j.egypro.2016.06.061

39. Rui Xiong, Yongzhi Zhang, Ju Wang et al. Lithium-Ion Battery Health Prognosis Based on a Real Battery Management System Used in Electric Vehicles. *IEEE Transactions on Vehicular Technology*. 2019. Vol. 68. Iss. 5, p. 4110-4121. DOI: 10.1109/TVT.2018.2864688

40. De Santis E., Pennazzi V., Luzi M., Rizzi A. Degradation mechanisms and differential curve modeling for non-invasive diagnostics of lithium cells: An overview. *Renewable and Sustainable Energy Reviews*. 2025. Vol. 211. N 115349. DOI: 10.1016/j.rser.2025.115349

41. Syrkin I.S., Buzunov N.V., Turgenev I.A. Battery sizes of low-voltage electrical equipment of dump trucks with payload capacity from 218 to 255 tons. *Journal of Mining and Geotechnical Engineering.* 2022. N 2 (17), p. 53-66 (in Russian). DOI: 10.26730/2618-7434-2022-2-53-66

42. Golubchik T., Kulikov A. Experimental tests results of lithium-iron-phosphate battery manufactured by LYOTECH under low-temperature conditions. *Electronics and Electrical Equipment of Transport.* 2021. N 1, p. 17-20 (in Russian).

43. Gursky A.S. Analysis of parameters of high-voltage batteries of electric buses in order to create algorithms for their general and element-by-element diagnostics using telematics systems. *Transport i transportnye sistemy: konstruirovanie, ekspluatatsiya, tekhnologii. Minsk: Belorusskii natsionalnyi tekhnicheskii universitet*, 2022. Iss. 4, p. 12-20 (in Russian).

44. Kuznetsov I.S., Sinoviev V.V., Nikolayev P.I., Starodubov A.N. Simulation modeling computer-based system for optimizing the parameters of open-pit excavator-dump truck complexes. *Mining Informational and Analytical Bulletin.* 2022. N 6-1, p. 304-316 (in Russian). DOI: 10.25018/0236_1493_2022_61_0_304

45. Voronov A.Yu. Optimization of operational performance indicators of shovel-truck systems in open-pit mines: Avtoref. dis. … kand. tekhn. nauk. Kemerovo: Kuzbasskii gosudarstvennyi tekhnicheskii universitet imeni T.F.Gorbacheva, 2015, p. 19 (in Russian).

***Authors*: Irina Yu. Semykina,** *Doctor of Engineering Sciences, Senior Researcher* (*T.F.Gorbachev Kuzbass State Technical University, Kemerovo, Russia*), *arinasemykina@gmail.com*, *https://orcid.org/0000-0001-6874-1735*, **Valery M. Zavyalov,** *Doctor of Engineering Sciences, Professor* (*T.F.Gorbachev Kuzbass State Technical University, Kemerovo, Russia*), *https://orcid.org/0000-0001-8485-9864*, **Yaroslava A. Nechiporenko,** *Postgraduate Student* (*T.F.Gorbachev Kuzbass State Technical University, Kemerovo, Russia*), *https://orcid.org/0009-0001-4686-4184*, **Elena N. Taran,** *Candidate of Engineering Sciences, Supplementary Education Teacher* (*Sevastopol Station of Young Technicians, Sevastopol, Russia*), *https://orcid.org/0009-0005-9656-9457*.

The authors declare no conflict of interests.

ISSN 2411-3336; e-ISSN 2541-9404

JOURNAL OF MINING INSTITUTE
Zapiski Gornogo instituta
Journal homepage: pmi.spmi.ru

Research article
Geotechnical Engineering and Engineering Geology

Application of machine learning to modeling Herschel – Bulkley drilling fluid parameters for optimizing wellbore cleaning

Vasiliy I. Nikitin ✉, Mikhail V. Dvoynikov, Kirill S. Kupavykh, Tatiana A. Panteleeva
Empress Catherine II Saint Petersburg Mining University, Saint Petersburg, Russia

***How to cite this article*:** Nikitin V.I., Dvoynikov M.V., Kupavykh K.S., Panteleeva T.A. Application of machine learning to modeling Herschel – Bulkley drilling fluid parameters for optimizing wellbore cleaning. Journal of Mining Institute. 2025. Vol. 275, p. 70-80.

Abstract
Water- and oil-based drilling fluids are polydisperse non-Newtonian systems, the stress state of which is adequately described by the Herschel – Bulkley rheological model. This study hypothesizes that cuttings transport efficiency can be improved by selecting the most effective combination of the three parameters of the rheological model – yield stress, consistency index, and flow behavior index – when designing drilling fluid properties. The effective parameter combination of the Herschel – Bulkley model for achieving a uniform velocity profile was determined using correlation and regression analysis methods as well as machine learning techniques. The computational part of the work was performed in the Wolfram Mathematica symbolic calculation package. Deterministic regions of the dependence of the velocity profile uniformity index on the rheological coefficients were identified. For practical engineering calculations, a linear mathematical model was constructed to represent the relationship between the modified excess coefficient and the parameters of the three-parameter Herschel – Bulkley rheological equation. The proposed methodology can be recommended for designing new drilling fluid systems and testing existing ones under given wellbore cleaning conditions.

Keywords
well drilling; drilling mud; wellbore cleaning; rheological models; cuttings removal quality; non-Newtonian fluid; neural network; machine learning; mathematical modeling

Received: 28.01.2025 ***Accepted: 02.07.2025*** ***Online: 10.10.2025*** ***Published: 31.10.2025***

Introduction

One of the most important functions of drilling fluids is to transport drilled cuttings to the surface. Cuttings transport efficiency is governed by annular flow velocity, fluid density, and its rheological characteristics. The correct selection of rheological parameters significantly enhances the rate of penetration [1]. Control of drilling fluid rheology is achieved through the selection of chemical additives and their concentrations [2, 3]. The velocity profile of drilling fluids has a significant impact on cuttings transport efficiency [4]. A flat velocity profile in the wellbore annulus provides a more uniform momentum transfer to the particles in the direction of flow. When fluids flow in pipes, the velocity profile exhibits a symmetric distribution with maximum velocity at the center of the flow [5]. In annular flow, however, the maximum velocity shifts toward the pipe axis. This leads to uneven cuttings transport and the formation of stationary cuttings beds along the wellbore walls [6, 7]. These effects are confirmed by both analytical and numerical solutions of the governing flow equations [8, 9]. Experimental data also validate the non-uniformity of velocity profiles in both pipes and annular geometries [10]. Research [11] demonstrates strong agreement between numerical simulations of cuttings-laden

flows and laboratory-scale experimental results. Similar solutions can be obtained using the control volume method implemented in software packages such as ANSYS Fluent and OpenFOAM [12, 13]. These computational tools also enable modeling of wellbore cleaning while accounting for drillstring rotation [14] and thermal effects [15]. Temperature effects become particularly significant during well construction and production operations in Arctic environments [16, 17]. Research [18] addresses the modeling of cuttings transport in deviated and horizontal wells under high-temperature and high-pressure conditions. At the same time, considerable attention is currently being given to drilling fluid losses. The calculation of flow velocities and pressures for specific wellbore conditions contributes to improving hole-cleaning practices in cases of drilling fluid loss [19].

When modeling the flow of drilling fluids, the choice of a rheological model plays a critical role. The rheological behavior of modern drilling fluids is best represented by the Herschel – Bulkley model [20-22]. This model is applicable both to fluids containing solid phases and to formulations without them [23]. The least-squares method is the most reliable approach for determining the coefficients of a rheological model. It is applied to approximate the experimental dependence of shear stress on shear rate [24]. The mathematical formulation of fluid flow in the wellbore annulus includes the governing equations of motion, the rheological model of the fluid, and boundary conditions. The choice of the rheological model is of particular importance, since adjusting its coefficients allows control over velocity and pressure distributions. The mathematical model of drilling fluid flow in the wellbore annulus was adopted from [24]. In this research, a numerical method is presented to determine the velocity distribution of a non-Newtonian fluid represented by the Herschel – Bulkley model in annular geometries. In contrast to the Ostwald – de Waale model, it contains three coefficients:

$$\tau = \pm\tau_0 + K\dot{\gamma}\left|\dot{\gamma}\right|^{n-1}, \tag{1}$$

where τ_0 – yield stress; $\dot{\gamma}$ – shear rate; K – consistency index; n – flow index.

The stationary modified Navier – Stokes differential equation for determining the velocity field:

$$\frac{\partial p}{\partial z} = -\rho g + \frac{1}{r}\frac{\partial r\tau}{\partial r},$$

where ρ – fluid density; r – radial coordinate; g – gravitational acceleration; $\partial p / \partial z$ – pressure gradient along the length L.

For the boundary conditions of the wellbore annulus:

$$w = 0; r = R_1; r = R_2,$$

where w – fluid layer velocity; R_1 – external radius of drill pipe; R_2 – well radius.

The assumptions include fluid incompressibility ρ = const, one-dimensional flow, and steady-state conditions:

$$\frac{\partial w}{\partial z} = 0. \tag{2}$$

Research [24] compared the solutions obtained under the Newtonian fluid approximation with the analytical solution for Poiseuille flow in an annular gap. The physical adequacy of the numerical solution was confirmed when varying the input parameters. The numerical solution was implemented in Wolfram Language as an interpolating function that enables velocity values to be represented as a

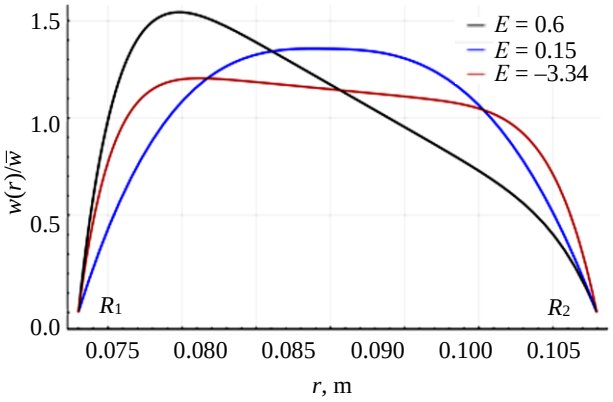

Fig.1. The flattest and most elongated velocity profiles

function of the coordinate. In addition, a numerical indicator of velocity profile uniformity, referred to as the modified excess coefficient, was introduced:

$$E = 3 - \frac{\mu_4}{\mu_2^2},$$

where μ_2, μ_4 – the central moments applied to the velocity distribution in the flow.

A minimum value of this parameter indicates the presence of the most uniform velocity profile. The use of program code makes it possible to obtain numerical solutions for the velocity profile. The corresponding modified excess coefficient characterizes the uniformity of the velocity distribution. For a more accurate visual assessment, the velocity distribution is plotted in a dimensionless form. This form represents the ratio of point velocity to the mean flow velocity – $w(r)/\bar{w}$. The plotting domain is located between the drill pipe wall R_1 and the wellbore wall R_2. Examples of velocity distributions and the corresponding values of the excess coefficient are shown in Fig.1. The most elongated and shifted profile corresponds to the highest value of parameter *E*.

It is known that in the Shvedov – Bingham model, the value of yield stress influences the uniformity of the velocity distribution, while plastic viscosity determines the average flow velocity. In the Ostwald – de Waale power-law model, a reduction in the flow behavior index *n* leads to the formation of a flatter velocity profile. A drawback of this approximation is that it does not account for the yield stress of the drilling fluid τ_0. The rheological equation of the power-law fluid is expressed as:

$$\tau = K\dot{\gamma}\left|\dot{\gamma}\right|^{n-1}.$$

Research [24] showed that in the Herschel – Bulkley model, no explicit correlation is observed between the parameters τ_0, *K*, *n* and the modified excess coefficient *E*. This confirms that the velocity distribution of the fluid cannot be controlled by adjusting τ_0, *K*, *n* independently of one another. Controlling only the flow behavior index *n*, as in the power-law model, does not yield a positive result [4, 8]. Considering these limitations, the objective of this work is to develop a method for determining the interrelations among the three rheological parameters of the Herschel – Bulkley model, with a tendency toward forming a more uniform velocity profile. The uniformity can be numerically assessed using the modified excess coefficient.

Methodology

To determine the effect of the parameter combination of the Herschel – Bulkley model (1) on the uniformity of the velocity profile, it is necessary to establish the dependence of the modified excess coefficient *E* on the parameters τ_0, *K*, *n*. Since *E* depends on the velocity distribution obtained from the numerical solution of the momentum equation with specified geometric conditions, pressure drops, and fluid parameters, the problem reduces to identifying the relationship among these numerical parameters. A nonlinear form of dependence is assumed:

$$E = f(\tau_0, K, n). \quad (3)$$

To establish such a dependence, it is necessary to construct a table of values for *E*, τ_0, *K*, and *n*, that correspond to the physical and technological parameters of the wellbore cleaning process.

When preparing this table, wide parameter ranges are proposed as constraints for τ_0, K, and n, corresponding to the properties of drilling fluids [25]: yield stress $0.1 \le \tau_0 \le 5$ Pa; consistency index $2 \le K \le 15$ Pa·s^n; and flow behavior index $0.15 \le n \le 1$. For the most promising fluids, rheological parameters are assumed that ensure efficient cuttings transport under laminar flow conditions. These parameters are calculated according to the methodology presented in [26]. Under laminar flow conditions, dynamic pressures are lower than in turbulent flow, which reduces the risk of formation fracturing during hole cleaning. Therefore, the critical velocity of the drilling fluid is calculated, above which the flow regime transitions from laminar to turbulent [27].

Next, the cuttings transport quality index for the critical velocity of the drilling fluid is calculated by determining the cuttings transport velocity based on the difference between the flow velocity and the particle settling velocity. Shear stresses and the flow regime in the vicinity of the particle, which may be either laminar or turbulent, must be taken into account. For the parameters τ_0, K, and n, corresponding to high values of the cleaning index, the velocity profile is calculated at pressures associated with the critical velocity of the drilling fluid. The calculated modified excess coefficient E is entered into a table for further processing.

The three-factor dependence $E = f(\tau_0, K, n)$ may exhibit a pronounced nonlinear character. The next task involves identifying the deterministic sections of dependence (2) with the possibility of determining linear segments, after which a linear multifactor regression can be constructed:

$$E = a_0 + a_1\tau_0 + a_2K + a_3n, \tag{4}$$

where a_i – the regression coefficients.

The advantage of isolating linear segments lies in the possibility of obtaining an analytical form of the dependence, which is preferred by drilling hydraulics designers for evaluating velocity profile uniformity when selecting a drilling fluid.

Machine learning methods have been successfully applied to describe multifactor nonlinear dependencies. For example, in [28] it is described the use of a neural network to evaluate equivalent circulating density based on large datasets. In [29], a neural network approach was employed to predict the plastic and effective viscosities of oil-based drilling fluids. Research [30] utilized a Gaussian process model to forecast drilling fluid rheological properties from six factors: Marsh funnel viscosity, density, volumetric content of water, oil and solids, and temperature. The coefficient of determination exceeded 0.9, indicating high predictive accuracy. The authors of [31] applied hybrid machine learning to achieve rapid prediction of rheological and filtration properties of water-based drilling fluids. Research [32] employed machine learning methods to predict porosity and permeability during drilling. Research [33] proposed a neural network training approach (Python programming language) for forecasting drilling fluid properties under high-pressure and high-temperature conditions. The results were compared with the Herschel – Bulkley and power-law rheological models. Yield stress values were predicted using three input parameters: shear rate, pressure, and temperature. In [34], the authors developed a script in Wolfram Language to implement a logarithmic-linear (L-L) mathematical model. Using this code, a mathematical model was realized for analyzing the rheological properties of drilling fluids, based on a nonlinear relationship between measured shear stress and shear rate values in fluids used for drilling oil and geothermal wells. Machine learning methods have also proven effective in addressing problems related to wellbore complications during field operations [35, 36]. Such approaches are particularly suitable for processing field data with high levels of noise caused by random factors.

Based on the objectives of this study, Wolfram Language was selected for the full calculation cycle, including the numerical solution of the momentum equation with respect to the velocity profile and the identification of deterministic sections of dependence (3). Using the Predict function, a machine learning method is selected – Random Forest, Nearest Neighbors, Decision Tree, and others [37]. A drawback of predictive models is the inability to construct an analytical form of the dependence. The identification of linear sections of the dependence makes it possible to transition to a linear multifactor regression model. The LinearRegression option within the Predict function enables the construction of multifactor linear dependencies of the form (4). To select the most effective method of the Predict function for processing the initially compiled data table, a predefined template is applied to test each method and compare the coefficient of determination R^2. For identifying deterministic sections potentially suitable for constructing the analytical form (4), the method with the highest R^2 value is used. The presence of deterministic sections can be readily determined by analyzing the ComparisonPlot and ResidualPlot graphs, which illustrate the deviation between actual and predicted values as well as the magnitude of deviation across different segments of the predicted values.

A methodology has been developed to determine the most effective parameter combinations of the Herschel – Bulkley model for ensuring high-quality wellbore cleaning, including through the formation of the most uniform velocity profile. The methodology consists of the following steps:

• Using the procedure for calculating the cuttings transport efficiency index, establish the initial requirements for the rheological characteristics of the drilling fluid under the power-law rheological approximation while maintaining laminar flow conditions.

• Determine the type of velocity profile by calculating the modified excess coefficient for a Herschel – Bulkley fluid with K and n values that satisfy the initial requirements.

• Identify the combinations of τ_0, K, and n that meet the requirement of high cuttings transport efficiency and provide a uniform velocity profile with the lowest value of the modified excess coefficient E.

• Apply machine learning methods to establish the relationship between τ_0, K, n and the quantitative indicator of velocity profile uniformity – the modified excess coefficient E.

• For the sections selected for constructing an analytical form of linear multifactor regression, calculate the regression coefficients.

• Develop methodological recommendations for the design of drilling fluids with effective combinations of rheological parameters τ_0, K, and n to ensure high-quality cuttings transport in laminar flow while maintaining a uniform velocity profile.

Discussion

Using Wolfram Language, 9235 combinations of the parameters τ_0, K, and n were generated within the specified bounds and step size Δ:

$$0.1 \le \tau_0 \le 5;\ \Delta_{\tau_0} = 0.25 \text{ Pa};$$
$$2 \le K \le 15;\ \Delta_K = 0.5 \text{ Pa·s}^n; \quad (5)$$
$$0.15 \le n \le 1;\ \Delta_n = 0.05.$$

The cuttings transport efficiency index was calculated for the critical velocity of the drilling fluid, defined as the velocity above which the fluid transitions to turbulent flow. This choice is justified by the requirement to remain within safe drilling parameters under laminar flow, which is characterized by significantly lower hydrodynamic pressures. The common input parameters for the

calculations are as follows: drilling fluid density – 1200 kg/m^3; cuttings density – 2300 kg/m^3; diameter of the spherical coarse cuttings model – 7.6 mm; wellbore diameter – 215.9 mm; and outer diameter of the drill pipe – 146 mm.

Out of the total combinations, 7980 provide cuttings transport efficiency greater than 70 %, while 7582 combinations exceed 80 %. The highest efficiency is observed at n = 1; however, modern drilling fluids for directional and horizontal wells exhibit pronounced pseudoplastic properties, and the parameter $n << 1$ [38]. A graph characterizing the trend of cuttings transport efficiency as a function of the rheological coefficients K and n is shown in Fig.2. With increasing values of the consistency index K and the flow behavior index n, the particle settling velocity decreases, since in the power-law rheological model the consistency index serves as an analogue of viscosity. Consequently, an increase in viscosity reduces the particle settling velocity due to the enhanced ability of the fluid flow to suspend particles. This conclusion is consistent with Stokes' theory through the viscous characteristics of the fluid [39].

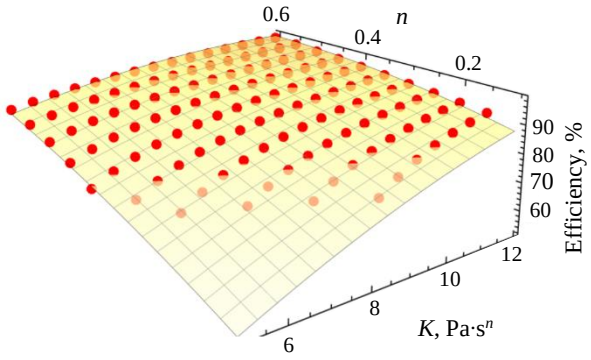

Fig.2. Dependences of the efficiency coefficient of cuttings transport on the coefficients K and n of the rheological model of a power-law liquid

The flow behavior index in the power-law rheological model reflects the non-Newtonian behavior of the medium: with increasing shear rate, viscosity decreases at low values of the exponent. Consequently, when $n \to 1$ viscosity shows a lower tendency to decline; at n = 1 viscosity remains constant; and when $n > 1$ the fluid can be considered dilatant, although such fluids are not used in drilling. An increase in viscosity enhances suspension capacity; therefore, its reduction, reflected by a decrease in the parameter n, is undesirable for cuttings transport. As these coefficients increase, the critical velocity of the drilling fluid also rises. The turbulent regime occurs at higher velocities, which is favorable for the drilling process, since the flow rate can be increased while avoiding transition to turbulent flow with high pressure [40].

The occurrence of turbulent flow is influenced by the hydraulic diameter of the wellbore annulus, the rheological characteristics of the drilling fluid, and its density. The most effective method for preventing the onset of turbulence is to reduce the drilling fluid flow rate and maintain its parameters within the range specified by the designed drilling hydraulics program. In well construction projects, pressure control is also carried out in terms of equivalent circulating density [41].

The values of the modified excess coefficient were calculated for each velocity distribution while varying the parameters τ_0, K, and n under pressure drops corresponding to the critical flow velocity. According to the two-sigma statistical rule, profiles with the most uniform velocity distribution were identified with a probability of 95 %. A total of 4845 cases with cuttings transport efficiency greater than 70 % and $n \leq 0.8$ correspond to the currently relevant formulations of drilling fluids. For these cases, the values of the velocity profile uniformity index were determined. The test was carried out for fluids with cuttings transport efficiency greater than 70 % and $n \leq 0.8$. The next step was to determine the dependence of type (3) of the modified excess coefficient on the parameters of the rheological model. Based on the results of [24], it can be assumed that the relationship is nonlinear. Due to the multifactorial nature of the approximation task, a machine learning method selection template was used. The data were randomly divided into training and test sets in an 80/20 ratio. The input parameters were $\tau_0, K, n,$ the output parameters were the modified kurtosis coefficient E. According to the coefficient of determination, the Neural Network method in Wolfram Language proved to be

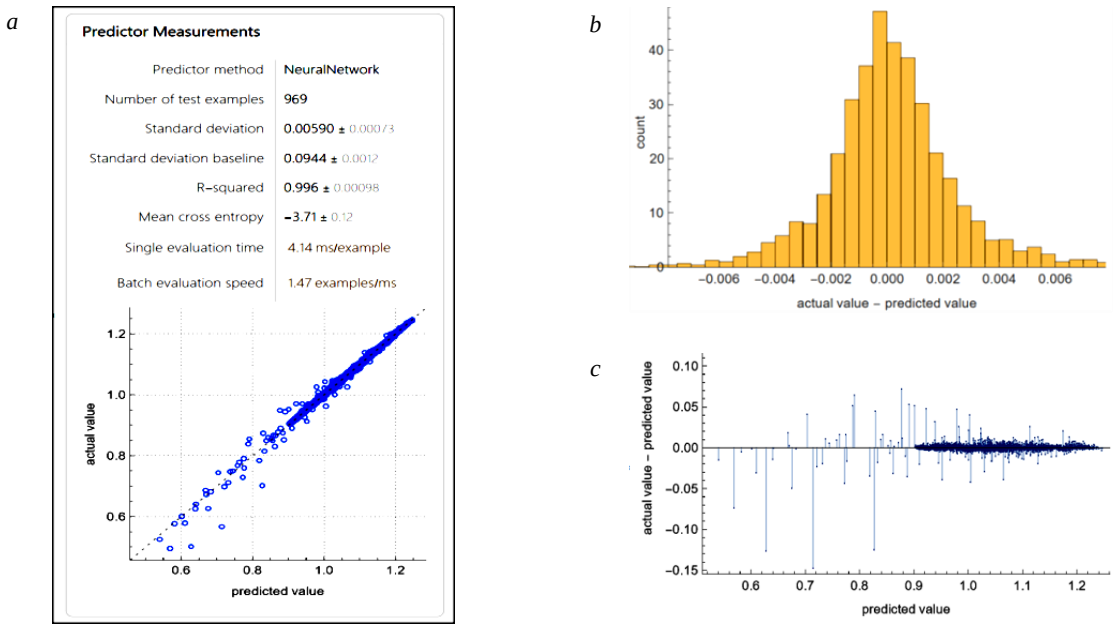

Fig.3. Characteristics of the neural network method: *a* – dialog of the method characteristics; *b* – histogram of deviations ResidualHistogram; *c* – distribution of deviations by areas ResidualPlot

the most effective for this task, with $R^2 = 0.996$ (Fig.3). The distribution of deviations (Fig.3, *b*) also indicates the high quality of the approximation. Analysis of the graphs showed that deterministic sequences were identified for the modified excess coefficient starting from 0.9. Further consideration of the problem continues exclusively within this interval.

The most uniform velocity profile from the deterministic values is $0.9 \le E \le 0.95$. The parameter constraints (5) become more stringent due to the requirements of achieving high cuttings transport efficiency:

$$0.35 \le n \le 0.8;$$
$$2.5 \le K \le 15 \text{ Pa·s}^n; \quad (6)$$
$$0.5 \le \tau_0 \le 5 \text{ Pa}.$$

According to [24], controlling these parameters independently within the Herschel – Bulkley rheological model to achieve a uniform velocity profile is not possible. Analysis of parameter combinations of the rheological model that are effective for cuttings transport under laminar flow with the presence of the most uniform velocity profiles showed the necessity of fulfilling conditions for n and τ_0 depending on K:

$$n \ge -0.02K + 0.65; \quad (7)$$
$$\tau_0 \ge -0.3182K + 5.2727.$$

Thus, it has been established that when using a bit and drill pipes with diameters of 215.9 mm and 146 mm, respectively, the most uniform velocity distributions of fluids modeled by the Herschel – Bulkley rheological model correspond to calculated parameter values in the range $0.9 \le E \le 0.95$. To achieve these values, the permissible limits of the rheological parameters were determined as (6) and (7).

The presented sequence of calculations requires sufficiently advanced engineering skills and specialized software for data processing, which makes its application challenging in industrial practice. Therefore, for the end user, such as a drilling fluids engineer, a final calculation formula accompanied by practical recommendations for its application would be of significant value.

In the deterministic range of values (6) within $0.9 \le E \le 0.95$, it is proposed to construct a linear multifactor regression model of type (4), which can be used to calculate the modified excess coefficient and predict the velocity profile when testing drilling fluid formulations. For the values satisfying conditions (6) and (7), the LinearModelFit function of Wolfram Language was applied to perform linear multifactor regression. The coefficient of determination was $R^2 = 0.83$, with the highest number of deviations recorded around zero. To predict the uniformity of the velocity profile in order to improve cuttings transport efficiency, the applicability of the constructed regression equation is confirmed:

$$E = 1.0658 - 0.0059\tau_0 - 0.0031K - 0.1636n. \quad (8)$$

The graphs (Fig.4) show projections of the four-dimensional model (8) onto three-dimensional space at fixed values of the rheological parameters. The response surfaces provide an approximation of the initial data in the examined regions. Low deviation values and $R^2 = 0.83$ are explained by the weak manifestation of nonlinearity in the vicinity of the response surface. Neglecting this minor nonlinearity, equation (8) can be used for sufficiently simple calculations. For the most uniform profile, E will assume the lowest values when conditions (6)-(7) are satisfied.

The proposed modeling method is validated by comparing two parameter sets of the rheological model for velocity distribution simulation: one obtained by numerical solution and the other using the control volume method in Ansys Fluent. The advantage of CFD software lies in its high calculation accuracy, which accounts for various influencing factors [42]. The calculation conditions are as follows: wellbore diameter – 215.9 mm; outer pipe diameter – 146 mm; fluid density – 1200 kg/m^3. For the Herschel – Bulkley model, two parameter sets are tested:

1) $\tau_0 = 3.5$ Pa, $n = 0.6$, $K = 7$, satisfying conditions (6), (7);

2) $\tau_0 = 2$ Pa, $n = 0.4$, $K = 7$, not satisfying conditions (6), (7).

When calculating the modified excess coefficient using the approximate formula (8), E = = 0.928 for parameter set 1 and $E = 0.967$ for parameter set 2. It has been established that the velocity profile of parameter set 1 is more uniform compared to parameter set 2. Analysis of the graphs (Fig.5) shows agreement between the solutions obtained by the numerical method and those obtained using the control volume method.

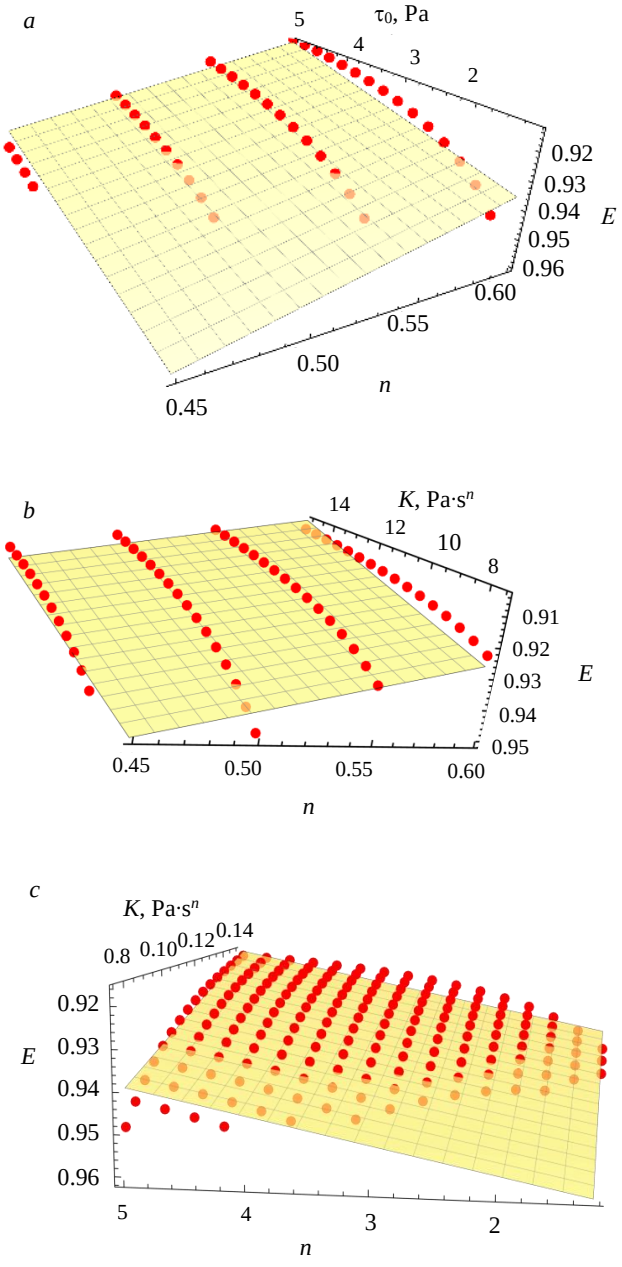

Fig.4. Three-dimensional projections of linear regression: a – τ_0, n, E at $K = 8$ Pa·s^n; b – K, n, E at $\tau_0 = 3$ Pa; c – K, τ_0, E at $n = 0.45$

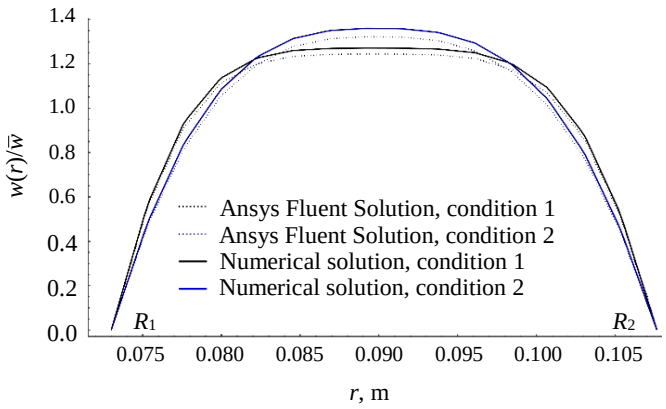

Fig.5. Comparison of velocity distributions obtained using a numerical solution and using the Ansys Fluent package

The minor deviation can be explained by differences between the computational algorithms of Wolfram Language, which constructs an interpolating function of the numerical solution, and the solver in Ansys Fluent. At the same time, it is evident that the hypothesis of a flatter velocity profile for parameter set 1 is confirmed by both calculation methods.

Conclusions

This work presents a method for establishing the relationship between the parameters of the Herschel – Bulkley model and the modified excess coefficient in order to ensure a uniform velocity profile of the drilling fluid in the wellbore annulus. The scientific novelty of this study lies in the simultaneous consideration of all three parameters of the Herschel – Bulkley rheological model and the derivation of compatibility conditions for them. The hypothesis concerning the possibility of controlling the velocity distribution of a non-Newtonian fluid in the wellbore annulus through the selection of parameter combinations of the rheological model is analyzed. Improving cuttings transport efficiency can be achieved by maintaining the most effective combination of Herschel – Bulkley model parameters when designing the properties of a drilling fluid to ensure a more uniform velocity profile.

The analysis of the influence of the Herschel – Bulkley model coefficients on the uniformity of the velocity profile revealed a qualitatively new behavior compared to the use of simplified rheological models. While in the Shvedov – Bingham model velocity profile uniformity is achieved by controlling the yield stress, and in the Ostwald – de Waale power-law model by the flow behavior index n, in the Herschel – Bulkley model the simultaneous influence of τ_0, K, n, has been established, which necessitates determining the interrelation among them.

This study demonstrates a method for determining the interdependence of the three rheological model parameters with the uniformity index of the velocity profile. As an example, combinations of the most favorable rheological parameters for cleaning the annular space between the pipe and the wellbore with diameters of 146 and 215.9 mm, respectively, are considered. Compatibility conditions have been defined for the flow behavior index τ_0, n with the consistency index K. A linear mathematical model $E = f(\tau_0, K, n)$, has been constructed, reflecting the relationship between the quantitative indicator used to evaluate velocity profile uniformity and the coefficients of the three-parameter Herschel – Bulkley rheological equation.

The implementation of these recommendations for designing drilling fluid parameters can result in the formation of a uniform velocity profile, thereby improving cuttings transport. The developed model makes it possible to numerically compare the uniformity of velocity profiles when testing potentially recommended fluids. For comparison of the calculation results, the Ansys Fluent package was used.

Using the described methodology, it is possible to analyze changes in the velocity profile for the most common combinations of annular space geometries. The presence of cuttings in the drilling fluid alters its density and rheological characteristics. Measuring the parameters of drilling fluid with cuttings under reservoir temperature ranges makes it possible to model the process under conditions close to those in the wellbore. These data can also be obtained using a continuous drilling fluid monitoring system at the rig. A promising direction is the development of nomograms for the rheological parameters of the Herschel – Bulkley model as a function of diameter ratios. The availability of such functional relationships enables more efficient selection of fluid parameters to ensure a uniform velocity profile in the wellbore annulus.

REFERENCES

1. Jalakani R., Tabatabaee Moradi S.S., Morenov V. Reliability Analysis of a Drilling Bit Penetration Model in Oil and Gas Wells: A Case Study. *International Journal of Engineering – Transactions B: Applications*. 2024. Vol. 37. Iss. 11, p. 2213-2222. DOI: 10.5829/ije.2024.37.11b.08

2. Raupov I., Rogachev M., Sytnik J. Design of a Polymer Composition for the Conformance Control in Heterogeneous Reservoirs. *Energies*. 2023. Vol. 16. Iss. 1. N 515. DOI: 10.3390/en16010515

3. Zubkova O.S., Kuchin V.N., Toropchina M.A., Ivkin A.S. Potential Application of Saponite Clay for Production of Drilling Fluids. *International Journal of Engineering – Transactions B: Applications*. 2024. Vol. 37. Iss. 11, p. 2142-2149. DOI: 10.5829/ije.2024.37.11b.01

4. Ferroudji H., Rahman M.A., Hadjadj A. et al. 3D numerical and experimental modelling of multiphase flow through an annular geometry applied for cuttings transport. *International Journal of Multiphase Flow*. 2022. Vol. 151. N 104044. DOI: 10.1016/j.ijmultiphaseflow.2022.104044

5. Ashena R., Badrouchi F., Elmgerbi A. et al. Stepwise mathematical derivation of the Herschel–Bulkley laminar fluid flow equations – in pipes. *Journal of Petroleum Exploration and Production Technology*. 2023. Vol. 13. Iss. 2, p. 625-643. DOI: 10.1007/s13202-022-01566-2

6. Belimane Z., Hadjadj A., Ferroudji H. et al. Modeling surge pressures during tripping operations in eccentric annuli. *Journal of Natural Gas Science and Engineering*. 2021. Vol. 96. N 104233. DOI: 10.1016/j.jngse.2021.104233

7. Chandrasekhar S.V. Annular Couette–Poiseuille flow and heat transfer of a power-law fluid – analytical solutions. *Journal of Non-Newtonian Fluid Mechanics*. 2020. Vol. 286. N 104402. DOI: 10.1016/j.jnnfm.2020.104402

8. Xiaofeng Sun, Kebo Zhang, Ye Chen et al. Study on the settling velocity of drilling cuttings in the power law fluid. *Powder Technology*. 2020. Vol. 362. P. 278-287. DOI: 10.1016/j.powtec.2019.11.025

9. Roberts T.G., Cox S.J. An analytic velocity profile for pressure-driven flow of a Bingham fluid in a curved channel. *Journal of Non-Newtonian Fluid Mechanics*. 2020. Vol. 280. N 104278. DOI: 10.1016/j.jnnfm.2020.104278

10. Lin Zhang, Yigang Wang, Dake Chen, Cheng Chen. Prediction and correction of scaling effects on velocity profile in hydraulic laboratory experiments. *Desalination and Water Treatment*. 2019. Vol. 149. 2019. P. 31-42. DOI: 10.5004/dwt.2019.23848

11. Sirui Tong, Bin Miao, Mengsong Shen et al. Experimental and numerical analysis of granular phase flow behavior in a rotary bed reactor: Velocity profile study. *Powder Technology*. 2024. Vol. 444. N 119992. DOI: 10.1016/j.powtec.2024.119992

12. Kharlamov S.N., Janghorbani M., Bryskin M.R. Aspects of Computer Simulation of Transport and Cleaning Processes from Cuttings in Horizontal Well Sections. *Mathematical Models and Computer Simulations.* 2023. Vol. 15. N 3, p. 502-519. DOI: 10.1134/S2070048223030080

13. Muangput B., Zin T., Namchanthra S. et al. CFD elucidation of high-pressure subcooled boiling flow towards effects of variable refrigerant properties using OpenFOAM empirical closures. *Applications in Engineering Science*. 2024. Vol. 19. N 100187. DOI: 10.1016/j.apples.2024.100187

14. Alade O., Mahmoud M., Al-Nakhli A. Rheological studies and numerical investigation of barite sag potential of drilling fluids with thermochemical fluid additive using computational fluid dynamics (CFD). *Journal of Petroleum Science and Engineering*. 2023. Vol. 220. Part A. N 111179. DOI: 10.1016/j.petrol.2022.111179

15. Gulraiz S., Gray K.E. A model for investigating wellbore hydraulics of thermo-thixotropic drilling fluids. *Geothermics*. 2021. Vol. 96. N 102214. DOI: 10.1016/j.geothermics.2021.102214

16. Litvinenko V.S., Dvoynikov M.V., Trushko V.L. Elaboration of a conceptual solution for the development of the Arctic shelf from seasonally flooded coastal areas. *International Journal of Mining Science and Technology*. 2021. Vol. 32. Iss. 1, p. 113-119. DOI: 10.1016/j.ijmst.2021.09.010

17. Leusheva E., Morenov V. Effect of Temperature Conditions in Arctic Offshore Oil Fields on the Rheological Properties of Various Based Drilling Muds. *Energies*. 2022. Vol. 15. Iss. 5. N 5750. DOI: 10.3390/en15155750

18. Al-Shargabi M., Davoodi S., Wood D.A. et al. Hole-cleaning performance in non-vertical wellbores: A review of influences, models, drilling fluid types, and real-time applications. *Geoenergy Science and Engineering*. 2024. Vol. 233. N 212551. DOI: 10.1016/j.geoen.2023.212551

19. Buslaev G.V., Belkin A.S. Development and Field Testing of the Downhole Multi-Purpose Thrusting Device for Drilling of Deep Vertical and Directional Wells. SPE Russian Petroleum Technology Conference, 26-28 October 2015, Moscow, Russia. OnePetro, 2015. N SPE-176539-MS. DOI: 10.2118/176539-MS

20. Abdullah A.H., Ridha S., Mohshim D.F., Maoinser M.A. An experimental investigation into the rheological behavior and filtration loss properties of water-based drilling fluid enhanced with a polyethyleneimine-grafted graphene oxide nanocomposite. *RSC Advances*. 2024. Vol. 14. Iss. 15, p. 10431-10444. DOI: 10.1039/D3RA07874D

21. Saasen A., Ytrehus J.D. Viscosity Models for Drilling Fluids – Herschel-Bulkley Parameters and Their Use. *Energies*. 2020. Vol. 13. Iss. 20. N 5271. DOI: 10.3390/en13205271

22. Bavoh C.B, Ofei T.N., Lai B. et al. Assessing the impact of an ionic liquid on NaCl/KCl/polymer water-based mud (WBM) for drilling gas hydrate-bearing sediments. *Journal of Molecular Liquids*. 2019. Vol. 294. N 111643. DOI: 10.1016/j.molliq.2019.111643

23. Leusheva E., Brovkina N., Morenov V. Investigation of Non-Linear Rheological Characteristics of Barite-Free Drilling Fluids. *Fluids*. 2021. Vol. 6. Iss. 9. N 327. DOI: 10.3390/fluids6090327

24. Nikitin V.I. Problem solution analysis on finding the velocity distribution for laminar flow of a non-linear viscous flushing fluid in the annular space of a well. *Journal of Mining Institute.* 2022. Vol. 258, p. 964-975. DOI: 10.31897/PMI.2022.93

25. Heidari M., Shahbazi Kh., Fattahi M. Experimental study of rheological properties of aphron based drilling Fluids and their effects on formation damage. *Scientia Iranica. Transactions C: Chemistry and Chemical Engineering*. 2017. Vol. 24. Iss. 3, p. 1241-1252. DOI: 10.24200/sci.2017.4108

26. Tabatabaee Moradi S.Sh. A probabilistic study on hole cleaning optimization. *Journal of Mining Institute.* 2022. Vol. 258, p. 956-963. DOI: 10.31897/PMI.2022.67

27. Nikolaev A., Goluntsov A., Breff A.T. Determination of the coefficient of hydraulic resistance when using anti-turbulence additives. *Reliability: Theory & Applications*. 2024. Vol. 19. Special Issue 6 (81), p. 107-124. DOI: 10.24412/1932-2321-2024-681-107-124

28. Alkinani H.H., Al-Hameedi A.T.T., Dunn-Norman S., Lian D. Application of artificial neural networks in the drilling processes: Can equivalent circulation density be estimated prior to drilling? *Egyptian Journal of Petroleum*. 2020. Vol. 29. Iss. 2, p. 121-126. DOI: 10.1016/j.ejpe.2019.12.003

29. Alsabaa A., Gamal H., Elkatatny S., Abdelraouf Y. Machine Learning Model for Monitoring Rheological Properties of Synthetic Oil-Based Mud. *ACS Omega*. 2022. Vol. 7. Iss. 18, p. 15603-15614. DOI: 10.1021/acsomega.2c00404

30. Song Deng, Bingzhao Huo, Shoukun Xu et al. Prediction of water-in-oil emulsion drilling fluids rheological properties based on GPR-Bagging ensemble learning. *Colloids and Surfaces A: Physicochemical and Engineering Aspects*. 2024. Vol. 686. N 133336. DOI: 10.1016/j.colsurfa.2024.133336

31. Davoodi S., Mehrad M., Wood D.A. et al. Hybridized machine-learning for prompt prediction of rheology and filtration properties of water-based drilling fluids. *Engineering Applications of Artificial Intelligence*. 2023. Vol. 123. Part C. N 106459. DOI: 10.1016/j.engappai.2023.106459

32. Jian Sun, Rongjun Zhang, Mingqiang Chen et al. Identification of Porosity and Permeability While Drilling Based on Machine Learning. *Arabian Journal for Science and Engineering*. 2021. Vol. 46. Iss. 7, p. 7031-7045. DOI: 10.1007/s13369-021-05432-x

33. Quitian-Ardila L.H., Garcia-Blanco Y.J., Rivera A. De J. et al. Developing a machine learning-based methodology for optimal hyperparameter determination – A mathematical modeling of high-pressure and high-temperature drilling fluid behavior. *Chemical Engineering Journal Advances*. 2024. Vol. 20. N 100663. DOI: 10.1016/j.ceja.2024.100663

34. Andaverde J.A., Wong-Loya J.A., Vargas-Tabares Y., Robles M. A practical method for determining the rheology of drilling fluid. *Journal of Petroleum Science and Engineering*. 2019. Vol. 180. P. 150-158. DOI: 10.1016/j.petrol.2019.05.039

35. Tananykhin D.S., Struchkov I.A., Khormali A., Roschin P.V. Investigation of the influences of asphaltene deposition on oilfield development using reservoir simulation. *Petroleum Exploration and Development*. 2022. Vol. 49. Iss. 5, p. 1138-1149. DOI: 10.1016/S1876-3804(22)60338-0

36. Podoprigora D.G., Byazrov R.R., Lagutina M.A. et al. A novel integrated methodology for screening, assessment and ranking of promising oilfields for polymer floods. *Advances in Geo-Energy Research*. 2024. Vol. 12. N 1, p. 8-21. DOI: 10.46690/ager.2024.04.02

37. Villalobos Alva J. Beginning Mathematica and Wolfram for Data Science. Apress, 2021, p. 416. DOI: 10.1007/978-1-4842-6594-9

38. Misbah B., Elgaddafi R., Malhas R.N. et al. Exploring the rheology characteristics of Flowzan and Xanthan polymers in drilling water based fluids at high-temperature and high-shear rates. *Geoenergy Science and Engineering*. 2024. Vol. 243. N 213309. DOI: 10.1016/j.geoen.2024.213309

39. Phirommark P., Namchanthra S., Chaiyanupong J. et al. CFD elucidation of microscopic particles in a low-volumetric classifier towards effects of Stokes number and density ratio. *International Journal of Thermofluids*. 2023. Vol. 20. N 100497. DOI: 10.1016/j.ijft.2023.100497

40. Singh R., Ahmed R., Karami H. et al. CFD Analysis of Turbulent Flow of Power-Law Fluid in a Partially Blocked Eccentric Annulus. *Energies*. 2021. Vol. 14. Iss. 3. N 731. DOI: 10.3390/en14030731

41. Badrouchi F., Rasouli V., Badrouchi N. Impact of hole cleaning and drilling performance on the equivalent circulating density. *Journal of Petroleum Science and Engineering*. 2022. Vol. 211. N 110150. DOI: 10.1016/j.petrol.2022.110150

42. Tananykhin D.S. Scientific and Methodological Support of Sand Management During Operation of Horizontal Wells. *International Journal of Engineering – Transactions A: Basics*. 2024. Vol. 37. Iss. 7, p. 1395-1407. DOI: 10.5829/ije.2024.37.07a.17

Authors: **Vasiliy I. Nikitin,** *Candidate of Engineering Sciences, Scientific Supervisor of Laboratory (Empress Catherine II Saint Petersburg Mining University, Saint Petersburg, Russia*), *nikitin_vi@pers.spmi.ru, https://orcid.org/0000-0002-1332-2485*, **Mikhail V. Dvoynikov**, *Doctor of Engineering Sciences, Scientific Supervisor of Scientific Center, Head of Department* (*Empress Catherine II Saint Petersburg Mining University, Saint Petersburg, Russia*), *https://orcid.org/0000-0002-3798-9938*, **Kirill S. Kupavykh,** *Candidate of Engineering Sciences, Executive Director of Scientific Center* (*Empress Catherine II Saint Petersburg Mining University, Saint Petersburg, Russia), https://orcid.org/0000-0002-6759-5614*, **Tatiana A. Panteleeva,** *Lead Engineer of Laboratory* (*Empress Catherine II Saint Petersburg Mining University, Saint Petersburg, Russia*), *https://orcid.org/0009-0000-7468-7528*.

The authors declare no conflict of interests.

ISSN 2411-3336; e-ISSN 2541-9404

JOURNAL OF MINING INSTITUTE
Zapiski Gornogo instituta
Journal homepage: pmi.spmi.ru

Research article *Geotechnical Engineering and Engineering Geology*

Permeability prediction of oil formations via machine learning-assisted simulation of well flow tests

Andrei V. Soromotin, Dmitrii A. Martyushev✉
Perm National Research Polytechnic University, Perm, Russia

***How to cite this article*:** Soromotin A.V., Martyushev D.A. Permeability prediction of oil formations via machine learning-assisted simulation of well flow tests. Journal of Mining Institute. 2025. Vol. 275, p. 81-93.

Abstract
We present an innovative approach to simulating flow tests of production wells operating in clastic reservoirs of oil fields in the Perm Region. To solve this issue, modern machine learning solutions (CatBoost, Random Forest, XGBoost, MLP, Gradient Boosting, etc.) were used, which allowed achieving high prediction accuracy. The main parameter for simulating and research is bottomhole pressure at various stages of its recovery during well flow testing. The use of the SHAP model interpretation method for the first time made it possible to assess the impact of geotechnical parameters on bottomhole pressure and identify key ones among them. Analysis of the bottomhole pressure recovery prediction model sensitivity to changes in initial parameters made it possible to evaluate the degree of their influence on the pressure recovery curves (PRC). The uniqueness of the proposed approach lies in studying the significance of parameters at various time stages of bottomhole pressure recovery during flow testing, which allows for a more detailed understanding of the processes occurring under formation conditions. The proposed algorithms made it possible to simulate PRC that are as close as possible to actual data, as well as to study the dynamics of permeability of the remote formation zone in real time. This approach opens up new horizons in simulating flow tests and allows for highly detailed and timely assessment of formation filtration properties across the entire production well stock simultaneously. The process engineering solution is aimed at promptly assessing filtration parameters of remote formation zones and provides the ability to monitor permeability changes, which helps to timely identify areas of reduced oil inflow and develop measures to restore well productivity. This approach significantly reduces economic risks associated with conducting expensive field tests while ensuring reliability and validity of predicted indicators with minimal resource and time costs.

Keywords
machine learning; permeability; well flow testing; pressure recovery curve; formation pressure; bottomhole pressure; bottomhole zone; formation filtration parameters

Funding
The research was supported by the Ministry of Science and Higher Education of the Russian Federation (project N FSNM-2024-0005).

Received: 24.12.2024 ***Accepted: 18.09.2025*** ***Online: 13.10.2025*** ***Published: 31.10.2025***

Introduction

Formation permeability and the bottomhole zone (BZ) state are key factors determining the efficiency of oil and gas production [1, 2]. The prediction and monitoring of these parameters allow optimizing field development [3], preventing operational complications during exploitation, and increasing the overall hydrocarbon recovery factor [4, 5].

Existing methods for determining permeability have numerous drawbacks. Empirical correlations depend on statistical relationships between core permeability measurements and petrophysical properties, making them unsuitable for application in various geological conditions [6, 7]. The Flow

Zone Indicator (FZI) method requires extensive core material analysis, resulting in a lengthy process, and the obtained results may not fully reflect the properties of the remote formation zone [8, 9]. Traditional methods based on empirical correlations for permeability estimation using petrophysical data often lead to inaccuracies, uncertainties, and can be time-consuming and expensive [10, 11]. Permeability prediction using machine learning interpretation of logging data is being actively studied, characterizing formation properties in close proximity to the wellbore [12-14]. Predicting permeability through image analysis and void space information using machine learning methods shows promise. However, this approach requires core samples and does not allow evaluating properties in remote formation zones [15].

One of the primary methods for assessing formation filtration parameters is the interpretation of well flow testing (WFT) under unsteady flow conditions using pressure recovery curves (PRC) and level recovery tests (LRT). The specific features of these methods include prolonged well shutting-in and associated reduction in oil production [16]. Accurate prediction of remote formation permeability is complicated by the peculiarities of WFT interpretation. It is necessary to identify the reasons for the low quality of a significant number of WFT in the Perm Region:

- difficulty in isolating the plane-radial flow section due to wellbore influence;
- insufficient duration of the testing period [17];
- impact of constant pressure boundary;
- well interference effects;
- low resolution of the telemetry system (TMS).

With the increasing application of downhole pressure sensors [18], it has become possible to widely utilize the pressure stabilization method (PSM) [19]. However, not all wells are equipped with TMS, which complicates the monitoring of reliable bottomhole pressure dynamics. Cases of abrupt changes and prolonged interruptions in pressure recording are observed. Another widely used method is decline curve analysis, also known as production history analysis (PHA). This empirical method is utilized for estimating hydrocarbon production, evaluating formation filtration parameters and well condition (skin factor). This procedure has several drawbacks: requirement for stable operation of neighbouring wells, uncertainty of filtration regimes in multilayer reservoirs with multiple types of void spaces, fluctuations in key parameters [20, 21]. The main advantages of PSM and PHA methods include the absence of the need to shut wells in. However, extending the duration of studies leads to uncertainty regarding the emergence of indirect factors and limitations [22].

Machine learning methods for estimating formation permeability are being actively studied and improved. The use of artificial neural networks (ANN) in studies [23-25] for permeability prediction showed better metrics compared to multiple linear regression (MLR) and multiple nonlinear regression (MNLR). The authors of [26] proposed an evolving ANN with a genetic algorithm (GA) optimizer, achieving higher accuracy than a standard ANN. Study [27] employed a combination of MLP (Multilayer Perceptron), RBF (Radial Basis Function), and GRNN (Generalized Regression Neural Network) networks optimized using GA, which improved prediction accuracy. The authors of [28] investigated PSO (Particle Swarm Optimization) and SSD (Social Ski-Driver) algorithms for permeability prediction, finding that the MLP-SSD model demonstrated the highest accuracy after feature selection using the SHAP (Shapley Additive Explanations) library. This library was also applied in studies [29, 30] for feature selection and interpretation, with the PSO-XGBoost model showing the best results.

Despite the promising nature of ANN, there is a significant issue of slow convergence – the training rate determines how quickly the model adapts to the task. A high training rate can lead to suboptimal solutions, while a low rate can slow down the convergence process, i.e., the adjustment of model weights to minimize error. Study [31] presents a solution to this issue using a Modular

Neural Network (MNN) model. The use of an RBF Neural Network [32] provided faster permeability prediction based on porosity compared to a standard fully connected network. Study [33] combines ANN with fuzzy logic, where the combination of their advantages resulted in improved permeability prediction accuracy compared to using the models separately. Work [34] utilized Nuclear Magnetic Resonance (NMR) in combination with logging data to enhance permeability prediction metrics. The application of a Functional Network (FN) [35] provided better results compared to ANN and regression methods. Researchers [36] employed Relevance Vector Regression (RVR) with GA optimization, which outperformed the Support Vector Machine (SVM) model. In [37], fuzzy logic was applied for effective permeability prediction. The proposed clustering technique confirmed its efficiency and accuracy. The author of [7] improved fuzzy logic through feature engineering for more accurate permeability predictions. This increased the coefficient of determination R^2 to 0.76 compared to linear regression (0.04) and fuzzy logic without feature engineering (0.41). Research [38] compared MLP, Support Vector Regression (SVR), and MLR models, with MLP and SVR demonstrating high accuracy. In [39], the authors used Least Squares Support Vector Machine (LSSVM) and Multilayer Extreme Learning Machine (MELM) models optimized with Cuckoo Optimization Algorithm (COA), PSO, and GA for permeability prediction. The MELM-COA hybrid showed superior metrics (Root Mean Square Error, RMSE – 0.56) compared to LSSVM and MELM with PSO and GA optimizers, as well as Convolutional Neural Network (CNN) (RMSE ranging from 0.72 to 1.24).

In [40], an ensemble machine learning model that demonstrated superior results compared to single configurations was proposed. The bagging method [15] for permeability prediction showed the best metrics. The application of ensemble models is also presented in several other studies [41-43]. The authors of [44] utilized an empirical formula and a new ensemble model for more accurate permeability prediction. The combination of SVM, ANN, and Adaptive Neuro-Fuzzy Inference System (ANFIS) models improved permeability prediction accuracy in heterogeneous oil fields [45]. Work [46] proposed a hybrid SVM-T2FL (Fuzzy Logic) with FN and feature selection, which demonstrated excellent permeability prediction model results. The authors of [47] proposed a unique MIRes (Multiple-Input deep Residual) CNN model for permeability prediction, utilizing the integration of digital and graphical data, which outperformed SIRes 1D-CNN, SIRes 2D-CNN (Single-Input deep Residual one (two) Dimensional CNN), GMDH (Group Method of Data Handling). A hybrid model using Random Forest, Lasso Regularization, and XGBoost [43] was developed for permeability prediction.

Analysis of scientific and technical literature demonstrates that the scientific community is actively developing machine learning (ML) methods for permeability estimation and prediction. However, most currently applied ML solutions rely on logging data [48]. The drawbacks of this approach include inability to estimate the average effective permeability of the well drainage zone, and requirement for up-to-date geophysical surveys on which the assessment is based.

This study is the first to utilize significant Big Data sets from well testing (pressure recovery curves, operational parameters before well shutting-in for testing, geological and physical properties of the formation and oil) conducted throughout the entire operation history of clastic deposits in oil fields of the Perm Region. The uniqueness of this work lies in the development of an approach for predicting bottomhole pressure during recovery, which in the future eliminates peculiarities and interpretation errors. The presented algorithm allows for real-time simulating of the pressure recovery curve in a well, significantly accelerating the determination of filtration parameters and enabling coverage of the entire well stock. The proposed approach contributes to more efficient and economically rational field development, ensuring resource optimization and improved decision-making in oil production. We do not suggest completely eliminating

flow testing, as it serves its intended purposes, including model refinement. Synthetic tests are necessary for describing processes occurring in the formation and predicting engineering and economic indicators.

Methods

A database of highly informative flow tests of clastic reservoirs in the Perm Region fields was formed. The following WFT were excluded from the sample: tests with significant interference from neighbouring wells, tests with low TMS resolution, tests with substandard bottomhole pressure recovery measurements. The proportion of WFT with these characteristics is approximately 15 %. Thus, the primary initial information for training consists of 85 % of all analysed WFT (≈3500), including well operational parameters, pressure recovery time, geological and physical properties of the formation and oil. Category features used include well profile (directional (DW), horizontal (HW), well completion procedure (hydraulic fracturing (HF), multi-stage hydraulic fracturing (MHF). Ranges of initial parameter variations: bottomhole pressure – 0.5-24 MPa; water cut – 0-99.9 %; flow rate – 0.1-244.8 m^3/day; formation volume factor – 1.0-1.7; formation compressibility – 1.1-4.6 $(MPa \cdot 10^4)^{-1}$; rock compressibility – 0.7-1.5 $(MPa \cdot 10^4)^{-1}$; gas content – 1.2-1210 m^3/t; oil compressibility – 2.5-26.2 $(MPa \cdot 10^4)^{-1}$; oil density – 0.6-1.2 g/cm^3; effective oil-saturated thickness – 0.4-19.6 m; oil viscosity – 0.5-114.1 mPa·s; formation pressure – 1.9-24.9 MPa; porosity – 4.6-34 %; saturation pressure – 3.9-22.9 MPa; bottomhole pressure at recovery start – 0.1-23.3 MPa; recovery time – 0-265,047 min. For handling the category feature containing four unique values, the One-Hot Encoding (OHE) method was applied. It converts the category feature into several binary columns, each corresponding to one of the unique values of the original feature. The recommended CatBoost model automatically processes category features without the need for prior encoding. The predicted parameter is the bottomhole pressure at each time period of pressure recovery curve (PRC) buildup. By sequentially predicting bottomhole pressure recovery at various test duration intervals, pressure recovery curve simulation is ensured.

To assess formation pressure, the results of computations in the Data Stream Analytics modular service [49] are used. This service determines formation pressure based on field geological data using machine learning methods for both retrospective periods and prospective periods up to one year ahead. This opens up the possibility of simulating pressure recovery curves at any moment, both retrospectively and in forecast without shutting-in wells during the survey period.

The following machine learning models were used for prediction:

• MLP Neural Network – an artificial neural network consisting of multiple layers of neurons (input, hidden, and output) that can simulate complex nonlinear relationships.

• Gradient Boosting – an ensemble method that creates a sequence of models, each correcting the errors of the previous ones. Typically used with decision trees and known for high accuracy.

• Random Forest – an ensemble algorithm that builds multiple decision trees on random subsets of data and features. Predictions are averaged (for regression) or determined by voting (for classification). Provides resistance to overtraining and works well with various data types.

• XGBoost – an optimized version of gradient boosting designed for high performance and accuracy. Includes regularization, parallel training, and other improvements.

• Decision Tree – an interpretable and simple algorithm that builds a tree-like model for decision-making. Branching is based on rules that minimize errors. However, it tends to overtraining without depth limitations.

• Linear Regression – a classical statistical method assuming a linear relationship between input features and the target variable. Known for simplicity, interpretability, and speed but limited in simulating complex nonlinear relationships.

• SVR – an algorithm that constructs a hyperplane that most accurately describes the relationship between features and the target variable while minimizing errors within a specified margin. Suitable for small datasets but requires significant computational resources.

• K-Nearest Neighbors – a method based on finding the nearest neighbours of a target. Prediction is based on the target variable values of the *k* closest targets. Simple and effective but sensitive to data size and noise.

• CatBoost – a gradient boosting algorithm that prevents overtraining and provides high performance and accuracy. Hyperparameters were tuned using the Optuna framework – a library for hyperparameter search in machine learning, providing a convenient interface for optimization using various search algorithms. The following parameters were varied: learning rate (learning_rate) – 0.01-0.3; L2 regularization coefficient (l2_leaf_reg) – 1e-8-100.0; bagging temperature (bagging_temperature) – 0.0-10.0; random noise strength (random_strength) – 1e-8-10.0; tree depth (depth) – 4-10; number of feature split borders (border_count) – 32-255; minimum number of targets in a leaf (min_data_in_leaf) – 1-100; tree growth policy (grow_policy) – SymmetricTree, Depthwise, Lossguide. Cross-validation was used to assess model accuracy on different subsets of training data. The best hyperparameters found were: 'depth' – 10; 'learning_rate' – 0,128; 'l2_leaf_reg' – 0,0117; 'bagging_temperature' – 6,509; 'random_strength' – 1,501; 'border_count' – 183; 'min_data_in_leaf' – 5; 'grow_policy' – 'Depthwise'.

The training digital dataset was formed as follows:

1. Verification and sequential selection of pressure recovery curves were performed. The absence of outliers, sharp jumps, and stepwise changes in bottomhole pressure recovery was checked.

2. For each PRC, duration of recovery and bottomhole pressure values were entered into the table. The table consisted of two columns: duration of recovery and bottomhole pressure (for each PRC point). The rows represented the results of PRC measurements, with each graph point being a table row.

3. For each point of the selected pressure recovery curve, the following constant parameters were added as new columns corresponding to the values before well shutting-in: flow rate, water cut, formation pressure, bottomhole pressure, BZ permeability, recovery time (time after well shutting-in), porosity, rock compressibility factor, formation compressibility factor, effective oil-saturated formation thickness, oil viscosity, gas content, oil density, oil compressibility factor, oil volume factor, saturation pressure. The model training utilized formation pressure values obtained from the interpretation of qualified well flow tests and from the Data Stream Analytics modular service.

A Spearman correlation matrix was constructed to determine relationships between features (Fig.1). The Spearman correlation measures the relationship between variables based on ranks rather than actual values. It is used to determine connections between variables, especially when data is not normally distributed or when the relationship is nonlinear. Analysis of the heatmap reveals that the following parameters have the strongest correlation with the pressure recovery pattern in the well: bottomhole pressure, formation pressure, and flow rate. The analysis also reveals strong relationships between initial parameters: direct dependence of the formation volume factor on gas content and oil compressibility, as well as inverse dependence on oil density and oil viscosity; the compressibility of the rock on porosity; the viscosity of oil on the density of oil. We see potential multicollinearity issues observed in Fig.1. Since the objective was to obtain a general understanding of the influence of selected parameters, possible distortions due to multicollinearity are considered acceptable within the scope of this study. To enhance the reliability of the results, a more detailed investigation of methods to reduce multicollinearity impact is planned, including selection of the most significant features, data normalization, and application of regularization techniques.

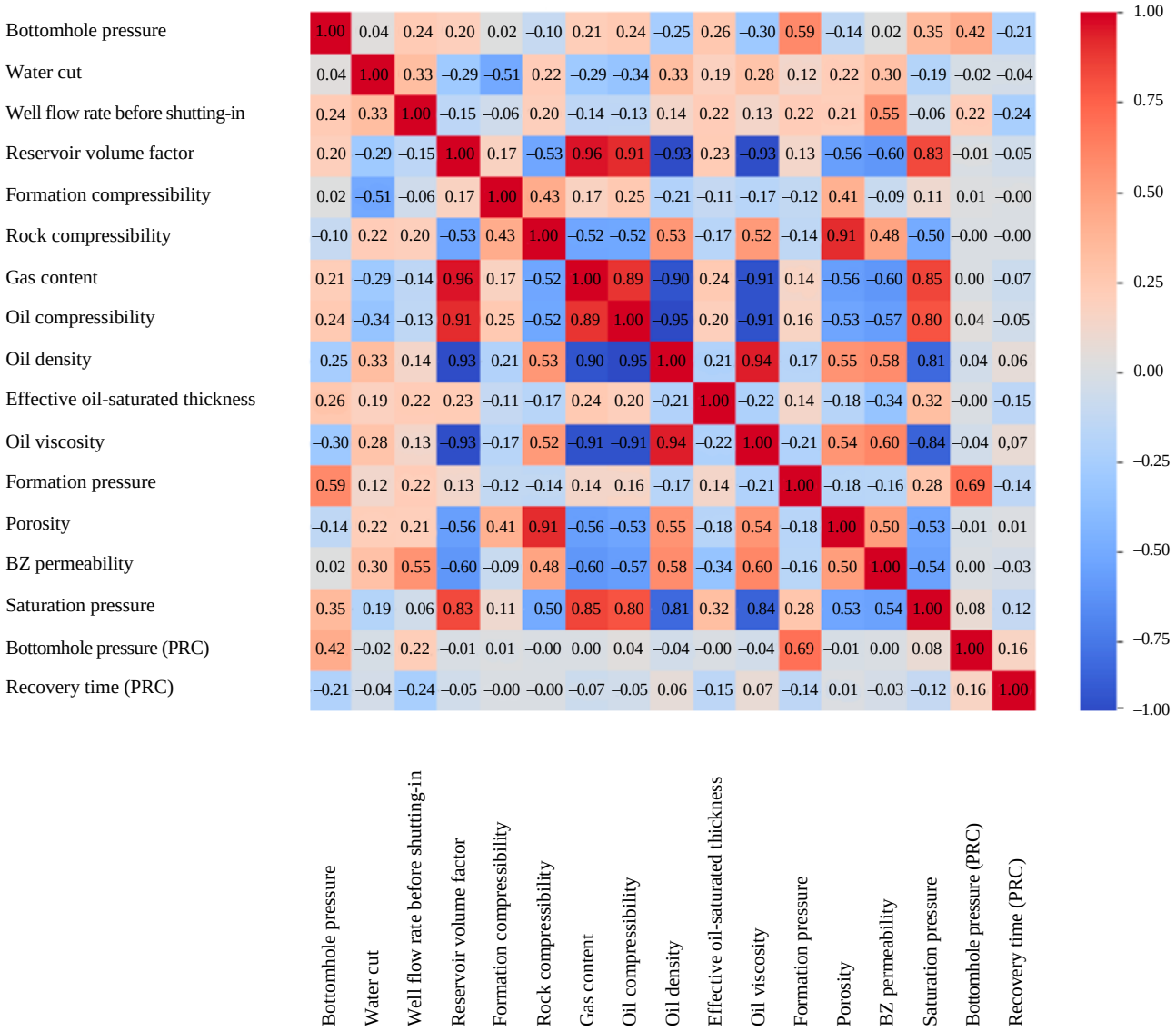

Fig.1. Spearman correlation matrix of the initial data

The proposed algorithm was applied to each PRC, sequentially forming a digital dataset. The predicted parameter is the bottomhole pressure at the recovery moment. The digital dataset was split into training set – 80 %, validation set – 10 %, and test set – 10 %. To equalize the contribution of features, MinMaxScaler scaling was used, which normalizes the data to the range from 0 to 1.

To tune and evaluate the models, statistical metrics were used – the coefficient of determination R^2 and RMSE

$$R^2 = 1 - \frac{\sum_{i=1}^{n}\left(y_i - \hat{y}_i\right)^2}{\sum_{i=1}^{n}\left(y_i - \bar{y}\right)^2};$$

$$\text{RMSE} = \sqrt{\frac{1}{n}\sum_{i=1}^{n}\left(y_i - \hat{y}_i\right)^2},$$

where y_i – actual value; $\hat{y}_i$ – predicted value; n – number of observations; $\bar{y}$ – mean value of actual data.

The procedure algorithm is built as follows:

1. Collection of data of flow studies of the entire well stock for the retrospective period, including initial parameters (properties of the formation, oil, and operational parameters), dynamics of bottomhole pressure recovery, and interpretation data (formation pressure).
2. Preparation, cleaning, and processing of data.
3. Training models to perceive the pattern of bottomhole pressure recovery depending on input parameters.
4. Obtaining a predictive simulated bottomhole pressure recovery curve for the current period based on a pre-trained model using retrospective flow studies conducted on wells and current field geological data.
5. Interpretation of the simulated bottomhole pressure recovery curve and obtaining a predicted value of permeability of the remote formation zone.

Results and discussion

Training and comparison of R^2 and RMSE metrics were performed, as shown in the Table, both for individual machine learning models for predicting bottomhole pressure at the moment of recovery, and for an ensemble of the best models for the validation sample. Analysis of the convergence of predicted and actual values of the selected models shows that the best result was obtained using CatBoost – an open-source gradient boosting library based on decision trees.

Machine learning model quality metrics

Model	R^2	RMSE
CatBoost	0.997	0.176
Random Forest	0.995	0.273
XGBoost	0.988	0.406
Decision Tree	0.987	0.432
MLP Neural Network	0.983	0.498
Ensemble	0.970	0.670
Gradient Boosting	0.878	1.354
Linear Regression	0.709	2.089
K-Nearest Neighbors	0.331	3.171
SVR	0.139	3.596

Figure 2, *a* shows the correlation field of predicted and actual values of bottomhole pressure at recovery moments. The linear correlation coefficient *r* between predicted and actual values for the test sample was 0.97, with RMSE of approximately 0.18. The simulated pressure recovery curve presented in Fig.2, *b* is close to the actual one, which demonstrates that machine learning models have the ability to train for solving the given task. It can be concluded that the application of these algorithms for estimating permeability of the remote formation zone through interpretation of simulated pressure recovery curves is promising.

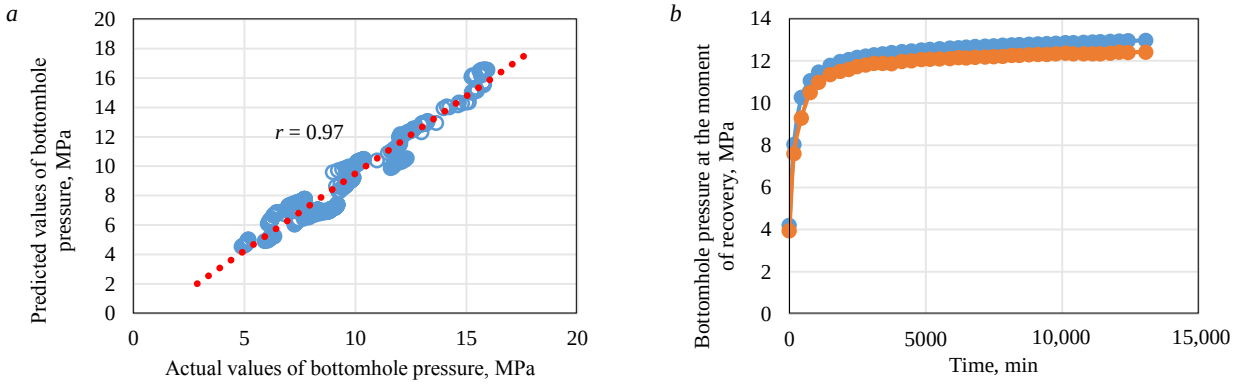

Fig.2. Scatter plot of predicted and actual pressure values at the moment of recovery (*a*); example of predicting the pressure recovery curve (*b*)

For a comprehensive study of the significance of initial parameters, gradient boosting was applied – a machine learning technique for classification and regression tasks that builds a prediction model in the form of an ensemble of weak predictive models, usually decision trees. The task was solved using the SHAP library and identifying the contribution of each feature to the final prediction of the target value – bottomhole pressure at the recovery moment. SHAP is a method based on the Shapley vector, which allows revealing the significance (measure of parameter influence on prediction result) of each feature. To determine the significance of a parameter, the model's predictions are evaluated with and without the given feature.

Feature significances for predicting pressure recovery for the sample: formation pressure, MPa – 0.309; bottomhole pressure, MPa – 0.209; recovery time, min – 0.193; flow rate, m^3/day – 0.053; water cut, % – 0.039; BZ permeability, μm^2 – 0.024; well profile and development procedure – 0.024; gas content, m^3/t – 0.024; effective oil-saturated thickness, m – 0.024; saturation pressure, MPa – 0.022; formation compressibility, $(MPa \cdot 10^4)^{-1}$ – 0.016; porosity, % – 0.013; oil viscosity, mPa·s – 0.013; oil compressibility, $(MPa \cdot 10^4)^{-1}$ – 0.011; rock compressibility, $(MPa \cdot 104)^{-1}$ – 0.011; oil density, g/cm^3 – 0.008; formation volume factor – 0.007. It is logical that formation pressure, bottomhole pressure, and recovery time have the greatest influence. However, an important feature is the impact of other parameters on pressure recovery in the well.

This approach was used for various durations of the study to investigate the nature of the pressure recovery process in the well. The time parameter was ranked from minimum to maximum values and divided into 10 sections to fully reflect the distribution of values and identify potential patterns. For each interval, a digital array was formed, and the SHAP library was used to assess the significance of parameters for pressure recovery in the well. Figure 3, *a* shows radar diagrams of the significance of initial parameters for different durations of recovery. The analysis shows that at the initial stage of pressure recovery, the formation compressibility parameter stands out. The flow rate influences all stages of recovery but shifts to later time intervals. The significance of gas content prevails at the initial stages of pressure recovery in the well. The significance of oil viscosity increases at high recovery time values. The significance of effective oil-saturated thickness is observed across all intervals of the PRC. An increase in the significance of water cut and rock compressibility is observed at high recovery duration values.

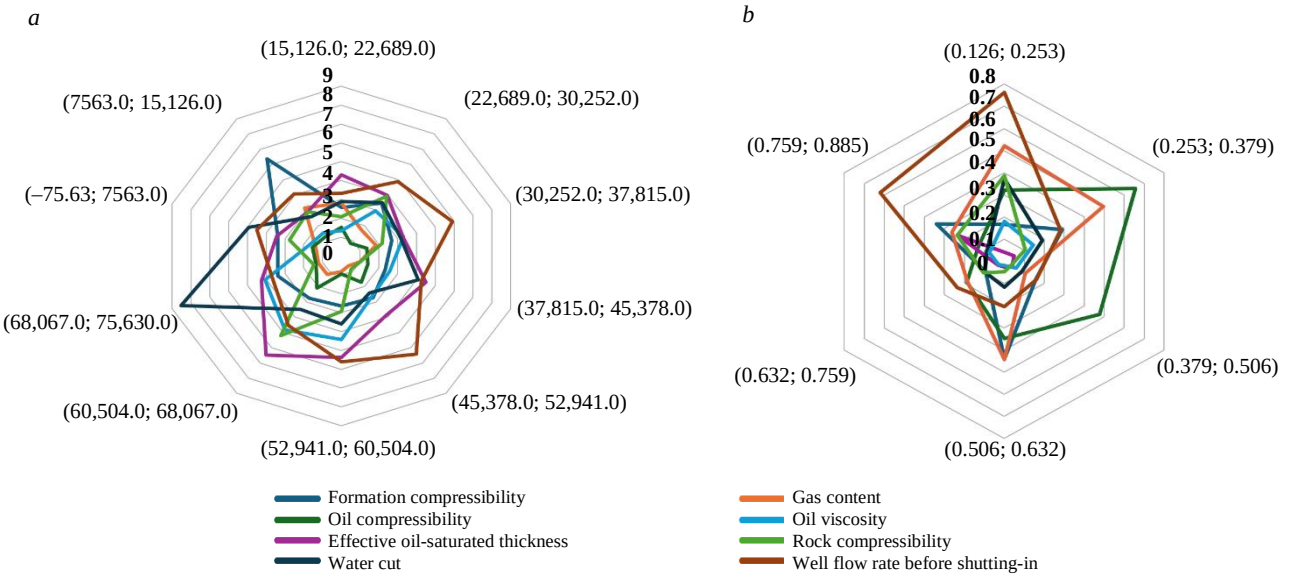

Fig.3. The significance of parameters for pressure recovery in the well at different time ranges (*a*) and at different recovery sites (*b*)

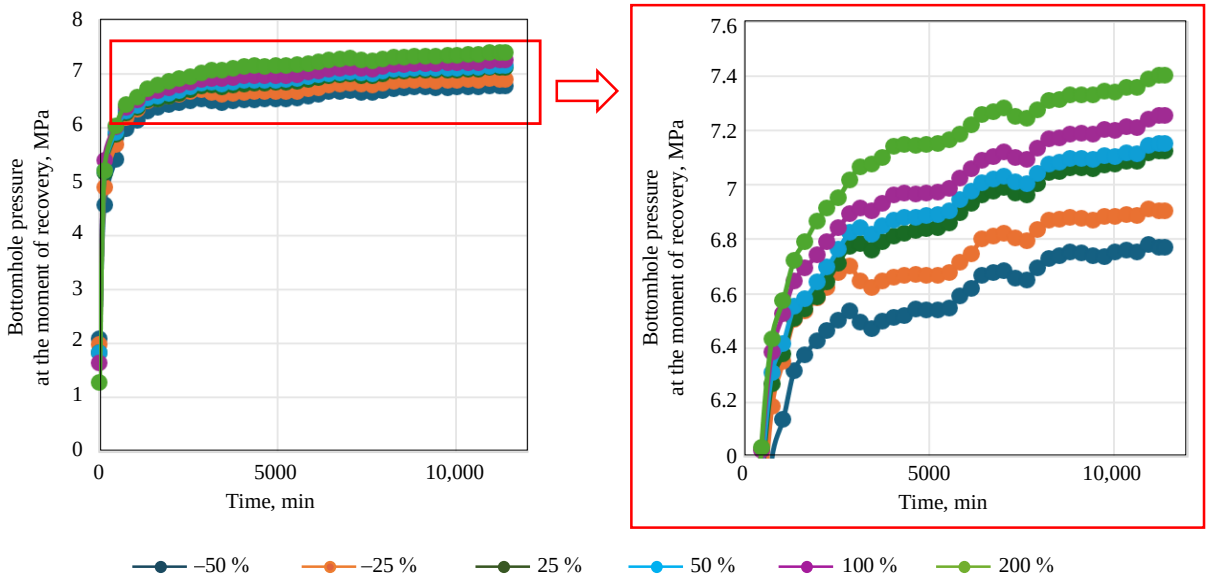

Fig.4. Analysis of the simulated pressure recovery curve sensitivity to changes in flow rate

A similar analysis was conducted at various stages of the PRC recovery. For this purpose, an additional variable was introduced, representing the ratio of bottomhole pressure at a certain recovery interval to formation pressure. Fig.3, *b* shows radar diagrams of the significance of initial parameters for different recovery sites. The analysis shows that at the initial stage of pressure recovery, the formation compressibility parameter stands out. The flow rate influences mainly the initial and final periods of the PRC. The significance of the gas content parameter prevails at the initial stage of pressure recovery in the well. At the final stage of the PRC, the effective oil-saturated thickness parameter is significant.

The next stage of analysis is the assessment of pressure recovery curve sensitivity to changes in initial parameters. Each initial parameter was varied sequentially from –50 to +200 % without changing the others, and based on this data, actual and predicted pressure recovery curves were constructed. It was found that the model trains and is sensitive to changes in each of the analysed parameters. The most important feature is the flow rate, and Fig.4 presents the analysis of bottomhole pressure recovery sensitivity to this parameter. Figure 4 shows that the model is trainable and the dynamics of pressure recovery responds to changes in flow rate.

The next step involved comparing the results of interpreting actual (not used in training) and simulated pressure recovery curves, as shown in Fig.5, which demonstrated high convergence of results (r is 0.95). This approach is promising for predicting filtration parameters of the remote formation zone and eliminates uncertainties associated with the peculiarities of flow studies interpretation.

Figure 6 shows the prediction of formation pressure in the Data Stream Analytics modular service for the retrospective (red line) and prospective (one year, purple line) periods. Thus, it is possible to simulate pressure recovery curves for a forecasted point in time to assess the permeability of the remote drainage zone of wells when the energy state of the formation changes.

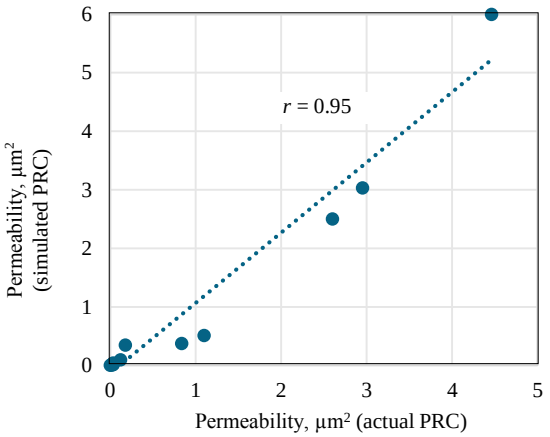

Fig.5. Comparison of the results of interpretation of actual and simulated PRC

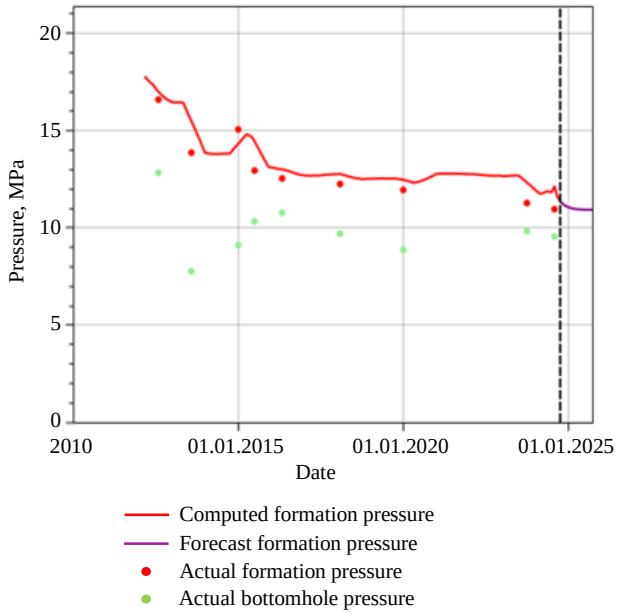

Fig.6. Forecasting formation pressure in the Data Stream Analytics modular service

Figure 7 shows the actual pressure recovery curve (as of 01.08.2024 – green line), simulated PRC for the current state (01.12.2024 – blue line) and the prospective period (01.10.2025 – red line), and the results of their interpretation. The application of these algorithms can enable real-time monitoring of filtration parameters and assessment of the impact of formation pressure on formation permeability for the prospective period. The forecasted formation pressure value of 10.86 MPa for 01.10.2025, computed in the Data Stream Analytics modular service (Fig.6, purple line), was used as the predicted formation pressure.

The analysis of Fig.7 shows high convergence between the actual (dark green line) and simulated (light green line) pressure recovery curves as of 1 August 2024. The results of interpreting the actual and simulated bottomhole pressure recovery curves characterize the negative predictive dynamics of permeability in the remote formation zone (from 0.0462 to 0.0348 μm^2), corresponding to a decrease in formation pressure (from 11.21 to 10.86 MPa).

The integration of machine learning methods and the use of real-time pressure recovery curves are promising for monitoring the development of hydrocarbon fields. These procedures will not only increase the accuracy of determining and predicting permeability but also reduce downtime associated with traditional well testing methods. The algorithms presented in this work will allow constructing dynamic maps of permeability distribution for the development target to identify filtration patterns and involve hydrocarbon reserves. As directions for future work, it is possible to note the expansion of the set of initial parameters and the generation of derivatives based on them, as well as the use of other algorithms for predicting PRC, including hybrid models.

Conclusion

Permeability of formations and the state of the bottomhole zone are key parameters affecting the efficiency of oil and gas field development. This paper proposes an innovative approach for predicting bottomhole pressure recovery and simulating the pressure recovery curve based on machine learning methods (CatBoost).

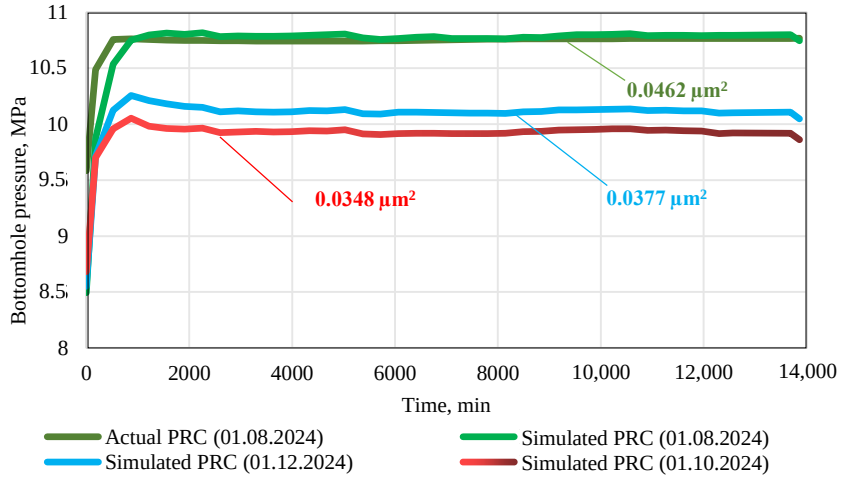

Fig.7. Simulated PRC in the period from 01.08.2024 to 01.10.2025 and the results of their interpretation

The developed algorithm, based on well flow research data and geological and physical parameters, improves the accuracy of permeability assessment. The use of the SHAP library allowed identifying the significance of initial parameters at various stages of pressure recovery. Sensitivity analysis confirmed the models' ability to account for parameter changes and their impact on the PRC.

The developed approach provided high convergence between predicted and actual pressure recovery curves, making it a promising tool for monitoring and optimizing field development. The linear correlation coefficient *r* between predicted and actual values for the bottomhole pressure recovery test sample was 0.97, with RMSE of approximately 0.18.

The high statistical metrics of the machine learning model, based on accumulated field geological data, demonstrate the ability to simulate PRC in real time and interpret them to assess changes in permeability of the remote formation zone simultaneously across the entire well stock. The linear correlation coefficient *r* between predicted and actual values when comparing the results of interpreting actual and simulated PRC is 0.95.

Permeability of the remote zone of the pay plays a key role in assessing the efficiency of oil production. The main method for determining it is well flow testing, which has significant limitations: incomplete coverage of the well stock, low measurement regularity, and the need to shut wells in.

The innovative approach proposed in the article provides for continuous assessment of filtration characteristics across the entire active well stock in real time. The developed method accelerates monitoring of the bottomhole zone state, ensuring timely identification of candidates for effective geotechnical interventions. The advantage of the algorithm is the use of conditioned measurements of bottomhole pressure at the recovery moment.

The algorithms are based on and validated using significant databases of well flow tests of clastic reservoirs from oil fields in the Perm Region. The described approach eliminates the peculiarities of the interpretation process and significantly speeds up the determination of filtration parameters, expanding coverage while ensuring timely and accurate model updates. This, in turn, will impact the improvement of forecasting processing and economic development indicators.

REFERENCES

1. Yazkov A.V., Kolbikov S.V., Shadchnev N.A. et al. Geological and Technological Challenges and Experience in Developing Hard-to-Recover Reserves. *Georesources.* 2024. Vol. 26. N 3, p. 7-12 (in Russian). DOI: 10.18599/grs.2024.3.1

2. Indrupskiy I.M., Ibragimov I.I., Tsagan-Mandzhiev T.N. et al. Laboratory, numerical and field assessment of the effectiveness of cyclic geo-mechanical treatment on a tournaisian carbonate reservoir. *Journal of Mining Institute.* 2023. Vol. 262, p. 581-593. DOI: 10.31897/PMI.2023.5

3. Kanin E., Garipova A., Boronin S. et al. Combined mechanistic and machine learning method for construction of oil reservoir permeability map consistent with well test measurements. *Petroleum Research.* 2025. Vol. 10. Iss. 2, p. 247-265. DOI: 10.1016/j.ptlrs.2024.09.001

4. Byrne M.T., McPhee C.A. The Extinction of Skin. SPE International Symposium and Exhibition on Formation Damage Control, 15-17 February 2012, Lafayette, LA, USA. OnePetro, 2012. N SPE-151807-MS. DOI: 10.2118/151807-MS

5. Al-Obaidi S.H., Khalaf F.H., Alwan H.H. Performance Analysis of Hydrocarbon Wells Based on the Skin Zone. *Technium.* 2021. Vol. 3. Iss. 4, p. 50-56.

6. Belhouchet H.E., Benzagouta M.S., Dobbi A. et al. A new empirical model for enhancing well log permeability prediction, using nonlinear regression method: Case study from Hassi-Berkine oil field reservoir – Algeria. *Journal of King Saud University – Engineering Sciences*. 2021. Vol. 33. Iss. 2, p. 136-145. DOI: 10.1016/j.jksues.2020.04.008

7. Xidong Wang, Shaochun Yang, Ya Wang et al. Improved permeability prediction based on the feature engineering of petrophysics and fuzzy logic analysis in low porosity–permeability reservoir. *Journal of Petroleum Exploration and Production Technology*. 2019. Vol. 9. Iss. 2, p. 869-887. DOI: 10.1007/s13202-018-0556-y

8. Mirzaei-Paiaman A., Asadolahpour S.R., Saboorian-Jooybari H. et al. A new framework for selection of representative samples for special core analysis. *Petroleum Research*. 2020. Vol. 5. Iss. 3, p. 210-226. DOI: 10.1016/j.ptlrs.2020.06.003

9. Mirzaei-Paiaman A., Saboorian-Jooybari H., Pourafshary P. Improved Method to Identify Hydraulic Flow Units for Reservoir Characterization. *Energy Technology*. 2015. Vol. 3. Iss. 7, p. 726-733. DOI: 10.1002/ente.201500010

10. Kochegurov A.I., Denisov V.I., Zadorozhnykh E.A. Analysis of applying machine learning methods in rock classification problems on core samples. *Bulletin of the Tomsk Polytechnic University. Geo Assets Engineering.* 2024. Vol. 335. N 9, p. 148-159. DOI: 10.18799/24131830/2024/9/4792

11. Soromotin A.V., Martyushev D.A., Pereira J.L.J. On the application of machine learning algorithms in predicting the permeability of oil reservoirs. *Artificial Intelligence in Geosciences*. 2025. Vol. 6. Iss. 2. N 100126. DOI: 10.1016/j.aiig.2025.100126

12. Bennis M., Torres-Verdín C. Automatic Multiwell Assessment of Flow-Related Petrophysical Properties of Tight-Gas Sandstones Based on the Physics of Mud-Filtrate Invasion. *SPE Reservoir Evaluation & Engineering*. 2023. Vol. 26. Iss. 3, p. 543-564. DOI: 10.2118/214668-PA

13. Ishola O., Vilcáez J. Machine learning modeling of permeability in 3D heterogeneous porous media using a novel stochastic pore-scale simulation approach. *Fuel*. 2022. Vol. 321. N 124044. DOI: 10.1016/j.fuel.2022.124044

14. Singh M., Makarychev G., Mustapha H. et al. Machine Learning Assisted Petrophysical Logs Quality Control, Editing and Reconstruction. Abu Dhabi International Petroleum Exhibition & Conference, 9-12 November 2020, Abu Dhabi, UAE. OnePetro, 2020. N SPE-202977-MS. DOI: 10.2118/202977-MS

15. Qing Kang, Kai-Qi Li, Jin-Long Fu, Yong Liu. Hybrid LBM and machine learning algorithms for permeability prediction of porous media: A comparative study. *Computers and Geotechnics*. 2024. Vol. 168. N 106163. DOI: 10.1016/j.compgeo.2024.106163

16. Jirjees A.Y., Abdulaziz A.M. Influences of uncertainty in well log petrophysics and fluid properties on well test interpretation: An application in West Al Qurna Oil Field, South Iraq. *Egyptian Journal of Petroleum*. 2019. Vol. 28. Iss. 4, p. 383-392. DOI: 10.1016/j.ejpe.2019.08.005

17. Martyushev D.A., Slushkina A.Yu. Assessment of informative value in determination of reservoir filtration parameters based on interpretation of pressure stabilization curves. *Bulletin of the Tomsk Polytechnic University. Geo Assets Engineering.* 2019. Vol. 330. N 10, p. 26-32 (in Russian). DOI: 10.18799/24131830/2019/10/2295

18. Kaleem W., Tewari S., Fogat M., Martyushev D.A. A hybrid machine learning approach based study of production forecasting and factors influencing the multiphase flow through surface chokes. *Petroleum.* 2024. Vol. 10. Iss. 2, p. 354-371. DOI: 10.1016/j.petlm.2023.06.001

19. Yudin V.A., Volpin S.G., Efimova N.P., Afanaskin I.V. Some features of pressure stabilization curve in the well located in the fault's dynamic influence zone. *Oilfield engineering.* 2020. N 12 (624), p. 15-22 (in Russian). DOI: 10.30713/0207-2351-2020-12(624)-15-22

20. Zhiping Chen, Jia Zhang, Daren Zhang et al. Enhanced permeability prediction in porous media using particle swarm optimization with multi-source integration. *Artificial Intelligence in Geosciences*. 2024. Vol. 5. N 100090. DOI: 10.1016/j.aiig.2024.100090

21. Zhuoheng Chen, Hannigan P. A shale gas resource potential assessment of Devonian Horn River strata using a well-performance method. *Canadian Journal of Earth Sciences*. 2016. Vol. 53. N 2, p. 156-167. DOI: 10.1139/cjes-2015-0094

22. Muslimov R.Kh. History and prospects of hydrodynamic methods for oil fields development in Russia. *Oil Industry Journal*. 2020. N 12, p. 96-100 (in Russian). DOI: 10.24887/0028-2448-2020-12-96-100

23. Piskunov S.A., Davoodi Sh. Horizontal well flow rate prediction applying machine-learning model. *Bulletin of the Tomsk Polytechnic University. Geo Assets Engineering*. 2024. Vol. 335. N 5, p. 118-130 (in Russian). DOI: 10.18799/24131830/2024/5/4553

24. Ben-Awuah J., Padmanabhan E. An enhanced approach to predict permeability in reservoir sandstones using artificial neural networks (ANN). *Arabian Journal of Geosciences*. 2017. Vol. 10. Iss. 7. N 173. DOI: 10.1007/s12517-017-2955-7

25. Elkatatny S., Mahmoud M., Tariq Z., Abdulraheem A. New insights into the prediction of heterogeneous carbonate reservoir permeability from well logs using artificial intelligence network. *Neural Computing and Applications*. 2018. Vol. 30. Iss. 9, p. 2673-2683. DOI: 10.1007/s00521-017-2850-x

26. Irani R., Nasimi R. Evolving neural network using real coded genetic algorithm for permeability estimation of the reservoir. *Expert Systems with Applications*. 2011. Vol. 38. Iss. 8, p. 9862-9866. DOI: 10.1016/j.eswa.2011.02.046

27. Bagheripour P. Committee neural network model for rock permeability prediction. *Journal of Applied Geophysics*. 2014. Vol. 104, p. 142-148. DOI: 10.1016/j.jappgeo.2014.03.001

28. Matinkia M., Hashami R., Mehrad M. et al. Prediction of permeability from well logs using a new hybrid machine learning algorithm. *Petroleum*. 2023. Vol. 9. Iss. 1, p. 108-123. DOI: 10.1016/j.petlm.2022.03.003

29. Xiaobo Zhao, Xiaojun Chen, Qiao Huang et al. Logging-data-driven permeability prediction in low-permeable sandstones based on machine learning with pattern visualization: A case study in Wenchang A Sag, Pearl River Mouth Basin. *Journal of Petroleum Science and Engineering*. 2022. Vol. 214. N 110517. DOI: 10.1016/j.petrol.2022.110517

30. Jing-Jing Liu, Jian-Chao Liu. Permeability Predictions for Tight Sandstone Reservoir Using Explainable Machine Learning and Particle Swarm Optimization. *Geofluids*. 2022. Vol. 2022. N 2263329. DOI: 10.1155/2022/2263329

31. Tahmasebi P., Hezarkhani A. A fast and independent architecture of artificial neural network for permeability prediction. *Journal of Petroleum Science and Engineering*. 2012. Vol. 86-87, p. 118-126. DOI: 10.1016/j.petrol.2012.03.019

32. Kumar A., Lin Liang, Ojha K. Simultaneous inversion of permeability, skin and boundary from pressure transient test data in three-dimensional single well reservoir model. *Petroleum Research*. 2024. Vol. 9. Iss. 2, p. 265-272. DOI: 10.1016/j.ptlrs.2024.01.004

33. Aïfa T., Baouche R., Baddari K. Neuro-fuzzy system to predict permeability and porosity from well log data: A case study of Hassi R'Mel gas field, Algeria. *Journal of Petroleum Science and Engineering*. 2014. Vol. 123, p. 217-229. DOI: 10.1016/j.petrol.2014.09.019

34. Chaves G.S., Ferreira Filho V.J.M. Enhancing production monitoring: A back allocation methodology to estimate well flow rates and assist well test scheduling. *Petroleum Research*. 2024. Vol. 9. Iss. 3, p. 369-379. DOI: 10.1016/j.ptlrs.2024.03.008

35. El-Sebakhy E.A., Asparouhov O., Abdulraheem A.A. et al. Functional networks as a new data mining predictive paradigm to predict permeability in a carbonate reservoir. *Expert Systems with Applications*. 2012. Vol. 39. Iss. 12, p. 10359-10375. DOI: 10.1016/j.eswa.2012.01.157

36. Gholami R., Moradzadeh A., Maleki S. et al. Applications of artificial intelligence methods in prediction of permeability in hydrocarbon reservoirs. *Journal of Petroleum Science and Engineering*. 2014. Vol. 122, p. 643-656. DOI: 10.1016/j.petrol.2014.09.007

37. Yanji Wang, Hangyu Li, Jianchun Xu et al. Machine learning assisted relative permeability upscaling for uncertainty quantification. *Energy*. 2022. Vol. 245. N 123284. DOI: 10.1016/j.energy.2022.123284

38. Guoyin Zhang, Zhizhang Wang, Huaji Li et al. Permeability prediction of isolated channel sands using machine learning. *Journal of Applied Geophysics*. 2018. Vol. 159, p. 605-615. DOI: 10.1016/j.jappgeo.2018.09.011

39. Sheykhinasab A., Mohseni A.A., Bahari A.B. et al. Prediction of permeability of highly heterogeneous hydrocarbon reservoir from conventional petrophysical logs using optimized data-driven algorithms. *Journal of Petroleum Exploration and Production Technology*. 2023. Vol. 13. Iss. 2, p. 661-689. DOI: 10.1007/s13202-022-01593-z

40. Campos D., Wayo D.D.K., De Santis R.B. et al. Evolutionary automated radial basis function neural network for multiphase flowing bottom-hole pressure prediction. *Fuel*. 2024. Vol. 377. N 132666. DOI: 10.1016/j.fuel.2024.132666

41. Anifowose F., Labadin J., Abdulraheem A. Improving the prediction of petroleum reservoir characterization with a stacked generalization ensemble model of support vector machines. *Applied Soft Computing*. 2015. Vol. 26, p. 483-496. DOI: 10.1016/j.asoc.2014.10.017

42. Anifowose F.A., Labadin J., Abdulraheem A. Ensemble model of non-linear feature selection-based Extreme Learning Machine for improved natural gas reservoir characterization. *Journal of Natural Gas Science and Engineering*. 2015. Vol. 26, p. 1561-1572. DOI: 10.1016/j.jngse.2015.02.012

43. Otchere D.A., Ganat T.O.A., Gholami R., Lawal M. A novel custom ensemble learning model for an improved reservoir permeability and water saturation prediction. *Journal of Natural Gas Science and Engineering*. 2021. Vol. 91. N 103962. DOI: 10.1016/j.jngse.2021.103962

44. Mkono C.N., Chuanbo Shen, Mulashani A.K., Nyangi P. An improved permeability estimation model using integrated approach of hybrid machine learning technique and Shapley additive explanation. *Journal of Rock Mechanics and Geotechnical Engineering*. 2025. Vol. 17. Iss. 5, p. 2928-2942. DOI: 10.1016/j.jrmge.2024.09.013

45. Shijia Ma, Jiangfeng Liu, Yuanjian Lin et al. Prediction of permeability of various geotechnical materials under different temperatures based on physical characteristics and machine learning. *Fuel*. 2025. Vol. 379. N 133109. DOI: 10.1016/j.fuel.2024.133109

46. Riyadi Z.A., Olutoki J.O., Hermana M. et al. Machine learning prediction of permeability distribution in the X field Malay Basin using elastic properties. *Results in Engineering*. 2024. Vol. 24. N 103421. DOI: 10.1016/j.rineng.2024.103421

47. Masroor M., Niri M.E., Sharifinasab M.H. A multiple-input deep residual convolutional neural network for reservoir permeability prediction. *Geoenergy Science and Engineering*. 2023. Vol. 222. N 211420. DOI: 10.1016/j.geoen.2023.211420

48. Lawal A., Yingjie Yang, Hongmei He, Baisa N.L. Machine Learning in Oil and Gas Exploration: A Review. *IEEE Access*. 2024. Vol. 12, p. 19035-19058. DOI: 10.1109/ACCESS.2023.3349216

49. Zakharov L.A., Martyushev D.A., Ponomareva I.N. Predicting dynamic formation pressure using artificial intelligence methods. *Journal of Mining Institute.* 2022. Vol. 253, p. 23-32. DOI: 10.31897/PMI.2022.11

***Authors*: Andrei V. Soromotin,** *Postgraduate Student* (*Perm National Research Polytechnic University*, *Perm*, *Russia*), *https://orcid.org/0000-0002-6535-6134*, **Dmitrii A. Martyushev,** *Doctor of Engineering Sciences*, *Professor* (*Perm National Research Polytechnic University*, *Perm*, *Russia*), *martyushevd@inbox.ru*, *https://orcid.org/0000-0002-5745-4375*.

The authors declare no conflict of interests.

ISSN 2411-3336; e-ISSN 2541-9404

JOURNAL OF MINING INSTITUTE

Zapiski Gornogo instituta

Journal homepage: pmi.spmi.ru

Research article *Geotechnical Engineering and Engineering Geology*

Interpretable machine learning to detect well integrity issues

Ildar M. Ishkulov[1,2] ✉, **Irik G. Fattakhov**[1]

[1] *Tatar Oil Research and Design Institute* (*TatNIPIneft*) *of PJSC TATNEFT, Almetyevsk, Republic of Tatarstan, Russia*

[2] *Almetyevsk State Technological University* "*Petroleum Higher School*", *Almetyevsk, Republic of Tatarstan, Russia*

***How to cite this article*:** Ishkulov I.M., Fattakhov I.G. Interpretable machine learning to detect well integrity issues. Journal of Mining Institute. 2025. Vol. 275, p. 94-109.

Abstract

The problem of timely and accurate evaluation of well integrity is becoming increasingly relevant in the context of mature field development, high wellstream water cut, and a growing number of old wells. For production casing diagnostics, geophysical methods are typically used to identify damage and determine its interval. However, high workload of field personnel hinders prompt deployment of wireline crews to survey the integrity of wells. This results in lost oil production, increased water cut, environmental risks, increased non-productive injected volumes, and reduced key economic indices. To address these challenges, a novel approach to evaluation of casing string integrity based on machine learning models has been proposed. The paper presents a procedure for application of interpretable machine learning to detect production casing leakage and provides a comparison of this approach with the ROC-AUC statistical analysis method. The novel approach integrates the LightGBM machine learning algorithm and SHAP analysis to evaluate contribution of key features to well integrity prediction and determine their threshold values. The model training was based on data from 14,318 well surveys conducted between 2000 and 2022. The results indicate that the most important features are sulfate content, solution supersaturation ratio, and water cut. The study confirms the efficiency of interpretable machine learning methods for diagnosing complex technical systems. These results show the potential for application of such models in well integrity monitoring and well workover planning. This approach can also be used in other oil and gas applications, such as prediction of various problems and optimization of well operation conditions.

Keywords

machine learning; casing leakage; data analysis; interpretation; surveys; oil production; oil field development

Received: 08.04.2025 ***Accepted: 18.09.2025*** ***Online: 17.10.2025*** ***Published: 31.10.2025***

Introduction

The problem of casing leakage is one of the most critical issues in oil field development. Loss of casing integrity results in oil production rate decrease, water cut increase, and significant environmental risks [1]. Conventional diagnostic methods for casing leakage typically involve well logging, water chemical analysis, and mathematical modeling [2-4]. However, all these methods have a number of disadvantages: high cost, complexity of data interpretation, and time-consuming studies [5, 6]. Magnetic pulsed inspection has limitations under high-temperature and high-pressure (HPHT) conditions, which reduces its efficiency in challenging downhole environment [5], while thermal convection monitoring requires precise calibration and specialized equipment, increasing diagnostic costs [6]. Consequently, there is a growing need in implementation of modern technologies for casing integrity monitoring, particularly machine learning methods which can enhance prediction accuracy and promptness of damage detection.

Geophysical surveys such as noise logging, temperature logging, and acoustic logging are the most common methods for detecting production casing leaks. For instance, tracer surveys enable efficient localization of behind-the-casing flow [7].

Produced water chemical analysis is an alternative, readily available diagnostic method. Changes in the concentration of chemical components, such as sulfates and chlorides, can indicate behind-the-casing flow and fluid inflow from other formations [8]. Water-oil ratio and well stream water cut analysis serve as important indicators of casing integrity failure [9, 10]. However, in case of complex geochemical sections, this method is less accurate than geophysical techniques.

Application of mathematical modeling makes it possible to forecast the development of behind-the-casing flow and optimize squeeze jobs. The paper [11] presents models considering the process dynamics during the waiting-on-cement period. The paper [12] proposes an innovative method for remedial cementing which minimizes economic risks and improves squeeze job efficiency. Thus, the combination of geophysical methods, chemical analysis, and mathematical modeling provides the basis for comprehensive diagnostics of production casing leakage. However, the limitations of conventional methods necessitate implementation of innovative approaches, such as machine learning. Machine learning methods make it possible to analyze large datasets, account for non-linear relationships, and enhance the accuracy of development parameter forecasting [11-14]. They are frequently used for predicting oil production rates, reservoir pressure, and other parameters. The paper [11] presents a procedure for predicting oil properties *in situ* using neural networks. The authors of paper [14] improved conventional decline curve analysis methods by applying Random Forest and Gradient Boosting algorithms, which allowed increasing the accuracy of forecasts. The paper [15] proposes a method for intake pressure recovery in wells equipped with electrical submersible pumps based on the analysis of water cut and other parameters.

The paper [16] discusses a multi-target regression based on the Random Forest algorithm to predict shale gas production. The use of ensemble approaches, such as ElasticNet and XGBoost, has demonstrated high accuracy of short-term production rate prediction [17-19]. Long short-term memory (LSTM) neural networks are used for time series processing to capture long-term data dependences [20-22].

Optimization of well operation conditions is another promising area for the application of machine learning. The paper [23] describes a hybrid method combining neural networks with a Particle Swarm Optimization algorithm, which improves the accuracy of well performance evaluation. Machine learning models are also used for integrated well modeling, where bottomhole pressure is simulated as a function of dynamic parameters [24].

Studies [25, 26] proposed a system for predicting optimum injection well operation conditions to maximize oil recovery. Deep learning is used for simultaneous prediction of oil, gas, and water production, as well as other dynamic parameters, which is particularly essential for unconventional assets [27, 28].

Machine learning methods are frequently used for predicting various problems and emergency situations. The paper [29] presents a pilot project for predicting incidents in injection wells, including behind-the-casing flow, abnormal pressure fluctuations, and equipment failure, using machine learning algorithms. Application of neural networks to identify abnormal behavior of drilling parameters is described in papers [30-32]. Furthermore, machine learning methods are used for process automation [33, 34] and well placement optimization. The paper [35] proposes a reinforcement learning model for the well pattern design optimization. Application of machine learning methods for log data interpretation to determine lithological types is described in the paper [36]. The paper [37] discusses PVT (pressure, volume, temperature) fluid properties determined by AI-based models. Neural networks and machine learning are used to model properties relationships.

A number of foreign publications discuss well integrity issues using machine learning methods. For instance, the study [38] employed machine learning models to analyze well integrity failures in artificial lift systems. Studies [39, 40] utilize machine learning for water quality prediction, which not only identifies changes in chemical composition but also reduces model uncertainty through advanced data processing techniques and time variation analysis.

Advanced machine learning techniques significantly enhance the accuracy of predicting development parameters, optimize well operation conditions, and automate processes. Their application, in combination with conventional geophysical and chemical methods, provides a comprehensive approach to addressing the problem of production casing leakage.

This study is aimed at determining absolute values of features affecting production casing integrity by using interpretable machine learning methods, as well as analyzing the actual model performance results.

The framework of this study is partially based on the approaches presented in papers [41, 42], which analyze the process of building and testing a machine learning model, as well as the key features affecting production casing integrity, including water chemical composition, well age, and operational dynamics.

This study advances the proposed procedure through a more in-depth analysis of machine learning model interpretability. SHAP analysis techniques [43] are employed as tools for assessing the impact of various features on predictions. This approach not only identifies important features but also their threshold values, exceeding of which is correlated with the increased probability of production casing leakage.

Furthermore, the aim of this study is to compare the feature values derived from statistical analysis of field data with the results of machine learning model interpretation.

Methodology

Under the field conditions, one of the primary methods to identify anomalies in produced fluids is taking samples for a six-component water chemical analysis which determines the concentration of six key ions: sodium, calcium, magnesium, chloride, bicarbonates, and sulfates. Changes in this six-component composition of the produced water are used for a preliminary appraisal of production casing integrity. Figure 1 shows the examples of produced water chemical analysis for field N wells.

The produced water analysis charts (Fig.1) show that ion concentration and total dissolved salts (TDS) in wells with leaking production casing are multiple times higher than in wells with leak-tight casing strings. Thus, chemical analysis of produced water has become a key factor to identify production casing leakage based on significant deviation of features from reference values.

One of the features used to determine well integrity failure is the Cl/Ca ratio. Analysis of this feature values typical for wells with leak-tight and leaking casing is presented in paper [42]. This serves as an example of determining well integrity failure. There can be a large number of such analyses, and studying the concentration ratios of various chemical components requires significant time and financial resources.

All computations and data analysis in this study were performed using the Python 3.10.5 programming language in a Jupyter Notebook environment launched through the Visual Studio Code v.1.99.3 integrated development environment. The scikit-learn v.1.2.2 library was used for data preprocessing, generating machine learning models, and evaluating their performance; the LightGBM v.4.1.0 library was used for implementing gradient boosting on decision trees; the shap v.0.44.1 library was used for interpreting model predictions and analyzing feature importance; the

pandas v.2.3.1 library was used for processing and analyzing tabular data; the numpy v.1.26.4 library was used for mathematical operations and data array handling; and the matplotlib v.3.8.4 and seaborn v.0.13.2 libraries were used for visualizing the results.

a

Normality of solution Hg	Correcting factor for Hg	Volume for Cl (ml)	Normality of trilon B solution	Correcting factor for trilon B	Volume for Ca,Mg (ml)	SO4 calculation procedure	Numerator	Denominator
0.05	0.9901	5	0.10	1.0000	50	Final value	0.0000	0.0000

Field: [redacted] Area: [redacted] Block: 8 Hor-n: Pashian horizon

Chemical analysis of produced water

Date: 04/11/2023 08:59 Density: 1.061 % of water: pH: 6.59 H2S : N/A

Parameter:	%	%%	mg/L	g/L	mg-eq/100	mg-eq/L	% equiv.
Chlorine	5.2899	52.8991	56163	56.1630	149.191	1583.965	49.92
Sulfates	0.0000	0.0001	0	0.0001	0.000	0.002	0.00
Hydrogen carbonate	0.0138	0.1375	146	0.1460	0.225	2.393	0.08
Calcium	0.6606	6.6064	7014	7.0140	32.966	349.999	11.03
Magnesium	0.1489	1.4891	1581	1.5810	12.246	130.017	4.10
Sodium, potassium	2.5009	25.0089	26552	26.5520	104.205	1106.344	34.87
Total dissolved salts	8.6141	86.1412	91456	91.4561	298.834	3172.720	100.00

Results of produced water chemical analysis

Palmer's classification

Primary salts	69.74
Second. salts	30.10
Prim. alkalis	0.00
Second. alkalis	0.16

Sulin's classification

(Na+K)/CL	0.70
CL-(Na+K)/Mg	3.67
Ca/Mg	2.69
SO4/Cl	0.000000

Iron (mg/dm3)	Barium (mg/dm3)	Strontium (mg/dm3)	Zink (mg/dm3)	Bromine (mg/dm3)
		0.000	0.000	0.000

Prediction of gypsum precipitation

Type of water	Solution ionic strength (mg-eq/L)	CaSO4 activity coefficient	Super saturation ratio
Calcium chloride	1.826	0.102	0.000

Prediction of CaCO3 precipitation: Negative

b

Normality of solution Hg	Correcting factor for Hg	Volume for Cl (ml)	Normality of trilon B solution	Correcting factor for trilon B	Volume for Ca,Mg (ml)	SO4 calculation procedure	Numerator	Denominator
0.05	1.0000	5	0.10	1.0000	50	Final value	0.0000	0.0000

Field: [redacted] Area: [redacted] Block: 8 Hor-n: Pashian horizon

Chemical analysis of produced water

Date: 09/10/2003 00:00 Density: 1.166 % of water: 99.0 pH: 6.40 H2S : N/A

Parameter:	%	%%	mg/L	g/L	mg-eq/100	mg-eq/L	% equiv.
Chlorine	9.7161	97.1612	113290	113.2900	274.024	3195.120	49.75
Sulfates	0.0592	0.5918	690	0.6900	1.225	14.280	0.22
Hydrogen carbonate	0.0086	0.0858	100	0.1000	0.138	1.610	0.03
Calcium	1.1175	11.1750	13030	13.0300	55.746	650.000	10.12
Magnesium	0.2607	2.6072	3040	3.0400	21.441	250.000	3.89
Sodium, potassium	4.7564	47.5643	55460	55.4600	198.200	2311.010	35.99
Total dissolved salts	15.9185	159.1852	185610	185.6100	550.774	6422.020	100.00

Results of produced water chemical analysis

Palmer's classification

Primary salts	71.97
Second. salts	27.98
Prim. alkalis	0.00
Second. alkalis	0.05

Sulin's classification

(Na+K)/CL	0.72
CL-(Na+K)/Mg	3.54
Ca/Mg	2.60
SO4/Cl	0.000000

Iron (mg/dm3)	Barium (mg/dm3)	Strontium (mg/dm3)	Zink (mg/dm3)	Bromine (mg/dm3)
0.000	0.000	0.000	0.000	0.000

Prediction of gypsum precipitation

Type of water	Solution ionic strength (mg-eq/L)	CaSO4 activity coefficient	Super saturation ratio
Calcium chloride	3.668	0.095	0.050

Prediction of CaCO3 precipitation: Negative

Fig.1. Results of water chemical analysis for wells with leak-tight (*a*) and leaking (*b*) production casing

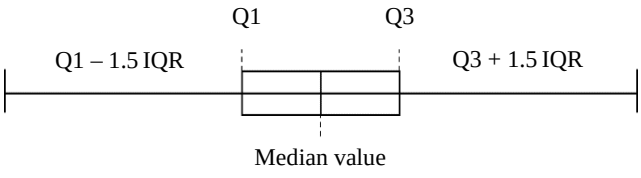

Fig.2. Range diagram

To assess distribution of the analyzed parameters by the field N areas, 14,318 well survey reports obtained from corporate databases for the 2000-2022 period were analyzed. The selected features included parameters characterizing water chemical composition, well performance, and well age.

Initially, distribution of each parameter was evaluated to analyze anomalies and outliers. Outliers are defined as data values that significantly deviate from the majority of other values in the dataset [44, 45]. The interquartile range (IQR) method [46] was selected for outlier detection.

Figure 2 shows a schematic representation of a range diagram, also known as a "box-and-whisker". This type of diagram displays all quartiles of the source data. Quartile Q1 is the value that separates the first quarter of the dataset, meaning that 25 % of the data are less than this value, and 75 % are greater. Next is the median value (the second quartile, Q2) which divides the dataset into two halves, meaning that 50 % of the data are less than this value and 50 % are greater. The third quartile, Q3, is the value that separates three quarters of the dataset, meaning that 75 % of the data are less than this value, and 25 % are greater. The distance between the third and first quartiles is called the interquartile range. The plot also has "whiskers" that extend leftward from the first quartile and rightward from the third quartile. The length of each whisker is equal to one and a half of the interquartile range. Any data points located beyond the whiskers can be considered as outliers.

Based on the described approach, outliers were analyzed across the areas of the N field. To begin with, let's consider outliers for wells with a leak-tight production casing string. Features with the highest average proportion of outliers include water chemical analysis, namely the Ca/Mg ratio 0.19, sulfate content 0.15, and Cl^-(Na+K)/Mg ratio 0.14.

As for parameters characterizing well performance, no outliers are observed, which indicates a reasonably good data representativeness. As for parameters characterizing water composition, the situation is not so straightforward. Features with proportion of outliers less than 10 % include water density, solution ionic strength, pH value, chloride content, bicarbonate content, calcium content, magnesium content, sodium content, total dissolved salts, (Na+K)/Cl ratio, and content of primary and secondary salts. Features with proportion of outliers over 10 % include $CaSO_4$ activity coefficient, supersaturation ratio, sulfate content, Cl^-(Na+K)/Mg ratio, Ca/Mg ratio, and content of secondary alkalis.

In the group of wells with a leaking casing string, the number of outliers is lower than in wells with a leak-tight casing string. Features with the highest proportion of outliers include content of secondary alkalis, fluid flow rate, and calcium concentration. In the entire dataset for wells with a casing leakage problem, the percentage of outliers does not exceed 10 %, which indicates sufficient dataset homogeneity.

The most interesting conclusions can be drawn for the dataset with a leak-tight casing string, which exhibits a higher percentage of outliers. It is possible that measurements were conducted incorrectly, and based on a number of parameters the well was classified as leaking, but all in all it was classified as leak-tight based on various studies and analyses. This discrepancy could be the reason for the outliers in the total dataset. The method proposed in this study allows for the analysis of multiple parameters and provides a correct assessment of well integrity.

The next step was filling the missing values. First, the missing values were filled using the previous value for each specific well, and then the remaining missing values for each specific well were filled from the bottom up, i.e., using the next subsequent value.

Following data preprocessing, a test for multicollinearity was performed using the Pearson correlation matrix. This matrix gives an insight into the strength and direction of the relationships between different features in the dataset [47].

The Pearson correlation matrix is based on the coefficients of linear correlation between all pairs of numerical variables in the dataframe:

$$r = \frac{\sum_{i=1}^{n}(x_i - \bar{x})(y_i - \bar{y})}{\sqrt{\sum_{i=1}^{n}(x_i - \bar{x})^2}\sqrt{\sum_{i=1}^{n}(y_i - \bar{y})^2}},$$

where x_i is the value of feature x in the i-th measurement; y_i is the value of feature y in the i-th measurement; $\bar{x}$ is the average value of feature x; $\bar{y}$ is the average value of feature y; n is the number of measurements.

Figure 3 presents the Pearson correlation matrix as a heat map for the features selected to analyze their impact on the loss of production casing integrity: F1 – area code; F2 – well age at the time of the study; Y – casing condition; F3 – water density; F4 – ionic strength; F5 – $CaSO_4$ activity coefficient; F6 – oversaturation ratio; F7 – pH; F8 – chloride; F9 – sulfates; F10 – bicarbonate; F11 – calcium; F12 – magnesium; F13 – sodium; F14 – total dissolved salts; F15 – (Na+K)/Cl ratio; F16 – Cl^-(Na+K)/Mg ratio; F17 – Ca/Mg ratio; F18 – primary salts; F19 – secondary salts; F20 – secondary alkalis; F21 – liquid rate; F22 – oil flow rate; F23 – water cut; F24 – reservoir pressure; F25 – bottomhole pressure; F26 – number of workover operations. The linear correlation coefficients are displayed at the intersection of the horizontal and vertical axes.

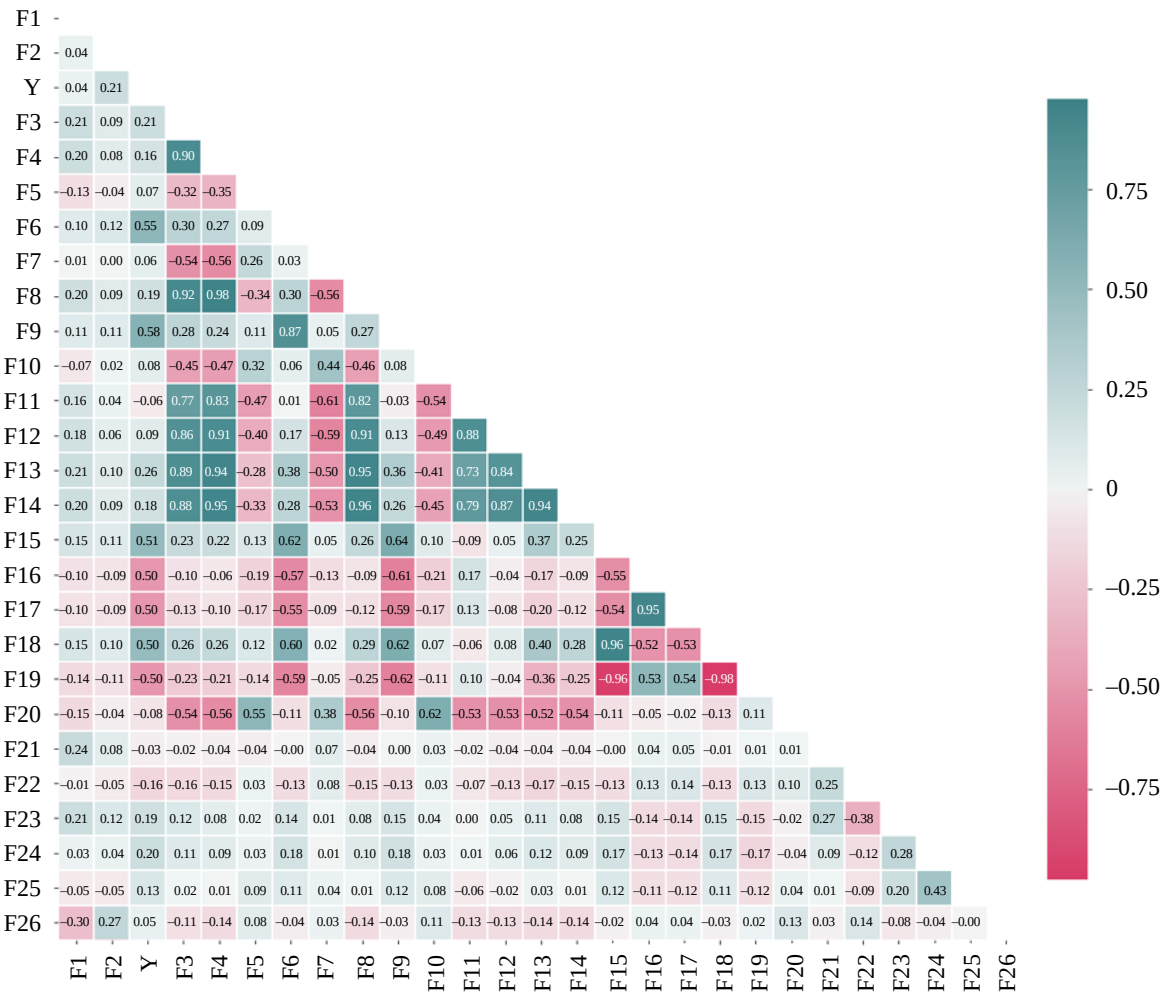

Fig.3. Feature correlation matrix in the dataset with regard to outlier processing

The strongest direct correlation is observed between the features that characterize water chemical composition (Fig.3). Due to the impact of strong feature correlation on model training and its subsequent application, a decision was made to remove one feature from each pair of dependent features. The following features were removed from the training dataset: solution ionic strength, chloride content, calcium content, magnesium content, sodium content, and the Ca/Mg ratio.

During the data processing stage, feature scaling was performed using the standardization method via the StandardScaler module from the scikit-learn library for the Python programming language [48]. Standardization is necessary due to the heterogeneity of feature values used for training. If standardization is not applied, the model will assume that features with larger values are more important than those with smaller values. The feature values were converted using the following equation:

$$z_i = \frac{x_i - \mu_i}{\sigma_i},$$

where z_i – a standardized value; x_i – initial value; μ_i – the average value (arithmetical average of all values); σ_i – standard feature deviation (measure of feature value spread relative to the average value).

At first, the average feature value is subtracted, which centers the distribution around zero. The second step is division by the standard deviation value, bringing the data to scale so that one standard deviation corresponds to a unit length. After standardization, we obtain a value that represents deviation of the original value from the average value in standard units.

A significant spread in values across different areas of the field is observed for a number of parameters, which is attributed to geological and physical characteristics of each production zone. In this context, the model training procedure was improved by incorporating the area feature and applying a knowledge transfer method [49]. This approach involves clustering of production zones based on water chemical analysis and using the silhouette method and the *K*-average algorithm. This made it possible to identify groups of similar production zones and consolidate data from zones with a small number of measurements with data from the analogous zones. The model was trained considering well clusters while recording the specific features of each production zone. This method increased prediction accuracy by 13 % and improved other model quality metrics. It also considered a specific production zone where the well was located when predicting production casing leakage.

To evaluate the importance of individual features and their ability to distinguish between leak-tight and leaking casings, the ROC-AUC (Receiver Operating Characteristic – Area Under the Curve) statistical analysis method was used [50]. It allows for evaluating feature importance based on their ability to distinguish between different classes. The process of AUC determining involves plotting of a ROC curve, which illustrates the relationship between True Positive Rate (TPR) and False Positive Rate (FPR) for a given feature. A higher AUC value indicates a better ability of the feature to distinguish between classes.

For each sample with a known feature value x_i and a class mark $y_i \in \{0, 1\}$, a binary classifier is defined based on the θ threshold value:

$$\hat{y}_i(\theta) = \begin{cases} 1, \text{ if } x_i \geq \theta; \\ 0, \text{ if otherwise,} \end{cases}$$

where $\hat{y}_i(\theta)$ is a predicted class for the *i*-th sample at a specified θ threshold; if $x_i \geq \theta$, the sample is considered positive, if otherwise it is considered negative.

For each θ point, sensitivity (TPR) and specificity (FPR) are calculated:

$$\mathrm{TPR}(\theta) = \frac{\mathrm{TP}(\theta)}{\mathrm{TP}(\theta) + \mathrm{FN}(\theta)};$$

$$\mathrm{FPR}(\theta) = \frac{\mathrm{FP}(\theta)}{\mathrm{FP}(\theta) + \mathrm{TN}(\theta)},$$

where TP(θ) is a number of wells truly classified as leaking; FN(θ) is a number of well falsely classified as leak-tight; FP(θ) is a number of wells falsely classified as leaking; TN(θ) is a number of wells truly classified as leak-tight.

With variation of the classification threshold θ across the entire range of the feature values, a ROC curve is plotted – TPR(θ) versus FPR(θ). The integral under this curve defines the AUC metric:

$$\mathrm{AUC} = \int_0^1 \mathrm{TPR}(f)\,df,$$

where f is a proportion of false-positive classifications (FPR); TPR(f) is sensitivity at specified FPR.

In addition to determining feature importance, it is necessary to establish feature threshold values. One of the statistical parameters used for determining threshold values is Youden's index [51]:

$$J(\theta) = \mathrm{TPR}(\theta) - \mathrm{FPR}(\theta).$$

The Youden's index allows finding the threshold value at which the maximum difference between the TPR and the FPR is achieved in binary classification problem:

$$\theta^* = argmax J(\theta),$$

where θ^* is an optimum classification threshold.

In addition to statistical methods, the ones based on machine learning models are also employed. One such method is SHAP analysis [52]. SHAP methods evaluate contribution of each feature to the model prediction, which helps identify the most significant factors affecting the result. This makes it a valuable tool for analyzing complex systems, such as well integrity diagnostics, where multiple factors contribute to the loss of integrity. Each point displayed on a SHAP plot represents the SHAP value for a specific case. The assembly of these points for each feature defines its distribution along the horizontal axis. Density of this distribution contains important information: broad dense areas on the plot indicate the range of SHAP values typical for the majority of measurements and reflect typical contribution of a feature. In contrast, narrow and elongated areas (the plot "tails") correspond to rare but potentially strong impact, which can be associated with outliers or specific feature interactions. Low feature values are displayed in blue, and high values in red. Position of the points relative to the zero line shows the direction and strength of the feature impact. If the values are on the right side, a positive class is more likely to be predicted, meaning well integrity failure. If the points are on the left side, a negative class is likely to be predicted, meaning well tightness. Impact of each feature is assessed as the difference between the model prediction with this feature and without it, ensuring a fair distribution of contribution of each feature.

Model prediction with consideration of feature contribution according to SHAP-analysis is calculated as follows:

$$f(x) = \phi_0 + \sum_{i=1}^{n} \phi_i(x), \quad (1)$$

where ϕ_0 is the base line; $\phi_i(x)$ is the SHAP value for the i-th feature; n is the number of features.

SHAP values are relative estimates of feature impact expressed in standardized units of deviation from the baseline ϕ_0. However, for the practical application of the model, it is crucial to understand which absolute values correspond to the key transition points between leak-tight and leaking wells.

In particular, there is a threshold value for any feature at which the SHAP contribution is close to zero, meaning the model prediction does not tend either towards the positive or negative class. Such values can be interpreted as cutoff values that separate the areas of "low-risk" and "high-risk" of leakage.

To obtain threshold values, the standardized features were reconverted back to their original physical scale. Based on scaling of each feature, the value corresponding to a neutral SHAP contribution is calculated by the following equation:

$$x_i^{(0)} = z_i^{(0)}\sigma_i + \gamma_i, \tag{2}$$

where $z_i^{(0)}$ is a standardized value at which the SHAP-contribution is equal to zero; $z_i^{(0)} = 0$; γ_i is an absolute threshold value.

The scientific novelty of this research consists in the development of an interpretable machine learning model based on the LightGBM algorithm [53] using SHAP analysis, which has been adapted for the first time to detecting production casing leakage. Unlike conventional implementations, LightGBM employs a tree growth strategy, which provides higher accuracy and training efficiency, and utilizes a histogram discretization method to accelerate computations and reduce memory consumption.

LightGBM is classified as a method of gradient boosting on decision trees. The model prediction is expressed as the sum of predictions from individual trees:

$$\hat{y}_i = \sum_{t=1}^{T} f_t(k_i); \quad f_t \in \mathcal{F},$$

where T is a number of trees in the assembly; f_t is a decision tree function built on the t-th iteration; $\mathcal{F}$ is the space of all possible decision trees; k_i is the i's feature vector.

SHAP analysis was applied as a post-processing method for the LightGBM model results to quantify the contribution of individual features to the model prediction. This enabled interpretation of the model performance and identification of key features that determine the probability of leakage.

The SHAP method calculates marginal contribution of each feature to the model prediction, considering all possible combinations of features. In this study, the feature importance was assessed based on the average absolute SHAP value across the entire dataset:

$$I_j = \frac{1}{N}\sum_{i=1}^{N}\left|\phi_{ij}\right|, \tag{3}$$

where ϕ_{ij} is SHAP value of j feature for i measurement; N is a number of samples.

The higher the value of I_j, the stronger the impact of a feature on the model prediction, on average.

Results and discussion

Figure 4 shows an example of the ROC analysis for sulfate content. This feature effectively distinguishes between leaking and leak-tight wells, as the area value under ROC curve is 0.8 f.u. The red dot indicates the optimal threshold for this feature according to Youden's index (2.08 mg-eq/l); wells with leaking casing are more often observed above this threshold, and wells with leak-tight casing are more often observed below it. The remaining features were analyzed in a similar manner. The results of the analysis are presented in Table 1.

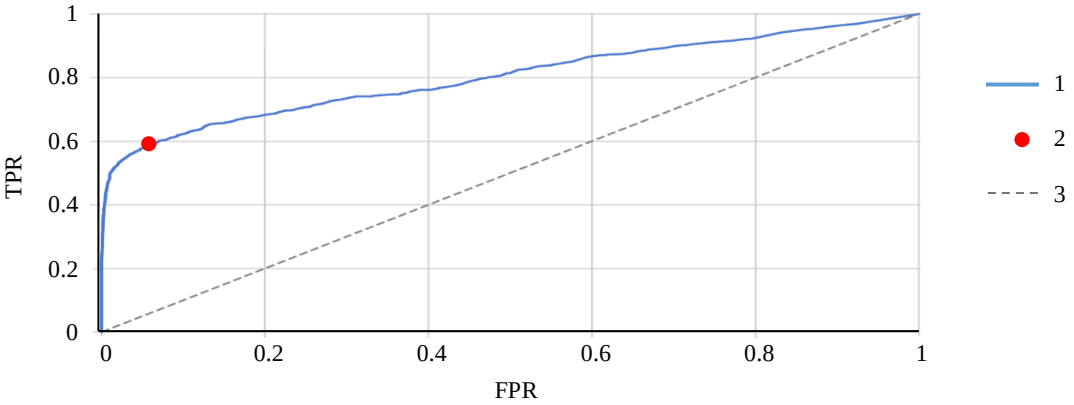

Fig.4. Example of sulfate content ROC analysis

1 – ROC-curve (AUC = 0.8); 2 – optimal threshold, AUC = 2.08; 3 – random guessing of actual model value

Table 1

AUC values and threshold values to distinguish between leak-tight and leaking wells based on ROC-AUC

Features	AUC, f.u.	Feature thresholds
Sulfates, mg-eq/l	0.802	2.082
Supersaturation ratio, f.u.	0.776	0.114
(Na+K)/Cl, f.u.	0.747	0.74
Primary salts, mg-eq/l	0.741	73.68
Water cut, %	0.647	93.83
Formation pressure, atm	0.647	158
Water density, g/cm^3	0.646	1.118
Well age, years	0.645	36
Total dissolved salts, mg-eq/l	0.627	5810.998
$CaSO_4$ activity coefficient, f.u.	0.619	0.101
Bottomhole pressure, atm	0.58	114
Hydrocarbonate, mg-eq/l	0.571	2.098
Number of workovers	0.558	10
pH value, f.u.	0.531	5.82
Fluid rate, m^3/day	0.503	13.145
Secondary alkalis, mg-eq/l	0.467	0.04
Oil rate, m^3/day	0.368	0.004
Secondary salts, mg-eq/l	0.257	38.62
Cl^-(Na+K)/Mg, f.u.	0.25	5.1

To interpret the predictive power of features, a qualitative scale was used [54], according to which AUC = 0.5 f.u. means classifier at the level of random guessing; AUC = 0.7-0.8 means acceptable; AUC = 0.8-0.9 means excellent; AUC > 0.9 means outstanding.

According to this scale, features such as sulfate content, solution supersaturation ratio, (Na+K)/Cl coefficient, and primary salts content are most important in statistical analysis, as the AUC value for the features is greater than 0.7. Features such as water content, formation pressure, and well age have a moderate impact on classification especially when combined with other factors. Features with the AUC value less than 0.6 f.u. have poor classification ability and are likely to play supporting role in well leakage prediction. However, this statistical analysis approach does not consider data nonlinear relationship and interaction between features, which may be critical for accurate prediction. ROC-AUC approach only evaluates the individual capacity of each feature to divide into classes, which limits its applicability in tasks such as well leakage detection.

Machine learning models combined with further SHAP analysis eliminate limitations of statistical methods.

Figure 5 shows SHAP analysis of feature importance calculated using equations (1) and (3). The features shown in the diagram are sorted by decreasing degree of impact on the model prediction.

The following features have the greatest impact on the leak occurrence as per the LightGBM model, based on the average absolute SHAP value: SHAP value of sulfate content – 0.872; SHAP value of solution supersaturation ratio – 0.644; SHAP value of water cut – 0.436; SHAP value of well age at the time of study – 0.420; SHAP value of hydrochemical ratio for Cl^{-}(Na+K)/Mg – 0.374.

In this study, absolute threshold values for features were determined from SHAP analysis using equation (2), changes in which can lead to an increased probability of leakage: sulfates – 2.36 mg-eq/l; supersaturation ratio – 0.10; water cut – 77.27 %; well age – 33 years; Cl^{-}(Na+K)/Mg – 3.86 f.u.; primary salts – 69.50 mg-eq/l; formation pressure – 151.14 atm; (Na+K)/Cl – 0.70 f.u.; secondary salts – 30.29 mg-eq/l; number of workovers – 15; water density – 1.10 g/cm^3; fluid rate – 27.04 m^3/day; $CaSO_4$ activity coefficient – 0.10 f.u.; total dissolved salts – 4776.53 mg-eq/l; pH value – 6.31 f.u.; oil rate – 3.13 m^3/day; secondary alkalis – 0.11 mg-eq/l; hydrogen carbonate – 2.19 mg-eq/l; bottomhole pressure – 95.86 atm.

Sulfates and the supersaturation ratio have the greatest impact on predicting leakage, with only a slight difference in the values of the features (Table 1). In both cases, primary salts, well age, water cut, and formation pressure are also highly important. According to ROC-AUC statistical analysis, the hydrochemical ratio Cl^{-}(Na+K)/Mg has the lowest impact on occurrence of leakage, while as per SHAP analysis, this feature is fifth in the order of importance. That is because SHAP analysis provides more accurate and interpretable threshold values, as it considers nonlinearities and combinations of features that are not detectable in simple ROC-AUC statistical analysis.

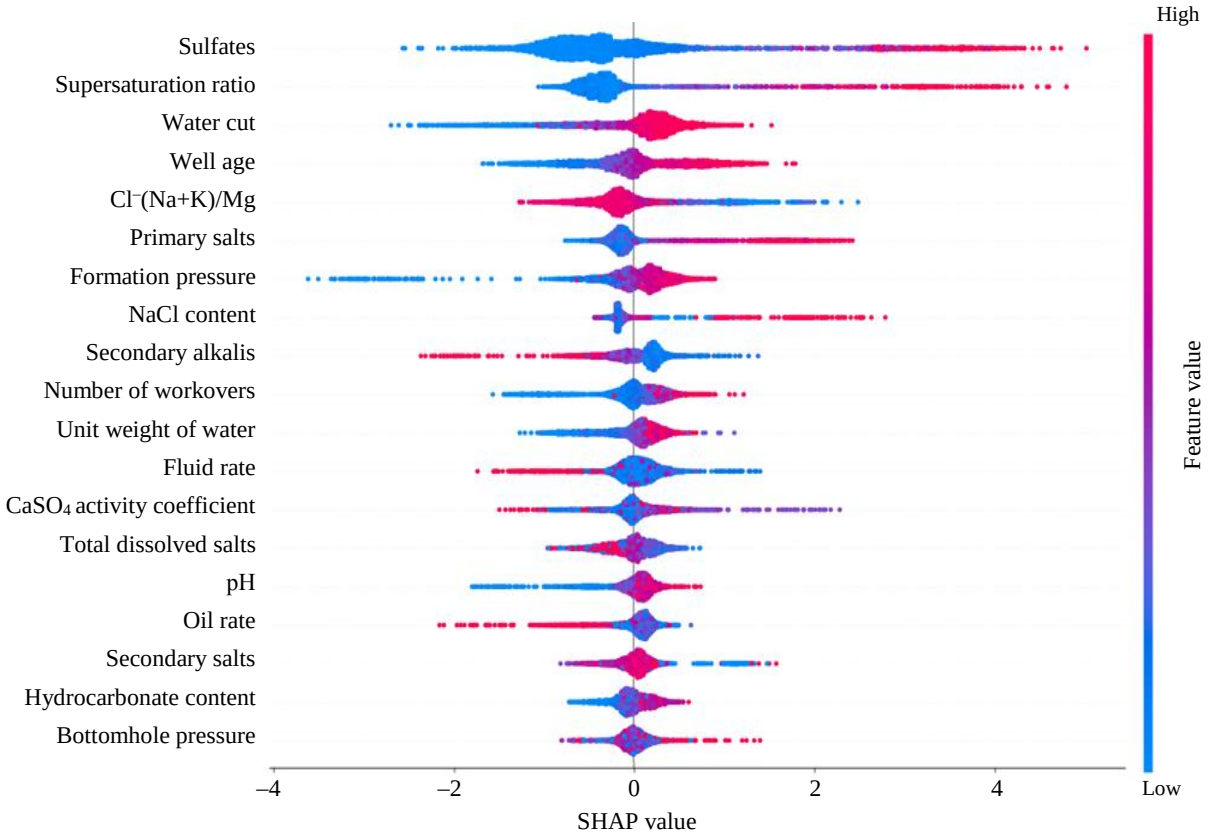

Fig.5. Evaluation of features impact on leakage occurrence

Figure 6 shows interpretation diagrams for five features that have the greatest impact on predicting well leakage.

The sulfate content value at which the SHAP value is neutral is 2.36 mg-eq/l (Fig.6, *a*), i.e., the values below this level reduce the likelihood of leakage, while the values above this level increase it.

As for supersaturation ratio, the threshold value is 0.1 (Fig.6, *b*). Higher values are more often observed in wells with leaking casing. As part of this study, the value of the supersaturation ratio in the terrigenous Devonian water was calculated. On average, it is 0.017, while the supersaturation ratio for the Lower and Middle Carboniferous ranges between 0 and 2.48, with an average of 0.69. Consequently, it can be concluded that as the supersaturation ratio in the water sample obtained from the well increases, there is high probability of fluid influx from the overlying horizons, from the Carboniferous sediments, in particular.

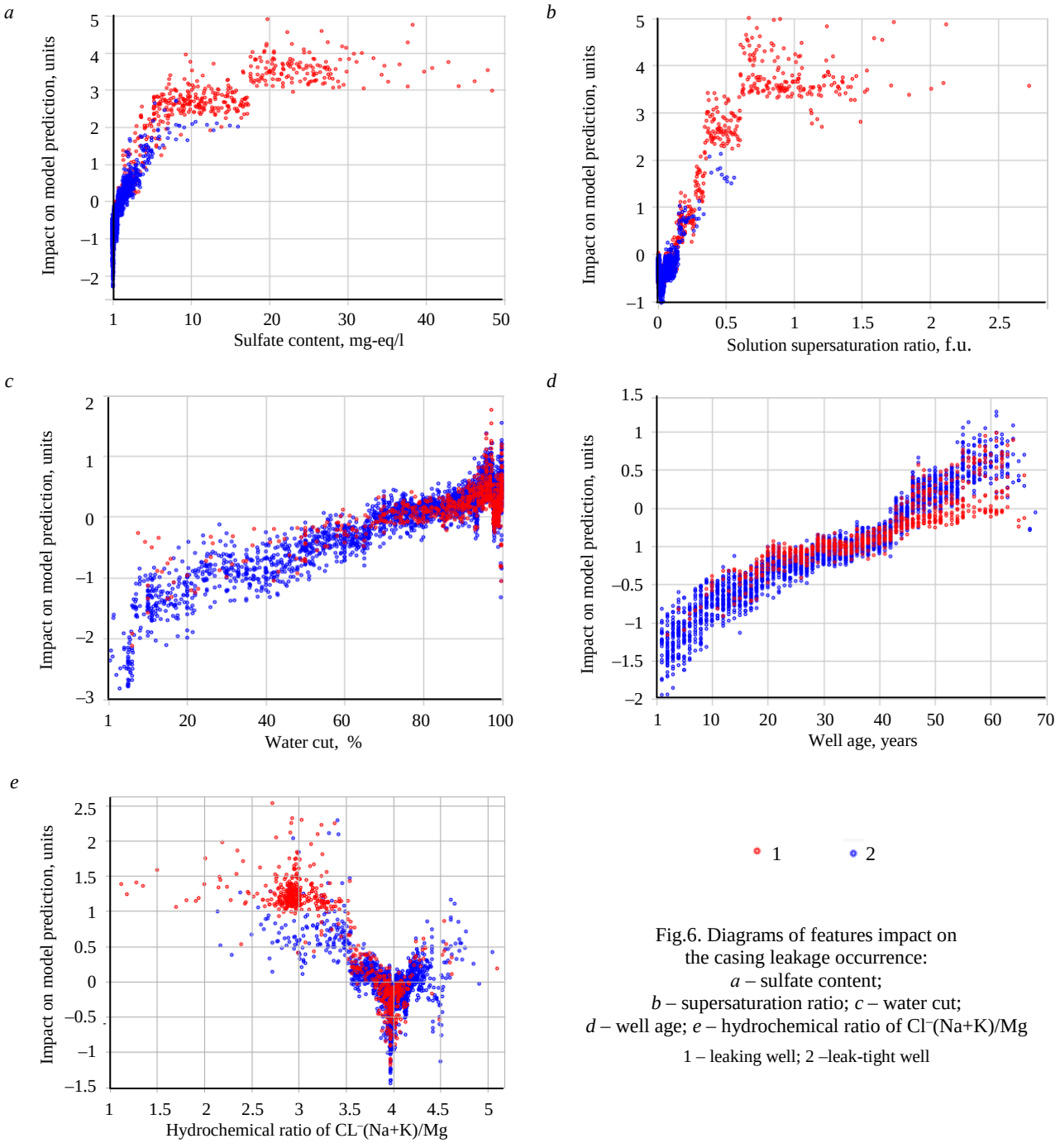

Fig.6. Diagrams of features impact on the casing leakage occurrence:
a – sulfate content;
b – supersaturation ratio; *c* – water cut;
d – well age; *e* – hydrochemical ratio of Cl^{-}(Na+K)/Mg
1 – leaking well; 2 –leak-tight well

As the water cut value increases, the probability of predicting well leakage also increases (Fig.6, *c*). The water cut value at which the SHAP value reaches its threshold is 77.27 %.

As the well age increases, the probability of predicting well leakage also increases (Fig.6, *d*). The well age threshold value according to SHAP analysis is 33 years.

As the value of hydrochemical ratio of Cl^-(Na+K)/Mg decreases, the probability of casing leakage increases (Fig.6, *e*). If the value of the hydrochemical ratio of Cl^-(Na+K)/Mg is around 3.86, there is a boundary zone between cases with leak-tight and leaking casings. As part of this study, the value of hydrochemical ratio of Cl^-(Na+K)/Mg in the terrigenous Devonian water was calculated – on average it is 4.08, while the value of Cl^-(Na+K)/Mg in the Lower and Middle Carboniferous water varies between 0.89 and 3.17, with an average of 2.40. When the value of the hydrochemical ratio of Cl^-(Na+K)/Mg in a sample obtained from the well decreases, there is a high probability of fluid influx from the overlying horizons, from the Carboniferous sediments, in particular.

Comparison of the threshold values determined by statistical methods and machine learning models with further SHAP analysis is presented in Table 2.

Table 2

Comparison of features threshold values as per ROC-AUC method and SHAP analysis

Features	Threshold value		Difference between values, %
	ROC-AUC	SHAP	
Sulfates, mg-eq/l	2.082	2.36	–13
Supersaturation ratio, f.u.	0.114	0.1	12
(Na+K)/Cl, f.u.	0.74	0.7	5
Primary salts, mg-e/l	73.68	69.5	6
Water cut, %	93.83	77.27	18
Formation pressure, atm	158	151.14	4
Water density, g/cm^3	1.118	1.1	2
Well age, years	36	33	8
Total dissolved salts, mg-eq/l	5810.998	4776.53	18
$CaSO_4$ activity coefficient, f.u.	0.101	0.1	1
Bottomhole pressure, atm	114	95.86	16
Hydrocarbonate, mg-eq/l	2.098	2.19	–4
Number of workovers	10	15	–50
pH value, f.u.	5.82	6.31	–8
Fluid rate, m^3/day	13.145	27.04	–106
Secondary alkalis, mg-eq/l	0.04	0.11	–175
Oil rate, m^3/day	0.004	3.13	–78,150
Secondary salts, mg-eq/l	38.62	30.29	22
Cl^-(Na+K)/Mg, f.u.	5.1	3.86	24

For 12 features, ROC-AUC statistical analysis shows higher threshold values compared to SHAP analysis (Table 2), e.g., for the supersaturation ratio those are 0.114 and 0.1, respectively. Conversely, for seven features ROC-AUC demonstrates lower values, e.g., for sulfate content – 2.082 and 2.36 respectively. In the first case, we can say that SHAP analysis focuses on recognizing even small changes in features. In the second case, ROC-AUC analysis attempts to cover the entire range of values that may be important for classification. For oil recovery rate there are significant differences in the threshold values depending on the analysis method. This is probably due to the fact that this feature has a nonlinear impact on the leakage prediction, and the ROC-AUC approach was unable to detect the relationship between the values of this feature and the leakage occurrence in the well.

Unlike previously used machine learning models and statistical methods, the proposed approach provides not only high prediction accuracy, but also interpretation of the threshold values of key features, such as sulfate content, supersaturation ratio, water cut, and well age. It also demonstrates

high importance of previously underestimated features identified by SHAP analysis, which was impossible using conventional ROC-AUC analysis.

Conclusion

In this study, applicability of machine learning methods for detecting well casing integrity issues was analyzed.

SHAP analysis allows identification of absolute threshold values of key features. For example, sulfate content threshold exceeding of which will likely result in casing leakage, is 2.36 mg-eq/l, supersaturation ratio threshold is 0.1, and water cut threshold is 77.27 %.

ROC-AUC analysis shows that some features, such as sulfate content and supersaturation ratio, exhibit high ability to distinguish between leak-tight and leaking wells. However, SHAP analysis provides a more in-depth model interpretation by taking into consideration nonlinearity and synergistic effects between features. This makes the SHAP analysis a valuable tool for analyzing complex systems, such as well operation, where multiple factors affect leakage occurrence. Thus, combination of machine learning methods and SHAP analysis increases prediction accuracy and reliability of results, providing a better basis for decision-making.

The practical significance of this study lies in the applicability of interpretable machine learning models to various tasks in the oil and gas industry, including monitoring of production casing integrity. This approach will facilitate prompt identification of risk zones and will mitigate environmental risks and economic losses during well logging and production operations.

REFERENCES

1. Chernenko A.V., Lyshko G.N. Prevention of Formation Fluids Flows in Anullar Space Based on Mathematical Modeling of Processes in the Well. *Neft. Gas. Novacii.* 2018. N 3 (208), p. 30-33 (in Russian).

2. Nabiullin A.Sh., Sinitsyna T.I., Vorontsov S.Yu. Studying the causes of casing leakages in production wells. Developing preventive methods for casing protection. *Exposition Oil Gas.* 2023. Iss. 8, p. 88-93 (in Russian). DOI: 10.24412/2076-6785-2023-8-88-93

3. Anikeev D.P., Zakirov S.N., Anikeeva E.S., Lysenko A.D. Well leakage is a global problem, not a local one. *Actual Problems of Oil and Gas.* 2019. Iss. 4 (27), p. 14 (in Russian). DOI: 10.29222/ipng.2078-5712.2019-27.art15

4. Trunov E.I., Ozdoeva A.Kh., Blotskaya A.I. et al. New approaches to the application of the acoustic method for continuous monitoring of well cementing integrity. *Oil Industry Journal.* 2024. N 2, p. 38-42 (in Russian). DOI: 10.24887/0028-2448-2024-2-38-42

5. Sharipov A.F., Volkov A.N. System for control and appraisal of well gas-condensate tests quality. *Vesti gazovoy nauki.* 2016. N 4 (28), p. 173-180 (in Russian).

6. Valiullin R.A., Sharafutdinov R.F., Fedotov V.Y. et al. The thermal convection study of behind-casing flow directed from up to down on a well model with induction heater. *Bulletin of Bashkir University.* 2017. Vol. 22. N 2, p. 325-329 (in Russian).

7. Patidar A.K., Joshi D., Dristant U., Choudhury Y. et al. A review of tracer testing techniques in porous media specially attributed to the oil and gas industry. *Journal of Petroleum Exploration and Production Technology*. 2022. Vol. 12. Iss. 12, p. 3339-3356. DOI: 10.1007/s13202-022-01526-w

8. Batista G. dos S., Takimi A.S., da Costa E.M. Chemical Changes in the Composition of Oil Well Cement with Core/Shell Nanoparticle Addition under CO_2 Geological Storage Conditions. *Energy & Fuels*. 2024. Vol. 38. Iss. 23, p. 22947-22958. DOI: 10.1021/acs.energyfuels.4c03686

9. Azamatov M.A., Shorokhov A.N. Production casing leakage determining method. *Nedropolzovanie XXI vek.* 2015. N 6 (56), p. 43-47 (in Russian).

10. Shcherbakova K.O. The problem of high water cut in the products of horizontal wells. *Proceedings of higher educational establishments. Geology and Exploration.* 2022. Vol. 64. N 6, p. 29-38 (in Russian). DOI: 10.32454/0016-7762-2022-64-6-29-38

11. Jabarov K.A. Mathematical modeling the processes of behind-casing fluid movement in the wells during waiting on cement. *Oil Industry Journal.* 2019. N 5, p. 67-71 (in Russian). DOI: 10.24887/0028-2448-2019-5-67-71

12. Burkova A.A. Application of a new technology for repair and insulation works. *Construction of oil and gas wells on land and sea.* 2022. N 8 (356), p. 39-44 (in Russian). DOI: 10.33285/0130-3872-2022-8(356)-39-44

13. Freiman O.A., Eremin N.A. Development of a methodology for predicting reservoir properties of oil using machine learning methods. *Exposition Oil Gas.* 2023. Iss. 7, p. 118-120 (in Russian). DOI: 10.24412/2076-6785-2023-7-118-120

14. Tadjer A., Hong A., Bratvold R.B. Machine learning based decline curve analysis for short-term oil production forecast. *Energy Exploration & Exploitation*. 2021. Vol. 39. Iss. 5, p. 1747-1769. DOI: 10.1177/01445987211011784

15. Pashali A.A., Azbukhanov A.F., Sukharev K.V., Topolnikov A.S. The pressure levels restoration at the pump suction on oil producing wells by the use of machine learning methods. *Petroleum Engineering.* 2022. Vol. 20. N 6, p. 165-172 (in Russian). DOI: 10.17122/ngdelo-2022-6-165-172

16. Liang Xue, Yuetian Liu, Yifei Xiong et al. A data-driven shale gas production forecasting method based on the multi-objective random forest regression. *Journal of Petroleum Science and Engineering*. 2021. Vol. 196. N 107801. DOI: 10.1016/j.petrol.2020.107801

17. Evseenkov A.S., Guz V.S., Shpetny D.N., Yudin E.V. Short-term forecasting of well flow rate based on probabilistic approach. *Oil Industry Journal.* 2023. N 2, p. 78-82 (in Russian). DOI: 10.24887/0028-2448-2023-2-78-82

18. Arief I.H., Tao Yang. A Machine-Learning Approach to Predict Gas-Oil Ratio Based on Advanced Mud Gas Data. *Petrophysics*. 2024. Vol. 65. Iss. 4, p. 433-454.

19. Negash B.M., Yaw A.D. Artificial neural network based production forecasting for a hydrocarbon reservoir under water injection. *Petroleum Exploration and Development*. 2020. Vol. 47. Iss. 2, p. 383-392. DOI: 10.1016/S1876-3804(20)60055-6

20. Gabitova S.I., Davletbakova L.A., Klimov V.Yu. et al. A new method of decline curve forecasting for project wells on the base of machine learning algorithms. *PROneft. Professionals about Oil.* 2020. N 4 (18), p. 69-74 (in Russian). DOI: 10.7868/S2587739920040102

21. Werneck R. de O., Prates R., Moura R. et al. Data-driven deep-learning forecasting for oil production and pressure. *Journal of Petroleum Science and Engineering*. 2022. Vol. 210. N 109937. DOI: 10.1016/j.petrol.2021.109937

22. Xuanyi Song, Yuetian Liu, Liang Xue et al. Time-series well performance prediction based on Long Short-Term Memory (LSTM) neural network model. *Journal of Petroleum Science and Engineering*. 2020. Vol. 186. N 106682. DOI: 10.1016/j.petrol.2019.106682

23. Ahmadi M.A., Soleimani R., Lee M. et al. Determination of oil well production performance using artificial neural network (ANN) linked to the particle swarm optimization (PSO) tool. *Petroleum*. 2015. Vol. 1. Iss. 2, p. 118-132. DOI: 10.1016/j.petlm.2015.06.004

24. Pechko K.A., Senkin I.S., Belonogov E.V. Well modeling using machine learning methods for integrated modeling. *PROneft. Professionals about Oil.* 2022. Vol. 7. N 2 (23), p. 114-120 (in Russian). DOI: 10.51890/2587-7399-2022-7-2-114-120

25. Vikara D., Khanna V. Application of a Deep Learning Network for Joint Prediction of Associated Fluid Production in Unconventional Hydrocarbon Development. *Processes*. 2022. Vol 10. Iss. 4. N 740. DOI: 10.3390/pr10040740

26. Ng C.S.W., Ghahfarokhi A.J., Amar M.N. Application of nature-inspired algorithms and artificial neural network in waterflooding well control optimization. *Journal of Petroleum Exploration and Production Technology*. 2021. Vol. 11. Iss. 7, p. 3103-3127. DOI: 10.1007/s13202-021-01199-x

27. Martyushev D.A., Ponomareva I.N., Zakharov L.A., Shadrov T.A. Application of machine learning for forecasting formation pressure in oil field development. *Bulletin of the Tomsk Polytechnic University. Geo Assets Engineering.* 2021. Vol. 332. N 10, p. 140-149 (in Russian). DOI: 10.18799/24131830/2021/10/3401

28. Ponomarev R.Yu., Migmanov R.R., Ziazev R.R. Assessment of the possibilities of using hybrid modeling to optimize the production potential of an oil and gas field. *Exposition Oil Gas.* 2023. Iss. 5, p. 64-68 (in Russian). DOI: 10.24412/2076-6785-2023-5-64-68

29. Mekhonoshin R.O., Vildanov T.F., Kordik K.E. et al. Prediction of incidents occurrence at injection wells using machine learning algorithms. *Oilfield engineering.* 2023. N 9 (657), p. 16-21 (in Russian). DOI: 10.33285/0207-2351-2023-9(657)-16-21

30. Chernikov A.D., Eremin N.A., Stolyarov V.E. et al. Application of artificial intelligence methods for identifying and predicting complications in the construction of oil and gas wells: problems and solutions. *Georesources.* 2020. Vol. 22. N 3, p. 87-96. DOI: 10.18599/grs.2020.3.87-96

31. Shibaev A.A., Shrago I.L., Vasinkin I.A., Chernyshov A.S. Application of machine learning methods in the task of analysis of anomal behavior of technological features, in the classification of technological operations, of the well construction cycle. *Burenie i neft.* 2023. N 7-8, p. 28-31 (in Russian).

32. Dexin Ma, Hongbo Yang, Zhi Yang et al. An Intelligent Method for Real-Time Surface Monitoring of Rock Drillability at the Well Bottom Based on Logging and Drilling Data Fusion. *Processes*. 2025. Vol. 13. Iss. 3. N 668. DOI: 10.3390/pr13030668

33. Shalyapin D.V., Bakirov D.L., Fattakhov M.M. et al. The applying of machine learning methods to improve the quality of well casing. *Oil and Gas Studies.* 2020. N 5 (143), p. 81-93 (in Russian). DOI: 10.31660/0445-0108-2020-5-81-93

34. Shlykov S.V. Application of machine learning methods to automate processes in the oil and gas industry. *Transport and storage of Oil Products and Hydrocarbons.* 2023. N 2, p. 46-53 (in Russian). DOI: 10.24412/0131-4270-2023-2-46-53

35. Maiorov K.N. Application of machine learning algorithms for solving problems in the oil and gas sector. *Intelligent Systems in Manufacturing.* 2021. Vol. 19. N 3, p. 55-64 (in Russian). DOI: 10.22213/2410-9304-2021-3-55-64

36. Sakhnyuk V.I., Novickov E.V., Sharifullin A.M. et al. Machine learning applications for well-logging interpretation of the Vikulov Formation. *Georesources*. 2022. Vol. 24. N 2, p. 230-238 (in Russian). DOI: 10.18599/grs.2022.2.21

37. Rammay M.H., Abdulraheem A. PVT correlations for Pakistani crude oils using artificial neural network. *Journal of Petroleum Exploration and Production Technology*. 2017. Vol. 7. Iss. 1, p. 217-233. DOI: 10.1007/s13202-016-0232-z

38. Salem A.M., Yakoot M.S., Mahmoud O. A novel machine learning model for autonomous analysis and diagnosis of well integrity failures in artificial-lift production systems. *Advances in Geo-Energy Research*. 2022. Vol. 6. N 2, p. 123-142. DOI: 10.46690/ager.2022.02.05

39. Sadiki N., Jang D.-W. Estimation of Hydraulic and Water Quality Features Using Long Short-Term Memory in Water Distribution Systems. *Water*. 2024. Vol. 16. Iss. 21. N 3028. DOI: 10.3390/w16213028

40. Xiaohui Yan, Tianqi Zhang, Wenying Du et al. A Comprehensive Review of Machine Learning for Water Quality Prediction over the Past Five Years. *Journal of Marine Science and Engineering*. 2024. Vol. 12. Iss. 1. N 159. DOI: 10.3390/jmse12010159

41. Ishkulov I.M., Vafin R.R., Takhauov D.D. et al. Production casing leak detection methods revisited. *Oil Industry Journal.* 2024. N 7, p. 56-60 (in Russian). DOI: 10.24887/0028-2448-2024-7-56-60

42. Ishkulov I.M., Tahauov D.D., Vafin R.R. et al. Well string leak detection using machine learning models. *Petroleum Engineering*. 2024. Vol. 22. N 4, p. 260-267 (in Russian). DOI: 10.17122/ngdelo-2024-4-260-267

43. Xianlin Ma, Mengyao Hou, Jie Zhan, Zhenzhi Liu. Interpretable Predictive Modeling of Tight Gas Well Productivity with SHAP and LIME Techniques. *Energies*. 2023. Vol. 16. Iss. 9. N 3653. DOI: 10.3390/en16093653

44. Smiti A. A critical overview of outlier detection methods. *Computer Science Review*. 2020. Vol. 38. N 100306. DOI: 10.1016/j.cosrev.2020.100306

45. Kiani R., Wei Jin, Sheng V.S. Survey on extreme learning machines for outlier detection. *Machine Learning*. 2024. Vol. 113. Iss. 8, p. 5495-5531. DOI: 10.1007/s10994-023-06375-0

46. Dash C.S.K., Behera A.K., Dehuri S., Ghosh A. An outliers detection and elimination framework in classification task of data mining. *Decision Analytics Journal*. 2023. Vol. 6. N 100164. DOI: 10.1016/j.dajour.2023.100164

47. Morais É.T., Barberes G.A., Souza I.V.A.F. et al. Pearson Correlation Coefficient Applied to Petroleum System Characterization: The Case Study of Potiguar and Reconcavo Basins, Brazil. *Geosciences*. 2023. Vol. 13. Iss. 9. N 282. DOI: 10.3390/geosciences13090282

48. Thippa Reddy G., Swarna Priya R.M., Parimala M. et al. A deep neural networks based model for uninterrupted marine environment monitoring. *Computer Communications*. 2020. Vol. 157, p. 64-75. DOI: 10.1016/j.comcom.2020.04.004

49. Ishkulov I.M., Safarov A.Kh., Fattakhov I.G., Dyakonov A.A. Application of knowledge transfer method for predicting wells integrity failure. *Oilfield engineering.* 2025. № 5 (677), p. 24-28 (in Russian).

50. Chicco D., Jurman G. The Matthews correlation coefficient (MCC) should replace the ROC AUC as the standard metric for assessing binary classification. *BioData Mining*. 2023. Vol. 16. N 4. DOI: 10.1186/s13040-023-00322-4

51. Starovoitov V.V., Golub Y.I. Comparative study of quality estimation of binary classification. *Informatics.* 2020. Vol. 17. N 1, p. 87-101 (in Russian). DOI: 10.37661/1816-0301-2020-17-1-87-101

52. Ishkulov I., Vafin R., Takhauov D. et al. Innovative approach to diagnostics of well integrity using machine learning. *Norwegian Journal of Development of the International Science*. 2024. N 144, p. 29-34. DOI: 10.5281/zenodo.14169109

53. Guolin Ke, Qi Meng, Finley T. et al. LightGBM: A Highly Efficient Gradient Boosting Decision Tree. Advances in Neural Information Processing Systems 30: 31st Annual Conference on Neural Information Processing Systems (NIPS 2017), 4-9 December 2017, Long Beach, CA, USA. Curran Associates Inc., 2018, p. 3147-3155. DOI: 10.5555/3294996.3295074

54. Hosmer D.W., Lemeshow S. Applied Logistic Regression. Wiley, 2000, p. 392. DOI: 10.1002/0471722146

***Authors*: Ildar M. Ishkulov,** *Engineer of the I Category* (*Tatar Oil Research and Design Institute* (*TatNIPIneft*) *of PJSC TATNEFT, Almetyevsk, Republic of Tatarstan, Russia*), *Postgraduate Student* (*Almetyevsk State Technological University* "*Petroleum Higher School*", *Almetyevsk, Republic of Tatarstan, Russia*), *ishkulovim@tatneft.ru, https://orcid.org/0009-0009-2598-0782*, **Irik G. Fattakhov,** *Doctor of Engineering Sciences, Director for Enhanced Oil Recovery, Wave Technology and Biotechnology* (*Tatar Oil Research and Design Institute* (*TatNIPIneft*) *of PJSC TATNEFT, Almetyevsk, Republic of Tatarstan, Russia*), *https://orcid.org/0000-0002-3086-4323*.

The authors declare no conflict of interests.

ISSN 2411-3336; e-ISSN 2541-9404

JOURNAL OF MINING INSTITUTE
Zapiski Gornogo instituta
Journal homepage: pmi.spmi.ru

Research article
Economic Geology

Cluster approach for industrial CO_2 capture and transport: savings via shared infrastructure

Pavel S. Tsvetkov
Empress Catherine II Saint Petersburg Mining University, Saint Petersburg, Russia

***How to cite this article*:** Tsvetkov P.S. Cluster approach for industrial CO_2 capture and transport: savings via shared infrastructure. Journal of Mining Institute. 2025. Vol. 275, p. 110-129.

Abstract
One promising avenue for reducing CO_2 emissions is through the use of carbon capture, utilization, and storage (CCU|S) technologies, which necessitate capital-intensive capture stage implementation. This study proposes implementing a cluster-based approach to its organization, which enables cost reduction through economies of scale achieved by integrating stationary emission sources into a single network with a shared infrastructure. To evaluate the economic effects of this organizational framework, an optimization model was developed utilizing algorithms (SLSQP, Nelder – Mead method, etc.) that account for: spatial distribution of emission sources, emission volumes, CO_2 partial pressure in flue gas streams. The model was tested using data from 533 Russian industrial enterprises in the energy, cement, and ferrous metallurgy sectors, with aggregate annual emissions exceeding 0.5 billion tons of CO_2. For a preliminary analysis of the spatial and technological data of these enterprises, a methodical approach was developed (based on the DBSCAN algorithm), which made it possible to identify 94 geographical areas of their increased concentration. Information about industrial enterprises forming six largest regions was utilized for modeling 90 configurations of carbon capture and transportation projects with shared infrastructure. The results demonstrated that the cluster-based approach reduced the cost of capture in the considered examples by 6.44-13.51 %, depending on the maximum radius of a cluster. An additional reduction in transportation costs due to the use of joint gas pipelines averaged 37.26 and 57.01 % for a 200 and 500 km distances, respectively. Under the same distances and with a maximum cluster radius of no less than 20 km, the average reduction in aggregate costs across the evaluated configurations amounted to 17.81 %. The results obtained confirm the importance of organizational solutions for scaling up CCU|S projects and establishing novel cross-sectoral technological chains. The proposed methodologies can be effectively employed to identify promising areas for the implementation of CCU|S pilot projects and to design highly efficient local networks for CO_2 capture and transportation with shared infrastructure.

Keywords
CO_2 capture; post-combustion capture; CO_2 transportation; shared infrastructure; cluster; SLSQP; Nelder – Mead method; CO_2 emissions; carbon dioxide emissions; CO_2 sequestration; low-carbon development; greenhouse gas emissions; decarbonization; CCS; CCUS; CCU

Received: 05.06.2025 ***Accepted: 25.08.2025*** ***Online: 08.09.2025*** ***Published: 31.10.2025***

Introduction

Climate change is a global challenge, the need to combat it, both in terms of reducing man-made greenhouse gas emissions and in terms of adapting to its negative consequences, has been noted in a number of international agreements [1] and recognized by the International Court of Justice[1]. To achieve these objectives, climate policy is being formulated at both governmental and international levels. The cornerstone of modern climate policy (with regard to emissions mitigation), driven by both objective and subjective factors [2], are renewable energy sources (RES). While RES undoubtedly hold significant long-term potential [3], they have proven insufficient in the recent past to reverse the

[1] Obligations of States in respect of Climate Change. Summary of the Advisory Opinion of 23 July 2025. URL: https://icj-cij.org/sites/default/files/case-related/187/187-20250723-sum-01-00-en.pdf (accessed 10.08.2025).

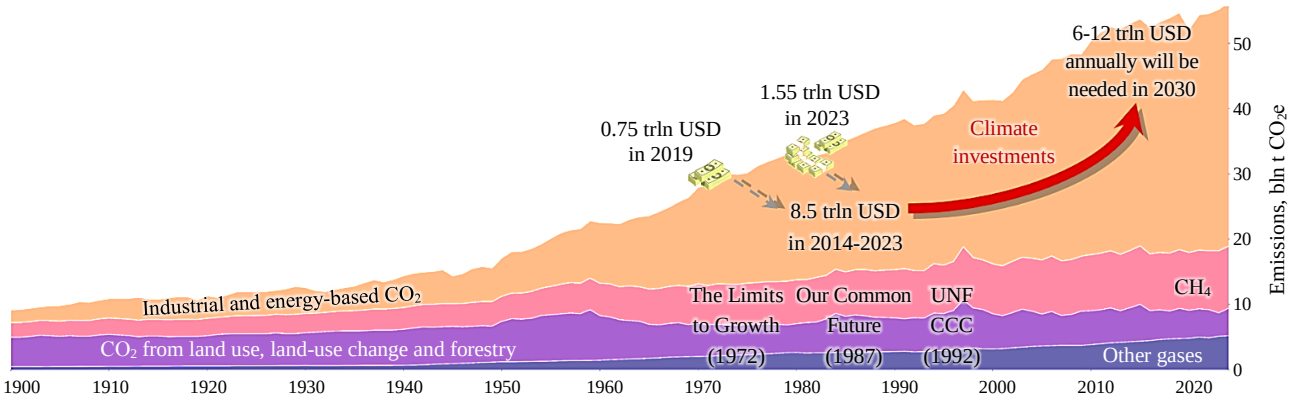

Fig.1. GHG emissions trend and climate investment data

upward trajectory of global greenhouse gas emissions (Fig.1)[2]. At the same time, the volume of climate investments is also growing rapidly, a significant part of which is unbalanced [4].

A possible solution to the problem of increasing the effectiveness of current climate policy is to diversify it by rethinking and re-evaluating alternative emission reduction processes [5, 6], which, in general, is already beginning to happen today. An example of this is the softening of the rhetoric of the European Union in 2024/25. Russia's position on this issue boils down to:

• Focusing on individual examples of energy efficiency improvement. With regard to such measures, it should be noted that attention should be paid to the energy efficiency of buildings [7] and housing and utilities infrastructure (including fostering a culture of rational consumption), rather than focusing exclusively on the industrial sector. While the industrial domain undoubtedly requires innovative solutions [8], it generally possesses significantly greater self-sufficiency in initiating processes to address specific energy intensity reduction challenges [9]. At the same time, even in the case of a real increase in energy efficiency, it should be taken into account that the results at a macrolevel are likely to be lower than expected due to the rebound effects [10] (e.g. the Jevons effect).

• Overreliance on forest-climatic projects as the main tool for reducing (offsetting) emissions, including through a reassessment of the entire emission inventory [11]. This area certainly has strengths and should be defended as an important part of the national decarbonization strategy; however, there are risks that require close attention:

– as temperatures continue to rise, the frequency of forest fires, which have become a seasonal but regular occurrence in recent decades, will increase;

– deforestation and export of forests are actively carried out;

– ignoring technological directions for reducing emissions is fraught with the loss of important competencies necessary for the development and commercialization of low-carbon technologies;

– focusing solely on non-technological compensation of emissions risks not receiving the support of partner countries, with which the formation of an international carbon trading systems is being discussed.

The objective strength of forest-climate projects is that they are not limited to the energy sector. Considering the structure of stationary CO_2 emissions in Russia[3], most of which, although related to energy generation [12], are still characterized by a significant proportion of other sources, it seems logical to overestimate the potential of equally flexible technologies applicable in a wide range of

[2] Climate Change Tracker. URL: https://climatechangetracker.org/igcc/yearly-human-induced-greenhouse-gas-emissions-in-CO_2-equivalent#data-source (accessed 10.08.2025).

[3] Russian Federation. 2024 National Inventory Document (NID). Biennial Transparency reports (BTR), GHG inventories. URL: https://unfccc.int/documents/645136 (accessed 10.08.2025).

industries, namely CO_2 sequestration (CCU|S). There are certainly many problematic issues regarding these groups of technologies, starting with the lack of sufficient real industrial data [13] applicable to Russian conditions, and ending with an almost complete lack of knowledge about the potential for CO_2 utilization and conversion into various types of products as a single focus, rather than individual projects. And it is precisely this lack of information about their effectiveness, as well as the lack of scientific research in this area, that is a barrier to Russia's development of a "balanced, economically sound and non-proactive" state climate policy [14], which includes CCU|S.

It is important that the starting point of all such projects is the stage of CO_2 capture, which has been gaining global interest in recent years. It is noteworthy that in 2008-2013, Russia was one of the world leaders in the number of patents in this field [15]. Thus, the scientific problem highlighted in this paper is that the current pace of development of CO_2 capture technologies required for all CCU|S projects does not give reasonable optimism about the imminent achievement of breakthrough results that can seriously reduce unit costs. With this in mind, it seems logical to develop not only technological, but also organizational approaches that can help improve this scientific and industry direction. Thus, the purpose of this study is to explore the possibility of using a cluster approach to the organization of a CO_2 capture project from stationary industrial sources. The goal defined the following research objectives:

• analysis of CO_2 capture methods and technologies, as well as various configurations of business models used in the implementation of CCU|S projects;

• development of a cluster approach to the implementation of a CO_2 capture project and a model for assessing its effects;

• testing of the proposed approach based on data from industrial sources of CO_2 emissions in the Russian Federation.

Problem statement

Carbon dioxide capture as a stage of CO_2 sequestration technologies

CCU|S is a group of technologies that, instead of preventing CO_2 emissions, involve it in various technological chains (Fig.2), which can be divided into three groups:

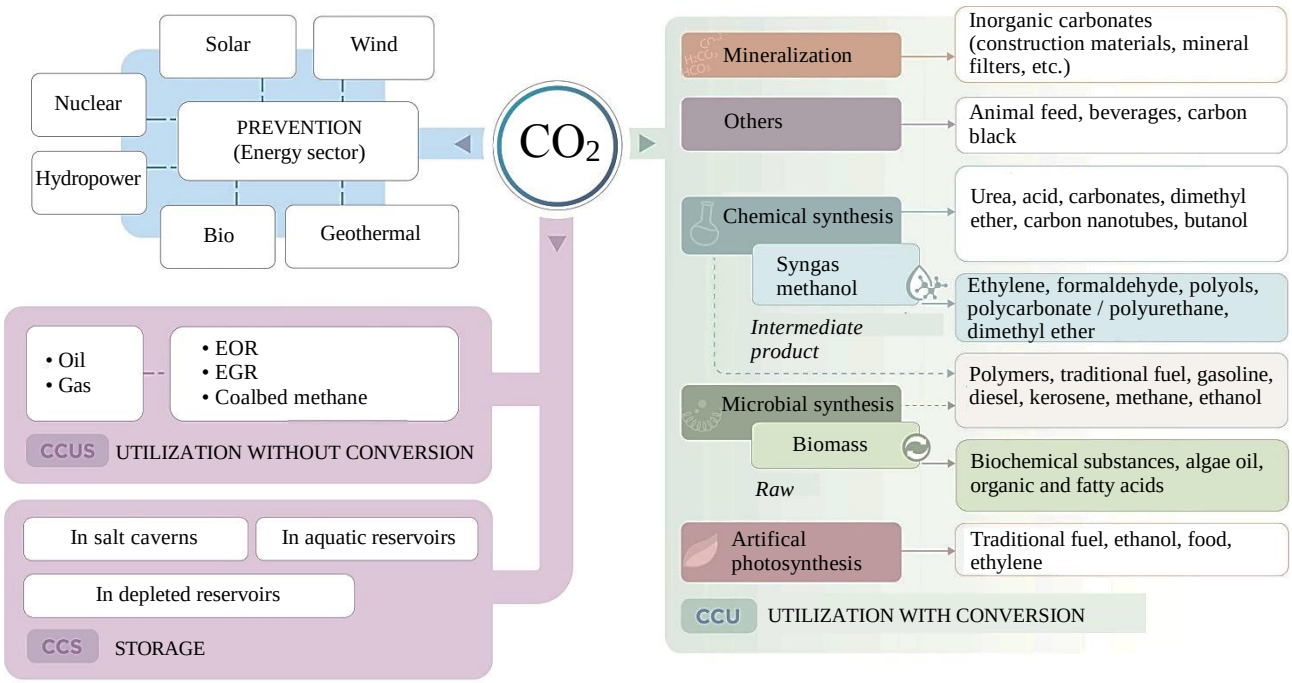

Fig.2. The diversity of CCU|S technologies

• Carbon capture and storage (CCS), which involves the capture and disposal of CO_2 in any geological formation, or by marine storage, without any application options with positive current cash flows.

• Carbon Capture, Utilization and Storage (CCUS) includes projects that use CO_2 to improve the efficiency of natural resource extraction processes (oil, natural gas, groundwater, geothermal energy, etc.) [16]. After the extraction stage, CO_2 is stored underground. Technologies for working with technogenic resources can also be attributed to this group. For example, relatively recently scientists at Saint Petersburg Mining University have proven the technological possibility of obtaining scandium concentrate from alumina production waste by carbonizing it with exhaust gases [17].

• Carbon capture and recycling (CCU) projects involve the capture and use of CO_2 in the production process as a raw material or chemical agent (i.e. these projects involve the "storage" of CO_2 in various commodities). The list of CO_2 disposal options shown in the Fig.2 is not exhaustive [18].

Despite their conceptual proximity, these technological chains have different goals, principles of implementation, effects, risks and prospects. In addition, the transition from one option to another leads to a change in the role of CO_2: it becomes not just a waste, but a resource that can be useful in industries, which is a clear example of the transition from a linear economy to a circular economy. Nevertheless, their common initial stage, which in fact opens up the fundamental possibility of implementing such technological schemes, is capture, to which this study is devoted.

First of all, it is important that the total amount of CO_2 emissions can be divided into:

• Not amenable to capture emissions. The sources of such emissions are some household processes, processes in natural ecosystems and agriculture. It can also include emissions from non-stationary sources (e.g. transport). At the current stage of development, the fight against such emissions from most sources can only be carried out by completely replacing technology (for example, switching to electric vehicles). In other cases, the measures are more promising and include removing CO_2 from ecosystems, adjusting the culture of resource consumption, developing geoengineering technologies, etc. Taking this into account, today there is a growing attention to compensation (offsetting) mechanisms, for example, implemented through forest-climatic projects [19].

• Capturable emissions occurring within several controllable natural and technological processes, e.g. industrial emissions. The methods of combating them are renewable energy technologies, energy efficiency improvement, etc. In the case of CCU|S projects, capture is carried out from stationary sources, the main of which include energy generation facilities (13.3 billion t of CO_2e per year), metallurgical (4.1 billion t of CO_2e per year), cement (3.7 billion t of CO_2e per year), chemical plants and oil refineries (1.1 billion t CO_2e per year), as well as hydrogen production (25 million t of CO_2e per year)[4]. There are already examples of successful implementation of industrial-scale technologies in almost all of these industries.

The costs and efficiency of the capture process at production facilities depend on many factors, however, one of the main ones is the partial pressure of CO_2 (in proportion to its percentage in the mixture) (Table 1). Some sources note [20] that the content of SO_x, NO_x, and some other impurities can also affect the qualitative and quantitative characteristics of the capture process.

The "target" efficiency of the process is also important (the proportion of CO_2 in the gas stream that can be captured), especially if we are talking about a difference of tens of percent, which can increase costs several times [21]. However, today, as a rule, it is customary to talk about high rates, i.e. 94±5 % of the efficiency of capture from the stream (Table 2), which somewhat reduces the spread of dependent values.

[4] Global Energy Perspective 2023: CCUS outlook. URL: https://www.mckinsey.com/industries/oil-and-gas/our-insights/global-energy-perspective-2023-ccus-outlook (accessed 10.08.2025).

Table 1

Characteristics of some emission sources [22, 23]

Industry	Source	Partial pressure, kPa[1]	Price range, USD/t
Cement	Flue gases from the furnace	18	37-118
	Pre-firing device	20-30	
Ferrous metallurgy	Lime firing	7.1-8.1	55-120
	Sintering plant	3.7-4.2	
Oil refining	Liquid catalytic cracking	10.1-14.2	45-120
	The heater	8.1-10.1	
	Steam cracking for ethylene production	7.1-12.2	
	Steam reforming of methane to produce hydrogen	300-480[2]	15-60
	Production of ethylene oxide	Over 92	5-35
Gas processing	Gas processing plant	Up to 5000[3]	5-35
Pulp and paper industry	Lime kiln	16	30-45
Energy industry	Coal-fired power plant	12.2-14.2	43-80
	Gas-fired power plant	3.8-4.6	59-107
Aluminum smelting	Aluminum plant	0.8-1.1	180-300
Fertilizer production	Coal gasification	750-2500[4]	5-40
	Synthesis gas from natural gas	300-1200[5]	

Notes: 1 – at standard atmospheric pressure (101.3 kPa), unless otherwise stated; 2 – 2-3 MPa; 3 – 0.9-8.2 MPa and above; 4 – 3-6 MPa; 5 – 2-3 MPa.

Table 2

Comparison of CO_2 capture technologies [24, 25]

CO_2 capture technology	Efficiency, %	Energy consumption, GJ/t	Cost of CO_2 capture, USD/t CO_2	Characteristics
Industrial gas separation	90	5.00	34.80-60.90	These technologies are common in the oil and gas and chemical industries, however, they require adaptation to the specifics of a particular gas component composition and are characterized by high energy consumption
Post-combustion	90	4.14	46-74	Technologies are suitable for upgrading existing industrial facilities, but require significant capital and operating costs
Pre-combustion	90	3.35	34-63	Highly efficient technology used in oil refining and hydrogen production processes. Application is not possible everywhere and requires a major reorganization of the production line
Oxy-fuel combustion	>90	4.05	52	The technology allows to obtain flue gases with a concentration of CO_2 up to 90 %, which simplifies subsequent capture. The technology is promising for cement and metallurgical plants, however, it requires expensive oxygen production equipment and a complete reconstruction of the production line. So far, there are only pilot projects
Chemical looping	96-99	0.95	<59.20	An innovative technology in the early stages of development, with good energy efficiency indicators, but, so far, characterized by rapid wear of carrier materials
Direct air capture	85-93	5.25	140-1000	In theory, this is a carbon-negative technology, but only if the problem with energy supply is solved. The same problem now leads to the uncompetitiveness of such solutions in terms of price

The difference between technologies may be aggravated by the specifics of the detection facility (Table 3). For example, if we talk about the cement industry, the difference in wet (5-7 GJ/ t of clinker) and dry (3-4 GJ/t of clinker) production methods can create a two-fold difference in energy consumption per unit of production[5].

Table 3

The average cost of CO_2 capture in various technological processes of the cement and metallurgical industries, without taking into account the specifics of the region [6, 7, 8]

Industry	CO_2 capture technology	Cost of CO_2 capture, USD/t CO_2	Increased production costs, USD/t of cement or steel*
Cement	Traditional chemical absorption	34-79	46-116
	Advanced absorption technologies	45	20
	Membranes	51-57	39
	Oxy-fuel	39-57	38-39
	Solid sorbents	40-74	40-74
Metallurgy	Traditional chemical absorption	7-23	31-110
	Advanced absorption technologies	7-13	36-37
	Vacuum pressure swing adsorption	11-15	40-45

* The estimated cost increase for cement is ~20-60 %, for steel – 5-25 %.

A general description of the capture technologies has been given more than once, both in Russian and in English-language literature. A fairly detailed and exhaustive scheme of the processes is available, for example, in the study [24].

It is also important to clarify the technologies for direct CO_2 capture from the air (DAC) as part of the review. The most efficient laboratory processes of this kind require electrical energy costs of the order of 1-2 GJ/t CO_2. In real operating conditions, this indicator can rise to 5 GJ/t CO_2 (taking into account the increase in electrical energy consumed), which is due to both natural factors and the need to process huge volumes of air [26]. At the same time, electricity costs are only about 10-20 % of the total energy costs. Other thermal energy is needed, for example, for the regeneration of sorption material. As a result, the energy needed for the DAC can be used more efficiently, for example, reducing direct emissions. There is no alternative to the situation when the already emitted CO_2 must be removed from the atmosphere.

The situation is much better with a multiple increase in the concentration of CO_2 in the treated gas. In most cases this value ranges from 4 to 30 %. At these levels, the total energy consumption for capture spans 1 to 5 GJ/t CO_2 [27], which, as a result, affects the cost of the process, in addition to the difference in the technologies themselves.

Another cost growth factor is evident when the transition from "catch-from-flow" planning to "catch-from-facility" is underway. The difference is that there may be several streams of CO_2-containing gas at a single facility from different processes with different component compositions. In such cases, it is possible either to combine gas flows, or to use several separate trapping plants (metallurgical plants, hydrogen production, etc.), and then the cost increase may be a multiple of the increase in the number of plants.

[5] IEAGHG Technical Report 2022-04: From Carbon Dioxide to Building Materials – Improving Process Efficiency. IEAGHG, 2022, p. 121. URL: https://publications.ieaghg.org/technicalreports/2022-04 %20From %20Carbon %20Dioxide %20to Building %20Materials %20– %20Improving %20Process %20Efficiency.pdf (accessed 10.08.2025).

[6] Ricome G., Guzzafame M., Degnan-Rojeski J., Jawa I. Cement's Carbon Footprint Doesn't Have to Be Set in Stone: The Future of Process Industries. URL: https://www.bcg.com/publications/2024/cement-industry-carbon-footprint (accessed 10.08.2025).

[7] IEAGHG Technical Review 2018-TR03: Cost of CO_2 capture in the industrial sector: cement and iron industries, IEAGHG, 2018, p. 65. URL: https://publications.ieaghg.org/technicalreports/2018-TR03 %20Cost %20of %20CO_2 %20capture in the industrial %20sector %20cement %20and %20iron %20and %20steel %20industries.pdf (accessed 10.08.2025).

[8] Sprenger T., Moritz M., Wild P., Çam E. Low-carbon steel. A global cost comparison. Institute of Energy Economics at the University of Cologne: official website, 45 slides. URL: https://www.ewi.uni-koeln.de/cms/wp-content/uploads/2022/12/221209_EWI_H2-Steel_Low-carbon-steel.pdf (accessed 10.08.2025).

For example, steam methane reforming plants capture CO_2 only in concentrated synthesis gas, which is why the capture efficiency of the entire plant is 50-80 %[9]. Taking into account less concentrated sources could lead to an increase in this value to 65-90 %, but the cost would also increase by 15-20 % (from about 40 to more than 50 USD/t). A similar situation is typical for the production of biodiesel (an increase from 78 to 96 % corresponds to an approximate increase in costs from 12 to 26 USD/t) and for the production of bioethanol (an increase from 12 to 91 % corresponds to an approximate increase in costs from 15 to 48 USD/t).

Given this, it is logical to assume that industries where such an approach is possible will form strategies for the transition to carbon-free production based on the gradual introduction of CO_2-reduced streams into the process, consistent with an increase in the carbon tax and/or strengthening other mechanisms to support such projects[10].

Development of business models of CCU|S technological chains

In addition to improving technological processes, CCU|S is also undergoing changes in organizational methods, models, and approaches. This is usually associated with the improvement of business models of projects, which are also a tool for developing and implementing corporate strategies. There are many approaches to creating a business-models (BM), each of which has its own unique features in terms of processes, elements, implementation mechanisms or organizational structure [28], however, the key elements of a successful BM are usually standard [29]. BM, as well as methods for their construction/validation, should strive for structural integrity, complexity, validity and feasibility [30]. If, with this in mind, it is possible to formulate a value proposition, analyze at least part of the cash flows and identify target market segments, then such a BM can be considered successful. As for CCU|S BM, they can be divided into two large groups[9].

BM projects of the complete technological chain. In many modern CCU|S projects, it is the full chain BM that is used, in which a single organization assumes responsibility for all stages of the project. In Fig.3 (extended and adapted version of schemes from[11]) it is shown in a green zone. These BM correspond to the specifics of "first-of-its-kind" (FOAK) innovative projects, which often require serious resource support from the state or other structures. The main advantages of this strategy are risk reduction and improved coordination through centralized management. However, this also implies that the operator is fully responsible and must have experience in all aspects of the process, which is rare.

In addition, such a BM has several significant disadvantages[11]. Firstly, it is almost impossible to scale (in terms of the rapid growth in the number of projects). The implementation of a complete chain requires significant investments in infrastructure, which makes it financially feasible only for large-scale industrial enterprises. This limits the possibilities of implementing CCU|S in small and medium-sized enterprises, preventing the introduction of technology in regions with less developed infrastructure and preventing companies from many sectors of the economy from fully participating in such projects.

Secondly, access to the project for external participants, such as independent technology providers or specialized service companies, is often limited. This hinders the formation of partnerships, which, in its turn, hinders the promotion of innovative technologies and CO_2 sequestration as an independent scientific and industrial area.

Thirdly, such a BM does not imply competition. As a result, there are no incentives to develop innovations, and the cost reduction process becomes more complicated. An alternative solution is to divide the CCU|S value chain between different participants, as suggested by the second group of BM.

[9] CCUS Policies and Business Models: Building a Commercial Market. International Energy Agency, 2023, p. 121. URL: https://iea.blob.core.windows.net/assets/d0cb5c89-3bd4-4efd-8ef5-57dc327a02d6/CCUSPoliciesandBusinessModels.pdf (accessed 10.08.2025).

[10] IEAGHG Technical Review 2019-TR02: CO_2STCap (Cutting cost of CO_2 Capture in Process Industry). IEAGHG, 2019, p. 28. URL: https://publications.ieaghg.org/technicalreports/2019-TR02%20CO2stCap%20(Cutting%20Cost%20of%20CO2%20Capture in%20Process%20Industry).pdf (accessed10.08.2025).

[11] Fattouh B., Muslemani H., Jewad R. Capture carbon, capture value: An overview of CCS business models. OIES Paper: CM, № 08. Oxford: The Oxford Institute for Energy Studies, 2024, p. 28. URL: https://www.econstor.eu/bitstream/10419/296651/1/1882397541.pdf (accessed 10.08.2025).

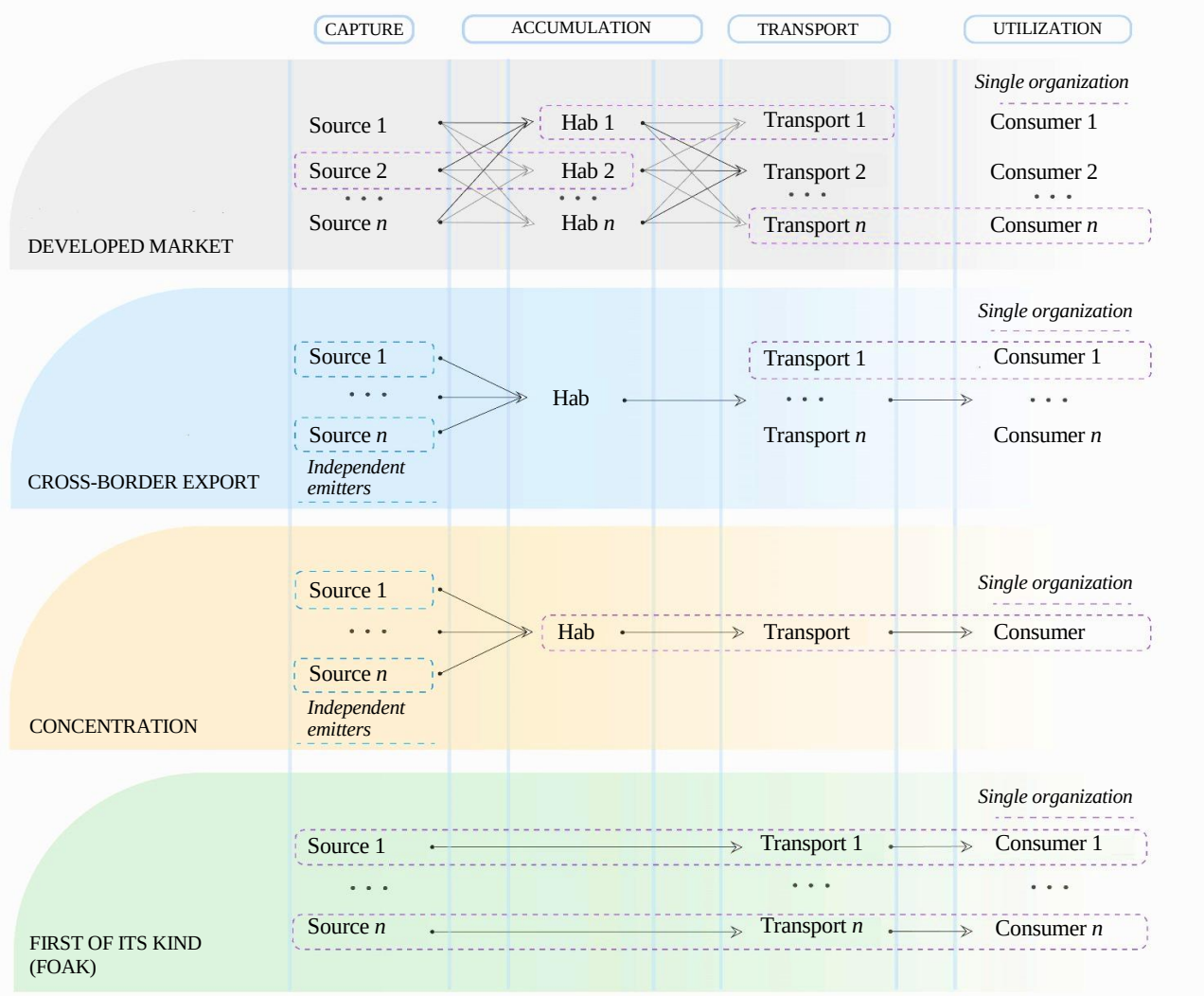

Fig.3. Various configurations of BM CCU|S. Green is the BM of the complete technological chain, other colors are the BM of partial technological chains

BM of partial chain projects – more flexible and more suitable for low-tonnage projects, such as CCU [12]. They allow businesses to delegate responsibilities for CO_2 capture, transportation, and storage to specialized firms. This is especially important when CO_2 capture is not included in the initial design of the technological process and requires a significant amount of additional equipment and new organizational solutions, unlike, for example, natural gas processing. As a result, new players may enter the CCU|S market, including companies from the metallurgical and machine-building sectors (equipment manufacturers), the chemical industry (as emitters or technology developers), as well as suppliers of infrastructure and engineering services. Despite the fact that CCU|S partial chain models are relatively new, high barriers to entry due to capital requirements and experience in the process have allowed some companies to take a leading position in the Capture as a service sector, for example: Aker Carbon Capture, Carbon Clean, Air Liquide, Svante, Entropy, Linde, etc.

It is also possible to implement the "Transportation as a Service" or "Storage as a Service" models. In the first case, the supplier may offer services for moving the captured CO_2 from emission sources to storage or disposal sites using various technological means. In the second case, only CO_2 storage

[12] CCUS Policies and Business Models: Building a Commercial Market. International Energy Agency, 2023, p. 121. URL: https://iea.blob.core.windows.net/assets/d0cb5c89-3bd4-4efd-8ef5-57dc327a02d6/CCUSPoliciesandBusinessModels.pdf (accessed 10.08.2025).

services are provided[13]. An example of a combination of these schemes is the Alberta Carbon project (Canada)[14], in which Wolf Carbon Solutions is a transportation service provider and Enhance Energy is responsible for storage. The Emirates Steel CCS (United Arab Emirates) project[15] is organized in a similar way, where CO_2 emissions are collected at the Emirates Steel Industries complex, and ADNOC reported their plans to carry out transportation and storage in the Rumaith and Bab oil fields.

Overall, separation of the chain increases flexibility, which accelerates the integration of new projects into CO_2 sequestration systems. In addition, the presence of competition helps to reduce and distribute costs due to the creation of shared infrastructure. At the same time, small and geographically distributed stationary sources of emissions can be easily integrated into these systems by creating nodes that combine the resources and expertise of various participants in the technological chain.

However, these BM are not without drawbacks. They are largely related to the need to coordinate the multitude of project participants, as each requires guarantees of demand for the products/ services they create. The solution to this problem is the active position of the state in terms of creating the necessary conditions. For example, providing financial support and reducing the risks of participating in a project is possible through a public-private partnership mechanism. An example of this approach is the activities of the Danish company Nordsofonden, which has a stake in many CO_2 storage projects[16]. Or the Porthos project (Netherlands, Port of Rotterdam), which has extensive support from both the national government and the European Union.

Partial chain BM also require strict antitrust regulation, since one company can have a significant impact on weaker players in an as-yet-unformed market. For example, the Stella Maris CCS project (Norway) uses a shared floating infrastructure for collecting, transporting and storing CO_2 in the North Sea. The planned capacity of the project is up to 10 million t of CO_2 per year, which is a significant amount, given the current level of technology development.

If the market can be considered formed, i.e. there are many independent companies with mature technologies (*n*-th of a kind, NOAK) operating in it, then government participation in it is minimized. As a rule, monitoring of legislative measures is necessary, but there is no need for substantial financial support for FOAK projects, which is urgently needed at the current stage due to their high cost, primarily due to the capture stage.

It can be concluded that the development of BM CCU|S leads, on the one hand, to the splitting of a single value chain, but, on the other hand, to the concentration of production activity in hubs (clusters). This corresponds to the general trend towards the decentralization of some industrial systems, which is being actively discussed, for example, in relation to distributed energy. It is important that the goal of this trend should not be the creation of separately located enterprises/production facilities, but the creation of many highly efficient local area networks, which, as technology develops, can be combined with higher-level networks [31].

Despite the growing interest in the CO_2 sequestration sector, many problems of further development of CCU|S projects are still far from being solved. In particular, this article focuses on the gaps in scientific knowledge related to the stage of CO_2 capture. As it was shown, the development of BM CCU|S proceeds towards the formation of cluster organizational structures; however, in the scientific literature, as a rule, we are talking about clusters of storage and/or transportation. The creation of

[13] Seyyed M., Williams E., Smith B., Murfet C. Business Models for CCS Hubs: Challenges and Opportunities with a Focus on MENA. Global CCS Institute, 2024, p. 82. URL: https://www.globalccsinstitute.com/wp-content/uploads/2024/09/Business-Models-for-CCS-Hubs-Challenges-and-Opportunities-with-a-Focus-on-MENA.pdf (accessed 10.08.2025).

[14] Enhance Energy and Wolf Midstream Sign Agreement to Finance and Construct the Alberta Carbon Trunk Line. URL: https://wolfmidstream.com/enhance-energy-and-wolf-midstream-sign-agreement-to-finance-and-construct-the-alberta-carbon-trunk-line/ (accessed 10.08.2025).

[15] Al Reyadah: Project Details. URL: https://www.geos.ed.ac.uk/sccs/project-info/622 (accessed 10.08.2025).

[16] Fattouh B., Muslemani H., Jewad R. Capture carbon, capture value: An overview of CCS business models. OIES Paper: CM, N 08. Oxford: The Oxford Institute for Energy Studies, 2024, p. 28. URL: https://www.econstor.eu/bitstream/10419/296651/1/1882397541.pdf (accessed 10.08.2025).

capture clusters has practically not been studied, although this may allow the use of organizational cost reduction mechanisms at this stage.

Methods

An approach to assessing the effects of organizing CO_2 capture clusters

The cost of capture from stationary industrial sources depends on the two key characteristics of the CO_2-containing stream mentioned earlier: CO_2 partial pressure and potential CO_2 capture capacity. Considering this, the following principles are proposed as the basis for combining emission sources into clusters with shared infrastructure (Fig.4, *a*):

• Increasing the capacity of the CO_2-containing gas flow, both at the facility and in the cluster as a whole. Clockwise movement from the upper-right graph. The transition from the upper-right graph to the cluster level (all other graphs) can be intuitively perceived as an association of many identical enterprises of the corresponding color, i.e. having the same capacity and partial pressure of CO_2 in the gas stream.

• Increase in the average partial pressure of CO_2 in the stream due to a combination of highly and weakly concentrated sources. Counterclockwise movement from the upper-right graph.

Based on these principles, as well as the information provided in the literature review, an analysis of the effect of economies of scale on capture costs for coal-fired power plants in the range of installed capacity from 100 MW to 1.5 GW was performed (Fig.4, *b*), as new economic strategies have been developed in recent years based on the likely growth of coal generation [32]. For each option considered, the reported costs of CO_2 capture were calculated based on modeling in the Integrated Environment Control Model software [17].

In addition, based on approximate GCCSI data [22] a generalized dependence of changes in the cost of capture on the partial pressure of CO_2 in the gas stream was constructed (Fig.4, *c*), as well as the dependence of pipeline transportation costs on the volume of gas. The presented approach allows to draw a number of conclusions that are significant from the point of view of the development of cluster organization schemes in the implementation of CO_2 capture projects with shared infrastructure:

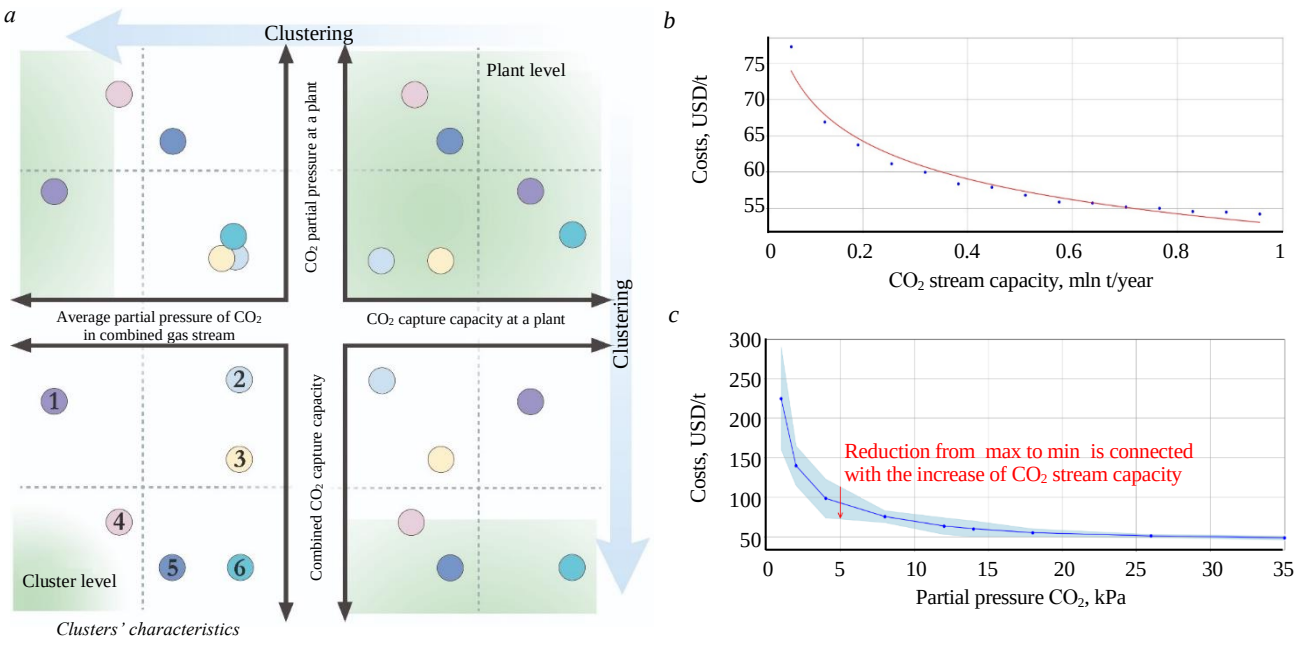

Fig.4. Principles of formation of capture clusters (*a*), estimation of the dependence of the cost of CO_2 capture in coal-fired power plants on partial pressure (*b*) and volume of emissions (*c*)

1 – the capacity shortage; 2, 3 – the shortage of capacity and partial pressure CO_2; 4 – promising cluster; 5, 6 – the shortage of partial pressure CO_2

[17] Integrated Environmental Control Model (IECM). Ver. 11.5. URL: https://www.uwyo.edu/iecm/download-iecm.html (accessed 10.08.2025).

• the effect of scale on the cost of capture is most significantly manifested with small amounts of emissions from emitting facilities;

• the effect of increasing partial pressure on the cost of capture is also more noticeable when combining small emitters;

• the combined effect of these two factors forms a wide range of unit costs for CO_2 capture, the maximum values of which can be many times higher than the minimum, which is consistent with similar estimates in international analytical reports [33].

To test the described approach, a model for the formation of CO_2 capture clusters and a software for working with it in the Python environment were developed [34]. It allows to find the optimal location of the hubs (shared CO_2 capture plant), where industrial gas flows are concentrated, obtained through onshore gas pipelines from other nearby enterprises. Centralized CO_2 capture can be carried out both at a stand-alone facility and, for example, at a large emitter in the geographical area under consideration, which can reduce costs, but requires greater trust from other network participants. To do this, such projects may require the participation of the state as a guarantor of the reliability of the project. Such examples are widely adopted in some industries [35].

The developed model evaluates the effect of using the described cluster approach, taking into account the above-mentioned characteristics of the emitting enterprises; the distance to the storage of CO_2; the cost of capture; transportation costs; the possibility of combining pipelines of several clusters. In this case, a storage facility is understood to mean either a production facility where CO_2 will be disposed of, or an underground reservoir in which it will be disposed of.

The location of the objects under consideration is either initially set in the Cartesian coordinate system (a unit segment is 1 km), or indicated using geographical coordinates. In the second case, the coordinates are converted to a Cartesian system using a local approximation, where 1° latitude corresponds to 111 km, and 1° longitude was calculated as 111 cos(φ) km, where φ is the average latitude of the region under study. This method provides acceptable accuracy for territories with linear dimensions up to 100 km. The location of the storage facility was set in five variants: in the "center of mass" (centroid) of all emitters (weighted average coordinates, taking into account emissions), as well as 50, 100, 200, and 500 km away from the center.

This model is based on an algorithm that includes three optimization tasks:

• Minimizing the overall system costs (*Greedy Algorithm*). This task is to choose a cluster configuration that maximizes overall system savings by prioritizing the formation of hubs around the largest sources of emissions, without taking into account how this choice may affect future opportunities for the formation of new clusters.

• Optimization of the hub location to minimize the total cluster costs (*Sequential Least Squares Programming, SLSQP*). While the "Greedy Algorithm" solves the combinatorial problem of which sources to group and which groups should be designated as clusters, SLSQP solves the problem of exactly where to place each hub, taking into account a fixed group of sources and minimizing the total cost of capture and transportation.

• Minimizing the total transportation costs of clusters (their estimation model is based on data from [18], the cost growth coefficient for crude gas is assumed 1.1) by searching for the optimal pipeline connection point (the Nelder – Mead method). This method uses as a basis the construction of a simplex, i.e. a geometric shape (a triangle in two-dimensional space). Constructed with the coordinates of the vertices of the simplex at the points of initial approximation, the algorithm searches for the optimal position by iteratively replacing the worst vertex. The algorithm searches for a point that minimizes the sum of transportation costs from all hubs to the merge point plus the cost of transporting the combined flow from the merge point to the storage. Simultaneously, at this stage, a determination is made regarding the potential integration of non-clustered emitters into the shared pipeline infrastructure.

[18] 2023 CCUS Cost Update: factors affecting levelised cost (LCOCCUS) to 2030 and beyond. Wood Mackenzie, 2023. URL: https://www.woodmac.com/reports/energy-markets-2023-ccus-cost-update-factors-affecting-levelised-cost-lcoccus-to-2030-and-beyond-150111848/ (accessed 10.08.2025).

The developed model can be described in such a way that it calculates costs in two configurations: the costs of decentralized capture and transportation; the costs of shared capture in clusters, taking into account the possibility of creating shared pipelines. Thus, having information about the mechanisms for reducing costs by creating clusters, the model allows optimizing the total costs of the system through the implementation of a series of iterative procedures (Fig.5) for each of the considered configurations (90 in total). Within this study, a configuration is formally defined as the combined dataset comprising: facility-level parameters for all enterprises within a specified geographic area; maximum cluster radius as the spatial boundary criterion; geological storage site coordinates.

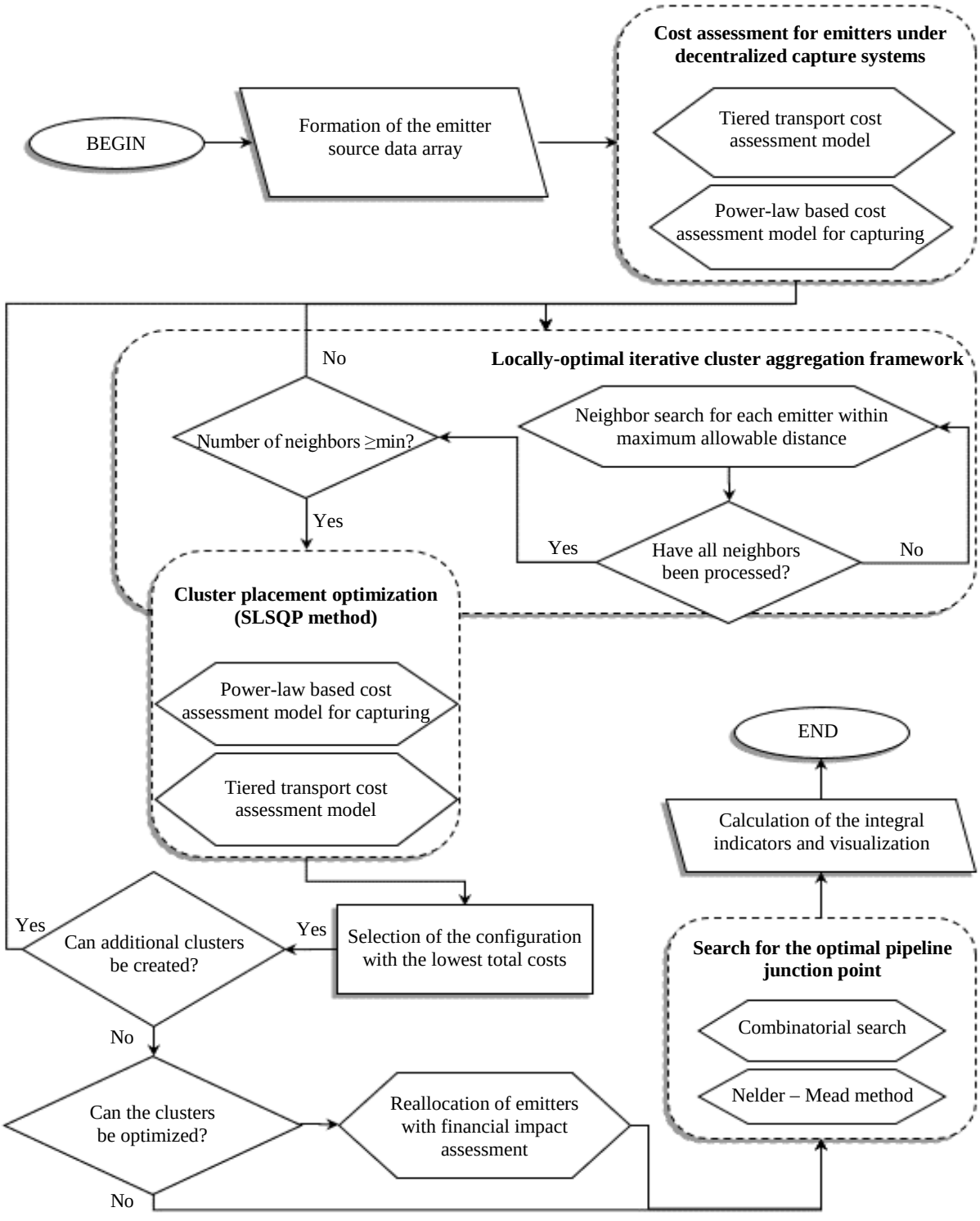

Fig.5. Algorithm of the model for searching the optimal cluster configuration

A model for preprocessing spatial data on industrial sources of CO_2 emissions

Approach to assessing the effects of organizing CO_2 capture clusters allows to evaluate the effects for a certain number of objects with specific geographical coordinates. It is applicable in a limited number of emitters, as well as a well-defined geographical area. Nevertheless, if we are talking about the scale of a country like Russia, which has an area of more than 17 million km^2, and the number of large industrial facilities is estimated at many hundreds, then performing all the necessary assessment procedures becomes an excessively resource-intensive task. In this regard, it is advisable to develop a mechanism for preprocessing spatial data. The purpose of such a mechanism is to search for geographical areas characterized by clusters of industrial facilities with high levels of CO_2 emissions. Such territories, for example, could be used to implement CCU|S pilot projects (similar to the Sakhalin experiment, but more localized) through the use of their cluster potential.

To search for such areas in Russia, information was collected on the technical and economic characteristics of 533 enterprises in the cement [36], energy [19] [37] and metallurgical (ferrous) [38] industries with annual emissions of 28.1, 382.2 and 125.9 million t of CO_2, respectively.

It is proposed to identify promising territories based on the developed model [39], the core of which is the density algorithm of spatial clustering with the presence of noise (DBSCAN).

Main steps of the model for analyzing spatial data on industrial CO_2 emission sources and identifying geographic areas of their concentration:

• collection and systematization of spatial and techno-economic data, calculation of the distance matrix;

• determination of cluster formation parameters (minimum number of neighbors (*n*), allowable radius);

• identification of core points (at least n neighbors), border points near them, and remaining points;

• recursive procedure for cluster formation;

• visualization of the map and calculation of integral parameters for each cluster.

The general principle of operation of this algorithm is to iteratively "bypass" all points to divide them into "cores" (the number of neighbors is greater than or equal to the minimum), "neighbors" and "noise" (i.e., not falling into the cluster unless a core point appears in the vicinity). The following parameters were used as assumptions: the maximum distance between enterprises in a cluster is 50 km; the minimum number of enterprises in a cluster is 2; the minimum amount of cluster emissions is 500 thousand t of CO_2 per year.

The convenience of the proposed approach using DBSCAN, as applied to solving the problem, lies in the fact that:

– it does not require you to set the number of clusters in advance;

– clusters can be of any shape;

– it is suitable for working with geographical data;

– the concept of "reachability" in DBSCAN intuitively corresponds to setting a maximum search radius for nearby objects.

Discussion of the results

Results of the allocation of geographical areas on the territory of the Russian Federation

An example of testing the proposed model for identifying regions of accumulation of industrial facilities (533 in total) that are promising from the point of view of organizing clusters of CO_2 capture for emitters of the cement (65 plants), metallurgical (79 plants) and energy (389 plants) industries in Russia is shown in the Fig.6.

[19] Global Power Plant Database. URL: https://github.com/wri/global-power-plant-database (accessed 10.08.2025).

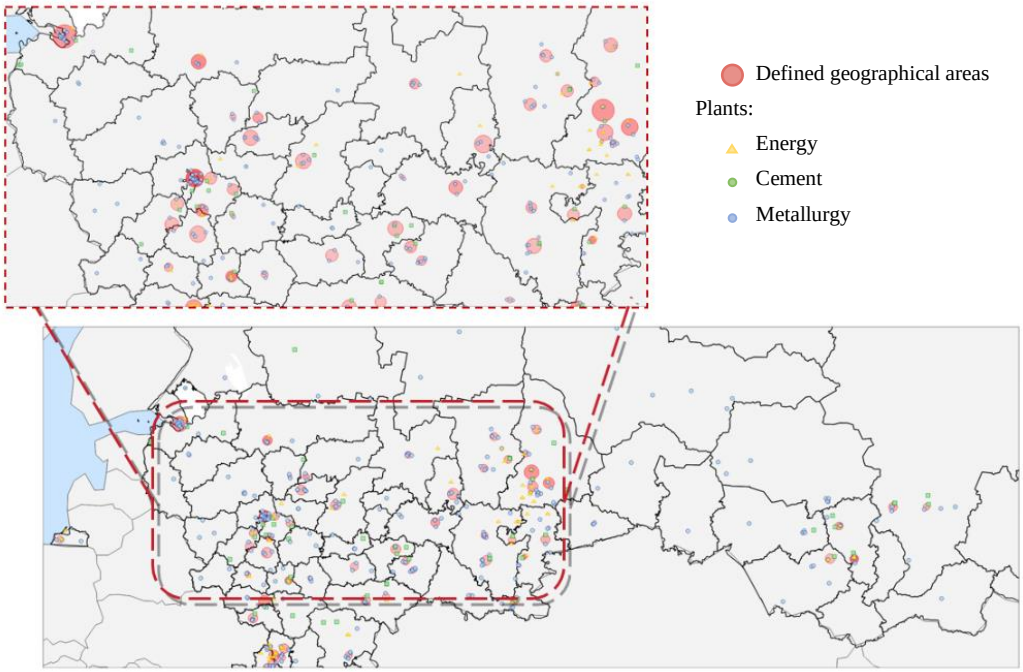

Fig.6. Visualization of search results for areas for the organization of CO_2 capture and transport clusters in the Russian Federation

It is noteworthy that in terms of the size of the area (by the number of objects included in it), large cities of Federal significance, as well as the regions of their location, play a visible role. On the one hand, this indicates the presence of additional social barriers that may arise during the implementation of CCU|S projects in these geographical areas [40]. On the other hand, this is another confirmation of the role of large cities in shaping the climate agenda [41, 42], as well as the relevance of the development of initiatives such as C40 Cities.

Nationwide, 94 regions were identified, covering 63.7 % of all reviewed facilities (cement – 46, metallurgical – 49, and energy – 252 plants) and 72.2 % of total emissions (Fig.7). Naturally, energy companies, due to their prevalence, are present in 88 identified areas, covering 65.7 % of their total emissions. For metallurgical and cement plants, the share of emissions coverage in the identified areas was 95.6 and 55 %, respectively.

In terms of districts of the Russian Federation, in addition to large cities the significant share of emissions falls on traditional industrially oriented subjects (taking into account the industry coverage of the enterprises considered), such as Chelyabinsk, Sverdlovsk, Kemerovo regions, Krasnoyarsk Territory, etc. These same regions are leaders in terms of CO_2 volumes concentrated in the designated geographic areas.

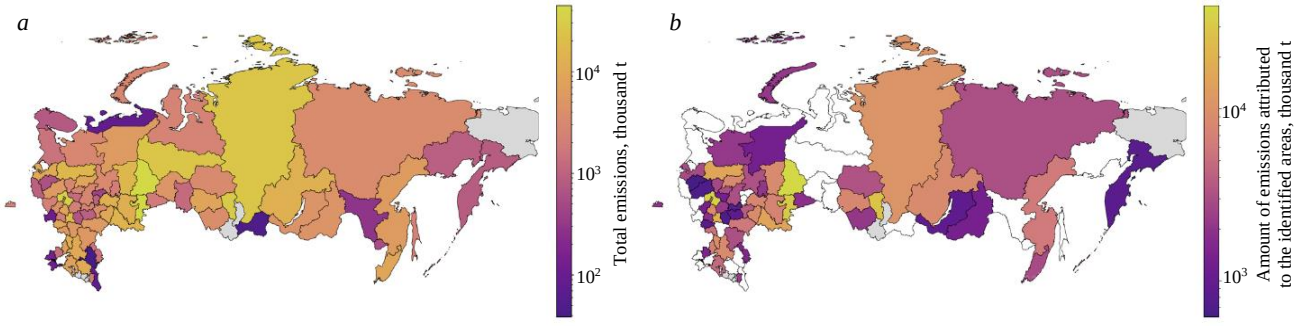

Fig.7. The results of the assessment of the total emissions of the districts (*a*) and the amount of emissions attributed to the identified areas in a specific district (*b*)

Journal of Mining Institute. 2025. Vol. 275. P. 110-129

Assessment of the effects of the cluster approach

The analysis performed in the previous section allows us to make a first approximation in terms of identifying geographical areas that are promising from the point of view of cluster organization. The next step is to directly assess the effects they create, according to the approach to assessing the effects of organizing CO_2 capture clusters. For this purpose, six areas were selected (out of 94 identified), characterized by different emissions, as well as the number of enterprises located in them (Table 4). The longitude and latitude values of all enterprises have been converted to the Cartesian coordinate system.

Table 4

Characteristics of geographical areas

Area	Number of plants			Total annual emissions, thousand t CO_2
	Energy	Metallurgy	Cement	
1	20	0	0	28876.8
2	4	3	0	22988.6
3	3	2	1	18745.1
4	2	2	1	12334.4
5	15	1	0	11346.6
6	2	1	2	11258.8

The results (Table 5) show that using a cluster approach in selected areas can reduce the total cost of CO_2 capture by an average of 13.51 % (with a maximum cluster radius of 30 km), 12.46 % (20 km) and 6.44 % (10 km). The potential for economies of scale through shared pipeline is marginal for short transport distances (storage ≤50 km from centroid), demonstrating cost reductions in only 22.2 % of evaluated configurations (36 total cases) with savings ranging 4.14-29.2 %. However, with changing the transportation distance to 100 km, cost reductions occur in 66.67 % of configurations (18 cases), achieving 1.67-52.10 % savings. For transportation at 200 and 500 km, cost reductions were achieved in all the considered cases and averaged 37.26 % and 57.01 %, respectively, the possibility of which is confirmed in study [43].

Table 5

Matrix of CO_2 capture and transportation cost changes* across different cluster configurations

Area	Distance from the cluster center, km**	Δ of capture costs, %			Δ of transportation costs, %			Δ of total costs, %		
		10 km***	20 km	30 km	10 km	20 km	30 km	10 km	20 km	30 km
1	0	–3.87	–16.10	–17.05	175.11	347.30	633.60	–2.58	–10.60	–9.48
	50				–4.14	147.64	228.38	–3.88	–11.91	–10.77
	100		–16.30		–41.15	42.43	79.89	–5.65	–13.50	–12.43
	200	–6.79		–17.04	–52.96	–14.67	–2.61	–10.71	–16.17	–15.82
	500	–5.44	–16.59	–17.42	–70.06	–52.70	–47.81	–17.50	–23.33	–23.09
2	0	–11.38	–14.81		168.61	286.91		–10.60	–13.50	
	50				–31.95	–13.32		–11.94	–14.77	
	100				–52.10	–42.62		–13.49	–16.25	
	200				–57.02	–51.56		–15.33	–17.99	
	500				–64.83	–62.67		–21.71	–24.06	
3	0	–8.44	–14.26	–12.52	245.59	561.19	772.84	–7.45	–12.00	–9.44
	50				–18.76	27.23	56.46	–8.72	–13.15	–10.68
	100				–41.69	–18.14	–2.96	–10.13	–14.45	–12.04
	200			–14.26	–50.38	–36.85		–12.03	–16.19	
	500			–11.56	–58.37	–52.94	–47.81	–17.87	–21.57	–18.41

End of Table 5

Area	Distance from the cluster center, km**	Δ of capture costs, %			Δ of transportation costs, %			Δ of total costs, %		
		10 km***	20 km	30 km	10 km	20 km	30 km	10 km	20 km	30 km
4	0	–2.66	–4.76	–6.16	–10.07	65.37	386.19	–2.73	–4.06	–2.27
	50			–13.53	–29.22	–17.43	93.25	–3.50	–5.16	–10.13
	100				–41.84	–35.36	19.97	–4.92	–6.52	–11.59
	200			–14.96	–59.31	–55.77	–18.05	–8.53	–10.04	–15.28
	500			–13.53	–62.15	–60.97	–48.97	–15.76	–17.14	–21.34
5	0	–10.99	–19.38		409.22	722.20		–7.37	–7.82	
	50				28.02	231.94		–9.52	–9.94	
	100				–27.18	76.29		–12.15	–12.49	
	200	–11.16	–18.53		–57.99	–0.66		–17.25	–16.21	
	500	–10.95			–74.54	–50.88		–28.07	–27.24	
6	0	–0.62	–5.88	–5.88	29.94	151.28	172.27	–0.35	–4.53	–4.35
	50	0.00	–5.26		0.00	30.27	46.42	0.00	–4.52	–4.79
	100					–10.47	–1.67		–5.48	–5.71
	200	–0.62	–5.88		–44.07	–40.88	–38.77	–4.01	–8.62	–8.45
	500			–1.94	–53.76	–53.10	–50.88	–9.95	–14.18	–10.54

* The change in all costs was estimated in relation to a situation where capture is decentralized, i.e. at each emission source facility, and transportation does not involve the construction of a single main pipeline.

** The location of the storage facility was set arbitrarily in 5 variants, taking into account both the possibility of organizing clusters near cities (the need to move the storage/CO_2 disposal facility outside the city/region) and the situation with the possible disposal of CO_2 in geological storage facilities, usually located far from industrial facilities 50, 100, 200 and 500 km away. This means that the storage facility is located at an appropriate distance from the "center of mass" of all emitters.

*** 10, 20 and 30 km is a maximal radius for cluster creation.

Total cost reductions were achieved in every configuration, averaging 12.02 %. With expanded cluster radii (≥20 km) and storage distances (≥200 km), the impact on total costs intensified – exceeding 16.18 % in most configurations (mean – 17.81 %). Some modeled cases demonstrated even higher performance. Such cases represent exceptions rather than the norm, as achieving reductions exceeding 25 % (Area 5) requires: high density of small emission sources; optimal spatial distribution of facilities; strategic storage site placement. The results demonstrate that while the cluster approach is not a panacea for CCU|S cost reduction, it can make a significant contribution to addressing this challenge, particularly for small emission sources. This finding is consistent with the conclusions of a similar study [44], conducted using the SimCCS^{PRO} software – a commercial version of the open software SimCCS [45].

It is also important that the more enterprises are involved in creating a cluster, the greater the effect it can have. The limiting factor in this case is the technological feasibility of combining remote facilities into a single network to create a shared infrastructure. As mentioned above, the concept of combining emitters into a CO_2 capture cluster (without taking into account its further transportation to storage), at the current level of technology development, can be considered on a scale of tens of kilometers.

It should also be noted that there may be no differences between individual configurations for the same area in terms of the amount of reduction of certain types of costs. The reason for this is that the cost of capture will change only if the formed clusters are restructured (Table 6). If the clusters do not change, then their effect remains the same.

Table 6

Characteristics of clusters formed under different configurations in each of the geographical areas

Area	Number of	
	clusters	clustered emitters
1	2-4	9-20
2	1	5-6
3	1-2	4-6
4	1-2	2-5
5	2-4	12-15
6	0-2	0-5

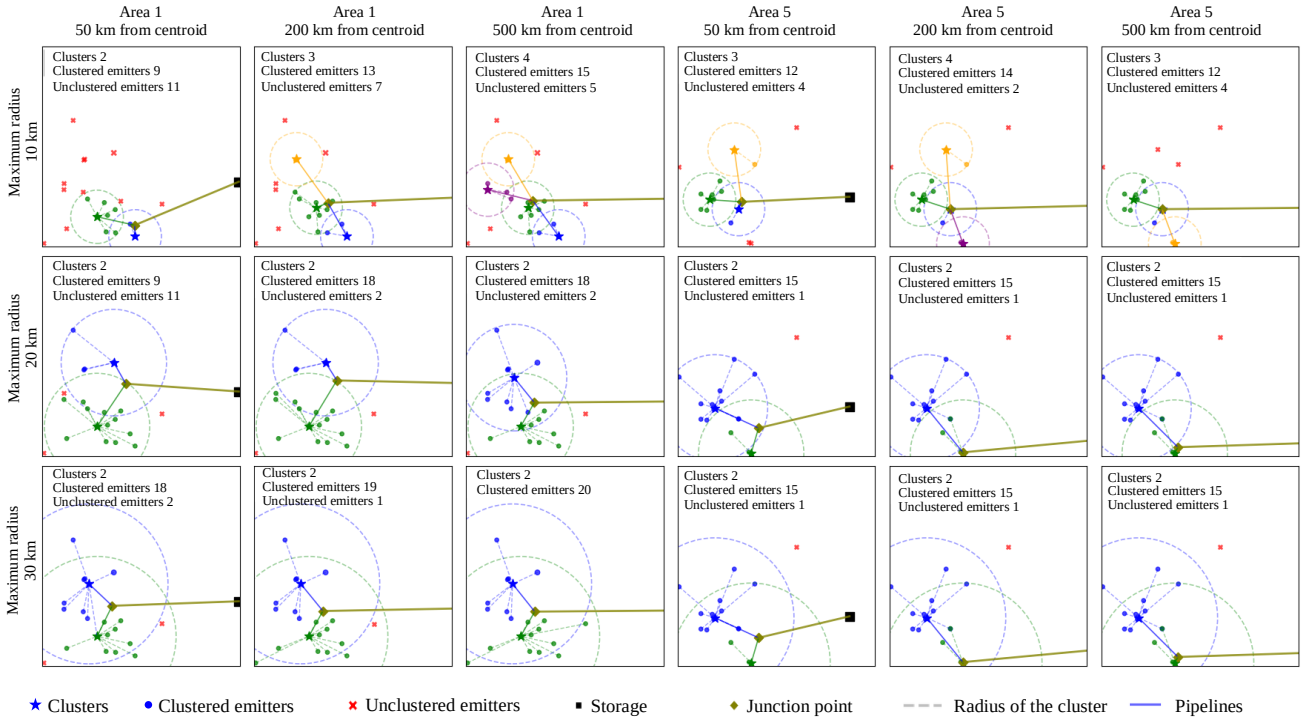

Fig.8. Visualization of clusters across selected configurations: storage locations at 50, 200, and 500 km from the centroid; and maximum cluster radii of 10, 20, and 30 km

Transportation costs are also related to cluster configuration. On the one hand, they influence the assessment of the feasibility of joining individual enterprises to clusters, since when removing the CO_2 storage, the share of transportation costs in the considered cases reached 17.6 % of total costs. On the other hand, the emergence of new/changing current clusters affects the process of finding a pipeline connection point, which also affects costs. Visualization of the spatial organization of clusters in areas 1 and 5 (selected based on the largest number of emitters) is shown in Fig.8.

Conclusion

CCU|S technologies are one of the promising options for reducing greenhouse gas emissions, which, unlike renewable energy, does not require an immediate transition from hydrocarbon energy and is more flexible in terms of potential implementation industries. Nevertheless, they are not without drawbacks, the main one of which is the high cost of such solutions. Despite the strengthening and intensification of technical research, they are currently insufficient to radically reduce the cost of both CO_2 capture and transportation.

A possible solution to this problem is the use of organizational schemes related to the formation of CO_2 capture clusters with shared infrastructure, which are practically ignored in the international literature, unlike transportation and storage clusters. The importance of this issue is determined by the fact that it is at the capture stage that 60-80 % of the total costs of most CCU|S projects are carried out.

To study this issue, a series of models was developed in this paper, which allowed, firstly, to identify 94 geographical areas in Russia that are promising in terms of organizing clusters of CO_2 capture. These areas are characterized by an increased accumulation of stationary industrial sources of emissions, among which 533 enterprises of the energy and cement industries, as well as ferrous metallurgy, were considered. The combined annual emissions of these enterprises amount to more than 0.5 billion t of CO_2.

Secondly, a model was developed to assess the effects of using the cluster approach in the organization of CO_2 capture and transportation through shared infrastructure. This model takes into

account the spatial characteristics of the sources, as well as the amount of CO_2 emissions and its partial pressure in the gas stream of enterprises. The model was tested based on information about industrial facilities in 6 geographical areas (out of 94 identified), selected based on the maximum cumulative annual emissions of CO_2.

The results showed the reduction of capture costs by an average of 6.44-13.51 %, depending on the maximum radius of cluster formation. An additional effect can be obtained in the case of shared gas pipelines, which made it possible to reduce the costs of this stage by an average of 37.26 % and 57.01 % for a 200 km and 500 km distances, accordingly. Under the same distance and with a maximum cluster radius of no less than 20 km, the average reduction in aggregate costs across the evaluated configurations amounted to 17.81 %.

The results show that for scaling CCU|S technologies, not only regulatory changes and technological innovations are important, but also effective organizational schemes that largely determine the business models for the implementation of such projects. These business models can become the basis for the formation of new cross-industry value chains that can give impetus to the development of the CO_2 sequestration industry and its large-scale shared infrastructure, if there is a sustained interest in this area from different stakeholders.

The approaches, algorithms, and models proposed in this article for identifying geographic areas, as well as evaluating the effects of cluster creation, can be used to identify promising areas for the implementation of CCU|S pilot projects in Russia. The developed toolkit also allows to answer the question of what is the effect of using the cluster approach with shared infrastructure in organizing the processes of CO_2 capture at stationary industrial facilities and its transportation to an arbitrarily located storage facility.

Nevertheless, this study has a number of limitations that should be taken into account in further research and in the practical use of its results:

• It is unlikely that objects located at multiple greater distances from each other than discussed in this article will cluster. This is due to the increasing costs of transporting crude gas (up to the stage of CO_2 separation).

• The developed toolkit is designed for rapid assessment of individual economic effects, but it is not sufficient to develop a detailed feasibility study of the project, which requires taking into account a significant number of additional factors, for example, the features of the natural landscape, the density of the current construction site (if we are talking about settlements), long-term infrastructure development plans, hydraulic regimes, etc. Similarly, further development of CCU|S cluster effects assessment models appears imperative.

• The testing was carried out within specific technological and industry boundaries, reflected in the text of the study. For example, only onshore pipeline delivery was considered, and only energy, cement, and metallurgical (ferrous metallurgy) enterprises were considered as sources of emissions.

• The results show that the cluster approach is an effective but not universal cost-cutting tool. Its effectiveness significantly depends on the specifics of emission sources, as well as on their relative location.

REFERENCES

1. Tsvetkov P., Andreichyk A. The Analysis of Goals, Results, and Trends in Global Climate Policy Through the Lens of Regulatory Documents and Macroeconomics. *Sustainability*. 2025. Vol. 17. Iss. 10. N 4532. DOI: 10.3390/su17104532

2. ÓhAiseadha C., Quinn G., Connolly R. et al. Energy and Climate Policy – An Evaluation of Global Climate Change Expenditure 2011-2018. *Energies*. 2020. Vol. 13. Iss. 18. N 4839. DOI: 10.3390/en13184839

3. Belsky A.A., Ngyen V.T., Sheikhi M.H., Starshaia V.V. Analysis of specifications of bifacial photovoltaic panels. *Renewable and Sustainable Energy Reviews*. 2025. Vol. 224. N 116092. DOI: 10.1016/j.rser.2025.116092

4. Tcvetkov P. Climate Policy Imbalance in the Energy Sector: Time to Focus on the Value of CO_2 Utilization. *Energies*. 2021. Vol. 14. Iss. 2. N 411. DOI: 10.3390/en14020411

5. Bashmakov I.A., Nilsson L.J., Acquaye A. et al. Industry. Climate Change 2022: Mitigation of Climate Change. Contribution of Working Group III to the Sixth Assessment Report of the Intergovernmental Panel on Climate Change. Cambridge University Press, 2022, p. 1161-1243. DOI: 10.1017/9781009157926.013

6. Makarov I. Does resource abundance require special approaches to climate policies? The case of Russia. *Climatic Change*. 2022. Vol. 170. Iss. 1-2. N 3. DOI: 10.1007/s10584-021-03280-0

7. Bashmakov I. Improving the Energy Efficiency of Russian Buildings: Forecast to 2050. *Problems of Economic Transition*. 2016. Vol. 58. Iss. 11-12. P. 1096-1128. DOI: 10.1080/10611991.2016.1316099

8. Rzazade U., Deryabin S., Temkin I. et al. On the Issue of the Creation and Functioning of Energy Efficiency Management Systems for Technological Processes of Mining Enterprises. *Energies*. 2023. Vol. 16. Iss. 13. N 4878. DOI: 10.3390/en16134878

9. Zhukovskiy Y., Koshenkova A., Vorobeva V. et al. Assessment of the Impact of Technological Development and Scenario Forecasting of the Sustainable Development of the Fuel and Energy Complex. *Energies*. 2023. Vol. 16. Iss. 7. N 3185. DOI: 10.3390/en16073185

10. Mashhadi Rajabi M. Dilemmas of energy efficiency: A systematic review of the rebound effect and attempts to curb energy consumption. *Energy Research & Social Science*. 2022. Vol. 89. N 102661. DOI: 10.1016/j.erss.2022.102661

11. Shirov A.A., Kolpakov A.Yu. Target Scenario of Low Greenhouse Gas Emissions Socio-Economic Development of Russia for the Period until 2060. *Studies on Russian Economic Development*. 2023. Vol. 34. N 6, p. 758-768. DOI: 10.1134/S1075700723060151

12. Litvinenko V. The Role of Hydrocarbons in the Global Energy Agenda: The Focus on Liquefied Natural Gas. *Resources*. 2020. Vol. 9. Iss. 5. N 59. DOI: 10.3390/resources9050059

13. Cherepovitcyn A.E. Economic and social aspects of CO_2 capture and storage technologies development in the oil and gas complex of Russia. *Journal of Mining Institute*. 2015. Vol. 211, p. 125-130 (in Russian).

14. Porfiriev B.N., Shirov A.A., Kolpakov A.Y., Edinak E.A. Opportunities and risks of the climate policy in Russia. *Voprosy ekonomiki*. 2022. N 1, p. 72-89 (in Russian). DOI: 10.32609/0042-8736-2022-1-72-89

15. Pal M., Karaliūtė V., Malik S. Exploring the Potential of Carbon Capture, Utilization, and Storage in Baltic Sea Region Countries: A Review of CCUS Patents from 2000 to 2022. *Processes*. 2023. Vol. 11. Iss. 2. N 605. DOI: 10.3390/pr11020605

16. Cherepovitsyna A., Kuznetsova E., Popov A., Skobelev D. Carbon Capture and Utilization Projects Run by Oil and Gas Companies: A Case Study from Russia. *Sustainability*. 2024. Vol. 16. Iss. 14. N 6221. DOI: 10.3390/su16146221

17. Pasechnik L.A., Pigai I.N., Skachkov V.M., Yatsenko S.P. Extraction of Rare Elements from Residual Sludge of Alumina Production with the Use of Flue Gas of Sintering Kilns. *Ecology and Industry of Russia*. 2013. N 6, p. 36-38 (in Russian). DOI: 10.18412/1816-0395-2013-6-36-38

18. Tcvetkov P., Cherepovitsyn A., Fedoseev S. The Changing Role of CO_2 in the Transition to a Circular Economy: Review of Carbon Sequestration Projects. *Sustainability*. 2019. Vol. 11. Iss. 20. N 5834. DOI: 10.3390/su11205834

19. Vaganov E.A., Porfiryev B.N., Shirov A.A. et al. Assessment of the contribution of Russian forests to climate change mitigation. *Economy of Region*. 2021. Vol. 17. N 4, p. 1096-1109. DOI: 10.17059/ekon.reg.2021-4-4

20. Roussanaly S., Berghout N., Fout T. et al. Towards improved cost evaluation of Carbon Capture and Storage from industry. *International Journal of Greenhouse Gas Control*. 2021. Vol. 106. N 103263. DOI: 10.1016/j.ijggc.2021.103263

21. Brandl P., Bui M., Hallett J.P., Mac Dowell N. Beyond 90 % capture: Possible, but at what cost? *International Journal of Greenhouse Gas Control*. 2021. Vol. 105. N 103239. DOI: 10.1016/j.ijggc.2020.103239

22. Kearns D., Liu H., Consoli C. Technology Readiness and Costs of CCS. Global CCS Institute, 2021, p. 49.

23. Technologies for carbon dioxide capture, useful use and storage (CCUS). Ed. by A.Osiptsova, I.Gaidy. Skolkovskii institut nauki i tekhnologii, 2022, p. 79 (in Russian).

24. Wan Yun Hong. A techno-economic review on carbon capture, utilisation and storage systems for achieving a net-zero CO_2 emissions future. *Carbon Capture Science & Technology*. 2022. Vol. 3. N 100044. DOI: 10.1016/j.ccst.2022.100044

25. Geweda A.E., Zayed M.E., Khan M.Y., Alquaity A.B.S. Mitigating CO_2 emissions: A review on emerging technologies/strategies for CO_2 capture. *Journal of the Energy Institute*. 2025. Vol. 118. N 101911. DOI: 10.1016/j.joei.2024.101911

26. Newman A.J.K., Dowson G.R.M., Platt E.G. et al. Custodians of carbon: creating a circular carbon economy. *Frontiers in Energy Research*. 2023. Vol. 11. N 1124072. DOI: 10.3389/fenrg.2023.1124072

27. Dowson G.R.M., Reed D.G., Bellas J.-M. et al. Fast and selective separation of carbon dioxide from dilute streams by pressure swing adsorption using solid ionic liquids. *Faraday Discussions*. 2016. Vol. 192, p. 511-527. DOI: 10.1039/C6FD00035E

28. Geissdoerfer M., Vladimirova D., Evans S. Sustainable business model innovation: A review. *Journal of Cleaner Production*. 2018. Vol. 198, p. 401-416. DOI: 10.1016/j.jclepro.2018.06.240

29. Osterwalder A., Pigneur Y. Business Model Generation: A Handbook for Visionaries, Game Changers, and Challengers. Wiley, 2010, p. 288.

30. Nevskaya M., Shabalova A., Kosovtseva T., Nikolaychuk L. Applications of simulation modeling in mining project risk management: criteria, algorithm, evaluation. *Journal of Infrastructure, Policy and Development*. 2024. Vol. 8. N 8. N 5375. DOI: 10.24294/jipd.v8i8.5375

31. Ponomarenko T.V., Gorbatyuk I.G., Cherepovitsyn A.E. Industrial clusters as an organizational model for the development of Russia petrochemical industry. *Journal of Mining Institute*. 2024. Vol. 270, p. 1024-1037.

32. Yashalova N.N., Potravny I.M. Tools to ensure carbon neutrality in the Russian coal business. *Ugol*. 2023. N 10 (1172), p. 66-71 (in Russian). DOI: 10.18796/0041-5790-2023-10-66-71

33. Barlow H., Shahi S.S.M., Kearns D.T. Advancements in CCS technologies and costs. Global CCS Institute, 2025, p. 65.

34. Tsvetkov P.S. Software Certificate of State Registration N 2025617009 (Russian Federation). Program for determining parameters of clusters for CO_2 capture from stationary industrial emission sources. Publ. 20.03.2025. Bul. N 3 (in Russian).

35. Litvinenko V.S., Petrov E.I., Vasilevskaya D.V. et al. Assessment of the role of the state in the management of mineral resources. *Journal of Mining Institute.* 2023. Vol. 259, p. 95-111. DOI: 10.31897/PMI.2022.100

36. Cuihong Chen, Ruochong Xu, Dan Tong et al. A striking growth of CO_2 emissions from the global cement industry driven by new facilities in emerging countries. *Environmental Research Letters*. 2022. Vol. 17. N 4. N 044007. DOI: 10.1088/1748-9326/ac48b5

37. Xinying Qin, Dan Tong, Fei Liu et al. Global and Regional Drivers of Power Plant CO_2 Emissions Over the Last Three Decades Revealed From Unit-Based Database. *Earth's Future*. 2022. Vol. 10. Iss. 10. N e2022EF002657. DOI: 10.1029/2022EF002657

38. Ruochong Xu, Dan Tong, Davis S.J. et al. Plant-by-plant decarbonization strategies for the global steel industry. *Nature Climate Change*. 2023. Vol. 13. N 10, p. 1067-1074. DOI: 10.1038/s41558-023-01808-z

39. Tsvetkov P.S. Software Certificate of State Registration N 2025662463 (Russian Federation). A program for the automated prospecting of territories suitable for the establishment of CO_2 capture clusters. Publ. 21.05.2025. Bul. N 6.

40. Tcvetkov P., Cherepovitsyn A., Fedoseev S. Public perception of carbon capture and storage: A state-of-the-art overview. *Heliyon*. 2019. Vol. 5. Iss. 12. N e02845. DOI: 10.1016/j.heliyon.2019.e02845

41. Porfiryev B.N., Bobylev S.N. Cities and Megalopolises: The Problem of Definitions and Sustainable Development Indicators. *Studies on Russian Economic Development.* 2018. Vol. 29. N 2, p. 116-123. DOI: 10.1134/S1075700718020119

42. Kumar P. Climate Change and Cities: Challenges Ahead. *Frontiers in Sustainable Cities*. 2021. Vol. 3. N 645613. DOI: 10.3389/frsc.2021.645613

43. Gunawan T.A., Gittoes L., Isaac C. et al. Design Insights for Industrial CO_2 Capture, Transport, and Storage Systems. *Environmental Science & Technology*. 2024. Vol. 58. Iss. 33, p. 14608-14617. DOI: 10.1021/acs.est.4c05484

44. Gunawan T.A., Hongxi Luo, Greig C., Larson E. Shared CO_2 capture, transport, and storage for decarbonizing industrial clusters. *Applied Energy*. 2024. Vol. 359. N 122775. DOI: 10.1016/j.apenergy.2024.122775

45. Middleton R.S., Yaw S.P., Hoover B.A., Ellett K.M. SimCCS: An open-source tool for optimizing CO_2 capture, transport, and storage infrastructure. *Environmental Modelling & Software*. 2020. Vol. 124. N 104560. DOI: 10.1016/j.envsoft.2019.104560

***Author* Pavel S. Tsvetkov,** *Candidate of Economics, Associate Professor* (*Empress Catherine II Saint Petersburg Mining University*), *pscvetkov@yandex.ru, https://orcid.org/0000-0002-3049-7893*.

The author declares no conflict of interests.

ISSN 2411-3336; e-ISSN 2541-9404

JOURNAL OF MINING INSTITUTE
Zapiski Gornogo instituta
Journal homepage: pmi.spmi.ru

Research article *Geotechnical Engineering and Engineering Geology*

Ontological modeling and management of digital transformation of mining enterprises architecture

Sergei A. Deryabin✉, **Igor O. Temkin**
National University of Science and Technology "MISiS", Moscow, Russia

How to cite this article: Deryabin S.A., Temkin I.O. Ontological modeling and management of digital transformation of mining enterprises architecture. Journal of Mining Institute. 2025. Vol. 275, p. 130-144.

Abstract
The paper is devoted to the conceptual formalization of the goals, objectives and criteria for managing the digital transformation of mining enterprises. The main idea is to define digital transformation as a process of minimizing or completely excluding human participation from the implementation of production processes in order to build an autonomously functioning cyber-physical industrial system. In order to determine the ways of building and functioning mechanisms of such systems, the necessity of forming an enterprise architecture model has been established, both ensuring the completeness and consistency of the knowledge embedded in it, and providing an instrumental numerical basis for self-organization and self-regulation of the system. The irrelevance of applying existing standards and frameworks for building architecture models is substantiated. Approaches to the construction of an ontological model and ways of its application in the management task of the digital transformation of mining enterprises are proposed. Under the results of the work, a basic ontological model of the mining enterprise architecture was formed based on the OWL descriptive logic language in the Protégé environment, applicable to geospatial natural and technical industrial systems with an open type of production environments. The resulting model was tested using the HermiT logical inference mechanism, confirmed its coherence and consistency, which indicates the potential correctness of the initial hypotheses of the study and the possibility of further research into the formation of a methodology for the digital transformation of mining enterprises.

Keywords
digital transformation; ontology; OWL; TOGAF 10; RAMI4.0; enterprise architecture; mining enterprise; autonomously functioning system; cyber-physical systems

Received: 15.04.2025 ***Accepted: 18.09.2025*** ***Online: 09.10.2025*** ***Published: 31.10.2025***

Introduction

Today, most industrial enterprises, with the support of engineering companies and research groups, are actively working in the field of digital transformation (DT) of production systems in the paradigm of the Industry 4.0 concept [1-3]. This activity includes:

• development, implementation, and pilot testing of robotic complexes with various levels of autonomy, including the use of unmanned aerial vehicles, unmanned transport systems and technological equipment [4-6];

• application of machine learning and data mining methods for a wide range of production management tasks [7-9] (predictive maintenance [10-12], planning of production indicators [13, 14], etc.);

• the organization of efficient transmission, storage and processing of large amounts of data [15, 16], coming from Internet of Things devices into a distributed computing environment [17, 18].

A relatively new direction is the work in the field of creating digital twins of technological processes and equipment, which are a highly accurate cybernetic model with two-way control communication with a physical analogue [19, 20].

Despite the success in solving certain scientific and practical tasks, the issues of conceptual goal-setting of such activities remain an obvious and critically important problem on the way to scaling the results and, in fact, the actual digital transformation of enterprises. At the declarative level, the result of digital transformation is understood as a transition to qualitatively new principles for the implementation of technological processes, which is difficult to formalize and quantify. Taking into account that automation is the previous stage of enterprise transformation, it should be assumed that the goal of digitalization can be formulated as minimizing or completely excluding (where possible) human participation in production processes through the use of Industry 4.0 methods and technologies. This means that the processes currently being implemented with direct human participation, including through information and automated systems, should be brought to an autonomously executable (software) form of management. Thus, the ultimate goal of digital transformation of enterprises is to build an effective autonomously functioning cyber-physical industrial system.

Based on goal-setting, it can be assumed that an autonomously functioning system, like some complexly configured rational agent [20-22], should have the ability to self-organize and self-regulate, and in some cases, to self-learn. In this regard, it is obvious that ensuring such requirements is possible only if the system has objective knowledge of its own functionality, criteria, and limitations of activity, as well as the structure and condition of its components. Such knowledge about the system is commonly referred to as an "architecture model" [23-25], and currently there are several international standards and frameworks regulating this concept with varying degrees of detail and practical applicability. The most relevant are the IEC PAS 63088:2017 "Smart manufacturing – Reference architecture model Industry 4.0 (RAMI4.0)" [26, 27] and the framework "The Open Group Architecture Framework 10 (TOGAF 10)" [28, 29]. Both standards specify the need for declarative knowledge in the form of an ontological (meta-) architecture models to reduce errors in managing the progress of the digital transformation of the enterprise. However, despite a number of really important methodological aspects, the proposed models cannot be directly used for the digital transformation of mining industries, do not regulate the construction of an autonomously functioning industrial system and, as a result, do not have the necessary tool base for formal computational procedures of knowledge manipulation. The purpose of the work is to formalize the type and mechanisms of the architecture model of an autonomously functioning cyber-physical industrial system to ensure the processes of digital transformation of mining enterprises.

Models and methods of the study

RAMI4.0 and TOGAF 10 regulate the need to represent an enterprise as a formalized architecture model that ensures transparency, controllability, consistency of views and actions of all stakeholders: from enterprise owners to software development teams. At the same time, it cannot be said that both standards are completely interchangeable, compatible or clearly complementary to each other, and the proposed architecture models provide a clear understanding of the actions necessary to realize the digital transformation of enterprises, especially mining industries.

RAMI4.0 is focused on industrial enterprises and largely develops the initial concept of Industry 4.0. In the RAMI4.0 enterprise architecture model, one of the most important aspects remains the use of the lifecycle and the products value chain integrated with the hierarchy levels of objects in the physical world (from products to the enterprise's connection to the external "connected" world) and layers of interaction (from assets to business). Of course, the use of PLM (Product Lifecycle Management) for continuous product management (from product type design to disposal of each specific instance) in order to improve the production process is a well-established practice [30]. The approach may be quite native when it comes to a machine-building enterprise, where processes can be considered as deterministic and discretized over time intervals, and where the product is a clearly delineated type

and instance of a product that can be equipped with devices that transmit information about its condition in real time. However, in the case of a mining enterprise, the formalization and, most importantly, the need for continuous changes in the types and specimens of the rock mass being produced are very unobvious. Moreover, an important component of the standard is the assumption of full observability, integration, and manageability of the production environment, provided by an appropriate set of sensors, controllers, and programs, which can be described as a closed type of production environment. Mining enterprises, on the other hand, are geotechnical spatially distributed systems subject to the effects of stochastic natural phenomena, and generally have a dynamically expanding configuration of the production environment that directly changes as a result of technological processes. In this regard, the constant saturation of a mining enterprise with all kinds of devices is not completely rational, and the production environment can be characterized as partially observable, without time-stable boundaries, and attributed to systems with an open type of production environment. As a result, the direct application of the RAMI4.0 standard for the digital transformation of mining enterprises is currently difficult to implement.

The TOGAF 10 framework represents a more general approach to digital transformation, extending to processes and organizations in any field of activity, including, for example, government agencies, medical institutions or construction sites. Universality entails a large number of generalizations that require serious adaptation to the conditions of specific DT facilities. Unlike RAMI4.0, TOGAF 10 has a more rigorous instrumental methodology (since it is not a standard, but a framework), declaring a set of actions and, above all, a clear list of results that are recommended to be obtained when forming an enterprise architecture model. Such results include a set of catalogs of enterprise components, matrices of communication between components and sets of diagrams in various notations (BPMN, UML, ERD, etc.), divided into four main types of architecture: business, data, applications and technologies. Despite the extensive and well-understood base of the resulting elements of the architecture model, TOGAF 10 leaves the processes of their formation, determination of accuracy, completeness, consistency, and order of implementation open and relies on the experience, knowledge, attentiveness and responsibility of participants in the digital transformation of specific enterprises. Of course, the compilation of any model is based on expert knowledge and is impossible without the participation of relevant specialists. However, in the case of large-scale industrial systems, which include mining enterprises, the lack of specific mechanisms for verifying the consistency of heterogeneous information embedded in the model entails at least high risks of disrupting the continuity of production processes. Moreover, some of the elements of the architecture model (especially diagrams in various notations) are aimed at making it easier for humans to perceive information, while digital transformation, the concept itself, and specific Industry 4.0 technologies are initially aimed at minimizing human participation in production processes. Therefore, it is impossible to speak with full confidence about the high practical applicability of the TOGAF 10 framework to obtain a model that provides any level of functional autonomy of the system.

Thus, the standards considered are largely irrelevant to the goals, objectives, and conditions of the digital transformation of mining enterprises. However, their main feature should be noted – an attempt to formalize the connection between fundamentally different components of enterprises, such as abstract concepts of business process organization (regulations, conditions, requirements, personnel roles, etc.), real-life objects of the physical world (sensors, equipment, products, resources, infrastructure elements), information (formal and informal expert knowledge; digital, analog, and neurophysiological signals measured by parameters, etc.) and software entities that implement a set of functional management tasks. In other words, in the context of building an enterprise architecture model, we are talking about the formation of knowledge about the system in order to build management mechanisms, that is, in fact, about an ontological model. Thus, the architecture model can be

informally defined by some ontology, which can be transformed into a knowledge base with mechanisms for proving the consistency and truth of statements embedded in it, as well as logical inference mechanisms for making enterprise management decisions.

The creation of ontologies and knowledge bases in various subject areas occupies a significant place in the history of artificial intelligence and, as a rule, is associated with the construction of expert systems capable of helping professionals solve problematic problems. As an example for mining industries, a number of works can be cited on the construction of formal classification systems for the types and properties of coal mining equipment [31], matching the terminology of IT systems and operated mining equipment [32, 33] or managing technical inspections and repairs of equipment [34]. Despite the high degree of detail of the taxonomy, the developed ontologies are aimed at solving highly specialized problems, and the expert systems obtained on their basis are designed exclusively for interaction with personnel in enterprise management processes. The coordination of specialized ontologies among themselves or with more general ontologies of knowledge can be quite difficult or impossible, which limits their scientific and practical significance.

At the same time, the concepts of "ontology" and "knowledge base" can be used both to formalize and verify knowledge when building an enterprise architecture model, and as tools for saturating (teaching) the system with knowledge about itself to build an autonomously functioning cyber-physical industrial system. Today, OWL (Open World Language or Web Ontology Language) is one of the most expressive, flexible and promising tools for building ontologies, recommended for creating Web 3.0 semantic networks and based on descriptive logic – a highly expressive and decidable formal logical language [35-37]. The basis of descriptive logic and OWL are: one-place and two-place atomic axiomatic statements – "concepts" and "roles"; hierarchical structures (classes or categories) of interrelations between statements; the reducibility of classes and super classes to instances with the possibility of assigning values (data); a finite set of properties of relations between statements (transitivity, reflexivity, etc.), obeying basic algebraic logic; as well as a set of "reasoners" – developed logical inference mechanisms to prove the completeness and consistency of ontology, deduction of hidden (obviously undeclared) axioms and for the purpose of dialog interaction with the knowledge base.

In this paper, we propose an approach to building an ontological architecture model using the OWL language and specialized Protégé software (ver. 5.6.3) in the process of digital transformation of mining enterprises. A feature of the proposed approach is the representation of the most general concepts in the form of hierarchical classes, and the final typical components of the enterprise architecture in the form of instances of such classes. The purpose of the obtained ontology is not dialogical work with the knowledge base, but the formation of a consistent semantic connection of various mining, geological, geotechnical, and physic-technological concepts, which further determine a finite set of atomic functional tasks that are unchangeable in time to identify the structure of the program components of an autonomously functioning cyber-physical industrial system. It should be noted that the proposed approach is aimed at forming a standardized model with unified and invariant concepts that are not tied to a specific enterprise, but due to the advantages of the OWL language, the model can be easily expanded both in width and depth of hierarchies, and the names of individual statements can be changed without violating logic.

Due to the specificity of the field under consideration and the lack of terminological and semantic consensus in it, we will first characterize the concepts used in this study and introduce a number of formulations.

The architecture of enterprise *A* is understood as a set of structural components and a configuration of the relationships between them that determine the actual form of the organization and the principles of management of production processes. Such components are concepts of a fundamentally different nature, which can be written as:

$$A = \left\langle C^1, C^2, C^3, C^4, R \right\rangle,$$

where C^1 – technological processes and operations – an ordered set of purposeful interactions of objects of the physical world, leading to a change in the states of these objects; C^2 – physical objects – objects of the technological environment interacting with each other when performing production tasks, which can be classified as equipment (dump trucks, excavators, etc.), infrastructure (geospatial facilities and technological zones), products (conventional units of rock mass) and resources (fuel and energy, etc.); C^3 – management agents – components of an enterprise capable of perceiving, processing and transmitting information about the states of physical objects to determine the order of technological processes and operations; C^4 – information – possible states of physical objects described by a set of measurable parameters and data forming such states; R – relations (mappings) – a set of possible types of relationships between components.

The architecture management task can be formulated as choosing a configuration that optimizes the integral efficiency indicator of the enterprise, which can select both the amount of profit received or the volume of useful desired (products) shipped, and a more relevant volume of profit for the mining enterprise in relation to the volume of processed ore,

$$F : A \to A'; \Pi_\Sigma \left(A' \right) \to \text{opt},$$

where F – a certain procedure for the transformation of architecture and the choice of its configuration, which would ensure the optimum of the integral criterion of enterprise efficiency Π_Σ.

To solve such a macro-optimization problem, a strict formal statement is necessary, which in turn requires taking into account a greater depth of detail of the factors, identifying their relationship, and clearly defined criteria and search conditions. An attempt to reduce this problem to a single mathematical function, i.e., to fully formalize it, seems extremely difficult (and probably with unsolvable computational complexity), and therefore it is necessary to find other ways to represent it – model abstraction. It is possible to formulate a hypothesis that there is a model Ω, that allows us to describe A, determine the type F, and reduce the architecture management problem to the optimization problem of the criterion Π_Σ. In this regard, for the sake of clarity, we will introduce a number of definitions and assumptions:

1. At any given time, the enterprise retains its main activity, which means that the list of technological processes and operations C^1, as well as the list of physical objects C^2 must be comparable and equivalent.

2. At any given time, the architecture of an enterprise should ensure the implementation of a complete list of technological processes and operations that explain and regulate the activities of such an enterprise.

3. Digital transformation is a continuous process of non-deterministic changes in the architecture of an enterprise aimed at improving integrated efficiency.

4. The integrated efficiency of an enterprise depends on the effectiveness of solving individual tasks of managing technological processes and operations.

5. Management tasks are solved by management agents $C_i^{3,j}$, which are staff $C_i^{3,j=1}$ and software systems $C_i^{\prime 3,j=0}$.

6. The efficiency of solving management tasks is defined as minimizing discrepancies between the planned values of production indicators and the actual ones ($\text{Accuracy}_{C_i^{3,j}}$) with minimal expenditure of time and/or resources ($\text{Performance}_{C_i^{3,j}}$).

7. Improved performance indicators for solving management problems can be achieved through the development and implementation of software components with more advanced (in terms of accuracy and performance) computing mechanisms.

Thus, digital transformation is understood as the process of replacing existing management agents with more advanced software components $C_i'^{3,j=0}$. The immediate criterion for changing the architecture is the availability (and the possibility of integration into the architecture) such a software component that performs the task of management at a level of efficiency not lower than the current management agent. Then the task of architecture management during digital transformation can be written as:

$$\begin{cases} \left\{F(A):\left\{C_i'^{3,j}\right\}\rightarrow\left\{C_i'^{3,j}\right\};\ i=1,I,\ j=[0;1]\right\} \\ \Pi_{\Sigma}(A')=\sum_{i=1}^{I} j_i\rightarrow\min \\ \forall\left\{C_i'^{3,j}\right\}:\dfrac{\text{Accuracy}_{C_i'^{3,j}}}{\text{Performance}_{C_i'^{3,j}}}\geq\dfrac{\text{Accuracy}_{C_i'^{3,j}}}{\text{Performance}_{C_i'^{3,j}}} \end{cases}. \quad (1)$$

It should be noted that the possibility of implementing (restrictions on changing the architecture) a new software component as a management agent should be determined by maintaining the functional integrity of the entire production system. Functional integrity should be understood as the ability of the system to solve a complete list of management tasks Φ,

$$R_0:\Phi\rightarrow C_i^{3,j},$$

where R_0 – display of a set containing a complete list of management tasks Φ and a set of management agents $C_i'^{3,j}$,

$$\vdash\left\{F\wedge R_0\right\}. \quad (2)$$

Due to the abstraction of management agents as components implementing the receipt, processing and transmission of information, regardless of their nature, the ability to solve a complete list of management tasks is considered as preserving the ability to produce a complete list and volumes of C^4 information necessary for the operation of such management agents, so equation (2) can be rewritten as:

$$\vdash\left\{F\wedge R_0\wedge\left(C^4\Leftrightarrow C'^4\right)\right\},$$

where C'^4 – a set of information produced by a set of management agents $C_i'^{3,j}$ obtained after a change in architecture F.

In other words, when implementing a new management agent, the functional integrity of the entire system should be tested to answer the following questions:

• Can the new management agent get the information needed for the job?

• Does the new management agent produce the information necessary to maintain the working capacity of all other management agents?

• Is it possible to exclude from the architecture a management agent that previously performed this management task?

• Is it possible to introduce a new management agent without excluding the current one?

The answers to these questions can be reduced to a number of mathematical procedures, and in combination with the proposed formalization, the architecture management tasks are relevant outside

the framework of discussing the digital transformation of enterprises, i.e. they are applicable not only to software systems, but also to personnel. However, in the context of this study, digital transformation is understood as the minimization or complete exclusion of human participation in the implementation of production processes, the construction of an autonomously functioning cyber-physical industrial system. This means that a multitude of physical objects C^2 must perform a multitude of technological processes and operations C^1 under the management of software agents C^3, operating with digital information C^4. In this case, the concept of enterprise architecture can be identified with the concept of software architecture, without being completely equivalent. Thus, technological processes and operations, as well as physical objects, although they can be represented by digital information objects or models in cybernetic space, nevertheless cannot become completely software entities and be excluded from the enterprise architecture. Accordingly, there is some substantial part of the architecture that is invariant for any arbitrary period of time, regardless of its changes caused by digital transformation, while part of the architecture, mainly related to management agents, can and should be modified. Based on the proposed definitions and assumptions 1 and 2, it can be concluded that as a part of the architecture model that remains unchanged over time, there should be a list of management tasks that, on the one hand, should be derived from the interconnection of the components of the architecture itself, and on the other, should be associated with specific management agents. Then the most important aspects of the digital transformation of architecture is to determine the full list of tasks implemented by management agents in order to identify their structural and functional relationship, the possibility and need for change; and procedures for manipulating management agents in terms of changing the structural configuration of the architecture.

The procedures for manipulating software components in automatic mode have been well studied and are implemented using a combination of understandable standard Git-CI/CD-Docker/Kubernetes technologies and analogues, as a result of which consideration of their implementation issues is beyond the scope of this study. However, it should be noted that the definition of the list of software components for filling Git repositories and their placement via Kubernetes on end nodes is carried out by developers and system architects. The de facto configuration of the architecture and the procedure for manipulating its structure are determined on the basis of an expert assessment of a person or group of persons operating with a certain model representation of the enterprise architecture. At the same time, the effectiveness of such procedures (non-violation of the functional integrity of the system) largely depends on the degree of elaboration of the model, its availability in general, and the ability to compare the initial architecture "as is" with what should be "to be".

Accordingly, the first step to begin digital transformation is to identify a list of tasks for management agents that does not depend on specific management agents and meets the requirement of full functional coverage of the system. The compilation of such a list is complicated by a number of problems:

• the degree of detail depth (tasks should be sufficiently "atomized", but not excessively decomposed to elementary operations);

• the degree of completeness (tasks should describe the entire production activity of the enterprise, including the one that is currently not a software function (implemented in the form of "mental" labor of personnel), but serves as an integral operation of the chain of technological processes);

• the degree of accuracy (the task should explain the interrelation of different types of architecture components and be equivalent to a formal computational procedure);

• the degree of consistency (the task must be unambiguous in its description and content, and also not be equivalent to another task).

It is possible to solve and obtain any quantitative estimates of the formulated problems using a model that would provide a representation of heterogeneous architectural components in the form of abstract concepts, connect them with formal logical rules and provide a computing device that guarantees the possibility of working with statements. Thus, it is proposed to consider ontological modeling as the type and mechanisms of building an architecture model.

Let A^0 be the initial type of enterprise architecture at the initial stage of DT, which can be described by the "as is" model – Ω^0; A', …, $A''^{\cdots\prime}$ are the types of enterprise architecture at individual stages of change, which can be described by the models Ω', …, $\Omega''^{\cdots\prime}$; and A^* is a type of enterprise architecture upon completion of digital transformation, which can be described by the "to be" model – Ω^*. At any arbitrary moment of time α the enterprise possesses some architecture A^α, the type of which can (and should) be determined through the representation of the model Ω^α. The continuous process of digital transformation of an enterprise $\overset{DT}{\rightarrow}$ can be represented as a set of discrete steps, non-deterministic in time, to change the A^α, carried out until its appearance becomes equivalent to A^*, which can be determined by comparing the Ω^α and Ω^* models.

At the initial step $\alpha = 0$ the view of architecture $A^{\alpha=0}$ should be determined, the model $\Omega^{\alpha=0}$ should be compiled, the final type of architecture A^* should be determined, and the corresponding immutable model Ω^* should be compiled. Next, starting from step $\alpha = 1$ to $\alpha = *$, it is necessary to evaluate the compliance of the current architecture model Ω^α with the required Ω^*, determine the need and possibility of modifying the architecture, and make decisions on making changes. Then the process of enterprise architecture management in the context of digital transformation *DT* can be written as:

$$F:\left(A^0 \not\Leftrightarrow A^*\right)\overset{DT}{\rightarrow}\left(A^\alpha \Leftrightarrow A^*\right),$$

where $\overset{DT}{\rightarrow}$ – a set of discrete steps to change the architecture (1) to bring the enterprise to the form of an autonomously functioning industrial system.

At the same time, the following conditions must be true at each stage:

$$\begin{cases} \Omega^{\alpha-1} \not\Leftrightarrow \Omega^\alpha \not\Leftrightarrow \Omega^{\alpha+1} \\ F_{\text{rule of inference}}:\Omega^\alpha \rightarrow \Phi \\ R_0{}^{\alpha-1} \Leftrightarrow R_0{}^\alpha \Leftrightarrow R_0{}^{\alpha+1} \end{cases}, \quad (3)$$

where $F_{\text{rule of inference}}$ – a mechanism for the logical derivation of a complete list of atomic tasks of management agents Φ from the ontological architecture model Ω^α. Then each atomic task $\varphi \in \Phi$ can be assigned a management agent $C_i^{3,j}$ that implements it as part of the architecture.

Also, achieving the fulfillment of (3), i.e. deducibility of the complete list of atomic tasks Φ from the Ω^α ontology, is possible only when the Ω^α ontology is consistent,

$$\vdash\left\{F_{\text{rule of inference}} \wedge \left(\Omega^\alpha \equiv 1\right)\right\}. \quad (4)$$

Consistency of ontology should be understood as the truth of all axiomatic statements embedded in it in the form of declared concepts and relations between them.

Therefore, it is necessary to compile a set of conceptual expressions that will form the basis of the ontological model of the mining enterprise architecture, link them with an appropriate set of relations that determine the company's activities, and check the obtained ontology for consistency in order to confirm the hypotheses outlined and the possibility of further work in the field of digital transformation.

Results and discussions

Due to the limitations of the presentation of all the theoretical concepts embedded in the proposed ontology of mining enterprise architecture, here are some key examples:

• an enterprise consists of technological processes, physical objects, management agents and information related to each other, having their own taxonomy (hierarchical classification) with end instances in the form of standard (uncountable and not having their own unique names) components;

• the physical objects are understood as elements of the production environment that do not have independent decision-making, including: equipment (outlined specimens – dump truck, conveyor, excavator, etc.), infrastructure (geospatial – road, board, dump; technical – loading area, warehouse, maintenance garage), devices (components of equipment – bucket, chassis, etc.), product (natural – rock mass block; geotechnical – roadbed; etc.), resource (energy – fuel, electricity; instrumental – water, explosive);

• each physical object has states, which are understood as abstract spatial, technological, operational and economic information properties described by a group of data in the form of measurable physical or economic quantities;

• the atomic task of the management agent $\varphi(C_i^{t3,j}) \in \Phi$ is understood as a class of computational procedure for determining changes in the state of a physical object during its pairwise interactions with other physical objects acceptable within the framework of a technological process at a certain point in time;

• as a class of computational procedure, the classical tasks of the theory of automated control systems are assumed: detection, identification, predicting, planning, and control.

The full set of common classes and the hierarchical structure of the resulting model is shown in Fig.1. The implementation of the ontology was carried out in the OWL language in the Protégé software environment ver. 5.6.3.

The proposed taxonomy is formed based on general interdisciplinary concepts, intentionally created in the form of a general-purpose ontology in order to enable potential alignment with other more general ontologies (time, physical quantities, etc.) or, conversely, special-purpose ones (including such as [32-35]). One of the important characteristic features of the taxonomy is its applicability to geospatial industrial systems in which natural and technical components act as the core of activity, starting from the production environment itself (spatial infrastructure facilities) to the products.

Including of individual instances in the form of well-understood and stable entities for each of the final taxonomy classes is a mandatory addition and a possible application of this ontology in the context of mining enterprises (currently mainly open-pit mining enterprises). Together with a set of properties-relationships between concepts explaining the roles of each instance and a set of data in the form of various measurable quantities (Fig.2) defining the concepts of "states" of physical objects, the resulting special-purpose ontology forms the basic architecture model of a mining enterprise. The lower part

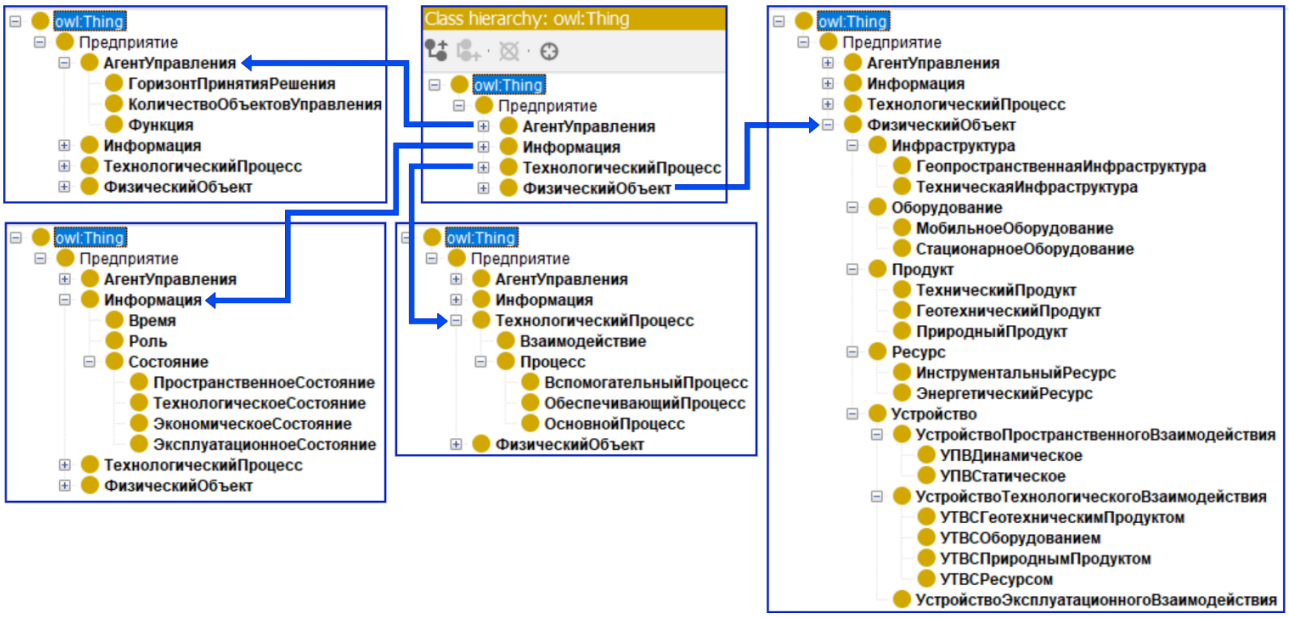

Fig.1. Hierarchy of classes of concepts of the ontological model of enterprise architecture

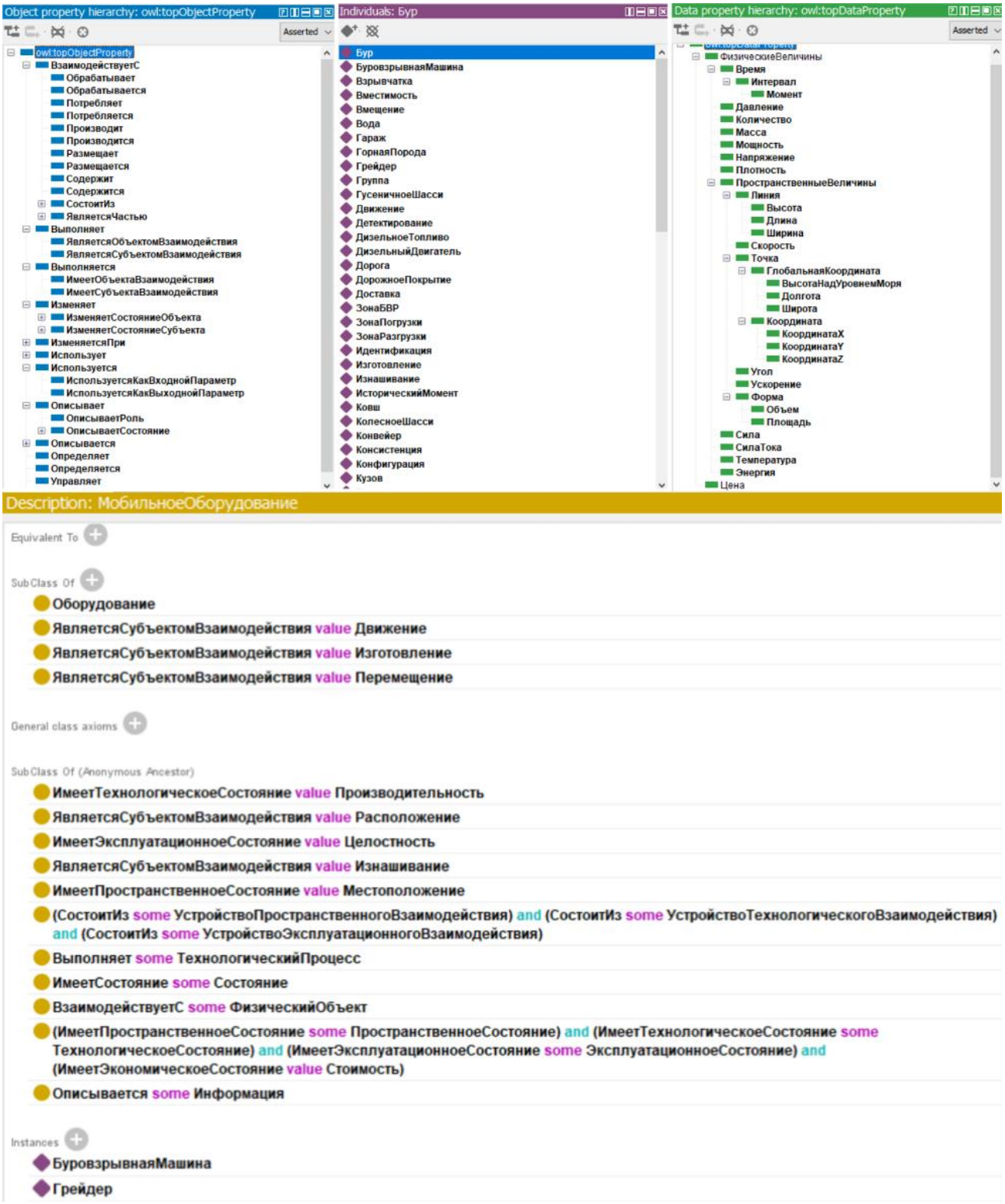

Fig.2. Fragments of the hierarchy table of relations between concept classes (Object property hierarchy, blue) and their instances; instance tables (Individuals, purple) and data hierarchy tables (Data property hierarchy, green); an example of the formation of initial (a priori) logical axioms for the concept class “Mobile Equipment” (Description, yellow)

of Fig.2 shows an example of assigning sets of a priori axiomatic relations to classes of a hierarchy with other classes and instances that determine the logical and semantic construction of the model. Note that the individual names in the current version of the ontology are illustrative in order to explain the proposed approach aimed at standardizing the way the architecture model is formed. Clear formulation

of specific names should be carried out by joint efforts of expert groups from among scientific and industry specialists during open discussions.

As a result of declaring all the axioms, the resulting ontological model can be represented as a semantic graph, where classes and their instances act as nodes, and the relationships between them act as edges (Fig.3, 4).

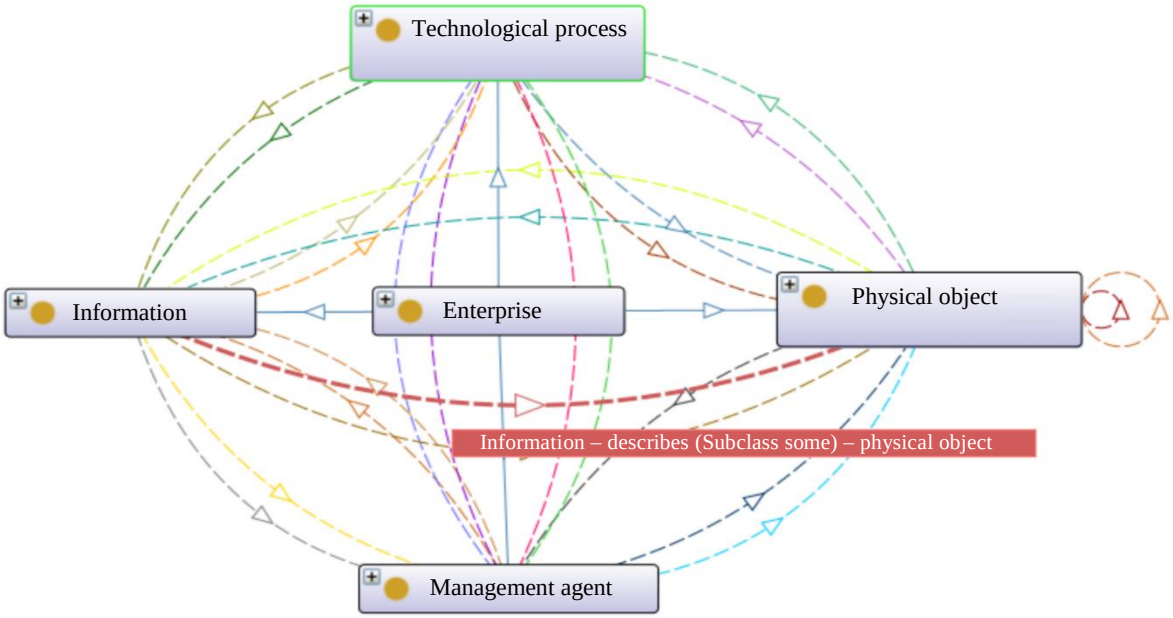

Fig.3. Fragment of the semantic graph of ontology

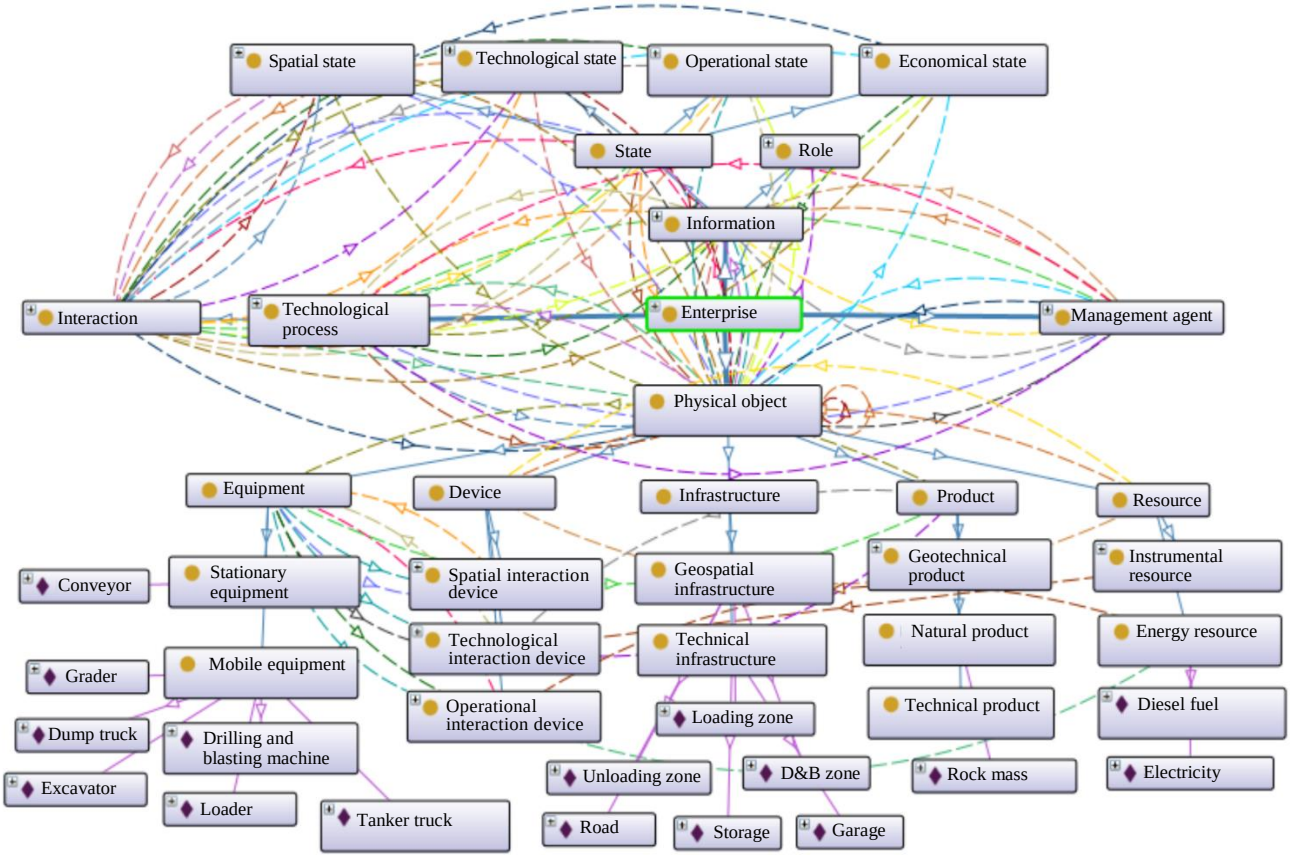

Fig.4. A fragment of the detail of the semantic graph of the ontology

Due to the high dimension of the resulting semantic graph, it is rather difficult to represent its full form in the framework of this work. For example, Fig.4 shows a fragment of the semantic graph detail when the “Physical object” branch is expanded to its final instances.

To determine the achievement of the key goal of this study, which is to confirm the consistency of the obtained ontology, one of the most traditional and developed methods of descriptive logic, HermiT ver. 1.4.3.456, was used [36]. Reasoner presents a logical inference mechanism to prove the completeness and consistency of the underlying axioms and to deduce hidden a posteriori relationships in the semantic graph.

Figure 5 shows a visualization of HermiT's work through the tools for testing and debugging ontologies. In the lower part of the screen, a message in a pop-up window indicates the confirmation of coherence (interconnectedness of all axioms) and consistency of the resulting ontology.

Figure 6 shows examples of visualization of the reasoner's work for deducing a posteriori relationships of class instances that were not declared “manually” at the stage of ontology formation.

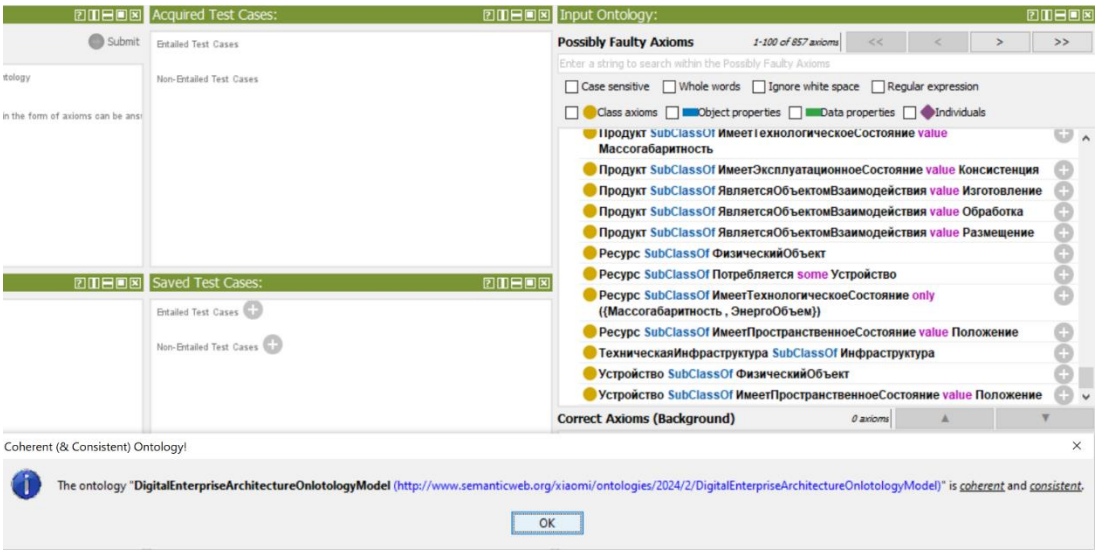

Fig.5. Confirmation of coherence and consistency of ontology by built-in axiom proof tools

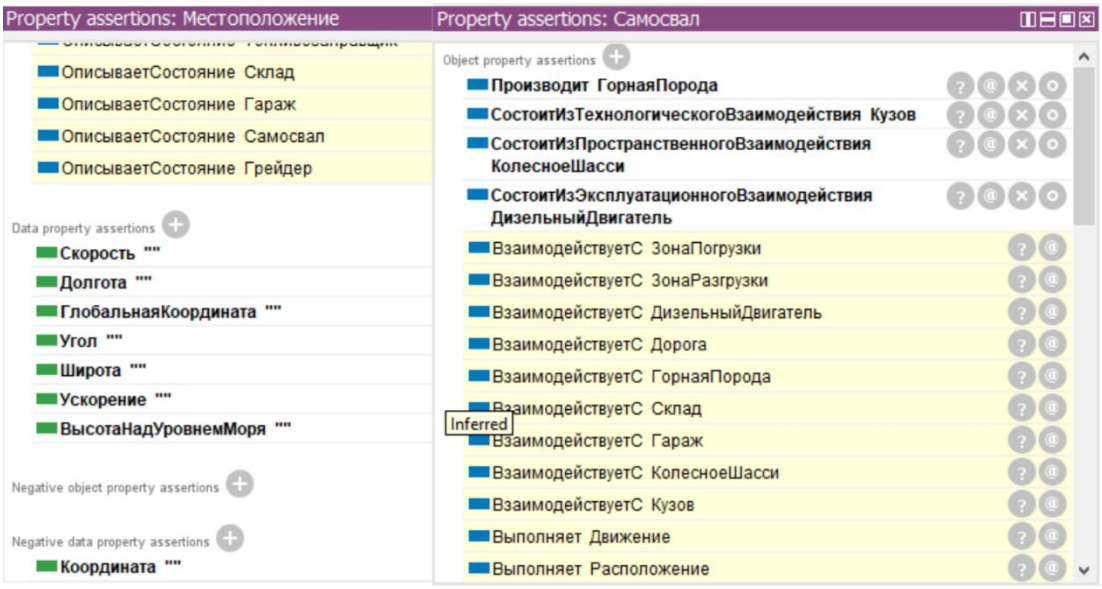

Fig.6. Visualization of the HermiT risoner's work results for the “Location” and “Dump truck” instances

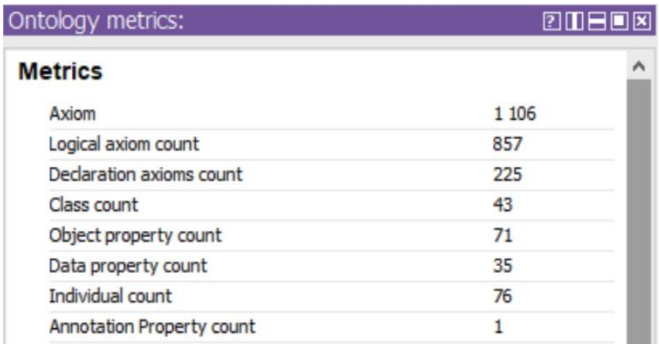

Fig.7. Metrics of ontology in terms of the number of axioms, classes, relationships, and instances

Figure 7 shows metric estimates of the number of axiomatic statements (including a priori declared and logically derived ones) for the current version of the ontology.

Thus, the achievability of the set research goal has been determined and the initial hypotheses about the possibility of building an enterprise architecture model based on ontology in order to ensure the digital transformation of mining industries have been confirmed. At the moment, a sufficient number of class instances have not been introduced into the ontology, which are the basic components of the architecture of mining enterprises. This is explained by the fact that the proposed ontology is aimed at unifying and standardizing the architecture model of mining industries, and therefore, the participation of a wide range of industry experts is necessary to ensure exhaustive depth, completeness, and uniformity of the taxonomy. The current model is proposed to be considered as a basic illustrative example of the formation of a comprehensive digital transformation methodology for building autonomously functioning geospatial industrial systems. In the future, based on the obtained model, it is planned to form a logical inference mechanism (3), (4), as well as a formal definition of the procedure for managing the structural configuration of the architecture in terms of management agents (1).

Conclusion

A number of conceptual statements of tasks and criteria for managing the digital transformation of mining enterprises are proposed, declaring the minimization or complete exclusion of human participation in the implementation of technological processes and, as a result, the construction of an autonomously functioning cyber-physical industrial system. The necessity of forming a knowledge model about the structural and functional properties of such a system in order to ensure self-organization and self-regulation is shown, and the requirements for the instrumental means of implementing the model are formulated.

It is determined that an enterprise architecture model should be understood as a knowledge model, regulating a set of key components with a complexly formalized heterogeneous essence and their interrelation. The impossibility of using existing standards and frameworks (RAMI 4.0, TOGAF 10) to build an enterprise architecture model to ensure the DT processes of geospatial natural and technical industrial systems with an open type of production environment is substantiated.

A number of principles and mechanisms for forming an architecture model of an independently functioning cyber-physical industrial system based on ontological modeling are formulated. The mechanism of application of the model in the management structure of the digital transformation of the enterprise is explained. In accordance with the proposed approach, the basic architecture model of a mining enterprise was formed in the form of general and special purpose ontologies in the OWL descriptive logic language in the Protégé environment. The resulting ontological model has undergone a formal coherence and consistency verification procedure, which suggests partial confirmation of the initial hypotheses and the possibility of further research into the formalization of methodological aspects of the digital transformation of mining industries.

Access to data

The resulting model is applied for the possibility of independent verification, as well as for the open participation of those interested in its development:

Supplement, https://pmi.spmi.ru/pmi/article/supplementary/16728/62861.

REFERENCES

1. Alkhalaf T., Durrah O., Alkhalaf M. Digital Transformation, Business Model, and Performance in the Context of Digital SMEs: Evidence From France // Digital Technologies for Sustainability and Quality Control. IGI Global Scientific Publishing, 2025. P. 101-120. DOI: 10.4018/979-8-3693-4373-9.ch005

2. Makarenko Ya.V., Solovyeva I.A. Digital transformation of the enterprise: key definitions, principles and approaches. *Bulletin of the South Ural State University. Series "Economics and Management"*. 2025. Vol. 19. N 1, p. 112-123 (in Russian). DOI: 10.14529/em250109

3. Litvinenko V.S. Digital Economy as a Factor in the Technological Development of the Mineral Sector. *Natural Resources Research*. 2019. Vol. 29. Iss. 3, p. 1521-1541. DOI: 10.1007/s11053-019-09568-4

4. Yong Fang, Xiaoyan Peng. Micro-Factors-Aware Scheduling of Multiple Autonomous Trucks in Open-Pit Mining via Enhanced Metaheuristics. *Electronics*. 2023. Vol. 12. Iss. 18. N 3793. DOI: 10.3390/electronics12183793

5. Sobolev A.A. Review of case history of unmanned dump trucks. *Gornyi zhurnal*. 2020. N 4, p. 51-55 (in Russian). DOI: 10.17580/gzh.2020.04.10

6. Temkin I.O., Deryabin S.A., Al-Saeedi A.A.K., Konov I.S. Operational planning of road traffic for autonomous heavy-duty dump trucks in open pit mines. *Eurasian Mining*. 2024. N 2, p. 89-92. DOI: 10.17580/em.2024.02.19

7. Vladimirov D.Ya., Klebanov A.F., Kuznetsov I.V. Digital Transformation of Surface Mining and New Generation of Open-Pit Equipment. *Mining Industry Journal*. 2020. N 6, p. 10-12 (in Russian). DOI: 10.30686/1609-9192-2020-6-10-12

8. Lukichev S.V., Nagovitsin O.V. Digital transformation of mining industry: Past, Present and Future. *Gornyi zhurnal*. 2020. N 9, p. 13-18 (in Russian). DOI: 10.17580/gzh.2020.09.01

9. Klebanov A.F., Bondarenko A.V., Zhukovsky Yu.L., Klebanov D.A. Establishing remote control centers of a mining operation: strategic prerequisites and implementation stages. *Russian Mining Industry*. 2024. N 4, p. 174-183 (in Russian). DOI: 10.30686/1609-9192-2024-4-174-183

10. Klebanov A.F., Sizemov D.N., Kadochnikov M.V. Integrated Approach to Remote Monitoring of Technical and Operating Conditions of Mine Dump Trucks. *Russian Mining Industry*. 2020. N 2, p. 75-81 (in Russian). DOI: 10.30686/1609-9192-2020-2-75-81

11. Koteleva N., Valnev V. Automatic Detection of Maintenance Scenarios for Equipment and Control Systems in Industry. *Applied Sciences*. 2023. Vol. 13. Iss. 24. N 12997. DOI: 10.3390/app132412997

12. Zhukovskiy Y.L., Kovalchuk M.S., Batueva D.E., Senchilo N.D. Development of an Algorithm for Regulating the Load Schedule of Educational Institutions Based on the Forecast of Electric Consumption within the Framework of Application of the Demand Response. *Sustainability*. 2021. Vol. 13. Iss. 24. N 13801. DOI: 10.3390/su132413801

13. Korolev N.A., Zhukovskiy Y.L., Buldysko A.D. et al. Energy resource evaluation from technical diagnostics of electromechanical devices in minerals sector. *Mining Informational and Analytical Bulletin*. 2024. N 5, p. 158-181 (in Russian). DOI: 10.25018/0236_1493_2024_5_0_158

14. Zhukovskiy Y., Koshenkova A., Vorobeva V. et al. Assessment of the Impact of Technological Development and Scenario Forecasting of the Sustainable Development of the Fuel and Energy Complex. *Energies*. 2023. Vol. 16. Iss. 7. N 3185. DOI: 10.3390/en16073185

15. Zakharov V.N., Kaplunov D.R., Klebanov D.A., Radchenko D.N. Methodical approaches to standardization of data acquisition, storage and analysis in management of geotechnical systems. *Gornyi zhurnal*. 2022. № 12, p. 55-61 (in Russian). DOI: 10.17580/gzh.2022.12.10

16. Sahal R., Breslin J.G., Ali M.I. Big data and stream processing platforms for Industry 4.0 requirements mapping for a predictive maintenance use case. *Journal of Manufacturing Systems*. 2020. Vol. 54. P. 138-151. DOI: 10.1016/j.jmsy.2019.11.004

17. López Martínez P., Dintén R., Drake J.M., Zorrilla M. A big data-centric architecture metamodel for Industry 4.0. *Future Generation Computer Systems*. 2021. Vol. 125, p. 263-284. DOI: 10.1016/j.future.2021.06.020

18. Deryabin S.A., Rzazade Ulvi Azar ogly, Kondratev E.I., Temkin I.O. Metamodel of autonomous control architecture for transport process flows in open pit mines. *Mining Informational and Analytical Bulletin*. 2022. N 3, p. 117-129 (in Russian). DOI: 10.25018/0236_1493_2022_3_0_117

19. Schmitt R., Borck C., Behm M., Böhnke J. Approach of an asset combination based on RAMI4.0 for the digital transformation and operation of a Digital Twin. *Procedia CIRP*. 2024. Vol. 130, p. 724-729. DOI: 10.1016/j.procir.2024.10.155

20. Deryabin S.A., Temkin I.O., Zykov S.V. About some issues of developing Digital Twins for the intelligent process control in quarries. *Procedia Computer Science*. 2020. Vol. 176, p. 3210-3216. DOI: 10.1016/j.procs.2020.09.128

21. Sakurada L., Leitao P., De La Prieta F. Agent-Based Asset Administration Shell Approach for Digitizing Industrial Assets. *IFAC-PapersOnLine*. 2022. Vol. 55. Iss. 2, p. 193-198. DOI: 10.1016/j.ifacol.2022.04.192

22. Reinpold L.M., Wagner L.P., Gehlhoff F. et al. Systematic comparison of software agents and Digital Twins: differences, similarities, and synergies in industrial production. *Journal of Intelligent Manufacturing*. 2025. Vol. 36. Iss. 2, p. 765-800. DOI: 10.1007/s10845-023-02278-y

23. Angreani L.S., Vijaya A., Wicaksono H. Enhancing strategy for Industry 4.0 implementation through maturity models and standard reference architectures alignment. *Journal of Manufacturing Technology Management*. 2024. Vol. 35. Iss. 4. p. 848-873. DOI: 10.1108/JMTM-07-2022-0269

24. Leitão P., Karnouskos S., Strasser T.I. et al. Alignment of the IEEE Industrial Agents Recommended Practice Standard With the Reference Architectures RAMI4.0, IIRA, and SGAM. *IEEE Open Journal of the Industrial Electronics Society*. 2023. Vol. 4, p. 98-111. DOI: 10.1109/OJIES.2023.3262549

25. Villar E., Martín Toral I., Calvo I. et al. Architectures for Industrial AIoT Applications. *Sensors*. 2024. Vol. 24. Iss. 15. N 4929. DOI: 10.3390/s24154929

26. Shirbazo A., Binghao Li, Ata S. et al. A Guideline for the Standardization of Smart Manufacturing and the Role of RAMI 4.0 in Digitising the Industrial Sector. *IEEE Internet of Things Journal*. 2025. Vol. 12. Iss. 12, p. 19090-19118. DOI: 10.1109/JIOT.2025.3559929

27. Esposito G., Romagnoli G. A Reference Model for SMEs understanding of Industry 4.0. *IFAC-PapersOnLine*. 2021. Vol. 54. Iss. 1, p. 510-515. DOI: 10.1016/j.ifacol.2021.08.166

28. Safitri S.R., Mulyana R., Fajrillah A.A.N. Developing enterprise architecture for BPRACo SMEs digital transformation by using TOGAF 10. *Jurnal Informatika dan Komputer*. 2024. Vol. 7. N 3, p. 165-174. DOI: 10.33387/jiko.v7i3.8629

29. Afarah S.F., Hindarto D., Wahyuddin M.I. Optimizing Automotive Manufacturing Systems through TOGAF Modelling. *SinkrOn*. 2024. Vol. 8. N 1, p. 414-425. DOI: 10.33395/sinkron.v9i1.13256

30. Khai Min Chew, Lee Wah Pheng. Product Life Cycle Data Management and Analytics in RAMI4.0 using the Manufacturing Chain Management Platform. *Journal of the Institution of Engineers*. 2021. Vol. 82. N 3, p. 101-108. DOI: 10.54552/v82i3.120

31. Baolong Zhang, Xiangqian Wang, Huizong Li, Miaomiao Jiang. Knowledge modeling of coal mining equipments based on ontology. *IOP Conference Series: Earth and Environmental Science*. 2017. Vol. 69. N 012136. DOI: 10.1088/1755-1315/69/1/012136

32. Stanković R.M., Obradović I., Kitanović O., Kolonja L. Towards a Mining Equipment Ontology. 12th International Conference "Research and Development in Mechanical Industry", 14-17 September 2012, Vrnjačka Banja, Serbia. SaTCIP, 2012, p. 10.

33. Kolonja L., Stanković R., Obradović I. et al. Development of terminological resources for expert knowledge: a case study in mining. *Knowledge Management Research & Practice*. 2016. Vol. 14. Iss. 4, p. 445-456. DOI: 10.1057/kmrp.2015.10

34. Vlasenko L., Lutska N., Zaiets N. et al. Core Ontology for Describing Production Equipment According to Intelligent Production. *Applied System Innovation*. 2022. Vol. 5. Iss. 5. N 98. DOI: 10.3390/asi5050098

35. Motik B., Shearer R., Horrocks I. Hypertableau Reasoning for Description Logics. *Journal of Artificial Intelligence Research*. Vol. 36, p. 165-228. DOI: 10.1613/jair.2811

36. Herron D., Jiménez-Ruiz E., Weyde T. On the Potential of Logic and Reasoning in Neurosymbolic Systems Using OWL-Based Knowledge Graphs. *Neurosymbolic Artificial Intelligence*. 2025. Vol. 1, p. 15. DOI: 10.1177/29498732251320043

37. Jiaoyan Chen, Pan Hu, Jimenez-Ruiz E. et al. OWL2Vec*: embedding of OWL ontologies. *Machine Learning*. 2021. Vol. 110. Iss. 7. p. 1813-1845. DOI: 10.1007/s10994-021-05997-6

***Authors*: Sergei A. Deryabin,** *Head of Laboratory* (*National University of Science and Technology "MISiS", Moscow, Russia*), *deryabin.sa@misis.ru, https://orcid.org/0000-0003-3165-7032,* **Igor O. Temkin,** *Doctor of Engineering Sciences, Head of Department* (*National University of Science and Technology "MISiS", Moscow, Russia*), *https://orcid.org/0000-0001-8150-6529*.

The authors declare no conflict of interests.

ISSN 2411-3336; e-ISSN 2541-9404

JOURNAL OF MINING INSTITUTE
Zapiski Gornogo instituta
Journal homepage: pmi.spmi.ru

Research article
Geotechnical Engineering and Engineering Geology

New approaches to mineral quality variability evaluation using big data for operational control of ore flows in mining operations

Egor A. Knyazkin[1]✉, **Dmitrii A. Klebanov**[1], **Roman O. Yuvakaev**[2]
[1] *Institute of Comprehensive Exploitation of Mineral Resources RAS, Moscow, Russia*
[2] *Piklema LLC, Moscow, Russia*

***How to cite this article*:** Knyazkin E.A., Klebanov D.A., Yuvakaev R.O. New approaches to mineral quality variability evaluation using big data for operational control of ore flows in mining operations. Journal of Mining Institute. 2025. Vol. 275, p. 145-154.

Abstract
This article examines the problem of managing ore flow quality at mining enterprises from the perspective of applying big data to improve the efficiency of mineral quality management. It is noted that assessing the feasibility of collecting and processing big data for ore flow quality control requires an optimal quantifiable weight parameter, which determines the data collection discreteness and the effectiveness of their processing. Currently, this parameter is the ore (or concentrate) batch. A scientific-practical approach to determining batch sizes at mining enterprises is proposed, based not on business process conditions, but on the analysis of the distribution of quality parameters within the ore body, considering subsequent methods of mineral raw material transportation. An analysis was conducted on the data from every technological process within the mining technical system, leading to the establishment of principles for calculating the minimum required data samples for each stage of the process. The applicability of the Kotelnikov theorem (Nyquist – Shannon sampling theorem) for determining the optimal quantifiable weight parameter of a mineral raw material batch within quality control frameworks is considered. To obtain a qualitative model, the required scope of quarry operation statistics should range from 16 to 52 months of excavator operation at the face. This range depends on the value of the mineral quality distribution coefficient at the mining enterprise. It was also established that for building a qualitative model, the mentioned coefficient must be considered; the higher its value, the lower the sampling frequency should be when collecting data from technological processing stages.

Keywords
mining engineering system; quality management; ore flow; big data; data analytics; production optimization

Funding
The research was funded by the Russian Science Foundation grant (project N 22-17-00142).

Received: 26.09.2024 ***Accepted: 02.07.2025*** ***Online: 09.10.2025*** ***Published: 31.10.2025***

Introduction

The management of ore flow quality is one of the key processes within a mining engineering system, determining its operational efficiency [1-3]. Consequently, justifying the frequency of data collection must be based on information regarding the qualitative and quantitative distribution of the mineral resource in the natural deposit, while also considering an analysis of data from the technological processes associated with the movement of mined rock from the point of natural rock mass breakage up to its transportation for processing [4, 5].

As of 2024, approximately 55 % of Russian IT companies have implemented big data analytics, while 31 % plan to do so. This signifies a shift in the perception of data, with its business value increasing notably, as new tools for data analysis create opportunities for optimizing business models. Leveraging big data on the rock mass, which reflects its qualitative characteristics, enables the justification

of technological process parameters and the development of recommendations for the sampling and accounting of mineral raw material samples. This facilitates tracking quality parameters from the excavation stage through to the production of final concentrate during the beneficiation process [6, 7].

The mining industry has well-established and thoroughly detailed methods for the sampling and preparation of samples for chemical analysis and moisture determination (technical sampling) during the stages of mineral storage and beneficiation. For instance, GOST 14180-80[1] is an essential document governing the sampling of both ore and concentrate batches. The primary limitation of the conventional approach lies in the fact that the key calculable parameter used – the "batch" – lacks strict definition. The operative definition of a "batch" is typically the volume of ore or concentrate moved during a specific loading (or unloading) period, with its size being established by contractual agreement. This stems from the standard's reliance on GOST R 50779.10[2] and GOST R 50779.11[3], which define the system of concepts and terminology in the field of probability theory and mathematical statistics. Within these referenced standards, the batch size is implicitly treated as a predefined variable, derived from the operational conditions of the applied processes within the mining engineering system. Furthermore, regulatory documentation typically defines a "batch" as the quantity of product units required to meet demand over a specific period, or the quantity produced within a single production cycle, accounting for production, storage, and logistics costs. This definition underscores that the concept is intrinsically linked to the attributes of business processes.

However, such definitions are suitable for the production of uniform commodity units with consistent quality parameters. In contrast, in mining, the batch size is influenced by the qualitative and quantitative distribution of the mineral component within the rock mass, as well as the applied method and conditions of rock transportation. This necessitates the calculation of an optimal sampling frequency for quality data collection [8]. Currently, mining enterprises commonly employ contractual agreements to determine batch size, which directly dictates the sampling frequency. Typically, this frequency is aligned with hourly intervals within a shift, a practice driven by tracking convenience.

The objective of this work is to develop a scientifically grounded methodology for determining the minimum required size of a transported rock mass batch, aiming to establish the optimal amount of data for predicting the quality of the supplied raw material [9]. To achieve this goal, it is necessary to define:

• the minimum data dimensions and collection frequency capable of characterizing the technological processes involved in mineral extraction;

• the quantitative values for the volume of data to be collected from each technological process.

This stated scientific and practical task is paramount for formulating the requirements and objectives for the digitalization of the mining engineering system.

Methods

Typically, the following formula is used to determine the sampling interval[1]

$$T = \frac{60M}{QN},$$

where M – mass of the sampled ore or concentrate batch, t; Q – throughput of the sampled stream, t/h; N – number of incremental samples,

$$N = 0.075V\sqrt{M};$$

V – coefficient of variation, %.

[1] GOST 14180-80. Ores and concentrates of non-ferrous metals. Methods of sampling and sample preparation for chemical analysis and moisture determination. Moscow: Standards Publishing House, 2010.

[2] GOST R 50779.10-2000 (ISO 3534-1:1993). Statistical methods. Probability and fundamentals of statistics. Terms and definitions. Moscow: Standards Publishing House, 2001.

[3] GOST R 50779.11-2000 (ISO 3534-2:1993). Statistical methods. Statistical quality control. Terms and definitions. Moscow: Standards Publishing House, 2002.

The formulas used in the standard demonstrate that the calculation of sampling frequency universally incorporates the mass characteristic of the sampled mineral raw material batch. Furthermore, the batch size depends on: the productivity of the mining and processing complex for ore delivery; the dispatch frequency of the batch constituent units (e.g., a truckload); the coefficient of variation of the mineral's quality; regulations for raw material blending, etc. The described methodology confirms that at mining enterprises, although regulations are developed based on the coefficient of variation of quality parameters, their implementation in practice is tied to hourly intervals within a shift due to contractual agreements.

Based on the classification of digital data sources in the mining engineering system by their object of acquisition, this study defines the rock mass from a «data» perspective and identifies the factors influencing it [4]. The qualitative indicators of the mineral raw material are associated with [10-12]:

• geological structure (the distribution of the raw material can depend on the deposit's structure, including the formation features and morphology of ore bodies, as well as folds, faults, and other elements);

• petrographic composition (the quality of the raw material can vary depending on the nature of the spatial relationships between rock-forming and accessory minerals, including the character of their alteration and intergrowths, which determines the recovery rates during beneficiation).

The distribution of mineral raw material quality within the rock mass can be represented by various models, such as a random distribution model (which posits that raw material quality is distributed randomly) and a zonal distribution model (where quality is distributed zonally, with distinct zones characterized by different mineral raw material qualities). When these distribution models are considered in conjunction with the technological features of rock mass extraction and transportation, the distribution of the valuable component over time can be conceptualized as an analog signal with a defined maximum amplitude. In the case of a zonal distribution, this amplitude becomes predictable [13].

The discretization of analog signals in electronics relies on the Kotelnikov theorem, known in Western literature as the Nyquist – Shannon sampling theorem. Formulated in the XX century, this theorem establishes that a continuous signal with a limited frequency spectrum can be perfectly reconstructed from its discrete samples provided the sampling rate is at least twice the highest frequency component of the signal. This implies that for transmitting such a signal through a communication channel, it suffices to send only instantaneous values (samples) at specific intervals rather than the complete continuous data set [14, 15]. In practical applications, recording devices capture a finite number of such measurements, resulting in discrete signal representations [16].

Mathematically, the Kotelnikov theorem can be expressed by the following formula:

$$f(t) = \sum \left(f(nT) \right) \frac{\operatorname{sinc}\left(\pi(t - nT)\right)}{T},$$

where $f(t)$ is the original continuous-time signal; $f(nT)$ – discrete samples of the signal; T – sampling period; $\operatorname{sinc}(x)$ – normalized sinc function.

The Kotelnikov theorem can be applied to the data generated during the management of the mining engineering system. When transmitting a signal originating from any technological process stage (drilling and blasting, excavation and transportation, storage, and beneficiation of solid minerals), it is not necessary to collect and transmit the complete continuous dataset. Application of the Kotelnikov theorem demonstrates that transmission of instantaneous samples is sufficient for signal reconstruction.

The methodology for testing the Kotelnikov theorem employed synthetic data – a dynamically scalable object generated according to predefined patterns derived from a trained machine learning model. The model was trained on two months of real sensor data from automated systems, utilizing, in this specific instance, the k-means clustering algorithm.

The developed methodology comprises the following stages:

• generation of a statistical distribution simulating the distribution of qualitative indicators of the mineral resource within the rock mass;

• modeling of the processes associated with drilling and blasting operations, excavation, and transportation of rock mass (for open-pit mining);

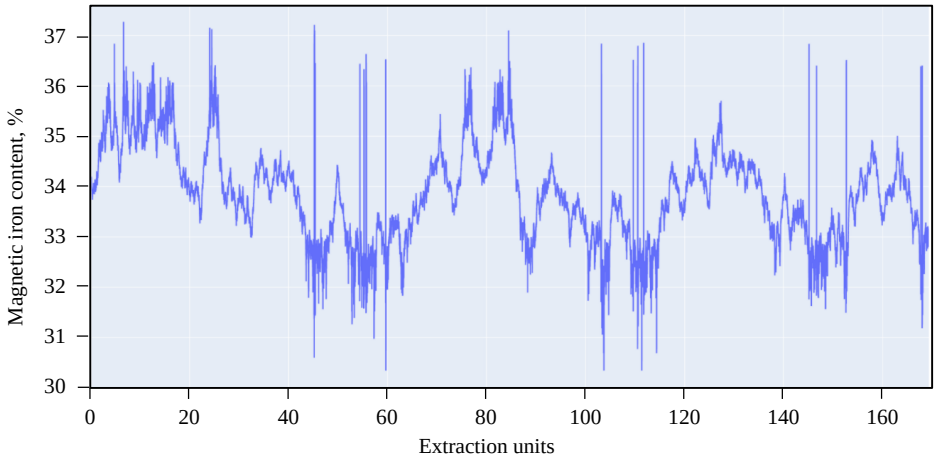

Fig.1. Initially generated distribution of qualitative characteristics within the rock mass volume

• modeling of dump truck unloading onto a stockpile or into a bin;

• modeling of belt conveyor operation, including the functioning of a sample cutting and division machine.

In accordance with the developed methodology, the research is directly linked to the physical processes of ore flow movement within the mining engineering system.

The following computational tools were employed for data array processing in this study: the NumPy library for signal analysis and processing, including filtration and Fourier transform operations; specifically, the library's fftfreq function was utilized, which returns the frequency array corresponding to the indices of the array obtained from the Fast Fourier Transform (FFT) [17].

The algorithm for generating the statistical distribution of mineral quality indicators within the rock mass was developed based on a reference dataset obtained from a dispatching automated system over a two-month period of operation at an iron ore enterprise conducting open-pit mining [18-20]. This resulted in a distribution (Fig.1) of the mineral quality indicators within the rock mass volume, representing 17 thousand excavator buckets [21, 22].

The resulting distribution was randomly assigned to the blast holes of extraction blocks according to the zonal distribution model [23]. This approach enabled the identification of multiple blocks with distinct quality characteristics, while maintaining consistent zoning within each block. In other words, within a single extraction block, closely spaced blast holes could not exhibit quality variations exceeding a step equivalent to 10 bucket loads (to the left or right), thereby conforming to the original distribution (Fig.1). This methodology successfully simulated a process where each loaded truck maintains a consistent quality parameter value in its payload during processes 1 and 2, as defined by the quality-aware ore delivery chain typical of mining enterprises (Fig.2) [24-27]. Processes 3 and 4 were simulated straightforwardly, as they are linear in nature, except for the blending stage. During this stage, the entire stockpiled volume undergoes mixing due to standard mining practices involving loading by front-end loaders or excavators [28, 29].

For data analysis, an experiment comprising several scenarios was conducted:

1. The Kotelnikov theorem was applied to the initial distribution (Fig.1), where the extraction unit is an excavator bucket. This scenario assumes the technical feasibility of monitoring the flow quality at Stage 4 (Fig.2) with a sampling frequency corresponding to each dispatched bucket. In this setup, the

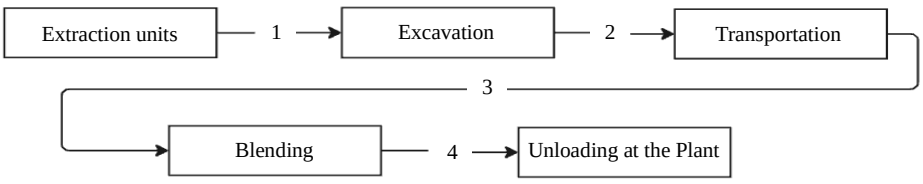

Fig.2. General simulated quality-aware ore delivery chain

blending process is disregarded, thereby simulating an ideal extraction and transportation process consisting of Stages 1, 2, and 4 (Fig.2).

2. The Kotelnikov theorem was applied to the weighted average value of the initial distribution, with the blending volume set as one truckload. In this scenario, the truck's nominal capacity was conditionally set at 7 bucket loads, with blending performed over this volume. At Stage 4, the quality recording interval changes according to the blending volume – one truckload or a weighted average over 14 bucket loads. Similar to Scenario 1, the final configuration of this scenario comprises Stages 1, 2, and 4 (Fig.2).

3. The Kotelnikov theorem was applied to the weighted average value of the initial distribution, with the blending volume set to 3 trucks or 42 bucket loads. This scenario simulates the unloading of trucks into a receiving hopper under a cyclic-flow transport scheme. The theorem is applied at Stage 4 during conveyor transport following the receiving hopper feeder (Fig.2).

4. The Kotelnikov theorem was applied to the weighted average value of the initial distribution, with the blending volume defined by a transfer stockpile. In this scenario, the blending volume amounted to 10 trucks or 140 excavator buckets, simulating a small section of a transfer point. The theorem was applied similarly to the previous scenarios, with the recorded volume being a stockpile section, and the flow scheme comprises all four stages.

It should be noted that considering larger blending volumes in subsequent scenarios is unnecessary, as most modern mining enterprises operate automated dispatching systems capable of dividing large-volume stockpiles into sections, effectively creating quality-based zoning. Furthermore, the point for reconstructing the original distribution from its discrete samples is the belt conveyor, which carries fragmented mineral raw material delivered by trucks of a specific volume. The primary objective of all scenarios is to compare the initial quality distribution with the newly obtained distribution derived via the Kotelnikov theorem and to draw conclusions regarding the theorem's applicability under different conditions.

Prior to the experiment, a decision was made to analyze the performance of the Kotelnikov theorem against variations in the distribution magnitude of the mineral within the rock mass. From the reference dataset obtained from an operating iron ore deposit, it was determined that the mineral quality distribution coefficient is 498 a.u. (spread = 498). Subsequently, based on this sample, initial distributions with spread = 1000 and 2000 were generated, simulating complex-structured, disturbed blocks. Thus, this part of the experiment was conducted without considering the rock mass delivery technology, and the Kotelnikov theorem was applied in its classical form – for reconstructing the original signal.

The Kolmogorov goodness-of-fit test was used as the metric to evaluate the conformity between the original distribution and the distribution obtained using the theorem. This method is widely used in practice as it is designed to test the hypothesis that a sample belongs to a specific distribution law, i.e., to assess the correspondence between an empirical distribution and a presumed model.

Results

Figure 3 shows the results of reconstructing the initial distribution according to the described methodology (Stage 1) for different initial quality distribution values – 498, 1000, and 2000.

The performance of the Kotelnikov theorem under ideal mining conditions is deemed acceptable, as the original distributions were reconstructed with sufficient accuracy; the corresponding evaluation metrics are presented in Table 1.

Interpreting the obtained results leads to an expected conclusion: the higher the initial spread value, the lower the sampling interval should be. For a spread of 498, the interval should be 104.95 s, meaning that for such a distribution, every 105th bucket must be sampled to achieve convergence, where the KS Statistic approaches zero and the P-value approaches one. For spreads of 1000 and 2000, it is necessary to sample every 43rd and 19th bucket, respectively.

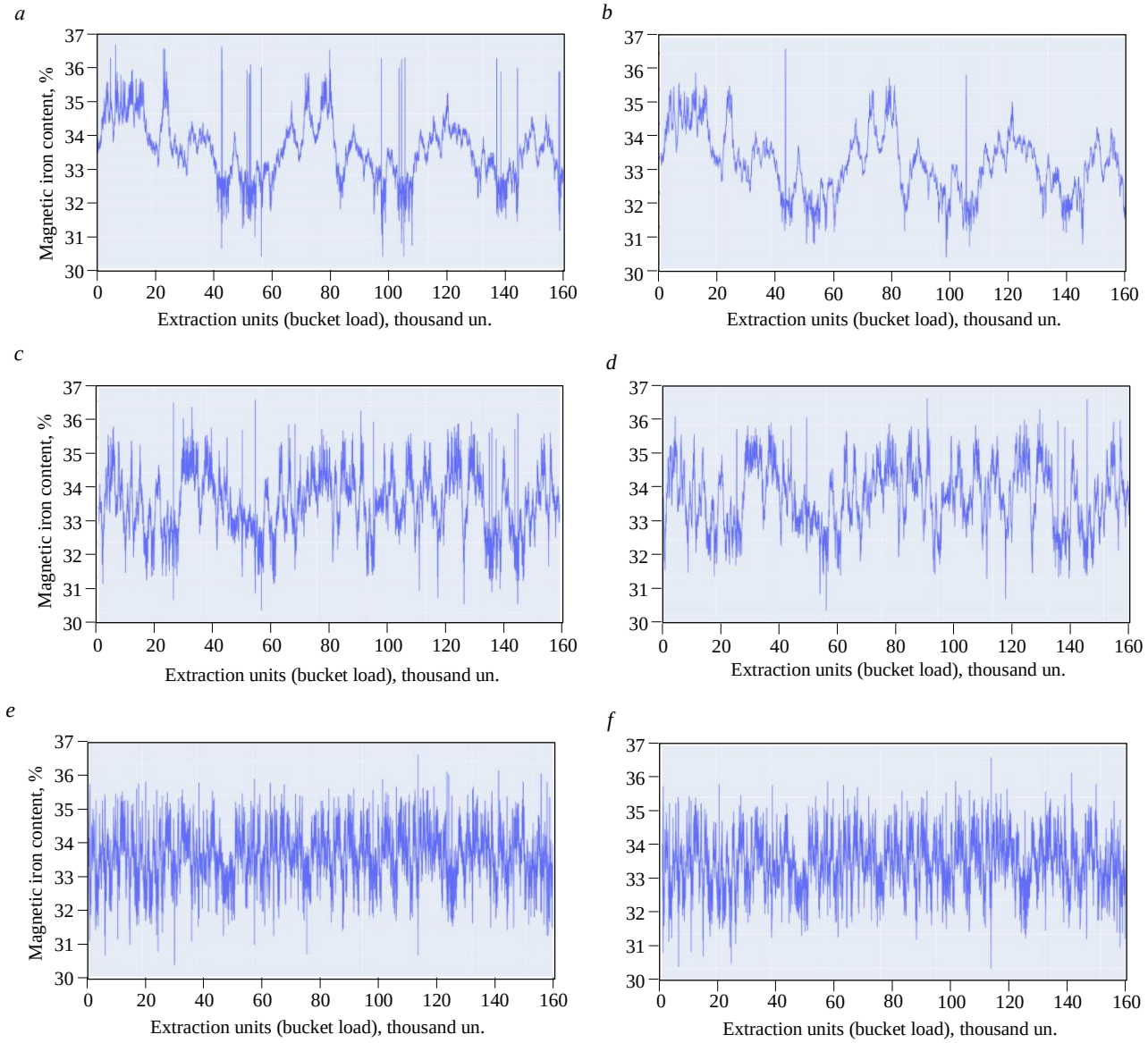

Fig.3. Original (*a*, *c*, *e*) and Kotelnikov theorem-reconstructed (*b*, *d*, *f*) distributions for spread = 498, 1000, and 2000

Table 1

Accuracy of distribution reconstruction via Kotelnikov theorem under different spread values

Distribution (spread)	Kolmogorov – Smirnov test		Sampling interval, s
	KS Statistic	P-value	
498	0.0055	0.9999	104.950
1000	0.0076	0.9768	43.256
2000	0.0029	0.9999	19.329

However, the considered ideal scenario is unattainable in real production conditions due to numerous constraints and uncertainties. A key factor among these is the blending of the mineral material that occurs in truck beds and at transfer blending stockpiles. To assess the degree of influence of the blending volume on the performance of the Kotelnikov theorem, situations were modeled where rock mass transportation involves blending of the conveyed raw material in volumes equivalent to 1, 3, and 10 trucks (Fig.4).

Based on Fig.4, it can be concluded that the performance of the Kotelnikov theorem in reconstructing the original distribution deteriorates as the blending volume increases. For instance, in the case of blending at the transfer point (Fig.4, *e*, *f*), the theorem only identifies the general trend [29]. Reconstructing the original distribution requires a more substantial sample size, as indicated by Table 2.

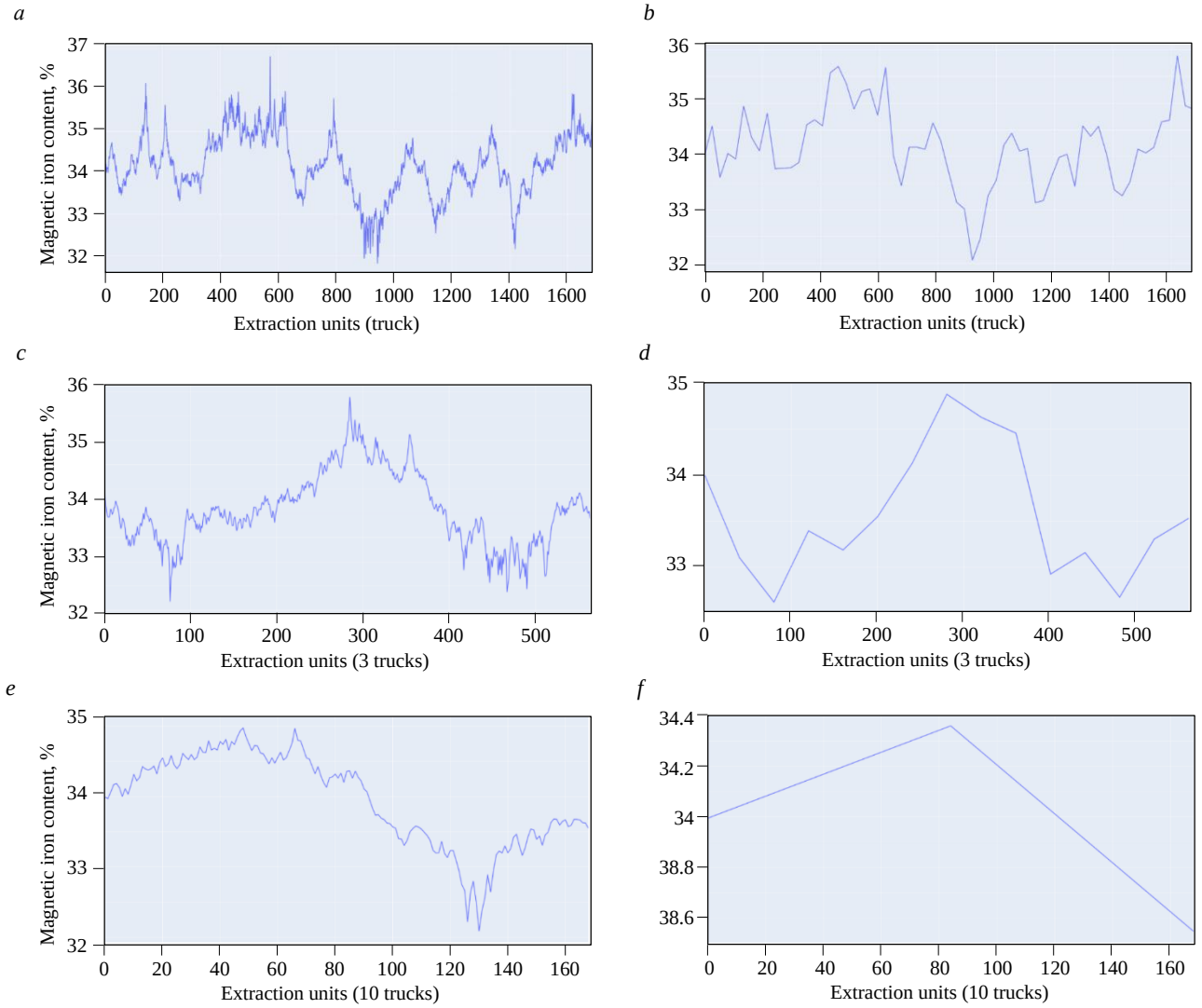

Fig.4. Original (*a*, *c*, *e*) and Kotelnikov theorem-reconstructed (*b*, *d*, *f*) distributions for blending volumes of 1, 3, and 10 trucks

A comparison presented in Table 2 demonstrates that for cases involving a fixed volume (e.g., a block or stope), the Kotelnikov theorem cannot be universally applied across all blending volumes. This limitation is most evident with the 10-truckload blending scenario, where the fidelity of the original distribution reconstruction is notably low [6].

Table 2

Accuracy of distribution reconstruction via Kotelnikov theorem under different blending scenarios

Blending volume	Kolmogorov – Smimov test		Sampling interval, s
	KS Statistic	P-value	
1 truck	0.0697	0.9092	27.323
3 trucks	0.1383	0.9064	40.286
10 trucks	0.3669	0.6945	84.500

The obtained results indicate that applying the Kotelnikov theorem without a thorough assessment of the mineral resource base quality is impractical. Training models and constructing high-quality forecasts for extracted raw material quality requires a substantial volume of statistical data, which must be collected from the mining engineering system through the implementation of digital solutions [30, 31]. Modern IT tools for data archiving and rapid retrieval significantly reduce the requirements for data storage media, thereby lowering the cost of maintaining large information volumes for subsequent analysis.

A series of comparative experiments was performed to assess how mineral characteristics influence the requisite data volume. These experiments demonstrate how the spread parameter affects the sampling interval and what data volume needs to be collected to achieve a specific KS Statistic under different blending schemes. For this experiment, a KS Statistic value of 0.07 was selected as indicative of

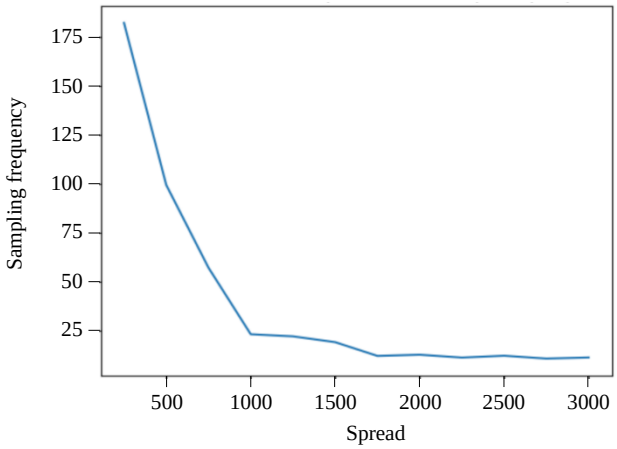

Fig.5. Dependence of sampling frequency on the spread parameter

a highly variable distribution (see Fig.3). It should be noted that the target KS Statistic can be set to any value and is contingent upon the specific conditions and requirements of the mining enterprise. For instance, this metric is influenced to varying degrees by factors such as: truck payload capacity and fleet size, the productivity of the mining complex, the method of mineral raw material delivery, the distribution of minerals within the rock mass, the structure of extraction blocks, and the processing flowsheet of the beneficiation plant, among others. Figure 5 illustrates the variation in sampling frequency as a function of the changing spread parameter.

Figure 5 demonstrates an inverse relationship between the spread parameter and the required sampling frequency, with frequency stabilizing into a plateau beyond the threshold of spread = 1700. This plateau indicates that at high spread values, the informational contribution of each subsequent data point diminishes. The resulting lower sampling rate produces a trend line that is less sensitive to local variations.

To determine the data volume required to achieve a KS Statistic of 0.07 under different blending schemes, graphical analyses were constructed for blending volumes of 10 and 100 trucks. This substantial difference in scale was selected to clearly demonstrate the influence of the blending volume on the requisite size of the initial dataset.

Figure 6 demonstrates that, despite substantial blending volumes, a requisite minimum volume of initial data can always be identified for model training. Specifically, to achieve a KS Statistic of 0.07 with a blending volume of 10 trucks requires 50,820 excavator buckets, while a volume of 100 trucks necessitates 203,280 buckets. This is equivalent to 4.5 and 18 months of enterprise operation (based on a single excavator's workload) for each quarry section type, characterized by the specific quality distribution within the rock mass.

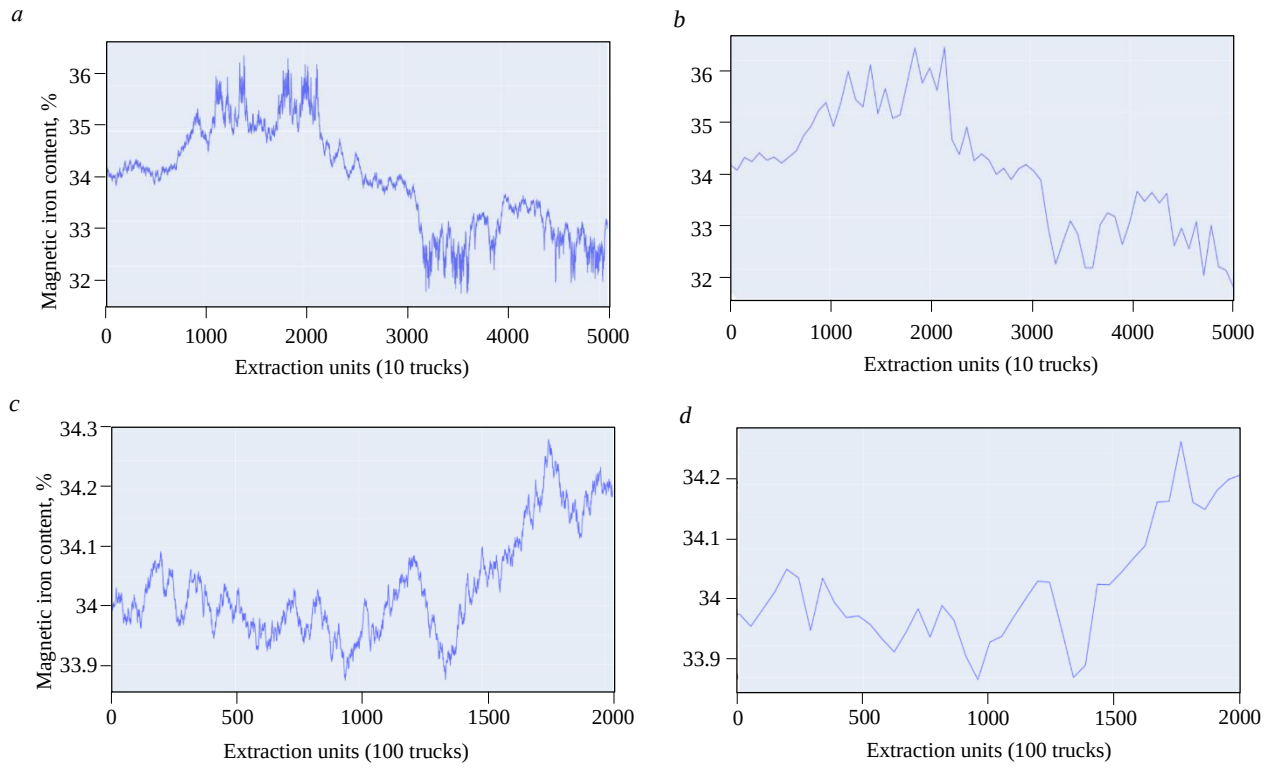

Fig.6. Original (*a*, *c*) and Kotelnikov theorem-reconstructed (*b*, *d*) distributions for blending volumes of 10 and 100 trucks at KS Statistic = 0.07

However, it is important to note that the numerical values obtained are valid only for the initial sample presented in Fig.6. Any modification of the source data could fundamentally alter the relationships illustrated in Fig.7.

To develop a high-fidelity model based on the Kotelnikov theorem for a rock mass delivery chain involving, for instance, a blending volume of 100 trucks, the required operational statistics range from 0.17 to 0.6 million bucket loads, equivalent to 16 to 52 months of continuous excavator operation [32-34]. This considerable variation is primarily governed by the value of the mineral's quality distribution coefficient.

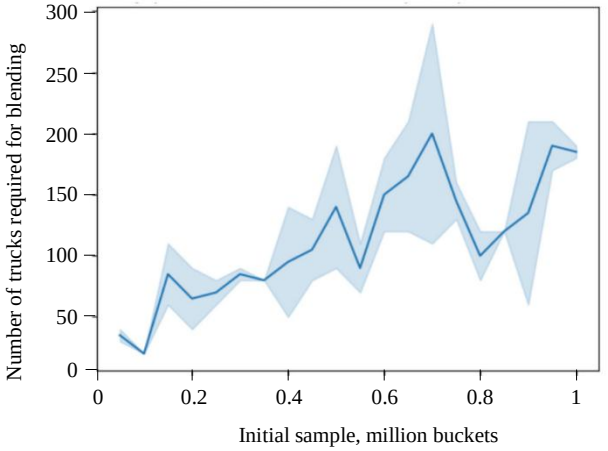

Fig.7. Blending volume versus initial sample size at a target KS Statistic of 0.07

Conclusion

Based on the conducted research following the outlined methodology, it has been established that the Kotelnikov theorem can be applied to determine the minimum batch size of transported mineral raw material, taking into account the productivity of technological equipment – specifically, the sampling frequency for recording quality parameters during rock mass transportation. Another significant outcome of applying the Kotelnikov theorem is the justification of the minimum required data volume necessary to describe each technological process within the mining engineering system. This information allows for the unambiguous determination of the requisite data collection frequency for various processes during the implementation of automation systems.

It was determined that the minimum data volume and the frequency of their recording and blending depend on the quality distribution of the mineral raw material in the original natural deposit, the structural features of the blocks, and the requirements set for the final product.

Data recording and collection must be performed for each technological process according to the rate of change of the structural properties of the mineral raw material within its boundaries. For instance, for the rock mass storage stage, quality and quantity indicators should be recorded at the moment of shipment or when the stockpile is being filled.

REFERENCES

1. Kaplunov D.R. Theory basis of designing of subsoil mastering: formation and development. *Gornyi zhurnal.* 2014. N 7, p. 49-51 (in Russian).

2. Turtygina N.A., Miroshnikova L.K., Volkov N.A., Karpenko I.O. The prospective forecasting method and research Norilsk deposits formed in order to control the quality of the extracted ores. *Mining Informational and Analytical Bulletin.* 2016. N 2, p. 313-319 (in Russian).

3. Kaplunov D.R., Rylnikova M.V., Yun A.B., Terenteva I.V. A new technological policy for integrated subsoil development in the conditions of depleting mineral reserves and resources. *Gornyi zhurnal.* 2019. N 4, p. 11-14 (in Russian). DOI: 10.17580/gzh.2019.04.02

4. Barnewold L., Lottermoser B.G. Identification of digital technologies and digitalisation trends in the mining industry. *International Journal of Mining Science and Technology*. 2020. Vol. 30. Iss. 6, p. 747-757. DOI: 10.1016/j.ijmst.2020.07.003

5. Rylnikova M.V., Vladimirov D.Ya., Pytalev I.A., Popova T.M. Robotic Geotechnologies as Way of Improving Efficiency and Ecologization of Mineral Resource Management. *Journal of Mining Science.* 2017. Vol. 53. N 1, p. 84-91. DOI: 10.1134/S1062739117011884

6. Zakharov V.N., Kaplunov D.R., Klebanov D.A., Radchenko D.N. Methodical approaches to standardization of data acquisition, storage and analysis in management of geotechnical systems. *Gornyi zhurnal.* 2022. N 12, p. 55-61 (in Russian). DOI: 10.17580/gzh.2022.12.10

7. Lomonosov G.G. Improving the quality of products of the mining production as a factor in increasing the effectiveness of the Russian mining and processing complex. *Mineral Mining & Concervation.* 2015. N 2, p. 51-61 (in Russian).

8. Sony M., Antony J., Douglas J.A. Essential ingredients for the implementation of Quality 4.0: A narrative review of literature and future directions for research. *The TQM Journal*. 2020. Vol. 32. Iss. 4, p. 779-793. DOI: 10.1108/TQM-12-2019-0275

9. Zhang Qi, Jiao ShouTao, Lu XinXiang. Discussion on causality and correlation in geological research. *Acta Petrologica Sinica*. 2018. Vol. 34. N 2, p. 275-280.

10. Turtygina N.A., Okhrimenko A.V., Kovalchuk A.A., Kalashnikov K.A. Planning of mining works as organizational method of quality management for mineral raw materials in mining system. *Mining Informational and Analytical Bulletin.* 2018. Special Issue 17, p. 3-11 (in Russian). DOI: 10.25018/0236-1493-2018-5-17-3-11

11. Kantemirov V.D., Yakovlev A.M., Titov R.S., Timokhin A.V. Improvement of Mineral Processing Methods in Mining Structurally-Complex Deposits. *Russian Mining Industry.* 2022. N 1S, p. 63-70 (in Russian). DOI: 10.30686/1609-9192-2022-1S-63-70
12. Ruihan Zhao, Liang Luo, Pengzhong Li, Jinguang Wang. An industrial heterogeneous data based quality management KPI visualization system for product quality control. *Assembly Automation*. 2022. Vol. 42. Iss. 6, p. 796-808. DOI: 10.1108/AA-05-2022-0139
13. Roberts F.S., Sheremet I.A. Resilience in the Digital Age. Springer, 2021, p. 199. DOI: 10.1007/978-3-030-70370-7
14. Xianming Liu, Guangyue Han. Information-Theoretic Extensions of the Shannon-Nyquist Sampling Theorem. ArXiv, 2018, p. 30 (Preprint). DOI: 10.48550/arXiv.1810.08089
15. Iudin S.V. Kotelnikov theorem and sampling periodicity for Schuhart maps. *News of the Tula state university. Technical sciences.* 2020. Iss. 10, p. 116-120 (in Russian).
16. Zhexuan Zeng, Jun Liu, Ye Yuan. A Generalized Nyquist-Shannon Sampling Theorem Using the Koopman Operator. *IEEE Transactions on Signal Processing*. 2024. Vol. 72, p. 3595-3610. DOI: 10.1109/TSP.2024.3436610
17. Shambina S.V., Shambin A.I. Scientific programming in Python. *Works of the Adygheya Republic Physical Society.* 2023. N 28, p. 42-52 (in Russian).
18. Cheskidov V.V., Manevich A.I., Lipina A.V. Big data obtaining and analysis in the mining structures state monitoring practice. *Russian Mining Industry.* 2019. № 2 (144), p. 86-88 (in Russian). DOI: 10.30686/1609-9192-2019-2-144-86-88
19. Rylnikova M.V., Klebanov D.A., Knyazkin E.A. Data analysis as a basis for improving the efficiency of mining equipment in open pit operations. *Russian Mining Industry.* 2023. N 1, p. 52-56 (in Russian). DOI: 10.30686/1609-9192-2023-1-52-56
20. Kupriyanov V.V. Modern problems of control on the basis of systems approach and the theory of information. *Mining Informational and Analytical Bulletin.* 2014. N 2, p. 273-280 (in Russian).
21. Le D.H., Temkin I.O., Do T.L., Agabubaev A.T. Optimization of scrapper conveyor run modes control based on the analysis of imitation modelling. *Caspian Journal: Control and High Technologies.* 2020. N 2 (50), p. 10-21 (in Russian). DOI: 10.21672/2074-1707.2020.50.2.010-021
22. Turtygina N.A., Okhrimenko A.V., Tsygankova D.N. Factors affecting the level of variability of the quality of extracted ore raw. *Scientific Bulletin of the Arctic.* 2022. N 13, p. 5-14 (in Russian). DOI: 10.52978/25421220_2022_13_5-14
23. Shvabenland E.E., Lapteva M.I. Principles of mineral raw material quality management in combined mining complex structural deposits. *News of the Tula state university. Sciences of Earth.* 2021. Iss. 3, p. 326-335 (in Russian). DOI: 10.46689/2218-5194-2021-3-1-320-329
24. Rylnikova M.V., Vlasov A.V., Makeev M.A. Justification of Conditions for Application of Automated Control Systems for Surface Mining during Construction of In Pit Crushing and Conveying System using Simulation Modeling. *Russian Mining Industry.* 2021. N 4, p. 106-112 (in Russian). DOI: 10.30686/1609-9192-2021-4-106-112
25. Teng Long, Zhangbing Zhou, Gerhard Hancke et al. A Review of Artificial Intelligence Technologies in Mineral Identification: Classification and Visualization. *Journal of Sensor and Actuator Networks.* 2022. Vol. 11. Iss. 3. N 50. DOI: 10.3390/jsan11030050
26. Deryabin S.A., Temkin I.O., Zykov S.V. About some issues of developing Digital Twins for the intelligent process control in quarries. *Procedia Computer Science*. 2020. Vol. 176, p. 3210-3216. DOI: 10.1016/j.procs.2020.09.128
27. Upadhyay S.P., Askari-Nasab H. Simulation and optimization approach for uncertainty-based short-term planning in open pit mines. *International Journal of Mining Science and Technology*. 2018. Vol. 28. Iss. 2, p. 153-166. DOI: 10.1016/j.ijmst.2017.12.003
28. Wengang Zhang, Jianye Ching, Goh A.T.C., Leung A.Y.F. Big data and machine learning in geoscience and geoengineering: Introduction. *Geoscience Frontiers*. 2021. Vol. 12. Iss. 1, p. 327-329. DOI: 10.1016/j.gsf.2020.05.006
29. Erkayaoglu M., Dessureault S. Improving mine-to-mill by data warehousing and data mining. *International Journal of Mining, Reclamation and Environment*. 2019. Vol. 33. Iss. 6, p. 409-424. DOI: 10.1080/17480930.2018.1496885
30. Pavlishina D.N., Shumilov P.A., Tereshchenko S.V. Working out a tool for formation efficient technological processes of ore flow quality stabilization. *Problems of Subsoil Use.* 2017. N 1 (12), p. 48-54 (in Russian). DOI: 10.18454/2313-1586.2017.01.048
31. Rylnikova M.V., Tsupkina M.V., Kirkov A.E. Technologies of big data collection and processing - the basis for increasing the reliability of primary information about rock massifs in the development of mineral deposits and technogenic formations. *News of the Tula state university. Sciences of Earth.* 2023. Iss. 1, p. 308-327 (in Russian). DOI: 10.46689/2218-5194-2023-1-1-308-327
32. Chong-chong Qi. Big data management in the mining industry. *International Journal of Minerals, Metallurgy and Materials*. 2020. Vol. 27. Iss. 2, p. 131-139. DOI: 10.1007/s12613-019-1937-z
33. Hui Yang, Yamei Luo, Xiaolei Ren et al. Risk Prediction of Diabetes: Big data mining with fusion of multifarious physical examination indicators. *Information Fusion*. 2021. Vol. 75, p. 140-149. DOI: 10.1016/j.inffus.2021.02.015
34. Yijiu Zhao, Houjun Wang, Yanze Zheng et al. High sampling rate or high resolution in a sub-Nyquist sampling system. *Measurement*. 2020. Vol. 166. N 108175. DOI: 10.1016/j.measurement.2020.108175

***Authors*: Egor A. Knyazkin,** *Candidate of Engineering Sciences, Researcher* (*Institute of Comprehensive Exploitation of Mineral Resources RAS, Moscow, Russia*), *knyazkin_e@ipkonran.ru*, *https://orcid.org/0009-0008-7750-0165*, **Dmitrii A. Klebanov,** *Candidate of Engineering Sciences, Head of Laboratory* (*Institute of Comprehensive Exploitation of Mineral Resources RAS, Moscow, Russia*), *https://orcid.org/0000-0002-3289-9212*, **Roman O. Yuvakaev,** *Senior Specialist* (*Piklema LLC, Moscow, Russia*), *https://orcid.org/0009-0006-4960-5387*.

The authors declare no conflict of interests.

ISSN 2411-3336; e-ISSN 2541-9404

JOURNAL OF MINING INSTITUTE
Zapiski Gornogo instituta
Journal homepage: pmi.spmi.ru

Research article *Geotechnical Engineering and Engineering Geology*

Scientific and methodological approaches in implementing the MGIS import substitution project at PJSC ALROSA

Sergei V. Lukichev[1]✉, **Oleg V. Nagovitsyn**[1,2]
[1] *Mining Institute, KSC of the RAS, Apatity, Russia*
[2] *MINEFRAME Lab LLC, Apatity, Russia*

***How to city this article*:** Lukichev S.V., Nagovitsyn O.V. Scientific and methodological approaches in implementing the MGIS import substitution project at PJSC ALROSA. Journal of Mining Institute. 2025. Vol. 275, p. 155-166.

Abstract
This article examines the experience of strategic cooperation between a mining software developer and a large mining company in adapting the Mining and Geological Information System (MGIS) to the company's corporate requirements. The market-out of foreign MGIS from Russia placed large companies in a particularly difficult situation, as they had been building solutions based on imported software products for many years. The task of software import substitution in the mining industry, which deals with complex geotechnical systems, should be considered as a managed interdisciplinary scientific and engineering process requiring a systematic methodological approach. We note the importance of assessing the level of digitalization of existing business processes for engineering support of mining operations in forming a rational plan for software adaptation and modification. Given the requirement for a quick solution to the import substitution issue, we must consider the internal development of MGIS when coordinating with the industrial partner a work plan for functionality modification. This ensures the development of a competitive digital system for engineering support of mining operations not only for the company but for the entire mining industry. We present the main directions for modifying the MGIS functionality in the fields of geology, mine surveying, and geotechnology, along with examples of developed digital tools. We note that experts have mostly resolved the tasks of developing MGIS to meet the requirements of PJSC ALROSA, and the priority has become the development of software tools f or medium-term and short-term planning of open-pit and underground mining operations. We provide a functional diagram of the planning unit. For the development of MGIS, we consider building the Mining Geological Digital Platform (MGDP). This platform provides the ability to create working tools (units) through the use of API functions and dynamic attachment of units to the MGDP system core.

Keywords
geology; mine surveying; geotechnology; mining and geological information system; planning; software; digital platform; modelling

Received: 01.04.2025 ***Accepted: 18.09.2025*** ***Online: 31.10.2025*** ***Published: 31.10.2025***

Introduction

As noted by many experts, the introduction of sanctions has had a dual impact [1, 2]. On the one hand, sanctions have restricted access to Western technologies, revealing the serious dependence of the domestic mining industry on imports. On the other hand, they have stimulated the development of Russian high-tech products that, for many years, were unable to compete equally with foreign counterparts due to the lack of investment in development. The situation in the domestic market of mining and geological information systems (MGIS) is particularly illustrative, where foreign developments dominate [3]. Large companies, which have been driving the adoption of digital technologies [4] and building their solutions based on imported software products for years, found themselves in a particularly difficult situation. One of the largest mining companies in

Russia, PJSC ALROSA[1, 2] [5], is among the first in the industry to adopt a comprehensive digital solution for operational mining tasks. The company was required to quickly switch to domestic solutions. It should be noted that MGIS and other related digital solutions in the field of mining are rich in specific functionality, the development of which requires appropriate personnel and scientific support. These are tools built on the use of methods for optimizing engineering solutions [6-8], simulation modelling [9-11], geostatistics [12-14], machine learning [15, 16], and big data processing [17].

As a result of analysing the functionality of few Russian MGIS, PJSC ALROSA selected a solution developed by MINEFRAME Lab LLC [18] in close collaboration with the Mining Institute of the KSC RAS [19] as its corporate system. The choice was determined by the presence of sufficiently advanced functionality in the fields of geology, mine surveying, and procedure for both open-pit and underground mining operations, implemented on the basis of 3D graphics and multi-user work with the database. In the summer of 2022, a memorandum on strategic cooperation in the field of information technology was signed between PJSC ALROSA and MINEFRAME Lab LLC. In this partnership, ALROSA acted as an industrial partner, while MINEFRAME Lab LLC served as a developer of digital solutions on the MINEFRAME MGIS platform. Given that ALROSA deals both with open-pit and underground mining operations, and the company has experience in implementation and a well-formed understanding of digital business processes, a detailed plan for the adaptation and development of MGIS functionality was prepared. This plan meets the requirements of both the industrial partner and the mining industry as a whole.

The substantial scope of work, which included not only the MGIS functionality development but also the transition to a new technology stack, required a significant increase in MINEFRAME Lab LLC staff and close interaction with the customer. One of the main requirements for business processes of engineering support for mining operations was their implementation in a unified digital space of mining procedure targets, formed on the basis of the MINEFRAME MGIS. At the same time, the customer specified strict requirements for information security and the implementation of a role-based user access model to data. Another key requirement was the transition to cross-platform solutions that would allow, if necessary, to switch to national operating systems in the near future.

Methods

The solution to the issue of software import substitution in the mining industry (an industry dealing with complex geotechnical systems) should be considered not as a routine process organizational operation, but as a managed interdisciplinary scientific and engineering procedure requiring a systematic methodological approach. This approach should be implemented within the framework of a digital lifecycle, combining elements of hybrid management (Agile + Waterfall) and focusing on the phased satisfaction of functional, engineering, and organizational requirements. The task was solved under significant constraints: complexity and diversity of geotechnical data, thorough coordination of individual design specifications, necessity for uninterrupted operation of existing processes, as well as limited timeframe of 2.5 years for adaptation and implementation. The implementation included several key stages:

• Assessment of the mining enterprise digital infrastructure maturity and identification of critical engineering gaps.

• Development of an architectural model for import-substituting software, considering functional, non-functional, and integration requirements.

[1] Diamonds are not forever: why Alrosa is venturing into gold mining and what investors should expect. RL: https://www.forbes.ru/investicii/519061-almazy-ne-navsegda-pocemu-alrosa-zajmetsa-zolotodobycej-i-cego-zdat-investoram (accessed 01.04.2025).

[2] Alrosa: does the company have prospects? URL: https://ru.investing.com/analysis/article-200311677 (accessed 01.04.2025).

• Adaptation and replatforming based on open standards, cross-platform solutions (e.g., Vulkan, PostgreSQL), and web-oriented architectures.

• Integration and validation in a production environment, including development of interfaces with external systems (mining and geological data management systems, geomechanical monitoring, dispatching, and ERP), unification of directories and classifiers, as well as testing of algorithms on real geological and engineering data while solving typical business tasks.

• Organizational and engineering support, including personnel training, development of operational regulations, and continuous technical support.

This approach is based on the principles of systems engineering and procedure change management, which ensures not only the system operability in principle but also its sustainable operation in production. To evaluate the effectiveness of the methodological approach implementation at real mining enterprises, the following metrics are proposed: degree of substitution of imported solutions, reduction in cost of ownership, increase in productivity of geological, mine surveying, and engineering departments, level of user satisfaction, response time to changes in mining conditions. Thus, the methodological approach transforms import substitution from a process modernization task into a scientifically organized digital transformation. This process contributes to the formation of a sustainable, secure, and technologically independent digital landscape of mining production.

Following the provisions of this methodological approach, prior to initiating the integration of the national mining and geological information system (MGIS) into the engineering support for mining operations, experts from MINEFRAME Lab LLC assessed the level of digital enablement across various divisions of PJSC ALROSA. This assessment formed the basis for developing an adaptation and software modification plan. Transition and target diagrams (to be) were developed for the most critical business processes (Fig.1).

The software incorporated in the MGIS was adapted and modified to meet PJSC ALROSA requirements simultaneously in several areas:

• Migration to PostgreSQL DBMS, integration of user authorization procedures and data access with Active Directory service.

• Expansion of data import tools for the most common CAD and MGIS formats, as well as data exchange in MS Excel format.

• Migration of the geological database editor to a Web platform, accompanied by development of data filtering and validation tools, implementation of the State Commission for Reserves (GKZ)

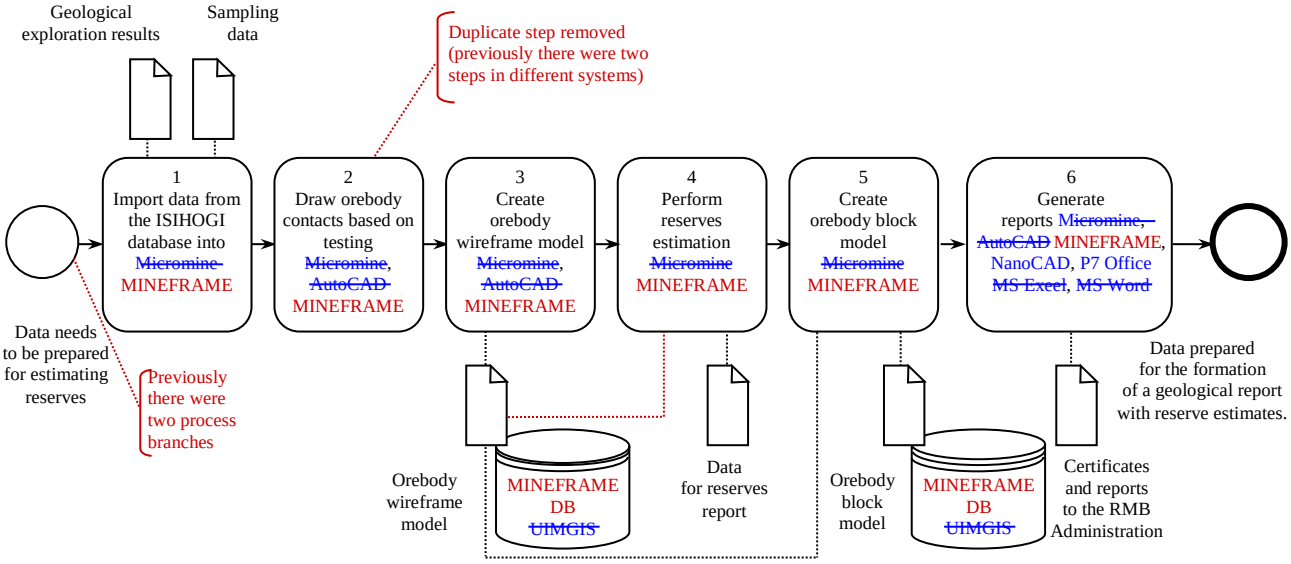

Fig.1. Fragment of the adaptation diagram of the business process “Deposit modelling, reserve assessment”

requirements for grade estimation, and introduction of capabilities for storing and processing geophysical data.

• Porting of the graphic editor (desktop application for solving mining and geological tasks in a 3D space) from DirectX API (Windows) to Vulkan (Windows, Linux).

• Enhancement of statistical and geostatistical research tools to a level capable of addressing most tasks encountered in the practice of prospecting and mining exploration [12, 20, 21].

• Implementation of functionality for working with block models containing hundreds of millions of blocks.

• Development of implicit (conditional) modelling functions [22, 12] for geological body surfaces based on a set of spatially distributed exploration data.

• Implementation of tools for working with point clouds [23-26] (based on results of laser scanning of underground workings, open pit slopes, and dumps), including construction of engineering facility models. A distinctive feature of MINEFRAME MGIS models is their structure, which is formed to solve engineering tasks rather than merely rendering their vector and wireframe models.

As an example of implementing functional requirements according to the MGIS adaptation plan, we can focus on the following tools.

Geology. Software was modified to provide experts with a set of tools capable of solving the entire range of geological tasks:

• Statistical data processing tools for geological exploration – statistical estimation for numerical components obtained from analytics and reserve estimation using block models; visualization of exploration data distribution, highlighting domains with high or top-cut grades on bar charts; emphasis of top-cut grades using multiple methods through various graphs, including decile analysis; construction of scatter plots for multiple components from a single data source; construction of box-and-whisker plots with estimation of median, quantiles, variance, and data asymmetry; Swath Plot displaying content distribution in multiple directions; formation of tonnage-average grade graphs based on cutoff grade variations in block models.

• Interactive tools for working with sample models to include or exclude them from the estimation of useful component content in a selected volume.

• Data comparison tools for adjacent exploration wells to identify and trace coeval complexes, horizons, beds, and interbeds.

• Spatial heterogeneity assessment tools (variography) using geostatistical methods and applying identified patterns during data interpolation with kriging techniques.

Mine surveying. One of the critical tasks of mine surveying support for underground mining operations is the development of mine working models based on survey data. Several methods are used for this purpose. One of the primary methods is tacheometric surveying of the mine working surface, which results in a list of 3D coordinates for a relatively small number of points defining the mine working limits. To improve the accuracy of mine working models, an algorithm was developed that allows for automated fitting of design cross-sections of mine workings into survey contours while linking the sections to surveyed points. This significantly enhances the accuracy of estimating mine working volumes based on modelling data. The improved algorithm simultaneously solves the issue of forming the mine working axis (required for transportation tasks during mining planning) in the presence of niches, rock falls, one-sided narrowings, and expansions.

Tools for creating actual working models based on point clouds obtained through scanning were further developed. An algorithm was implemented for transitioning from a point cloud describing the mine working surface to a set of its cross-sections. This has significantly reduced the "weight" of vector and wireframe models while making them more informative in the field of engineering graphics.

Geotechnology. The evolution of methods for modelling underground mine workings indicates a transition to more detailed representation of their cross-sections and junctions. In both foreign and

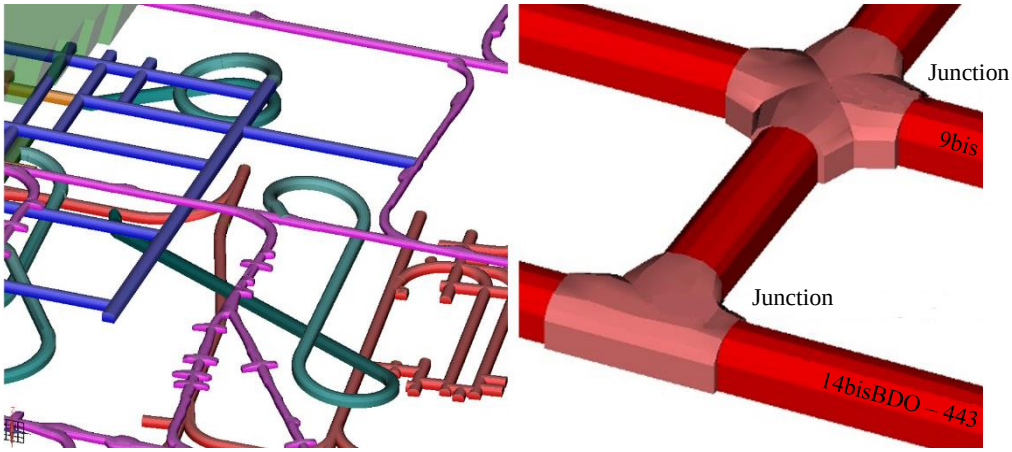

Fig.2. Automated design of workings and their junctions based on typical sections

national MGIS systems, automation of the design process for workings is generally absent, which affects the speed of design and accuracy of models. To automate this process, a set of tools was developed in MINEFRAME that provides parametric modelling of workings and their junctions based on a set of cross-sections (Fig.2), for the creation of which standard or user formulas for estimation are used. Shape control for the selected type of cross-sections is implemented by setting the width and height of the working. Cross-sections are linked to the working axis and positioned along linear sections and curves through defining parameters of the generated models.

An important part of the design process for workings is the selection of support type and estimation of its parameters. An algorithm was developed for automated selection of working support passports based on mining, geological, and geomechanical conditions of mining operations. While developing the algorithm, we analysed instructions for supporting mine workings used at mining enterprises. This allowed generalizing existing experience and presenting it in the form of a set of digital solutions.

The range of tools for open-pit mining design was expanded, focusing on automated development of structural elements for the open-pit mine. To achieve this, we implemented an algorithm that allows creating brake platforms of specified length and width based on the edge line of the bench (upper or lower) and the outline of an already constructed ramp. The tool considers the possibility of connecting ramps with different and equal widths, allows for sequential construction of multiple ramps and platforms, automatically determines various elements of the open pit, and significantly reduces design time.

Tools for estimating tonnage based on volumetric and quality indicators in models of geological and engineering facilities were developed. The developed approaches allow for highly accurate estimation of volumetric and quality indicators based on attributes of block models in selected volumes of the simulated space. Such volumes can include reserves of horizons, blocks, individual extraction units. The modified functionality allows for operation with values of density and other properties of the massif, creating conditions for more accurate accounting of its characteristics.

As an example of interaction with third-party developer solutions, we can consider integration with specialized software[3] [27]. This software is designed for 3D modelling and estimation of engineering indicators for mineral extraction using underground mining in a sublevel caving system with end drawing of ore. This integration allows for synchronization of data on deposit attitude, modelling

[3] From kimberlite deposits to data deposits. URL: https://b2partner.ru/modules/article/ot_kimberlitovih_massivov__k_massivam_informatsii?ysclid=m84905domb750533797 (accessed 01.04.2025).

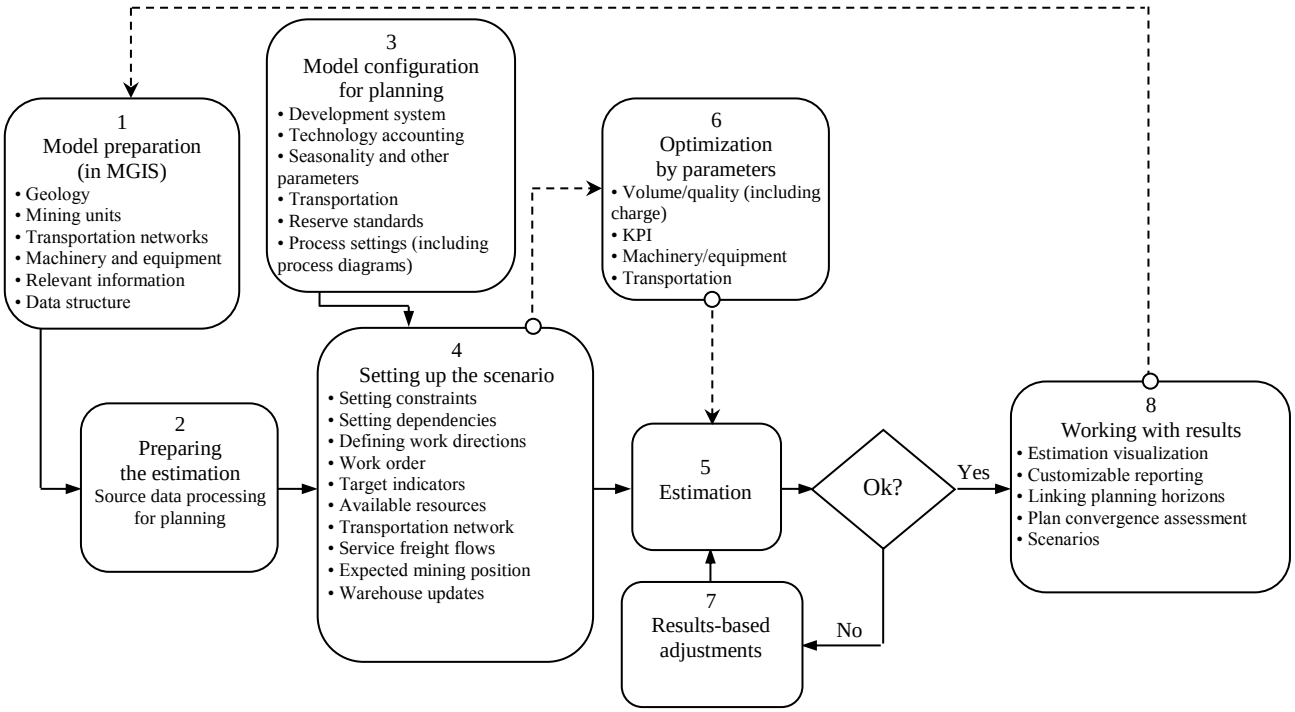

Fig.3. Design of the automated mining planning unit

results, estimation of recovery rates during rock mass drawing. This improves the accuracy of mining planning. Through integration, a data exchange solution was implemented to ensure uninterrupted mining design and planning processes.

Mining operations planning. A separate major area is the development of units for medium- and short-time planning for both open-pit and underground mining methods. In close collaboration with the PJSC ALROSA working group, we formulated the requirements for functionality that should provide automated development of technologically sound plans for periods ranging from two years to weekly-daily schedules.

The planning unit for open-pit and underground mining operations is based on a unified optimization algorithm within the framework of constraint programming [28-32] and simulation modelling methods (Fig.3). The main principles of its operation are as follows:

• seamless integration with mining and geological models within the MGIS environment;

• automated generation of extraction units;

• calendar planning of mining operations for various time periods with the ability to divide them into time intervals: year, quarter, month, week, day;

• end-to-end planning procedure integrating medium- and short-term horizons, and in the future – the strategic level;

• estimation and visualization of mining operation scenarios based on limiting factors (extraction sequence, equipment productivity, repairs/downtimes, process constraints), with display/editing, comparison/analysis of scenarios;

• generation of user documentation, including equipment operation schedules, based on mining operation plan estimations.

Basic requirements for underground mining planning tools (Fig.4):

• duration accounting of process cycles (filling, second mining, driving, etc.);

• assessment of volumes of preparatory and cutting works based on planned ore volumes, considering the prepared reserves coefficient;

• determination of sequence of extraction volumes according to the development system regulations;

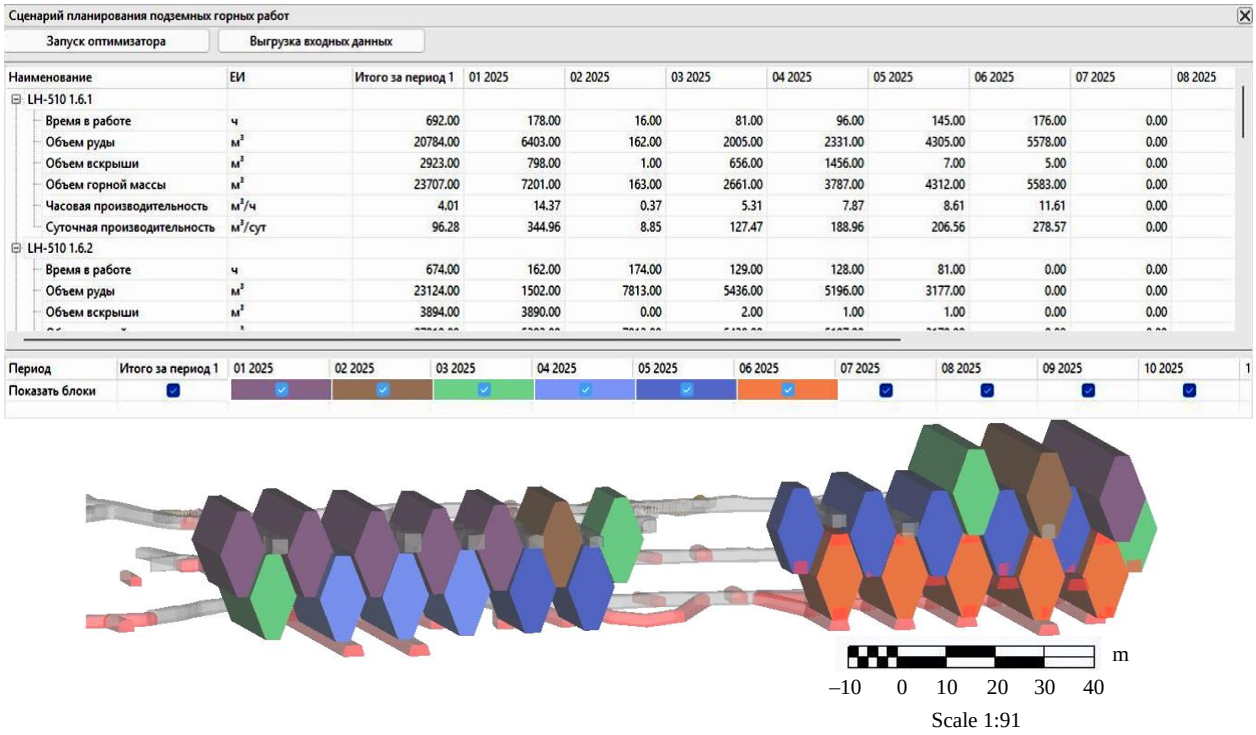

Fig.4. Planning of underground mining operations with extraction unit modelling

• planning scenario implementation based on specified conditions and driving speeds of mine workings, including near hazardous zones and faults;

• construction of transportation network with assignment of trafficability and storage capacity (e.g., ore pass) for its individual elements;

• evaluation of equipment productivity and its optimal quantity depending on operating conditions.

Basic requirements for open-pit mining planning tools (Fig.5):

Количественные показатели	Сводный	Блок 2	Блок 3	Блок 4	Блок 5	Блок 6	Блок 7	Блок 8	Блок 9	Блок 1
Объем (м³)	1 962 635.99	207 723.91	225 472.90	194 194.52	72 291.07	281 334.30	225 000.45	225 000.00	225 046.87	120
Тоннаж (т)	4 814 188.75	515 542.37	552 845.64	475 276.70	180 373.68	694 369.95	536 704.72	537 615.60	558 862.97	297
Плотность (т/м³)		2.35	2.35	2.35	2.35	2.35	2.35	2.35	2.35	
Влажность (%)		10	10	10	10	10	10	10	10	
Объем Высокий сорт (м³)	107 380.00	0.00	1 224.00	1 296.00	0.00	1 992.00	78 996.00	23 872.00	0.00	
Тоннаж Высокий сорт (т)	252 343.00		2 876.40	3 045.60		4 681.20	185 640.60	56 099.20		
Объем Низкий сорт (м³)	508 628.00	25 116.00	71 020.00	66 768.00	2 360.00	57 780.00	92 980.00	142 024.00	25 028.00	18
Тоннаж Низкий сорт (т)	1 195 275.80	59 022.60	166 897.00	156 904.80	5 546.00	135 783.00	218 503.00	333 756.40	58 815.80	43
Объем Пустая порода (м³)	1 346 627.99	182 607.91	153 228.90	126 130.52	69 931.07	221 562.30	53 024.45	59 104.00	200 018.87	101
Тоннаж Пустая порода (т)	3 366 569.95	456 519.77	383 072.24	315 326.30	174 827.68	553 905.75	132 561.12	147 760.00	500 047.17	254

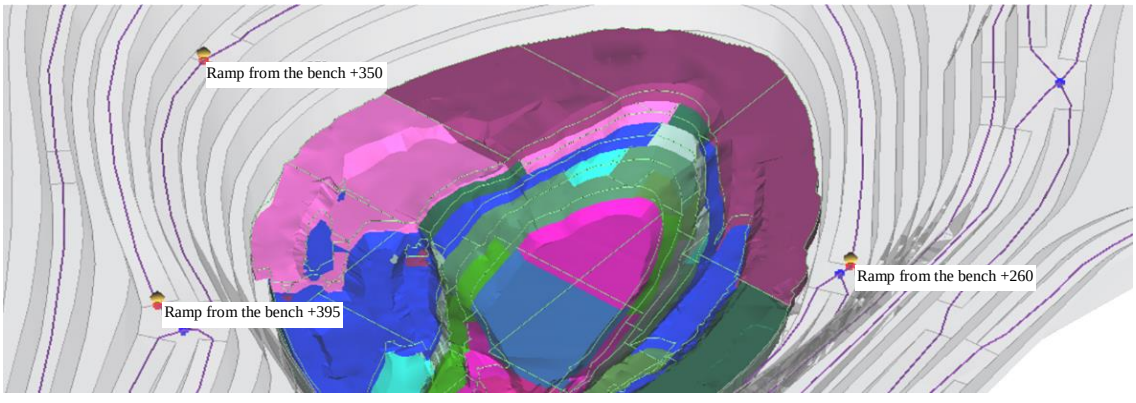

Fig.5. Open-pit mining planning with cut modelling

• consideration of engineering features of stripping and mining operations when operating excavator-truck complexes, as well as bulldozer equipment;

• compliance with safety conditions for conducting mining operations;

• determination of sequence for extracting units at different levels;

• construction of transportation network including temporary ramps;

• accounting of mining and transportation equipment productivity based on traffic conditions in each section of the transportation network.

Development of a mining digital platform. One of the key development vectors of the MINEFRAME MGIS is a mining digital platform (MDP) based on it, which implements the following operation principles:

• separation of system tools (development, visualization, editing, saving, and loading of models) and working tools (solving specific mining and geological tasks), achieved through the development of a cross-platform core and dynamically connected units;

• simplification of new functionality development by providing developers with documented high-level API functions for accessing object model classes and system functions for working with them;

• increased stability of operation by restricting developers of working tools from making changes to the MDP core;

• enhanced database performance by reducing traffic associated with saving only modified parts of models;

• implementation of local (user) – remote (corporate) database connection to simplify the procedure for connecting and interaction between experts;

• provision of model development history display in a time-based perspective, achieved through saving all model changes in the database.

The MDP architecture (Fig.6) provides multi-user work with a collaborative controlled access database. The relational principle of database arrangement maintains data integrity, preservation, and quick response to requests requiring data transfer. Data import, export, and analysis tools are integrated with other programs at mining enterprises. The ability to use third-party digital data and models is even more relevant because, with foreign software vendors market-out from Russia, mining enterprises are extremely interested in preserving information they have been collecting over years [33].

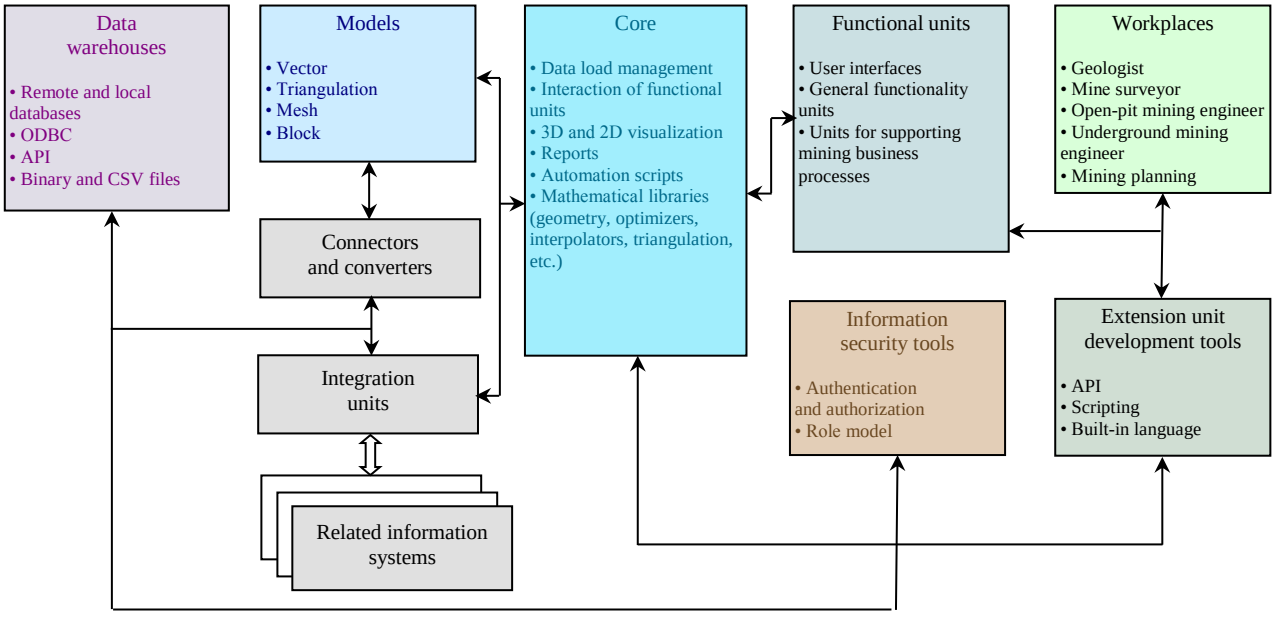

Fig.6. MINEFRAME MDP architecture

For MINEFRAME, tools are developed that allow seamless data importing in formats of the most widespread in Russia foreign MGIS systems into the MDP environment.

Discussion

To date, adapting the MGIS to the PJSC ALROSA requirements has been mostly completed, with verification and refinement of individual working tools underway. The main focus shifted tothe development of open-pit and underground mining planning units, which, according to the functionality stated in the design specification, must meet the best foreign counterparts and surpass them in terms of universality.

The project scale can be assessed by several indicators: our team conducted over 1,500 working meetings between customer and developer employees. We assigned 106 major tasks, which were transformed into more than 3,000 elementary development tasks. As we implemented and presented the developed functionality to the customer, we identified and addressed over 150 comments.

Analysis of successful interaction practices with PJSC ALROSA and other representatives of the mining industry, which have requirements for deep software customization, allows formulating key theoretical and applied conclusions:

• Specificity of developing industry-specific MGIS software solutions. Software of this class is characterized by complex architecture formed under the influence of internal engineering and methodological processes of the developer. This is due to the need to adapt specialized algorithms and software units to the unique production conditions of the customer. It is critically important for the customer to consider the developer's expert position during the stages of identifying design specification requirements and coordinating the project implementation schedule. Ignoring this aspect leads to an imbalance between the parties' expectations, incorrect task formulation, and, consequently, reduced quality and functional stability of the final product.

• Role of communicative and creative components in software development management. Development of software solutions for the mining industry is a complex process combining elements of system design, research activities, and creative approach. Normalization of labour costs in such projects is complicated by the need to solve non-standard engineering tasks, as well as dependence on the level of involvement of customer's experts in iterative development stages. Clear formulation of business goals, combined with a deep understanding of the process platform's capabilities, allows minimizing risks of time and resource costs. This is achieved through early identification of critical project nodes, prioritization alignment, and implementation of advanced project management methodologies. This combination reduces software time-to-market and increases return on digitalization investments.

• Critical importance of documenting processes and requirements. Successful implementation of projects for adapting both MGIS and other complex digital systems is impossible without detailed recording of requirements, business logic, and engineering specifications. Neglecting the documentation stage leads to discrepancies between customer expectations and developer task interpretation and complicates system maintenance at the post-project stage. It is recommended to use combined approaches – supplement text descriptions with visual models, use cases, and examples of source data. This reduces the risk of ambiguity in design specifications.

• Necessity of training and knowledge transfer. Effective software implementation requires not only engineering adaptation but also training of customer employees. There is often a gap between the functional capabilities of the system and the competency level of its users. To minimize this gap, it is necessary to provide training sessions focused on practical tasks specific to the particular enterprise, develop instructions and video tutorials adapted to the customer's business processes, as well as implement a feedback system for prompt response to training gaps and identified needs for software functionality improvements.

• Strategic role of post-project support and development. The cycle of interaction does not end with project completion. Mining companies facing dynamic external conditions (changes in legislation, engineering innovations, expansion of production capacities) require software flexibility. This implies building long-term partnership relations between the customer and the developer; incorporating into contractual obligations provisions for functionality updates, error corrections, and system scaling; use of modular software architecture allowing implementation of new components without reworking the entire system.

• Expectation management and balance of parties' interests. Conflicts in projects often arise due to discrepancies between customer expectations and real process capabilities or resource limitations. To prevent them, it is necessary to conduct an audit of the customer's digital maturity and infrastructure, analysis of analogous solutions at the project initiation stage; clearly differentiate mandatory and desirable functions for implementation; define intermediate acceptance stages for results (for example, the minimum viable product stage) to timely adjust the development direction.

• Consideration of industry specifics and regulatory requirements. The mining industry is characterized by strict safety standards, environmental regulations, and requirements of supervisory authorities. The developer needs to integrate into software tools for automated reporting in accordance with regional and international standards; provide functions for risk monitoring, including geomechanical and hydrogeological aspects; ensure data protection that complies with industry regulations and digital infrastructure of mining holdings.

• Risk analysis and flexibility in project management. The high complexity and probabilistic nature of geological data, elements of uncertainty in mining operations require developers to account for risks such as incomplete or contradictory initial data from the customer; technical limitations of the existing IT landscape; periodic changes in external conditions (e.g., adjustment of regulatory framework). To minimize consequences, it is necessary to apply risk management methodologies and incorporate backup mechanisms into schedule plans (buffer periods, budget reserve).

Conclusion

Effective collaboration between mining companies and developers of both MGIS and similar systems requires a systematic approach that combines engineering expertise, communication management, and adaptation to industry challenges. The success of projects is determined not only by engineering implementation but also by the ability of the parties to build a dialogue based on mutual trust, transparency, and readiness to jointly solve non-standard tasks.

The experience of practically implementing the MGIS import substitution project at PJSC ALROSA has allowed achieving the following indicators:

• information security requirements are fully implemented, data synchronization is configured according to a schedule, and data loss resulting from file access outside the user's role is eliminated;

• more than 250 trained experts;

• seven network databases deployed, with 35 engineering projects organized across implementation sites;

• over 200 user accounts registered in the MGIS role-based model;

• foreign software replaced by 95 %.

Engineering support for mining operations was implemented at six deposits, with implementation underway at five more sites. Thus, the successful implementation of projects to adapt the MGIS required synergy between the technical experience of the developer and the engineering experience of the customer. This is confirmed both by IT project management models and by the practical results presented in the article.

REFERENCES

1. Tverdov A.A. Western sanctions policy's impact on solid minerals sector. *Nedropolzovanie XXI vek.* 2022. N 6 (98), p. 14-17 (in Russian).
2. Lyutyagin D.V., Zabaikin Yu.V., Bogachev M.Yu. et al. Transformation of approaches to efficiency management for mining enterprises facing risks of sanctions. *Economics: Yesterday, Today and Tomorrow.* 2019. Vol. 9. N 3B, p. 613-628 (in Russian).
3. Lukichev S.V., Nagovitsyn O.V. Digital transformation and technological independence of the mining industry. *Russian Mining Industry.* 2022. N 5, p. 74-78 (in Russian). DOI: 10.30686/1609-9192-2022-5-74-78
4. Barnewold L., Lottermoser B.G. Identification of digital technologies and digitalisation trends in the mining industry. *International Journal of Mining Science and Technology*. 2020. Vol. 30. Iss. 6, p. 747-757. DOI: 10.1016/j.ijmst.2020.07.003
5. Bobova M. ALROSA experts: ignoring digitalization is running away from problem-solving. *Dobyvayushchaya promyshlennost.* 2024. N 4 (46), p. 156-160 (in Russian).
6. Mai L., Saw Z. Chapter 10 – Optimization of large mining supply chains through mathematical programming. Applications of Artificial Intelligence in Mining and Geotechnical Engineering. Elsevier, 2024, p. 165-182. DOI: 10.1016/B978-0-443-18764-3.00022-9
7. Furtado e Faria M., Dimitrakopoulos R., Pinto C. Stochastic stope design optimisation under grade uncertainty and dynamic development costs. *International Journal of Mining, Reclamation and Environment*. 2022. Vol. 36. Iss. 2, p. 81-103. DOI: 10.1080/17480930.2021.1968707
8. Nelis G., Morales N. A mathematical model for the scheduling and definition of mining cuts in short-term mine planning. *Optimization and Engineering*. 2022. Vol. 23. Iss. 1, p. 233-257. DOI: 10.1007/s11081-020-09580-1
9. Rylnikova M.V., Vlasov A.V., Makeev M.A. Justification of Conditions for Application of Automated Control Systems for Surface Mining during Construction of In Pit Crushing and Conveying System using Simulation Modeling. *Russian Mining Industry.* 2021. N 4, p. 106-112 (in Russian). DOI: 10.30686/1609-9192-2021-4-106-112
10. Hadizadeh Ghaziani H., Monjezi M., Mousavi A. et al. Design of Loading and Transportation Fleet in Open-Pit Mines using Simulation Approach and Metaheuristic Algorithms. *Journal of Mining and Environment*. 2021. Vol. 12. Iss. 4, p. 1177-1188. DOI: 10.22044/jme.2022.11450.2131
11. Manríquez F., Pérez J., Morales N. A simulation–optimization framework for short-term underground mine production scheduling. *Optimization and Engineering*. 2020. Vol. 21. Iss. 3, p. 939-971. DOI: 10.1007/s11081-020-09496-w
12. Avalos S., Ortiz J.M. Recursive convolutional neural networks in a multiple-point statistics framework. *Computers & Geosciences*. 2020. Vol. 141. N 104522. DOI: 10.1016/j.cageo.2020.104522
13. Madani N. Multi-collocated cokriging: An application to grade estimation in the mining industry. Mining goes Digital. Proceedings of the 39th International Symposium "Application of Computers and Operations Research in the Mineral Industry", 4-6 June 2019, Wroclaw, Poland. CRC Press, 2019, p. 158-167. DOI: 10.1201/9780429320774
14. Deveci M., Varouchakis E.A., Brito-Parada P.R. et al. Evaluation of risks impeding sustainable mining using Fermatean fuzzy score function based SWARA method. *Applied Soft Computing*. 2023. Vol. 139. N 110220. DOI: 10.1016/j.asoc.2023.110220
15. Valencia J., Emami E., Battulwar R. et al. Blasthole Location Detection Using Support Vector Machine and Convolutional Neural Networks on UAV Images and Photogrammetry Models. *Electronics*. 2024. Vol. 13. Iss. 7. N 1291. DOI: 10.3390/electronics13071291
16. Levinson Z., Dimitrakopoulos R. A reinforcement learning approach for selecting infill drilling locations considering long-term production planning in mining complexes with supply uncertainty. *Mining Technology*. 2024. Vol. 133. Iss. 2, p. 176-187. DOI: 10.1177/25726668241244930
17. Badiezadeh T., Saen R.F., Samavati T. Assessing sustainability of supply chains by double frontier network DEA: A big data approach. *Computers & Operations Research*. 2018. Vol. 98, p. 284-290. DOI: 10.1016/j.cor.2017.06.003
18. Laptev V.V., Gurin K.P. Automated Planning of Underground Mining Operations with Regard to Geological and Geotechnical Constraints. *Journal of Mining Science.* 2023. Vol. 59. N 3, p. 490-496. DOI: 10.1134/S106273912303016X
19. Kornienko A.V., Gurin K.P., Stepacheva A.V. Application of modern approaches for software development on an example of mining-and-geological information system MINEFRAME. *The North and the Market: Forming the Economic Order*. 2019. N 1 (63), p. 153-160 (in Russian). DOI: 10.25702/KSC.2220-802X.1.2019.63.153-160
20. Araújo C. da P., Bassani M.A.A., Koppe V.C. et al. Geostatistical simulations with heterotopic hard and soft data without modeling the linear model of coregionalization. *REM – International Engineering Journal*. 2021. Vol. 74. Iss. 2, p. 269-278. DOI: 10.1590/0370-44672020740075
21. Chilès J.-P., Desassis N. Fifty Years of Kriging. Handbook of Mathematical Geosciences. Springer, 2018, p. 589-612. DOI: 10.1007/978-3-319-78999-6_29
22. Huang L., Balamurali M., Silversides K.L. Machine learning classification of geochemical and geophysical data. Mining goes Digital. Proceedings of the 39th International Symposium "Application of Computers and Operations Research in the Mineral Industry", 4-6 June 2019, Wroclaw, Poland. CRC Press, 2019, p. 101-105. DOI: 10.1201/9780429320774
23. Vystrchil M.G., Baltyzhakova T.I., Savina A.V. Algorithm for assessing the accuracy of polygonal TIN surfaces, obtained from sparse point clouds. *Vestnik of the Siberian State University of Geosystems and Technologies.* 2024. Vol. 29. N 3, p. 5-19 (in Russian). DOI: 10.33764/2411-1759-2024-29-3-5-19
24. Kolesatova O.S., Krasavin A.V. Enhancing the effectiveness of mine surveying measurements to determine the volumes of underground mined-out areas through mobile scanning systems. *Globus.* 2020. N 5 (64), p. 76-78 (in Russian).
25. Ferrero A.M., Migliazza M.R., Umili G. Rock mass characterization by means of advanced survey methods. Rock Engineering and Rock Mechanics: Structures in and on Rock Masses. CRC Press, 2014, p. 17-27. DOI: 10.1201/b16955
26. Buyer A., Schubert W. Calculation the Spacing of Discontinuities from 3D Point Clouds. *Procedia Engineering*. 2017. Vol. 191, p. 270-278. DOI: 10.1016/j.proeng.2017.05.181

27. Shekhar G., Gustafson A., Hersinger A. et al. Development of a model for economic control of loading in sublevel caving mines. *Mining Technology*. 2019. Vol. 128. Iss. 2, p. 118-128. DOI: 10.1080/25726668.2019.1586371

28. Van Hentenryck P., van Hoeve W.-J. Constraint Programming. Encyclopedia of Optimization. Springer, 2023. p. 16 DOI: 10.1007/978-3-030-54621-2_713-1

29. Zuenko A.A., Fridman O.V., Zuenko O.N. Constraint programming paradigm in solving scheduling problems: an analytical survey. *Proceedings of Voronezh State University. Series: Systems Analysis and Information Technologies.* 2022. N 4, p. 156-179 (in Russian). DOI: 10.17308/sait/1995-5499/2022/4/156-179

30. Morales N., Nancel-Penard P., Espejo N. Development and analysis of a methodology to generate operational open-pit mine ramp designs automatically. *Optimization and Engineering*. 2023. Vol. 24. Iss. 2, p. 711-741. DOI: 10.1007/s11081-021-09702-3

31. Nancel-Penard P., Morales N., Rojas V., González T. A heuristic approach for scheduling activities with 'OR'-precedence constraints at an underground mine. *International Journal of Mining, Reclamation and Environment*. 2020. Vol. 34. Iss. 10, p. 748-762. DOI: 10.1080/17480930.2020.1734152

32. Rivera Letelier O., Espinoza D., Goycoolea M. et al. Production Scheduling for Strategic Open Pit Mine Planning: A Mixed-Integer Programming Approach. *Operations Research*. 2020. Vol. 68. Iss. 5, p. 1425-1444. DOI: 10.1287/opre.2019.1965

33. Tsepina A. Mining industry digitalization – 2024: dreams and reality. *Dobyvayushchaya promyshlennost*. 2024. N 4 (46), p. 24-30 (in Russian).

***Authors*: Sergei V. Lukichev,** *Doctor of Engineering Sciences*, *Corresponding Member of the RAS*, *Director* (*Mining Institute, KSC of the RAS, Apatity, Russia*), *s.lukichev@ksc.ru*, *https://orcid.org/0000-0002-2944-1913*, **Oleg V. Nagovitsyn,** *Doctor of Engineering Sciences*, *Deputy Director* (*Mining Institute, KSC of the RAS, Apatity, Russia*), *General Director* (*MINEFRAME Lab LLC, Apatity, Russia*), *https://orcid.org/0000-0002-0115-8411*.

The authors declare no conflict of interests.

ISSN 2411-3336; e-ISSN 2541-9404

JOURNAL OF MINING INSTITUTE
Zapiski Gornogo instituta
Journal homepage: pmi.spmi.ru

Research article
Geotechnical Engineering and Engineering Geology

Alternative frameworks for equipment positioning in mining operations

Mikhail S. Nikitenko✉, **Danila Yu. Khudonogov**, **Sergei A. Kizilov**
Federal Research Center of Coal and Coal Chemistry of Siberian Branch of the RAS, Kemerovo, Russia

***How to cite this article*:** Nikitenko M.S., Khudonogov D.Yu., Kizilov S.A. Alternative frameworks for equipment positioning in mining operations. Journal of Mining Institute. 2025. Vol. 275, p. 167-178.

Abstract
The purpose of the work is to review and consider alternative frameworks for object position determination, including for solving dispatching and navigation tasks in technological areas for the operation of highly automated autonomous vehicles without the use of satellite navigation equipment. The main problems associated with the use of satellite navigation equipment for the positioning of vehicles equipped with an automated driving system, as well as loading equipment interacting with them, are considered. The promise and relevance of developing alternative systems and methods for positioning the automated transport component during open-pit mining are shown. The review of technologies is presented, confirming the concept of current research direction related to the digital transformation of the mining industry, ensuring the positioning and position determination of mining equipment at mining enterprises without the use of satellite navigation means. An analysis of existing solutions, their advantages and disadvantages, is carried out. It is proposed to implement the solution to the problem based on machine vision algorithms, the radio direction-finding method, and laser range finding means. Options for the interaction of auxiliary and correcting devices in solving the problems of object orientation in a local coordinate system are provided. The results of field and laboratory studies of radio direction-finding and machine vision methods are presented. A patented, detailed algorithm for determining object coordinates in a designated area, developed by the authors, is described; based on this algorithm, a method for determining the position of loading equipment when interacting with transport vehicles equipped with an automated driving system without the use of global navigation satellite systems is proposed.

Keywords
technological process; mining equipment; autonomous vehicle; positioning; position determination; machine vision

Funding
The work was carried out within the framework of the State assignment of the Federal Research Center of Coal and Coal Chemistry of Siberian Branch of the RAS, project FWEZ-2024-0025 “Development of scientific foundations for the creation of autonomous and automated mining machines, equipment, technical and control systems based on promising digital and robotic technologies (prolongation)” (N 125013101207-7).

Received: 10.04.2025 ***Accepted: 09.10.2025*** ***Online: 31.10.2025*** ***Published: 31.10.2025***

Introduction

Open-pit mining with truck haulage is characterized by high operational costs compared to other methods of mineral deposit development[1]. For instance, loading and hauling operations alone can account for up to 40 % of all costs per unit volume of mined mineral [1]. Climatic conditions and hazardous factors associated with open-pit mining [2] lead to a shortage of qualified personnel at mining enterprises[2]. In response to this situation, mining companies in the Russian Federation and abroad

[1] Typical technological schemes for conducting mining operations in open-pit coal mines. Moscow: Nedra, 1982, p. 405 (in Russian).
[2] Kuchumova A. Quarry “drones”. *Dobyvayuschaya promyshlennost*. 2020. N 1 (19), p. 64-68 (in Russian).

are striving to reduce dependence on the human factor through the automation of the haulage technological process, which can increase the productivity of the haulage component by up to 30 % [3]. According to published data, by the second quarter of 2022, a fleet of more than a thousand haul trucks equipped with an automated driving system (ADS) was in operation worldwide. Forecasts indicate that the number of haul trucks equipped with such systems globally will only increase [4, 5], and by the second half of 2026, the market volume for such mining equipment will exceed 4 billion dollars, confirming the relevance of developing the ADS and its components for quarry transport [6].

An important condition for the effective operation of quarry mining equipment equipped with ADS is its precise positioning within the automated area, which is closely related to localization and routing [7, 8]. Currently, modern ADS and dispatching systems perform position determination of controlled objects using global navigation satellite systems (GNSS), such as the American Global Positioning System (GPS) and the Russian Global Navigation Satellite System (GLONASS) [9-11]. With ground infrastructure, GPS can provide positioning accuracy of up to several tens of centimeters[3]; however, without ground infrastructure, the positioning accuracy decreases[4] to 15-20 m. For GLONASS[5] the declared error in the position determination of stationary objects using ground infrastructure is 1 m.

However, there exists a number of industrial and technological positioning tasks for which the solution by conventional methods is inefficient. These include positioning for open-underground mining technological processes, as well as operation in northern regions with an unstable satellite signal level [7, 12, 13]. It is known that in the Arctic and Antarctic, satellite navigation systems have errors in the position determination of objects [7, 12, 13]. At the same time, these territories possess significant mineral reserves [14-16] and are a priority for development[6].

Despite the advantages of GNSS, the application of the system has a number of features that can be considered disadvantages. Specifically, these include the necessity of ground infrastructure for high accuracy, as well as the low power of the signal received from satellites in conditions of insufficient coverage. For example, on average, the GPS signal power at the earth's surface is only –160 dB (1 W) [17], which makes it vulnerable to intentional jamming [18-20]. The signal can be completely jammed or spoofed, in which case the navigation equipment will determine incorrect coordinates [17, 21]. Furthermore, signals from satellite navigation systems can be distorted and lost without external influence due to the effect of metal structures and terrain relief [22-24].

The aim of the research is to review and consider alternative frameworks for the position determination of objects, including for solving dispatching and navigation tasks within the technological process areas of highly automated mining equipment without the use of navigation equipment. The development and implementation of alternative methods for the position determination and navigation of mining equipment with an ADS are relevant scientific and technical tasks [7, 20, 25].

Methods

The literature describes the application of optical [26, 27] and non-optical [26, 28, 29] methods for solving the task of spatial orientation of objects in a local coordinate system. However, a detailed consideration of the application options of these methods for the positioning of mining equipment with an ADS requires an analysis of the interaction between the elements of the excavator – truck system during loading. One of the main conditions for achieving maximum productivity of technological

[3] BenchManager high-precision positioning system for quarry machinery. URL: https://rit-it.com/2015/03/21/sistema-vysokotochnogo-pozicionirovanija-benchmanager-dlja-karernoj-tehniki/ (accessed 10.04.2025).

[4] Lebedev V. Active safety systems in the mining industry. *Gold and Technology*. 2022. N 4 (58), p. 106-110.

[5] High-precision positioning using GNSS GLONASS. URL: https://russianspacesystems.ru/bussines/navigation/sdkm/vysokotochnoe-mestoopredelenie/ (accessed 10.04.2025).

[6] Order of the Ministry of Natural Resources and Environment of the Russian Federation dated June 9, 2023, N 357 "On approval of the Program for licensing hydrocarbon resource sites in the Arctic zone of the Russian Federation for the period up to 2035, the resource base of which can potentially ensure the utilization of the Northern Sea Route" (in Russian).

process areas for the operation of highly automated mining equipment is the coordinated work of the excavator and the haul truck. For this purpose, there exists a methodology for the approach and positioning of a haul truck with an ADS, which regulates the spatial and temporal parameters of the process to rationalize the loading cycle and ensure safety. The methodology supports the rationality of the positioning configuration, has a recommendatory nature, and is based on an analysis of industrial practice and standard schemes[7]. A key parameter is the orientation of the haul truck parallel to the pit face axis. This arrangement minimizes the time for approach and positioning for loading, as well as the rotation angle of the excavator's boom. Furthermore, positioning is carried out on the right side of the excavator, which ensures safe loading from the side or from behind. Although positioning the haul truck at an angle to the pit face axis may in some cases reduce the boom rotation angle, this configuration is not rational, as it increases the duration and complexity of vehicle maneuvering, negating the potential time savings. The orientation of the haul truck parallel to the pit face axis allows for the standardization of the truck's trajectory in the loading zone, as well as for the automatic determination of the excavator's position based on the application of object spatial orientation methods.

Among the alternative methods for the position determination of objects for dispatching and routing in transport sections, two approaches can be distinguished – determining the object's position on the ground (using a dedicated area of known size referenced to an object on the ground) and in geodetic coordinate systems, such as WGS-84[8], PZ-90[9], and their analogs [30]. In this case, the object's coordinates can be linked to coordinates in geodetic coordinate systems.

From the set of methods ensuring the position determination of objects in geodetic coordinate systems, one can distinguish astronomical navigation [31], object identification on the ground using machine vision [7, 32] and real-time positioning systems based on wireless data transmission technologies [33-35].

Astronomical navigation is one of the oldest methods for the position determination of objects. In the modern world, astronomical navigation is used as a backup method for position determination at sea and in the air [31]. Progress in the field of machine vision, the increase in computational power of compact computers, and the search for solutions to replace GNSS in zones of unstable operation have renewed researchers' interest in astronomical navigation. As a result, prototypes began to appear, combining methods of astronomical navigation and machine vision, embodied in compact, low-cost devices [20].

Position determination of objects by their identification on the terrain using machine vision is a group of methods with various approaches, to both the collection and formation of a database of objects on the earth's surface, the recognition of which is necessary for position determination, and to the detection and identification of objects [7, 32]. In general, this group of methods allows for extracting an object with precisely known coordinates in geodetic coordinate systems from a video data stream and referencing the position of the unmanned autonomous vehicle from which the observation is conducted by the machine vision system to it [7, 32].

Among the real-time positioning methods based on wireless data transmission technologies, position determination via triangulation of GSM communication base station signals can be highlighted as the primary one [33], whereas other methods within this group are more often used for position determination in local coordinate systems [36-38]. In such systems, measurements of signals from Wi-Fi network access points [39-41], Bluetooth transmitters, Active RFID, and UWB [36, 37] are used for position determination of objects. Combined methods based on machine vision are also applied [42, 43].

The implementation of position determination methodologies in a local coordinate system, based on measuring the signal from Wi-Fi access points; Bluetooth, Active RFID, and UWB transmitters, has several

[7] Typical technological schemes for conducting mining operations in open-pit coal mines. Moscow: Nedra, 1982, p. 405 (in Russian).
[8] World Geodetic System 1984. URL: https://www.unoosa.org/pdf/icg/2012/template/WGS_84.pdf (accessed 10.04.2025).
[9] Coordinate system PZ-90. URL: https://astro.tsu.ru/TGP/text/1_3_7.htm (accessed 10.04.2025) (in Russian).

approaches, and all of them are generally based on measuring signal power [35, 41, 44]. In [41], an approach is presented where preliminary recording of signal parameters in each square of the local coordinate system is performed, and in [35] the authors indicate that the distance to a Wi-Fi network access point installed at a location with known coordinates is calculated based on the power of the detected signal.

With the use of mechanical measuring instruments for celestial navigation and conducting all measurements manually, an accuracy of approximately 1 nautical mile (1852 m) or ±1 angular minute is achieved [31, 45], which is used in maritime and air transport as a backup method for vessel position determination. The application of modern technologies, such as machine vision and neural network image analysis, has allowed for the development of a compact celestial navigation device based on a modern single-board computer without the use of complex mechanical and optical systems; the theory and operating principles of which are described in [46, 47]. A functional prototype of a celestial navigation device with positioning accuracy almost two times higher than when using the manual method (1050 m) is described in [20]. Furthermore, the NAS-14V2 navigation system, developed in the USA in the 1960s, which allowed for determining coordinates using celestial navigation with an accuracy of up to 90 m, is known and described in the literature [48]. Despite progress, over centuries of application, the method of position determination by the location of celestial bodies does not allow achieving accuracy comparable to GNSS and has a serious drawback for use on ground transport – the necessity of constant visibility of the celestial bodies in the sky, by whose position the coordinates of the object being positioned are determined [20].

Different approaches are practiced for the position determination of unmanned autonomous vehicles using machine vision methods in areas with known coordinates. In [32], the authors propose forming a database of objects for identification using satellite imagery, which remain in large volumes after remote sensing of the earth's surface from space. In [7] the authors propose creating special markers on the surface with precise reference to geodetic coordinate systems, similar to those described in [49]. An option involving equipping roads with special markers recognized by machine vision (so-called Smart roads) [50] using masks and contours [51] is also considered. At the moment, such navigation systems are under development and have significant potential for advancement [7, 32]. The universality of this group of position determination methods allows for their testing on scaled models. Machine vision has a number of application peculiarities in conditions of a constantly changing environment due to the necessity of determining the coordinates of stationary, unchangeable objects; however, it demonstrates effectiveness when working in conjunction with auxiliary guiding and adjusting devices and systems [25, 43].

Another group of alternative methods for position determination of objects is real-time positioning based on wireless data transmission technologies. For determining the coordinates of an object (in the case of a cell phone or modem) in geodetic coordinate systems, only methods based on studying signals from GSM communication base stations are well-suited [33], predominantly, methodologies built on the triangulation of GSM communication base station signals are used[10] [33].

The application of methods based on Bluetooth technology reduces the error in object positioning to 1-2 m [35, 41]. Similar error rates are provided by Active RFID technology – 2 m [35, 41]. The most accurate solution with an error of about 0.3 m is the method based on the use of UWB technology [35, 41]. At the same time, the operating range relative to the base station is less than 100 m for all the listed methods [35, 41], which is insufficient for their use in the ADS. As of 2025, the possibility of using UWB-based methods within the territory of the Russian Federation has not been officially confirmed by the State Commission for Radio Frequencies[11].

[10] Martinka J. Locating mobile phones using signal strength measurements: Master's Thesis. Brno: Masaryk University, 2019, p. 59. URL: https://is.muni.cz/th/asrql/433615_thesis.pdf (accessed 10.04.2025).

[11] Apple AirTags are useless for Russians. Their main feature is banned throughout Russia. URL: https://www.cnews.ru/news/top/2021-04-26_metki_apple_airtag_pochti_polnostyu (accessed 10.04.2025).

As a result of analyzing the features of methods permissible for hardware implementation in the ADS, their advantages and disadvantages have been identified from the perspective of application in the mining industry for solving tasks of dispatching and navigation within technological process sections for the operation of highly automated vehicles without the use of navigation equipment. Based on existing methods, an original approach to the position determination of machinery at mining enterprises using a combination of radio direction finding, machine vision, and laser rangefinding is proposed. Conceptually, the approach consists of the sequential application of radio direction-finding equipment and a machine vision system for devices determining the position of a moving object relative to a stationary one within a local coordinate system, followed by the application of laser rangefinding means and the determination of angular movements.

Discussion

The task of determining the coordinates of an excavator is a technological process requirement aimed at reducing downtime and increasing the readiness factor of mining equipment for open-pit operations. The input data for solving the research problem was the requirement to ensure a positioning error of no more than 1 m for every 200 m of distance to the moving object (excavator), moving within an allocated local site of limited size relative to a stationary one (the mast of the entrance gate). For the site to which the local coordinate system is applied, restrictions have been established – the site where navigation is carried out has a flat surface (designed in accordance with the requirements of regulatory documentation) and a slope of no more than 5 %. Significant elevation differences of the site's surface exceeding standard values can lead to an increase in error and the failure of the proposed approach.

To solve the problem, a local coordinate system associated with a stationary object, relative to which the coordinates of the moving one were determined, was introduced. Taking into account the assumption that the allocated site is flat and has no elevation changes, a Cartesian coordinate system is proposed for the local site. Since the task of position determination is considered in the context of controlling a vehicle by the ADS, the entrance gate to the site is defined as the stationary object relative to which the coordinates of the moving object are determined. The entrance gates consist of two masts installed on the right and left sides of the technological process road used for entering the site, such that the line drawn through the centers of the entrance gate masts is strictly perpendicular to the road surface.

The entrance gate masts are the reference points for the local coordinate system on the site. Thus, a virtual grid with the required step is superimposed on the entire site. The virtual abscissa axis passes through the center of each gate mast. The intersection point of the abscissa and ordinate axes is chosen so that the entire site is located in the first quadrant of the coordinate plane formed by the virtual axes. The distance from the intersection point of the virtual coordinate axes to the center of the entrance gate mast, from which the hypotenuse of the right triangle will be constructed, is set when building the virtual axes.

A graphical method for solving the analytical problem was applied for determining the coordinates in the Cartesian system. The sequence of actions when determining the coordinates of a moving object in the Cartesian coordinate system inscribed in the allocated local site is demonstrated in Fig.1.

Using the graphical method, it is shown that any point located in the first quadrant of the coordinate plane and not belonging to the coordinate axes can be the vertex of a right triangle, one side of which will be located on the virtual abscissa axis. Then the hypotenuse of this triangle will be the segment laid from the center of one of the masts to the point whose coordinates need to be determined. After measuring the angle between the hypotenuse and the abscissa axis, the lengths of the two unknown legs are calculated based on the properties of a right triangle. Then the coordinate of the point in the local coordinate system will be the distance from the intersection point of the coordinate axes to its projection on the axes. Thus, to determine the coordinate of a point on the local site, it is necessary to measure the hypotenuse and the angle between the hypotenuse and the virtual abscissa axis, which forms two measured quantities.

Journal of Mining Institute. 2025. T. 275. P. 167-178

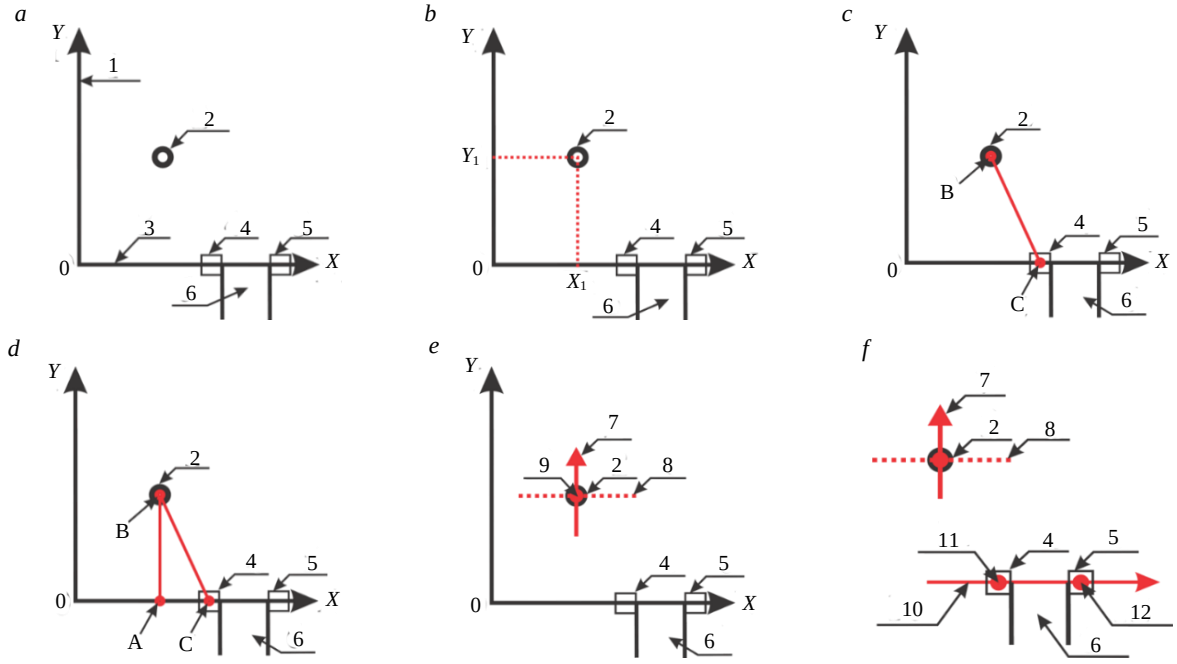

Fig.1. Sequence of determining the coordinates of a moving object in the Cartesian coordinate system on a designated local area: *a* – location of the virtual coordinate axes and the entry gate masts relative to the haul road; *b* – example of determining the coordinates of a moving object (coordinates X_1, Y_1); *c* – location of the hypotenuse CB of the virtual triangle between the coordinate determination devices; *d* – location of the virtual lines AB and AC (coordinates of the moving object); *e* – example of the encoder's zero point location on the moving object in the coordinate determination device; *f* – example of the zero position of the encoder of the coordinate determination device in the entry gate mast

1 – virtual axis 0*Y*; 2 – moving object; 3 – virtual axis 0*X*; 4 – left entry gate mast; 5 – right entry gate mast; 6 – haul road; 7 – zero position of the coordinate determination device's encoder on the moving object; 8 – longitudinal axis of the moving object; 9 – location of the coordinate determination system's encoder on the moving object; 10 – zero position of the coordinate determination device's encoder in the left entry gate mast; 11 – location of the coordinate determination system's encoder in the center of the left entry gate mast; 12 – center of the right entry gate mast

The distance between the object, whose coordinates need to be determined, and the entrance gate mast is proposed to be measured using the laser rangefinding method, which can provide a measurement error at a distance of 200 m of less than 0.005 m for modern device models. Also, Fig.1, *d* allows us to understand that the greatest error in determining the coordinates of a moving object is caused by the resolution of the encoder when measuring angle ACB. In this regard, to determine the sufficient accuracy of the encoder, the maximum deviations of the projection values of point A when measuring angle ACB were calculated, and a diagram of the dependence of these deviations in the calculated size of segment AB (coordinate of the 0*Y* axis) on the resolution of the encoder at a distance of 200 m to the moving object was obtained (Fig.2). It should be considered that the cost of an encoder increases depending on its resolution – the number of measurement points (equal steps) per one revolution.

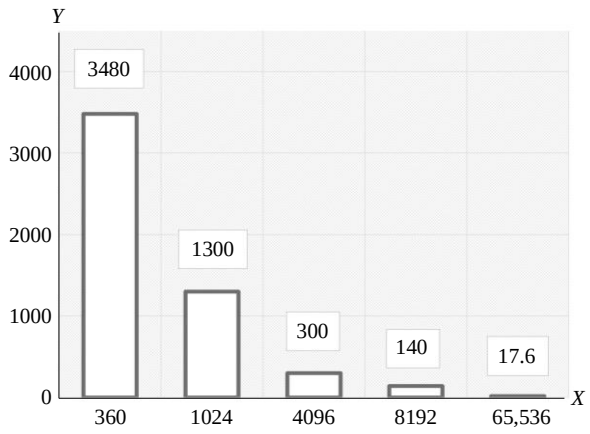

Fig.2. Plot of projection value deviations of point A when measuring angle ACB in the calculated length of segment AB (0*Y* axis coordinate) on the encoder resolution at a distance of 200 m to the moving object; *X* – typical resolution values of commercially available absolute encoders, steps per revolution; *Y* – maximum deviation from the calculated distance to the moving object between encoder steps at 200 m range, mm

The values of the second measured quantity – the angle between the abscissa axis and the hypotenuse of the triangle – are proposed to be measured by an absolute encoder using an opto-mechanical

measurement method, where a unique digital position code is provided for each shaft position, read by an optical system from a code disk.

Subsequently, based on the obtained angle value and the distance to the object measured by the laser rangefinder, the calculation of the object's coordinates *X* and *Y* is performed.

The radio direction-finding method and machine vision, when applied sequentially, allow for orienting a motorized platform equipped with a laser rangefinder and an absolute encoder for measuring the described quantities (the hypotenuse of the right triangle and the angle between the hypotenuse and the leg lying on the abscissa axis).

An array of sensitive photodiodes is installed on the moving object, onto which the laser rangefinder beam is directed. To simplify the operation of machine vision algorithms, it is proposed to install bright point light sources as markers along the perimeter. The radio direction-finding method is used for the primary targeting of the motorized platform, which includes a laser rangefinder and a video camera of the machine vision system. This approach allows for a significant reduction in the region of interest for machine vision. It should be considered that weather conditions can introduce distortions into the results and require the development of additional measures and technical means to compensate for their influence. If one of the components fails, an alarm signal must be generated by the self-diagnostic means.

An experimental verification of the proposed concept was carried out in simulated conditions. Field studies related to radio direction-finding measurements were conducted in an open area, located more than 40 km from the city boundary, outside the influence zone of high-voltage power lines and cellular operator base stations, according to the following methodology:

1. Installation of the receiving device in the line of sight of the transmitting device.

2. Measurement of the accuracy characteristics of the azimuth deviation of the signal's angle of arrival for distances from 1 to 50 m using amplitude modulation, binary phase-shift keying, and quadrature phase-shift keying.

3. Execution of a right turn and assessment of the deviation direction from the transmitting module. Measurement of the accuracy characteristics of the azimuth deviation of the signal's angle of arrival for distances from 1 to 50 m using amplitude modulation, as well as binary phase-shift keying and quadrature phase-shift keying.

4. Return of the receiving device to the line-of-sight zone. Measurement of the accuracy characteristics of the azimuth deviation of the signal's angle of arrival for distances from 1 to 50 m using amplitude modulation, binary phase-shift keying, and quadrature phase-shift keying.

5. Execution of steps 1-4 when moving the receiving device to the left.

Figure 3 shows the direction-finding spectra of signal direction angles in the binary phase-shift keying operation mode. A phased antenna array consisting of four whip antennas was used during the experiment. The angle values were obtained based on the method of signal phase difference on each receiving antenna using the MUSIC (MUltiple SIgnal Classification) algorithm[12,13]. The results of the accuracy characteristics for the used modulation types are presented in the Table.

During the experiment, a periodic deviation of the angle azimuth in the range from 35 to 50° for amplitude modulation and from 10 to 15° for quadrature phase-shift keying generation was observed. The distance from the receiving device to the stationary signal source transmitting device varied from 1 to 50 m, while the accuracy characteristics of the angle azimuth deviation for binary phase-shift keying changed within deviations of 5-7°. This method has potential in combination with machine vision for determining the coordinates of objects in a local coordinate system.

Furthermore, during the conducted experiments under laboratory conditions, testing of the positioning of the machine vision camera relative to a marker with installed point light sources – coordinate positioning markers (CPM) – was carried out. The marker image represents a geometric shape

[12] MUSIC Super-Resolution DOA Estimation. URL: https://www.mathworks.com/help/phased/ug/music-super-resolution-doa-estimation.html (accessed 10.04.2025).

[13] High Resolution Direction of Arrival Estimation. URL: https://www.mathworks.com/help/phased/ug/high-resolution-direction-of-arrival-estimation.html (accessed 10.04.2025).

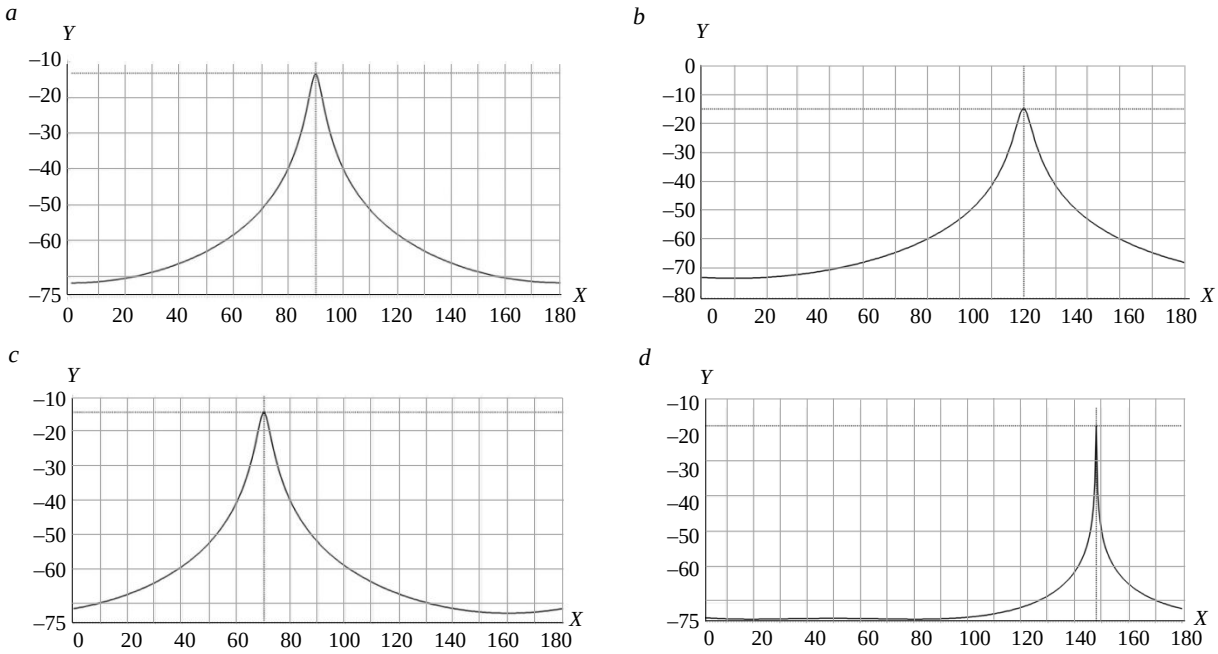

Fig.3. Front panel views during field studies:
a – direct line of sight to the object, azimuth 90°; *b* – object located to the right at a 120° angle;
c – object located to the left at a 70° angle; *d* – object located at a 148° angle;
X – signal strength, dBm; *Y* – directional spectrum of the signal arrival angle, deg

(a circle) and, from the standpoint of machine vision methods, is a vector gradient at the contour points [29] with distinctly bright pixels inside the contour. The Hough transform algorithm was chosen as the most accurate tool for determining the geometric correspondence of contours (Shape Detection) to the given shape.

Modulation types accuracy characteristics

Distance to signal source, m	Radio signal source angle azimuth, deg				
	Modulation type				
	Amplitude modulation	Root mean square deviation	Binary phase-shift keying	Quadrature phase-shift keying	Root mean square deviation
1	–	–	–	–	–
2	35-40	1.87	5	10-15	2.02
3	35-41	2.27	5	11-15	1.63
4	32-40	4.85	5	9-15	2.44
5	31-39	3.02	6	12-16	1.35
6	32-42	3.84	5-6	10-15	1.89
7	32-35	1.05	3	11-16	2.02
8	33-36	1.03	5	9-14	1.62
9	39-45	3.36	6	10-14	1.58
10	36-47	4.32	7	12-15	1.23
20	33-50	6.36	6	12-14	0.88
50	35-50	6.24	5	10-12	0.92

The installation of the central coordinate point in the allocated region of the reference light markers of the light board on the video image is defined as the central coordinate, relative to which the recognition of the contours of the circles of the horizontal and vertical CPM (three on the left or right) is carried out. Figure 4 shows an example of the image processing sequence when determining the

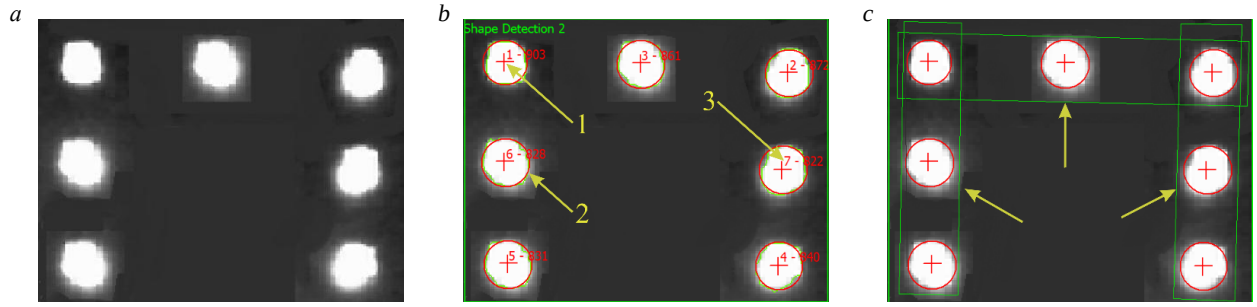

Fig.4. Image processing sequences for CPM recognition:
a – binarization of the original image (extraction of gray tones); *b* – the CPM image after processing with Hough algorithms; *c* – the result of determining horizontal and vertical correspondences

1 – recognized circle centers; 2 – recognized circle contours; 3 – determination of the CPM quantity

contours of the circles of the coordinate markers and their quantity under an illumination of 300 lm from a distance of 8 m by an NI 1742 Smart Camera with the following characteristics: matrix type – monochrome CCD, resolution – 640×480 pixels, pixel size – $7.4 \cdot 10^{-6}$ m by $7.4 \cdot 10^{-6}$ m, lens aperture – F/1.4.

The process of checking the position of the CPM control points horizontally and vertically by the machine vision system determines them so that the quantitative composition of all markers is within the rectangular area of the region of interest, both horizontally and vertically.

The control position is determined based on the region of interest, a rectangular allocated area in the video data stream. Accordingly, if the control position of the point light sources is determined with horizontal deviations, it is shifted by a specified angle. The control position of the point light sources is checked vertically in the same manner. A fragment of determining the CPM control position is shown in Fig.5. This is how the precise targeting of the laser rangefinder and the rotation of the absolute encoder shaft towards the marker installed on the moving object is performed.

The described method of position determination is shown in Fig.6 as an algorithm, where: S1 – start; O1 – construction of virtual coordinate axes; O2 – preparation and startup of the position determination devices; O3 – determination of the bearing to the moving object; D1 – decision "Bearing to the moving object found?"; M1 – message "Error in bearing detection. Repeat search?"; Mi1 – manual input "Yes/No"; E2 – end/stop; O4 – alignment of the position determination device on the moving object and the entrance gate mast along one axis according to the bearing data using motorized drives; O5 – fine-tuning of the direction using the machine vision system data via motorized drives; O6 – precise direction adjustment using the array of sensitive photodiodes and the laser emitter via motorized drives; O7 – measurement of the segment CB (see Fig.1, *c*) by the laser rangefinder and the rotation angle of the laser rangefinder ACB (see Fig.1, *d*) by the encoder of the position determination device in the left entrance gate mast; O8 – calculation of the moving object's coordinates; Ou1 – input of the moving object's coordinates into the control system.

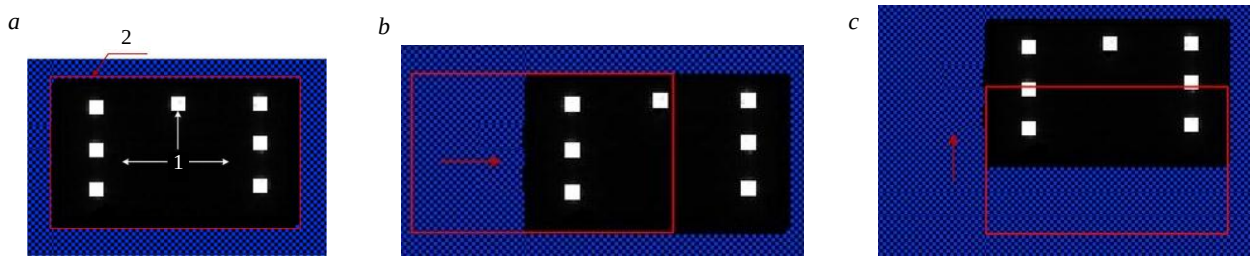

Fig.5. Verification of the reference position of point light sources by the machine vision system:
a – reference position of the CMP; *b* – horizontal region of interest definition;
c – vertical region of interest definition

1 – reference position of the fiducial markers; 2 – rectangular region of interest

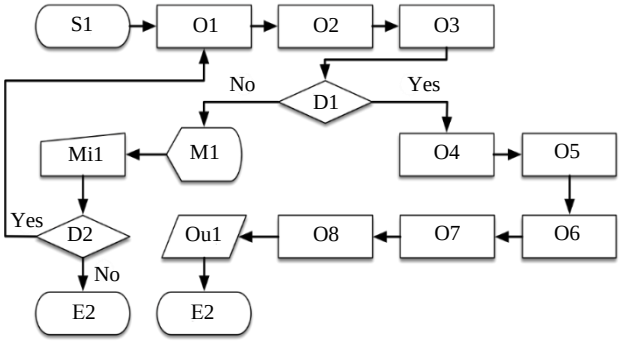

Fig.6. Algorithm for determining the coordinates of a moving object in the Cartesian coordinate system on a designated local area

Thus, the proposed approach, based on the application of a combination of machine vision methods, radio direction finding, laser rangefinding, and means for determining angular movements with sufficient resolution, allows for determining the position of equipment with a positioning error of no more than 1 m for every 200 m of distance between objects.

Conclusion

The analysis of the most common classical and alternative methods for positioning objects has shown the relevance of developing methods for the precise position determination of equipment in automated areas without the use of satellite navigation.

The proposed and described method for the mutual orientation of objects in a local coordinate system, using the example of determining the location of a stationary object relative to a moving one, which consists in using a machine vision system and a complex of auxiliary optical and direction-finding equipment by means of motorized rotary supports, allows, through the combined application of machine vision algorithms, the radio direction-finding method based on the MUSIC algorithm, and laser rangefinding means, to solve the problems of determining the coordinates of objects. Machine vision using the Hough method in recognizing CPM determines the specified number of light markers within the established region of interest.

The proposed method for the position determination of a loading machine, based on the application of machine vision methods, the direction-finding method, and laser rangefinding means, has demonstrated the operational capability of the proposed solutions. Collectively, the described solutions can be considered as a basis for building digital twins of the excavator-truck complex and can be applied to solve the problems of reducing downtime, increasing safety, and improving the transport logistics efficiency of mining enterprises.

REFERENCES

1. Damrin M.E. Evaluation of efficiency and increase of performance of mining equipment fleet for open pit mine operations. *Transport, mining and construction engineering: science and production.* 2024. N 27, p. 99-106 (in Russian). DOI: 10.26160/2658-3305-2024-27-99-106

2. Burakov A.M., Panishev S.V., Alkova E.L., Khosoev D.V. Experience of using hydraulic excavators in difficult mining, geological and climatic conditions. *Russian Mining Industry.* 2022. N 2, p. 90-96 (in Russian). DOI: 10.30686/1609-9192-2022-2-90-96

3. Klebanov D.A., Makeyev M.A., Sizemov D.N. Use of autonomous and remotely operated equipment in surface mining. *Russian Mining Industry.* 2020. N 6, p. 14-18 (in Russian). DOI: 10.30686/1609-9192-2020-6-14-18

4. Li Zhang, Wenxuan Shan, Bin Zhou, Bin Yu. A dynamic dispatching problem for autonomous mine trucks in open-pit mines considering endogenous congestion. *Transportation Research Part C: Emerging Technologies*. 2023. Vol. 150. N 104080. DOI: 10.1016/j.trc.2023.104080

5. Sizemov D.N., Temkin I.O., Deryabin S.A., Vladimirov D.Ya. On some aspects of increasing the target productivity of unmanned mine dump trucks. *Eurasian Mining*. 2021. N 2, p. 68-73. DOI: 10.17580/em.2021.02.15

6. Sishi M.N., Telukdarie A. Implementation of Industry 4.0 technologies in the mining industry – a case study. *International Journal of Mining and Mineral Engineering*. 2020. Vol. 11. Iss. 1, p. 1-22. DOI: 10.1504/IJMME.2020.105852

7. Chuprov S., Belyaev P., Gataullin R. et al. Robust Autonomous Vehicle Computer-Vision-Based Localization in Challenging Environmental Conditions. *Applied Sciences*. 2023. Vol. 13. Iss. 9. N 5735. DOI: 10.3390/app13095735

8. Cotroneo D., Russo S., Cornevilli F. et al. Implementing positioning services over an ubiquitous infrastructure. Second IEEE Workshop on Software Technologies for Future Embedded and Ubiquitous Systems, 11-12 May 2004, Vienna, Austria. IEEE, 2004, p. 14-18. DOI: 10.1109/WSTFES.2004.1300407

9. Gaber T., El Jazouli Y., Eldesouky E., Ali A. Autonomous Haulage Systems in the Mining Industry: Cybersecurity, Communication and Safety Issues and Challenges. *Electronics*. 2021. Vol. 10. Iss. 11. N 1357. DOI: 10.3390/electronics10111357

10. Nguyen H.A.D., Ha Q.P. Robotic autonomous systems for earthmoving equipment operating in volatile conditions and teaming capacity: a survey. *Robotica*. 2023. Vol. 41. Iss. 2, p. 486-510. DOI: 10.1017/S0263574722000339

11. Hamada T., Saito S. Autonomous Haulage System for Mining Rationalization. *Hitachi Review*. 2018. Vol. 67. N 1, p. 87-92.

12. Akl M.N. Elements of a methodology for modernizing a satellite geodetic network in a geologically unstable area. *Uspekhi sovremennogo estestvoznaniya*. 2023. N 6, p. 113-121. DOI: 10.17513/use.38061

13. Yastrebova A., Höyhtyä M., Boumard S. et al. Positioning in the Arctic Region: State-of-the-Art and Future Perspectives. *IEEE Access*. 2021. Vol. 9, p. 53964-53978. DOI: 10.1109/ACCESS.2021.3069315

14. Lassila M. The Arctic mineral resource rush and the ontological struggle for the Viiankiaapa peatland in Sodankylä, Finland. *Globalizations*. 2021. Vol. 18. Iss. 4, p. 635-649. DOI: 10.1080/14747731.2020.1831818

15. Dmitrieva D., Solovyova V. A Taxonomy of Mineral Resource Projects in the Arctic: A Path to Sustainable Financing? *Sustainability*. 2024. Vol. 16. Iss. 11. N 4867. DOI: 10.3390/su16114867

16. Seregin S.N., Gasanova Kh.N., Tazetdinov R.R. Resource potential of the Russian Arctic: possible facets of connecting mineral resources and water bioresources. *Economics, labor, management in agriculture.* 2023. N 3 (97), p. 150-161 (in Russian). DOI: 10.33938/233-150

17. Meggs R.W., Watson R.J. Spoofing and Jamming of GNSS Signals: Are They Real and What Can We Do About Them? Proceedings of the International Ship Control Systems Symposium (iSCSS), 6-8 October 2020, Delft, Netherlands. Institute of Marine Engineering, Science and Technology, 2020, p. 8. DOI: 10.24868/issn.2631-8741.2020.005

18. Zhijun Wu, Yun Zhang, Yiming Yang et al. Spoofing and Anti-Spoofing Technologies of Global Navigation Satellite System: A Survey. *IEEE Access*. 2020. Vol. 8, p. 165444-165496. DOI: 10.1109/ACCESS.2020.3022294

19. Cardellach E., Elósegui P., Davis J.L. Global distortion of GPS networks associated with satellite antenna model errors. *Journal of Geophysical Research: Solid Earth*. 2007. Vol. 112. Iss. B7. N B07405. DOI: 10.1029/2006JB004675

20. Teague S., Chahl J. An Algorithm for Affordable Vision-Based GNSS-Denied Strapdown Celestial Navigation. *Drones*. 2024. Vol. 8. Iss. 11. N 652. DOI: 10.3390/drones8110652

21. Psiaki M.L., Humphreys T.E., Stauffer B. Attackers can spoof navigation signals without our knowledge. Here's how to fight back GPS lies. *IEEE Spectrum*. 2016. Vol. 53. Iss. 8, p. 26-53. DOI: 10.1109/MSPEC.2016.7524168

22. von Hünerbein K. Detection and Monitoring of Jamming and Spoofing of GPS/GNSS Signals in Harbours and Industrial Areas. The European Test and Telemetry Conference, 11-13 June 2024, Nuremberg, Germany. AMA Association for Sensors and Measurement, 2024, p. 54-60. DOI: 10.5162/ETTC2024/A3.2

23. Keyuan Jiao, Maozhong Song, Xiaolong Tang et al. Two-Dimensional Differential Positioning with Global Navigation Satellite System Signal Frequency Division Relay Forwarding to Parallel Leaky Coaxial Cables in Tunnel. *Applied Sciences*. 2024. Vol. 14. Iss. 22. N 10288. DOI: 10.3390/app142210288

24. Kundiladi M.S., Rahim S.M.S.A., Rishad M.S. Secure Autonomous Vehicle Localization Framework using GMCC and FSCH-KMC under GPS-Denied Locations. *Annals of Emerging Technologies in Computing*. 2024. Vol. 8. N 3, p. 64-74. DOI: 10.33166/AETiC.2024.03.001

25. Kizilov S.A., Nikitenko M.S., Khudonogov D.Yu. Technical implementation of a method for excavator positioning in a face without using a satellite navigation. *Modern Science: actual problems of theory and practice. Series Natural and Technical Sciences.* 2024. N 12-2, p. 46-52 (in Russian). DOI: 10.37882/2223-2966.2024.12-2.11

26. Zakharov A.A., Tuzhilkin A.Y., Vedenin A.S. The algorithm for determining the position and orientation of three-dimensional objects from video images on the basis of a probabilistic approach. *Fundamental research.* 2014. N 11-8, p. 1683-1687 (in Russian).

27. Nikitenko M.S., Khudonogov D.Y., Popinako Y.V. Autonomous vehicle positioning approach based on machine vision and direction finding. *Modern Science: actual problems of theory and practice. Series Natural and Technical Sciences.* 2023. N 12-2, p. 84-86 (in Russian). DOI: 10.37882/2223-2966.2023.12-2.20

28. Molodtsov V., Kureev A. Experimental study of the applicability of the MUSIC algorithm for determining the direction of signal arrival. Informatsionnye tekhnologii i sistemy 2019 (ITIS 2019): Sbornik trudov 43-i mezhdistsiplinarnoi shkoly-konferentsii IPPI RAN, 17-22 sentyabrya 2019, Perm, Russia. Institut problem peredachi informatsii im. A.A.Kharkevicha RAN, 2019, p. 123-129.

29. Korobkov M.A., Petrov A.S. Direction of arrival estimation algorithms. *Electromagnetic Waves and Electronic Systems.* 2015. N 4, p. 3-32 (in Russian).

30. Barzegari V., Edrisi A. Optimal number and location of parking facilities in presence of autonomous vehicles. *Numerical Methods in Civil Engineering*. 2022. Vol. 7. Iss. 1, p. 70-83. DOI: 10.52547/nmce.2022.401

31. Mostafa A. The Principles of Celestial Navigation. Arab Academy for Science, Technology & Maritime Transport, 2019, p. 211.

32. Kramarov S.O., Mityasova O.Yu., Temkin I.O., Khramov V.V. Delaunay triangulation-based methodology of intelligent navigation and control of mobile objects. *Mining Informational and Analytical Bulletin.* 2021. N 2, p. 87-98 (in Russian). DOI: 10.25018/0236-1493-2021-2-0-87-98

33. Bansal S.K. Advancements in Digital Forensics: A Quantitative Analysis of Cell Tower Triangulation Techniques. *International Journal of Current Science Research and Review*. 2024. Vol. 7. Iss. 10, p. 7947-7954. DOI: 10.47191/ijcsrr/V7-i10-54

34. Zandbergen P.A. Accuracy of iPhone Locations: A Comparison of Assisted GPS, WiFi and Cellular Positioning. *Transactions in GIS*. 2009. Vol. 13. Iss. s1, p. 5-25. DOI: 10.1111/j.1467-9671.2009.01152.x

35. Stewart J., Hassan M.N., Sudin S. Location Based Systems over Wi-Fi Networks: Current Challenges and Future Directions. 3rd International Conference on Advanced Materials Engineering & Technology, 4-5 December 2014, Ho Chi Minh, Vietnam. 2014.

36. Lachvajderova L., Fil'o M. Real-Time Location Systems Across the Industries – Literature Review and Case Studies. *Acta Mechanica Slovaca*. 2024. Vol. 28. Iss. 3, p. 42-48. DOI: 10.21496/ams.2024.017

37. Sullivan B.P., Ghafoorpoor Yazdi P., Thiede S. Total Cost of Ownership of Real-Time Locating System (RTLS) Technologies in Factories. *Procedia CIRP*. 2023. Vol. 120, p. 822-827. DOI: 10.1016/j.procir.2023.09.082

38. Ermolaev V.T., Semenov V.Yu., Flaksman A.G. et al. Two-dimensional direction finding with super-resolution in an automotive MIMO radar under target correlation conditions. *Elektrosvyaz*. 2022. N 8, p. 45-52. DOI: 10.34832/ELSV2022.33.8.006

39. Yu-Chung Cheng, Yatin Chawathe, Anthony LaMarca, John Krumm. Accuracy characterization for metropolitan-scale Wi-Fi localization. MobiSys '05: Proceedings of the 3rd international conference on Mobile systems, applications, and services, 6-8 June 2005, Seattle, WA, USA. Association for Computing Machinery, 2005, p. 233-245. DOI: 10.1145/1067170.1067195

40. Bouguebrine C., Mikhailov A.V., Kazakov Yu.A. Control of excavator bucket positioning using sensors. *Transport, mining and construction engineering: science and production.* 2024. N 25, p. 169-175 (in Russian). DOI: 10.26160/2658-3305-2024-25-169-175

41. Núñez Fernández D. Implementation of a WiFi-based indoor location system on a mobile device for a university area. 2019 IEEE XXVI International Conference on Electronics, Electrical Engineering and Computing (INTERCON), 12-14 August 2019, Lima, Peru. IEEE, 2019, p. 4. DOI: 10.1109/INTERCON.2019.8853556

42. Khudonogov D.Yu., Nikitenko M.S., Kizilov S.A. Direction finding methods application for autonomous vehicles orientation in closed technological area. *Modern high technologies.* 2023. N 12-2, p. 239-245 (in Russian). DOI: 10.17513/snt.39888

43. Kizilov S.A., Nikitenko M.S., Khudonogov D.Yu. Determining excavator location in the face relative to a dump truck issue without using satellite navigation. *Modern high technologies.* 2024. N 12, p. 41-47 (in Russian). DOI: 10.17513/snt.40242

44. Ramtohul A., Khedo K.K. Mobile Positioning Techniques and Systems: A Comprehensive Review. *Mobile Information Systems*. 2020. Vol. 2020. N 3708521. DOI: 10.1155/2020/3708521

45. Venkat R. Challenges to overcome limitations of human centric practices in celestial navigation at sea. *International Journal of Health Sciences*. 2022. Vol. 6. N S6, p. 11080-11093. DOI: 10.53730/ijhs.v6nS6.13034

46. Teague S., Chahl J. Imagery Synthesis for Drone Celestial Navigation Simulation. *Drones*. 2022. Vol. 6. Iss. 8. N 207. DOI: 10.3390/drones6080207

47. de Almeida Martins F., Carrara V., D'Amore R. Positionless Attitude Estimation With Integrated Star and Horizon Sensors. *IEEE Access*. 2024. Vol. 12, p. 2340-2348. DOI: 10.1109/ACCESS.2023.3348077

48. Malkin R. Understanding the Accuracy of Astro Navigation. *The Journal of Navigation*. 2013. Vol. 67. Iss. 1, p. 63-81. DOI: 10.1017/S0373463313000520

49. Olson E. AprilTag: A robust and flexible visual fiducial system. 2011 IEEE International Conference on Robotics and Automation, 9-13 May 2011, Shanghai, China. IEEE, 2011, p. 3400-3407. DOI: 10.1109/ICRA.2011.5979561

50. Ryghaug M., Haugland B.T., Søraa R.A., Skjølsvold T.M. Testing Emergent Technologies in the Arctic: How Attention to Place Contributes to Visions of Autonomous Vehicles. *Science & Technology Studies*. 2022. Vol. 35. N 4, p. 4-21. DOI: 10.23987/sts.101778

51. Romashev A.O., Nikolaeva N.V., Gatiatullin B.L. Adaptive approach formation using machine vision technology to determine the parameters of enrichment products deposition. *Journal of Mining Institute*. 2022. Vol. 256, p. 677-685. DOI: 10.31897/PMI.2022.77

***Authors*: Mikhail S. Nikitenko,** *Candidate of Engineering Sciences, Head of Laboratory* (*Federal Research Center of Coal and Coal Chemistry of Siberian Branch of the RAS, Kemerovo, Russia*), *ltd.mseng@gmail.com*, *https://orcid.org/0000-0001-8752-1332*, **Danila Yu. Khudonogov,** *Researcher* (*Federal Research Center of Coal and Coal Chemistry of Siberian Branch of the RAS, Kemerovo, Russia*), *https://orcid.org/0000-0002-0208-790X*, **Sergei A. Kizilov,** *Candidate of Engineering Sciences, Senior Researcher* (*Federal Research Center of Coal and Coal Chemistry of Siberian Branch of the RAS, Kemerovo, Russia*), *https://orcid.org/0000-0003-2554-1383*.

The authors declare no conflict of interests.

ISSN 2411-3336; e-ISSN 2541-9404

JOURNAL OF MINING INSTITUTE

Zapiski Gornogo instituta

Journal homepage: pmi.spmi.ru

Research article

Geotechnical Engineering and Engineering Geology

Optimisation of blast-induced rock fragmentation using hybrid artificial intelligence methods at Orapa Diamond Mine (Botswana)

Onalethata Saubi✉, Rodrigo S. Jamisola Jr., Raymond S. Suglo, Oduetse Matsebe

Botswana International University of Science and Technology, Palapye, Botswana

***How to cite this article*:** Saubi O., Jamisola Jr. R.S., Suglo R.S., Matsebe O. Optimisation of blast-induced rock fragmentation using hybrid artificial intelligence methods at Orapa Diamond Mine (Botswana). Journal of Mining Institute. 2025. Vol. 275, p. 179-195.

Abstract

This study demonstrates various artificial intelligence methods to predict and optimise blast-induced rock fragmentation at Orapa Diamond Mine in Botswana. These techniques include an artificial neural network (ANN), an adaptive neuro-fuzzy inference system (ANFIS), a genetic algorithm with ANN (GA-ANN), and particle swarm optimization with ANN (PSO-ANN). A collection of data from 120 blasting events with nine input parameters at the mine was utilized for this task. The results indicate that the PSO-ANN model outperforms other models in predicting blast-induced fragmentation. We used the optimal PSO-ANN model to optimise fragmentation, identified using the Monte Carlo method. The optimal model consists of nine inputs, two hidden layers with 65 and 30 neurons, and one output (7-65-30-1). Using gradient descent, we navigated this ten-dimensional solution space to determine the optimised blast design parameters and achieved an optimal fragmentation value of approximately 86 %. Sensitivity analysis results reveal that the most influential input parameters on fragmentation are rock factor (15.3 %), blastability index (14.7 %), and spacing-to-burden ratio (14.7 %). In contrast, the stiffness ratio has the least influence on fragmentation (6.3 %).

Keywords

optimisation; prediction; blasting; rock fragmentation; artificial intelligence; sensitivity analysis; diamond mine

Funding

This research project was was funded by Debswana Diamond Company with grant N P00064.

Received: 03.10.2024 ***Accepted: 25.08.2025*** ***Online: 31.10.2025*** ***Published: 31.10.2025***

Introduction

Drilling and blasting are recognized as the most effective methods for rock fragmentation in the mining and civil engineering industries. This means that production blasting in mining plays a significant role in the subsequent operations, including loading, hauling, and crushing. Generating fragments with an optimal particle size distribution enhances the efficiency of these downstream processes [1]. Hence, the precise prediction of rock fragmentation following blasting is crucial in enhancing the overall economics of mining and plant operations [2]. Both controllable and uncontrollable parameters influence rock fragmentation. The controllable factors are the blasting design parameters and explosive properties, whereas uncontrollable parameters include the geomechanical properties of the rock [3, 4].

There are numerous empirical models designed to predict rock fragmentation [5-7]. Yet, these models often lack reliability and accuracy as they cannot capture the non-linear relationships among

all relevant parameters. This led to the application of artificial intelligence methods in mining engineering and rock mechanics [8-13]. N.Ghaeini et al. [14] used mutual information method (MI) for forecasting rock fragmentation from blasting at the Meydook Copper Mine. The Kuznetsov – Rammler model (KuzRam) was also used for comparison purposes. The model inputs involved ten input parameters with a dataset of 36 blasts. The study found the MI method was the most effective with an R^2 = 0.81. In a different study, S.Shams et al. [15] used a fuzzy inference system (FIS), multiple regression analysis (MRA), and empirical models by Kuznetsov and SveDeFo for predicting rock fragmentation. The FIS model outperformed the statistical and empirical models, achieving a coefficient of determination R^2 = 0.922.

P.Asl et al. [16] applied artificial neural network (ANN) aided by "firefly algorithm" (FFA) for predicting and optimizing rock fragmentation caused by blasting in the Tajareh limestone mine. The parameters that were considered for the study were (burden, blast-hole, spacing, hole length, sub-drilling, stemming, powder factor, charge in each delay and geological strength index (GSI). The R^2 value for the ANN from the study was 0.94 and sensitivity analysis showed that GSI and burden had the most influence on fragmentation. L.Dimitraki et al. [17] used a dataset from 100 blasts to predict the particle size from blast-induced fragmentation. They employed ANN, with powder factor, blastability index and quantity of blasted rock pile as inputs. The ANN had an R^2 value of 0.80 in predicting fragmentation. The SVR yielded superior results with the highest accuracy and the lowest error, while the Kuznetsov method had the lowest accuracy and highest error. Lastly, E.Ebrahimi et al. [18] employed ANN and an artificial bee colony (ABC) algorithm for predicting and optimizing back-break and rock fragmentation. As a benchmark, an empirical model (KuzRam) was used to predict the mean fragment size. The findings showed the ABC algorithm's superior capability to optimize rock fragmentation compared to the other models.

This work brings several contributions to the field. First, it applies blasting data from Debswana Diamond Company in Orapa, Botswana. Second, the study utilsises a dataset drawn from 120 blasting events. Third, it includes nine input parameters: spacing-to-burden ratio *S*/*B*, stiffness ratio *H*/*B*, stemming *T*, hole diameter *D*, powder factor *Pf*, the charge per delay *C*, and hole depth *L*, rock factor *Rf*, and blastability index *BI*. Fourth, it employs four machine learning techniques: ANN, adaptive neuro-fuzzy inference system (ANFIS), GA-ANN, and PSO-ANN. Fifth, the study models an eight-dimensional solution surface using PSO-ANN to predict, optimise and find inverse solution of blast-induced rock fragmentation with the gradient descent method. Lastly, a sensitivity analysis is performed using the network weights of the PSO-ANN model and validated through the SHapley Additive exPlanations (SHAP) method. The methodology proposed in this paper is compared with two related studies.

M.Hasanipanah et al. [19] predicted the rock fragmentation resulting from blasting activities in the Shur River dam region, situated in the Southern part of the Kerman province, Iran. They used a dataset comprising 72 blasts and five input parameters, namely, the maximum charge per delay, stemming, burden (RMR), spacing, and specific charge. Their study employed three machine learning algorithms, ANFIS, PSO-ANFIS, and SVR, along with a statistical non-linear multiple regression method. They carried out sensitivity analysis using the cosine amplitude method.

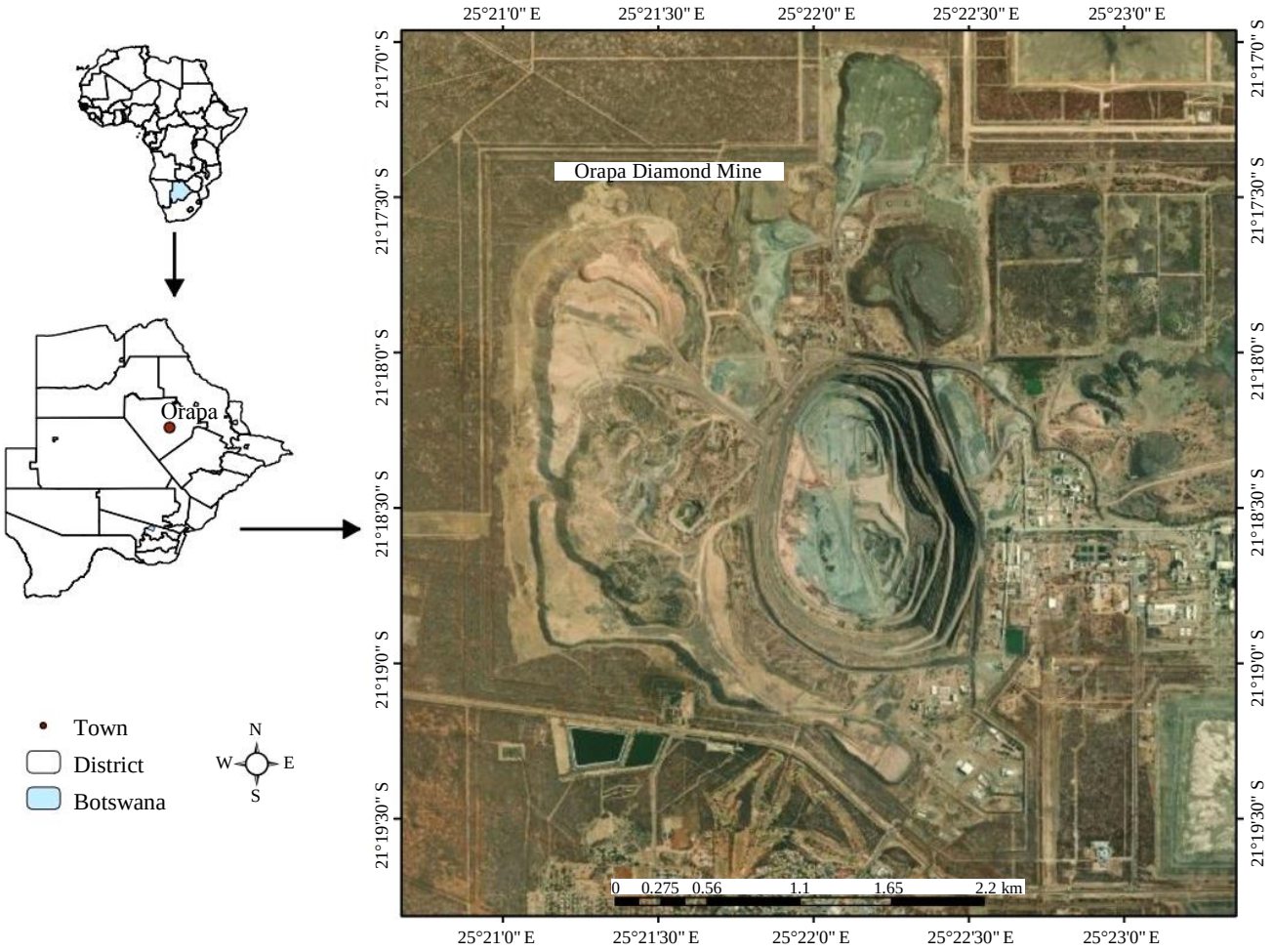

Fig.1. Orapa Diamond Mine

J.Zhou et al. [20] predicted blast-induced rock fragmentation in the Shur River dam region of Iran. They utilized a dataset involving 88 blasts and six input parameters, namely, maximum charge per delay, burden, powder factor, spacing, stemming, and rock mass rating RMR. They implemented five machine learning algorithms, specifically, ANFIS-GA, ANFIS-firefly algorithm (FFA), ANFIS, SVR, and ANN. They conducted a sensitivity analysis using the cosine amplitude method.

Mine Case Study. Orapa Diamond Mine is situated in Botswana, Southern Africa (Fig.1). The mine's resources include a single volcanic pipe that splits into deep north and south pipes, penetrating through Transvaal strata and Karoo sediments formed over 200 million years ago. The blasting operations employ a staggered pattern and primarily use two types of explosives: A and B. The bench height is 15 m, with blast holes that have diameters of 127, 165, and 250 mm. A typical row contains between 40 and 60 holes, and each blast involves 15 to 25 rows. Shovels, excavators, and rear dump trucks handle the blasted materials within the pit. Presently, the mining operations at Orapa reach a depth of 305 m and are projected to attain a depth of 350 m by 2026. Production fluctuates per mining plan, averaging about 2000 kg annually.

Methods

This section explores the dataset and methodologies employed in this study, focusing on the datasets collected from the mining operation, the machine learning techniques applied, and the optimization processes implemented.

Dataset. Blasting data with 120 blasting events was collected from the mine records for training and testing the models proposed in this research. An overview of the parameters and their ranges considered in this study is provided in Table 1.

Table 1

Input and output parameters

Parameter	Type	Min	Max
Stiffness ratio *H*/*B*	Input	2.5	3.75
Spacing to burden ratio *S*/*B*	Input	1.17	1.25
Stemming length *T*, m	Input	4	5
Hole depth *L*, m	Input	12.73	15.34
Hole diameter *D*, mm	Input	165	250
Charge per delay *C*, kg	Input	235.71	634.88
Powder factor *Pf*, kg/m^3	Input	0.3	1.2
Rock factor *Rf*	Input	3.26	7.62
Blastability index *BI*	Input	22	66
Fragmentation *Fr*, %	Output	70	81

Data preprocessing was first performed to ensure the quality and consistency of the dataset. This included cleaning, where missing or inconsistent values were handled, and normalisation, which scaled all input parameters to a uniform range to prevent features with larger magnitudes from dominating the learning process. The dataset was split into two subsets: 80 % for training and 20 % for testing. The training portion was further subjected to 6-fold cross-validation, where the data was partitioned into six equal folds (approximately 20 samples per fold). In this approach, five folds were used for training the model, while the remaining fold was used for validation, and the process was repeated six times to ensure that every sample contributed to both training and validation. The data pre-processing also includes a correlation matrix and principal components analysis. The performance indices used to assess the models are RMSE, R^2, and mean absolute error (MAE). Split Desktop software was used to analyse and produce the particle size distribution (PSD) curve for fragmentation using images captured with a digital camera. The quality of fragmentation at the mine is assessed based on 76 % passing the 150 mm sieve size, less than 50 mm is considered undersize while above 150 mm is considered oversize. Figure 2 shows an image of the muck pile and the PSD curve from the Split Desktop software.

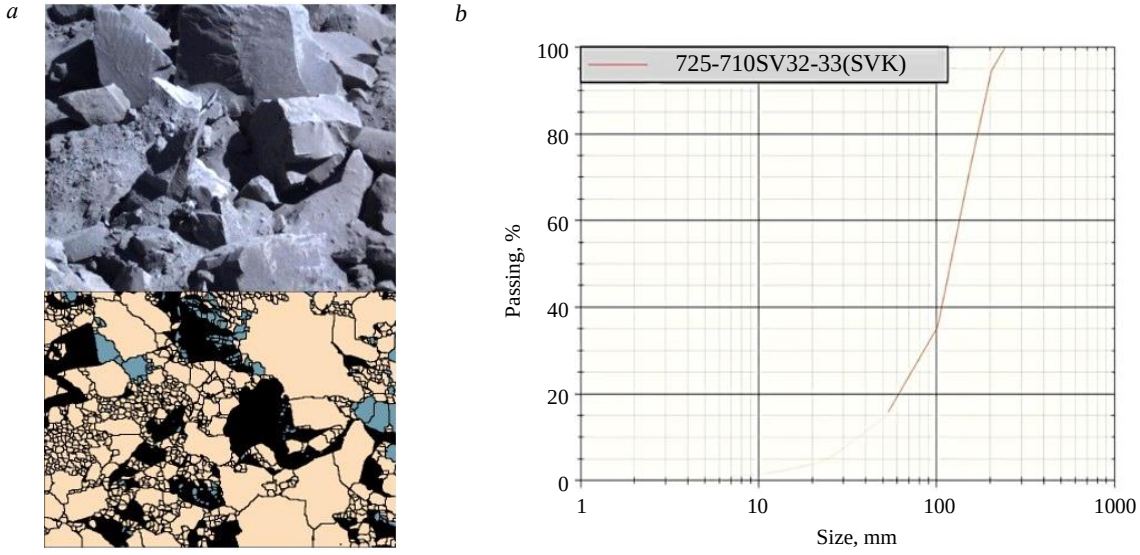

Fig.2. Muck pile image (*a*) and the Split Desktop PSD curve (*b*)

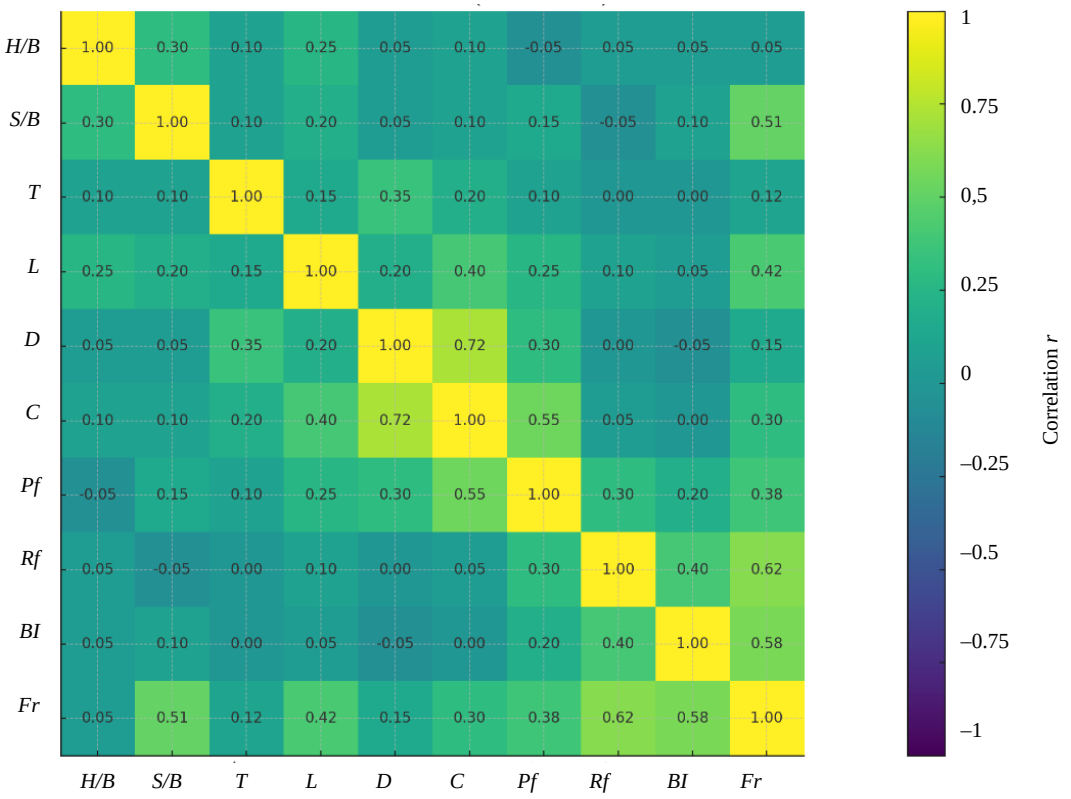

Fig.3. Correlation matrix

The correlation matrix (Fig.3) provides a linear snapshot of how rock and design variables relate to fragmentation *Fr*. The strongest positive links are with rock factor *Rf* ($r \approx 0.62$) and blastability index *BI* ($r \approx 0.58$), indicating that more favourable rock mass conditions tend to deliver finer breakage under comparable designs. Geometry also matters: spacing-to-burden *S*/*B* ($r \approx 0.51$) is moderately high, consistent with better burden relief and crack interaction across rows within the tested window. Energy delivery terms support these trends – hole depth *L* ($r \approx 0.42$) and powder factor *Pf* ($r \approx 0.38$) increase with finer product, reflecting a longer charged column and higher energy per unit rock. By contrast, the stiffness ratio *H*/*B* ($r \approx 0.05$) is near zero in this range, and hole diameter *D* shows only a small direct link to *Fr*, plausible where effective energy is governed more by charge *C* and *Pf*, and where decoupling or decking practices dilute any simple diameter effect.

Relationships among inputs align with practical design linkages. *D*-*C* ($r \approx 0.72$) is highest because larger holes accommodate higher charge mass; *C*-*Pf* ($r \approx 0.55$) follows since *Pf* scales with charge per rock volume. *T*-*D* ($r \approx 0.35$) reflects scaling of stemming to hole size to preserve gas sealing, while *H*/*B*-*S*/*B* ($r \approx 0.30$) co-moves because both ratios share the burden term. Overall, the matrix suggests that rock characteristics (*Rf*, *BI*) set the baseline fragmentation response, while geometry *S*/*B* and energy intensity (*Pf*, *L*, via *C*) act as the primary controllable levers. As this is a linear summary, non-linear or threshold effects common in blast geometry may be under-represented, so these correlations should be read as transparent guidance for design tuning rather than strict causal claims.

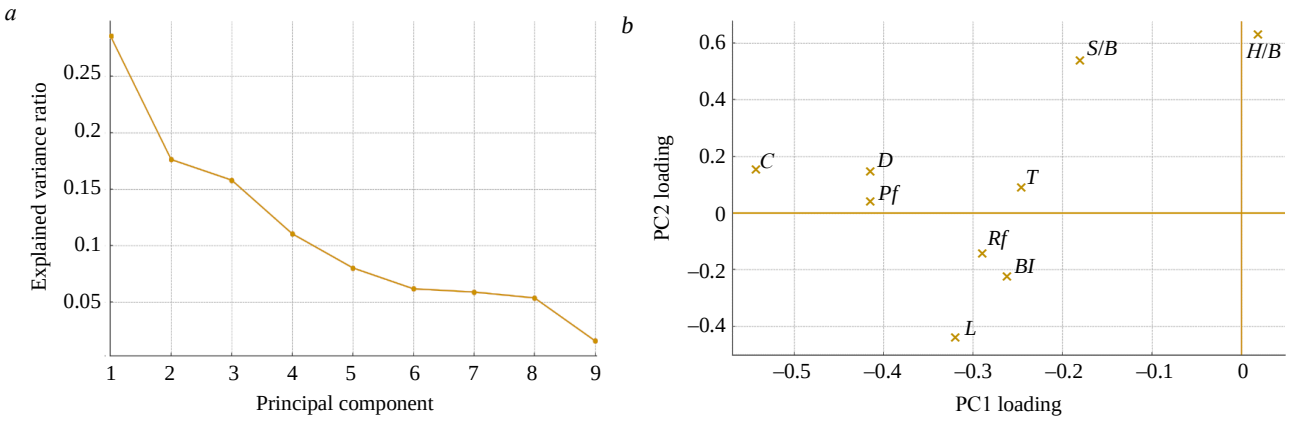

Fig.4. Principal component analysis: *a* – explained variance of the PCA components; *b* – PC1 and PC2 loadings

Principal component analysis (PCA) was applied to the nine input variables to summarise multicollinearity and reveal dominant blast design and rock factors. The first two components captured most of the input variance as shown by the scree plot in Fig.4, *a*. In Fig.4, *b*, PC1 is defined by large-magnitude loadings from *C*, *D*, *Pf* (and, to a lesser extent, *T* and *L*), representing an energy-scale axis (meaning greater hole, greater charge settings and more delivered energy). The PC2 contrasts relief ratios (*H*/*B*, *S*/*B*) against rockability indices (*Rf*, *BI*, negative), representing a rock-relief axis, meaning, given the same relief, tougher rockability needs more energy or design adjustment to hit the same fragmentation *Fr*. These results are consistent with the correlation matrix in Fig.3 in which relief/rockability variables (*S*/*B*, *BI*, *Rf*) dominate, with energy variables (*Pf*, *L*, *C*, *D*) providing a secondary, controllable influence.

AI methods. Several advanced machine learning techniques were utilised to predict rock fragmentation: ANN, PSO-ANN, ANFIS, and GA-ANN. Sensitivity analysis is conducted using the network weights of the best PSO-ANN model to determine the relative influence of input parameters on the output. The Monte Carlo method was utilised to systematically explore and evaluate various neural network architectures by varying the number of hidden layers (from one to three) and the corresponding number of neurons within each layer. This probabilistic sampling identified the optimum neural network architecture. Subsequently, gradient descent was applied to navigate the solution space and find the optimum value of rock fragmentation and the corresponding input parameters. To obtain a stable estimate of training runtime, the models were trained repeatedly for n = 10,000 cycles. At the start of the 10,000 cycles, we record the t_{start}. And at the end of the 10,000 cycles, we record t_{end}. The average cycle time was computed as $\overline{T} = (t_{end} - t_{start})/n$. All timings were measured on an HP ProBook 455 G8 (laptop-class Ryzen 7 5800U CPU, 8 GB RAM, integrated Radeon graphics) under Python 3.11/TensorFlow 2.19. No discrete GPU acceleration was used.

The final cleaned sample of n = 120 blasts (from 2016-2024) is appropriate for the study's objectives and parameter dimensionality (nine inputs), and it is in line with prior drill and blast modelling in the literature (Table 2), where high predictive accuracy has been achieved with datasets of similar or smaller size. To mitigate finite-sample risk and selection bias, we enforced a strict train/test separation with no leakage, used six-fold cross-validation only within the training set for model selection. On the blind test set, the best model (PSO-ANN) attains R^2 = 0.96 and RMSE = 0.17,

MAE = 0.30, consistent with the accuracy range reported for comparable sample sizes. Collectively, the dataset scale, alignment with published practice, and the validation/diagnostic controls support that the data are sufficient and fit-for-purpose for the modelling claims made.

Table 2

Performance indices from other studies

Best model	Other models	Inputs	Dataset	R^2	Reference
PSO-ANFIS	ANFIS; SVM; MNLR	*SC*, *T*, *S*, *B*, *MC*	72	0.89	[1]
ANN		*D*, *L*, *B/S*, *T*, *Nr*, *Pf*, *RD*, *Tc*	250	0.98	[2]
BPNN	BPNN; RBFNN	*B*, *S*, *L*, *T*, *SC*, *SD*	103	0.90	[4]
FIS	FIS	*B*, *S*, *D*, *SHRN*, *DJ*, *Pf*, *T*	185	0.92	[15]
FIS	MVRA	*B*, *S*, *L*, *SD*, *T*, *MC*, *RD*, *Pf*	415	0.80	[16]
ANN	SVR; ANN; MVRA; Kuznetsov	*S/B*, *L/B*, *B/D*, *T/B*, *Pf*, *E*, *Xb*	90	0.96	[17]
ANN	ABC	*B*, *S*, *L*, *T*, *Pf*	34	0.78	[18]
RES	MVRA	*B*, *MIC*, *SC*, *S/B*, *T/B*, *H/B*, *Nr*, *INCL*, *D*, *B/D*	52	0.86	[19]
FFA-ANFIS	GA-ANFIS; ANFIS; SVR; ANN	*B*, *S*, *T*, *Pf*, *MC*, *RMR*	88	0.98	[20]
FFA-ANN	FFA-ANN; FFA-ANFIS; SVM; GPR; SVM; KNN	*Pf*, *MC*, *S*, *T*, *B*, *H*	136	0.98	[2]
GPR	SVM; ANFIS; PSO-ANFIS	*B*, *S*, *Pf*, *T*, *E*	72	0.95	[21]
ANN	SVR; Kuznetsov	*S/B*, *L/B*, *B/D*, *T/B*, *Pf*, *E*, *Xb*	102	0.87	[22]
ANN	MVRA	*D, Pf, TC, L, T, D, S/B*	180	0.99	[23]
JSO-LGBM		*B*, *S*, *Pf*, *T*, *L*, *SD*	234	0.99	[24]
ANN		*S*, *B*, *T*, *Pf*, *Lc*, *D*, *L*	70	0.88	[25]
FFA-BGAM	FFA-ANN; ANFIS; SVM; GPR; KNN	*Pf*, *MC*, *S*	136	0.98	[26]
RES		*B*, *S/B*, *Pf*, *MH*, *H/B*, *HIL*, *HDVD*, *J/B*, *BI*, *IS*, *BHP*, *B/D*	64	0.93	[27]

Note. BGAM – boosted generalized additive model; BPNN – back propagation neural network; MVRA – multi-variate linear regression; RES, rock engineering system; JSO-LGBM, jellyfish search optimizer-light gradient boosting machine; *MIC* – maximum instantaneous charge; *INCL* – hole inclination; GPR – Gaussian process regression; *B*/*D* – burden to hole diameter; *L*/*B* – hole depth to burden; *T*/*B* – stemming to burden; *Xb* – *in situ* block size; *SC* – specific charge; *SD* – sub-drilling; *RD* – rock density; *J* – density of joints; *SHRN*, Schmidt hammer rebound number; *Nr* – number of rows; *PLI* – point load index; *Dr* – delay between rows; *MC* – maximum charge; *TC* – total charge per delay; *E* – elastic modulus; *UCS* – uniaxial compressive strength; *MH* – maximum holes per delay; *HIL* – hole inclination; *HDV* – hole deviation; *IS* – initiation sequence; *BHP* – blast hole pattern.

The highest-performing model in Table 2 is the jellyfish search optimizer-light gradient boosting machine (JSO-LGBM,) by M.Yari et al. [24], which achieved an R^2 of 0.99 using 234 datasets with six inputs (*B, S, Pf, T, L, SD*). This model's superior performance can be attributed a large dataset, and the optimisation capabilities of the Jelly fish search optimizer (JSO) combined with GBM, which likely captures non-linearities more effectively than other models. The lowest-performing model is the ANN by E.Ebrahimi et al. [18] with an R^2 of 0.78 using 34 datasets and five inputs (*B, S, L, T, Pf*). The limited dataset size and potentially less complex model architecture might have restricted the model's ability to generalize and capture the variability in the data, leading to lower predictive accuracy.

In the middle range, the GPR model by W.Gao et al. [21] achieved an R^2 of 0.95 using 72 datasets with five inputs (*B, S, Pf, T, E*) due to its ability to capture complex non-linear relationships using kernel functions like the radial basis function (RBF). Its uncertainty quantification makes it robust to noise, particularly in small-to-medium datasets like the 72 samples used. The GPR's smooth predictions, hyperparameter optimization, and flexibility in modeling intricate dependencies contributed to its strong performance.

Comparing these with our results, our PSO-ANN model achieved an R^2 of 0.96 with 90 datasets and seven inputs. It performs well and aligns closely with other high-performing models, such as the ANN by L.Dimitraki et al. [17], which achieved an R^2 of 0.96 with 90 blasting events. However, hybrid models that use advanced techniques and larger datasets, including FFA-ANN (R^2 = 0.98, Q.Fang et al. [2]) and ANN with larger datasets (R^2 = 0.97, M.Yari et al. [24]), perform slightly better than our model. These results imply that the accuracy and generalizability of model can be improved by increasing the dataset size and adding more inputs, allowing it to capture more complex interactions and improve generalizability, as seen in the highest-performing models.

Implementation of ANN. A three-layer feed-forward artificial neural network (ANN) was trained using the stochastic gradient descent method. To identify the optimal configuration for the network, a grid search combined with 6-fold cross-validation was performed. Several parameters were explored during grid search, including the number of hidden neurons (ranging from 5 to 50); learning rates (between 0.01 and 0.1); different activation functions such as rectified linear unit (ReLU), Sigmoid, and Tanh. Among these, the ReLU function consistently outperformed the others in terms of convergence and predictive accuracy. Table 2 demonstrates that a configuration with 15 neurons and a learning rate of 0.1 achieved the lowest RMSE across the folds. Training the three-layer ANN converged in 8 s for 100 epochs. Its dominant cost term is $O(N \cdot H)$, where N is the number of training samples processed per epoch; H is the number of hidden neurons (i.e., trainable weights), so that runtime increases with the increase in either N or H. When retraining, a warm start fine-tuning on an additional 10 % of new data was completed in ≈ 5 s.

Implementation of ANFIS. The ANFIS combines the principle of fuzzy logic into the neural network. The neural network constructs the *if – then* statements, acting as the rule building expert [28]. Grid search was used to tune the number of membership functions (ranging from 2 to 7), the type of membership function (Gaussian, triangular, and generalized bell), the learning rate (from 0.01 to 0.1), and the number of training epochs (50 to 150). A hybrid optimisation strategy, combining gradient descent with least squares estimation, was employed to fine-tune both premise and consequent parameters.

As illustrated in Table 2, the best model performance was achieved with three Gaussian membership functions and a learning rate of 0.1 across 100 epochs. Training the ANFIS model converged in 75 s. Its dominant cost term is $O(N \cdot R \cdot M)$, where R is the number of fuzzy rules created during learning; M is the number of membership functions assigned to each input variable. Because every sample is evaluated against every fuzzy rule, training samples, and membership functions, runtime rises quickly if more data, rules, or functions are added. When retraining, ANFIS did not support quick fine-tuning, and any new data require rebuilding and retraining the full rule set.

Implementation of GA-ANN. According to the literature, ANN performance has been effectively improved using GA [29, 30]. The GA is a stochastic search method capable of avoiding entrapment in local minima, a common drawback of ANNs. Due to the significant advantage of GA in performing multi-directional searches, it can find global minima and improve the prediction capability of ANN [31]. Therefore, the weights and biases of the ANN were updated using GA. To overcome local minima problems often encountered in backpropagation-based ANN training, a hybrid model combining GA and ANN was implemented.

A comprehensive grid search explored key GA parameters such as population size (10-50), mutation rates (1-10 %), number of generations (50-150), and crossover strategies (single-point and uniform). During cross-validation, each parameter set was evaluated based on average RMSE to ensure the robustness of the selected configuration. Table 2 shows that a population size of 20, a mutation rate of 5 %, and 100 generations yielded the lowest error, and highest accuracy.

Training the GA-ANN (population – 20, generations – 100) took 115 s. Its dominant cost term $O(P \cdot G \cdot H)$ depends on the genetic-algorithm population size P, the number of generations G, and the number of hidden neurons (weights) H in each network. Runtime therefore grows very fast if the population is enlarged, more generations are run, or a wider network is used. When retraining, because the genetic the search explores a new fitness landscape, a full retrain is usually needed whenever the data distribution changes.

Implementation of PSO-ANN. One of the shortcomings of ANN is that it can become stuck in the existence of local minima [32]. The PSO algorithm can search over a far larger space and locate global minima. As a result, the weights and biases of the neural network are updated to use the best positions discovered by the PSO method.

A three-layer back-propagation neural network was initialized with ten neurons in the hidden layer. Grid search was applied to explore a wide range of hyperparameters, including swarm size (10-50 particles), cognitive learning factor C_1 (1.0-2.0), social learning factor C_2 (1.5-2.0), inertia weight w (0.6-0.8), and the number of iterations (up to 150). The ANN architecture included a single hidden layer, and the number of neurons in this layer was also varied during the search. Table 3 reveals that the best-performing configuration used 30 particles, $C_1 = 1.3$, $C_2 = 1.8$, and an inertia weight of 0.8 over 100 iterations.

From Table 3, across all cross-validation metrics (R^2, RMSE, and MAE), the hybrid optimisation models consistently outperformed the standalone ANN and ANFIS models. PSO-ANN achieved the highest predictive accuracy with the lowest error values, followed closely by GA-ANN, while ANFIS showed moderate improvement over ANN.

Table 3

Cross-validation results for all the models

Model	Best parameters	Parameter (mean ± SD)		
		R^2	RMSE	MAE
ANN	Neurons – 15; LR – 0.01	0.87 ± 0.03	1.15 ± 0.28	1.67 ± 0.19
ANFIS	MF – 3; epochs – 200	0.89 ± 0.05	1.13 ± 0.32	1.34 ± 0.25
GA-ANN	Neurons – 15; generations – 100; population – 20	0.93 ± 0.02	1.08 ± 0.21	1.12 ± 0.14
PSO-ANN	Neurons – 15; particles – 30	0.95 ± 0.01	0.95 ± 0.17	0.85 ± 0.11

All the models exhibited low standard deviation (CD) values across the cross-validation folds, indicating that their performance remained stable and consistent regardless of how the data was partitioned. This consistency, combined with the progressive improvement observed in the hybrid models, highlights the effectiveness of incorporating metaheuristic optimisation in enhancing model generalisation and reducing prediction errors. Training the PSO-ANN (swarm = 30 particles, iterations = 100) completed in 105 s. The dominant cost term $O(S \cdot I \cdot H)$ shows very fast growth with the increase in swarm size S, the number of position-velocity update iterations I, and the hidden-layer size H. When retraining, the swarm's last positions can be warm started, so an incremental update on fresh data is quicker than the initial run. Table 4 summarises the complexity or dominant cost expressions alongside the measured training time and the retraining considerations.

Table 4

Computational profile of the evaluated AI models: runtime, complexity, and retraining considerations

Model	Train time	Dominant cost	Retraining note
ANN	8 s (100 epochs)	$O(N{\cdot}H)$	Fine-tune on 10 % new data – 5 s
ANFIS	75 s	$O(N{\cdot}R{\cdot}M)$	Must retrain full rule-sets
GA-ANN	115 s (population – 100; generations – 20)	$O(P{\cdot}G{\cdot}H)$	Retrain required when data distribution shifts
PSO-ANN	105 s (swarm – 30; iterations – 100)	$O(S{\cdot}I{\cdot}H)$	Incremental update possible via warm start

Sensitivity analysis. A sensitivity analysis was performed to assess the impact of input parameters on fragmentation using the network weights of the best-performing algorithm [33]:

$$Ij = \frac{\sum_{m=1}^{m=Nh}\left(\left(\frac{W_{jm}^{ih}}{\sum_{k=1}^{Ni}\left|W_{jm}^{ih}\right|}\right) X \left|W_{mn}^{ho}\right|\right)}{\sum_{k=1}^{k=Ni}\left\{\sum_{m=1}^{m=Nh}\left(\frac{\left|W_{jm}^{ih}\right|}{\sum_{k=1}^{Ni}\left|W_{jm}^{ih}\right| X \left|W_{mn}^{ho}\right|}\right)\right\}},$$

where Ij indicates the relative importance of the j-th input variable on the output variable, ranging 0-1; N_i, N_h denote the number of neurons in the input and hidden layers, respectively. The network weights are represented by W; the superscripts i, h, o – correspond to the input, hidden, and output layers, respectively, while the subscripts k, m, n – denote the neuron numbers in the input, hidden, and output layers, respectively.

***Gradient descent optimisation*.** This study employs gradient descent optimization alongside the Monte Carlo technique to fine-tune the architecture of the PSO-ANN used. The goal is to optimize a model with seven inputs, one output, and two hidden layers, specifically to determine the optimal number of neurons, which are 50 in the first layer and 25 in the second. Gradient descent, a widely used iterative optimisation algorithm in computational and machine learning applications, was employed to efficiently search the solution space to achieve maximum fragmentation and determine optimal blast-design parameters [34]. The underlying principle of gradient descent involves iteratively updating parameters by moving them in the direction opposite to the gradient of the objective function, thereby gradually converging towards the optimum. In this study, the gradient descent algorithm updates each input parameter according to the following rule:

$$P_i^{\text{new}} = P_i - \eta * \left(\frac{f\left(P_i,...,P_{i,}\ldots,P_N\right) - f\left(P_i,\ldots,P_i^{\text{old}},\ldots,P_N\right)}{P_i - P_i^{\text{old}}}\right),$$

where P_i represents the current value of the parameter being optimised; the term P_i^{old} denotes the parameter's value from the previous iteration, allowing the numerical calculation of the gradient via finite differences; the learning rate is represented as η, a small positive value controlling the magnitude of each update step, thus influencing both the stability and speed of convergence; the function f represents the PSO-ANN, which predicts rock fragmentation based on the blast design parameters.

Specifically, we set the learning rate η = 0.05 to ensure stable yet sufficiently rapid convergence. The iterative updates continued until the change in predicted fragmentation between consecutive iterations became less than 10^{-4}, with a maximum allowable number of iterations set at 200 to prevent indefinite computations. Furthermore, by explicitly fixing the random seed at 42, this optimisation process is rendered fully reproducible.

Results and discussion

Three key performance indices were employed to assess each predictive model's efficacy: RMSE, MAE, and R^2:

$$\text{RMSE} = \sqrt{\frac{1}{n}\sum_{i=1}^{n}\left(y_i - y_i'\right)^2};$$

$$\text{MAE} = \frac{1}{n}\sum_{i=1}^{n}\left|y_i - y_i'\right|;$$

$$R^2 = 1 - \frac{\sum_{i=1}^{n}\left(y_i - y_i'\right)^2}{\sum_{i=1}^{n}\left(y_i - \bar{y}_i\right)^2},$$

where n is the number of observations; y_i and y_i' are the measured and predicted values of the i-th observation, respectively; and $\bar{y}_i$ is the mean value.

Table 5 presents the performance indices of the best-performing configurations of each model on both the training and testing datasets. Across all metrics, the results demonstrate notable variations in predictive capability depending on the chosen modelling approach and hyperparameter configuration. The PSO-ANN model stands out as the best performer, achieving the highest R^2 values (0.94 for training and 0.96 for testing) and the lowest error metrics (RMSE = 0.13 and 0.17; MAE = 0.25 and 0.30 for training and for testing). This indicates that the particle swarm optimisation algorithm effectively fine-tuned the ANN parameters, enabling the model to learn complex input-output relationships while maintaining excellent generalisation to unseen data. The GA-ANN model also performed strongly, with R^2 values of 0.93 in both training and testing and comparably low RMSE and MAE values, confirming the benefit of using genetic algorithms for parameter optimisation.

Table 5

Best models calculated performance indices on the training and testing set

Model	Parameter	Training			Testing		
		R^2	RMSE	MAE	R^2	RMSE	MAE
ANN	Neurons – 15	0.87	0.45	0.50	0.85	1.75	1.57
GA-ANN	Population – 10	0.93	0.15	0.80	0.93	0.80	0.47
PSO-ANN	Particle size – 30	0.94	0.13	0.25	0.96	0.17	0.30
ANFIS	MF – 3	0.91	0.42	0.50	0.87	1.36	1.08

The ANFIS model, although not the top performer, achieved solid results with R^2 values of 0.91 (training) and 0.87 (testing). This shows that its hybrid neuro-fuzzy approach can capture nonlinear relationships in the blasting data effectively, even without metaheuristic optimisation. In contrast, the ANN model exhibited the lowest predictive capability, with R^2 values of 0.87 (training) and 0.85 (testing) and higher error metrics, suggesting that the basic network struggled to capture the data complexity compared to the hybrid approaches.

All models achieved high R^2 values during training, indicating they learned the patterns in the dataset well. The testing performance also remained strong, especially for the hybrid models (GA-ANN and PSO-ANN), demonstrating good generalisation and minimal overfitting. The progression in results clearly highlights the impact of metaheuristic optimisation in improving predictive accuracy and stability for blast fragmentation modelling.

Figure 5, *a* illustrates that the predictions made by PSO-ANN model closely align with the actual fragmentation measurements, thus highlighting the model's superiority in predicting fragmentation when compared with other models. The PSO-ANN model performs better than GA-ANN, ANFIS, and ANN due to the efficiency of PSO in exploring the search space and avoiding local minima, its capability to dynamically adjust velocity and position, and its computational efficiency. The PSO's simpler update mechanisms allow it to find optimal solutions faster and more accurately than GA while avoiding the scalability issues of ANFIS. This hybrid approach leverages the strengths of both PSO and ANN, optimizing the neural network weights more effectively and leading to higher prediction accuracy.

Figures 5, *b-d* display the correlations between the observed and estimated fragmentation for each model. The majority of data points lie reasonably close to the best-fit line for all models, indicating their potential for fragmentation prediction. Among all the models, the ANN model's data points diverge most from the best-fit line, therefore it has the lowest coefficient of determination R^2. This shows that optimization algorithms can improve the performance of the ANN model, as all the optimized models (ANFIS, GA-ANN, PSO-ANN) perform better than the standalone ANN.

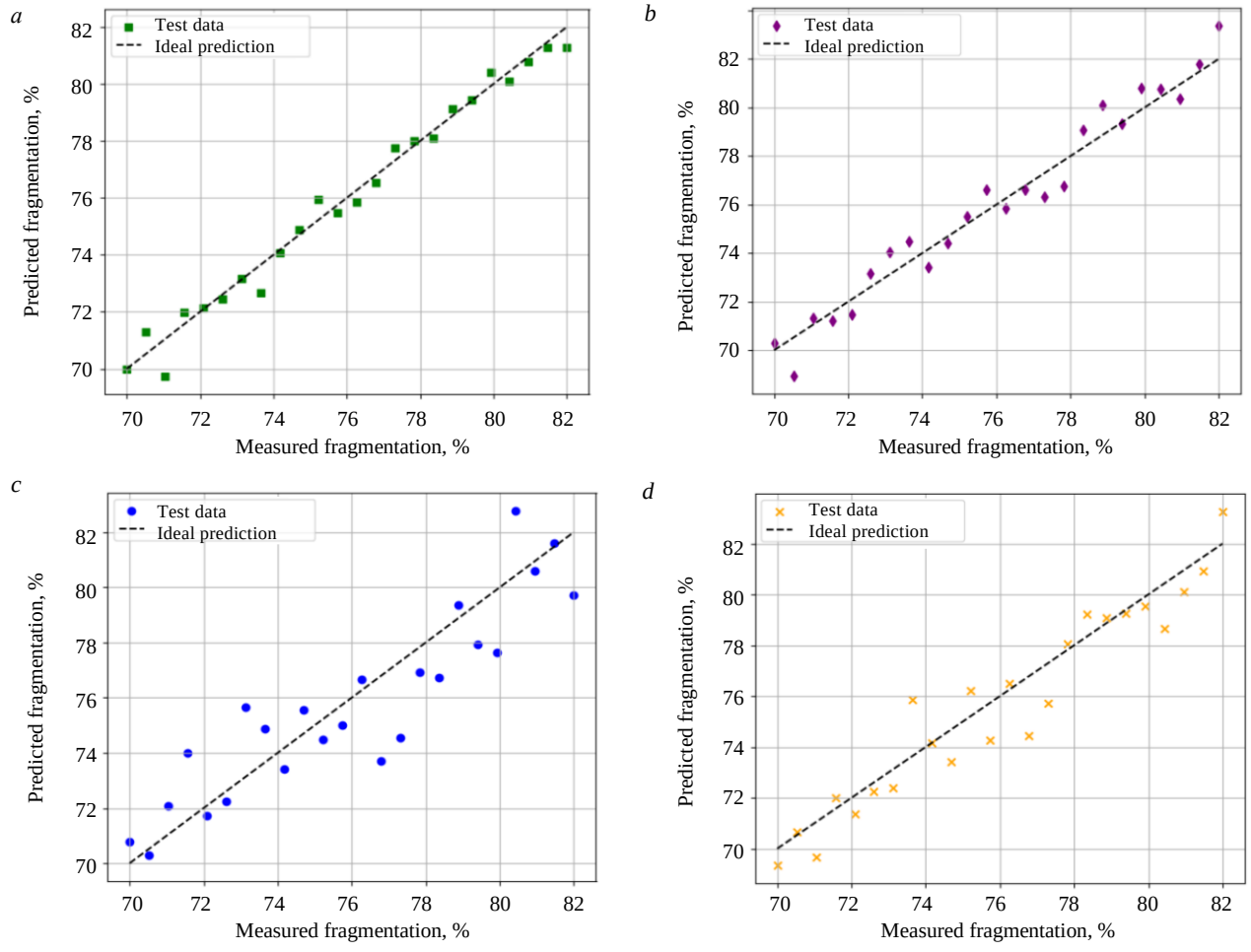

Fig.5. Scatter plots for the study models: *a* – PSO-ANN; *b* – GA-ANN; *c* – ANN; *d* – ANFIS

Sensitivity analysis. Figure 6, *a* shows a radar chart, each axis of the chart represents one of the input parameters (*H*/*B*, *S*/*B*, *T*, *L*, *D*, *C*, *Pf*, *Rf*, *BI*), the strength index I_j values are plotted along these axes. The area enclosed by the blue polygon reflects the relative sensitivity of each parameter. The blastability index *BI*, rock factor *Rf*, spacing-to-burden ratio *S*/*B* are the most influential input parameters, accounting for 15.3, 14.7 and 14.7 %, respectively, as indicated by the longest extension of the blue polygon. The stiffness ratio is the least effective parameter *H*/*B* (6.3 %) on fragmentation, with the shortest extension of the blue polygon. The sensitivity analysis highlights the critical role of the S/B ratio in influencing fragmentation [35-37]. These parameters should be given priority during the blast design process. The high sensitivity of the *BI*, *Rf* and especially *S*/*B* ratio as a controllable parameter, suggests that even minor adjustments can lead to significant changes in rock fragmentation, providing a powerful lever for engineers to control blast outcomes. On the other hand, the relatively low sensitivity of the *H*/*B* ratio indicates that it can be considered a secondary factor, allowing engineers to focus their optimisation efforts on more influential parameters. These sensitivity rankings are consistent with the correlation analysis, which also indicates strong positive associations for *BI*, *Rf* and *S*/*B* and a near-zero association for *H*/*B*.

Figure 6, *b* presents the mean absolute SHAP values for fragmentation *Fr*, illustrating the average contribution of each input parameter to the model's prediction. SHAP is a unified framework based on cooperative game theory that explains individual predictions by computing the contribution of each feature relative to a baseline expectation [38]. From the figure, rock factor *Rf* emerges as the most influential parameter, followed by hole depth *L*, blastability index *BI*, and powder factor *Pf*. Other parameters such as stemming *T*, stiffness ratio *H*/*B* and hole diameter *D* have lower impacts.

These findings are consistent with the sensitivity analysis in Fig.6, *a* and the correlation matrix, confirming the robustness of the results. The agreement between SHAP and the sensitivity approach enhances confidence in the model's interpretability and aligns with known blast physics, where rock properties and hole design factors dominate fragmentation outcomes.

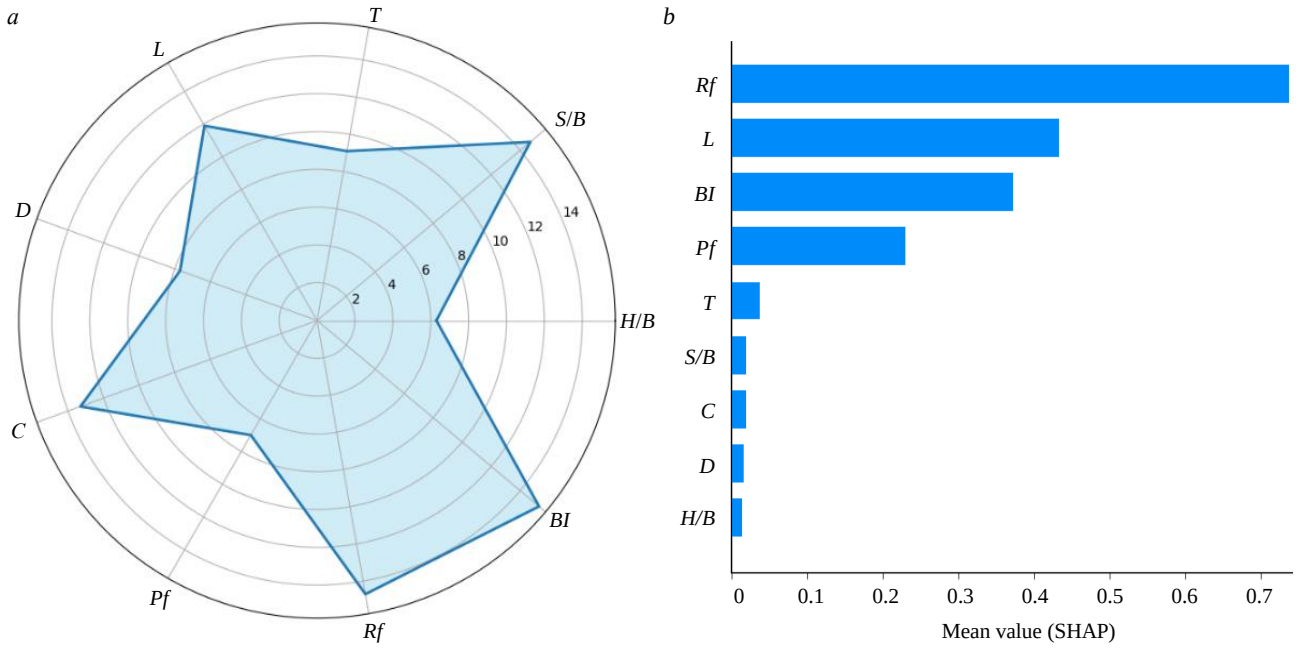

Fig.6. Sensitivity analysis (*a*) and mean absolute SHAP values (average impact on model output magnitude) for fragmentation (*b*)

Optimisation to maximize fragmentation. Figures 7, *a-d* illustrate the outcomes of the optimisation process, starting with seven initial points (represented as red dots) selected randomly and converging towards the optimised value (shown as blue dot). This optimisation enhanced fragmentation to about 86 %, with the refined input parameters being: powder factor *Pf* 0.56; charge per delay *C* 374; spacing to burden ratio *S*/*B* 1.2; stiffness ratio *H*/*B* 2.5; stemming *T* 4.6; hole depth *L* 15.5; diameter *D* 191; rock factor *Rf* 8 and blastability index *BI* 65.

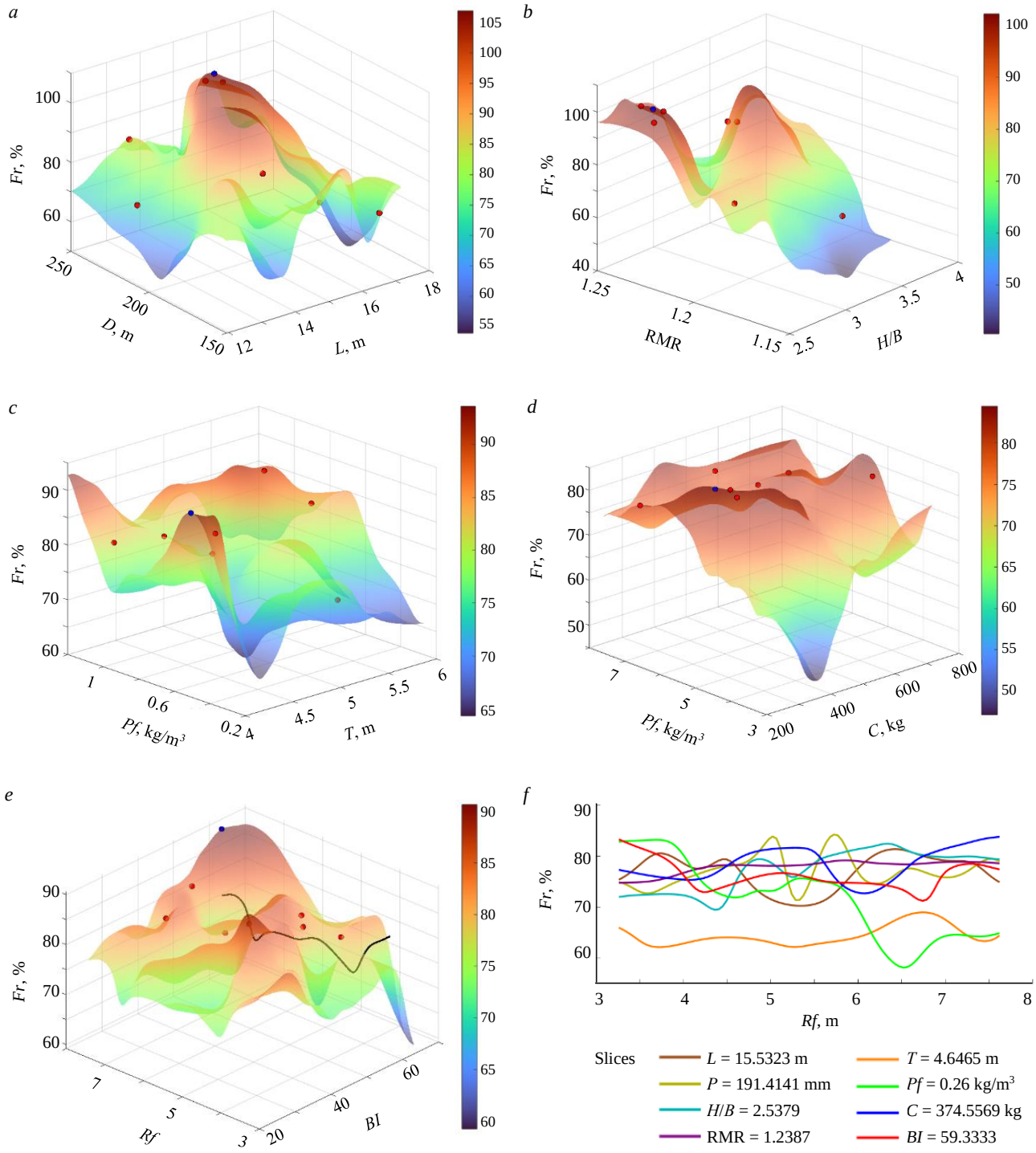

Fig.7. Solution space for rock fragmentation as the output parameter with input parameters, taken two at a time dependencie of hole diameter and hole dept on fragmentation *Fr* (*a*); spacing to burden ratio and stiffness ratio on *Fr* (*b*); powder factor and stemming on *Fr* (*c*); rock factor and charge per delay on *Fr* (*d*); rock factor and blastability on *Fr* (*e*) and combined plot for the 2-dimensional slices (*f*)

The highest point on the solution surface corresponds to the maximum value of rock fragmentation predicted by the model (approximately 86 %). Every point in the solution surface has ten components, i.e., nine components of the input parameters plus the output component of rock fragmentation. The solution surface is capable of prediction, optimisation and inverse solution. At the same time, the solution surface affords a visualisation of the interactions of the different parameters with the output.

In Fig.7, *e*, increasing the rock factor while keeping the blastability index (the blastability index is kept constant in the traced curve that includes the blue dot which is the minimum point) fixed results in fragmentation gradually decreasing and then increasing with fluctuations to an optimal value of fragmentation.

Figure 7, *f* shows rock fragmentation versus rock factor, the most influential input parameter, presented in a 2D plot. The values of the other nine input parameters at the optimal point are kept constant, while rock factor is plotted in its entire range.

The solution space also confirms the results of the sensitivity analysis. As shown in Fig.7, *f*, generated by varying the rock factor fixing all the other parameters, and taking a slice through the highest, optimised point in the solution space. Blastability index and spacing to burden ratio are the second most influential input parameters after rock factor and have sharp fluctuations/variations ranging from about. This indicates a high sensitivity, as changes in spacing to burden ratio significantly impact fragmentation. The stiffness ratio is the least influential parameter, this parameter shows gentle fluctuations, also suggesting lower sensitivity.

This optimisation has several practical benefits: it enhances efficiency by reducing the energy and time needed for crushing and grinding, lowers blasting operation costs by using explosives more effectively, improves safety by ensuring stable blasting conditions, reduces environmental impact through lower vibrations, and optimizes resource management by accurately utilizing drilling and blasting resources. These optimized parameters significantly enhance the operational efficiency, safety, and cost-effectiveness of the blasting process.

Conclusions

This study presents a methodology for predicting and optimising the particle size distribution of muck piles resulting from blasting operations at the Orapa Mine in Botswana, managed by Debswana. In this research, various artificial intelligence techniques were employed, including ANN, GA-ANN, ANFIS, and PSO-ANN. These models were trained using data from 120 blasting events. Nine input parameters were selected to predict and optimise fragmentation.

The results indicate that the PSO-ANN model out- performed the others, achieving the highest R^2 value of 0.96 and the lowest RMSE and MAE values of 0.17 and 0.30, respectively for the test set. Consequently, the PSO-ANN hybrid model proved to be the most suitable for predicting fragmentation. Optimisation of fragmentation through gradient descent, aided by the Monte Carlo method to find the optimal architecture, enhanced the fragmentation to approximately 86 %. The optimal architecture derived from the Monte Carlo method is 7-65-30-1. The optimal input parameters are: powder factor Pf – 0.56 kg/m^3, charge per delay C – 374 kg, spacing to burden ratio RMR – 1.2, stiffness ratio H/B – 2.5, stemming T – 4.6 m, hole depth L – 15.5 m, diameter D – 191 mm, rock factor Rf – 8 and blastability index BI – 65. Sensitivity analysis results reveal that the most influential input parameters on fragmentation are rock factor, blastability index, and spacing-to-burden ratio, with 15.3, 14.7 and 14.7 %, respectively. In contrast, the stiffness ratio 6.3 % has the least influence on fragmentation.

The modelling framework developed in this study is designed to be scalable and adaptable to other mining sites. The results obtained here can serve as a baseline model, which can then be refined by incorporating site-specific data. Through iterative recalibration and validation, the model's parameters can be adjusted until prediction errors are minimised, ensuring that the adapted model accurately represents the conditions of the new site.

The authors would like to thank Orapa Diamond Mine for supplying the data in this research. Special appreciation is extended to Mr. Thuso Mogotsi and Mr. Matenga Joe Chite from Debswana for their help in coordinating this research project.

REFERENCES

1. Hasanipanah M., Amnieh H.B., Arab H., Zamzam M.S. Feasibility of PSO–ANFIS model to estimate rock fragmentation produced by mine blasting. *Neural Computing and Applications*. 2018. Vol. 30. Iss. 4, p. 1015-1024. DOI: 10.1007/s00521-016-2746-1
2. Qiancheng Fang, Hoang Nguyen, Xuan-Nam Bui et al. Modeling of rock fragmentation by firefly optimization algorithm and boosted generalized additive model. *Neural Computing and Applications*. 2021. Vol. 33. Iss. 8, p. 3503-3519. DOI: 10.1007/s00521-020-05197-8
3. Bakhtavar E., Khoshrou H., Badroddin M. Using dimensional-regression analysis to predict the mean particle size of fragmentation by blasting at the Sungun copper mine. *Arabian Journal of Geosciences*. 2015. Vol. 8. Iss. 4, p. 2111-2120. DOI: 10.1007/s12517-013-1261-2
4. Zhi Yu, Xiuzhi Shi, Xianyang Qiu et al. Optimization of postblast ore boundary determination using a novel sine cosine algorithm-based random forest technique and Monte Carlo simulation. *Engineering Optimization*. 2021. Vol. 53. Iss. 9, p. 1467-1482. DOI: 10.1080/0305215X.2020.1801668
5. Esmaeili M., Salimi A., Drebenstedt C. et al. Application of PCA, SVR, and ANFIS for modeling of rock fragmentation. *Arabian Journal of Geosciences*. 2015. Vol. 8. Iss. 9, p. 6881-6893. DOI: 10.1007/s12517-014-1677-3
6. Dumakor-Dupey N.K., Arya S., Jha A. Advances in Blast-Induced Impact Prediction – A Review of Machine Learning Applications. *Minerals*. 2021. Vol. 11. Iss. 6. N 601. DOI: 10.3390/min11060601
7. Jian Zhou, Yulin Zhang, Yingui Qiu. State-of-the-art review of machine learning and optimization algorithms applications in environmental effects of blasting. *Artificial Intelligence Review*. 2024. Vol. 57. Iss. 1. N 5. DOI: 10.1007/s10462-023-10636-8
8. Kaklis K., Saubi O., Jamisola R., Agioutantis Z. Machine Learning Prediction of the Load Evolution in Three-Point Bending Tests of Marble. *Mining, Metallurgy & Exploration*. 2022. Vol. 39. Iss. 5, p. 2037-2045. DOI: 10.1007/s42461-022-00674-1
9. Saadati G., Javankhoshdel S., Javad Mohebbi Najm Abad et al. AI-Powered Geotechnics: Enhancing Rock Mass Classification for Safer Engineering Practices. *Rock Mechanics and Rock Engineering*. 2024, p. 1-31. DOI: 10.1007/s00603-024-04189-7
10. Kaklis K., Saubi O., Jamisola R., Agioutantis Z. A preliminary application of a machine learning model for the prediction of the load variation in three-point bending tests based on acoustic emission signals. *Procedia Structural Integrity*. 2021. Vol. 33, p. 251-258. DOI: 10.1016/j.prostr.2021.10.031
11. Taihua Yang, Tian Wen, Xing Huang et al. Predicting Model of Dual-Mode Shield Tunneling Parameters in Complex Ground Using Recurrent Neural Networks and Multiple Optimization Algorithms. *Applied Sciences*. 2024. Vol. 14. Iss. 2. N 581. DOI: 10.3390/app14020581
12. Zhiheng Ma, Jinguo Wang, Yanrong Zhao et al. Research on Multi-Objective Optimization Model of Foundation Pit Dewatering Based on NSGA-II Algorithm. *Applied Sciences*. 2023. Vol. 13. Iss. 19. N 10865. DOI: 10.3390/app131910865
13. Lawal A.I. A new modification to the Kuz-Ram model using the fragment size predicted by image analysis. *International Journal of Rock Mechanics and Mining Sciences*. 2021. Vol. 138. N 104595. DOI: 10.1016/j.ijrmms.2020.104595
14. Ghaeini N., Mousakhani M., Amnieh H.B., Jafari A. Prediction of blasting-induced fragmentation in Meydook copper mine using empirical, statistical, and mutual information models. Arabian Journal of Geosciences. 2017. Vol. 10. Iss. 18. N 409. DOI: 10.1007/s12517-017-3189-4
15. Shams S., Monjezi M., Majd V.J., Armaghani D.J. Application of fuzzy inference system for prediction of rock fragmentation induced by blasting. *Arabian Journal of Geosciences*. 2015. Vol. 8. Iss. 12, p. 10819-10832. DOI: 10.1007/s12517-015-1952-y
16. Asl P.F., Monjezi M., Hamidi J.K., Armaghani D.J. Optimization of flyrock and rock fragmentation in the Tajareh limestone mine using metaheuristics method of firefly algorithm. *Engineering with Computers*. 2018. Vol. 34, p. 241-251. DOI: 10.1007/s00366-017-0535-9
17. Dimitraki L., Christaras B., Marinos V. et al. Predicting the average size of blasted rocks in aggregate quarries using artificial neural networks. *Bulletin of Engineering Geology and the Environment*. 2019. Vol. 78. Iss. 4, p. 2717-2729. DOI: 10.1007/s10064-018-1270-1
18. Ebrahimi E., Monjezi M., Khalesi M.R., Armaghani D.J. Prediction and optimization of back-break and rock fragmentation using an artificial neural network and a bee colony algorithm. *Bulletin of Engineering Geology and the Environment*. 2016. Vol. 75. Iss. 1, p. 27-36. DOI: 10.1007/s10064-015-0720-2
19. Hasanipanah M., Armaghani D.J., Monjezi M., Shams S. Risk assessment and prediction of rock fragmentation produced by blasting operation: a rock engineering system. *Environmental Earth Sciences*. 2016. Vol. 75. Iss. 9. N 808. DOI: 10.1007/s12665-016-5503-y

20. Jian Zhou, Chuanqi Li, Arslan C.A. et al. Performance evaluation of hybrid FFA-ANFIS and GA-ANFIS models to predict particle size distribution of a muck-pile after blasting. *Engineering with Computers*. 2021. Vol. 37. Iss. 1, p. 265-274. DOI: 10.1007/s00366-019-00822-0

21. Wei Gao, Karbasi M., Hasanipanah M. et al. Developing GPR model for forecasting the rock fragmentation in surface mines. *Engineering with Computers*. 2018. Vol. 34. Iss. 2, p. 339-345. DOI: 10.1007/s00366-017-0544-8

22. Amoako R., Jha A., Shuo Zhong. Rock Fragmentation Prediction Using an Artificial Neural Network and Support Vector Regression Hybrid Approach. *Mining*. 2022. Vol. 2. Iss. 2, p. 233-247. DOI: 10.3390/mining2020013

23. Tiile R.N. Artificial neural network approach to predict blast-induced ground vibration, airblast and rock fragmentation: A Thesis Presented to the Faculty of the Graduate School of the Missouri University of Science and Technology in Partial Fulfillment of the Requirements for the Degree Master of Science in Mining Engineering. Missouri, 2016. N 7571, p. 99.

24. Yari M., He B., Armaghani D.J. et al. A novel ensemble machine learning model to predict mine blasting–induced rock fragmentation. *Bulletin of Engineering Geology and the Environment*. 2023. Vol. 82. Iss. 5. N 187. DOI: 10.1007/s10064-023-03138-y

25. Koopialipoor M., Armaghani D.J., Haghighi M., Ghaleini E.N. A neuro-genetic predictive model to approximate overbreak induced by drilling and blasting operation in tunnels. *Bulletin of Engineering Geology and the Environment*. 2019. Vol. 78. Iss. 2, p. 981-990. DOI: 10.1007/s10064-017-1116-2

26. Hosseini S., Poormirzaee R., Hajihassani M. An uncertainty hybrid model for risk assessment and prediction of blast-induced rock mass fragmentation. *International Journal of Rock Mechanics and Mining Sciences*. 2022. Vol. 160. N 105250. DOI: 10.1016/j.ijrmms.2022.105250

27. Hosseini S., Mousavi A., Monjezi M., Khandelwal M. Mine-to-crusher policy: Planning of mine blasting patterns for environmentally friendly and optimum fragmentation using Monte Carlo simulation-based multi-objective grey wolf optimization approach. *Resources Policy*. 2022. Vol. 79. N 103087. DOI: 10.1016/j.resourpol.2022.103087

28. Jelušič P., Ivanič A., Lubej S. Prediction of Blast-Induced Ground Vibration Using an Adaptive Network-Based Fuzzy Inference System. *Applied Sciences*. 2021. Vol. 11. Iss. 1. N 203. DOI: 10.3390/app11010203

29. Mohamad E.T., Armaghani D.J., Hasanipanah M. et al. Estimation of air-overpressure produced by blasting operation through a neuro-genetic technique. *Environmental Earth Sciences*. 2016. Vol. 75. Iss. 2. № 174. DOI: 10.1007/s12665-015-4983-5

30. Yilmaz A., Poli R. Successfully and efficiently training deep multi-layer perceptrons with logistic activation function simply requires initializing the weights with an appropriate negative mean. *Neural Networks*. 2022. Vol. 153, p. 87-103. DOI: 10.1016/j.neunet.2022.05.030

31. Chen Z., Zhu L., Lu H. et al. Research on bearing fault diagnosis based on improved genetic algorithm and BP neural network. *Scientific Reports*. 2024. Vol. 14. N 15527. DOI: 10.1038/s41598-024-66318-0

32. Temeng V.A., Ziggah Y.Y., Arthur C.K. A novel artificial intelligent model for predicting air overpressure using brain inspired emotional neural network. *International Journal of Mining Science and Technology*. 2020. Vol. 30. Iss. 5, p. 683-689. DOI: 10.1016/j.ijmst.2020.05.020

33. Pizarroso J., Portela J., Muñoz A. NeuralSens: Sensitivity Analysis of Neural Networks. *Journal of Statistical Software*. 2022. Vol. 102. Iss. 7, p. 36. DOI: 10.18637/jss.v102.i07

34. Armaghani D.J., Hasanipanah M., Mahdiyar A. et al. Airblast prediction through a hybrid genetic algorithm-ANN model. *Neural Computing and Applications*. 2018. Vol. 29. Iss. 9, p. 619-629. DOI: 10.1007/s00521-016-2598-8

35. Hosseini M., Khandelwal M., Lotfi R., Eslahi M. Sensitivity analysis on blast design parameters to improve bench blasting outcomes using the Taguchi method. *Geomechanics and Geophysics for Geo-Energy and Geo-Resources*. 2023. Vol. 9. Iss. 1. N 9. DOI: 10.1007/s40948-023-00540-4

36. Mboyo H.L., Bingjie Huo, Mulenga F. K. et al. Assessing the Impact of Surface Blast Design Parameters on the Performance of a Comminution Circuit Processing a Copper-Bearing Ore. *Minerals*. 2024. Vol. 14. Iss. 12. N 1226. DOI: 10.3390/min14121226

37. Singh P.K., Roy M.P., Paswan R.K. et al. Rock fragmentation control in opencast blasting. *Journal of Rock Mechanics and Geotechnical Engineering*. 2016. Vol. 8. Iss. 2, p. 225-237. DOI: 10.1016/j.jrmge.2015.10.005

38. Lundberg S.M., Su-In Lee. A Unified Approach to Interpreting Model Predictions. 31st Conference on Neural Information Processing Systems (NIPS 2017), Long Beach, CA, USA, December, 2017, p. 10. DOI: 10.48550/arXiv.1705.07874

***Authors*: Onalethata Saubi,** *MEng Mining, Research Assistant* (*Botswana International University of Science and Technology, Palapye, Botswana*), *so13000604@biust.ac.bw*, *https://orcid.org/0000-0001-7724-6170*, **Rodrigo S. Jamisola Jr.,** *PhD Electronics and Communication, Lecturer* (*Botswana International University of Science and Technology, Palapye, Botswana*), *https://orcid.org/0000-0002-6481-1545*, **Raymond S. Suglo,** *PhD Mining, Head of Department* (*Botswana International University of Science and Technology, Palapye, Botswana*), *https://orcid.org/0000-0002-5031-5655*, **Oduetse Matsebe,** *PhD Robotics and Mechatronics, Head of Department,* (*Botswana International University of Science and Technology, Palapye, Botswana*), *https://orcid.org/0000-0001-6052-7320*.

The authors declare no conflict of interests.

ISSN 2411-3336; e-ISSN 2541-9404

JOURNAL OF MINING INSTITUTE

Zapiski Gornogo instituta

Journal homepage: pmi.spmi.ru

Research article

Geotechnical Engineering and Engineering Geology

Application of digital simulation methods for predicting parameters of blasted rock muckpile

Sergei V. Khokhlov

Empress Catherine II Saint Petersburg Mining University, Saint Petersburg, Russia

***How to cite this article*:** Khokhlov S.V. Application of digital simulation methods for predicting parameters of blasted rock muckpile. Journal of Mining Institute. 2025. Vol. 275, p. 196-204.

Abstract

The paper considers the features of simulating the blasted rock muckpile formation. We describe various applied approaches and algorithms, as well as discuss the further development of national digital technologies in the mining industry. The study addresses key challenges in simulating explosive impact on rock mass. Due to the significant complexity of mathematical description of rock mass and explosive destruction processes, simulation requires various assumptions that inevitably affect its quality in terms of correspondence to real-world processes. The research compares two approaches to rock fragment dispersion: classical solution based on Newton's laws and alternative approach assuming that the blasted rock moves as a single indivisible volume at the initial moment of time and fractures only upon contact with the surface. The study demonstrates that, given identical explosive impact and different rock mass representations (2D model with pieces of different sizes and densities), the resulting muckpiles differ significantly. The closest in shape muckpiles for both computation methods are obtained for rock mass simulated with 50 and 100 mm fragments. The obtained results suggest that under certain conditions, it is feasible to use a simplified (alternative) method for simulating the muckpile formation. This approach involves treating the rock movement after explosive impact as a single piece with subsequent fragmentation upon landing.

Keywords

explosion; mathematical modelling; muckpile; blasted rock; physics engines; digital technology development

Received: 27.01.2025 ***Accepted: 18.09.2025*** ***Online: 22.10.2025*** ***Published: 31.10.2025***

Introduction

The introduction of various digital solutions in the mining industry is taking place across all areas used in mineral extraction [1, 2], starting with deposit digitalization [3], process simulation [4-6], risk assessment [7, 8], organization of stable and secure communication [9], application of artificial intelligence methods [10, 11], creation of digital twins, introduction of digital assistants, development of automation systems [12, 13], equipment condition diagnostics [14, 15], and ending with the development of full-fledged software packages that store all information about the deposit and stages of its development with full or partial use of Industry 4.0 tools [16, 17].

The computing power of modern computers allows us to return to various mining production tasks that were posed by researchers in the middle of the 20th century, at the dawn of the computer technology era, but could not be solved at that time.

One of these global tasks is predicting the formation of the blasted rock muckpile, which has evolved over time into a more specific task – predicting the location of each point of the blasted block in the muckpile. Thus, the initial task of determining the geometric parameters of the muckpile (width, length, and height) has evolved into a full-scale simulation of rock mass movement during blasting,

with determination of any block point's location at any moment in time. Over the past 50-60 years, there has been a clear trend towards increasing complexity both in problem formulation and in applied solutions. Initially, efforts began with determining 2D or 3D geometry of the muckpile shape and approximate maps of useful component distribution [18], with empirical coefficients (values determined individually for each target) accounting for the influence of blasting parameters and rock mass characteristics. Today, complete simulation of all destruction processes is performed (explosive detonation, stress wave propagation, explosive destruction of the rock mass, and muckpile formation) [19-21], yielding a complete muckpile profile and detailed distribution of the useful component [22] within it. The rock mass was simulated as a matrix of circles (spheres) or squares (cubes) [23, 24], represented as separate blocks (templates), whose dynamics was computed in advance [21, 25, 26]. Various simplifications were introduced to represent the structure of the real rock mass, considering it as an isotropic medium, etc. [27, 28]. The analysis showed that the mechanism of energy transfer from the explosion to the surrounding environment, the specifics of its occurrence [29, 30], and distribution across work types largely determine the formation of the blasted rock muckpile.

Methods

Mathematical modelling of blasted rock muckpile should consider numerous aspects. However, this article focuses on the most essential ones, without which the simulation would be meaningless. These are mathematical descriptions of the research target and the simulated process, which should realistically describe the target's behaviour in the real world. Otherwise, the simulation results could only be used in the gaming industry or for presentation purposes (visual representations).

For the task under consideration, the research target is a rock mass prepared for blasting (the blasted block or its part); the process is the movement of the blasted rock (movement of each piece). As is known, explosive destruction occurs in several stages [31-33]. In this regard, it is necessary to simulate each stage of the blast. This raises the following issues:

1. Different approaches are used when simulating each stage, and the stages overlap in time (they do not occur sequentially).

2. Simulation of the research target. Currently, from a simulation perspective, almost nothing is known about the rock mass. For quality simulation, it is necessary to know the rock mass structure (fracturing or initial fragmentation), physical and mechanical properties of each initial rock mass piece (jointing), and its position in space.

3. Mathematical description of the rock mass after explosive impact (before movement begins).

While the second problem can still be attempted to be solved using modern technical means (sounding, etc.), the state of the rock mass at the moment of movement is unlikely to be determined experimentally. Many scientists have attempted to perform a complete simulation of the explosion and its impact on the rock mass, but due to the noted complexities, the task has not been solved yet. Therefore, during simulation, researchers resort to major assumptions that, although they allow computations to be performed within an acceptable timeframe, do not always reflect the actual state of things. For example, they represent the rock mass in the form of cubic particles measuring 1×1×1 or 2×2×2 m and simulate the muckpile formation. In real conditions, it is difficult to imagine that the muckpile forms precisely from such particles of blasted rock.

The representation of the rock mass in the form of particles of equal size is considered the most common approach to simulation, used by many researchers (companies like Geomix, Blast Maker, etc.). Simulating the formation of detonation products (impact on the target under study – rock), the propagation of stress waves, and the associated explosive destruction of rocks requires a separate description and is not presented in this article. We use only the final result of these studies. Explosive

impact can be simulated differently in various software, therefore it is not specified in the article, just as the blasting parameters used are not mentioned.

The process of rock mass movement is directly related to the mechanism of energy transfer from the explosion to the rock mass. That is, the dispersion of blasted rock occurs due to the pressure exerted on the rock mass by detonation products (gases). With conditionally known explosive impact on the rock mass (pressure of explosion products) and conditionally known state of the rock mass at the initial moment of movement (initial fragmentation), it is possible to simulate the movement of each piece of blasted rock. For this purpose, various libraries are used (physics engines, LS-DYNA, SIMULIA Abaqus, Rocky DEM), actively applied in scientific and gaming computer industries. These tools ensure that target movement strictly follows Newton's classical mechanics laws [34] and appears quite realistic. With proper tuning of input parameters, good convergence with experimental data can be achieved.

Simulation of blasted block

The main elements used to construct a model of a rock mass prepared for blasting:

• Particle (body) – a rigid target where the distance between any two points remains constant. Bodies can represent ground surface, undisturbed rock mass (static bodies), as well as movable targets (dynamic targets), e.g., fragmented rock pieces.

• Shape – a geometric target that follows the body's contour, necessary for assigning properties to targets (e.g., elasticity, density) and checking body interactions (collisions).

• Special constraints required for simulating friction between bodies and preventing mutual penetration of bodies, which is permissible in simulation but not in real life.

• Computation module determines body movement over time according to all constraints using discrete time steps.

When resolving one constraint, we violate others, so to obtain an acceptable solution, it is necessary to iterate through all constraints several times (the most resource-intensive task). To simplify the model, the rock mass prepared for blasting is usually simulated from dynamic targets of the same size (square for solving a planar problem, cube for solving a volumetric problem). Each target is placed geometrically so that it describes the contour of the blasted block or its part. The target size can vary, but it is necessary to consider the fact that reducing the size increases the complexity and computation time. Therefore, most often the targets are made with a side equal to 1 or 0.5 m. In this case, we will simulate the target under study in the Rocky software package (the result will be exactly the same in other software packages, since they all use the laws of classical mechanics).

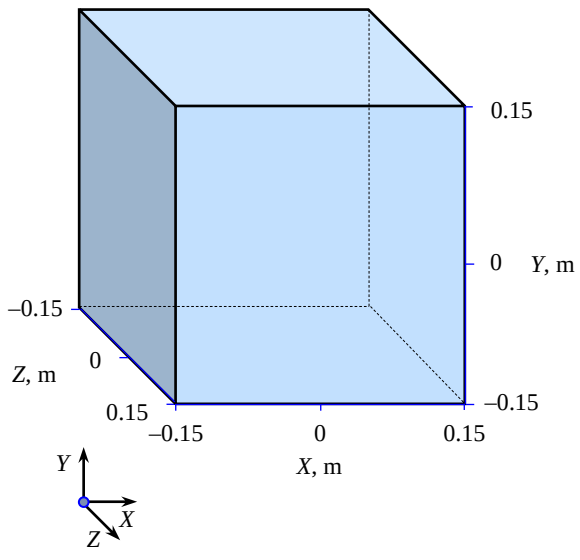

Fig.1. Simulated particle with a size of 0.3 m

The model under study was constructed as part of a blasted block, limited by the bench and the first row of blastholes. The bench height was 10 m, the slope angle was 70°, the toe burden was 5.6 m, and the first row to the bench edge distance was 2 m. The influence of rock conditions, blasting parameters, and delay intervals are not presented in this article.

The model was always formed from identical particles of different sizes – ranging from 0.5 to 0.05 m (Fig.1). Since the software used does not

provide cubic particles, they were created in an external software (Space Claim graphic editor) and subsequently integrated into the Rocky software. The behaviour of particles with two density values was studied: 1800 and 2500 kg/m^3; elastic modulus of 1 GPa; Poisson's ratio of 0.24; friction coefficient of 0.8; dynamic friction coefficient of 0.7. Particle coordinates were set via CSV files, which specified coordinates and indicated the time of particle appearance in the simulation (Fig.2). The final graphical representation of the models is shown in Fig.3.

	A	B	C	D
1	x	y	z	release
2	0	0,15	-1,5	0
3	0	0,45	-1,5	0
4	0	0,75	-1,5	0
5	0	1,05	-1,5	0
6	0	1,35	-1,5	0
7	0	1,65	-1,5	0
8	0	1,95	-1,5	0
9	0	2,25	-1,5	0
10	0	2,55	-1,5	0
11	0	2,85	-1,5	0
12	0	3,15	-1,5	0
13	0	3,45	-1,5	0

Fig.2. Fragment of CSV file with particle coordinate information

In this case, the colour scheme does not carry any semantic meaning and serves purely for presentation purposes. However, all similar software provides the ability to track the movement of individual parts of the rock mass. Despite the fact that the particles were set as solid bodies, in this particular case, a planar problem was solved. To prevent particle movement in the third dimension, two transparent walls with a zero friction coefficient were artificially added to the model, between which the particles moved. The already blast-destroyed rock mass is being simulated, so the fact that blastholes are overdrilled and rock masses below the bench toe are exposed to blast impact is ignored.

Simulation of dispersion

After developing the rock mass model, it is necessary to simulate the explosive impact. For this purpose, the applied physics engine (similar in others) provides the following capabilities: setting force, torque, and impulse. Full-scale simulation of blasted rock fragment dispersion and muckpile formation is quite a challenging task. This study compares two methods of muckpile simulation: classical and with assumptions (alternative):

• Particle dispersion along ballistic trajectories with determination of particle coordinates at any moment in time (classical problem).

• Initial movement of rock mass as a single piece with subsequent dispersion at the moment of landing (simplified problem).

Our study tests the hypothesis about the formation of the muckpile as the movement of the entire volume of blasted rock to a certain distance, followed by dispersion of rock mass fragments upon

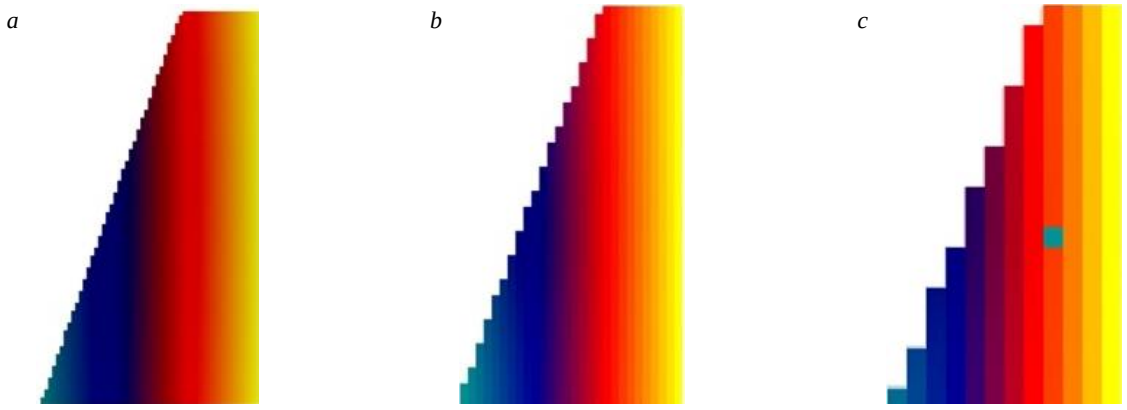

Fig.3. Models formed from particles of different sizes:
a – 0.1 m; *b* – 0.2 m; *c* – 0.3 m

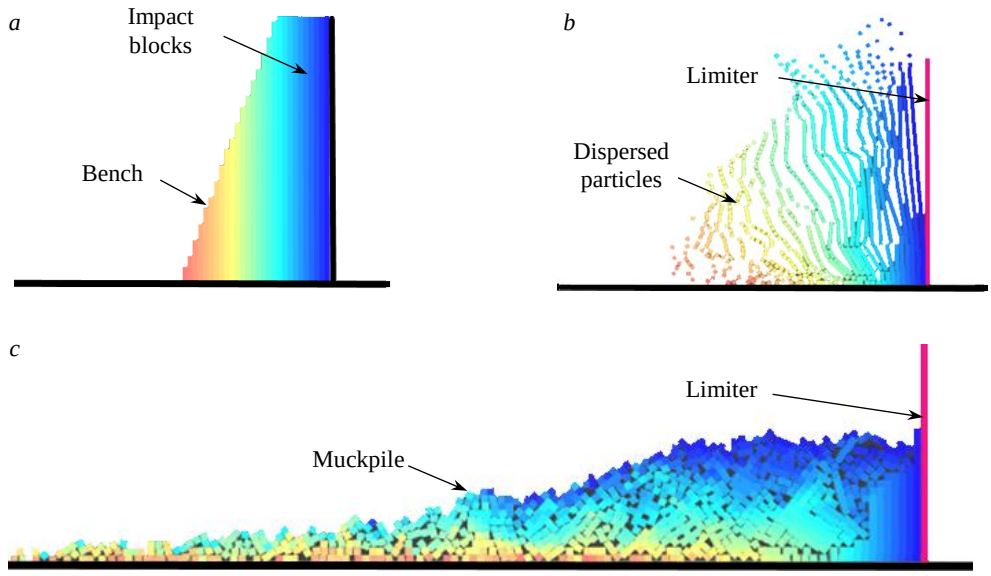

Fig.4. Simulation stages according to the classical variant [35]

impact with the surface. This assumption was based on the analysis of high-speed camera video recordings of explosions made during research work at one of the deposits in Yakutia.

Experiments

Particle dispersion along ballistic trajectories with determination of particle coordinates at any moment in time. In the classical case, the explosive impact on particles (setting rocks in motion) was specified through the Motion Frames function. After the start of movement, a special limiter was created to prevent particles from dispersion to the right, towards the undisturbed rock mass. The initial state of the model (before the start of movement) (Fig.4, *a*), the moment of particle dispersion (Fig.4, *b*), and the final state (muckpile) (Fig.4, *c*) are presented.

Initial movement of rock mass as a single piece with subsequent dispersion at the moment of landing. This alternative task considers the movement of the block as a single piece. In this case, after explosive impact, the block moves as a single piece and destroys into parts only at the moment of its contact with the surface. The movement of rocks is specified using a platform that moves the centre

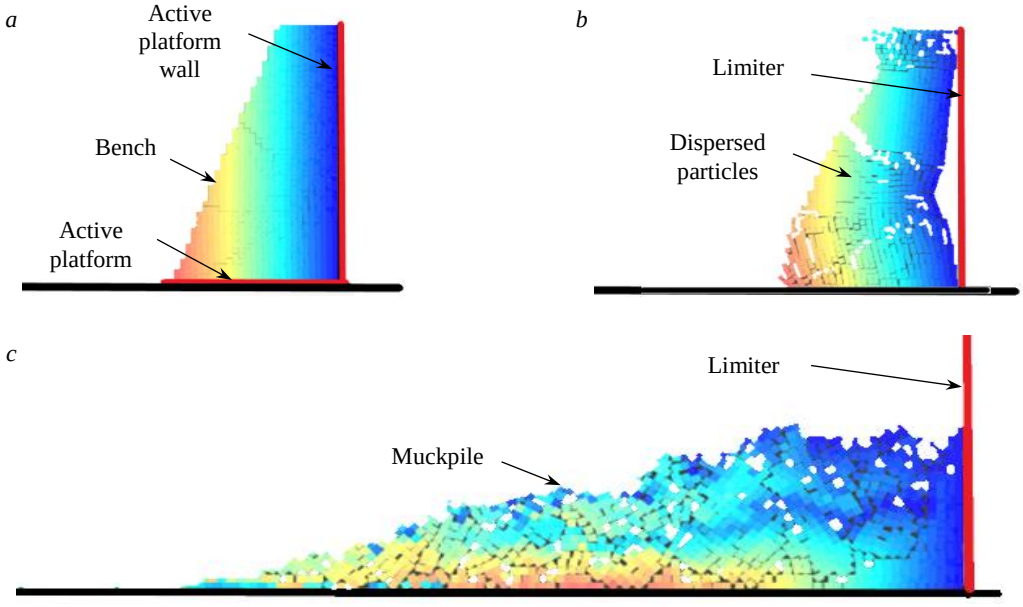

Fig.5. Simulation stages according to the alternative variant [35]

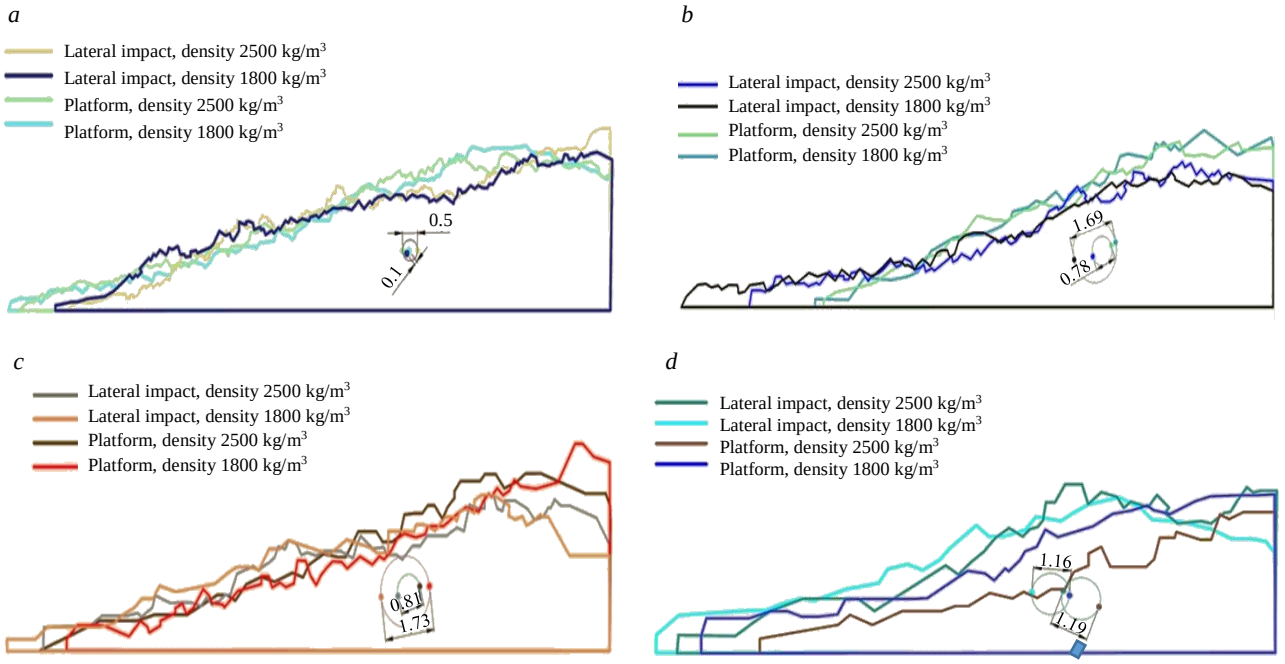

Fig.6. Comparison of muckpile contours and centres of mass [35] for particles of different sizes: *a* – 0.1 m; *b* – 0.2 m; *c* – 0.3 m; *d* – 0.5 m

of gravity of the block at an angle of 45° with a speed of 2 m/s along the vertical and horizontal axes (Fig.5, *a*). After 0.05 s, the impact ceased, the block continued to move under the influence of inertial forces and dispersed upon contact with the surface. As in the first case, a special limiter was created to prevent particles from dispersion to the right, towards the undisturbed rock mass (Fig.5, *b*). Figure 5, *c* presents the final state of the rocks.

Research results

When comparing muckpiles obtained using different methods, the following parameters were selected as criteria: muckpile width, height, and angle; distance to the muckpile centre of mass; difference between centres of mass, and time required for simulation. The centre of gravity coordinates of the muckpiles were determined using the Space Claim software, while the contour of the obtained muckpiles was traced in AutoCAD. The parameters of the muckpiles obtained in this way are presented in Fig.6. The numbers in the figures show the difference in metres between the centres of mass of the muckpiles obtained using different methods. For example, the difference in centres of mass of the muckpiles for particles measuring 100 mm with a density of 2500 kg/m^3 is 0.5 m (Fig.6, *a*). For particles measuring 0.05 m, the muckpiles were simulated only under the condition that their density was 1800 kg/m^3 (Fig.7). The results of discrepancies in the parameters of the muckpile obtained using different methods for particles of the same size and density are presented in the Table.

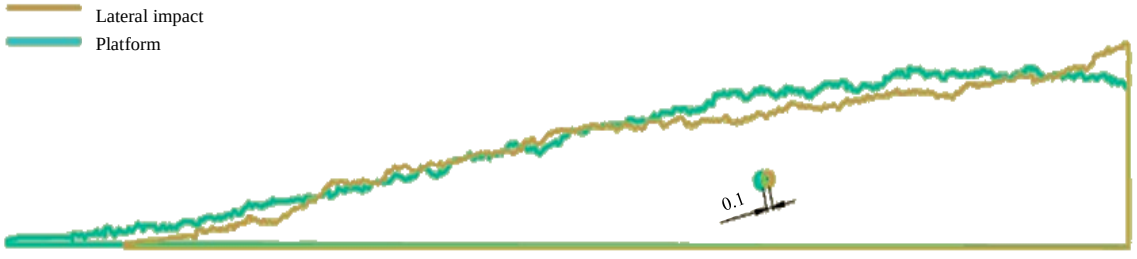

Fig.7. Comparison of muckpile contours and centres of mass distribution [35]

Simulation results

Particle size, m	Density, kg/m^3	Difference between centres of mass, m	Difference in muckpile height, m	Difference in muckpile width, m	Difference in muckpile height, %	Difference in muckpile width, %
0.5	1800	1.16	0.06	1.39	1.36	7.29
0.5	2500	1.19	0.79	2.57	16.53	13.92
0.3	1800	1.73	0.37	2.10	9.76	9.86
0.3	2500	0.81	0.52	0.15	13.72	0.75
0.2	1800	1.69	0.81	5.49	22.50	23.71
0.2	2500	0.78	0.84	2.58	21.71	12.54
0.1	1800	0.10	0.02	1.14	0.53	6.08
0.1	2500	0.50	0.05	1.85	1.28	10.05
0.05	1800	0.10	0.01	1.15	0.32	5.24

Discussion

The results of simulation strongly depend on the specified boundary conditions. For example, under identical conditions, the muckpile height for particles measuring 0.5×0.5 m is 4.41-4.47 m, while for particles measuring 0.1×0.1 m it is 3.9-3.95 m. The results of simulating muckpile formation using various approaches showed that as the piece size and density decrease, the difference between the centres of mass of the muckpiles formed according to the first and second problems decreases. The smallest deviation of 0.1 m is observed for particle density of 1800 kg/m^3 and particle sizes of 0.05 and 0.1 m. The remaining parameters for these particles differ by no more than 5 %.

This allowed us to conclude that under certain conditions, muckpile formation can be carried out using a simplified method – considering the movement of the rock mass as a single piece with subsequent dispersion at the moment of landing. This approach was implemented in the developed software [36]. In the first approximation, the problem was solved in a planar formulation, which is a very significant assumption [37]. Modern computing capabilities make it possible to perform this research in a 3D formulation. Currently, these works are being actively conducted at the Educational Centre of Digital Technologies of the Mining University*.

Due to the market-out of foreign companies from Russia, there is a shift towards software packages developed by Russian experts. The simplest and fastest way is to copy all existing solutions. In this process, both solutions and terms used in the original product are copied into software packages. It should be noted that Russian legislation prohibits the use of foreign words when Russian equivalents exist**.

A simple replacement of foreign software with a similar Russian development (which copies the foreign product) will not increase enterprise efficiency. It is necessary to create new software products with solutions that surpass existing foreign developments. A technological and scientific breakthrough will occur through the joint efforts of all developers (at least in terms of standardization and data exchange). Without this, it is impossible to create an advanced software package with functionality that meets the needs of the entire mining industry. To use complex software packages effectively, it is necessary to have a deep understanding of all the intricacies of mining production processes, which is impossible without receiving quality specialized education [38].

While digital technologies are transforming our world, they remain merely tools for accomplishing our goals. Recently, mining science was considered an art form [39], with many uncertainties that are difficult to describe in mathematical terms. Often, in the author's opinion, it is necessary to simply listen to one's intuition and to people who work directly in production and know all the intricacies of

* Educational Centre of Digital Technologies. URL: https://nc-digital.spmi.ru/ (accessed 17.02.2025).

** Federal Law N 52-FZ of 28 February 2023 "On Amendments to the Federal Law "On the State Language of the Russian Federation".

the work. It seems that the final adjustment of the used software package together with such people is the right management decision for leaders.

Conclusion

From a scientific point of view, the most correct solution for simulating the muckpile (the final stage of explosive destruction) is to estimate the movement of each individual piece of blasted rock based on classical Newtonian mechanics. However, this requires significant computational resources, and the rock pieces must be of different sizes and shapes. The use of alternative approaches, such as those presented in this article, requires firstly scientific justification, secondly, a description of the boundaries of use (it may not be suitable for all conditions), as well as mandatory industrial validation.

The formation of the blasted rock muckpile is a complex and still unsolved problem. Currently, there are only certain simplifications of the classical problem solution. If the boundary conditions are incorrectly specified, researchers will obtain results that differ from reality. Simplification of the problem should be based on knowledge [38] about explosive destruction processes; otherwise, researchers will go down the wrong path. When implementing any solution using software tools, all simplifications and assumptions used must be communicated to potential users.

The author expresses gratitude to A.V.Bazhenova and A.P.Kirkin, Candidates of Engineering Sciences, Senior Researchers at Gipronickel Institute LLC for their assistance in developing and configuring the models.

REFERENCES

1. Makhovikov A.B., Filyasova Yu.A. Information technologies for solid mineral extraction in the Arctic. *Sustainable Development of Mountain Territories.* 2024. Vol. 16. N 3, p. 1110-1117 (in Russian). DOI: 10.21177/1998-4502-2024-16-3-1110-1117
2. Fomin S.I., Govorov A.S. Strategy of formation of operating space in open pit mines based on cut-off grade control. *Mining Informational and Analytical Bulletin.* 2024. N 11, p. 165-179 (in Russian). DOI: 10.25018/0236_1493_2024_11_0_165
3. Egorov A.S., Kalinin D.F., Sekerina D.D. Geotectonic model of the deep structure of the Zmeinogorsky ore district of Rudny Altai according to geological interpretation of geophysical survey complex. *Bulletin of the Tomsk Polytechnic University. Geo Assets Engineering.* 2024. Vol. 335. N 8, p. 148-160 (in Russian). DOI: 10.18799/24131830/2024/8/4431
4. Bagautdinov I.I., Belyakov N.A., Sevryukov V.V., Rasskazov M.I. Hardening soil model in prediction of plastic deformation zone in soft rock mass of Yakovlevo iron ore deposit. *Gornyi zhurnal.* 2022. N 12, p. 16-21 (in Russian). DOI: 10.17580/gzh.2022.12.03
5. Zhukovskiy Yu.L., Suslikov P.K. Assessment of the potential effect of applying demand management technology at mining enterprises. *Sustainable Development of Mountain Territories.* 2024. Vol. 16. N 3, p. 895-908 (in Russian). DOI: 10.21177/1998-4502-2024-16-3-895-908
6. Galimyanov A.A., Kazarina E.N. Clarification of the formula for the relevance of well collection. *Bulletin of the Kuzbass State Technical University.* 2025. N 2 (168), p. 94-100 (in Russian). DOI: 10.26730/1999-4125-2025-2-94-100
7. Shojaee Barjoee S., Rodionov V. Mathematical modeling and optimization of workplace illumination in ceramic industries (Iran) using DIALux evo. *Journal of Infrastructure, Policy and Development.* 2024. Vol. 8. N 15. N 5918. DOI: 10.24294/jipd5918
8. Shojaee Barjoee S., Rodionov V.A. Respirable Dust in Ceramic Industries (Iran) and its Health Risk Assessment using Deterministic and Probabilistic Approaches. *Pollution*. 2024. Vol. 10. Iss. 4, p. 1206-1226. DOI: 10.22059/POLL.2024.376043.2360
9. Makhovikov A.B., Kryltsov S.B., Matrokhina K.V., Trofimets V.Ya. Secured communication system for a metallurgical company. *Tsvetnye metally.* 2023. N 4, p. 5-13 (in Russian). DOI: 10.17580/tsm.2023.04.01
10. Sekerina D.D., Saitgaleev M.M., Senchina N.P. et al. Role of strike-slips and graben-rifts in controlling oil and gas reservoirs in deep horizons of the Russko-Chaselsky Ridge (West Siberian Province). *Mining Science and Technology.* 2025. Vol. 10. N 2, p. 109-117. DOI: 10.17073/2500-0632-2025-02-399
11. Zaytseva E.V., Kochneva A.A., Katuntsov E.V., Kiba M.R. Approaches to digital image processing in the mining industry. *XXI Century: Resumes of the Past and Challenges of the Present plus.* 2024. Vol. 13. N 1 (65), p. 62-67 (in Russian).
12. Romashev A.O., Nikolaeva N.V., Gatiatullin B.L. Adaptive approach formation using machine vision technology to determine the parameters of enrichment products deposition. *Journal of Mining Institute.* 2022. Vol. 256, p. 677-685. DOI: 10.31897/PMI.2022.77
13. Rasskazov I.Yu., Fedotova Yu.V., Anikin P.A. et al. Improvement of the automated system of geomechanical monitoring and early prevention of dangerous geodynamic phenomena. *Mining Informational and Analytical Bulletin.* 2022. N 12-1, p. 106-121 (in Russian). DOI: 10.25018/0236_1493_2022_121_0_106
14. Koteleva N., Korolev N. A Diagnostic Curve for Online Fault Detection in AC Drives. *Energies*. 2024. Vol. 17. Iss. 5. N 1234. DOI: 10.3390/en17051234

15. Koteleva N., Valnev V. Automatic Detection of Maintenance Scenarios for Equipment and Control Systems in Industry. *Applied Sciences*. 2023. Vol. 13. Iss. 24. N 12997. DOI: 10.3390/app132412997

16. Klebanov A.F., Bondarenko A.V., Zhukovsky Yu.L., Klebanov D.A. Establishing remote control centers of a mining operation: strategic prerequisites and implementation stages. *Russian Mining Industry.* 2024. N 4, p. 174-183 (in Russian). DOI: 10.30686/1609-9192-2024-4-174-183

17. Lukichev S.V., Nagovitsyn O.V. Digital transformation and technological independence of the mining industry. *Russian Mining Industry.* 2022. N 5, p. 74-78 (in Russian). DOI: 10.30686/1609-9192-2022-5-74-78

18. Yang R.L., Kavetsky A. A three dimensional model of muckpile formation and grade boundary movement in open pit blasting. *International Journal of Mining and Geological Engineering*. 1990. Vol. 8. Iss. 1, p. 13-34. DOI: 10.1007/BF00881125

19. Zhi Yu, Xiu-Zhi Shi, Zong-Xian Zhang et al. Numerical Investigation of Blast-Induced Rock Movement Characteristics in Open-Pit Bench Blasting Using Bonded-Particle Method. *Rock Mechanics and Rock Engineering*. 2022. Vol. 55. Iss. 6, p. 3599-3619. DOI: 10.1007/s00603-022-02831-w

20. Wei Fu, Furtney J., Valencia J. Blast Movement Simulation Through a Hybrid Approach of Continuum, Discontinuum, and Machine Learning Modeling. 57th U.S. Rock Mechanics/Geomechanics Symposium, 25-28 June 2023, Atlanta, GA, USA. OnePetro, 2023. N ARMA-2023-0831. DOI: 10.56952/ARMA-2023-0831

21. Zhixian Hong, Ming Tao, Mingsheng Zhao et al. Numerical modelling of rock fragmentation under high in-situ stresses and short-delay blast loading. *Engineering Fracture Mechanics*. 2023. Vol. 293. N 109727. DOI: 10.1016/j.engfracmech.2023.109727

22. Yanitskii E.B., Kabelko S.G., Dunaev V.A., Rakhmanov R.A. Computer simulation of displacement of rock mass and estimation of ore dilution as a result of massive explosion in the open mining. *Explosion technology.* 2018. N 120/77, p. 94-108 (in Russian).

23. Kucewicz M., Łukasz M., Baranowski P. et al. Numerical modeling of blast-induced rock fragmentation in deep mining with 3D and 2D FEM method approaches. *Journal of Rock Mechanics and Geotechnical Engineering*. 2024. Vol. 16. Iss. 11, p. 4532-4553. DOI: 10.1016/j.jrmge.2024.01.017

24. Sellers E., Furtney J., Onederra I., Chitombo G. Improved understanding of explosive–rock interactions using the hybrid stress blasting model. *The Journal of The Southern African Institute of Mining and Metallurgy*. 2012. Vol. 112. Iss. 8, p. 721-728.

25. Vasylchuk Y.V., Deutsch C.V. Approximate blast movement modelling for improved grade control. *Mining Technology.* 2019. Vol. 128. Iss. 3, p. 152-161. DOI: 10.1080/25726668.2019.1583843

26. Cundall P.A., Strack O.D.L. A discrete numerical model for granular assemblies. *Géotechnique*. 1979. Vol. 29. Iss. 1, p. 47-65. DOI: 10.1680/geot.1979.29.1.47

27. Hosseini S., Poormirzaee R., Hajihassani M. An uncertainty hybrid model for risk assessment and prediction of blast-induced rock mass fragmentation. *International Journal of Rock Mechanics and Mining Sciences*. 2022. Vol. 160. N 105250. DOI: 10.1016/j.ijrmms.2022.105250

28. Zharikov I.F., Zakharov V.N., Norel B.K. Strength passport and relation equation between stress and strain invariants for inhomogeneous rocks under volumetric stress state. *Izvestiya Rossiiskoi akademii nauk. Mekhanika tverdogo tela*. 2015. N 6, p. 49-60 (in Russian).

29. Moldovan D.V., Chernobay V.I., Yastrebova K.N. The influence of composite material in the stemming design on its operability. *Mining Informational and Analytical Bulletin.* 2023. N 9-1, p. 110-121 (in Russian). DOI: 10.25018/0236_1493_2023_91_0_110

30. Moldovan D.V., Chernobay V.I., Sokolov S.T., Bazhenova A.V. Design concepts for explosion products locking in chamber. *Mining Informational and Analytical Bulletin.* 2022. N 6-2, p. 5-17 (in Russian). DOI: 10.25018/0236_1493_2022_62_0_5

31. Kazakov N.N., Viktorov S.D., Shlyapin A.V., Lapikov I.N. Rock crushing by blasting in open-pit mines. Moscow: Rossiiskaya akademiya nauk, 2020, p. 520 (in Russian).

32. Kurinnoi V.P. Theoretical foundations of explosive rock destruction. Dnepr, 2018, p. 280 (in Russian).

33. Peng Xu, Renshu Yang, Jinjing Zuo et al. Research progress of the fundamental theory and technology of rock blasting. *International Journal of Minerals, Metallurgy and Materials*. 2022. Vol. 29. Iss. 4, p. 705-716. DOI: 10.1007/s12613-022-2464-x

34. Verbilo P., Karasev M., Belyakov N., Iovlev G. Experimental and numerical research of jointed rock mass anisotropy in a three-dimensional stress field. *Rudarsko-geološko-naftni zbornik*. 2022. Vol. 37. N 2, p. 109-122. DOI: 10.17794/rgn.2022.2.10

35. Bazhenova A.V. Forecasting ore contour displacement during blasted rock muckpile formation in open-pit mines: Avtoref. kand. dis. … tekhn. nauk. Saint Petersburg: Sankt-Peterburgskii gornyi universitet, 2023, p. 20 (in Russian).

36. Koteleva N.I., Khokhlov S.V., Bazhenova A.V. Certificate of state registration of computer program N 2024660948 of the Russian Federation. Program for determining ore contour displacement during blasted rock muckpile formation. Publ. 14.05.2024. Bul. N 5 (in Russian).

37. Engmann E., Ako S., Bisiaux B. et al. Measurement and Modelling of Blast Movement to Reduce Ore Losses and Dilution at Ahafo Gold Mine in Ghana. *Ghana Mining Journal*. 2013. Vol. 14, p. 27-36.

38. Litvinenko V.S. Digital Economy as a Factor in the Technological Development of the Mineral Sector. *Natural Resources Research*. 2020. Vol. 29. Iss. 3, p. 1521-1541. DOI: 10.1007/s11053-019-09568-4

39. Rudnik S.N., Afanasev V.G., Samylovskaya E.A. 250 years in the service of the Fatherland: Empress Catherine II Saint Petersburg Mining University in facts and figures. *Journal of Mining Institute.* 2023. Vol. 263, p. 810-830.

***Author* Sergei V. Khokhlov,** *Candidate of Engineering Sciences, Associate Professor* (*Empress Catherine II Saint Petersburg Mining University, Saint Petersburg, Russia*), *khokhlov_sv@pers.spmi.ru, https://orcid.org/0000-0003-1040-8328.*

The author declares no conflict of interests.